IOWA STATE UNIVERSITY
Digital Repository

1978

Spectral analysis methods for noisy sampled-data systems

Steve Forrest Russell
Iowa State University

Follow this and additional works at: https://lib.dr.iastate.edu/rtd

Part of the Electrical and Electronics Commons

Recommended Citation

INFORMATION TO USERS

This material was produced from a microfilm copy of the original document. While the most advanced technological means to photograph and reproduce this document have been used, the quality is heavily dependent upon the quality of the original submitted.

The following explanation of techniques is provided to help you understand markings or patterns which may appear on this reproduction.

1. The sign or "target" for pages apparently lacking from the document photographed is "Missing Page(s)". If it was possible to obtain the missing page(s) or section, they are spliced into the film along with adjacent pages. This may have necessitated cutting thru an image and duplicating adjacent pages to insure you complete continuity.

2. When an image on the film is obliterated with a large round black mark, it is an indication that the photographer suspected that the copy may have moved during exposure and thus cause a blurred image. You will find a good image of the page in the adjacent frame.

3. When a map, drawing or chart, etc., was part of the material being photographed the photographer followed a definite method in "sectioning" the material. It is customary to begin photoing at the upper left hand corner of a large sheet and to continue photoing from left to right in equal sections with a small overlap. If necessary, sectioning is continued again — beginning below the first row and continuing on until complete.

4. The majority of users indicate that the textual content is of greatest value, however, a somewhat higher quality reproduction could be made from "photographs" if essential to the understanding of the dissertation. Silver prints of "photographs" may be ordered at additional charge by writing the Order Department, giving the catalog number, title, author and specific pages you wish reproduced.

5. PLEASE NOTE: Some pages may have indistinct print. Filmed as received.

7813242

RUSSELL, STEVE FORREST
  SPECTRAL ANALYSIS METHODS FOR NOISY
  SAMPLED-DATA SYSTEMS.

IOWA STATE UNIVERSITY, PH.D., 1978

Spectral analysis methods for noisy

sampled-data systems

by

Steve Forrest Russell

A Dissertation Submitted to the

Graduate Faculty in Partial Fulfillment of

The Requirements for the Degree of

DOCTOR OF PHILOSOPHY

Major: Electrical Engineering

Approved:

Signature was redacted for privacy.

In Charge of Major Work

Signature was redacted for privacy.

For the Major Department

Signature was redacted for privacy.

For the Graduate College

Iowa State University
Ames, Iowa

1978

TABLE OF CONTENTS

PREFACE

Although there are copious publications available that address the topic of spectral analysis in general and many that address time series data in particular, it is difficult to find information on how to apply the general theory to practical data processing. User oriented application techniques and computer programs are seldom published and canned routines leave the researcher uneasy as to their biasing effect on the results. This research was done in an effort to provide a complete system of applied spectral analysis. Special attention was given to describing the effects of measurement and sampling error, observer bias, and interpretation of results.

Much of the text is basically tutorial and, as such, is not original but the organization and presentation are unique. Except for Chapter XIX, the original contributions are discussed in the introduction. The author is especially happy with Chapter XIX because it represents several ideas on interpretation he believes to be unique. To the fullest extent possible, authors of works already published have been gratefully acknowledged by the many references.

The author's major professor, John Basart, has contributed greatly to this work through his helpful technical discussions, objective criticism of important ideas, and diligent proofreading. His original interest in the Maximum Entropy Technique and conviction that it would provide an important dissertation topic are the embryos of this work. It could not have been completed without his continuing encouragement and patience.

I. INTRODUCTION

The analysis of empirical data for the purpose of determining funda-
mental parameters for a physical system is a basic goal for much applied
research. One of the most important characteristics to be determined is
the frequency spectrum of the recorded data. Spectral analysis plays an
important role in many scientific fields such as radio astronomy, meteo-
rology, geophysics, mechanics, statistics, communication signal processing,
econometrics, physics, and biology. Probably the most important research
applications of spectral analysis are presently in the fields of geophysics
and astronomy. The most advanced work on the spectral analysis of noisy
empirical data is being published by geophysicists in connection with oil
exploration geology. The search for new sources of oil in deeper domes
and offshore has placed severe requirements on the available methods of
data processing. To improve the spectral resolution of the measured spec-
trum, these researchers have developed many sophisticated techniques with
the most advanced being maximum entropy spectral analysis.

Maximum entropy spectral analysis (MEM) has stirred the interest of
radio astronomers because its claims for better spectral resolution with
limited amounts of data creates a promise of better sky brightness maps for
radio sources. However, both the theory and application of MEM are not well-
developed and, consequently, this tool is not available to most researchers.
Initially, the goal for this research was to develop the theory and prac-
tical implementation of the maximum entropy spectral analysis method for
estimating the power spectral density function when the autocorrelation
data are incomplete. As the research progressed it became apparent that

many problems and barriers existed between theory and application of spectral analysis. These problems were further investigated and it was concluded that a more general approach to spectral analysis should be taken. This approach led to a more user oriented thesis. Such topics as estimation theory, frequency domain analysis, system analysis techniques, sampling theory, and Fourier analysis were investigated. The selection of a method of spectral estimation as well as the mathematical behavior of the most common methods was developed.

The author's original contributions are a collection of smaller topics scattered throughout the text. Chapter X, the Hilbert space vector formulation of digital Fourier transform analysis, is independent work that constitutes the mathematical framework used to develop the spectral mixing formula discussed in Chapter XI. The discovery of a companion function to the time autocorrelation function is original work and is discussed in Chapter XV. The mathematical development of the calculus of variations technique used for this derivation was developed independently and is given in Chapter XXI, Part J. Much of the development of digital Fourier transform spectral estimation given in Chapter XII is unique to this text. The author's approach is one of analysis and interpretation while most published material concentrates on the computational details of the fast Fourier transform (FFT). The chapter on methods of spectral analysis is original work designed to aid researchers in selecting appropriate estimation techniques and to help in understanding the problems common to all spectral estimators. Although the topics of sampling theory presented in Chapter VI are not new, the presentation and derivations are specifically

designed to relate the effects of sampling to spectral analysis. The discussion of MEM is not original but the computer program and interpretation of results have not been previously published.

Much work remains to be done in this research area. More theoretical study of MEM is needed to determine optimum series lengths and more efficient methods of spectral calculation. Data reduction schemes and better interpretation of estimated spectra need further research work. Probably the most needed future research is on the problem of unequally spaced data samples and undersampled data.

Most of the mathematics and terminology used in the text are those commonly used in current publications in the spectral analysis area. One of the author's more fundamental contributions has been to unite the terminology used by geophysicists, statisticians, and electrical engineers to provide a common basis for communication. Where more than one terminology exists for a given concept, every effort has been made to define and use the varied terminology. The term time function is used to denote a continuous function of time that can be completely described in mathematical terms. A time series is a sampled or discrete time function and may be ideal or empirical. The term data function is used by the author to denote either a time function or time series that is being numerically processed. The author defines collective parameters as those characteristics of a data function that are used to describe the process that generated the data. An asterisk is used to denote complex conjugation, a script F operator denotes Fourier transformation ($\mathcal{F}\{x(t)\} = X(\omega)$), and convolution is abbreviated by the product; $y(t) = x(t) * h(t)$.

This research and resulting thesis are most directly suited for use by the researcher who must do very serious spectral studies. The casual user is better served by applying readily available "canned" approaches to spectral analysis. This distinction and the possible alternatives available are discussed in Section D of Chapter IX.

It will become apparent to the reader doing a detailed study of this work that the techniques of autoregressive spectral estimation, maximum entropy spectral estimation, and recursive digital filtering all have similar mathematical forms. They do share a common mathematical and theoretical basis but they produce different spectral estimates because they employ different criteria-of-goodness and numerical algorithms. These similarities were useful in helping to better define the properties of these estimators.

It must be emphasized that this work has a wide range of applicability. It is useful for any empirical work involving the Fourier transform or the autocorrelation function. The variables of time and frequency are used for convenience but others such as space and momentum are equally valid. All the methods of analysis presented involve some type of model fitting. In estimation theory, a truly "parameter free" method is not possible. The selection of a model is the most important task in spectral analysis. Chapter IX was written to help clarify the selection of a model and the computing method.

II. TIME AND FREQUENCY CHARACTERIZATION OF TIME
FUNCTIONS AND SERIES

A time function or time series can always be specified by enumerating all possible function values in the time domain. For the continuous time function, this is done by representing the function by a mathematical equation. For the discrete time series, the entire description can be given by an autoregressive equation or difference equation. This complete description often involves mathematical completeness in the sense that the mathematical representation is valid over the entire time domain and is well behaved. In many scientific applications, this complete description is not necessary. Quite often it is sufficient to specify more collective parameters such as average value, mean-square value, or power spectrum. Such collective descriptions often give valuable insight into the physical nature of the process which generated the observed data. For this reason it is desirable to discuss some of these collective characterizations.

For theoretical purposes, a time function or time series can be considered as being a sample function of a real process. This process can generate a time function which has both periodic components and random components. Often a statistical description involving probability density functions and higher order moments is considered suitable. For most circumstances, the observable in this system is some time function or series and it is the analysis of this time data that must be used to study the process. The definition of many of the collective parameters of a real process involve the use of statistical definitions. To be able to obtain these same parameters from time data it is usually necessary to assume that the

process is ergodic. With this assumption it is possible to avoid the use of statistical descriptions of the process and obtain the collective parameters directly from the time data. Most of the theory that is presented in this dissertation will be concerned with time functions that are sample functions of real ergodic processes. The use of probability descriptions will usually be limited to those that are necessary for a better theoretical understanding. None of the actual signal processing techniques will involve the direct use of any probabilistic descriptions.

In the time domain, a data function can be characterized by its time average value, mean-square value, and variance. These collective parameters can be related to the statistical description of the function and yet do not require any transformations or use of statistical parameters. The time domain analysis of a data function can also involve the computation of the time autocorrelation function (Appendix I, Part E). The time autocorrelation function is a measure of how well the function correlates with itself in time and also can be used to determine the mean-square value of the function and detect any periodic components of the process.

In the frequency domain, a data function can be characterized by its amplitude spectrum or its power spectrum. The amplitude spectrum is obtained by taking the Fourier transform of the data function. The existence of an amplitude spectrum depends upon the existence of the Fourier transform. In many cases, the amplitude spectrum of a random process does not exist. The power spectral density function for a data function is obtained by taking the Fourier transform of the autocorrelation function. This definition is superior to the use of the amplitude spectrum because it elim-

inates the problem of existence. The power spectrum of a data function is often the desired physical information that is needed to solve a problem or verify some scientific hypothesis. For discrete data the power spectrum can be determined from the discrete form of the autocorrelation function or by using the autoregressive power spectrum.

In theoretical discussions of the characterization of data functions, it is possible to give a mathematical formulation which describes the function over the entire domain of the independent variable. When the data function is obtained from a physical process, the mathematical description becomes only an _estimate_ for the "true" function. The various collective parameters which are used to characterize the data function are derived with the infinite domain assumption. Measured data can be described by collective parameters only when mathematical estimates of the entire data function are assumed. For example, a finite time series can be represented by a discrete Fourier series or by an autoregressive series. Both of these representations assume that the data function can be defined for all time. In Fourier analysis this is referred to as the periodic extension assumption.

Once a mathematical description of the data function is obtained, the various collective parameters such as average value, mean-square value and power spectrum can be calculated from the theory. As a consequence, these representations are only valid for the infinite domain assumption. It is important to realize that a concept such as power spectrum is totally dependent on the mathematical definition and is not related directly to a physical concept. The mathematical definitions for the various collective parameters are given in Chapter IV.

III. OBSERVABLES AND ESTIMATION THEORY

The mathematical description of an area of physical theory such as quantum mechanics or spectral analysis often involves the use of transformations into other domains. When working with this theory, it is important to realize that quantities defined in domains other than the time domain do not have a real physical significance and hence are not physical observables. Quantities such as amplitude spectra or power spectra depend upon a mathematical definition for their existence. The definition is usually chosen so that it helps to give additional useful information about the physical process that is described by the function. As an example, for a periodic function, the amplitude spectrum obtained by taking the Fourier transform gives the complex amplitude coefficients of the Fourier series which describe the time behavior of the function.

A time function can be defined for all time but a real observable can be defined only for a finite time. This causes problems with definitions which involve the use of infinite time functions. Transform domain functions such as amplitude and power spectra are defined only for functions which exist for all time. These definitions must be modified to accommodate the "finiteness" of a real observable. The modification is usually designed so that it gives a good approximation of the "true" value. Another approach is to use mathematical models to approximate the observed function with a mathematical function which is defined for all time. The study of how to formulate mathematical functions which describe data that is obtained empirically is called estimation theory.

The simplest forms of estimation theory are concerned with the selection of an approximating function to "fit" a set of empirical data and the selection of a criterion to judge the "goodness" of that fit. A function or computational scheme that is used to describe some property of the empirical data is referred to as an <u>estimator</u>. Estimators can be as simple as a single sine function or as complicated as a digital Fourier transform. The three estimation processes most commonly used are those of signal filtering or smoothing, prediction or extrapolation, and interpolation. These processes are typically used in conjunction with a desired mathematical process such as numerical intergration or Fourier transformation. The estimation processes of smoothing, extrapolation, and interpolation are all useful in spectral analysis.

Estimation theory is used to help solve the common problems of numerical integration, difference equations, and the representation of empirical data by exact functions. These methods are discussed in books on estimation theory and numerical analysis. A partial list of these methods would include for interpolation; Lagrange interpolation, Hermite interpolation, divided differences, Newton's forward and backward differences, Gaussian interpolation, Stirling's interpolation, and methods due to Bessel, Everett, and Steffenson, and for numerical integration; Riemann summation, Cote's formulas, Simpson's rule, Romberg's method, Filon's formula, Gauss-Sidel method, Gauss-Laguerre method, Gauss-Hermite method, Chebyshev's formulas, and aid-of differences, and finally for curve-fitting of empirical data; least-squares polynomial, orthogonal polynomials, trigonometric functions (Fourier series), exponential functions, Chebyshev polynomials,

continued fractions, and rational functions.

Why are there so many approximation methods? The reason is that estimation theory cannot specify a unique method of estimation for every class of problem. All of the listed methods incorporate assumptions about the measured data that make that estimate optimum in some sense. For every criterion of goodness, a slightly different estimator can be determined.

Estimation methods often derive their name from the criterion used in their selection as "optimum". Such schemes as the method-of-least-squares, the method-of-moments, and the method-of-maximum-likelihood are often seen in the literature. Estimators can also be classified according to such characteristics as linearity, bias, sufficiency, efficiency, and asymptotic efficiency.

The selection of an estimate as "best" is strictly a matter of user definition. Experience with the use of practical estimators has shown that certain criteria produce good results for a variety of tasks. One of the most popular criterion-of-goodness is to minimize the least-square error between data values and estimated values. The sum given in Equation 3-1 is often referred to as the total mean-square error or "residue" of the estimate:

$$\text{mean-square error} = \frac{1}{N} \sum_{n=1}^{N} (\hat{x}_n - x_n)^2 \qquad (3\text{-}1)$$

The data set is represented by the x_n values and the estimations by the $\hat{x}_n$ values.

Estimation theory is an important part of the theory of spectral analysis of empirical data because of the finite observations involved. Estimation theory can be applied to truncated functions to provide the "best" possible spectral estimate for a given amount of data. Criteria of goodness for spectral estimators are often not well-defined and an attempt will be made to discuss this problem for each of the various estimation schemes.

A rigorous background in estimation theory is not necessary for the study of spectral analysis but it does help to clarify the goals of the various schemes and puts the selection of a particular scheme on a rational basis. For the reader who is interested in a good introductory text on estimation theory, the book by Deutsch (1965) is recommended.

IV. TIME AND FREQUENCY DOMAIN ANALYSIS

The time and frequency domain analysis of a time function or time series can be done on a theoretical basis or on an empirical basis. The theory for this analysis has been well worked out and is widely published in communication theory books and statistics books. The empirical analysis of a data function involves the use of estimation theory and criteria of goodness and is not well defined for the user. Empirical analysis also involves many subjective decisions and a priori assumptions about the process which generated the data. These factors make it easy for the observor to bias and influence the computed results. This has been especially true in spectral analysis where the experimenter often must choose among several techniques which give dissimilar results. In this chapter we will attempt to summarize the theory and equations that are used to characterize a data function and make special emphasis on the differences between theoretical definitions and estimations.

A. Theoretical Definitions

A data function is completely described by an equation or recursive relation which specifies all values in the time domain. Although this complete description is adequate, it is often more meaningful to describe the data function by such collective parameters as average (mean or expected value) value, mean-square value, variance, autocorrelation function, amplitude spectrum, and power spectrum. A discussion of the theoretical definitions for these parameters will now be given. It will be assumed that

the data function is defined for all time and is well-behaved so that there are no mathematical problems with the definition. The theoretical definitions will depend on a knowledge of the probability density function for the process and on the assumed ability to define the function over the entire domain of the independent variable. Most of the theory to be given can be applied to deterministic functions as well as random time functions. The discussion will emphasize the random aspects of the data function but it will be assumed that the reader will see the analogy for deterministic functions.

The expectation (or average) value for a random variable is defined as:

$$E\{x\} = \int_{\text{all } x} x\, p(x)dx \tag{4A.1}$$

This theoretical definition depends on a complete knowledge of the probability density function $p(x)$ and the existence of the integral.

For a periodic function, the average value for one Fourier period is computed from the integral:

$$\overline{x(t)} = \frac{1}{T} \int_{-T/2}^{+T/2} x(t)dt \tag{4A.2}$$

The mean-square value for a random variable is defined as the second moment integral:

$$E\{x^2\} = \int_{\text{all } x} x^2 p(x)dx \tag{4A.3}$$

For a periodic function, the mean-square value for one Fourier period is:

$$\overline{x^2(t)} \quad \frac{1}{T} \int_{-T/2}^{+T/2} x^2(t)dt \qquad (4A.4)$$

The square root of this value is called the root-mean-square value of the periodic function. The mean-square value for a random variable or periodic time function is often called the "power" of the function because it is a measure of the second moment and is used to calculate the power in an electrical circuit.

The variance of a random function is a measure of the variability of the values of the function. The variance is defined as:

$$\sigma_x^2 = \int_{all\ x} (x - E\{x\})^2 p(x)dx \qquad (4A.5)$$

The variance is often referred to as the "ac power" in the function because it is a measure of the variability after removal of the average or "dc" part. An equivalent definition for the periodic function could be developed but is rarely used. Quite often the average value is subtracted from the total function and a "zero average" function is defined. This is done explicitly in the definition of the variance. A good example of this approach is the use of a zero-mean autocorrelation to define a power spectrum. Blackman and Tukey (1958) use the term <u>autocovariance</u> for this zero-mean function. Other descriptive parameters such as higher order moments could be defined but these are not often used. This completes the discussion of time descriptions and we now go to the autocorrelation function.

The time autocorrelation function for a data function is defined by the following multiplication and integration process:

$$R_x(\tau) = \lim_{T \to \infty} \frac{1}{T} \int_{-T/2}^{T/2} x(t)x(t+\tau)dt \qquad (4A.6)$$

The autocorrelation function has two very important uses. First, it can be used to describe the "coherence" of a function because it is a measure of how well the data function correlates with itself after a shift in time. The process of shift-multiply-average emphasizes periodic features in the data function and is useful for determining any periodic structure in a data function which would normally appear to be stochastic in nature. Second, it is used to define the power spectrum of a stochastic process. The Wiener-Khinechine relations (Appendix I, Part F) define the power spectrum of a random function as the Fourier transform of its autocorrelation function.

We refer to the autocorrelation function as the representation of the time function in the "autocorrelation domain." The domain variable τ is called the lag time or simply the lag. The lag time is the amount of shift between the two functions. The autocorrelation function cannot be used to derive a unique time function because of the integration process. This means that the autocorrelation function is not unique with respect to the time function. For any given autocorrelation function, an infinite number of time functions could have been used to derive it.

The frequency domain descriptions for a data function are limited to the amplitude spectral function, the power spectral density function, and the autoregressive spectral function. Other spectral representations such as using a filter transfer function are valuable for special applications but are really just special cases of the three general methods.

The amplitude spectral function is defined as the Fourier transform of the data function:

$$X(\omega) = \int_{-\infty}^{+\infty} x(t)e^{-j\omega t}dt \qquad\qquad (4A.7)$$

The amplitude spectrum will exist only when the Fourier transform exists. It is most applicable for periodic functions and single pulses in the time domain. It also forms the basis for discrete Fourier transform analysis of sampled data functions where the function is assumed periodic beyond the sampling interval.

The power spectral density function is defined as the Fourier transform of the autocorrelation function. These two functions form a Fourier transform pair as given by the Wiener-Khinchine relations:

$$S_x(\omega) = \int_{-\infty}^{+\infty} R_x(\tau)e^{-j\omega\tau}d\tau \qquad\qquad (4A.8)$$

$$R_x(\tau) = \frac{1}{2\pi} \int_{-\infty}^{+\infty} S_x(\omega)e^{+j\omega\tau}d\omega \qquad\qquad (4A.9)$$

In theory, a knowledge of either function implies a complete knowledge of the other. In empirical analysis, this assumption is rarely true because of finite data. Consequently, the various estimators and algorithms will have an important effect on computed results. It is the development of the theory describing these various estimators that is the primary goal of this research.

B. Estimations

When working with empirical data, the data function is only an estimate of the "true" function and all collective parameters that are calculated from the empirical data set are <u>estimated</u> parameters. If the data set is large and the estimator is well chosen, the estimated parameters are very close to the true parameters. For theoretical reasons, and also for asthetic reasons, most estimators are chosen so that they are unbiased and converge to the true values as the amount of data becomes infinite. There are important cases where the estimate that is used does not converge to the theoretical value but still gives an acceptable estimate. This occurs often in commonly used techniques of spectral analysis. The estimators that will now be presented are widely used in the analysis of empirical data.

The average value for a time series or set of random variable values is estimated by the sum

$$\bar{x}_k = \frac{1}{N \sum_{k=1} p_k} \sum_{k=1}^{N} x_k p_k \tag{4B.1}$$

where the p_k are the discrete probabilities associated with each data sample x_k. It is commonly assumed that all of the samples, x_k, are equally likely which means that the p_k are all equal. For N equally likely random samples of x, the average value is the simple arithematic average given by

$$\bar{x}_k = \frac{1}{N} \sum_{k=1}^{N} x_k \tag{4B.2}$$

where $p_k = \frac{1}{N}$.

For a periodic function, the average is estimated by the integral

$$\overline{x(t)} = \frac{1}{T} \int_{-T/2}^{+T/2} x(t)dt \tag{4B.3}$$

where T is called the period of the average. Generally this period is not equal to the Fourier period because the Fourier period is unknown. The Riemann sum approximation for this integral is given by Equation 4B.2.

The mean-square value for a discrete random variable is estimated by:

$$\overline{x^2} = \frac{1}{\sum_{k=1}^{N} P_k} \sum_{k=1}^{N} x_k^2 P_k \tag{4B.4}$$

When all N samples are equally likely, the mean-square value reduces to:

$$\overline{x^2} = \frac{1}{N} \sum_{k=1}^{N} x_k^2 \tag{4B.5}$$

For a periodic function, the mean-square value is estimated by

$$\overline{x^2(t)} = \frac{1}{T} \int_{-T/2}^{+T/2} x^2(t)dt \tag{4B.6}$$

where, again, T is called the period of the average (or estimate). The Riemann sum approximation for this integral is given by Equation 4B.5.

The variance of a random function is estimated by using a weighted average summation approximation for Equation 4A.5. This estimate is:

$$\hat{\sigma}_x^2 = \overline{(x - \overline{x})^2} = \overline{x^2} - (\overline{x})^2 \tag{4B.7}$$

When all samples are equally likely, (4B.7) is estimated by the sum:

$$\hat{\sigma}_x^2 = \frac{1}{N} \sum_{k=1}^{N} (x_k - \overline{x})^2 \tag{4B.8}$$

The estimation procedures used for autocorrelation functions, auto-covariance functions, amplitude spectra, power spectra, and autoregressive spectra are the most important aspects of spectral analysis and are the main themes of this dissertation. The procedure for selecting a particular estimation method and its application to empirical data will be discussed in Chapter IX. The details of the estimation algorithms will be presented in the appropriate later chapters.

V. SYSTEM ANALYSIS TECHNIQUES

There are several important system theorems and mathematical tools used in spectral analysis. Many of these are associated with system analysis in electrical engineering and are also broadly applicable to many other physical systems. For completeness, and to familiarize the reader with many of the concepts to be used later, these analysis techniques will now be discussed.

A. Convolution Theorem

The time output response, y(t), of a physical system can be related to the time input, x(t), by convolving the system impulse response, h(t), with the input. A simple system is shown in Figure 5A-1. For a linear,
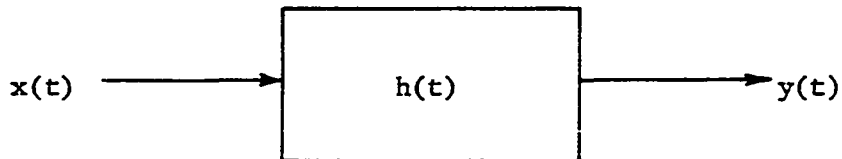
Figure 5A-1. A Simple Operating System for Illustrating Convolution

time-invariant system, the <u>convolution integral</u> relating the input and output is written as:

$$y(t) = \int_{-\infty}^{+\infty} h(t - \tau)x(\tau)d\tau \qquad (5A.1)$$

or in shorthand notation:

$$y(t) = h(t) * x(t) \qquad (5A.2)$$

All functions are assumed to be defined for all time and $h(t-\tau)$ is the impulse response of the system occurring at delay time, $t=\tau$.

The impulse response of a system is defined as the system output response when the input is a unit impulse (Dirac delta function). This can be shown by using the convolution integral of Equation 5A.1 and the sifting property of the Dirac delta function.

The impulse response of a system can also be obtained by first computing the system transfer function, $H(\omega)$, and taking the inverse Fourier transform. It is important to realize that $H(\omega)$ and $h(t)$ form a Fourier transform pair: —

$$H(\omega) = \int_{-\infty}^{+\infty} h(t)e^{-j\omega t}dt \qquad (5A.3)$$

$$h(t) = \frac{1}{2\pi} \int_{-\infty}^{+\infty} H(\omega)e^{+j\omega t}d\omega \qquad (5A.4)$$

This relationship is frequently used in electrical engineering to help analyze and synthesize electrical networks and systems. It is often easier to synthesize an electrical network in the frequency domain and then use the inverse Fourier transform to determine its time response. These equations all assume infinite time functions and do not take into effect the requirement of causality in the system.

For $h(t)$ to be <u>causal</u> (no output prior to there being an input), the impulse response must be zero prior to zero time; $h(t)=0$, $t<0$. Also, if the system is to be stable, the impulse response must be absolutely integrable (the response must die out as time goes on). The true limits of the convolution integral are actually the "overlap" of $x(t)$ and $h(t-\tau)$.

Only for the theoretical case where both exist for all delay time, τ, do

the limits become infinite. At a specific observation time, $t = t_1$, the

output will have a value corresponding to the value of the convolution

integral:

$$y(t_1) = \int_a^b h(t_1 - \tau)x(\tau)d\tau \qquad (5A.5)$$

A typical graphical interpretation of this convolution integral is shown

in Figure 5A-2.
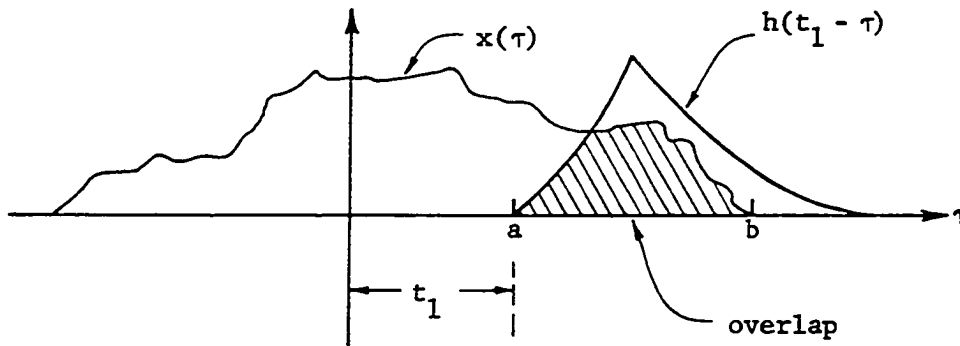
Figure 5A-2. A Typical Graphical Interpretation of Convolution
Showing Limits of Integration

For physically realizable systems with causal impulse response, the

convolution integral is usually written as (Schwartz, 1970, p. 87):

$$y(t) = \int_{-\infty}^{t} h(t - \tau)x(\tau)d\tau \qquad (5A.6)$$

For both $x(t)$ and $h(t)$ causal, the convolution integral relating the

system output with its causal input and causal impulse response becomes:

$$y(t) = \int_0^t h(t - \tau)x(\tau)d\tau \qquad (5A.7)$$

This representation of the system response most closely represents the true circumstances when a signal x(t) is applied to a system h(t). The system output, y(t), can be interpreted as a superposition of past values of x(τ) weighted by the system impulse response, h(τ). A widely used graphical interpretation for the convolution of two causal functions is given in Figure 5A-3. The impulse response h(t - τ) represents the true system response after it has been "folded over" and extended into past time. The system response, y(t), at observation time t, is the input function, x(τ), from τ = 0 to τ = t weighted by the "folded over" impulse response, h(t - τ).

The convolution integral of Equation 5A.7 is used in linear systems analysis to develop the Laplace transform method of solving system responses (Cheng, 1959, p 227). If x(t) and h(t) are both Laplace transformable, the Laplace transform of the output is equal to the product of the Laplace transforms of x(t) and h(t):

$$Y(s) = X(s)H(s) \tag{5A.8}$$

This important result is called the convolution theorem.

The convolution of finite time signals or periodic time functions with a causal system can be analyzed using the concepts of the amplitude transform, both Fourier and Laplace, but the analysis of the response of a system to a random time function must be done using autocorrelation functions and power spectra. This theory will now be summarized.

x(t)
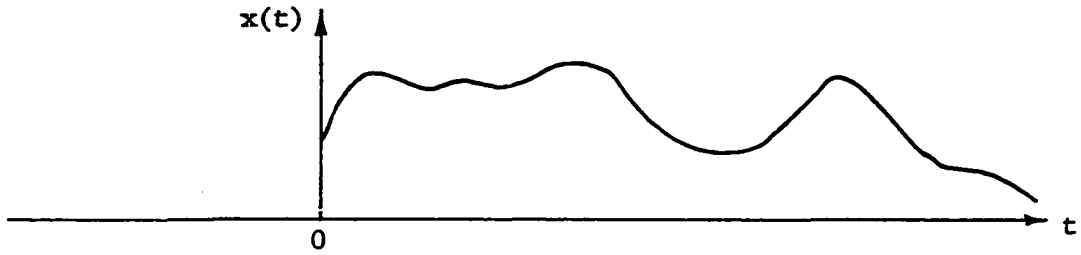
a) Causal input function

h(t)
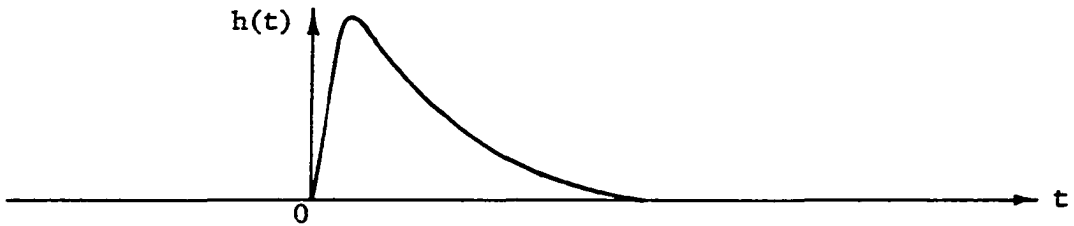
b) Causal filter response

$h(t - \tau)$ $x(\tau)$

0   t τ

t

past | future

present
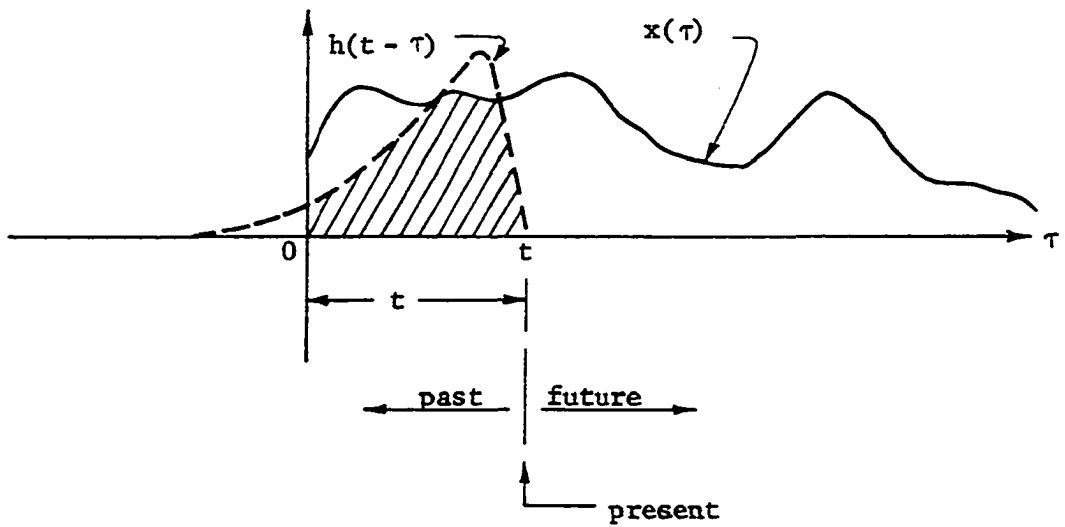
c) Convolution for causal functions

Figure 5A-3. Graphical Interpretation for the Convolution of
Two Causal Functions

B. System Response to Random Time Inputs

A linear, time-invariant system, $h(t)$, operating on a sample time function of a random process, $x(t)$, defines a new sample function, $y(t)$, that is related to the "old" function and the system impulse response by the following convolution integral:

$$y(t) = \int_{-\infty}^{+\infty} h(u)x(t-u)\,du \qquad\qquad (5B.1)$$

This integral is equivalent to that given in Equation 5A.1 and we see that the concept of convolution is valid even for random inputs. This alternate form of the convolution integral was chosen to make the following derivations simpler. This result is very important because it will facilitate the derivation of important relationships between the input and output sample functions.

If we assume the input process is both stationary and ergodic, the time autocorrelation function can be used to determine the power spectra of input and output. The time autocorrelation function for the output is defined as:

$$R_y(\tau) = \lim_{T \to \infty} \frac{1}{T} \int_{-T/2}^{+T/2} y(t)y(t+\tau)\,dt \qquad\qquad (5B.2)$$

The output at time t and at time $(t + \tau)$ can be written in terms of the convolution integral of Equation 5B.1 as

$$y(t) = \int_{-\infty}^{+\infty} h(u)x(t-u)\,du \qquad\qquad (5B.3)$$

$$y(t+\tau) = \int_{-\infty}^{+\infty} h(v)x(t+\tau-v)\,dv \qquad\qquad (5B.4)$$

where u and v are dummy variables of integration. If these relationships are substituted into Equation 5B.2, and the time average of the product $x(t-u)x(t+\tau-v)$ is identified as the autocorrelation function of the input with argument $(\tau-v+u)$, the autocorrelation of the output can be written in terms of the system impulse response and the autocorrelation of the input as (Carlson, 1968, p. 80):

$$R_y(\tau) = \int_{-\infty}^{+\infty} \int_{-\infty}^{+\infty} h(u)h(v)R_x(\tau-v+u)\,dv\,du \qquad (5B.5)$$

Equation 5B.5 is an important intermediate result because it expresses the relationship between the input and output autocorrelation functions. It can be thought of as the autocorrelation domain equivalent of the time domain convolution integral of Equation 5B.1.

To obtain the power spectral density function for both the input and output processes, we take the Fourier transform of both sides of Equation 5B.5. The resulting triple integral can be separated by rearranging the exponential of the transform to give an argument equal to the argument of the input autocorrelation function (Carlson, 1968, p. 81). This gives:

$$\mathcal{F}\{R_y(\tau)\} = \int_{-\infty}^{+\infty} h(u)e^{+j\omega u}\,du \int_{-\infty}^{+\infty} h(v)e^{-j\omega v}\,dv \int_{-\infty}^{+\infty} R_x(\tau-v+u)e^{-j\omega(\tau-v+u)}\,d\tau$$

$$(5B.6)$$

The last integral is the Fourier transform of the input while the first two are the Fourier and inverse Fourier transforms of the impulse response. These transforms can be written in abbreviated form as:

$$\mathcal{F}\{R_y(\tau)\} = \mathcal{F}^{-1}\{h(u)\}\mathcal{F}\{h(v)\}\mathcal{F}\{R_x(\tau)\} \qquad (5B.7)$$

Using the Wiener-Khinchine relations and recognizing that the product of

the two transforms of h(t) is equal to the absolute value squared of the Fourier transform, we obtain the important relationship between input and output power spectra:

$$S_y(\omega) = |H(\omega)|^2 S_x(\omega) \qquad \text{(5B.8)}$$

Equation 5B.8 is widely used in the analysis of linear systems and their response to random inputs (Thomas, 1969, p. 145). It clearly illustrates the effect of a linear filter on the spectrum of an input function. It is also used to determine filter shape for optimum design and spectral shaping. This relationship is also used in prewhitening and in the design of a linear predictive filter as needed in maximum entropy spectral analysis.

C. Digital Convolution

Digital convolution can be performed with two discrete functions by adapting the convolution integral for causal functions as given in Equation 5A.7. Since digital operations involve finite input data sets and digital filters of finite length, the convolution and filtering operations can always be thought of as involving causal functions. Approximating the continuous convolution integral with a Riemann sum gives

$$y_t = \Delta t \sum_{k=0}^{t} h_{t-k} x_k \qquad \text{(5C.1)}$$

where:

t = the output or observation time index.

Δt = the sampling interval.

The correspondence between discrete and continuous variables is given below:

$$y(t) : y(t\Delta t) = y_t$$
$$h(t - \tau) : h(t\Delta t - k\Delta \tau) = h_{t-k} \qquad (5C.2)$$
$$x(\tau) : x(k\Delta \tau) = x_k$$

An example for a digital filter of length five and a time series of length six will now be given. Figure 5C-1 illustrates a graphical interpretation of digital convolution. The outputs for the example are:

$$y_0 = \Delta t(h_0 x_0)$$
$$y_1 = \Delta t(h_1 x_0 + h_0 x_1)$$
$$y_2 = \Delta t(h_2 x_0 + h_1 x_1 + h_0 x_2)$$
$$y_3 = \Delta t(h_3 x_0 + h_2 x_1 + h_1 x_2 + h_0 x_3)$$
$$y_4 = \Delta t(h_4 x_0 + h_3 x_1 + h_2 x_2 + h_1 x_3 + h_0 x_4)$$
$$y_5 = \Delta t(h_4 x_1 + h_3 x_2 + h_2 x_3 + h_1 x_4 + h_0 x_5)$$
$$y_6 = \Delta t(h_4 x_2 + h_3 x_3 + h_2 x_4 + h_1 x_5 + h_0 x_6)$$
$$y_7 = \Delta t(h_4 x_3 + h_3 x_4 + h_2 x_5 + h_1 x_6)$$
$$y_8 = \Delta t(h_4 x_4 + h_3 x_5 + h_2 x_6)$$
$$y_9 = \Delta t(h_4 x_5 + h_3 x_6)$$
$$y_{10} = \Delta t(h_4 x_6)$$

These outputs represent the numerical computation of the digital outputs for observation times starting at zero and ending at $10\Delta t$. The outputs y_0 through y_3 represent the transient response of the filter to the input, y_4 through y_6 represent the steady-state output, and y_7 through y_{10} represent the "ringing down" of the filter.
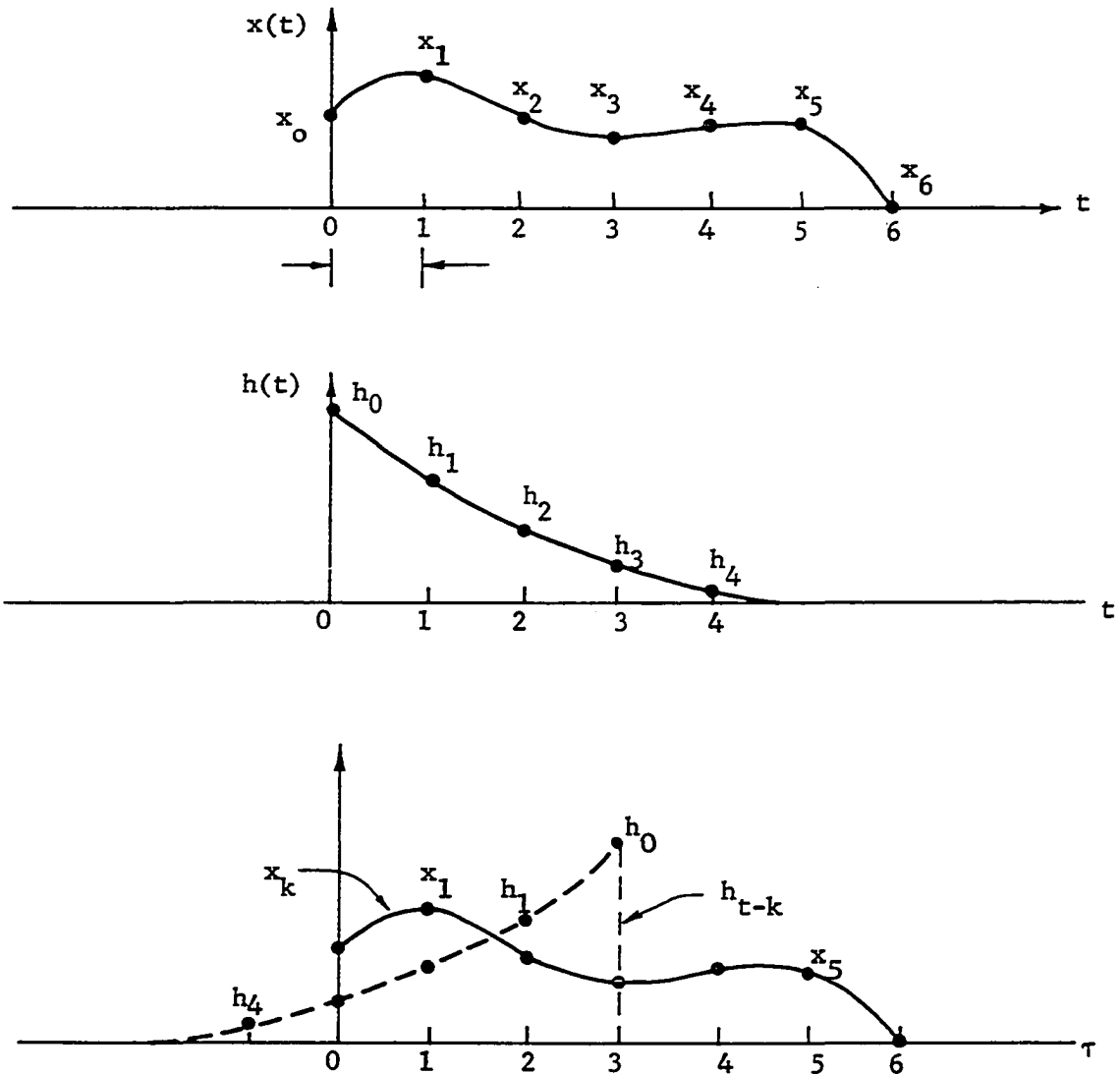
Figure 5C-1. Graphical Interpretation for the Digital Convolution
of a Time Series and a Digital Filter Showing the
Output Conditions at y_3

Digital convolution or filtering can also be thought of as the weighted superposition of past values of $x(\tau)$. As time goes forward, the past values are represented by smaller values of t. If this weighting is represented by coefficients a_0, a_1, a_2, ... a_M, the convolution can be written as:

$$y_t = \Delta t \sum_{k=0}^{t} a_{t-k} x_k \qquad (5C.3)$$

The digital convolution concept does not depend upon having a filter with as many coefficients, a_i, as there are data values, x_i. As a general rule, the filter is of length M and the time series is of length N. It is desirable to have N much larger than M so that filter transient response will be minimized.

The most commonly used formulation for digital convolution is given by Equation 5C.4:

$$y_t = \Delta t \sum_{k=0}^{M} a_k x_{t-k} \qquad (5C.4)$$

The ranges on the indices are

$$t = 0, 1, 2, 3, 4, \ldots (N+M)$$

$$k = 0, 1, 2, 3, 4, \ldots M$$

and the values for x with indices less than zero are assumed to be zero (causality). The response of the filter and the resulting output can be separated into three distinct observation time intervals:

1. y_t for $0 \leq t \leq (M-1)$ is the transient response of the filter near the starting time.

2. y_t for $M \leq t \leq N$ is the steady-state response.

3. y_t for $(N+1) \leq t \leq (N+M)$ is the "ringing down" or decay response after removal of the input.

Digital filtering and convolution can also be formulated with matrices. This procedure is straight forward if one uses Equation 5C.4.

D. Digital Deconvolution

A general method for solving the convolution integral and obtaining a unique solution does not exist. In special cases, the convolution integral can be solved but the required boundary conditions and class of functions are such that these special circumstances do not apply to most practical cases. For discrete data and digital filters, deconvolution is really a matter of definition and is an "unraveling" of the weighting applied by the filter coefficients. For most cases, digital deconvolution can be performed using the following method.

Digital convolution was represented by Equation 5C.1. If the y's are measured and the h's are known, it is possible to use the set of $(N+M+1)$ equations defined by (5C.1) to solve for the x's. This can be done recursively by solving the following system of equations:

$$x_n = \frac{1}{\Delta t a_o} y_n - \frac{1}{a_o} \sum_{k=0}^{N-1} a_{n-k} x_k \qquad (5D.1)$$

These recursive equations can also be expressed exclusively in terms of the y's. When this is done, the resulting set of equations can be

thought of as a deconvolution filter with weights, b_i. The "deconvolution" using this special filter is obtained from:

$$x_n = \frac{1}{\Delta t} \sum_{k=0}^{N} b_{n-k} y_k \qquad (5D.2)$$

The b's or filter weights are obtained from the a's of the original filter by using the following recursive formulas:

$$b_0 = \frac{1}{a_0}$$

$$b_1 = \frac{a_1}{a_0} b_0 \qquad (5D.3)$$

$$b_n = \frac{a_n}{a_0} b_0 - \frac{1}{a_0} \sum_{k=1}^{n-1} a_{n-k} b_k \qquad (n = 2, 3, \ldots M)$$

VI. SAMPLING THEORY AND SAMPLED DATA FUNCTIONS

In the usual sense, sampling theory is applied to sampled data systems in communication theory. In this application the user must consider such aspects as digital data transmission and reconstruction. The parameters of the system are usually under the control of the designer and can be optimized to suit a particular need. The signal is usually sampled at a rate well above the Nyquist rate and is sampled long enough to give any desired accuracy for the reconstruction.

Sampling theory as applied to spectral analysis must be approached from a somewhat different viewpoint. First of all, the parameters of the transmitting system are not under the control of the experimenter. The "received signal" is usually a data function generated by some physical process that is being investigated. Since the nature of the received signal is being investigated for its unknown spectral properties, it is difficult to determine what sampling rate is necessary. Also, the amount of data needed to resolve an unknown spectrum cannot be determined in advance. The experimenter must solve this problem in an iterative manner by making reasonable assumptions about the spectrum to be measured. The sampling technique can then be studied to see if these assumptions are valid. A widely used technique for spectral analysis of an unknown spectrum involves the use of prefiltering to limit the spectral input to the sampler. This method is most successful if the sampling system can be adjusted to produce a range of filtered spectrums and sampling rates. As can be seen from the theory that will be discussed, the prefiltering method will produce an accurate estimate of the input spectrum that is within the filter passband.

A time function or time series generated by a real physical process can be generally represented in the frequency domain by a spectrum containing both continuous and line components. Because of the "uncertainty principle" between time and frequency, this function is theoretically limited in spectral bandwidth by the physical process of measurement. Drawing on an analogy from quantum mechanics, the process of observation will introduce a perturbation which limits the observed spectral bandwidth. Even if the process has an infinite bandwidth, any measurement of a data function would involve the convolution of that function with a "filter" inside the measuring system.

Because of this effect, every data function or set of empirical data will be bandlimited. To assure the user that the signal input to the sampler is bandlimited, it is wise to use the method of prefiltering. The method of data sampling can have a profound effect on an empirically derived power spectrum. The conditions of sampling such as sampling rate and number of samples are important parameters to be analyzed. The sampling technique is such a fundamental part of the measurement of a power spectrum that it is difficult to separate its effects from the actual power spectrum estimation technique.

The basic concepts of sampling theory as applied to spectral analysis will be discussed in this chapter. It will not be possible to discuss all aspects of this broad topic but the most important ideas will be covered. Specific applications of sampling theory to the various aspects of spectral estimation will be presented in appropriate later chapters.

A. Sampling Theory - Basic Definitions

The important parameters of a sampling system are the spectral band-width of the data function to be sampled, the sampling rate, the pulse shape of the sampling function, the output filtering for the sampler, and the amount of data measured. Figure 6B-1 shows a block diagram of a sampling system that will be used for the system analysis of the sampler. It is assumed that prefiltering has already been applied to the data function and that post-sampling reconstruction or filtering will be applied at a later stage. For purposes of discussion it will be assumed that the process being examined produces a continuous time function.

The time function to be measured, $x(t)$, is called the sampled function. It is assumed to be continuous, bandlimited, and defined for all time. The spectral bandwidth of $x(t)$ will be assumed to be limited to $2\omega_b$. The output of the sampler is denoted by $y(t)$ and is obtained by multiplying the sampled function, $x(t)$, by the sampling function, $m(t)$. $m(t)$ is characterized by a repetitive pulse shape, $p(t)$, and is a periodic function that can be represented by a Fourier series. The sampling system can also be modeled by the convolution of a Dirac comb function and a single pulse, $p(t)$, which represents the basic pulse shape of the sampler. The system is modeled with system blocks such as multiplication and convolution so that the system analysis techniques given in Chapter V can be used in the derivations.

The important relationship between the sampling rate (or frequency) and the Nyquist sampling rate (or frequency) can be discussed with the help of Figure 6A-1. The Nyquist frequency depends upon the spectral content of
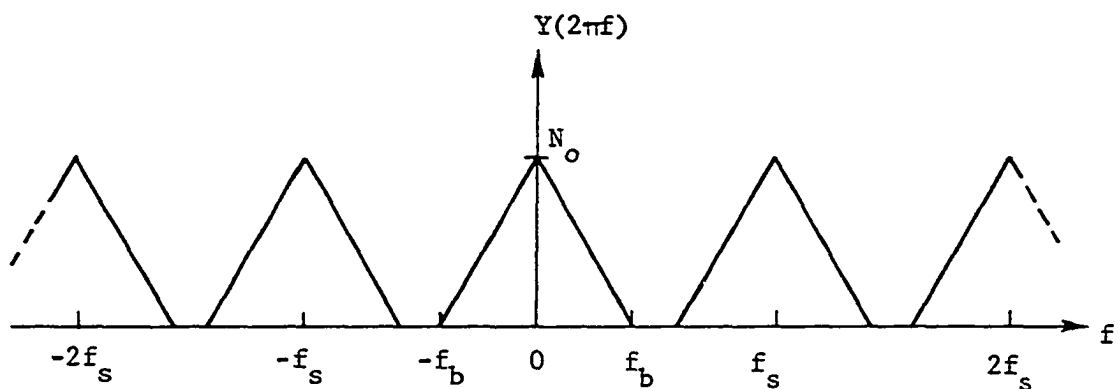
a) Sampling frequency greater than the Nyquist frequency.
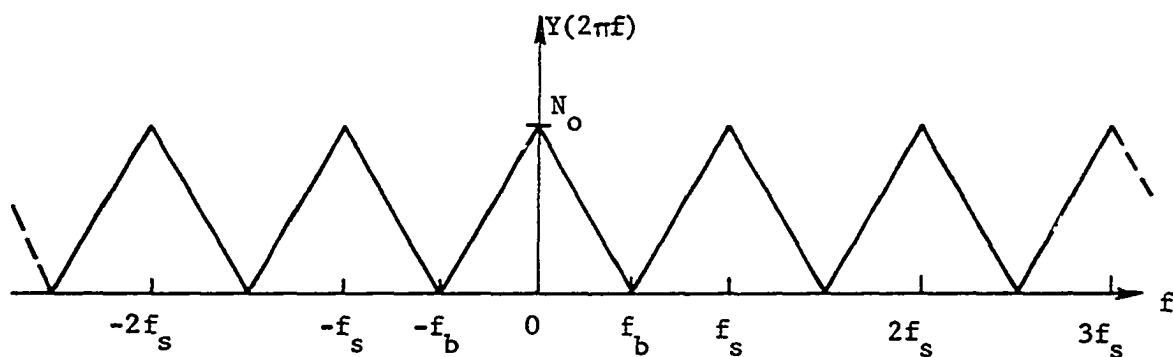
b) Sampling frequency equal to the Nyquist frequency.
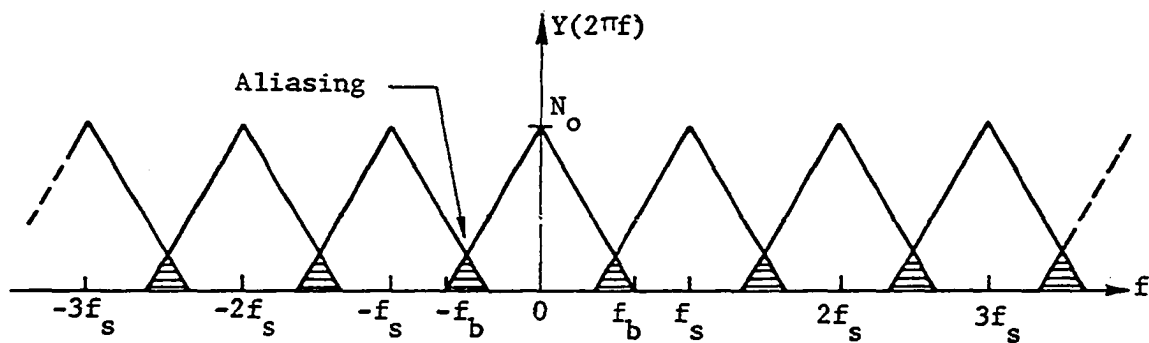
c) Sampling at less than the Nyquist frequency (undersampling).

Figure 6A-1. Output Spectra for an Ideal Sampler Showing the Effects of Sampling Rate and Aliasing

the signal being sampled and is defined to be twice the highest frequency

for which a nonzero spectral component of x(t) exists (Schwartz, 1970,

p. 119). For the present discussion, the spectral components in x(t) will

be limited to frequencies less than f_b so the Nyquist frequency is $f_N = 2f_b$.

The time interval between samples, $\frac{1}{2f_b}$, is called the Nyquist sampling

interval.

The sampler is characterized by the sampling frequency, sampling in-

terval, and folding frequency. The time interval between samples (sampling

interval) is T_s and the sampling frequency is defined as the reciprocal of

the sampling interval, $f_s = \frac{1}{T_s}$. In this dissertation, the folding frequency

will be defined to be one-half of the sampling frequency, $f_f = \frac{1}{2} f_s$. The

folding frequency is a characteristic of the sampler and is the highest

frequency that can be sampled without aliasing effects. This definition

and concept is important to the discussion of the theory of sampling.

Other authors appear to define it in a different manner (Blackman and Tukey,

1958, p. 32).

If a signal is sampled at exactly the Nyquist rate, the Nyquist fre-

quency and the sampling frequency will be equal and the folding frequency

and the frequency of highest spectral content will be equal. This condi-

tion is often used as an example in discussions of sampling but does not

illustrate the important differences between the characteristics of the

sampled signal and the characteristics of the sampling device.

The sampling rate can have a drastic effect on the spectral output of

the sampler. The sampling rate must be greater than the Nyquist rate

or serious spectral distortion will occur. From the viewpoint of the

sampling device, this is equivalent to saying that the input signal cannot have any spectral components above the folding frequency or aliasing will occur. This phenomenon, which is called aliasing, is illustrated in Figure 6A-1. The input spectrum to the sampler is assumed to be triangular. Figure 6A-1a shows the spectrum of the output, y(t), when the sampling frequency is greater than the Nyquist frequency of the input. Figure 6A-1b shows the output spectrum when the sampling frequency is equal to the Nyquist frequency and Figure 6A-1c shows the aliasing effect when the sampling frequency is less than the Nyquist frequency. Sampling at a rate that is less than the Nyquist sampling rate causes the output spectra to overlap. This overlap or "folding back" of the spectra creates erroneous spectral components or "aliasing" of the true spectrum. It is important to note that not all of the spectral information is rendered useless by aliasing. The spectral components below a frequency of $(f_s - f_b)$ remain unaffected.

B. Sampling Theory - The System Equations

Figures 6B-2 and 6B-3 represent the sampling system in both the time and frequency domains. Both representations are used because both provide useful system information. The solution for the output spectrum of the sampler will be obtained by solving the convolution interals by means of the Fourier transform.

The sampling function, m(t), can be represented as the convolution of the pulse shape of the sampler with a Dirac comb function (See Equation 6C.2):

$$m(t) = \int_{-\infty}^{+\infty} p(\tau)\text{Comb}(t - \tau)d\tau \qquad (6B.1)$$

x(t) = Sampled Signal

multiplication

y(t)

p(t) = Pulse Shape of Sampler

m(t)

comb(t) = Dirac Comb

x(t)

y(t)

m(t)

p(t)

Convolution

Comb(t)

$-T_s$ 0 T_s

$-T_s$ 0 T_s

39
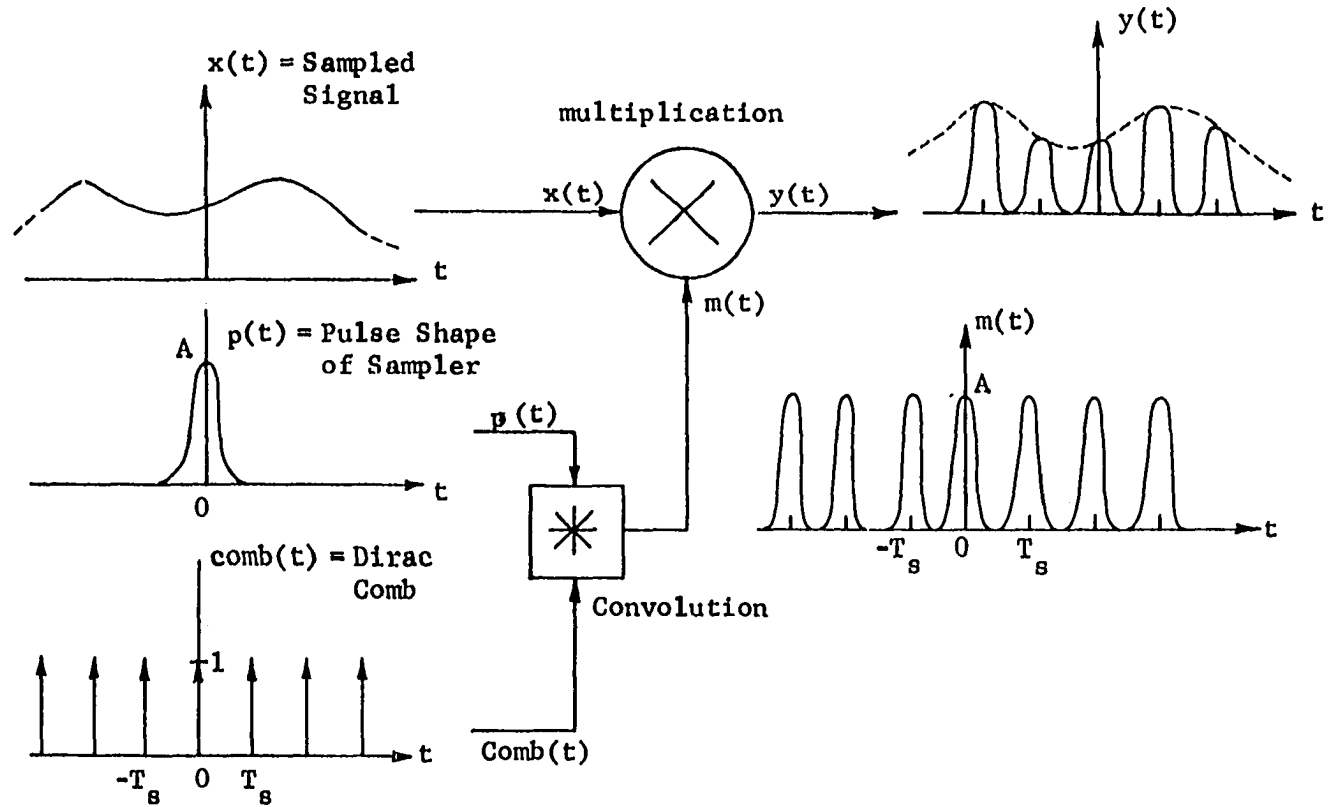
Figure 6B-1.   Time Domain System Diagram for a Multiplying Sampler
Showing Signal Waveforms
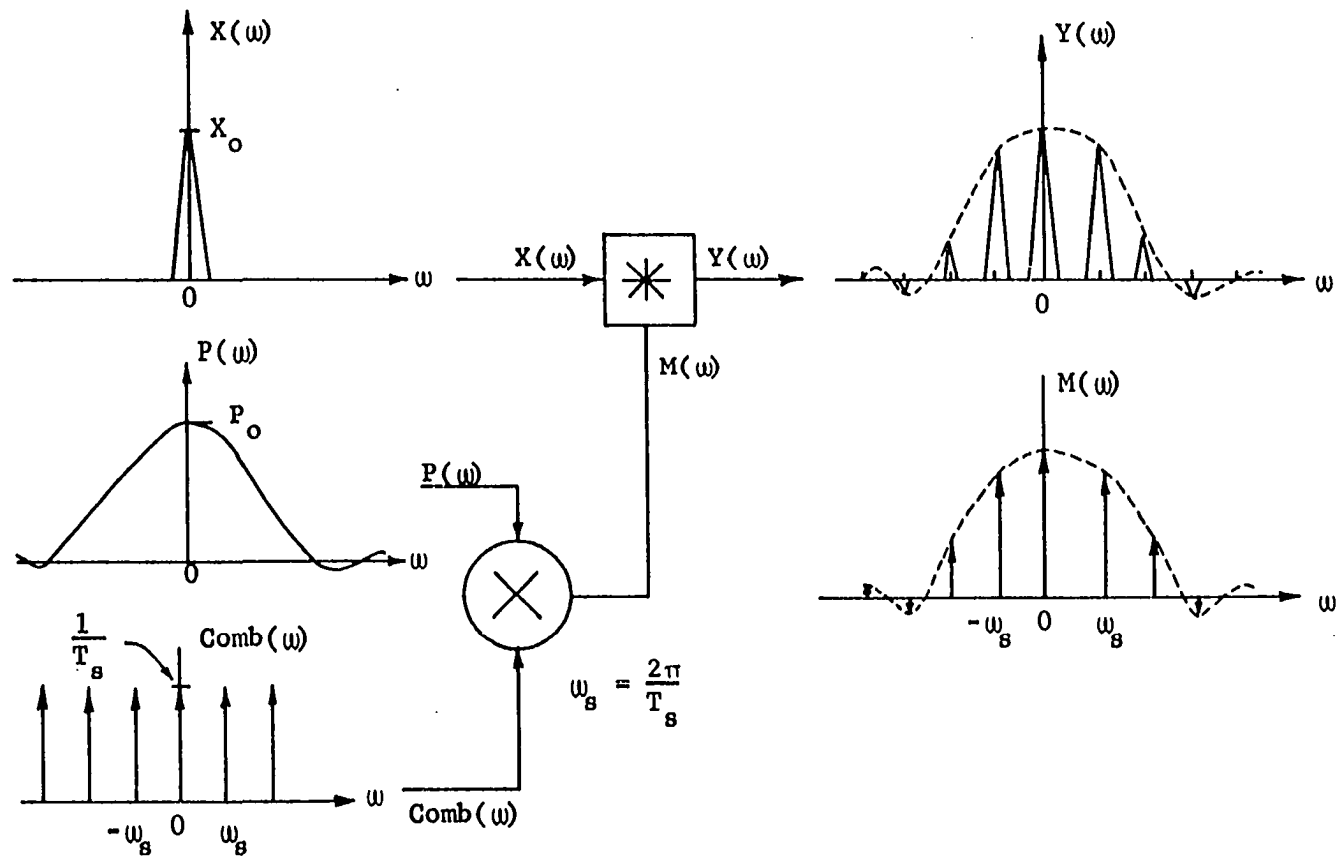
Figure 6B-2. Frequency Domain System Diagram for a Multiplying Sampler
Showing Amplitude Spectra

The sampling function is even and periodic so it can be represented by an even Fourier series

$$m(t) = \frac{1}{2} C_o + \sum_{n=1}^{\infty} C_n \cos\left(\frac{2\pi n}{T_s} t\right) = \sum_{n=-\infty}^{+\infty} p(t - nT_s) \qquad (6B.2)$$

where $C_o/2$ is the average value and T_s is the sampling rate.

The output of the sampler is obtained by multiplying the sampling function, $m(t)$, and the sampled function, $x(t)$. The resulting output can be written in two ways:

$$y(t) = x(t)m(t) = x(t) \sum_{n=-\infty}^{+\infty} p(t - nT_s) \qquad (6B.3)$$

In the frequency domain, the convolution integral representing $m(t)$ is replaced by multiplication of the Fourier transforms of $p(t)$ and $Comb(t)$

$$M(\omega) = P(\omega)Comb(\omega) \qquad (6B.4)$$

where:

$$M(\omega) = \mathcal{F}\{m(t)\}$$
$$P(\omega) = \mathcal{F}\{p(t)\}$$
$$Comb(\omega) = \mathcal{F}\{Comb(t)\}$$

Also in the frequency domain, the multiplication of $x(t)$ and $m(t)$ is replaced by the convolution of their respective Fourier transforms:

$$Y(\omega) = \frac{1}{2\pi} \int_{-\infty}^{+\infty} X(\lambda)M(\omega - \lambda)d\lambda \qquad (6B.5)$$

These system equations describe the operation of the sampler and will now be used to derive equations for the output frequency spectrum and the reconstructed signal.

C. Output Frequency Spectrum

The output frequency spectrum of the sampler can be obtained by making use of the special properties of the Dirac comb function or by expressing the sampling function as a Fourier series. Each method will now be briefly presented.

The reason for expressing the periodic sampling function, $m(t)$, as the convolution of a single pulse, $p(t)$, and a Dirac comb function is that the spectrum of $m(t)$ can be expressed as the product of the spectrum of $p(t)$ and the spectrum of $Comb(t)$. Since the spectrum of a Dirac comb function is another Dirac comb function, the convolution integral of Equation 6B.5 is easily solved by using the sifting property of delta functions. First, the amplitude spectral density function for $m(t)$ is:

$$M(\omega) = P(\omega)Comb(\omega) \tag{6C.1}$$

The Dirac comb function is written in the time domain as:

$$Comb(t) = \sum_{n=-\infty}^{+\infty} \delta(t - nT_s) \tag{6C.2}$$

The Fourier transform of the Dirac comb function is itself a Dirac comb function (Reference Data for Radio Engineers, 1968, p. 42-2):

$$\mathcal{F}\{Comb(t)\} = Comb(\omega) = \frac{2\pi}{T_s} \sum_{n=-\infty}^{+\infty} \delta(\omega - n\,\frac{2\pi}{T_s}) \tag{6C.3}$$

Since the output spectral function is obtained from the convolution of $M(\omega)$ and $X(\omega)$, we can write $Y(\omega)$ as

$$Y(\omega) = \frac{1}{2\pi} \int_{-\infty}^{+\infty} X(\lambda)P(\omega-\lambda)Comb(\omega-\lambda)d\lambda \tag{6C.4}$$

where $M(\omega - \lambda) = P(\omega - \lambda)\text{Comb}(\omega - \lambda)$. Explicitly writing out the series for the Dirac comb function and replacing $\frac{2\pi}{T_s}$ with ω_s, the convolution integral of Equation 6C.4 becomes:

$$Y(\omega) = \frac{1}{2\pi} \int_{-\infty}^{+\infty} [x(\lambda)p(\omega - \lambda)\omega_s \sum_{n=-\infty}^{+\infty} \delta(\omega - \lambda - n\omega_s)]d\lambda \qquad (6C.5)$$

Equation 6C.5 is reduced by cancelling common factors and interchanging summation and integration to give:

$$Y(\omega) = \frac{1}{T_s} \sum_{n=-\infty}^{+\infty} \int_{-\infty}^{+\infty} X(\lambda)P(\omega - \lambda)\delta(\omega - \lambda - n\omega_s)d\lambda \qquad (6C.6)$$

The integral can be eliminated by making use of the sifting property (Appendix II, Part E) of the Dirac delta function. Using the sifting property for Equation 6C.6, the convolution integral becomes

$$\int_{-\infty}^{+\infty} X(\lambda)P(\omega - \lambda)\delta(\lambda - \omega + n\omega_s)d\lambda = X(\omega - n\omega_s)P(n\omega_s) \qquad (6C.7)$$

and the output spectrum for the sampler can be written as:

$$Y(\omega) = \frac{1}{T_s} \sum_{n=-\infty}^{+\infty} P(n\omega_s)X(\omega - n\omega_s) \qquad (6C.8)$$

The term $P(n\omega_s)$ represents the Fourier transform of the sampling pulse, $p(t)$, as it is periodically sampled at values $n\omega_s$ in the frequency domain. Since this amplitude function is a constant with respect to the frequency variable, ω, and is only dependent on the sampling frequency ω_s, it can be replaced by a real coefficient defined by:

$$P_n = \frac{1}{T_s} P(n\omega_s) \qquad (6C.9)$$

The output spectrum can now be represented by the infinite series

$$Y(\omega) = \sum_{n=-\infty}^{+\infty} p_n X(\omega - n\omega_s) \tag{6C.10}$$

with constant coefficients p_n and a periodic repetition of the amplitude spectrum of the sampled data function, $x(t)$. Before interpreting the meaning of the output spectrum, the alternate derivation using the Fourier series representation for the sampling function, $m(t)$, will be given.

The sampling function is represented by the Fourier series of Equation 6B.2. The Fourier transform of this series given by

$$M(\omega) = \pi C_0 \delta(\omega) + \sum_{n=1}^{\infty} C_n \pi [\delta(n\omega_s - \omega) + \delta(n\omega_s + \omega)] \tag{6C.11}$$

is used in the convolution integral for the output spectrum given by Equation 6B.5. The Fourier transform for $m(t)$ is substituted into (6B.5) and integration and summation are interchanged to give the integrals:

$$Y(\omega) = \frac{1}{2} C_0 \int_{-\infty}^{+\infty} X(\lambda) \delta(\lambda - \omega) d\lambda$$

$$+ \frac{1}{2} \sum_{n=1}^{\infty} C_n \int_{-\infty}^{+\infty} X(\lambda) [\delta(\lambda - \omega + n\omega_s) + \delta(\lambda - \omega - n\omega_s)] d\lambda \tag{6C.12}$$

The sifting property of the Dirac delta functions is used to eliminate the integrals and give an output spectrum of:

$$Y(\omega) = \frac{1}{2} C_0 X(\omega) + \sum_{n=-\infty}^{1} C_n X(\omega - n\omega_s) + \frac{1}{2} \sum_{n=1}^{\infty} C_n X(\omega - n\omega_s) \tag{6C.13}$$

The first term represents the original spectral function centered about zero frequency and amplitude scaled by a factor of $C_0/2$. The second term is the series of all the negative frequency spectral terms and the third series represents all of the positive spectral terms. If these series are identified term by term with the previous result given by Equation 6C.10 we

see that the coefficients are related as:

$$P_o = C_o/2$$

$$C_n = \frac{2}{T_s} P(n\omega_s) \tag{6C.14}$$

$$P_n = C_n/2$$

The function $P(n\omega_s)$ is even so the coefficients, P_n or C_n, form an even array ($P_n = P_{-n}$ or $C_n = C_{-n}$).

A simple example will now be given to illustrate the application of the derived equations. Consider a sampler whose sampling function consists of a pulse train of narrow rectangular pulses as illustrated by Figure 6C-1. The amplitude spectrum of $x(t)$ will assume the arbitrary but bandlimited form shown in the figure. The amplitude spectrum of a single pulse of $m(t)$ is given by the Fourier transform of a narrow rectangular pulse:

$$\mathcal{F}\{p(t)\} = \int_{-\frac{\Delta T_s}{2}}^{+\frac{\Delta T_s}{2}} A e^{j\omega t} dt = \frac{2A}{\omega} \sin(\frac{\Delta T_s}{2} \omega) \tag{6C.15}$$

This equation can be written with a sinc function:

$$P(\omega) = A \Delta T_s \left[\frac{\sin(\frac{\Delta T_s}{2} \omega)}{\frac{\Delta T_s}{2} \omega} \right] \tag{6C.16}$$

The pulse height of the sampler, A, is called the gain of the sampler and ΔT_s is the pulse width. The product $A\Delta T_s$ is the area under the rectangular pulse. For purposes of analysis, the pulse area is often set equal to unity. The spectrum of $p(t)$, sampled at intervals corresponding to $n\omega_s$, is used to obtain the coefficients, P_n. These coefficients are calculated

from:

$$P(n\omega_s) = A \, \Delta T_s \left[\frac{\sin(\frac{\Delta T_s}{2} n\omega_s)}{\frac{\Delta T_s}{2} n\omega_s} \right] \tag{6C.17}$$

The output spectrum for the rectangular sampler can be calculated from Equation 6C.10 and the corresponding amplitude coefficients from (6C.17) and (6C.9). The output spectrum for the rectangular pulse example is shown in Figure 6C-2.

As the pulse width of the rectangular pulse is made narrower, and the pulse height increased so that the pulse area remains constant, the rectangle function approaches a delta function. If the sampling function, $m(t)$, is a Dirac comb function, the amplitude spectrum of a single delta function is a constant and the output spectrum simply becomes

$$Y(\omega) = A \, \frac{\Delta T_s}{T_s} \sum_{n=-\infty}^{+\infty} X(\omega - n\omega_s) \tag{6C.18}$$

because all the p_n coefficients are equal. The original spectrum is reproduced periodically with an amplitude scaling factor of $A \frac{\Delta T_s}{T_s}$. This type of sampler is called an ideal sampler. The sampler that directly multiplies the incoming signal by a rectangular pulse shape is called a "natural" sampler, an exact-scanning sampler, or a multiplying sampler. When the data function or input signal is sampled with a sample-and-hold circuit, it is referred to as square-topped sampling. A similar analysis of the square-topped sampler yields an output spectrum which is given by:

$$Y(\omega) = \frac{1}{T_s} P(\omega) \sum_{n=-\infty}^{+\infty} X(\omega - n\omega_s) \tag{6C.19}$$
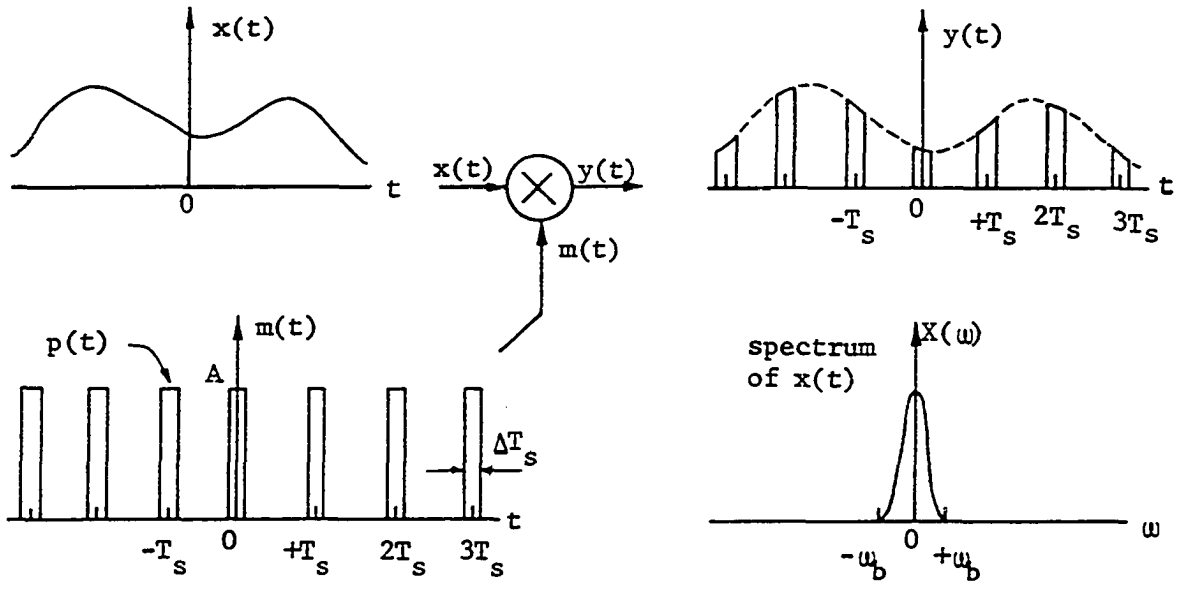
Figure 6C-1. Waveforms and Input Spectrum for Rectangular
Sampling Pulses in a Multiplying Sampler
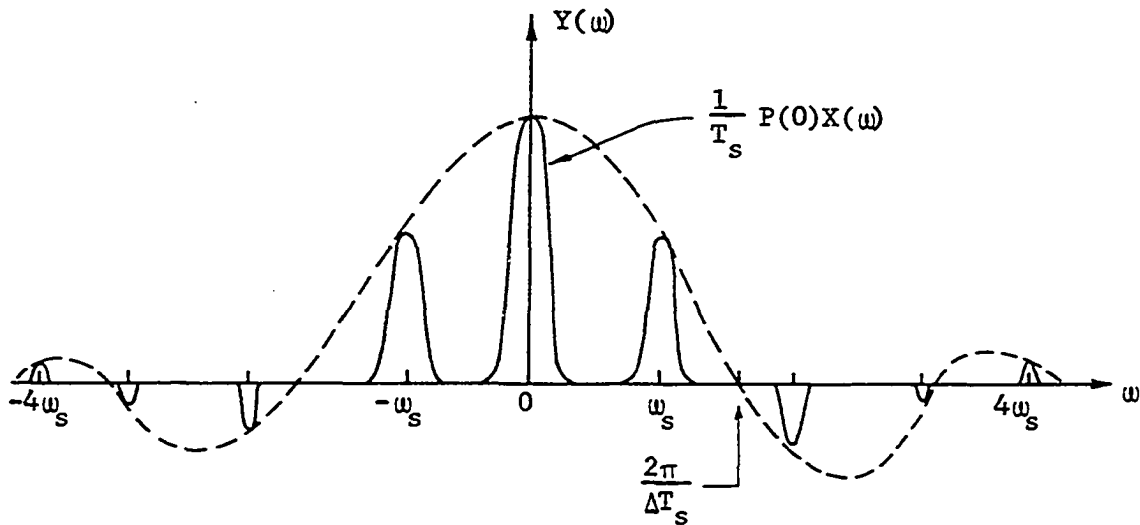
Figure 6C-2. Output Amplitude Spectrum for a Multiplying Sampler
with a Rectangular Multiplying Function

This spectrum differs from that of the exact-scanning spectrum in that the Fourier transform of the sampling pulse is now an explicit function of the frequency, ω. This can be interpreted as a weighting function on the periodic spectrum that tends to lowpass filter the spectrum that would be produced by an ideal sampler. If m(t) is a rectangle function, the weighting function will be a sinc function. This effect may or may not be desired and certainly must be taken into account if a sample-and-hold circuit is used.

From the general theory of sampling that has been presented it is possible to summarize some of the important features of a sampling system. The ideal or Dirac comb type of sampler produces a periodic output spectrum which has a fundamental shape corresponding to the spectrum of the input signal. This type of output is illustrated in Figure 6A-1. The effect of a finite linear sampling time in a multiplying sampler is to introduce a scale factor of $P(n\omega_s)$ into the periodic spectrum of $X(\omega - n\omega_s)$. This factor is not a function of frequency but its effect is to scale the amplitude of each term in the series. The shape of the pulse in this type of sampler does not affect the spectral shape of the baseband spectrum or any of the higher order spectra in the series. It does, however, affect the amplitude factor for each term. The sample-and-hold type of sampler, on the other hand, actually changes the spectral shape of the sampled input spectrum. This effect is easily accounted for by determining the Fourier transform of p(t). The output spectrum of a sampler is not a physical observable and is usually processed by lowpass filtering to reproduce the original input signal. This filtering process is called reconstruction.

D. Data Function Reconstruction

The input data function can be reconstructed at the output of the sampler by lowpass filtering the output spectrum. This is equivalent to convolving the output time function, y(t), with the impulse response, h(t) of the lowpass filter. The reconstructed signal is represented by an estimate of the original input, x(t). The reconstructed output is given by the convolution integral:

$$\hat{x}(t) = \int_{-\infty}^{+\infty} h(\tau) y(t - \tau) d\tau \qquad (6D.1)$$

In the frequency domain, this filtering is represented by the multiplication of the output spectrum with the amplitude frequency response of the filter (Equation 6C.8):

$$\hat{X}(\omega) = H(j\omega)Y(\omega) = \frac{1}{T_s} H(j\omega) \sum_{n=-\infty}^{+\infty} P(n\omega_s)X(\omega - n\omega_s) \qquad (6D.2)$$

The convolution integral can also be written in terms of the original input signal and the sampling function as:

$$\hat{x}(t) = \int_{-\infty}^{+\infty} h(\tau)x(t - \tau)m(t - \tau) d\tau \qquad (6D.3)$$

The solution for the output estimate, $\hat{x}(t)$, is now obtained by solving these system equations.

The convolution integral of Equation 6D.3 can be solved for the ideal sampler by replacing m(t) with a Dirac comb function and using the sifting property of the Dirac delta function as was done in Equation 6C.7. For the ideal sampler, the estimated output in the time domain becomes:

$$\hat{x}(t) = \sum_{n=-\infty}^{+\infty} x(nT_s)h(t - nT_s) \qquad (6D.4)$$

This equation has an interesting mathematical form that is worth discussing because it gives insight into the sampling and reconstruction process. This series for the estimated function, x(t), uses a vector basis set which is derived from the impulse response of the lowpass filter. The amplitude coefficients are simply the data samples at times, nT_s. It is significant to realize that _any_ bandlimited signal, x(t), can be represented by an infinite series with amplitude coefficients corresponding to the samples of x(t) at times nT_s and basis vectors corresponding to the impulse response of an _arbitrary_ lowpass filter. The only requirement on the reconstruction filter is that it completely removes the higher order spectral components of y(t). This requirement is satisfied if the transfer function for h(t) is zero for frequencies above ω_b.

A commonly used example for a lowpass filter that is frequently seen in textbooks is that of the ideal rectangular lowpass filter. The impulse response of this type of filter is obtained by taking the Fourier transform of a rectangle function with height N_o and "double-sided" spectral bandwidth $2\omega_b$. This transform is the well-known sinc function and can be written as:

$$h(t) = \frac{N_o}{2\pi} 2\omega_b \left[\frac{\sin(\omega_b t)}{\omega_b t}\right] \qquad (6D.5)$$

This impulse response is used in the series of Equation 6D.4 to give the well known result

$$\hat{x}(t) = 2 N_o f_b \sum_{n=-\infty}^{+\infty} x(nT_s) \frac{\sin 2\pi f_b(t - nT_s)}{2\pi f_b(t - nT_s)} \qquad (6D.6)$$

where f_b is the "single-sided" spectral bandwidth, in Hz, of the lowpass filter.

In most cases, the results obtained for the ideal sampler can be directly applied to "exact-scanning" and "flat-topped" samplers. Usually only the amplitude factor is affected. For exact-scanning, the estimated output spectrum is obtained by lowpass filtering the spectrum given by Equation 6D.2:

$$\hat{X}(\omega) = \frac{1}{T_s} P(0)H(\omega)X(\omega) \qquad |\omega| \leq \omega_b \qquad (6D.7)$$

The inverse Fourier transform is taken to give the output in the time domain. The resulting equation will be the convolution of the impulse response of the filter and the input signal. The final result is given by Equation 6D.4 and the addition of a scaling factor to account for the finite gain of the sampler:

$$\hat{x}(t) = \frac{P(0)}{T_s} \sum_{n=-\infty}^{+\infty} x(nT_s)h(t - nT_s) \qquad (6D.8)$$

$P(0)$ is the Fourier transform of the pulse shape of the sampling function evaluated at zero frequency. For the previous example of a rectangle function, this factor is, $P(0) = A\Delta T_s$.

The flat-topped sampler introduces an additional complicating factor because the output power spectrum after lowpass filtering still contains the weighting function $P(\omega)$. This result is shown by filtering the spectrum given by Equation 6C.19 with a lowpass filter to give the estimated output spectrum as:

$$\hat{X}(\omega) = H(\omega)Y(\omega) = \frac{1}{T_s} H(\omega)P(\omega)X(\omega) \qquad |\omega| \leq \omega_b \qquad (6D.9)$$

The solution in the time domain involves two convolution integrals and cannot be solved in general. If the width of the sampling pulse is sufficiently small so that $P(\omega)$ is essentially a constant over the frequency interval 0 to ω_b, the output in the time domain will be the same as that given by Equation 6D.8. This approximation is valid for most practical samplers.

It is of practical interest to compute the spectral output of the lowpass filter by taking the Fourier transform of the estimated output given by Equation 6D.8. Since the only time dependent term in the equation is the time shifted impulse response, the Fourier transform is simply the infinite series composed of the Fourier transform of h(t) and the shifting theorem phase factor:

$$\hat{X}(\omega) = \frac{P(0)}{T_s} H(\omega) \sum_{n=-\infty}^{+\infty} x(nT_s)e^{-jn\omega T_s} \qquad |\omega| \le \omega_b \qquad (6D.10)$$

The infinite series part of (6D.10) is exactly the form of a digital Fourier series with infinite sampling. This important result shows how the continuous spectrum given by Equation 6D.7 can be obtained from the lowpass filter spectrum and the discrete samples of x(t). Both of these quantities are known in a practical sampling system.

If the lowpass filter has a rectangular passband, its amplitude spectral function, $H(\omega)$, will be a constant over the spectrum of x(t) and the output spectrum, $\hat{X}(\omega)$, can be computed, within a scale factor, by a digital Fourier series with infinite sampling.

E. Sampling Theory - Finite Record Lengths

In practical sampling situations, the length of the input data function is either limited in time or else the data can be observed for only a finite time. This situation can be adequately modeled by using a sampling function which exists only over a finite time interval. For a total of $2N+1$ observations of the input signal, the sampling function is defined as:

$$m(t) = \int_{-\infty}^{+\infty} p(\tau) \sum_{n=-N}^{+N} \delta(t - \tau - nT_s) d\tau \qquad (6E.1)$$

or in terms of the periodic pulse train as:

$$m(t) = \sum_{n=-N}^{+N} p(t - nT_s) \qquad (6E.2)$$

The sampling function is periodic only over the interval of the defined pulses. In effect, the sampling function has been multiplied by a rectangular window function of width $(2N+1)T_s$. This forces the amplitude spectrum of m(t) to be infinite and continuous. This effect does not cause a problem with the analysis of the system but does force the observer to accept, at best, only an _estimate_ of the "true" input spectrum.

The amplitude spectrum of the sampling function can be obtained by taking the Fourier transform of the finite pulse train of Equation 6E.2. The transform is simply the transform of the pulse, p(t), with a phase factor determined by the shifting theorem. This result may be written as:

$$M(\omega) = P(\omega) \sum_{n=-N}^{+N} e^{-jn\omega T_s} \qquad (6E.3)$$

If m(t) is modeled by an infinite pulse train multiplied by a window

function, the resulting amplitude spectrum is obtained by convolving the amplitude spectrum of the window function with the amplitude spectrum of the infinite series. The infinite series can be written as a Fourier series so its Fourier transform has already been given by Equation 6C.11. The Fourier transform of a window function of unity amplitude and width $(2N+1)T_s$ is the same as that for a rectangular pulse. This transform is given in Equation 6C.16 where $A = 1$ and $\Delta T_s = (2N+1)T_s$. The convolution integral can be solved by using the sifting property of the Dirac delta function to give:

$$M(\omega) = (\frac{2N+1}{2})T_s \sum_{n=-\infty}^{+\infty} C_n \left[\frac{\sin(\frac{2N+1}{2})T_s(\omega - n\omega_s)}{(\frac{2N+1}{2})T_s(\omega - n\omega_s)} \right] \qquad (6E.4)$$

The amplitude coefficients, C_n, are determined from the amplitude spectrum of the pulse shape as given in Equation 6C.14. When this substitution is made into (6E.4), the desired alternate form for the spectrum of the multiplying function is obtained as:

$$M(\omega) = (2N+1) \sum_{n=-\infty}^{+\infty} P(n\omega_s) \left[\frac{\sin(\frac{2N+1}{2})T_s(\omega - n\omega_s)}{(\frac{2N+1}{2})T_s(\omega - n\omega_s)} \right] \qquad (6E.5)$$

Equations 6E.3 and 6E.5 represent two equivalent series representations for the amplitude spectrum of m(t). Both of these representations have their usefulness in certain applications and insight into the properties of the sampling function can be obtained from both. The sampler output spectrum will now be computed using the representation of (6E.3). The output spectrum of the sampler, before filtering, is a series of 2N + 1 functions obtained by convolving the spectrum of x(t) with the spectrum of p(t)

and a multiplicative phase factor:

$$Y(\omega) = \sum_{n=-N}^{+N} \frac{1}{2\pi} \int_{-\infty}^{+\infty} X(\lambda) P(\omega - \lambda) e^{-j(\omega-\lambda)nT_s} d\lambda \qquad (6E.6)$$

If the sampler is ideal, the Fourier transform of the sampling pulse will be a constant and the convolution integral for the output spectrum of (6E.6) will be reduced to:

$$Y(\omega) = \frac{1}{2\pi} \sum_{n=-N}^{+N} e^{-j\omega nT_s} \int_{-\infty}^{+\infty} X(\lambda) e^{+j\lambda nT_s} d\lambda \qquad (6E.7)$$

The integral in (6E.7) is the inverse Fourier transform of the amplitude spectrum of $x(t)$. If we identify the inverse domain variable as nT_s, the output spectrum can be simplified to the finite series:

$$Y(\omega) = \sum_{n=-N}^{+N} x(nT_s) e^{-j\omega nT_s} \qquad (6E.8)$$

In the frequency range of $|\omega| \leq \omega_b$, $Y(\omega)$ is an estimate of the amplitude spectrum, $X(\omega)$. As the number of samples of the input function becomes large, the estimate converges to the "true" value. This expression for $Y(\omega)$ is identical to that of a discrete Fourier transform for a bandlimited spectrum.

The output spectrum computed using Equation 6E.8 involves an infinite series of convolution integrals which convolve the sinc function in $M(\omega)$ with the "true" spectrum $X(\omega)$. This convolution in the frequency domain tells us that the spectrum of $X(\omega)$ is smoothed by the finite observation process. Spectral smoothing reduces the spectral resolution of the observation and limits the ability of the measurement process to resolve two

closely spaced line spectra. The problem of spectral smoothing will be discussed in detail in several later chapters.

Other discussions of sampling theory as applied to communication systems can be found in (Carlson, 1968, Ch. 7), (Thomas, 1969, Ch. 7), and (Schwartz, 1970, Ch. 3).

VII. THE FIRST PRINCIPLE OF DATA REDUCTION

The reduction of real physical data often requires estimation schemes which include, either overtly or covertly, algorithms which modify the data. Often the selection of a particular estimation scheme results in observer bias being introduced into the data processing. A common example of this type of observer bias occurs in the selection of a <u>lag window</u> as is done in the Blackman-Tukey method of spectral analysis. Merely by selecting different types of lag windows, the observer can compute different estimated power spectra from the same observed data. In theory, we say that the autocovariance function and the power spectral density function form a Fourier transform pair. When using a lag window, the inverse transform of the computed power spectrum will not "give back" the initial autocovariance function. This type of processing is in violation of the First Principle of Data Reduction (Ables, 1974):

> "The result of any transformation imposed on the experimental data shall incorporate and be consistent with all relevant data and be maximally non-committal with regard to unavailable data."

By the very nature of data processing and estimation it is ordained that the FIRST PRINCIPLE will be violated to some degree. The fact that all sampled data is finite in length causes this violation. Whenever real physical data is modeled by a mathematical function and a criterion of goodness is chosen, it follows that certain assumptions must be made about how the model fits outside the domain of measurement.

The first example of this is the modeling of a finite time series with a Fourier series. The complex amplitudes are computed by assuming

that the length of the observed series is the Fourier period, that the

observed time series is periodic outside the interval of observation, and

that the sampling rate is more than the Nyquist rate. If the observer

has not sampled the data in such a way that these assumptions are valid,

the computed complex amplitudes may be poor estimates of the "true" complex

amplitudes. Observer bias has entered into the scheme by the method of

data taking and by the tacit assumptions involved in using the digital

Fourier transform. The irony of this situation is that the computed com-

plex amplitudes can be used to generate the observed time series exactly.

Of course we must realize that an infinite number of Fourier series may be

used to describe a finite time series but only one was computed.

A second example of time series modeling is the autoregressive-moving

average time series. In maximum entropy spectral analysis, a least-square

error criterion is applied to fit the observed time series. The assumptions

in this method are that the process can be represented by an nth-order

autoregressive-moving average time series and that the observation time

was long enough to permit an exact calculation of the autoregressive co-

efficients. Also, it is assumed that the infinite time series can be

computed from the estimated series. This is analogous to the assumption

of periodicity in Fourier analysis.

Although the first principle can never be ideally achieved it is worth

striving for and any proposed data processing scheme should try to minimize

its effects. Techniques which try to minimize the effects of data windows

are referred to as "data adaptive spectral analysis" (Lacoss, 1971).

VIII.   DATA ADAPTIVE SPECTRAL ANALYSIS

The study of spectral analysis using only hypothetical or ideal data functions provides little insight into the practical problems involved in the study and analysis of empirical data sets. The reason for this is that a strictly mathematical analysis of data functions and spectral functions depends on the existence of infinite domains and infinite amounts of data. Attempts to modify the theory of spectral functions to apply to finite empirical data sets have been plagued by many problems. The theory that applies to infinite domains must be greatly modified to handle finite data sets. Spectral analysis methods for empirical data sets involve the definition and selection of various estimation procedures that, hopefully, result in realistic estimates of the "true" spectrum. A study of the various estimation procedures for spectral analysis constitutes the majority of effort in this type of research. A brief discussion of commonly used spectral analysis estimates will now be given and are used as an illustration of why data adaptive procedures are being sought.

In most applications of spectral analysis, the goals are to determine the existence of "peaks" in the frequency spectrum, the location of these peaks, and their spectral power. The reason that the peaks are sought is that they contain the interesting information needed for scientific analysis. Using definitions from information theory, a spectrum which is flat would be called a maximum entropy spectrum while a spectrum containing only one amplitude value would contain zero information.

Often, the amplitude spectrum is estimated directly by taking the fast Fourier transform of the empirical data. This procedure produces a discrete amplitude spectrum which is based on the assumptions that the data is periodic and spectrally limited both in the number of spectral components and the frequency of the highest component (See Chapter XII). In statistical studies of spectral functions derived from sample functions of a real process, the amplitude spectrum is avoided for theoretical reasons because it may not exist or it will not give a power spectrum estimate that converges. For this reason an alternate definition is often chosen.

This alternate definition is the famous Wiener-Khinechine relations (Appendix I, Part F) using the autocorrelation function. This definition is preferred because of the previously given theoretical reasons. There are severe problems associated with the use of an autocorrelation function for empirical data. First, the estimated autocorrelation is badly truncated. If the spectrum is estimated by taking the Fourier transform of this truncated function, many additional frequency components are introduced that are not in the original spectrum. Second, this estimate is obtained from only one sample function of the process. For statistical reasons, many samples are needed to make the autocorrelation function converge to the "true" value. Third, the algorithm used to determine the estimated function uses less data as the lag value increases. This causes the function to be a poor estimate for large values of lag. Practical schemes for estimating the power spectrum of a random process must take these undesirable effects into account and minimize their effect on the

accuracy of the estimate.

The most commonly used method of spectral analysis of empirical data is the Blackman-Tukey method (Blackman and Tukey, 1958). This method uses the autocorrelation definition for the power spectral density of a random process. Their approach to the problems associated with the estimated autocorrelation function was to introduce a lag window function which would be multiplied with the estimated autocorrelation function. The lag window function was chosen so that it would weight the autocorrelation values in such a way that values near zero would be emphasized and large lag values would be removed or smoothed to zero. Their fundamental assumption was that the modified estimate of the autocorrelation function would give a respectable estimate of the smoothed values of power spectral density even though the weighting process actually produced a poor estimate of the "true" autocorrelation function. This assumption has been surprisingly effective in a number of practical applications and accounts for the success of this method.

Although the Blackman-Tukey method is probably the best method in common use, it has serious drawbacks in many scientific applications. First, for limited amounts of data, the estimated autocovariance function is severely truncated and the process of "windowing" further reduces the range of useful lag values. The method recommends that only about 5 to 10 percent of the estimated autocovariance function be used. This procedure effectively removes much valuable data that might otherwise be used in the estimation of the spectrum. Second, the selection of a lag window introduces bias into the data and tempts the observer to "select" a window function that produces the "most agreeable" spectrum. The use of a lag window

function is also found to be objectional on theoretical grounds because it causes "negative" power spectra to be produced. Third, in many practical situations, the goal of spectral analysis is to detect and resolve two closely spaced spectral peaks but the Blackman-Tukey method of using a lag window produces a smoothed estimate of the "true" spectrum resulting in a loss of spectral resolution. The most obvious questions to be asked are: 1) How can the data be processed to use all of it and still avoid the problem of truncation and 2) How can the smoothing effect associated with "windowing" be minimized to produce the best spectral resolution? Data adaptive spectral analysis methods are an attempt to answer these questions.

The discussion of the drawbacks in the Blackman-Tukey method should not be viewed by the reader as an attempt to discourage the use of this method. On the contrary, there are many practical situations where this method gives very good results. It is important that the reader be aware of the problems attendant to the use of a lag window and the possible alternatives to its use. As is often the case, the user will probably try several methods and compare the results with his a priori knowledge about the measured process.

There has been much work done on the selection of an "optimum" window function and many window functions are in common use (Otnes and Enochson, 1972). The primary goals of this work have been to retain as much spectral resolution as possible and still minimize the production of "negative" power spectra. One cannot escape the fact that the concept of a window function will always be valuable in the discussion and applications of power spectrum estimation techniques. Windowing can, however, be ap-

proached in entirely different ways if alternate modeling techniques are employed such as those used in data adaptive spectral analysis.

In recent years, data adaptive methods of spectral analysis have received increasing attention from experimentalists. These methods attack the problem of limited data and are producing surprisingly good spectral estimates using data that cannot be easily processed by the Blackman-Tukey method. Data adaptive methods are based upon assumptions which allow limited degrees of smoothing and extrapolation to be applied to the estimated autocorrelation function. Within the limits of the various assumptions, this technique essentially produces an infinite function which can be easily handled by conventional theory. This approach essentially circumvents the need to select a window function but has not eliminated the theoretical requirement that a truncated autocorrelation function needs some type of "windowing". The way in which a truncated autocorrelation function may be smoothed and extrapolated is governed by the criterion that is selected for the particular estimation routine used. Data adaptive methods are so named because the empirical data actually governs the optimization criterion used for smoothing and extrapolation. It can be said that the problem of windowing adapts itself to fit the nature of the data.

Lacoss (1971) published a widely referenced paper in which he discusses the mathematical formulation of such data adaptive techniques as maximum likelihood and maximum entropy. His use of a matrix formulation of the methods adds a valuable dimension to their understanding and provides the reader with more theoretical insight than can be obtained by studying the algorithms only. This paper is highly recommended reading because it com-

pares the data adaptive methods with more "conventional" methods.

This discussion has been given to provide the reader with the necessary insight into the problems associated with the estimation of power spectra. It should be emphasized again that the problem of truncated data is not considered by conventional theory and that various estimation techniques must be used. These estimation techniques involve either the direct use of a windowing function as in the Blackman-Tukey method or smoothing and extrapolation as done in the data adaptive techniques. The selection of a particular technique of spectral analysis is discussed in Chapter IX. The implementation of some of these various techniques is discussed in later chapters.

IX. METHODS OF SPECTRAL ANALYSIS

The selection and application of a particular method of spectral analysis is a very complicated task and offers many challenges for the potential user. The development of a method usually begins by selecting known estimators and then modifying them to fit the conditions of the problem. This process of development often requires a unique mixture of theory, art, and "luck" before a suitable solution is obtained.

Estimators obtained from the theory of spectral functions can be greatly improved if as much information as possible is incorporated into the development of a technique. Physical boundary conditions, a priori assumptions, and other information should be used. Modifying the estimator in these ways can be thought of as a type of model fitting. It should be apparent that effort expended in obtaining the best starting model will pay off in producing the best final results.

It is ironic that the selection of a "best" spectral estimator often depends upon a priori assumptions that may or may not be valid for the empirical data to be analyzed. For example, the computation of an amplitude spectrum by Fourier analysis techniques depends upon the assumption that the function is periodic and that it has been observed for exactly one Fourier period. This assumption is seldom true but the amplitude spectrum is estimated this way by most users. Another example is the representation of empirical data by an autoregressive series. It must be assumed that the process produces a sample function that is an autoregressive series before the autoregressive spectral estimator can be used. Again this assumption is seldom true but the autoregressive spectral esti-

mator is used with good success and can give very good approximations to the spectrum of a periodic function provided the autoregressive series has enough coefficients. The validity of these various assumptions will affect the accuracy of the spectral estimate and offers a basis for judging the "goodness" of a particular technique. The effect of the various assumptions will be discussed in detail in later chapters.

A data function is characterized in the frequency domain by its amplitude spectrum or its power spectrum. These spectrums are estimated by applying various filtering techniques and using the theory of spectral functions given in Chapter IV. Since spectral estimation theory is based on the use of filtering, Fourier transforms, and autocorrelation functions, the development of suitable estimators is primarily concerned with obtaining good approximations to the integrals in these techniques. Estimators for the amplitude spectrum are based on the discrete Fourier series or transform. Estimators for the power spectral density function are based on filtering and/or the autocorrelation function and its transform. The autoregressive spectral estimator is based on the discrete form of the autocorrelation companion function discussed in Chapter XV. The various estimators can also be described in terms of linear predictive filtering and recursive digital filtering.

A. Computing Methods

It is difficult to place the various spectral analysis methods into distinct categories because of the large number of variations that can be applied. For the benefit of the reader, a brief listing will be given in

an order that seems the most logical to the author. Other methods of presentation based on different viewpoints would be equally logical. The amplitude spectrum can be obtained by computing the Fourier transform of the data function. This scheme seems suitable and no other methods are commonly used. The computation of the power spectrum is quite a different matter. Most schemes are based on the autocorrelation function, recursive digital filtering, or the autoregressive spectral estimator. Methods which avoid the explicit use of a window function are called data adaptive methods (See Chapter VIII). Estimators for the power spectrum include:

1. The Blackman-Tukey method (autocorrelation function, window function).

2. The direct Fourier transform method (amplitude spectrum squared).

3. Recursive digital filtering.

4. Data adaptive methods,

   a) maximum likelihood method.

   b) maximum entropy method, Burg algorithm.

   c) maximum entropy method, Levinson algorithm.

5. Bartlett estimator.

6. Autoregressive spectral estimator.

These various estimators do not represent completely independent methods. For example, the data adaptive methods and the autoregressive method can be formulated with the same mathematics that is used to describe recursive digital filtering. Likewise, the autocorrelation function and lag window function can be represented by analogous equations representing the digital

filter. The Blackman-Tukey method could then be formulated with the proper selection of a recursive filter. The selection of a particular representation often depends on the viewpoint adopted by the user or his estimation of the most "economical" approach.

B. Data Collection and Experimental Design

The observation and collection of data can have an important interactive effect with the chosen method of spectral estimation. The experimenter should consider the effects of data collection on the errors intrinsic to a particular spectral estimator. An observation system model for spectral analysis studies is shown in Figure 9B-1. A hypothetical sample function, s(t), is used to model a ergodic real process. It is assumed that s(t) will generally contain both random and periodic components and is properly well-behaved so that its autocorrelation function and power spectrum exist and are well-defined. In theory, the "true" sample function

Multiplier

```
┌──────────────┐   ┌────────┐      ┌──────────────┐   ┌───────────┐
│Stationary real│──│Filter  │──⊗──│Sampled - data│──│Spectral   │
│process, s(t) │   │h(t)    │   ↑  │Function, d(t)│   │Estimation │
└──────────────┘   └────────┘   │  └──────────────┘   └───────────┘
                             ┌──────────────────┐
                             │Sampling Function │
                             │m(t)              │
                             └──────────────────┘
```
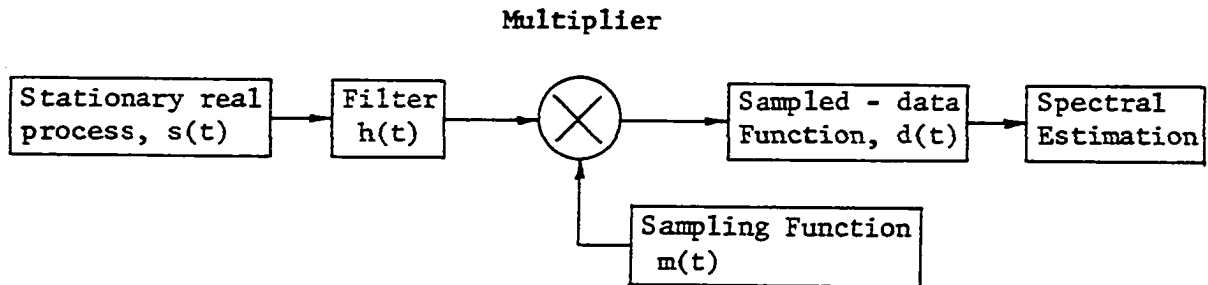
Figure 9B-1. Observation System Model for Spectral Analysis Studies

of a process is inaccessible to direct observation. This is because the observation process limits the observation bandwidth and total number of data samples. This has the effect of limiting the spectral bandwidth and resolution of any spectral estimator.

The inherent bandwidth limiting effects are modeled by a filter with impulse response, $h(t)$. This filter may represent the time constants associated with probes, cables and other electrical conductors or it may represent the use of prefiltering for the sampler. Prefiltering is necessary for the successful operation of a practical data sampler. This filter is designed to have a sharp cutoff characteristic to limit the maximum spectral component that is transferred to the sampler. The filter should be designed so that it effectively attenuates all frequencies above the folding or aliasing frequency, $f_a = \frac{1}{2T_s}$. The filter passband and the sampling rate can be properly designed to make the problem of aliasing negligible compared to spectral mixing errors in the estimator.

The effects of finite data sampling are modeled by a multiplying or "natural" sampler. The effects of data sampling on the spectrum of an input function were discussed in Chapter VI. The observable function, $d(t)$, at the output of the sampler will be called the data function. This will be the function that represents the actual data used by the spectral estimation routine. The data function represents all that is observed about the generating process and its sample function, $s(t)$. All estimates of the spectrum of the process will depend on the observed data in the data function.

The spectrum of $d(t)$ can be considerably different than the spectrum of $s(t)$ if proper experimental design is not used. First, the observation

filter will pass only those spectral components of s(t) which are in the filter passband and will attenuate or reject those components outside the passband. The filter output is the convolution of the sample function, s(t), and the filter impulse response, h(t). If the spectral estimator is capable of producing highly accurate estimates of the spectrum of d(t), it may be necessary for the experimenter to deconvolve or "inverse-filter" the output to obtain a better estimate of the spectrum of s(t). Second, the sampler will introduce frequency multiplication and some aliasing of the spectrum passed by the filter. Third, the limited number of available data samples will limit the spectral resolution of the estimator. All of these effects must be accounted for if acceptable estimates are to be obtained.

Many of the problems caused by the observation and sampling of a process can be minimized by proper experimental design. For example:

1. The filter bandwidth can be made wide enough to pass all significant spectral components of s(t).
2. The sampling rate can be made high enough to avoid aliasing problems.
3. The output of the sampler can be digitally filtered so only the baseband spectrum (also called the principle alias) is determined.

Even with careful experimental design, the estimated spectrum of a process can never converge to the "true" spectrum because of the intrinsic spectral estimation errors. A finite, sampled-data function will always be corrupted by aliasing, leakage, spectral smoothing, and statistical variability.

C. Data Preprocessing and Intrinsic Spectral Estimation Errors

Empirical data that must be used for spectral studies often is corrupted with errors that are due to the observation technique or are inherent to the estimation process. The user can minimize these effects by properly preprocessing the data and choosing an estimation method that will minimize intrinsic effects. The following data preprocessing techniques can be used, when needed, to improve the accuracy of a chosen spectral estimator:

1. Wild point editing.

2. Trend removal.

3. Remove average value ("dc" value).

4. Smoothing and decimation.

5. Prewhitening.

6. Rejection filtering.

Wild point editing is necessary when the observation procedure is likely to introduce data values that are erroneous and not related to the "true" data. These types of errors are usually due to equipment malfunctions and gross errors committed by the observer. A "wild" data value can cause considerable trouble in an estimation routine if the amount of data is limited. For instance, a least-squares fit can be greatly influenced by a data value that is far removed from the mean. The least-squares method would place great importance on the value because it has a small probability of occurrence. The selection of an editing scheme is largely a matter for user definition and depends on the type of data to be collected. A scheme

that rejects data points with large variance is discussed in Otnes and Enochson (1972, p. 56).

Trend removal is an euphemism for treatment of nonstationary data that has a mean value that varies over the interval of observation. This violation of the assumption of stationarity is not serious if the rate of variation of the mean is very slow compared with the rate of fluctuation of the data. This slow variation in the mean value can be removed by model fitting with a low-order polynomial, partial sinewave, exponential function or other estimation schemes listed in Chapter III. Trend removal causes an irrevocable change in the low frequency spectrum of the data and cannot be used if low-frequency spectral estimation is important. Trend removal can be treated as a process of highpass filtering and appropriate filtering techniques can be applied.

The removal of the average value from the data function is really a simple form of trend removal where the "dc" spectral component is "filtered" out. The accuracy of most spectral estimators can be improved by removing the average value because this minimizes the "spectral mixing" effect (Chapter XI). This "spilling over" or "leakage" of one spectral component onto the frequency of another is an important source of estimation error and "dc" removal is almost always recommended.

Smoothing and decimation can be applied to data functions that are sampled at several times the Nyquist rate. As discussed in Chapter VI, oversampling increases the spectral bandwidth and the total number of data samples. If the total spectral bandwidth is not needed to display the desired spectrum, it is often desirable to filter or smooth the unwanted

spectrum. This will minimize the effects of spectral mixing and reduce any high frequency noise that may have been introduced in the measurement process. Decimation (Blackman and Tukey, 1958, p. 45) refers to the process of reducing the total number of data points by selecting only every second or third sample. This process has the effect of reducing the sampling rate and increasing the sampling interval to $2\Delta T$, $3\Delta T$, etc. Decimation is practical only when the data are highly oversampled and the desired spectral bandwidth is well-defined. Oversampling of data has some desirable features such as improved estimation accuracy and minimization of aliasing problems that should not be overlooked. Decimation should only be applied when the reduction of the total number of data samples is absolutely necessary due to processing efficiency problems.

One of the most frequent causes of errors in spectral analysis is that due to spectral mixing (called intermodulation distortion by Blackman and Tukey). This problem is especially severe when the data spectrum contains one or more peaks which have a high spectral power. Some of this power will "leak" into another part of the spectrum and give an erroneous contribution to the spectral amplitude. The leakage power can be so high as to cause the true spectrum to be completely "masked" by the leakage contribution. The spectral mixing problem is greatly reduced for a data spectrum which is essentially flat or "white". It is often observed that spectral estimators give the most accurate results for a "white noise" spectrum. Prewhitening refers to the process of adding a synthetic signal to the measured data signal that will add to the data spectrum to make it essentially flat. This "prewhitened" signal is then spectrum analyzed

and the resulting spectrum corrected for the added spectrum.

Prewhitening essentially corrupts the data with additional noise and may cause the "purist" to reject its use. This should not be the case, however, because it is designed to improve the _estimation_ and not the theory of spectral analysis. There is a strange aspect of prewhitening that needs further discussion. This involves the design of a filter or other processor that is used to prewhiten the data. One might suppose that the technique used to determine the required synthetic spectrum might also be suitable for estimating the data spectrum directly. This is indeed the situation and the data adaptive techniques that employ recursive digital filtering are used to compute a "prewhitening filter" that is used directly to estimate the data spectrum. The prewhitening filter concept is the basis for the autoregressive spectral estimator and the maximum entropy spectral estimator.

Rejection filtering is yet another attempt at reducing the effects of spectral mixing. This preprocessing technique should be used if the data spectrum has an unusually strong peak. The amplitude of this peak can be reduced by notch filtering to make it comparable with the rest of the spectrum. The application of this technique usually requires at least one "run" of the data function through a spectral estimator that will detect this strong peak. The characteristics of the rejection filter must be retained in the processor so that the spectral peak may be "reconstituted" in the final estimate.

The preprocessing of empirical data and the careful selection of a spectral estimator are necessary for successful spectral analysis. These processing and selection techniques are designed to minimize the effects

of <u>intrinsic spectral estimation errors</u>. Intrinsic errors are those which are present for all estimation methods. These errors often do not appear explicitly in the analysis of the estimation method and may cause unexpected problems if the user is not aware of them. The most common errors are listed as follows:

1. Aliasing (undersampling).

2. Spectral mixing (intermodulation distortion or "leakage").

3. Spectral smoothing.

4. Statistical variability.

5. Lack of stationarity.

<u>Aliasing</u> or frequency fold-over is caused by undersampling or sampling at a rate that is less than the Nyquist rate. Aliasing will be present to some extent in all practical sampling systems. The undesirable effects of aliasing can be minimized by the use of sharp cutoff filters and adequate sampling rates. Every attempt should be made to make the effects of aliasing negligible compared to the effects of spectral mixing. Aliasing is discussed in detail in Chapter VI.

<u>Spectral mixing</u> is the most severe problem in spectral analysis. Most estimators are designed to minimize its effects but it still causes problems when the data spectrum has one or more high spectral peaks. This problem can be described by a "leakage" of the power at one spectral frequency into another frequency. Lag window functions that are used in the Blackman-Tukey method are usually chosen to minimize leakage. The term leakage is derived from the analogy between a window function and the

field pattern of an antenna. The one-dimensional aperture distribution and the far-field power pattern for a beam antenna are reciprocal Fourier transforms as are the lag window function and the spectral window function. The minor lobes of the antenna cause "leakage" of the power that is wanted in the main beam. Likewise, the lag window function causes leakage of the spectral power at the observed frequency into adjacent frequencies. The problem of spectral mixing is present whenever the observed data function is truncated. This is true for all known estimators. In most practical schemes, the problem of leakage can be traded off against the problem of spectral smoothing.

Spectral smoothing is also caused by the truncation of the observed data function. The lack of enough data to resolve closely spaced spectral components causes two nearby peaks to be "smeared" together. The only solution to the smoothing problem is to observe the data function for a longer period. In the Blackman-Tukey method, spectral smoothing is an obvious result of the convolution of the spectral window function with the "true" spectrum. As the period of observation increases, the spectral window function becomes very narrow and approaches a Dirac delta function. When this happens, the estimated spectrum converges to the true spectrum. In filtering and data adaptive techniques, the spectral smoothing effect is not so obvious. It is introduced indirectly when the data function is smoothed and processed to obtain estimates of the filter coefficients or autoregressive coefficients. Data adaptive spectral estimators such as the maximum entropy estimator are superior to the Blackman-Tukey method in their ability to minimize the effects of spectral smoothing and to give

better spectral resolution. This improved resolution is due to the fact that the adaptive methods utilize all of the data while the Blackman-Tukey method is restricted to about 5 to 10 percent of the total lag values. The reason for limiting the useful range of lag values in the Blackman-Tukey method is to minimize the effects of statistical variability in the estimate.

The statistical variability of the estimate is caused by the finite observation time for the data function. The time autocorrelation function definition for power spectra is valid only if the process is both stationary and ergodic. The definition of the time autocorrelation function depends on an infinite time. If the data function is observed for a finite time, the time autocorrelation function is only an estimate of the "true" function. This introduces statistical variability into the estimated autocorrelation function that directly carries over into the estimate of the power spectrum. The effects of statistical variability can be reduced only by making many observations of the process to obtain and "average" autocorrelation function. A large number of truncated estimates of the autocorrelation function will sufficiently reduce the effects of statistical variability but will have no effect on the spectral smoothing problem. Spectral smoothing can only be reduced by increasing the length of time the samples are observed.

If an observed process is not stationary, most spectral theory and commonly used spectral estimates will not apply. The power spectrum of the process will be a function of time and can only be obtained from the ensemble definition of the autocorrelation function. If the time variation

is slow enough so that the spectrum is essentially constant for the time interval of observation, a "quasi-stationary" estimate can be obtained. In this instance, the deleterious effects of a short observation time must be traded against those of a time varying spectrum. The display of time varying spectra can be accomplished by a power spectral density profile plot (Otnes and Enochson, 1972, p. 415).

The multitude of effects involved in the preprocessing of the data function, the sampling process, and the intrinsic spectral estimation errors must be collectively considered in the process of method selection.

D. Method Selection

Method selection should begin with a detailed study of the physical process that generates the data function. The purpose of this initial study is to discover and incorporate as many constraints as possible into the process model. The constraints will help to improve the accuracy and/or efficiency of the estimator and often mean the difference between success and failure. After the constraints are determined, the next step is to see how the various possible estimators compare in efficiency, accuracy, bias, and other appropriate characteristics. For these comparisons, the user must define a criterion of goodness and determine what estimator is "best" for his application. This determination will often involve a detailed mathematical analysis of the estimator coupled with several tests using hypothetical data samples from a "known" process. Finally, once an estimator is chosen, the spectra produced by this estimator must be interpreted as to its accuracy and ability to minimize such

effects as aliasing, leakage, and spectral smoothing.

It is very difficult to develop a step-by-step procedure for the spectral analysis of data. Each problem presents its own unique set of boundary conditions and each experimenter must choose a criterion of goodness that is suitable for his purpose. Spectral analysis "by the numbers" is not possible under these circumstances. Some general guide-lines are possible if the reader is willing to accept loosely defined boundary conditions and criteria of goodness. These guidelines will now be presented along with an examination of the more fundamental processes involved in spectral estimation. These fundamental characteristics are discussed in Section E of this chapter.

A flowchart of some commonly used spectral analysis schemes is shown in Figure 9D-1. The top flowchart shows the possible theoretical analysis methods for the theoretical data function, s(t). There are essentially three ways of obtaining a spectral function. First, for a periodic function, the amplitude spectrum is determined by the complex amplitude coefficients of the Fourier series. The spectrum is bandlimited and discrete for all real data functions. The amplitude spectrum can be used to reconstruct the original data function. Second, the spectrum of a single time pulse can be specified by taking the Fourier transform. The resulting amplitude spectrum is both continuous and infinite. As before, the time pulse can be reconstructed by taking the inverse Fourier trans-form. Third, for random processes, the power spectrum is defined as the Fourier transform of the autocorrelation function of the process. For many theoretical data functions that represent sample functions of a real

Theoretical Data Function s(t)	Amplitude Spectrum (for periodic fcns)	Fourier Series	Fourier Coefficients Bandlimited Discrete Spectrum
	Amplitude Spectrum (for time pulses	Fourier Transform	Amplitude Spectrum Continuous
	Autocorrelation Function	Fourier Transform	Power Spectrum

Theoretical Data Function s(t)	Blackman-Tukey Method	Estimated Autocovariance	Lag Window Function	Fourier Transform	Estimated Power Spectrum
Sampling and Preprocessing	Recursive Digital Filtering	Convolution or Filtering	Mean-Square Output or Total Filter Power		Estimated Power Spectrum
Empirical Data Function d(t)	Data Adaptive Techniques	Autocorrelation Function Smoothing and Extrapolation	Autoregressive Coefficients		Autoregressive Spectral Estimator
	Direct Fourier Transform Method	Discrete Fourier Transform	Absolute Magnitude Squared		Estimated Power Spectrum
	Autoregressive Series Method	Estimate Autoregressive Coefficients	Autoregressive Spectral Estimator		

Figure 9D-1. A Flowchart of Spectral Analysis Methods

process, the amplitude spectral function is not defined because the Fourier transform of the data function does not exist. For these functions, the original time function cannot be reconstructed from either the autocorrelation function or the power spectrum. The autocorrelation function definition for the power spectrum is widely accepted as the most useful for random processes and can also be applied, if one accepts the use of the Dirac delta function, to periodic functions and single time pulses.

The bottom flowchart in Figure 9D-1 shows several commonly used spectral estimators and their most important processing steps. The Blackman-Tukey method, the data adaptive techniques, and the autoregressive spectral estimator all use the autocorrelation function definition for the power spectrum. The recursive digital filter methods defines the power spectrum by computing the power output of the filter. The direct Fourier transform method defines the power spectrum by computing the absolute magnitude squared of the complex Fourier coefficients obtained by taking the digital Fourier transform of the empirical data function.

A typical empirical data function is made up of $2N + 1$ samples of the theoretical data function. Since this time series is limited both in the total number of samples and the length of observation time, it can be exactly represented by a Fourier series with $2N + 1$ complex amplitude coefficients (double sided spectrum). The coefficients can be used to determine both the amplitude spectrum and the power spectrum. The accuracy of this estimate will depend on the nature of the "true" data function.

Likewise, this same data function can be represented by an autoregressive series of any order from order one to order $2N + 1$. The power

spectrum can be estimated by using the autoregressive spectral estimator or the autoregressive series can be used to generate the discrete auto-covariance function and then the discrete Fourier transform used. This scheme can be applied to any truncated and discrete data function. The accuracy of the spectral estimate will again depend upon the nature of the "true" data function.

In still another way, this empirical data function can be used to determine the estimated autocovariance function for use in the Blackman-Tukey method of spectral estimation. The accuracy of this method will depend upon the amount of data available for obtaining the autocovariance estimate and the window function selected for smoothing. As the amount of data becomes large and the observation time increases, the Blackman-Tukey estimate will converge to the "true" autocorrelation function definition of the power spectrum. This property of the Blackman-Tukey method makes it the "best" estimator in terms of adherence to the autocorrelation definition of power spectra.

It may be difficult for the reader to accept the fact that these methods may all be considered "exact" for the purposes of representing the empirical data function. In this sense, any of the methods could be used to <u>define</u> the spectrum of an empirical data function. The only way to validate a particular method as being the "best" estimator is to apply some a priori knowledge about the process that generated the data. In other words, <u>if absolutely nothing is known about the process that generated the empirical data function none of the spectral estimators can be selected as a "best" estimate.</u>

The a priori knowledge needed to select a best estimator does not have to be very detailed or specific. Usually, a very general assumption can be used that will help. As an example, we consider the assumptions needed to justify the more common spectral estimators. To use the auto-regressive spectral estimator it is necessary only to assume that the data function can be represented by an autoregressive series because the process is autoregressive. This assumption is surprisingly good for many practical data functions. The digital Fourier series representation is exact if the data function is assumed to be periodic and if the period of observation is exactly equal to one Fourier period. The maximum entropy estimator is valid if it is assumed that the process is autoregressive and that the resulting spectrum has maximum spectral entropy. An additional boundary condition on this estimator is that the autocorrelation function and power spectral density function be exact reciprocal transforms (no window function).

The Blackman-Tukey estimator differs from most of the other estimators in that it converges to the "true" spectrum for random processes as increasing amounts of data are taken. This circumstance is brought about because of the choice of the definition for the apparent autocovariance function. The assumptions required for validating this method are:

1. The Fourier transform of the modified apparent autocovariance function is a respectable estimate of the smoothed values of the "true" spectrum.

2. The statistical variability of the estimate is small enough to be acceptable.

In theory, the Blackman-Tukey estimator is capable of giving the best spectral estimate when the data function is well-sampled.

When nothing is known about the process that generated the data function, it is safest to select an estimator that requires the weakest assumptions about the process. Recent work by researchers in geophysics, astronomy, and other scientific areas that require the tools offered by digital spectral analysis has shown that the maximum entropy spectral analysis method offers higher spectral resolution and improved estimation accuracy over previous methods. If large amounts of data are available, the Blackman-Tukey method can also be successfully used.

Figure 9D-2 is a data processing flow diagram that illustrates how data might be processed to obtain a spectral estimate. The diagram is based on the consideration of several characteristics of the spectral analysis problem. These are:

1. The process model.

2. Discrete or continuous output.

3. Amount of available data.

4. Sampling rate.

5. Desired accuracy of estimate.

"Real data" represents the actual signal output from the process. If it is continuous, an analog spectrum analyzer can give the desired spectrum. If the output is analog but has a finite duration, the data record will usually be sampled and preprocessed. The proper experimental design should be observed so that the finite record is sampled above the Nyquist rate
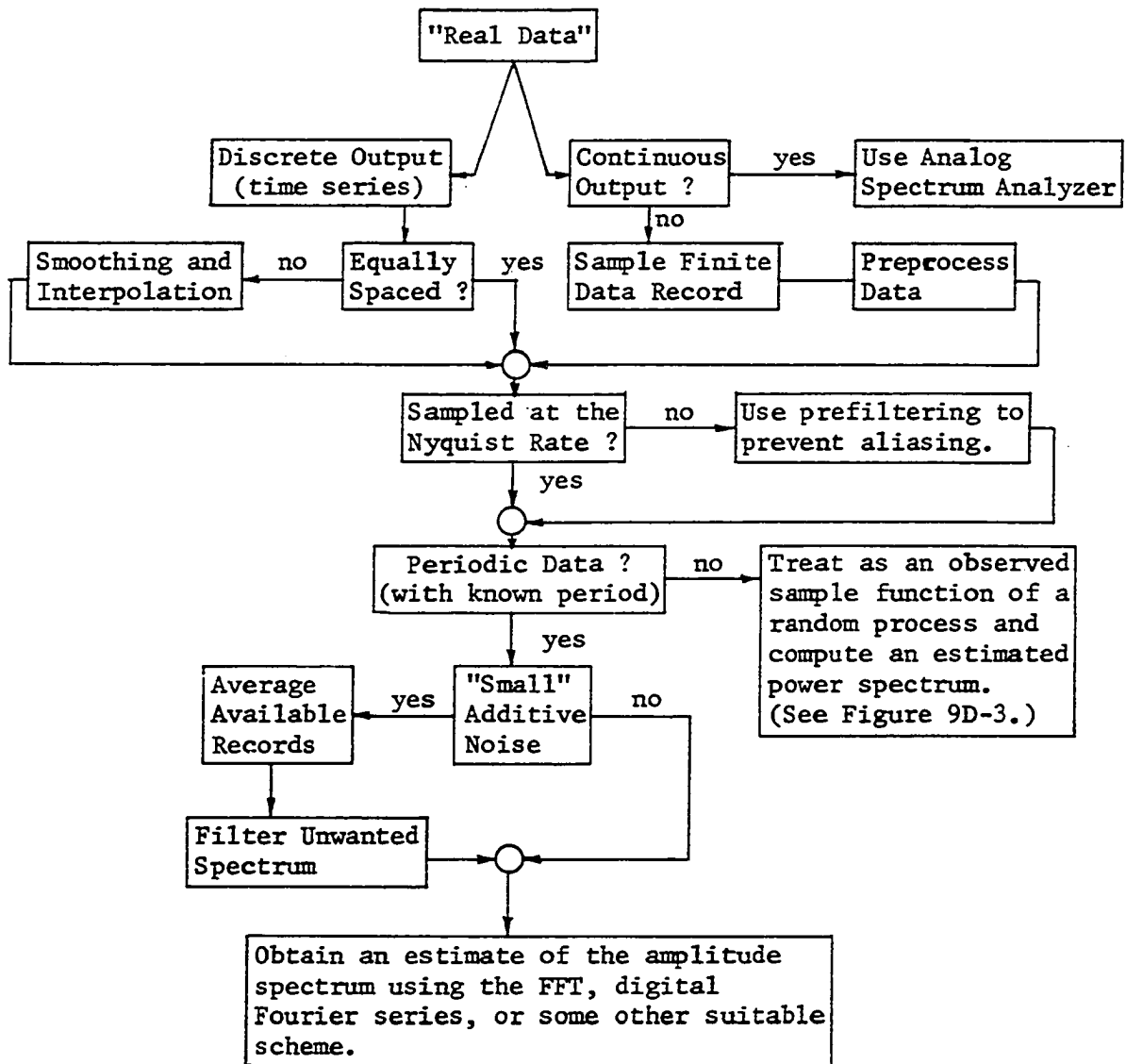
Figure 9D-2. Data Processing Flow Diagram for Illustrating a
Possible Scheme of Spectral Analysis

and prefiltering should be used. If the data output are already in the form of a time series, the experimenter cannot exercise control over the sampling process. If the data are undersampled, the spectrum of the time series will be aliased and spectral accuracy may be seriously degraded.

If the data is periodic or "almost" periodic, it can be processed using the amplitude spectral estimator. A knowledge of the period of the function allows the use of some strong model constraints that can improve the statistical variability of the estimate by reducing random effects due to sampling or noise. If the data is not periodic or if the noise level is so high as to make the data function appear to be random, the data must be treated accordingly.

Figure 9D-3 shows one possible scheme for selecting a spectral estimator for the empirical data function obtained from a random process. The decision as to what kind of estimator to use essentially depends upon how much is known about the process model and how much data is available for processing. A selection of possible estimators is shown. If a large amount of data is available for analysis and the process model is unknown, the Blackman-Tukey method can be used to give the most accurate estimate. The computational efficiency will be considerably reduced from the direct FFT method but this sacrifice may be desirable if the experimenter needs the improved estimation accuracy.

If large amounts of data are available, there is a scheme that appeals to the author that is not shown in the diagram. The scheme essentially would be used when high accuracy estimates are needed. The Blackman-Tukey estimator would be used to make iterative calculations of the power spectrum as the amount of data is increased for each estimate. The power
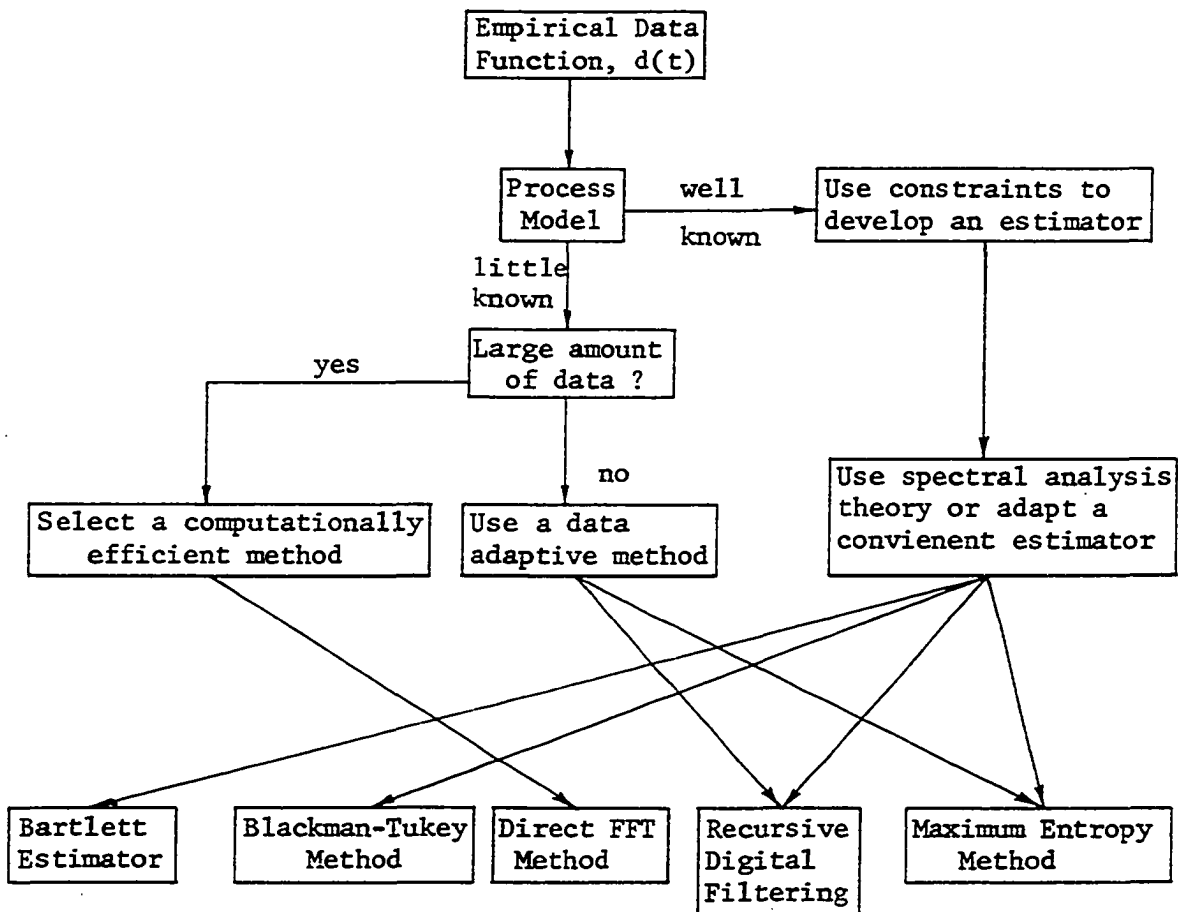
Figure 9D-3. Data Processing Flow Diagram for Illustrating a
Possible Scheme of Spectral Analysis for a
Random Process

spectrum would be seen to converge and the rate of convergence and the variance of the final estimate would give a measure of the statistical variablilty of the estimate. This variability could be traded off against the resolution of the selected spectral window to give a user defined "best" estimate. The scheme can be described as the use of smaller subsets of data to obtain an estimate of the variance of the spectral estimate that used all available data. The author has not seen this scheme developed in the literature and has not had time to develop it in this research. Further study could be done to develop criteria for evaluating the limits on statistical variance and spectral resolution.

The ultimate decision about the use of a particular spectral estimation scheme must be made by the user after serious consideration of the need for the estimate and the scientific consequences or conclusions to be made from the estimate. The occasional or casual user of spectral analysis and spectral estimation methods does not usually have the time to devote to a detailed analysis of possible estimation schemes. As a consequence, the casual user should be warned against placing great scientific importance on the results of the estimate. He should use well-developed estimators as discussed in this chapter or as given in Blackman and Tukey (1958) or Otnes and Enochson (1972). Any presentation of an estimated spectrum and scientific conclusions based on that estimate should be well-supported by a discussion of the details of the estimation scheme used. It is especially important to list all assumptions necessary to make the estimator valid.

It would appear to this author that maximum entropy spectral analysis will become an increasingly important technique in future years. Its a-daptibility to the data and its improved spectral resolution over other methods should establish it as the method most recommended to the casual user. It is especially useful when the amount of experimental data is limited. At the present time, the practical implementation of this technique is not well-discussed in the literature. The reader is referred to Chapter XV and Appendix III for a further discussion.

The experienced or serious user of spectral analysis theory and theory of spectral estimators must devote a considerable amount of time to the study of estimation theory and the criteria of goodness associated with the selection of a "best" method. He must especially be familiar with the strengths and weaknesses of each method and the attendant assumptions. In most cases, more than one spectral estimator should be used to analyze the empirical data function of a real process. The use of more than one estimator can help to reduce the effect of intrinsic estimation errors and provide more confidence in the estimate.

A typical scheme for analyzing the spectrum of an unknown process is shown in Figure 9D-4. This scheme employs more than one kind of estimator and illustrates what the author considers a reasonable approach to a detailed spectral analysis study. A theoretical data function is prefiltered, sampled, and preprocessed to obtain an empirical data function. This empirical data function is used to do a spectral study of the process. Since the properties of the process are unknown, a process model cannot be developed and estimation techniques that do not depend heavily on a particu-

```
            ┌─────────────────┐
            │ Theoretical Data│
            │ Function, s(t)  │
            └────────┬────────┘
                     │
                     ▼
            ┌─────────────────┐
            │ Prefilter, Sample,│
            │ and Preprocess  │
            └────────┬────────┘
                     │
                     ▼
            ┌─────────────────┐
            │ Empirical Data  │
            │ Function, d(t)  │
            └────────┬────────┘
              ┌──────┴───────┐
              ▼              ▼
   ┌───────────────┐   ┌──────────────────┐
   │ Direct FFT    │   │ Blackman-Tukey   │
   │ Method        │   │ Method           │
   └───────────────┘   └──────────────────┘
```
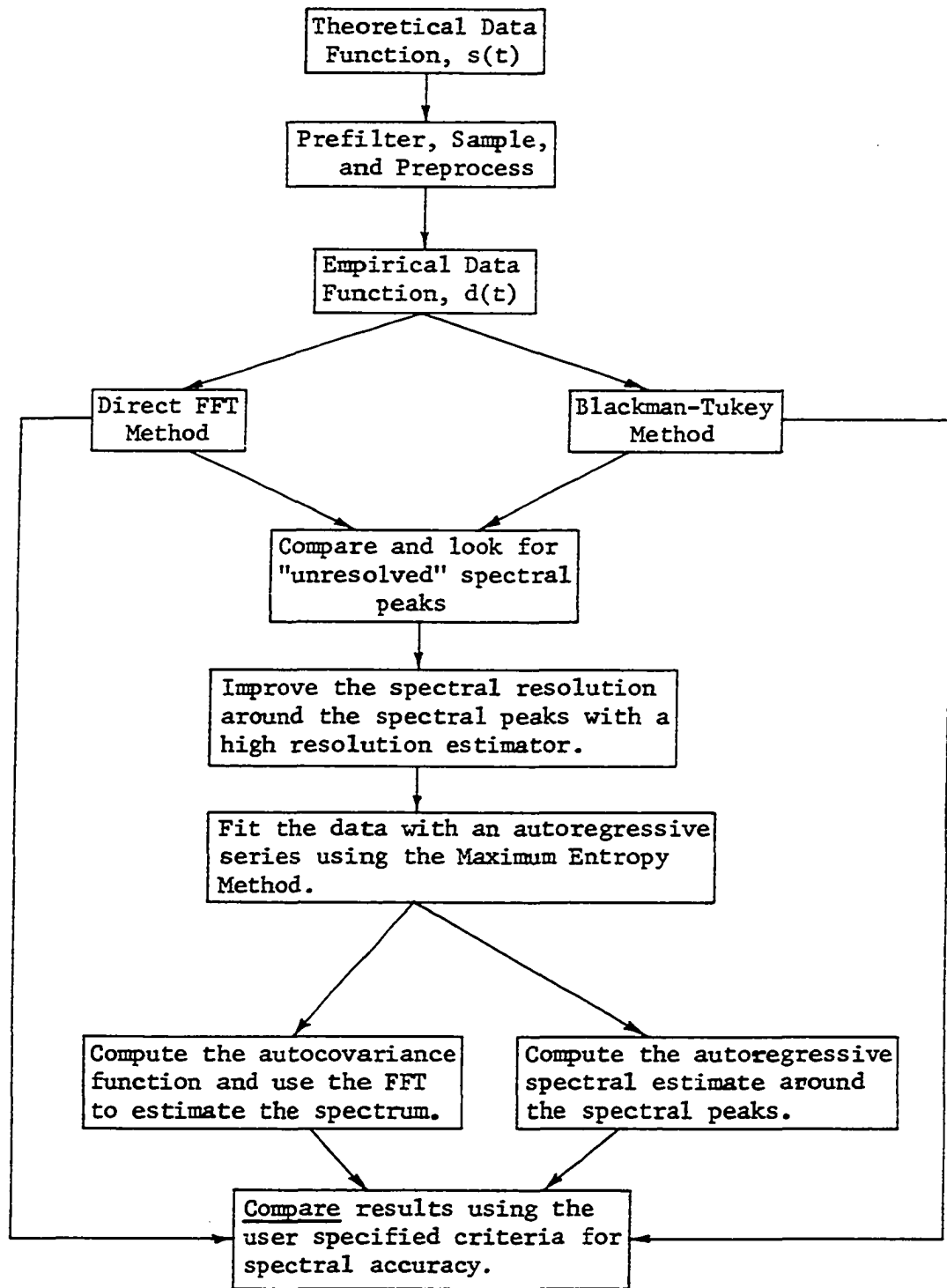

Figure 9D-4. A Typical Scheme for a Detailed Analysis
of the Spectrum of an Unknown Process

lar model should be used. First, the spectrum is estimated by the direct FFT method. This estimator is very computationally efficient and can provide a good first idea of the spectral shape. If the data is sufficient to warrant its use, the Blackman-Tukey estimator should be tried as it will give an estimate that converges (In theory, the direct method cannot). If the spectrum contains spectral peaks that may not be resolved, the spectral resolution can be improved by using the maximum entropy method. The spectrum can be computed by either the FFT or by using the autoregressive spectral estimator. To reduce computation time, the autoregressive spectral estimator need only be evaluated at frequencies near the spectral peaks. The results of these estimations should be compared and additional processing applied as needed.

If the data is very limited, it appears that the use of the maximum entropy spectral estimator is the best choice for obtaining maximum spectral resolution. A summary of the fundamental properties of spectral estimators will help to illustrate their applicability and help the user to make a wise selection.

E.   Fundamental Characteristics of Spectral Estimators

Spectral estimators are usually developed by starting with the various theoretical definitions for a spectral function and applying suitable estimations and numerical approximations. A spectral estimator is usually designed to minimize the intrinsic estimation errors caused by finite data sampling. The various methods appear to differ because they represent different viewpoints concerning the "best" way to represent empirical data.

These different viewpoints usually are the result of selecting different criteria of goodness and starting with different a priori assumptions. By carefully analyzing the commonly used spectral estimators, one can reach the conclusion that they do not represent entirely different approaches to the estimation problem. Because they are all derived from the same theoretical basis, the various estimators share many common characteristics.

When developing a suitable spectral estimator, there are essentially three commonly held viewpoints concerning the best way to treat the problem of finite data. These viewpoints have been developed by the author from reading the literature in this area and they may not represent the breakdown that another author might choose. This author believes that this separation adapts itself nicely to the discussion of method selection. The three methods are:

1. "Lag windowing" of the estimated autocorrelation function.

2. Smoothing and extrapolation of the autocorrelation function.

3. Recursive digital filtering.

The use of a lag window function to give a smoothed estimate of the power spectral density function represents the approach taken by Blackman and Tukey (1958). The use of smoothing and extrapolation to obtain an estimate of the autocorrelation function is the method chosen by those who prefer data adaptive methods which do not have fixed window functions. Data adaptive methods such as maximum entropy and maximum likelihood (Lacoss, 1971) smooth and extrapolate using their respective criteria. The truncated autocorrelation function can also be smoothed and extrapolated using purely mathematical means such as model fitting with some exact function.

This can be done using the straightforward techniques common to numerical analysis (Chapter III) or by using more exotic orthonormal expansions such as angular prolate spheroidal wave functions (Veltman et al., 1972). Recursive digital filtering gives an estimate of the frequency spectrum by computing the average power over the bandwidth of the filter. The filtering method adds the flexibility of choosing the bandwidth of the estimate (within certain limits) but still suffers from problems such as leakage and computational efficiency. Recursive filtering has the tutorial advantage of being able to represent a wide variety of discrete spectral estimators including the important maximum entropy estimator.

The use of a lag window and the autocorrelation function definition of a power spectrum is treated in great detail in Blackman and Tukey (1958). A brief summary of this method showing how the use of a window function reduces the effects of statistical variability and produces a smoothed estimate of the spectrum will now be presented. In discussing the Blackman-Tukey method we will use the autocovariance function instead of the autocorrelation function.

An unbiased estimate for the autocovariance function (Appendix I, Part I) is defined by

$$C_o(\tau) = \frac{1}{T_N - |\tau|} \int_{-(T_N - |\tau|)/2}^{+(T_N - |\tau|)/2} x(t - \tau/2)x(t + \tau/2)dt \qquad (9E.1)$$

where $x(t)$ is a sample record of the process that has been observed for a time T_N. $C_o(\tau)$ is called the apparent autocovariance function because it

is obtained from only one sample realization of the process. For each observed record, x(t), there will be a corresponding function, $C_o(\tau)$. Because $C_o(\tau)$ is an unbiased estimate, its expectation value for lag times between $\pm T_N$ will be equal to the "true" autocovariance function, $C(\tau)$. If several sample records are available, the corresponding apparent autocovariance functions can be averaged to give a better estimate. Lag times near zero will show the least statistical variation because the most data is used for the estimate. As the lag value approaches $\pm T_N$ the amount of data used for the estimate becomes very small and the statistical variance becomes very large.

To avoid the use of lag values with large variances and to reduce problems associated with the truncation of the autocovariance function, Blackman and Tukey chose to multiply the apparent autocovariance function by a lag window function, $D(\tau)$. The resulting function is called the modified apparent autocovariance function:

$$\hat{C}(\tau) = D(\tau)C_o(\tau) \tag{9E.2}$$

Although it is purely arbitrary, the lag window function is usually chosen so that it will give the most weighting to lag values near zero and smoothly reduce the weighting factor to zero at lag values approaching 5 to 10 percent of the total record.

For this discussion, $\hat{C}(\tau)$ will be called the estimated autocovariance function because it is this function that is used to obtain the estimate of the power spectrum. To examine the accuracy of this estimate, we first take the expectation value of $\hat{C}(\tau)$ as given by:

$$E\{\hat{C}(\tau)\} = D(\tau)E\{C_o(\tau)\} = D(\tau)C(\tau) \qquad\qquad |\tau| < T_N \qquad (9E.3)$$

Since, by definition, the expectation of $C_o(\tau)$ is equal to the "true" autocovariance for lag values between $\pm T_N$, the expectation of $\hat{C}(\tau)$ is equal to the "true" autocovariance multiplied by the chosen lag window function.

The estimated power spectral density function is obtained by taking the Fourier transform of the expectation value of $\hat{C}(\tau)$. The result is:

$$\mathcal{F}\{E\{\hat{C}(\tau)\}\} = E\{\mathcal{F}\{\hat{C}(\tau)\}\} = E\{\hat{P}(f)\} \qquad (9E.4)$$

$\hat{P}(f)$ is the Fourier transform of one particular estimate of the autocovariance and $E\{\hat{P}(f)\}$ is the expectation value of all possible realizations. The Fourier transform of the expectation value of $\hat{C}(\tau)$ is equal to the Fourier transform of the product $D(\tau)C(\tau)$ as given in Equation 9E.3. The transform of the product is the convolution of the transforms of $D(\tau)$ and $C(\tau)$. The final result is that the expected value for all possible realizations of the estimated spectrum is equal to the convolution of the "true" power spectrum with the spectral window function $Q(f)$

$$E\{\hat{P}(f)\} = \int_{-\infty}^{+\infty} Q(f - \lambda)P(\lambda)d\lambda \qquad (9E.5)$$

where $Q(f)$ is the Fourier transform of the lag window function (Appendix I, Part I). The best we can do with a finite data function is to give a smoothed estimate of the "true" power spectrum. Increasing the number of data records will help to reduce the problem of statistical variance but only an increase in observation time can help to improve the spectral resolution.

Under certain circumstances, it is theoretically possible to solve the convolution integral (deconvolution) to give the "true" power spectrum, $P(f)$, when the spectral window function, $Q(f)$, is known. For most practical analyses this is not done because, with only a few sample records, the error due to statistical variance is great enough to more than offset any improvement derived from deconvolution.

A simple example will be given to illustrate the smoothing and leakage problems associated with the use of a lag window. For simplicity, we choose a periodic sample function, $x(t)$, made up of three sinewave components. Many sample observations of $x(t)$ are taken and the corresponding apparent autocovariance functions computed. These values are then averaged to produce a close estimate of the "true" autocovariance function for lag values between $\pm T_N$. This averaging reduces the statistical variance for the apparent autocovariance function. The "true" autocovariance is not known for lag values greater than T_N because the sample function was not observed for time intervals greater than this.

The average (or expected) value for the time autocovariance function is shown in Figure 9E-1. This truncated function is multiplied by a rectangular window function to produce the estimated autocovariance function, $\hat{C}(\tau)$. The width of the window function must be chosen narrow enough to minimize the effect of statistical variation in the observed sample functions. Blackman and Tukey recommend that the width of the lag window be no more than 5 to 10 percent of the total lag record. In our example, the width is much wider because the statistical variance has been reduced by averaging multiple observations. For this example and others to follow,

continuous functions will be illustrated. Usually the actual data processing will be done digitally but the continuous functions more clearly illustrate the results without the additional complication of sampling.

The spectral functions associated with the Blackman-Tukey method and this example are shown in Figure 9E-2. The effects of windowing and truncation can be illustrated by comparing the "true" spectrum, $P(f)$, with the estimated spectrum, $\hat{P}(f)$. The estimated power spectrum has been obtained by convolving the spectral window function, $Q(f)$, with the "true" spectrum, $P(f)$. The spectral window function is a sinc function obtained by taking the Fourier transform of the rectangular lag window function. The estimated spectrum is the superposition of many sinc functions. Each line spectrum in $P(f)$ will generate a sinc function of corresponding amplitude in the estimated spectrum, $\hat{P}(f)$. These sinc functions are shown separately in the last plot of Figure 9E-2. Spectral smoothing has caused the two closely spaced components at f_1 and f_2 to be smeared together. The smaller spectral component at f_2 has been obscured by this loss of spectral resolution and most likely would go undetected. Also, the spectral component at f_3 has been smeared out and leakage has caused considerable error in the estimated amplitude of the lower frequency components. Not shown is a dc component in the spectrum caused by the net average value in the estimated autocovariance.

The window function has also introduced some negative power spectra. "Negative power" is not possible physically and its presence in this estimation routine is one of the major complaints of the users of this method. The generation of negative components in the power spectrum can be reduced
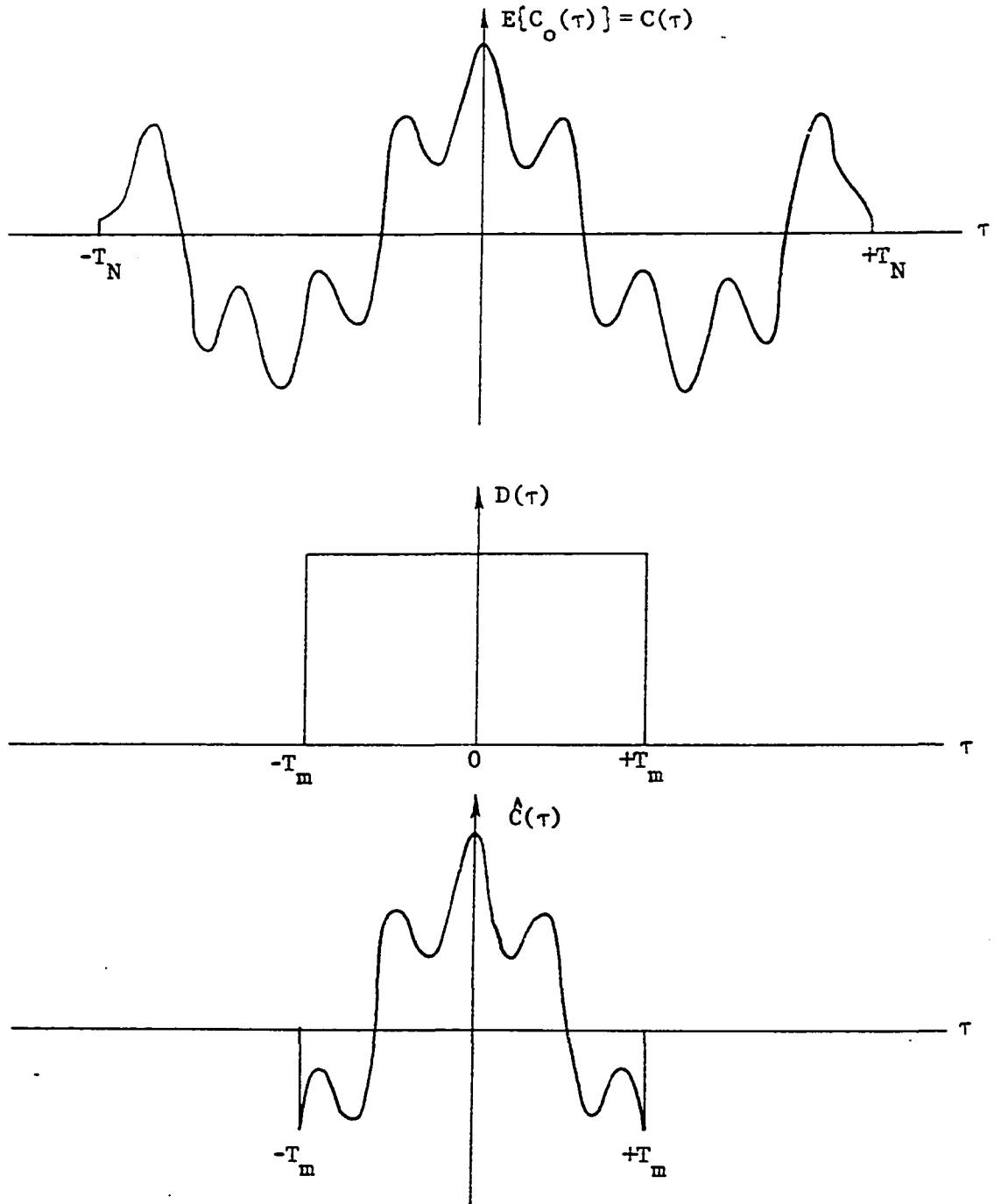
Figure 9E-1.   The Estimated Autocorrelation Function Obtained from a
Rectangular Lag Window
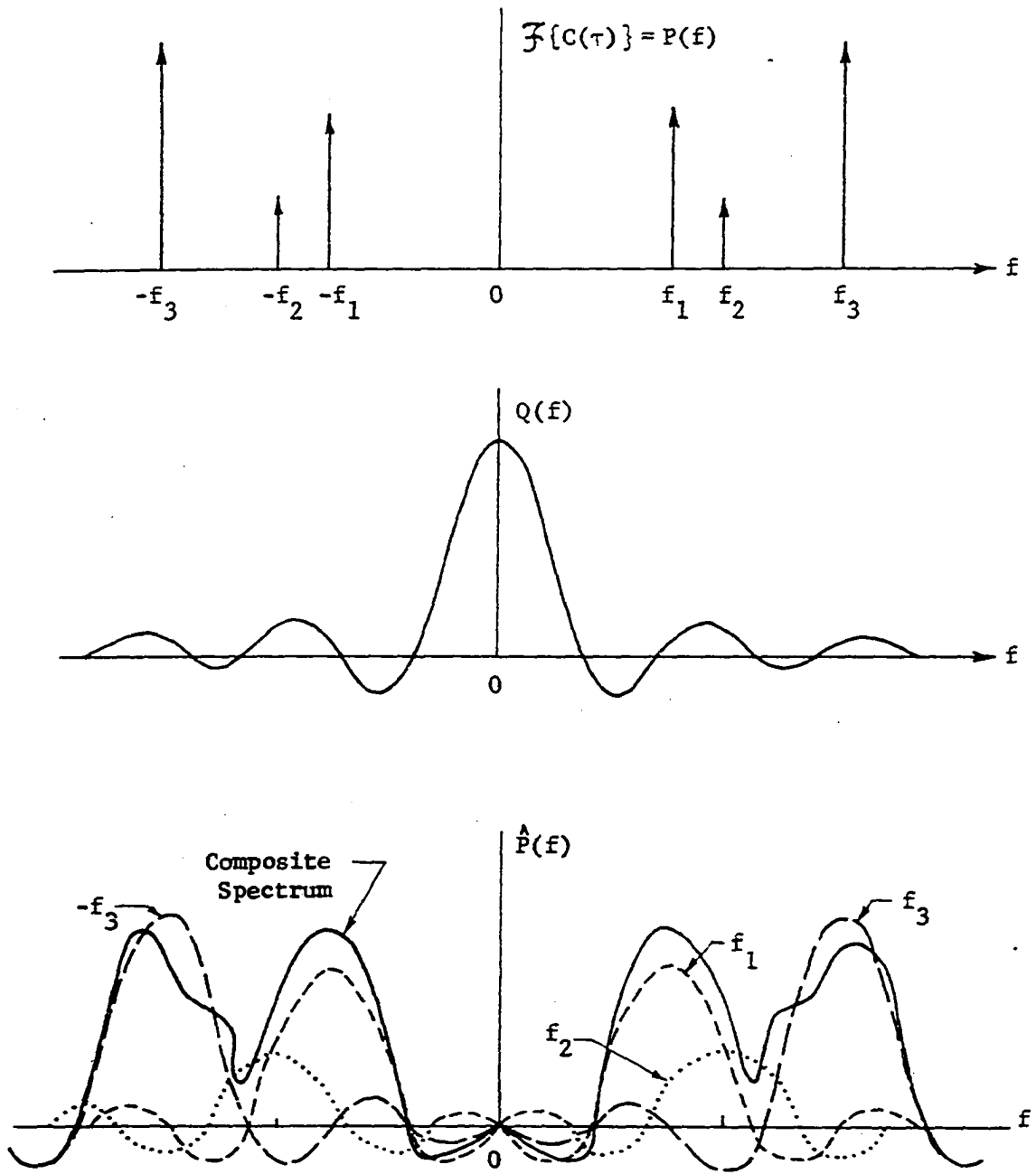
Figure 9E-2. Example Spectral Functions that Illustrate the Blackman-Tukey Method

by the proper selection of a lag window function. The rectangular window function is seldom used because it causes such a severe leakage problem. It does, however, have the best spectral resolution. Other window functions such as the Hanning window or Hamming window (Otnes, 1972, p. 258) have much smaller leakage with only a small sacrifice in spectral resolution.

In many ways, the Blackman-Tukey method of spectral analysis can be viewed as a "fix-up" approach for handling a "difficult" apparent autocovariance function. They use essentially a three step approach to obtain a spectral estimator. First, they define one estimate of the time autocorrelation function that they call the apparent autocovariance function, $C_0(\tau)$. While this estimator has desirable theoretical properties, it also has serious practical shortcomings. Second, the practical shortcomings of this estimator are minimized by using a lag window to obtain a second estimator for the "true" autocovariance function. This second estimator, which Blackman and Tukey call the modified apparent autocovariance function and the author calls the estimated autocovariance, is the function that must represent the "true" autocovariance function for spectral estimation purposes. Third, the Fourier transform of the estimated autocovariance function, $\hat{C}(\tau)$, is used to obtain the estimated spectrum. This three step approach has good and bad aspects that will now be summarized.

For theoretical purposes, the Blackman-Tukey definition of the apparent autocovariance function has many desirable characteristics needed for a good estimator. It converges to the "true" function as the record length becomes infinite and hence is unbiased. Also, its expectation value is

equal to the "true" function for lag values between $\pm T_N$.

For practical purposes, these desirable characteristics are often overshadowed by the problem of statistical variation. This can introduce a "dc" component not present in the "true" function. It can also make the estimate very poor for large values of lag. This happens because the estimator (Equation 9E.1) uses very little data for lag values approaching $\pm T_N$.

A lag window function can be used to reduce the effects of statistical variance by removing the larger lag values. This effectively reduced the statistical variance in the estimated spectrum but it also introduces spectral smoothing effects. The selection of a suitable lag window becomes a tradeoff choice between spectral resolution and statistical variation. A lag window removes valuable data that, although it may have a large variance, could still be used to give some improvement in the spectral estimate.

A technique that avoids the problem of choosing a lag window function and that attempts to use all of the observed data has a lot of practical appeal. Such techniques come under the broad category of data adaptive techniques and apply methods of smoothing and extrapolation to obtain an "acceptable" estimate for the autocovariance function. Conceptually, smoothing and extrapolation are more difficult to justify than the use of a lag window. A criterion of goodness must be defined and its effect on the accuracy of the spectral estimate must be determined. It is entirely possible that an acceptable rational for smoothing or extrapolation may lead to a very unacceptable spectral estimate.

Generally speaking, two different viewpoints have been adopted concerning the "best" way to achieve smoothing and extrapolation. The first adopts a purely mathematical viewpoint and proceeds on the basis of well established numerical techniques for fitting numerical data with exact functions. This approach is often called a parameter free procedure (Veltman et al., 1972) because it does not depend upon any a priori assumptions about the observed process or the resulting data. The resulting spectral estimate is independent of any model for the process. The second viewpoint insists that an estimate of the "true" autocovariance function should be developed by assuming a reasonable and acceptable model for the process or the data.

The parameter free procedure for smoothing and extrapolation is not well-suited for spectral analysis applications because it does not allow for the input of important information that may be known about the process. Also, numerical analysis techniques employ criteria of goodness that cannot be easily related to the determination of the accuracy of the spectrum. In practical applications, the addition of known information about the process can be used as a powerful tool to improve the spectral estimate. For these reasons, it is usually better to choose a method based on some model.

Estimation procedures that employ some type of process model do not have to be as restrictive as one might imagine. It usually turns out that, for purposes of general spectral analysis applications, the process model is designed to have wide applicability and only very modest restrictions on the data function are needed. If a considerable amount of model infor-

mation is known about the process, the user is well-advised to design a spectral estimator that incorporates all of this information. This unusual situation precludes the use of a "standard" procedure.

Process models that have been very successful for obtaining smoothed and extrapolated autocovariance functions are those used in autoregressive spectral estimation and maximum entropy spectral estimation. These techniques operate directly on the observed data function to produce both the estimated autoregressive coefficients and the estimated autocovariance function. The power spectrum can then be estimated by using either the autoregressive spectral estimator (Chapter XIV) or by taking the Fourier transform of the estimated autocovariance function.

For the autoregressive estimator, it is assumed that the observed data can be modeled by an nth order autoregressive series. Once the series coefficients have been determined by some appropriate smoothing and fitting technique, they are used in the spectral estimator. In the maximum entropy method, it is assumed that the process produces a spectrum that has maximum spectral entropy subject to the constraints that the process can be modeled by an autoregressive series and that the estimated autocovariance and the estimated power spectral density form an exact transform pair (no window function).

The estimated autocorrelation function produced by these methods satisfies all of the theoretical requirements set forth in the discussion on frequency domain analysis in Chapter IV. It is discrete but it obeys a well-defined mathematical equation and is defined for all lag values. This estimate can be considerably different from the one obtained using

the Blackman-Tukey method. It is now generally accepted that the maximum entropy method of spectral analysis has a spectral resolution superior to that of the Blackman-Tukey method.

It is difficult to see just how these techniques develop a smoothed and extrapolated estimate unless the autoregressive series approach to the characterization of a random time series is studied in considerable detail. This is not necessary for our purposes and the interested reader is referred to a book by Koopmans (1974). It is important for the reader to realize that these techniques can be described by the mathematics associated with the recursive digital filter. For example, the maximum entropy algorithm can be described as a method for the design of a filter that prewhitens the input spectrum. The filter coefficients can then be used to obtain a spectral estimate (Ulrych, 1972b). This is also commonly referred to as prediction-error filtering (Peacock and Treitel, 1969). The Burg algorithm for determining the maximum entropy spectrum is a recursive procedure for calculating the prediction-error filter and the error power of the prediction (Smylie et al., 1973).

The maximum entropy method, in particular, assumes that the process can be accurately described by an all-pole filter model (a "purely recursive" digital filter) and that the error power is minimized by a least-square-error criterion. These assumptions also apply to the smoothed and extrapolated estimate of the autocovariance function.

An excellent discussion of smoothing and extrapolation techniques for estimating autocorrelation functions with several examples is given in a paper by Veltman et al. (1972).

A third method of developing a spectral estimator involves the use of recursive digital filtering. It was stated in the previous discussion that a recursive digital filter could be used to obtain a maximum entropy spectral estimate by using the concept of prewhitening. It can also be used in the more classical sense as a digital filter operating directly on the observed data.

An analog spectrum analyzer sweeps a narrowband filter through the spectrum of the incoming signal and the detected power output of the filter is displayed as a function of frequency. For digital spectral analysis, the digital filter must be "stepped" through the desired frequency range and the "power output" determined at each step. At each new frequency step, the filter coefficients must be changed and the data processed through the filter. The method operates as though the actual time function were passed through an electrical filter and the resulting output detected to determine the average spectral power over the passband of the filter. Adopting this viewpoint will help the user to understand that the digital filter has all of the "real" problems associated with the analog filter.

There are several problems associated with the use of digital filtering for spectral analysis. The transient response or "ringing" of the filter and its finite bandwidth reduce the accuracy of the spectral estimate. The transient response is especially troublesome if the data record is so short that the filter never reaches "steady state". The required modification of the filter coefficients for each frequency step and the repeated running of the data through the stepped filter may require large amounts of computation time. Finally, the user must develop a filter

and a criterion of goodness that is suitable for his purpose and that produces an acceptable estimator.

This last task is probably the most difficult one facing the potential user. If he is forced to use one of several "canned" procedures, he loses the ability to incorporate known information about the process. This is a serious disadvantage if model information is reasonably accurate. Unless a digital filtering technique has obvious advantages for a particular process model, it is usually advisable for the user to select another method of analysis. A discussion of the application of digital filtering to the estimation of power spectra is given in Otnes and Enochson (1972).

X. HILBERT SPACE VECTOR FORMULATION OF DIGITAL FOURIER TRANSFORM ANALYSIS

When this research was started and the mathematical forms for Fourier series and Fourier analysis were being investigated, the author noted the mathematical similarity between the Fourier analysis equations and those of Hilbert space vector analysis. Having just completed a quantum mechanics course, it seemed worthwhile to use the now familiar Hilbert space vector analysis to investigate the properties of digital Fourier analysis. The vector formulation that will follow was worked out in detail by the author and proved to be extremely useful in some of the subsequent mathematical derivations. Since that time, the author has discovered other references to this Hilbert space - Fourier analysis analogy but has not seen the mathematical details presented. The material that will now be presented was subsequently used to derive the spectral mixing formula and to describe many of the properties of digital Fourier analysis.

The complex representation of a Fourier series is written as

$$f(x) = \sum_{n=-\infty}^{+\infty} C_n e^{+j\frac{2\pi}{T}nx} \tag{10.1}$$

which has complex amplitudes defined by:

$$C_n = C(\frac{2\pi}{T}n) = \frac{1}{T}\int_{-T/2}^{+T/2} e^{-j\frac{2\pi}{T}nx} f(x)dx \tag{10.2}$$

The function $f(x)$ is periodic with a Fourier period of T. The independent variable, x, ranges over $\pm\infty$ but the principal range of x is $\pm T/2$. Since $f(x)$ is periodic it is completely specified by its values over the principal range of x. Since $f(x)$ is not bandlimited, it may theoretically take an

infinite number of complex amplitudes to describe it.

In Hilbert space vector notation, the complex representation of a Fourier series is written as:

$$f(x,T) = \sum_{n=-\infty}^{+\infty} a_n \alpha_n(x,T) = \sum_{n=-\infty}^{+\infty} (\alpha_n, f) \alpha_n(x,T) \tag{10.3}$$

The **orthonormal basis set** of eigenvectors is given by

$$\alpha_n(x,T) = e^{+j\frac{2\pi}{T}nx} \tag{10.4}$$

where the vector "direction" is specified by the parameter n/T. The Hilbert space vector $f(x,T)$ is an infinite linear combination of eigenvectors $\alpha_n(x,T)$. The **complex expansion coefficients** which are the eigenvalues of $f(x,T)$ are defined by the **vector inner product** as:

$$a_n = (\alpha_n, f) = \frac{1}{T} \int_{-T/2}^{+T/2} \alpha_n^*(x) f(x) dx \tag{10.5}$$

The "direction" of the Hilbert space vector is analogous to the Fourier period and the complex expansion coefficients are analogous to the Fourier complex amplitudes.

The vector norm for Hilbert space vectors is given by:

$$(f,f) = \frac{1}{T} \int_{-T/2}^{+T/2} f^*(x) f(x) dx = \sum_{n=-\infty}^{\infty} |a_n|^2 \tag{10.6}$$

The derivation of the complex coefficients from the definition of the vector inner product will now be done because it is important for later work. The vector inner product given in Equation 10.5 is written with Equation 10.3 substituted for $f(x,T)$ as

$$I_n = \frac{1}{T} \int_{-T/2}^{+T/2} \alpha_n^*(x) [\sum_{k=-\infty}^{+\infty} (\alpha_k, f) \alpha_k(x)] dx \tag{10.7}$$

where the dummy index k has replaced n. Interchanging summation and integration and grouping the variables in x, we obtain the expression:

$$I_n = \sum_{k=-\infty}^{+\infty} (\alpha_k, f) \frac{1}{T} \int_{-T/2}^{+T/2} \alpha_n^*(x) \alpha_k(x) dx \tag{10.8}$$

The integral in (10.8) represents the vector inner product of the eigenvectors α_n and α_k but since these form an orthonormal basis set, their inner product is the Kronecker delta function. These steps are summarized as:

$$I_n = \sum_{k=-\infty}^{+\infty} (\alpha_k, f)(\alpha_n, \alpha_k) = \sum_{k=-\infty}^{+\infty} (\alpha_k, f)\delta_{nk} \tag{10.9}$$

The Kronecker delta operating on the inner product (α_k, f) contracts to give the inner product (α_n, f) and this was the original definition of the complex coefficients:

$$I_n = (\alpha_n, f) = a_n \tag{10.10}$$

The derivation of the <u>vector norm</u> is shown in the same way by starting with the definition given in (10.6). Equation 10.3 is substituted for $f(x,T)$ to give:

$$(f,f) = \frac{1}{T} \int_{-T/2}^{+T/2} \sum_{n=-\infty}^{+\infty} (\alpha_n, f)^* \alpha_n^*(x) \sum_{k=-\infty}^{+\infty} (\alpha_k, f)\alpha_k(x) dx \tag{10.11}$$

Grouping variables in x and interchanging summation and integration gives:

$$(f,f) = \sum_{n=-\infty}^{+\infty} (\alpha_n, f)^* \sum_{k=-\infty}^{+\infty} (\alpha_k, f) \frac{1}{T} \int_{-T/2}^{+T/2} \alpha_n^*(x) \alpha_k(x) dx \tag{10.12}$$

As before, the integral defines the vector inner product (α_n, α_k) which reduces to the Kronecker delta to give:

$$(f,f) = \sum_{n=-\infty}^{+\infty} (\alpha_n, f)^* \sum_{k=-\infty}^{+\infty} (\alpha_k, f) \, \delta_{nk} = \sum_{n=-\infty}^{+\infty} (\alpha_n, f)^* (\alpha_n, f) \qquad (10.13)$$

The vector inner products, (α_n, f), define the complex amplitude coefficients, a_n, and the final result becomes:

$$(f,f) = \sum_{n=-\infty}^{+\infty} a_n^* a_n = \sum_{n=-\infty}^{+\infty} |a_n|^2 \qquad (10.14)$$

These same equations which have been derived in Hilbert space notation will also be derived using the notation for Fourier series given in Appendix II. The physical and mathematical significance of these various quantities as related both to the Fourier series and Hilbert space vectors will be presented.

A periodic function can be represented by a series expansion around some vector basis set. The complex representation of a Fourier series is one such expansion that can be written in the form:

$$f(x,T) = \sum_{n=-\infty}^{+\infty} (\alpha_n, f)\alpha_n(x,T) = \sum_{n=-\infty}^{+\infty} c_n e^{+j\frac{2\pi}{T}nx} \qquad (10.15)$$

The orthonormal basis set of eigenvectors for a Fourier series expansion is defined by Equation 10.4. The complex expansion coefficients, a_n, are represented by the Fourier complex amplitudes, c_n, and both are defined by the vector inner product, (α_n, f).

The vector inner product can be used to calculate the complex Fourier amplitudes and also to simplify mathematical derivations involving Fourier series. It is this latter function that the author found very useful. To show that the complex amplitudes can be derived from the vector inner product of the eigenvector operating on the state function, we evaluate

the following integral:

$$I_n = \frac{1}{T} \int_{-\infty}^{+\infty} e^{-j\frac{2\pi}{T}nx} \left[\sum_{k=-\infty}^{+\infty} c_k e^{+j\frac{2\pi}{T}k} \right] dx \qquad (10.16)$$

$$= \sum_{k=-\infty}^{+\infty} c_k \frac{1}{T} \int_{-T/2}^{+T/2} e^{-j\frac{2\pi}{T}nx} e^{+j\frac{2\pi}{T}kx} dx \qquad (10.17)$$

$$= \sum_{k=-\infty}^{+\infty} c_k \frac{1}{T} \int_{-T/2}^{+T/2} e^{+j\frac{2\pi}{T}(k-n)} dx \qquad (10.18)$$

The integral in (10.18) is recognized as one form of the Kronecker delta function discussed in Appendix II, Equation A2.33. Replacing the integral with the Kronecker delta function, the contraction of δ_{kn} and c_k gives the complex amplitudes:

$$(\alpha_n, f) = I_n = \sum_{n=-\infty}^{+\infty} c_k \delta_{kn} = c_n \qquad (10.19)$$

These complex amplitudes are used to reconstruct the original time function, compute the average power, and determine the discrete amplitude spectrum.

The vector norm is used to determine the mean-square voltage or "average" power in the periodic time function. The vector norm is also an alternate representation of Parsaval's theorem. The derivation of the vector norm for a Fourier series is summarized below:

$$(f,f) = \frac{1}{T} \int_{-T/2}^{+T/2} \sum_{n=-\infty}^{+\infty} c_n^* e^{-j\frac{2\pi}{T}nx} \sum_{k=-\infty}^{+\infty} c_k e^{+j\frac{2\pi}{T}kx} dx \qquad (10.20)$$

$$= \sum_{n=-\infty}^{+\infty} c_n^* \sum_{k=-\infty}^{+\infty} c_k \frac{1}{T} \int_{-T/2}^{+T/2} e^{-j\frac{2\pi}{T}nx} e^{+j\frac{2\pi}{T}kx} dx \qquad (10.21)$$

$$= \sum_{n=-\infty}^{+\infty} c_n^* \sum_{k=-\infty}^{+\infty} c_k \, \delta_{kn} = \sum_{n=-\infty}^{+\infty} c_n^* c_n \qquad (10.22)$$

This expression for the vector norm can also be written in the more usual form:

$$(f,f) = \sum_{n=-\infty}^{+\infty} |c_n|^2 \qquad (10.23)$$

Parseval's Theorem for Fourier transformable functions is given by (Cooper, 1971, p. 133):

$$\int_{-T}^{+T} x^2(t)dt = \frac{1}{2\pi} \int_{-\infty}^{+\infty} |X(\omega)|^2 d\omega \qquad (10.24)$$

For a Fourier series it is (Thomas, 1969, p. 600):

$$\frac{1}{2} a_o^2 + \sum_{n=1}^{\infty} (a_n^2 + b_n^2) = \frac{1}{T} \int_{-T/2}^{+T/2} f^2(t)dt = (f,f) \qquad (10.25)$$

In Equation 10.25 the sin-cos expansion coefficients are used. If these are replaced by the complex coefficients, this expression is equivalent to the vector norm equation. To show this we expand the vector norm equation using (10.6) to give

$$\frac{1}{T} \int_{-T/2}^{+T/2} f^2(x)dx = \sum_{n=-\infty}^{+\infty} |c_n|^2 \qquad (10.26)$$

where it is assumed that $f^*(x) = f(x)$.

XI. SPECTRAL MIXING FORMULA

A bandlimited time function, $x(t)$, with period T_F can be <u>exactly</u> specified for all time by a Fourier series

$$x(t) = \sum_{n=-M}^{+M} c_n e^{+j\frac{2\pi}{T_F}nt} \qquad -\infty < t < +\infty \qquad (11.1)$$

with complex amplitudes:

$$c_n = \frac{1}{T_F} \int_{-T_F/2}^{+T_F/2} x(t) e^{-j\frac{2\pi}{T_F}nt} dt \qquad -M \le n \le M \qquad (11.2)$$

The following quantities are defined:

T_F = The period of $x(t)$ which will be referred to as the Fourier period.

$\omega_F = \frac{2\pi}{T_F}$, the Fourier frequency which is also the lowest possible frequency component in $x(t)$.

c_o = The average or "dc" value of $x(t)$.

c_n = The complex spectral amplitude of the nth frequency component corresponding to $n\omega_F$.

$M\omega_F$ = The highest frequency component in $x(t)$.

The complex spectral amplitudes are specified by the integral of Equation 11.2 but this representation can only be used to develop the theory or when $x(t)$ is specified as a mathematical function. For empirical data, the integral must be approximated numerically. Suppose we define a hypothetical experiment where $x(t)$ is sampled at a rate exactly equal to the Nyquist rate and we assume that the total number of samples taken is sufficient to completely determine the complex spectral amplitudes, c_n.

For these conditions, the sampling interval is defined as $\Delta t = T_F/(2M+1)$ and the total number of samples is $2M+1$. This means that the function has been sampled for exactly one Fourier period.

The complex amplitudes will be estimated by using a Riemann sum approximation for the integral of Equation 11.2. This approximation can be written as follows (Appendix I, Part A):

$$\hat{I}_n = \frac{1}{T_F} \Delta t \sum_{k=-M}^{+M} x(k\Delta t) e^{-j\frac{2\pi}{T_F} nk\Delta t} \tag{11.3}$$

Since the total number of samples taken is $2M+1$, there are a total of $2M+1$ segments to be summed. If the sampling interval is replaced by, $\Delta t = T_F/(2M+1)$, the Riemann approximation can be written as:

$$\hat{I}_n = \frac{1}{2M+1} \sum_{k=-M}^{+M} x(k\Delta t) e^{-j\frac{2\pi}{2M+1} nk} \tag{11.4}$$

Does this Riemann sum approximation for estimating the complex amplitudes give accurate estimates for these sampling conditions? This answer can be obtained by computing the vector inner product using the estimate. The The procedure is the same as that used to derive Equation 10.19. Substituting Equation 11.1 for $x(k\Delta t)$ into (11.4) gives:

$$\hat{I}_n = \frac{1}{2M+1} \sum_{k=-M}^{+M} e^{-j\frac{2\pi}{2M+1} nk} \sum_{L=-M}^{+M} c_L e^{+j\frac{2\pi}{2M+1} Lk} \tag{11.5}$$

This expression is modified by interchanging summation and combining the exponents to give:

$$\hat{I}_n = \sum_{L=-M}^{+M} c_L \{ \frac{1}{2M+1} \sum_{k=-M}^{+M} e^{+j\frac{2\pi}{2M+1}(L-n)k} \} \tag{11.6}$$

or by applying trignometric substitutions, the alternate form is:

$$\hat{I}_n = \sum_{L=-M}^{+M} c_L \left\{ \frac{1}{2M+1} [1 + 2 \sum_{k=1}^{M} \cos \frac{2\pi}{2M+1}(L-n)k] \right\} \qquad (11.7)$$

It has been determined that the quantities in the brackets represent the Kronecker delta function (Appendix II, Equations A2.36 and A2.37). To prove this, a computer program was written for the expression in brackets and this expression was evaluated for various combinations of the integers L and n. The double precision program showed that for integers restricted to $(L-n) \leq 2M$, the representation is exact. This discovery was used to conclude that:

$$\hat{I}_n = \sum_{L=-M}^{+M} c_L \delta_{Ln} = c_n \qquad (11.8)$$

In other words, when the time function is sampled in this very special way, the Riemann sum estimation for the integral gives the _exact_ values of the complex spectral amplitudes. Hence, the digitally computed complex amplitudes can be used in the series of Equation 11.1 to _exactly_ reproduce the original _continuous_ time function.

Since the reproduction is exact for the continuous function, it is also exact for the sampled function, $x(k\Delta t)$. If Equation 11.4 is used as a _definition_ for the complex amplitudes and Equation 11.1 is written in a discrete form, these two equations become a basis for the definition of a _digital Fourier transform pair_:

$$x(k\Delta t) = \sum_{n=-M}^{+M} c_n e^{+j\frac{2\pi}{2M+1}nk} \qquad (11.9)$$

$$c_n = \frac{1}{2M+1} \sum_{k=-M}^{+M} x(k\Delta t) e^{-j\frac{2\pi}{2M+1}nk} \qquad (11.10)$$

The digital Fourier series and the digital Fourier transform (Bergland, 1969) have the same mathematical form. From the data processing viewpoint, they are equivalent.

Discrete Fourier transform (DFT) routines including the fast Fourier transform (FFT) are designed to produce M independent frequency components and a "dc" term from $2M+1$ samples of a data function. If the ideal sampling conditions previously described are achieved, the DFT will give exact values for the c_n. If these conditions are not achieved, it will give only an estimate. When the discrete transform is arbitrarily applied to $2M+1$ data values, the resulting discrete amplitude spectrum will be such that the data values can be exactly reproduced. For this reason, the transform pair given above is called an exact transform pair. In general an estimator for the complex amplitudes will not produce a series that will give back the exact data values.

A mathematical examination of the effect of sampling on the estimation of a discrete amplitude spectrum has led to the development of the author's spectral mixing formula. In this derivation, the vector inner product was used to define the complex amplitudes and a Riemann sum was used to approximate the integral in (11.2). The goal of this analysis was to determine the effect of sampling interval and number of samples on the accuracy of the estimate.

Suppose a time function which can be exactly specified by Equations 11.1 and 11.2 is sampled over an arbitrary observation interval, T_N. It is assumed that the observer is unaware of the exact value of the Fourier period, T_F. It is also assumed that there are $2N+1$ samples in the interval

T_N and that the arbitrary sampling interval is Δt.

First, we define an estimated amplitude spectral function as the digital Fourier transform of the time series $\{x(k\Delta t): k = 0, \pm 1, \pm 2, \ldots, \pm N\}$:

$$\hat{X}(\omega) = \Delta t \sum_{k=-N}^{+N} x(k\Delta t)e^{-j\omega k\Delta t} \qquad (11.11)$$

It should be noted that this estimate produces a continuous function of ω despite the fact that $x(k\Delta t)$ is discrete. The continuous nature of $\hat{X}(\omega)$ is a result of the definition of the estimation procedure. In some cases, this continuous estimate can be exploited to produce better results than a discrete estimate.

Second, the complex spectral amplitudes associated with the time series above are defined to be:

$$\hat{c}_n = \frac{1}{T_N} \Delta t \sum_{k=-N}^{+N} x(k\Delta t)e^{-j\frac{2\pi}{T_N}nk\Delta t}$$

$$= \frac{1}{2N+1} \sum_{k=-N}^{+N} x(k\Delta t)e^{-j\frac{2\pi}{2N+1}nk} \qquad (11.12)$$

These complex amplitudes are related to the estimated amplitude spectral function for $x(k\Delta t)$ as follows:

$$\hat{c}_n = \frac{1}{T_N} \hat{X}(\frac{2\pi}{T_N} n) \qquad\qquad T_N = (2N+1)\Delta t \qquad (11.13)$$

In other words, $\hat{c}_n$ is obtained from $\hat{X}(\omega)$ by sampling at intervals corresponding to $\omega_n = 2\pi n/T_N$ and dividing by the observation interval. Before continuing with the derivation, the following observations about the estimation process should be made:

1. Under very special circumstances the $\hat{c}_n$'s are exactly equal to the "true" complex amplitudes, c_n, and hence can be used to generate the continuous time function $x(t)$ from the samples $x(k\Delta t)$.

2. For any given data set $\{x(k\Delta t): k = 0, \pm 1, \pm 2, \ldots, \pm N\}$, the estimated coefficients $\hat{c}_n$ specify a Fourier series given by

$$\hat{x}(t) = \sum_{n=-N}^{+N} \hat{c}_n e^{+j\frac{2\pi}{T_N}nt} \tag{11.14}$$

which is periodic with period T_N and which __exactly__ reproduces the sample values $x(k\Delta t)$. From this we realize that $\hat{x}(t)$ and $x(t)$ are equal at the times $t = k\Delta t$ but, in general, are unequal everywhere else in the time domain. For this reason it is concluded that there are an infinite number of $x(t)$ functions which will fit a discrete data set. Any particular $\hat{x}(t)$ is completely specified by the sampling interval Δt and the total number of samples, $2N + 1$. The desired goal of the estimation scheme is to obtain $\hat{x}(t)$ and its amplitude spectral estimate as close as possible to $x(t)$ and $\mathcal{F}\{x(t)\}$.

3. For $2N + 1$ samples of $x(t)$ there are $2N + 1$ values of $\hat{c}_n$ computed in a digital Fourier analysis scheme. In the "true" spectrum there are $2M + 1$ coefficients. This means that for oversampling there may be many more estimated coefficients than "true" coefficients while undersampling produces just the opposite.

We now proceed to derive the spectral mixing formula. For convenience, a continuous complex spectral amplitude estimate will be defined as:

$$\hat{C}(\omega) = \frac{1}{2N+1} \sum_{k=-N}^{+N} x(k\Delta t)e^{-j\omega k\Delta t} \tag{11.15}$$

where $\Delta t = T_N/(2N+1)$. This continuous function gives the discrete coefficients when sampled at intervals corresponding to $n\Delta\omega = \frac{2\pi}{T_N} n$.

To determine the accuracy of this spectral estimator it is convenient to compare the "true" complex amplitudes with the estimate. This may be done by evaluating the vector inner product using the estimator. Substituting the "true" Fourier series given by (11.1) into Equation 11.15 gives the following estimate in terms of the "true" amplitude coefficients:

$$\hat{C}(\omega) = \frac{1}{2N+1} \sum_{k=-N}^{+N} \sum_{L=-M}^{+M} c_L e^{+j\frac{2\pi}{T_F}Lk\Delta t} e^{-j\omega k\Delta t} \tag{11.16}$$

This equation can be manipulated into the form:

$$\hat{C}(\omega) = \sum_{L=-M}^{+M} c_L \{\frac{1}{2N+1} \sum_{k=-N}^{+N} e^{+jk(L\omega_F-\omega)\frac{T_N}{2N+1}}\} \tag{11.17}$$

Using trigonometric substitutions it can also be written as:

$$\hat{C}(\omega) = \sum_{L=-M}^{+M} c_L \{\frac{1}{2N+1}[1+2\sum_{k=1}^{N} \cos(L\omega_F-\omega)k\frac{T_N}{2N+1}]\} \tag{11.18}$$

$$= \sum_{L=-M}^{+M} c_L \hat{\delta}(L\omega_F-\omega) \tag{11.19}$$

Equation 11.18 is one form of the spectral mixing formula. In this form, it describes the mixing effect of sampling on the continuous complex spectral amplitude estimate. In another form it will be used to describe the spectral mixing effect for the discrete spectral amplitudes, $\hat{c}_n$. The quantity in brackets has a very special significance and will be represented

by $\hat{\delta}(L\omega_F - \omega)$. As far as the author is aware, this concept has not been previously developed. It will be called the <u>estimated Kronecker delta function</u> because when it is used to describe the discrete case, its functional behavior is similar to a Kronecker delta function. It could also reasonably be called a Dirac delta function except its amplitude is normalized to unity and it is primarily used in estimating the spectral amplitudes in the discrete function.

The estimated spectral function at any particular frequency is composed of the sum of all the "real" components after they have been weighted by the estimated Kronecker delta function. In many ways this weighting can be thought of as a convolution of the discrete spectrum with the estimated delta function. This viewpoint suggests an analogy between this process and the convolution with a window function as encountered in the Blackman-Tukey method. The concept of an estimated Kronecker delta function can be applied to other spectral estimators. The one derived here is valid only for the Riemann sum approximation.

The "filtering" effect of the estimated Kronecker delta function is shown with the help of Figure 11-1. The delta function becomes "peaked" about a frequency corresponding to $\omega = L\omega_F$. This weighting tends to "sift out" the discrete amplitude corresponding to the observed frequency, ω, and deemphasize the other components. When the amount of observed data becomes large, the estimated Kronecker delta function converges to the "true" function. When the hypothetical sampling circumstances described earlier are achieved, the estimate becomes exact.
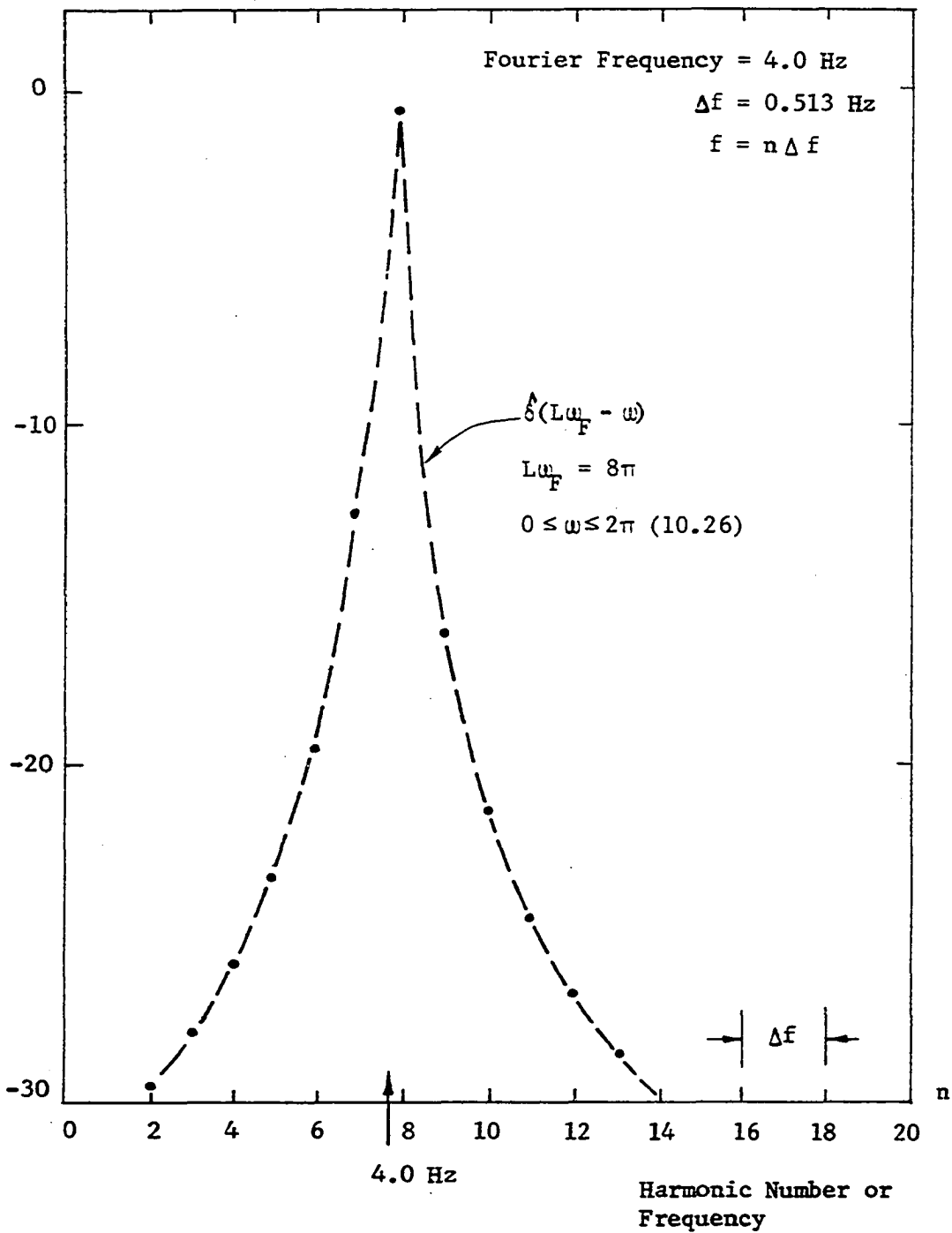
Figure 11-1. A Plot of the Estimated Kronecker Delta
Function Showing the Filtering Effect

The spectral mixing formula for the discrete spectral amplitudes is obtained by sampling the continuous complex spectral amplitude estimator at frequencies corresponding to $n\Delta\omega = \frac{2\pi}{T_N} n$. The resulting equation is:

$$\hat{C}(\frac{2\pi}{T_N} n) = \hat{c}_n = \sum_{L=-M}^{+M} c_L \{\frac{1}{2N+1}[1 + 2\sum_{k=1}^{N} \cos \frac{2\pi k}{2N+1}(\frac{L}{T_F} - \frac{n}{T_N})T_N]\} \quad (11.20)$$

The estimated discrete complex amplitudes are the same as those that would be calculated by the discrete Fourier transform. If the observation interval and the Fourier period are equal, $T_F = T_N$, the estimate is exact.

The discrete form of the spectral mixing formula relates the "true" spectral amplitudes, c_n, to the estimated amplitudes, $\hat{c}_n$, for any given set of sampling conditions. The parameters of the sampler are the total number of samples, $2N+1$, the observation interval, T_N, and the sampling interval, $\Delta t = \frac{T_N}{2N+1}$. The parameters of the input signal are the Fourier period, T_F, and the complex amplitudes, c_n. The effect of changes in the sampling parameters can be studied by using the mixing formula.

More research needs to be done to further develop the mixing formula into an analytical tool. Since it relates the estimated coefficients to the "true" coefficients, it seems possible that an algorithm can be developed that will improve the spectral estimate by "unmixing" the mixing effect. This procedure would involve an optimal search for the Fourier period by some appropriate criterion placed on the resulting spectrum.

Such a routine has not been worked out by the author but some preliminary ideas were developed. These ideas are generally expressed in Hilbert space notation and employ some assumptions that have not been shown to be valid.

The basic problem will now be formulated. Suppose an observed $x(t)$ is recorded for a time T_N but it is assumed that the Fourier period is unknown. Using Hilbert space representations, suppose that the "direction" of the vector is changed until some "optimum" direction is found that gives as "best" estimate of the time series. This analysis would produce a period T_{opt} which would approximate the Fourier period and complex coefficients (α_n, f) based upon the desired criteria.

The <u>state vector of the system</u> is defined as the infinite series:

$$\psi(x,T_m) = \sum_{m=1}^{\infty} f(x,T_m) = \sum_{m=1}^{\infty} \sum_{n=-\infty}^{+\infty} (\alpha_n,f)\alpha_n(x,T_m) \qquad (11.21)$$

It will be assumed that an operator, $\hat{A}$, exists which will yield an "optimum" time series when operating on ψ. A second assumption, based upon intuition and the need for a suitable criterion of goodness, is that the "optimum" period is the one which concentrates the spectral power into the fewest possible spectral components. This a priori assumption is, in effect, forcing the estimate to agree with the empirical data by approximating the data with the "least complicated" spectrum. To formulate this idea, we normalize the complex amplitudes such that the vector norm is unity:

$$\sum_{n=-\infty}^{+\infty} |c_n|^2 = 1 \qquad (11.22)$$

The entropy measure for the spectrum will be defined as:

$$H = - \sum_{n=-\infty}^{+\infty} |c_n| \log |c_n| \qquad (11.23)$$

To produce the fewest possible spectral components, we will want to min-
imize the entropy, H. The problem can be summarized as trying to find an
operator, $\hat{A}$, which operates on ψ to yield an "optimum" time series,
$f(x,T_{opt})$, which is the best estimate of the observed time series. The
constraint for this optimization is that the entropy is minimized. Time
did not permit the author to develop the details of this analysis or even
to prove the basic assumptions. For the reader interested in developing
this idea further, the author recommends using a calculus of variations
with constraints. One example of this type of procedure has been given in
Appendix I, Part J.

Examples of the use of the spectral mixing formula and a further
discussion of the use of the digital Fourier transform for the spectral
analysis of finite time series will be presented in Chapter XII.

XII. FOURIER TRANSFORM SPECTRAL ESTIMATION

A. Infinite Periodic Time Functions

A sample record of an infinite periodic time function with period T_F is shown in Figure 12A-1. It is assumed that the function is bandlimited and that it can be characterized by $2M+1$ complex amplitudes.
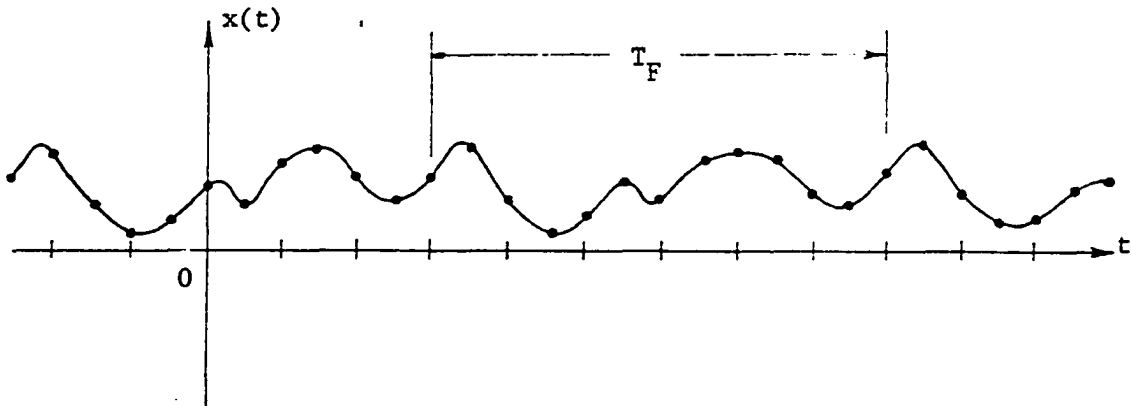
Figure 12A-1. A Sample Record of an Infinite
Periodic Time Function with Period T_F

This bandlimited function can be **exactly** specified for all time by a complex Fourier series

$$x(t) = \sum_{n=-M}^{+M} c_n e^{+j \frac{2\pi}{T_F} nt} \qquad -\infty \leq t \leq +\infty \qquad (12A.1)$$

with complex amplitudes:

$$c_n = \frac{1}{T_F} \int_{-T_F/2}^{+T_F/2} x(t) e^{-j \frac{2\pi}{T_F} nt} dt \qquad -M \leq n \leq +M \qquad (12A.2)$$

The following quantities are defined:

T_F = The period of x(t) referred to as the Fourier period.

$\omega_F = \dfrac{2\pi}{T_F}$, the Fourier frequency, also the lowest frequency component in x(t).

c_o = The average value of x(t).

c_n = The complex spectral amplitude or Fourier coefficient corresponding to the nth frequency component, $n\omega_F$.

$M\omega_F$ = The highest frequency component in x(t).

The actual number of complex amplitudes that are needed to describe a particular x(t) can be very deceiving. In a practical situation it may take hundreds of c_n's to characterize x(t) but many times only a few of them are nonzero.

1. Fourier analysis

The Fourier analysis of an infinite periodic function consists of determining the complex amplitudes, c_n, and the amplitude spectrum, $X(\omega)$. The complex amplitudes are determined from Equation 12A.2 and the amplitude spectral function is the Fourier transform of x(t):

$$\mathcal{F}\{x(t)\} = \int_{-\infty}^{+\infty} \sum_{n=-M}^{+M} c_n e^{+j\omega_F n t} e^{-j\omega t} dt$$

$$= \sum_{n=-M}^{+M} c_n \int_{-\infty}^{+\infty} e^{+j(n\omega_F - \omega)t} dt \qquad (12A.3)$$

The expression in brackets is recognized as a form of the Dirac delta function (Appendix II, Part E) and the final result is:

$$\mathcal{F}\{x(t)\} = X(\omega) = \sum_{n=-M}^{+M} c_n 2\pi \delta(n\omega_F - \omega) \qquad (12A.4)$$

The use of a delta function allows for the existence and definition of the amplitude spectrum of an infinite periodic time function.

2. Autocorrelation function

By applying the definition given in Appendix I for a time autocorrelation function and using Equation 12.1 for $x(t)$, the time autocorrelation function for an infinite periodic time function is easily determined to be:

$$R_x(\tau) = \sum_{n=-M}^{+M} |c_n|^2 e^{+jn\omega_F \tau} \qquad (12A.5a)$$

$$= |c_o|^2 + 2 \sum_{k=1}^{M} |c_k|^2 \cos(k\omega_F \tau) \qquad (12A.5b)$$

$R_x(\tau)$ has an average value of $|c_o|^2$ and is periodic with period T_F.

3. Power spectral density function

The power spectral density function for an infinite periodic time function is determined by taking the Fourier transform of the time autocorrelation function:

$$\mathcal{F}\{R_x(\tau)\} = S_x(\omega) = \sum_{n=-M}^{+M} |c_n|^2 \, 2\pi\delta(n\omega_F - \omega) \qquad (12A.6)$$

For this ideal condition, the amplitude spectrum and power spectrum both consist of $2M+1$ line components of amplitude c_n and $|c_n|^2$ respectively. They both give essentially the same spectral information about $x(t)$.

4. Total spectral power

The total power in the spectrum of $x(t)$ is obtained by integrating the power spectral density function over all frequency:

$$\text{Total Power} = \frac{1}{2\pi} \int_{\text{all } \omega} S_x(\omega) d\omega = \sum_{n=-M}^{+M} |c_n|^2 \qquad (12A.7)$$

The total power is also obtained by evaluating the time autocorrelation function at zero lag:

$$\text{Total Power} = R_x(0) = \sum_{n=-M}^{+M} |c_n|^2 \qquad (12A.8)$$

5. Vector norm

The vector norm is used to determine the mean-square voltage or "average" power in the periodic time function. It is also a particular form of Parseval's Theorem. For the complex Fourier series it is given by

$$\text{Average Power} = \frac{1}{T_F} \int_{-T_F/2}^{+T_F/2} x^*(t) x(t) dt = \sum_{n=-M}^{+M} |c_n|^2 \qquad (12A.9)$$

From this representation we see that the total power in the frequency spectrum is determined by the mean-square value of $x(t)$ averaged over one Fourier period.

6. Ideal sampling

If $x(t)$ is sampled by an ideal sampler and at a rate exceeding the Nyquist rate (see Chapter VI), the sampled function can be exactly reconstructed using the following infinite orthonormal series:

$$x(t) = \sum_{k=-\infty}^{+\infty} x(k\Delta t) \left[\frac{\sin \frac{\pi}{\Delta t}(t - k\Delta t)}{\frac{\pi}{\Delta t}(t - k\Delta t)}\right] \qquad (12A.10)$$

This formula can be used for exact interpolation between sampled values provided the sampling interval is less than the Nyquist sampling interval, $\Delta t < \frac{T_F}{2M}$.

B. Finite Periodic Time Functions

The infinite periodic time function x(t) is now observed for a finite time, T_N, as illustrated in Figure 12B-1. It will be assumed that the observer is unaware of the exact value of the Fourier period, T_F. Although
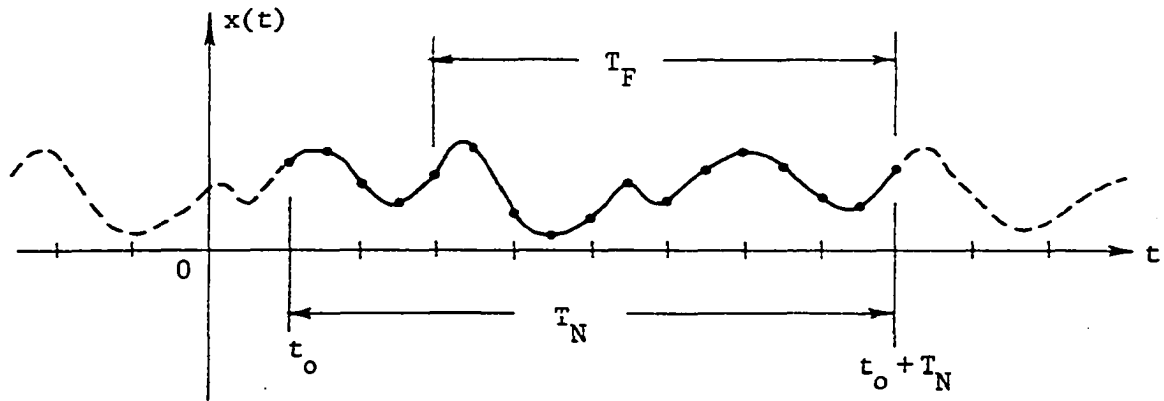
Figure 12B-1. Truncated Time Sample of an
Infinite Periodic Time Function

x(t) is infinite, a truncated time function can be defined using a rectangular observation window function such that

$$\hat{x}(t) = u(t)x(t) \tag{12B.1}$$

where

$$u(t) = \begin{cases} 1 & t_o \le t \le t_o + T_N \\ 0 & \text{otherwise} \end{cases} \tag{12B.2}$$

or:

$$\hat{x}(t) = \begin{cases} x(t) & t_o \le t \le t_o + T_N \\ 0 & \text{otherwise} \end{cases} \tag{12B.3}$$

For purposes of presentation, the origin in Figure 12B-1 will be shifted so that $t_o = -T_N/2$ and the sample length is symmetrical about the vertical axis.

1. Fourier analysis

Since the truncated function is absolutely integrable,

$$\int_{-\infty}^{+\infty} |\hat{x}(t)| \, dt = \int_{-T_N/2}^{+T_N/2} |x(t)| \, dt < \infty \tag{12B.4}$$

the amplitude spectral function exists and is obtained by taking the following Fourier transform:

$$\hat{X}(\omega) = \mathcal{F}\{\hat{x}(t)\} = \int_{-T_N/2}^{+T_N/2} x(t) e^{-j\omega t} \, dt \tag{12B.5}$$

If $x(t)$ in the above integral is replaced by Equation 12A.1 and the integration performed, the resulting estimated amplitude spectral density becomes:

$$\hat{X}(\omega) = \sum_{n=-M}^{+M} c_n T_N \left[\frac{\sin(n\omega_F - \omega)T_N/2}{(n\omega_F - \omega)T_N/2} \right] \tag{12B.6}$$

As the observation interval becomes very large, $T_N \to \infty$, this estimate converges to the "true" amplitude spectral density given in Equation 12A.4:

$$\lim_{T_N \to \infty} \hat{X}(\omega) = \sum_{n=-M}^{+M} c_n 2\pi \, \delta(n\omega_F - \omega) \tag{12B.7}$$

The interested reader can verify this limit by applying Equation A2.49 given in Appendix II.

For the very special circumstances where the period of observation, T_N, is an exact multiple of the Fourier period, $T_N = qT_F$, and if we are interested only in the amplitude spectrum sampled at multiples of the Fourier frequency, $\omega_F = 2\pi/T_F$, we get:

$$\hat{X}(k\omega_F) = \sum_{n=-M}^{+M} c_n qT_F \left[\frac{\sin \pi(n-k)}{\pi(n-k)}\right] \tag{12B.8}$$

The sinc function in the brackets is actually a special form of the Kronecker delta function given in Appendix II. Replacing the sinc function with the Kronecker delta and using the contraction property gives:

$$\hat{X}(k\omega_F) = qT_F \sum_{n=-M}^{+M} c_n \delta_{nk} = qT_F c_k \tag{12B.9}$$

From this derivation we can see that, for these special circumstances, the complex spectral amplitudes can be exactly computed from the samples of $\hat{X}(\omega)$ by:

$$c_n = \frac{1}{qT_F} \hat{X}(n\omega_F) \tag{12B.10}$$

This special relationship between the complex amplitudes, c_n, and sample values of the estimated amplitude spectral function, $\hat{X}(\omega)$, suggests a curious interpretation for Equation 12B.6. Except for a scale factor, T_N, this equation is identical in form to the reconstruction equation (6D.6) discussed in Chapter VI. From this it is concluded that the amplitude spectral function for a truncated continuous time function can be obtained by a series expansion involving the "true" complex coefficients and an appropriate orthornormal sinc function.

For a periodic time function, the amplitude spectral function can also be computed by applying the convolution theorem:

$$\hat{x}(t) = u(t)\, x(t) \tag{12B.11a}$$

$$\hat{X}(\omega) = U(\omega) * X(\omega) \tag{12B.11b}$$

The Fourier transform of the rectangular window function is a sinc function and $X(\omega)$ is given by Equation 12A.4. The convolution of the sinc function with a series of Dirac delta functions gives the same series as Equation 12B.6. This convolution technique cannot generally be applied if $x(t)$ has any random components because $X(\omega)$ may not exist. The approach to use for random functions is discussed in Part C of this chapter.

2. Estimated autocorrelation function

There are two possible definitions for the estimated time autocorrelation function, $\hat{R}_x(\tau)$. The first definition is valid for lag values much smaller than the observation period, $\tau \ll T_N$. This definition is consistent with the usual assumptions applied in the Blackman-Tukey method:

$$\hat{R}_x(\tau) = \frac{1}{T_N} \int_{-T_N/2}^{+T_N/2} x^*(t)x(t+\tau)\,dt \qquad \tau \ll T_N \tag{12B.12}$$

This definition also yields the simplest results

$$\hat{R}_x(\tau) = \sum_{k=-M}^{+M} \sum_{L=-M}^{+M} \alpha_{kL}\, e^{+j\omega_F k\tau} \tag{12B.13}$$

$$= \sum_{k=-M}^{+M} \beta_k\, e^{+j\omega_F k\tau} \tag{12B.14}$$

where

$$\alpha_{kL} = c_k^* c_L \left[\frac{\sin \pi (k - L)\frac{T_N}{T_F}}{\pi(k - L)\frac{T_N}{T_F}} \right] \qquad (12B.15)$$

and

$$\beta_k = \sum_{L=-M}^{+M} \alpha_{kL} \qquad (12B.16)$$

The amplitude constants, β_k, in Equation 12B.14 play the same role as the amplitude constants, $|c_n|^2$, in Equation 12A.5. In this sense, the auto-correlation function for the truncated time function is no more complicated than that for the infinite case. The very definite difference between the two is that the estimated autocorrelation is itself a random function. As the window function moves with respect to $x(t)$, it gives different sample realizations and thus generates a randomness in $\hat{R}_x(\tau)$. This randomness is a direct result of the observation and sampling process.

If the period of observation is again an exact multiple of the Fourier period (as in Equation 12B.8), the sinc function reduces to a Kronecker delta and the complex amplitudes reduce to

$$\alpha_{kL} = c_k^* c_L \delta_{kL} \qquad (12B.17)$$

and:

$$\beta_k = \sum_{L=-M}^{+M} c_k^* c_L \delta_{kL} = |c_k|^2 \qquad (12B.18)$$

The net result is that the estimated autocorrelation function is identical to the "true" function for these sampling conditions:

$$\hat{R}_x(\tau) = \sum_{k=-M}^{+M} |c_k|^2 e^{+jk\omega_F \tau} = R_x(\tau) \tag{12B.19}$$

The second definition for the estimated time autocorrelation function is the one which will converge to the "true" function and hence is not biased. It is also valid for all lag values, $|\tau| < T_N$. This estimate is more complicated than the previous one and does not lend itself to an easy interpretation. The estimate we will work with is given by:

$$\hat{R}_x(\tau) = \frac{1}{T_N - |\tau|} \int_{-\frac{1}{2}(T_N - |\tau|)}^{+\frac{1}{2}(T_N - |\tau|)} x^*(t - \tau/2) x(t + \tau/2) dt \tag{12B.20}$$

This autocorrelation estimate can be expressed in terms of the complex Fourier coefficients by replacing the $x(t)$'s with Equation 12A.1 and doing the integration. After many detailed algebraic manipulations we obtain

$$\hat{R}_x(\tau) = \sum_{n=-M}^{+M} |c_n|^2 e^{+j\omega_F n \tau}$$

$$+ \sum_{\substack{k=-M \\ k \neq L}}^{+M} \sum_{L=-M}^{+M} c_k^* c_L q_{kL}(\tau) e^{+j\omega_F(k+L)\tau/2} \tag{12B.21}$$

where:

$$q_{kL}(\tau) = \frac{1}{T_N - |\tau|} \int_{-\frac{1}{2}(T_N - |\tau|)}^{+\frac{1}{2}(T_N - |\tau|)} e^{+j\omega_F(L-k)t} dt \tag{12B.22}$$

$$= \frac{\sin\left\{\frac{1}{2}\omega_F(L-k)(T_N - |\tau|)\right\}}{\frac{1}{2}\omega_F(L-k)(T_N - |\tau|)} \tag{12B.23}$$

The function $q_{kL}(\tau)$ is even and represented by two sinc functions which are

mirror images of each other. Attempts at further analysis of $q_{kL}(\tau)$ have not been successful. The Fourier transform of $q(\tau)$ involves a sine integral. For $|\tau| \ll T_N$, $q_{kL}(\tau)$ reduces to the sinc function in Equation 12B.15 and the two estimates agree.

3. Estimated power spectral density function

For the autocorrelation estimate given by Equation 12B.12, the estimated power spectral density function is

$$\hat{S}_x(\omega) = \mathcal{F}\{\hat{R}_x(\tau)\} = \sum_{n=-M}^{+M} \beta_n 2\pi\delta(n\omega_F - \omega) \qquad (12B.24)$$
$$(\tau \ll T_N)$$

where

$$\beta_n = \sum_{k=-M}^{+M} c_k^* c_n \left[\frac{\sin \pi (k-n)\dfrac{T_N}{T_F}}{\pi(k-n)\dfrac{T_N}{T_F}} \right] \qquad (12B.25)$$

and again if T_N is an exact multiple of T_F, the amplitude coefficient simplifies to $\beta_n = |c_n|^2$.

For the autocorrelation estimate given by Equation 12B.21, the power spectral density function involves the Fourier transform of $q_{kL}(\tau)$ which has not been determined. This estimate may be written as:

$$\hat{S}_x(\omega) = \sum_{n=-M}^{+M} |c_n|^2 2\pi\delta(n\omega_F - \omega)$$

$$+ \sum_{\substack{k=-M \\ k \neq L}}^{+M} \sum_{L=-M}^{+M} c_k^* c_L \, \mathcal{F}\{q_{kL}(\tau)e^{+j\omega_F(k+L)\tau/2}\} \qquad (12B.26)$$

4. Total power estimate

The total spectral power for each estimate is obtained by integrating the spectral density over all frequency. This gives for $|\tau| \ll T_N$,

$$\text{Total Power} = \frac{1}{2\pi} \int_{-\infty}^{+\infty} \hat{S}_x(\omega)\,d\omega = \sum_{n=-M}^{+M} \beta_n \qquad (12B.27)$$

and for all $|\tau| < T_N$:

$$\text{Total Power} = \sum_{n=-M}^{+M} |c_n|^2$$

$$+ \sum_{\substack{k=-M \\ k \neq L}}^{+M} \sum_{L=-M}^{+M} c_k^* c_L \frac{1}{2\pi} \int_{-\infty}^{+\infty} \mathcal{F}\{q_{kL}(\tau) e^{+j\omega_F(k+L)\tau/2}\}\,d\omega \qquad (12B.28)$$

It can be shown that the sum in Equation 12B.27 is positive and real.

5. Vector norm

The vector norm or Parseval's Theorem for the truncated function is similar in form to that for the infinite periodic time function. The major differences are that the mean-square value is averaged over the observation interval and not over the Fourier period and the amplitudes, $|c_n|^2$, are replaced by the amplitudes, β_n. The approximation to Parseval's Theorem becomes:

$$\frac{1}{T_N} \int_{-T_N/2}^{+T_N/2} x^*(t)x(t)\,dt = \sum_{n=-M}^{+M} \beta_n = \frac{1}{2\pi} \int_{-\infty}^{+\infty} \hat{S}_x(\omega)\,d\omega \qquad (12B.29)$$

6. Frequency resolution and spectral mixing

The ability to resolve line spectra and avoid false spectral peaks is of great concern when doing high resolution spectral analysis of periodic

signals. These topics can be studied by assuming a reasonable model for the spectrum of a periodic signal and then doing Fourier spectral analysis on the model. A convenient spectral model is shown in Figure 12B-2. The
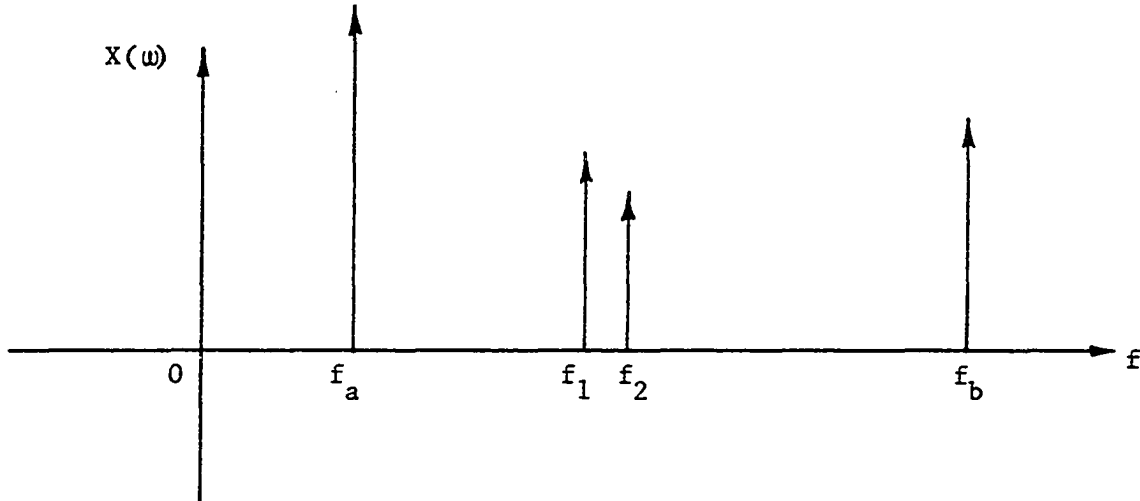
Figure 12B-2. A Convenient Spectral Model
for Resolution Studies

periodic time function can be modeled by a Fourier series of four terms:

$$x(t) = A_a \cos (2\pi f_a t + \phi_a) + A_b \cos (2\pi f_b t + \phi_b)$$

$$+ A_1 \cos (2\pi f_1 t + \phi_1) + A_2 \cos (2\pi f_2 t + \phi_2) \qquad (12B.30)$$

A complete Fourier series representation would involve determining integers, m, and a Fourier period T_F such that:

$$f_a = m_a \frac{1}{T_F} \qquad\qquad f_1 = m_1 \frac{1}{T_F}$$

$$\qquad\qquad\qquad\qquad\qquad\qquad (12B.31)$$

$$f_b = m_b \frac{1}{T_F} \qquad\qquad f_2 = m_2 \frac{1}{T_F}$$

The time function would then be modeled by a Fourier series such as in Equation 12A.1 where many of the complex amplitudes would be zero.

To be able to compute a Fourier series for the periodic waveform requires a knowledge of the Fourier period, T_F. If this is not known, it is difficult to determine the integers m_a, m_b, m_1, and m_2.

The time autocorrelation function for an infinite record of $x(t)$ is computed using Equation 12A.5 as:

$$R_x(\tau) = \frac{1}{2} A_a^2 \cos (2\pi f_a \tau) + \frac{1}{2} A_b^2 \cos (2\pi f_b \tau)$$

$$+ \frac{1}{2} A_1^2 \cos (2\pi f_1 \tau) + \frac{1}{2} A_2^2 \cos (2\pi f_2 \tau) \tag{12B.32}$$

If the infinite autocorrelation function were now truncated it would be a straightforward matter to use a lag window function and continue the analysis. The data function, however, is terminated with a data window and this complicates the analysis considerably. The estimated autocorrelation function should be computed using Equation 12B.21.

The complicated mathematical analysis of the estimated autocorrelation function will not be presented. Even the simple example of a single sine-wave burst discussed in Part 7 of this section involves a considerable amount of mathematical manipulation. Further spectral analysis for this section will be done using the amplitude spectral function.

The amplitude spectral function for the infinite time function is computed using Equation 12A.4. For the four term series this becomes:

$$X(\omega) = \pi A_a [e^{+j\phi_a} \delta(\omega_a + \omega) + e^{-j\phi_a} \delta(\omega_a - \omega)]$$

$$+ \pi A_b [e^{+j\phi_b} \delta(\omega_b + \omega) + e^{-j\phi_b} \delta(\omega_b - \omega)]$$

$$+ \pi A_1 [e^{+j\phi_1}\delta(\omega_1 + \omega) + e^{-j\phi_1}\delta(\omega_1 - \omega)]$$

$$+ \pi A_2 [e^{+j\phi_2}\delta(\omega_2 + \omega) + e^{-j\phi_2}\delta(\omega_2 - \omega)] \qquad (12B.33)$$

We can say that infinite spectral resolution has been achieved in Equation 12B.33 because of the Dirac delta functions. For a finite observation period, the spectral resolution becomes finite.

For mathematical convenience, the finite time function can be thought of as the infinite time function being observed through a finite data window. We write the observed function as the product of a rectangular window function and the infinite time function as:

$$\hat{x}(t) = u(t)x(t) \qquad (12B.34)$$

The rectangular window function was defined in Equations 12B.2 and 12B.11. The amplitude spectral function for $\hat{x}(t)$ can be obtained from the convolution of the Fourier transforms of $u(t)$ and $x(t)$. The relationship is:

$$\hat{X}(\omega) = \frac{1}{2\pi} \int_{-\infty}^{+\infty} U(\omega - \lambda)X(\lambda)d\lambda \qquad (12B.35)$$

The Fourier transform of a rectangular window function with unity height and width T_N is:

$$U(\omega) = T_N \left[\frac{\sin \omega \frac{T_N}{2}}{\omega \frac{T_N}{2}} \right] \qquad (12B.36)$$

The convolution integral is evaluated using (12B.33) and (12B.36) to give:

$$\hat{X}(\omega) = A_a\left[\frac{\sin(\omega_a + \omega)\frac{T_N}{2}}{(\omega_a + \omega)} + \frac{\sin(\omega_a - \omega)\frac{T_N}{2}}{(\omega_a - \omega)}\right]$$

$$+ A_b\left[\frac{\sin(\omega_b + \omega)\frac{T_N}{2}}{(\omega_b + \omega)} + \frac{\sin(\omega_b - \omega)\frac{T_N}{2}}{(\omega_b - \omega)}\right]$$

$$+ A_1\left[\frac{\sin(\omega_1 + \omega)\frac{T_N}{2}}{(\omega_1 + \omega)} + \frac{\sin(\omega_1 - \omega)\frac{T_N}{2}}{(\omega_1 - \omega)}\right]$$

$$+ A_2\left[\frac{\sin(\omega_2 + \omega)\frac{T_N}{2}}{(\omega_2 + \omega)} + \frac{\sin(\omega_2 - \omega)\frac{T_N}{2}}{(\omega_2 - \omega)}\right] \qquad (12B.37)$$

The phase factors have all been omitted for simplicity because we are only interested in the amplitude of the spectral function.

The spectral estimate above becomes exact when the observation interval goes to infinity because the sinc functions converge to Dirac delta functions. This is illustrated in Equation A2.49 in Appendix II. A typical spectral term in the estimator is represented by:

$$\hat{\delta} = A_a\frac{T_N}{2}\left[\frac{\sin(\omega_a - \omega)\frac{T_N}{2}}{(\omega_a - \omega)\frac{T_N}{2}}\right] \qquad (12B.38)$$

The "spread" or width of this spectral component is characterized by the width between first nulls of the sinc function,

$$\text{bandwidth-between-first-nulls} = \Delta\omega_{FN} = \frac{4\pi}{T_N} \qquad (12B.39a)$$

or by the bandwidth between the points where the amplitude is down by a factor of $(2)^{\frac{1}{2}}$:

$$BW_{3dB} \simeq \frac{16\pi}{9T_N} \qquad (12B.39b)$$

If we were to do a Fourier series analysis of $\hat{x}(t)$ and we knew the exact Fourier period we could set the observation interval equal to T_F and obtain an exact answer. This criterion of observation can be applied to the Fourier transform to determine the spectral resolution. If $T_N = T_F$, and we examine the typical frequency component at ω_a, the period of observation can be replaced by

$$T_N = \frac{m_a}{f_a} \tag{12B.40}$$

where m_a is one of the integers discussed for Equation 12B.31. When this is substituted into Equation 12B.37, the result becomes:

$$\overset{\wedge}{\delta} = A_a \frac{m_a}{2f_a} \left[\frac{\sin (2\pi f_a - 2\pi f) \frac{m_a}{2f_a}}{(2\pi f_a - 2\pi f) \frac{m_a}{2f_a}} \right] \tag{12B.41}$$

The ratio m_a/f_a is multiplied through and, the sin term reduced to give:

$$\overset{\wedge}{\delta} = A_a \left[\frac{\sin \left[\pi m_a (1 - \frac{f}{f_a}) \right]}{2\pi(f - f_a)} \right] \tag{12B.42}$$

The amplitude of the typical spectral component is evaluated by taking the limit:

$$\lim_{f \to f_a} \overset{\wedge}{\delta} = A_a \frac{m_a}{f_a} = A_a T_F = A_a T_N \tag{12B.43}$$

The bandwidth-between-first-nulls is

$$\Delta \omega_{FN} = \frac{2\omega_a}{m_a} \quad \text{or} \quad \Delta f_{FN} = \frac{2f_a}{m_a} \tag{12B.44}$$

and the 3dB bandwidth is:

$$Bw_{3dB} = \frac{8\omega_a}{9m_a} \tag{12B.45}$$

At this point a resolution quality factor or "Q" could be defined as:

$$Q_a = \frac{f_a}{\Delta f_{FN}} = \frac{m_a}{2} \tag{12B.46}$$

We are now able to draw several conclusions from this example. First, if the Fourier period is exactly known, the Fourier series technique gives infinite spectral resolution. Second, the width of a typical spectral component in the Fourier transform is directly related to the frequency, f_a, of the spectral component and the number of cycles, m_a, that particular component has been observed. The spectral bandwidth in percent of the observed frequency is directly related to m_a, the number of cycles observed. Third, for a given observation period, the higher frequencies will get the better percentage resolution because more cycles have been observed. This results in a higher "Q".

The spectral resolution for the frequency components f_1 and f_2 can be determined by examining the amplitude spectrum near these frequencies:

$$\hat{x}(\omega) \Big|_{\omega \simeq \omega_1 \simeq \omega_2} \simeq A_1 \left[\frac{\sin (\omega_1 - \omega) \frac{T_N}{2}}{(\omega_1 - \omega)} \right]$$
$$+ A_2 \left[\frac{\sin (\omega_2 - \omega) \frac{T_N}{2}}{(\omega_2 - \omega)} \right] \tag{12B.47}$$

Since ω_1 and ω_2 are nearly equal, the two spectral components have approximately the same spectral bandwidth. For equal amplitude spectra we define the _Rayleigh resolution_ as one-half the bandwidth-between-first-nulls:

$$\text{Rayleigh resolution} = \frac{1}{2} \, \Delta\omega_{F_N} = \frac{2\pi}{T_N} \tag{12B.48}$$

Using this criterion, the two spectral peaks are just resolved. For the case where the observation period, T_N, is equal to the Fourier period, T_F, the Rayleigh resolution is:

$$\frac{1}{2} \, \Delta f_{FN} \simeq \frac{f_1}{m_1} \simeq \frac{f_2}{m_2} \tag{12B.49}$$

Again we see that the more cycles observed, the better the resolution. We will also define a _Fourier resolution_ as equal to the bandwidth-between-first-nulls:

$$\text{Fourier resolution} = \Delta\omega_{FN} = \frac{4\pi}{T_N} \tag{12B.50}$$

For this spectral separation we say that the spectral components are completely resolved.

The resolution criterion must take into account differences in spectral amplitudes because a large component near a small one may obscure the identity of the smaller component. A criterion is difficult to establish for dissimilar amplitudes. The "leakage" of spectral power from the large component onto the frequency of a smaller component can be fairly well-defined. For a Fourier resolution criterion we will say that a component has been resolved if the estimated spectral amplitude is larger than twice the amplitude of the leakage spectra. In terms of the example, this means that:

$$\hat{X}(\omega_2) > 2A_1 \left[\frac{\sin(\Delta\omega_{FN}) \frac{T_N}{2}}{\Delta\omega_{FN}} \right] \tag{12B.51}$$

The criteria used to select an appropriate observation interval will now be summarized. First, to resolve the lowest frequency component, f_a, the number of cycles to be observed depends upon the absolute frequency and the desired bandwidth between first nulls:

$$\text{\# of cycles observed} = m_a = \frac{2f_a}{\Delta f_{FN}} \tag{12B.52}$$

The needed observation length for distinguishing the lowest spectral component from zero frequency is obtained by equating one-half of the bandwidth-between-first-nulls to f_a. This gives, $m_a = 4$. Second, to resolve two closely spaced sinewaves by the Fourier resolution criterion requires an observation period of:

$$T_N > \frac{2}{\Delta f_{FN}} \tag{12B.53}$$

Third, to determine the observation period required to resolve the bandwidth, $f_b - f_a$, into m_s increments of frequency resolution it is necessary to compute the bandwidth-between-first-nulls as the ratio of the total bandwidth to the total number of increments. This is used in (12B.53) to give:

$$T_N > \frac{2m_s}{f_b - f_a} \tag{12B.54}$$

7. Sinewave burst spectral analysis

In somewhat of a digression from the material in the previous section, we consider a single frequency sinewave observed through a data window of width, T_N. The phase of the sinewave with respect to the origin of the data window is arbitrary and contributes a random aspect to the sampling

observation. The observed function illustrated in Figure 12B-3 is some-
times referred to as a sinewave burst. The infinite cosinusoid is ex-
pressed in the phase angle representation as

$$x(t) = A \cos (\omega_o t + \phi_o) \qquad (12B.55)$$

with amplitude spectrum, time autocorrelation function, and power spectrum
respectively:

$$X(\omega) = \pi A [e^{+j\phi_o} \delta(\omega_o + \omega) + e^{-j\phi_o} \delta(\omega_o - \omega)] \qquad (12B.56)$$

$$R_x(\tau) = \frac{1}{2} A^2 \cos \omega_o \tau \qquad (12B.57)$$

$$P_x(\omega) = \frac{\pi}{2} A^2 [\delta(\omega_o + \omega) + \delta(\omega_o - \omega)] \qquad (12B.58)$$
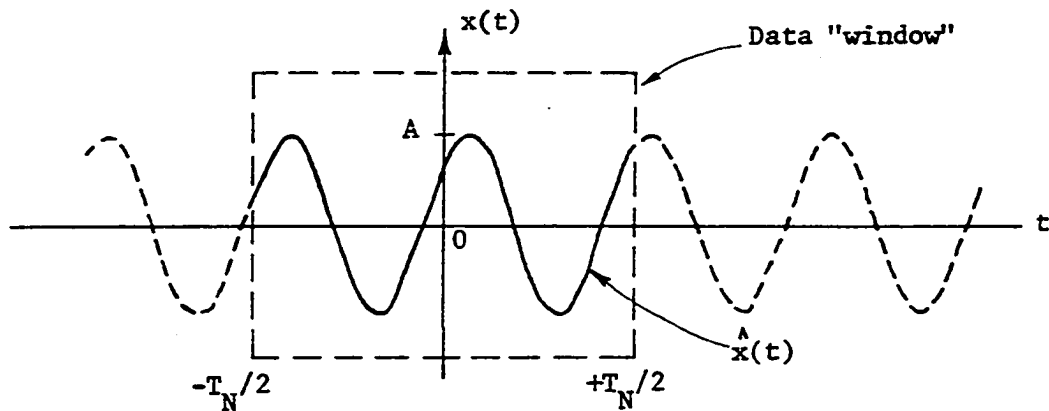
Figure 12B-3. Sinewave Burst or Single-Frequency
Sinewave Observed Through a Data
Window

For the Fourier spectral analysis of a sinewave burst of arbitrary

reference phase, we can model the observed function as the product of a

rectangular window function and the infinite time function:

$$\hat{x}(t) = u(t)x(t) = u(t)A \cos (\omega_o t + \phi_o) \tag{12B.59}$$

The rectangular window function $u(t)$ was defined in Equations 12B.2 and

12B.11. The amplitude spectrum of $\hat{x}(t)$ is obtained from the convolution

of the Fourier transforms of $u(t)$ and $x(t)$. The relationship is:

$$\hat{x}(\omega) = \frac{1}{2\pi} \int_{-\infty}^{+\infty} U(\omega - \lambda)X(\lambda)d\lambda \tag{12B.60}$$

The Fourier transform of the rectangular window function is

$$U(\omega) = T_N \left[\frac{\sin \omega \frac{T_N}{2}}{\omega \frac{T_N}{2}} \right] \tag{12B.61}$$

and the convolution integral becomes:

$$\hat{x}(\omega) = A \left[e^{+j\phi_o} \frac{\sin (\omega_o + \omega)\frac{T_N}{2}}{(\omega_o + \omega)} + e^{-j\phi_o} \frac{\sin (\omega_o - \omega)\frac{T_N}{2}}{(\omega_o - \omega)} \right] \tag{12B.62}$$

This is the familiar amplitude spectral function previously presented in

Equation 12B.37. The sinewave burst may be effectively analyzed with this

function. If one applies the autocorrelation concept to the sinewave burst

in an attempt to obtain the power spectral density function, the mathe-

matics becomes very complicated.

For the sinewave burst, the estimated time autocorrelation function

can be computed using either the definition in Equation 12B.20 and inte-

grating directly or by applying Equation 12B.21. For this discussion we will apply Equation 12B.21 to demonstrate its usefulness to the reader. In complex notation, the sinewave is written as

$$x(t) = c_- e^{-j\omega_0 t} + c_+ e^{+j\omega_0 t} \tag{12B.63}$$

where (see Appendix II):

$$c_- = \frac{1}{2} A e^{-j\phi_0} \qquad c_+ = \frac{1}{2} A e^{+j\phi_0} \tag{12B.64}$$

Applying (12B.21) we get

$$\hat{R}_x(\tau) = |c_-|^2 e^{-j\omega_0 \tau} + |c_+|^2 e^{+j\omega_0 \tau}$$
$$+ c_-^* c_+ q_{-+}(\tau) + c_+^* c_- q_{+-}(\tau) \tag{12B.65}$$

with:

$$q_{-+}(\tau) = q_{+-}(\tau) = \frac{\sin \omega_0 (T_N - |\tau|)}{\omega_0 (T_N - |\tau|)} \tag{12B.66}$$

Simplifying terms and adding we can obtain the estimated time autocorrelation function for the sinewave burst as a function of both lag and observation period

$$\hat{R}_x(\tau, T_N) = \frac{1}{2} A^2 \cos \omega_0 \tau$$
$$+ \frac{1}{2} A^2 \cos 2\phi_0 \left[\frac{\sin \omega_0 (T_N - |\tau|)}{\omega_0 (T_N - |\tau|)} \right] \tag{12B.67}$$

where it must always be remembered that the lag must be less than the observation period, $|\tau| < T_N$, and that the autocorrelation is zero for lags larger than T_N.

$\hat{R}_x(\tau,T_N)$ is really a function of the random variable, ϕ_o, introduced by the randomness of observation. The expectation value of the estimate is:

$$E\{\hat{R}_x(\tau,T_N)\} = R_x(\tau) \qquad |\tau| < T_N \qquad (12B.68)$$

The last term in (12B.67) is the direct result of not having an infinite record to average over time and thus represents a distortion in the auto-correlation function obtained for an infinite sinewave. We now examine $\hat{R}_x(\tau,T_N)$ to determine the effect and seriousness of the distortion.

The two terms of the sum in (12B.67) are plotted in Figure 12B-4. The most serious distortion of the ideal cosinusoidal shape of the auto-correlation function occurs within a distance, T_o, of the observation interval, T_N. For small observation intervals, the sinc function will "mask" the identity of the sinusoid. For large observation intervals, the effect of the added sinc function is reduced to a small percentage. We will look at two limiting conditions for $\hat{R}_x(\tau,T_N)$ and compute the limiting effect on the amplitude estimate and the spectral estimate. For lag values much smaller than the observation interval and for an observation interval much larger than the period of the cosinusoid:

$$\hat{R}_x(\tau,T_N) \simeq \frac{1}{2} A^2 \cos \omega_o \tau = R_x(\tau) \qquad \begin{array}{c} |\tau| \ll T_N \\ T_N \gg T_o \end{array} \qquad (12B.69)$$

This result is expected because we want the estimate to converge and be unbiased for large observation intervals. Next we look at the estimate of the total power because it is used to obtain the estimate for the mean-square value of the cosinusoid which is in turn used to estimate the amplitude, A. For zero lag, the total power estimate is:
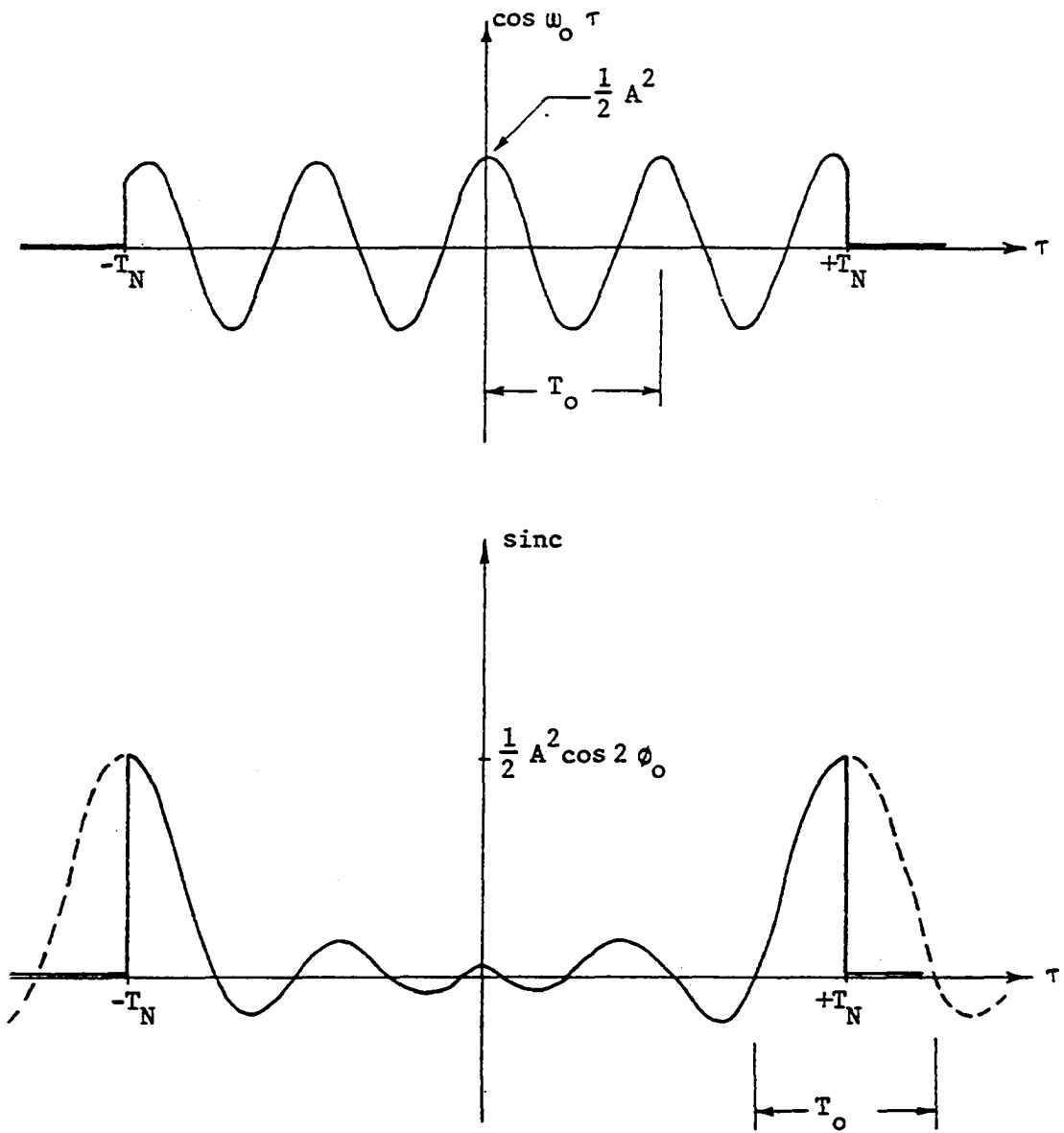
Figure 12B-4. Two Components for the Estimated
Autocorrelation Function of a Sinewave
Burst

$$\text{Total Power} = \hat{R}_x(0,T_N) = \frac{1}{2} A^2 [1 + \cos 2\phi_o \frac{\sin \omega_o T_N}{\omega_o T_N}] \qquad (12B.70)$$

A plot of this function is shown in Figure 12B-5 to illustrate how the total power estimate converges as the observation interval increases.
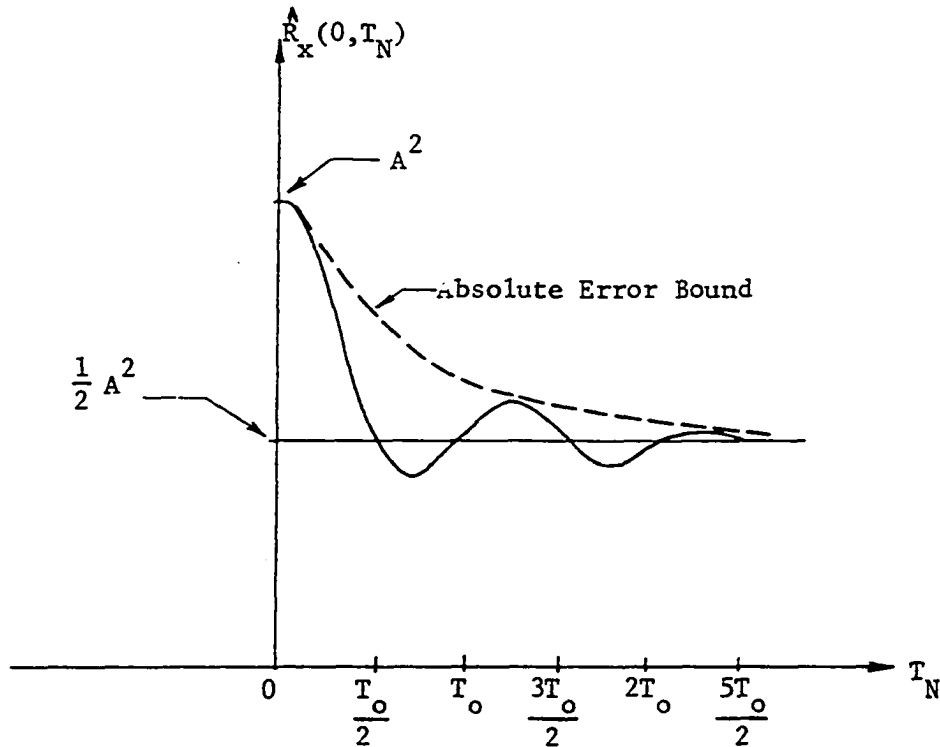
Figure 12B-5. Convergence Function for the Total
Power Estimate of a Sinewave Burst

The maximum error in total power is 2 or a factor of 3 db. The absolute percentage error for worst case phase and frequency is obtained by evaluating:

$$\frac{1}{2} A^2 [1 \pm \frac{1}{\omega_o T_N}] \qquad (12B.71)$$

Table 12B-1 shows the observation interval as some multiple of the period T_o and the resulting percentage error in total power. It must be remembered that these are absolute worst case values and actual results may be considerably better for observation periods exceeding T_o. Also, the randomness of the initial phase of the cosinusoid will have the effect of producing a randomness in the estimate.

Table 12B-1. Percentage Amplitude Error as a Function of Observation Interval

Observation Interval	Percentage Error
$T_N = 1.59\,T_o$	$\pm\ 10\%$
$T_N = 3.18\,T_o$	$\pm\ 5\%$
$T_N = 15.9\,T_o$	$\pm\ 1\%$
$T_N = 159\,T_o$	$\pm\ 0.1\%$

The Fourier transform of $\hat{R}_x(\tau, T_N)$ is used to obtain an estimate of the power spectral density function for the sinewave burst. The power spectrum can be represented by two components

$$\{\hat{R}_x(\tau, T_N)\} = \tilde{S}_1(\omega) + \tilde{S}_2(\omega) \qquad (12B.72)$$

where the integrals over the interval $\pm\ T_N$ become:

$$\tilde{S}_1(\omega) = \frac{1}{2} A^2 \int_{-T_N}^{+T_N} \cos \omega_o \tau\, e^{-j\omega\tau} d\tau \qquad (12B.73)$$

$$\tilde{S}_2(\omega) = \frac{1}{2} A^2 \cos 2\phi_0 \int_{-T_N}^{+T_N} \frac{\sin \omega_0 (T_N - |\tau|)}{\omega_0 (T_N - |\tau|)} e^{-j\omega\tau} d\tau \qquad (12B.74)$$

The analysis could be continued using these definitions but much more insight into the processing problem can be gained by introducing a lag window function, $D(\tau, T_L)$. A plot of the estimated autocorrelation function showing the application of a rectangular window function is shown in Figure 12B-6. The estimated power spectral density function becomes

$$\hat{S}_x(\omega) = \hat{S}_1(\omega) + \hat{S}_2(\omega) \qquad (12B.75)$$

where:

$$\hat{S}_1(\omega) = \frac{1}{2} A^2 \int_{-T_L}^{+T_L} \cos \omega_0 \tau \, e^{-j\omega\tau} d\tau \qquad (12B.76)$$

$$\hat{S}_2(\omega) = \frac{1}{2} A^2 \cos 2\phi_0 \int_{-T_L}^{+T_L} \frac{\sin \omega_0 (T_N - |\tau|)}{\omega_0 (T_N - |\tau|)} e^{-j\omega\tau} d\tau \qquad (12B.77)$$

These estimates will converge to those in (12B.73) and (12B,74) when $T_L \rightarrow T_N$. Since both parts of $\hat{R}_x(\tau, T_N)$ are even, the cosine transform can be applied to give:

$$\hat{S}_1(\omega) = \frac{1}{2} A^2 T_L \left[\frac{\sin(\omega_0 - \omega)T_L}{(\omega_0 - \omega)T_L} + \frac{\sin(\omega_0 + \omega)T_L}{(\omega_0 + \omega)T_L} \right] \qquad (12B.78)$$

$$\hat{S}_2(\omega) = \frac{1}{2} A^2 \cos 2\phi_0 \int_{-T_L}^{+T_L} \frac{\sin \omega_0 (T_N - |\tau|)}{\omega_0 (T_N - |\tau|)} \cos \omega\tau \, d\tau \qquad (12B.79)$$
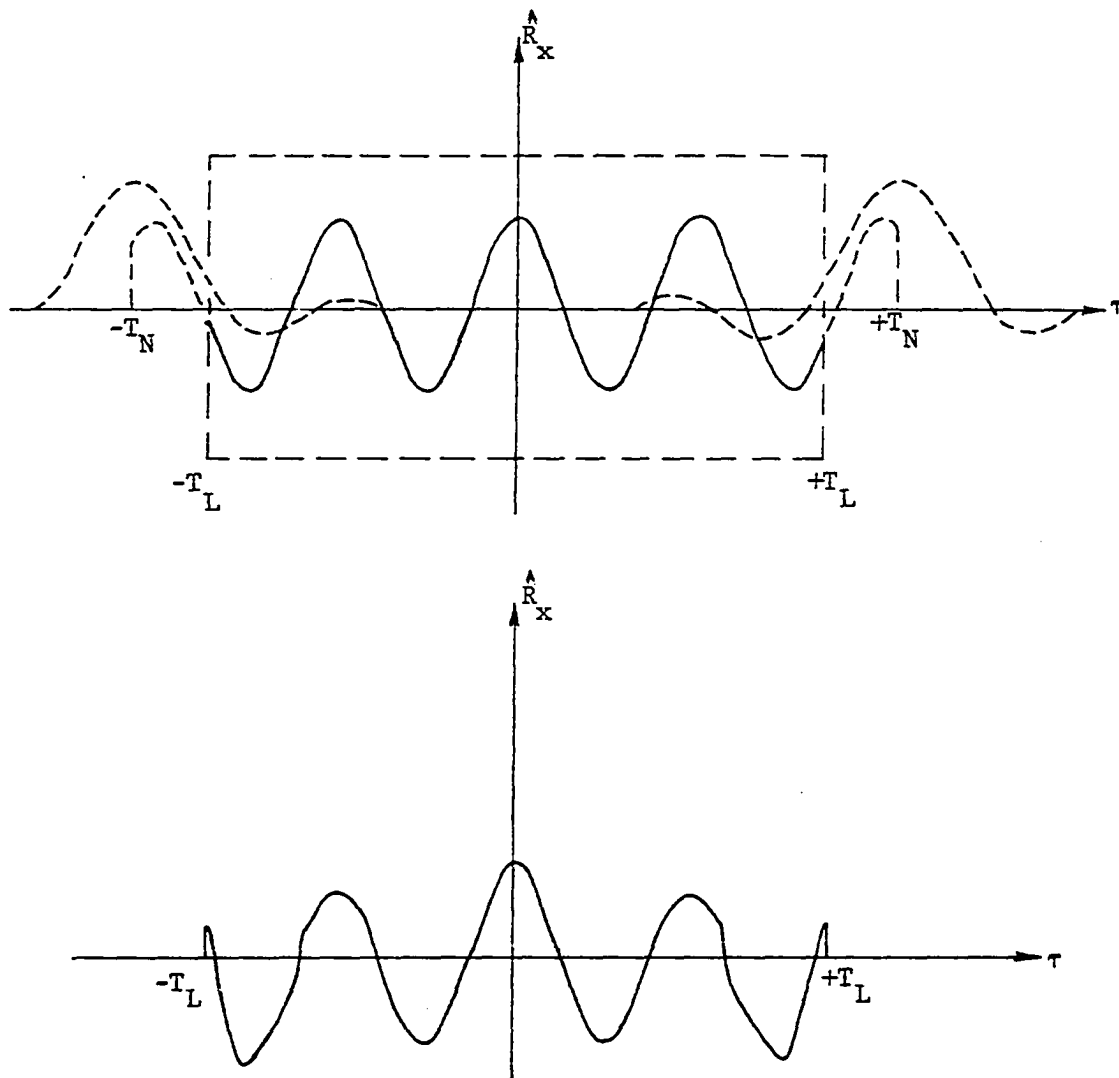
Figure 12B-6. A Rectangular Lag Window Function Applied to
Estimated Autocorrelation Function of a Sine-
wave Burst.

These two spectral components must be analyzed to determine the accuracy of the estimate. The $\hat{S}_1(\omega)$ component is exactly what would be obtained from applying a rectangular window function to an infinite autocorrelation function obtained from an infinite time function. In this sense, $\hat{S}_1(\omega)$ represents the "true" spectrum obtained by a finite observation. The $\hat{S}_2(\omega)$ component represents the additional spectrum generated because the <u>time</u> function was truncated before the autocorrelation function was computed.

The expression for $\hat{S}_2(\omega)$ given in (12B.79) could not be integrated directly because an analysis of the integral by a change of variables showed that it was a sine integral and could only be solved by numerical techniques. If it is assumed that the lag window width is much smaller than the observation interval, $T_L \ll T_N$, the spectrum represented by $\hat{S}_2(\omega)$ can be written as

$$\hat{S}_2(\omega) = \frac{1}{2} A^2 \cos 2\phi_0 \frac{\sin \omega_0 T_N}{\omega_0 T_N} \int_{-T_L}^{+T_L} \cos \omega\tau \, d\tau \qquad (12B.80)$$
$$T_L \ll T_N$$

$$= A^2 T_L \cos 2\phi_0 \left[\frac{\sin \omega_0 T_N}{\omega_0 T_N}\right]\left[\frac{\sin \omega T_L}{\omega T_L}\right] \qquad (12B.81)$$

The power spectral density function for this special case is plotted in Figure 12B-7. The effect of truncated data and a rectangular data window on the sinewave burst power spectrum is an added sinc function term at zero frequency and a distortion of the total power estimation. The amplitude of the dc term is a factor of

$$2 \cos 2\phi_0 \left[\frac{\sin \omega_0 T_N}{\omega_0 T_N}\right] \qquad (12B.82)$$

$$\hat{S}_x(\omega) = \hat{S}_1(\omega) + \hat{S}_2(\omega)$$

$\frac{1}{2} A^2 T_L$

$A^2 T_L \cos 2\phi_o \left[\dfrac{\sin \omega_o T_N}{\omega_o T_N}\right]$

$-\omega_o$

0

ω_o

ω

$\dfrac{2\pi}{T_L}$

$\dfrac{2\pi}{T_L}$
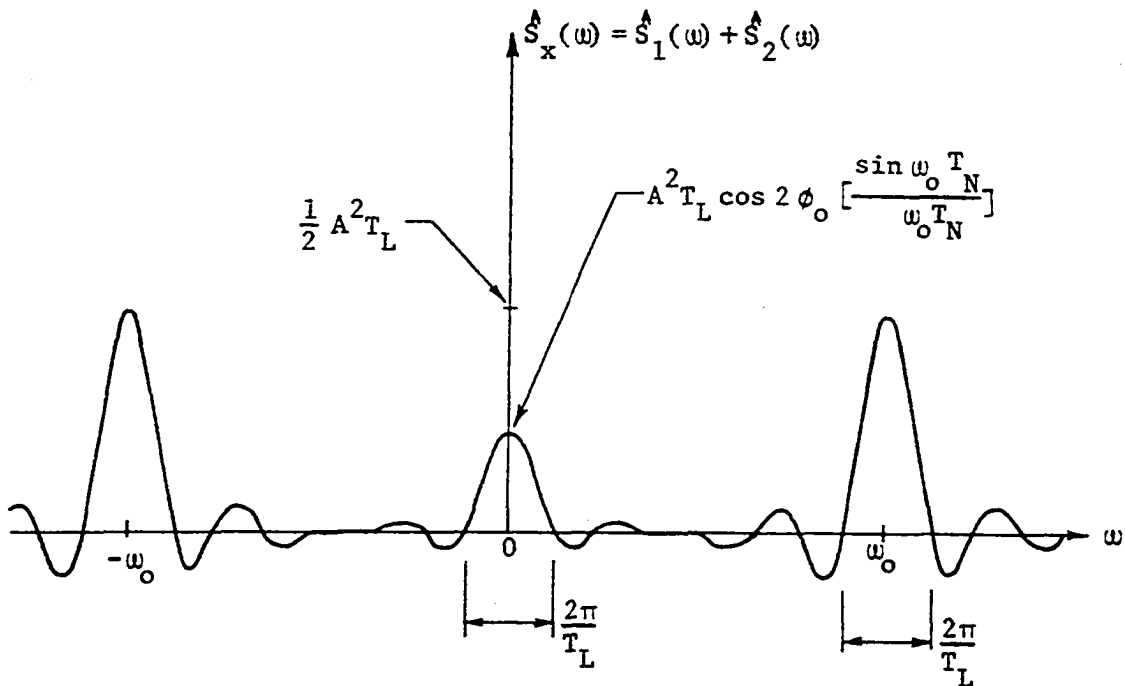
Figure 12B-7. Power Spectral Density Function for a Sinewave Burst where $T_L \ll T_N$

smaller than the "true spectral amplitude of $\hat{S}_1(\omega)$. For practical situations, $T_N \gg T_o$, and the worst case value for this factor becomes:

$$\frac{2}{\omega_o T_N} = \frac{T_o}{\pi T_N} \tag{12B.83}$$

For a dc amplitude of less than one-percent of the "true" amplitude, the

sinewave burst must be observed for more than 31.8 cycles.

These derivations for a simple time function such as a sinewave burst help illustrate the mathematical difficulty associated with trying to calculate the power spectrum for a truncated periodic function. These problems are usually solved numerically.

8. Errors in amplitude spectral estimation

A continuous but finite record of a noiseless periodic waveform with Fourier period T_F is sampled for a time T_N. The accuracy of the Fourier coefficients calculated from this sample record will depend upon the length of the sample and the relative amplitude of each frequency component in the spectrum. The Fourier transform estimate of the amplitude spectrum is given by Equation 12B.5. This estimate can also be written in terms of the Fourier frequency, the "true" complex amplitudes, and the observation interval as given in Equation 12B.6.

There are actually four stages of estimation which may be considered in determining the accuracy of our estimate. Stage-1 is represented by the actual Fourier transform given by Equations 12B.5 and 12B.6. These estimates are continuous functions and do not directly represent the complex amplitudes. Stage-2 is the discrete spectral estimate obtained from doing a discrete Fourier transform such as the FFT. The discrete spectrum obtained by this approach is represented by:

$$\hat{X}(k \frac{2\pi}{T_N}) = \int_{-T_N/2}^{+T_N/2} x(t) e^{-j \frac{2\pi}{T_N} kt} \, dt \qquad (12B.84)$$

or by modifying (12B.6):

$$\hat{X}(k\frac{2\pi}{T_N}) = \sum_{n=-M}^{+M} c_n T_N \left[\frac{\sin(\frac{n2\pi}{T_F} - \frac{k2\pi}{T_N})T_N/2}{(\frac{n2\pi}{T_F} - \frac{k2\pi}{T_N})T_N/2} \right] \qquad (12B.85)$$

This discrete spectrum may or may not correspond to the spectral frequencies representing the "true" Fourier spectrum. If the Fourier frequency were known, a stage-3 estimate would be defined such that

$$\hat{X}(k\omega_F) = \int_{-T_N/2}^{+T_N/2} x(t)e^{-j\omega_F t} dt \qquad (12B.86)$$

or:

$$\hat{X}(k\omega_F) = \sum_{n=-M}^{+M} c_n T_N \left[\frac{\sin\pi(n-k)\frac{T_N}{T_F}}{\pi(n-k)\frac{T_N}{T_F}} \right] \qquad (12B.87)$$

Equation 12B.87 can be solved to give an exact expression for the k-th complex amplitude as:

$$c_k = \frac{1}{T_N} \hat{X}(k\omega_F) - \sum_{\substack{n=-M \\ n\neq k}}^{+M} c_n \left[\frac{\sin\pi(n-k)\frac{T_N}{T_F}}{\pi(n-k)\frac{T_N}{T_F}} \right] \qquad (12B.88)$$

The second term on the right-hand side of (12B.88) can be thought of as an error correction factor for the Fourier transform estimator. If the Fourier transform approximations for the complex amplitudes in the error correction factor are substituted into (12B.88), the stage-4 complex amplitude estimator is obtained:

$$\hat{c}_k = \frac{1}{T_N} \hat{X}(k\omega_F) - \frac{1}{T_N} \sum_{\substack{n=-M \\ n\neq k}}^{+M} \hat{X}(n\omega_F) \left[\frac{\sin \pi (n-k)\frac{T_N}{T_F}}{\pi(n-k)\frac{T_N}{T_F}} \right] \qquad (12B.89)$$

This estimator is not practical unless the Fourier frequency is known or can be accurately approximated.

The unknown parameters for the estimation problem are T_F and c_n. These must be determined from $x(t)$ by using T_N and Equations 12B.5 or 12B.84. The error associated with the amplitude spectral estimate is mostly dependent on the observation time, T_N. Equation 12B.10 showed that, if T_N was an exact multiple of T_F, the complex amplituded could be computed exactly. When T_N is not an exact multiple, we can use Equation 12B.87 to estimate the error. First let

$$T_N = qT_F + \Delta T \qquad (12B.90)$$

where: $q = 1, 2, 3, \ldots$ and $0 \leq \Delta T < T_F$.

This is substituted into 12B.87 and after many manipulations we obtain:

$$\hat{X}(k\omega_F) = \sum_{n=-M}^{+M} c_n qT_F \cos \pi(n-k) \frac{\Delta T}{T_F} \left[\frac{\sin \pi (n-k)q}{\pi(n-k)q} \right]$$

$$+ \sum_{n=-M}^{+M} c_n qT_F \cos \pi(n-k)q \left[\frac{\sin \pi (n-k)\frac{\Delta T}{T_F}}{\pi(n-k)q} \right] \qquad (12B.91)$$

This can be further reduced to:

$$\hat{X}(k\omega_F) = qT_F \sum_{n=-M}^{+M} c_n \cos \pi(n-k)\frac{\Delta T}{T_F} [\delta_{nk}]$$

$$+ \Delta T \sum_{n=-M}^{+M} c_n \cos \pi(n-k)q \, \text{sinc}[(n-k)\frac{\Delta T}{T_F}] \qquad (12B.92)$$

The first term on the right-hand side of (12B.92) is reduced to $qT_F c_k$ by using the sifting property of the delta function. The second term is an error term caused by not sampling at an exact multiple of the Fourier period. The principal error term is $\Delta T c_k'$ and is found by letting $n = k$. The estimate of (12B.93) is now written as:

$$\hat{X}(k\omega_F) = (qT_F + \Delta T)c_k + \Delta T \sum_{\substack{n=-M \\ n \neq k}}^{+M} c_n \cos \pi(n-k)q \, \text{sinc}[(n-k)\frac{\Delta T}{T_F}]$$

$$(12B.93)$$

This equation reduces to Equation 12B.9 when $\Delta T \to 0$. As the number of periods of observation increases, the term qT_F dominates and the estimate converges.

C. Finite Random Time Functions

A sample time function for a random process exists for all time, $-\infty \leq t \leq +\infty$. A truncated time function is defined from this sample by multiplying it with a rectangular window function such that

$$x_T(t) = u_T(t)x(t) \qquad (12C.1)$$

where $u_T(t)$ was defined in Equation 12B.2. For this condition, $x_T(t)$ is absolutely integrable and an amplitude spectrum exists and is defined as:

$$\hat{X}_T(\omega) = \int_{-\infty}^{+\infty} x_T(t) e^{-j\omega t} dt = \int_{-T/2}^{+T/2} x(t) e^{-j\omega t} dt \qquad T < \infty \qquad (12C.2)$$

One might expect to apply the convolution theorem to obtain $\hat{X}_T(\omega)$ but this requires the existence of the Fourier transform of the infinite time function, $x(t)$. For random processes, this transform generally does not exist.

This conceptual dilemma can be resolved through the use of <u>Parseval's theorem</u>. The power spectral density function sought is the distribution of average power over frequency so for the previous estimations this is:

$$\frac{1}{T} \int_{-\infty}^{+\infty} x_T^2(t) dt = \frac{1}{T} \frac{1}{2\pi} \int_{-\infty}^{+\infty} |\hat{X}_T(\omega)|^2 d\omega \qquad T < \infty \qquad (12C.3)$$

The term on the left is an estimate of the mean-square value of $x_T(t)$ averaged over a time, T. Both this estimate and $\hat{X}_T(\omega)$ are random because they are derived from only one sample function of the process and hence are not ensemble averages.

These estimates of average power can be used to derive the power spectral density estimate by first taking the expected value of both sides of (12C.3) and then taking the limit as $T \to \infty$:

$$\lim_{T \to \infty} \frac{1}{T} \int_{-T/2}^{+T/2} E\{x_T^2(t)\} dt = \frac{1}{2\pi} \int_{-\infty}^{+\infty} \lim_{T \to \infty} \frac{1}{T} E\{|\hat{X}_T(\omega)|^2\} d\omega \qquad (12C.4)$$

We know, for a stationary process, that the total power is determined by:

$$E\{x^2(t)\} = \frac{1}{2\pi} \int_{-\infty}^{+\infty} S_x(\omega) d\omega = R_x(0) \qquad (12C.5)$$

The expectation of $x_T^2(t)$ can be reduced as follows:

$$E\{x_T^2(t)\} = u_T^2(t) \; E\{x^2(t)\} = u_T^2(t)R_x(0) \qquad (12C.6)$$

This can be used to reduce the left-hand side of Equation 12C.4) and from identification with (12C.5) we can conclude that:

$$S_x(\omega) = \lim_{T \to \infty} \frac{1}{T} E\{|\hat{X}_T(\omega)|^2\} \qquad (12C.7)$$

This gives the power spectral density function in terms of the estimate of the amplitude spectrum.

To show the relationship of this estimate to the autocorrelation function definition of spectral power, the Fourier transform relationship for $\hat{X}_T(\omega)$ is substituted into (12C.7) to give:

$$S_x(\omega) = \lim_{T \to \infty} \frac{1}{T} E\{ \int_{-T/2}^{+T/2} x(t_1)e^{+j\omega t_1} dt_1 \int_{-T/2}^{+T/2} x(t_2)e^{-j\omega t_2} dt_2 \} \qquad (12C.8)$$

$$= \lim_{T \to \infty} \frac{1}{T} E\{ \int_{-T/2}^{+T/2} \int_{-T/2}^{+T/2} x(t_1)x(t_2)e^{-j\omega(t_2 - t_1)} dt_1 dt_2 \} \qquad (12C.9)$$

This double integral is further simplified by using the variable substitution, $\tau = t_2 - t_1$, and then, $t_1 = t$:

$$S_x(\omega) = \lim_{T \to \infty} \frac{1}{T} \int_{-T/2-t}^{+T/2-t} \int_{-T/2}^{+T/2} E\{x(t)x(t+\tau)\}e^{-j\omega\tau} dt\, d\tau \qquad (12C.10)$$

For a stationary process, the expected value inside the integral is the time autocorrelation function $R_x(\tau)$ and since it is independent of reference time, t, the integral equation reduces to:

$$S_x(\omega) = \lim_{T \to \infty} \int_{-T-t}^{+T-t} R_x(\tau)e^{-j\omega\tau} d\tau$$

$$= \int_{-\infty}^{+\infty} R_x(\tau)e^{-j\omega\tau} d\tau \qquad (12C.11)$$

Equation 12C.11 shows that the estimate for power spectral density given by (12C.7) converges and is unbiased for large observation times.

All of the estimation techniques which have been developed for amplitude spectral analysis can be modified and applied to finite random time functions by using Equation 12C.7. An estimator for power spectral density for an observation time T would be:

$$\hat{S}_x(\omega) = \frac{1}{T} E\{ |\hat{X}_T(\omega)|^2 \}$$

(12C.12)

D. Finite Periodic Time Series

The previous analysis of periodic time functions and random time functions could be applied to discrete time functions by "digitizing" all of the continuous equations and functions. This approach can be taken when the collected data is continuous and the desired degree of numerical resolution may be chosen. This technique is equivalent to a numerical solution for the continuous case.

Another approach to the analysis of discrete data is to treat the data directly as though it is a time series. The author prefers this approach because it results in the use of superior data processing techniques. Data in the time domain will be treated in discrete form even though it would be possible to generate a continuous function using the sampling theorem of Equation 6D.6.

A periodic time function, $x(t)$, is sampled for a finite observation time, T_N, with a sampling interval, Δt. This process will generate a time series $x(k\Delta t)$. The sampled function is shown in Figure 12D-1 and

we observe the following definitions:

Δt = The sampling interval.

$f_s = \dfrac{1}{\Delta t}$, The sampling frequency.

$2N + 1$ = The number of samples of $x(t)$ in the interval T_N.

T_N = The length of the observation interval.

T_F = The Fourier period of $x(t)$.

$M\omega_F = M\dfrac{2\pi}{T_F}$, The highest frequency component in $x(t)$.

$f_F = \dfrac{1}{2} f_s$, The folding frequency.

$2\pi f_N = 2M\omega_F$, f_N is the Nyquist frequency.
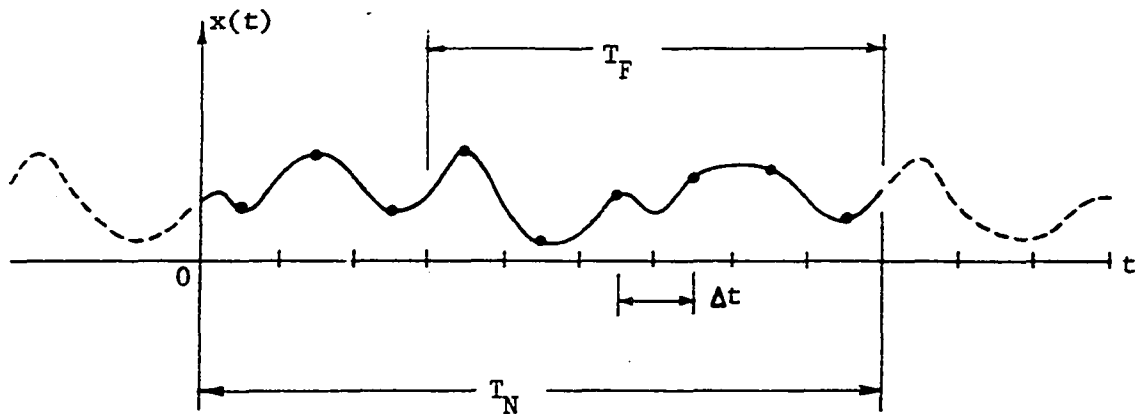
Figure 12D-1. A Sample Record of a Finite Periodic Time Series

It will be assumed that $x(t)$ is sampled at a rate greater than or equal to the Nyquist rate so that aliasing is prevented. Also, the number of samples will be assumed to be odd so that; $(2N + 1)\Delta t = T_N$.

1. Fourier analysis

The discrete Fourier transform has been briefly discussed in Chapter XI and Appendix II. The discrete transform pair in the time domain can be represented by:

$$x(k\Delta t) = \frac{1}{T_F} \sum_{n=-N}^{+N} X(n\frac{2\pi}{T_F})e^{+j\frac{2\pi}{T_F}nk\Delta t} \qquad (12D.1)$$

$$X(n\frac{2\pi}{T_F}) = \Delta t \sum_{n=-N}^{+N} x(k\Delta t)e^{-j\frac{2\pi}{T_F}nk\Delta t} \qquad (12D.2)$$

If the periodic function is sampled such that, $\Delta t = T_F/(2N+1)$, the discrete transform pair becomes

$$x_k = \sum_{n=-N}^{+N} \frac{1}{T_F} X_n e^{+j\frac{2\pi}{2N+1}nk} \qquad (12D.3)$$

$$\frac{1}{T_F} X_n = \frac{1}{2N+1} \sum_{n=-N}^{+N} x_k e^{-j\frac{2\pi}{2N+1}nk} \qquad (12D.4)$$

where the arguments $k\Delta t$ and $n\frac{2\pi}{T_F}$ have been replaced by the indices k and n.

Most discussions of the discrete Fourier transform actually use the complex Fourier coefficients, c_n, as the amplitude spectral component when actually it should be X_n. This is done in Bergland (1969) and in Equations 11.9 and 11.10 of this text. As a practical matter it makes little difference as they differ only by the scale factor T_F. This can be seen by comparing Equations 11.9 and 11.10 with 12D.3 and 12D.4. For a given time series $\{x_k: k = 0, \pm 1, \pm 2, \ldots, \pm N\}$, the complex amplitudes computed by (12D.4) represent those which are needed to __exactly__ reproduce the original

time series using Equation 12D.3. This feature of the discrete Fourier transform is discussed in Chapter XI. In the discussions to follow, we will use the circumflex accent over x_k and X_n to denote that they are really estimates and the exact Fourier period, T_F, will be replaced by the observation period, T_N. Also, in most cases we will work with the complex Fourier amplitudes, $c_n = X_n/T_N$.

The theory behind the discrete Fourier analysis of a finite time series must be studied to determine the interpretation of the estimated spectrum. Given a finite time series $\{x(k\Delta t): k = 0, \pm 1, \pm 2, \ldots, \pm N\}$ we have $2N+1$ ordered data pairs $\{x_k, k\}$. This data set can be used to define $2N+1$ complex Fourier coefficients according to the following algorithm:

$$\hat{c}_n = \frac{1}{2N+1} \sum_{k=-N}^{+N} x_k e^{-j \frac{2\pi}{2N+1} nk} \tag{12D.5}$$

These complex coefficients are actually approximations to the "true" coefficients representing $x(t)$. These estimates are then used to <u>define</u> a bandlimited Fourier series of the form:

$$\hat{x}(t) = \sum_{n=-N}^{+N} \hat{c}_n e^{+j \frac{2\pi n}{T_N} t} \qquad\qquad T_N = (2N+1)\Delta t \tag{12D.6}$$

This estimated Fourier series has the following properties:

1. $\hat{x}(t)$ is continuous and periodic with period, $T_N = (2N+1)\Delta t$.

2. The highest frequency component present in $\hat{x}(t)$ is, $2\pi f_N = N \frac{2\pi}{T_N} = 2\pi \frac{N}{2N+1} f_s$.

3. The average value of $\hat{x}(t)$ is $\hat{c}_o$.

4. The mean-square value of $\hat{x}(t)$ is computed by:

$$\overline{x^2} = \sum_{n=-N}^{+N} |c_n|^2 \tag{12D.7a}$$

5. The critical frequencies of the discrete transform are:

$$f_n = \frac{n}{T_N} = \frac{n}{2N+1} f_s \quad (n = \pm1, \pm2, \ldots, \pm N) \tag{12D.7b}$$

The most important feature of $\hat{x}(t)$ is the fact that the values of $\hat{x}(t)$ at $t = k\Delta t$ are __exactly__ equal to the data set values $x(k\Delta t)$, in other words:

$$\hat{x}(k\Delta t) = x(k\Delta t), \quad k = 0, \pm1, \pm2, \ldots, \pm N \tag{12D.8}$$

The complex spectral amplitudes in Equation 12D.5 represent the spectrum of $\hat{x}(t)$ exactly while $\hat{x}(t)$ approximates $x(t)$. It seems reasonable to assume that if enough samples of $x(t)$ are taken so that it is very closely approximated by $\hat{x}(t)$, the spectral estimate, $\hat{c}_n$, will approximate the true spectrum, c_n.

The continuous function, $\hat{x}(t)$, generated from the $\hat{c}_n$ by Equation 12D.6 and hence from the finite time series $\{x(k\Delta t): k = 0, \pm1, \pm2, \ldots \pm N\}$ can be said to be "optimum" in the sense that $\hat{x}(t)$ at $t = k\Delta t$ exactly reproduces the original time series with a Fourier series bandlimited to N/T_N. This bandwidth limitation provides the "smoothest" extrapolation between data points consistent with the restriction that $\hat{x}(t)$ be periodic with period, T_N. The fact that $\hat{x}(t)$ is both periodic and bandlimited provides considerable mathematical convenience for analysis purposes.

To illustrate the discrete Fourier transform we will look at a simple example. PROGRAM 01 in Appendix III has been written for the example. The line spectrum subroutine in this example is a straightforward digital transform. For large amounts of data processing, the FFT should be used. Consider a time series obtained by sampling a continuous time function represented by (see Appendix II)

$$x(t) = 4 \cos(2\pi t) + 1 \sin(6\pi t) \qquad (12D.9a)$$

where, $a_1 = 4$ volts, $f_1 = 1$ Hz., $b_3 = 1$ volt, and $f_2 = 3$ Hz. The Fourier frequency is 1 Hz. and the highest frequency is 3 Hz. The complex amplitudes are calculated to be:

$$c_0, \ c_2 = 0$$
$$c_1 = c_{-1}^* = 2$$
$$c_3 = c_{-3}^* = \frac{1}{2} e^{-j\frac{\pi}{2}} = -j\frac{1}{2} \qquad (12D.9b)$$

The data inputs to the program are the a's and b's, the Fourier period, the period of observation, and the number of data points. The program generates $x(t)$ sampled at the intervals $\Delta t = T_N/(2N+1)$ and calculates the magnitude and phase of $\hat{c}_n$ for, $n = 0, 1, 2, \ldots N$. The magnitude of $\hat{c}_n$ with respect to a chosen reference is also given. Finally the calculated $\hat{c}_n$ are used to generate the estimated series $\hat{x}(t)$ where $\hat{x}(t)$ is sampled four times as often as $x(t)$.

By varying T_N and $2N+1$ it is possible to see the effect of sampling on the computed discrete spectrum for the time series $\{x(k\Delta t) : k = 0, \pm 1, \pm 2, \ldots \pm N\}$. Figure 12D-2 shows the effect of observing for less than a
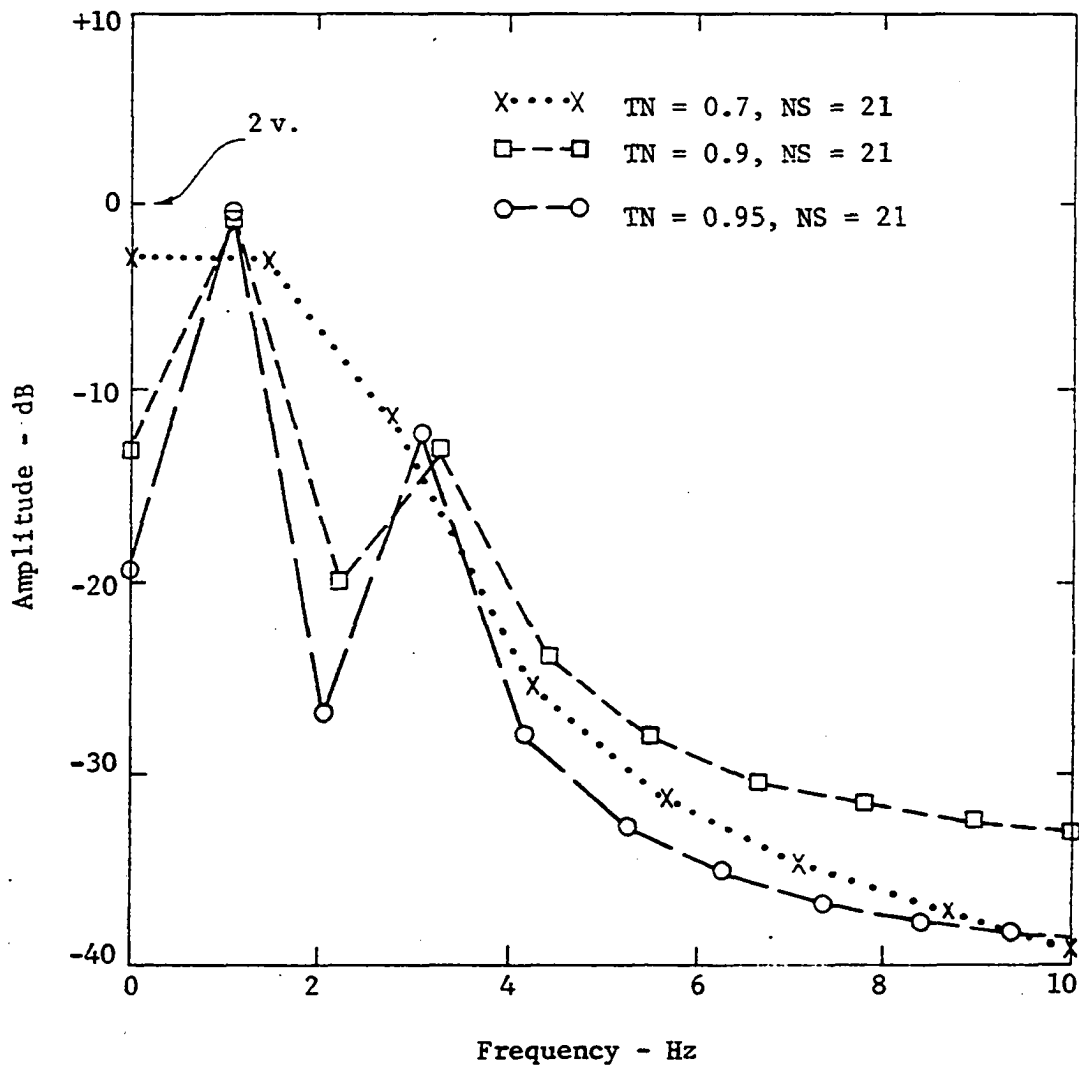
Figure 12D-2. Discrete Spectrum Plots Showing
the Effect of a Varying Observation
Period

Fourier period and also shows how the spectrum converges as T_N approaches T_F. Several computer runs where T_N was an exact multiple of T_F showed that the calculated spectrum was exact within computational accuracy. The magnitude of the complex amplitude was plotted in dB with a two volt reference. A dB plot is necessary because of the wide range of amplitude values. It is important to note that the plot for $T_N = 0.7$ shows no peaks. This may be described as a shift of spectral power toward dc.

Figure 12D-3 shows the calculated spectrum for a variety of sampling conditions. It is important to note that the spectral resolution of 81 data points and $T_N = 10.5$ is little better than the resolution of 21 data points and $T_N = 3.1$. This illustrates the very important effect of obtaining and observation period as close to a multiple of T_F as possible. The reader may experiment with these effects by using PROGRAM 01 to study a variety of sampled functions and sampling conditions. For large data sets, a Fast Fourier Transform subroutine should be used in place of SUBROUTINE LNSPTM. The high degree of spectral selectivity observed as T_N is varied was the reason for the discussion at the end of Chapter XI of the selection of an optimum observation period. This procedure has much potential in terms of improving the discrete Fourier transform. This theory needs to be worked out.

2. Spectral mixing

A discussion of spectral mixing and the derivation of the spectral mixing formula were given in Chapter XI. In this section we discuss the use of the spectral mixing formula
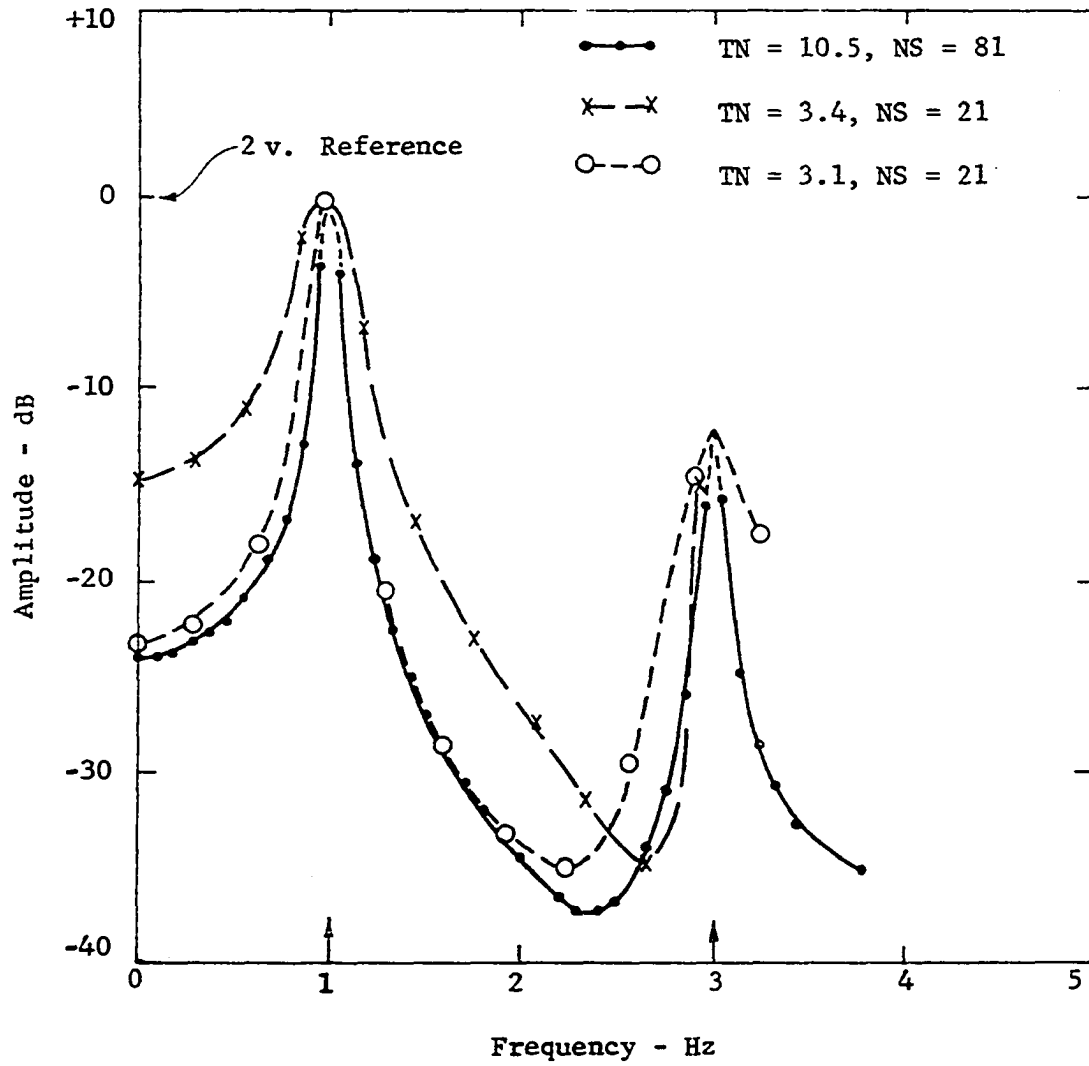
Figure 12D-3. Discrete Spectrum Plots Showing the
Effects of Long Observation Times and
Increased Number of Samples

$$\hat{c}_q = \sum_{r=-M}^{+M} c_r \, \hat{\delta}_{rq}(N,T_N,T_F) \qquad (12D.10)$$

where the estimated Kronecker delta function is defined by:

$$\hat{\delta}_{rq}(N,T_N,T_F) = \frac{1}{2N+1}\left[1 + 2\sum_{k=1}^{N} \cos\frac{2\pi k}{2N+1}\left(\frac{r}{T_F}-\frac{q}{T_N}\right)T_N\right] \qquad (12D.11)$$

The estimated Kronecker delta has the following properties:

$$\hat{\delta}_{rq} = \begin{cases} 1 & r = q \\ 0 & r \neq q \text{ and } T_N = T_F \end{cases} \qquad (12D.12)$$

$$\hat{\delta}_{rq} \simeq 0 \qquad r \neq q \text{ and } T_N \gg T_F \qquad (12D.13)$$

The ranges on the indices are:

$$r = 0, \pm 1, \pm 2, \ldots, \pm M$$

$$q = 0, \pm 1, \pm 2, \ldots, \pm N \qquad (12D.14)$$

PROGRAM 02 was written to verify the formula for the estimated Kronecker delta function. RUN #1 shows all values for the condition TF = TN = 1. and M = N = 5. Within a high degree of accuracy, Equation 12D.11 is verified for the conditions specified by Equation 12D.12. For a large number of samples, the estimated Kroneker delta converges to the "true" delta function. This can be verified using PROGRAM 02 by increasing N and TN. The interested reader is encouraged to experiment with the properties of $\hat{\delta}_{rq}(N,T_N,T_F)$ by using the program.

There are a variety of ways the spectral mixing formula can be applied to the analysis of the spectrum of a time series. A particular application is needed before a specific use can be specified. One of the most useful

applications is the determination of the amplitude resolution limit for an estimated spectrum. The determination of resolution limits will be discussed in Chapter XIX.

3. Spectral resolution and accuracy

A discrete frequency spectrum derived from digitally processing a time series can be viewed as a sampled frequency spectrum. Because of sampling, the spectrum will have a limited resolution and accuracy and it will be finite. For a periodic time function, $x(t)$, the maximum and minimum frequencies present are:

$$\omega_{max} = \frac{2\pi}{T_F} M \qquad\qquad f_{max} = \frac{1}{T_F} M \qquad\qquad (12D.15)$$

$$\omega_{min} = \frac{2\pi}{T_F} \qquad\qquad f_{min} = \frac{1}{T_F} \qquad\qquad (12D.16)$$

For a time series with sampling interval, Δt, and observation interval, $T_N = (2N+1)\Delta t$, the maximum and minimum frequency components detected by the digital transform are:

$$\omega_{max} = \frac{2\pi}{T_N} N \qquad\qquad f_{max} = \frac{N}{2N+1} \frac{1}{\Delta t} \qquad\qquad (12D.17)$$

$$\omega_{min} = \frac{2\pi}{T_N} \qquad\qquad f_{min} = \frac{1}{T_N} \qquad\qquad (12D.18)$$

The digital transform can be viewed as generating discrete frequency "boxes" or frequency bands into which the computed power in the sampled signal is distributed. A continuous spectral function is generated from the discrete spectrum by expanding in a series of sinc functions (see Equation 12B.6):

$$\hat{c}(f) = \sum_{n=-N}^{+N} c_n \left[\frac{\sin \pi (f - f_n)T_N}{\pi (f - f_n)T_N} \right] \tag{12D.19}$$

The bandwidth between first nulls is:

$$BWFN = \frac{2}{2N+1} f_s = \frac{2}{T_N} \tag{12D.20}$$

The center frequencies for the "boxes" of the discrete transform are

$$f_n = \frac{n}{2N+1} \frac{1}{\Delta t} = \frac{n}{2N+1} f_s = \frac{n}{T_N} \tag{12D.21}$$

where f_s is the sampling frequency. A convenient technique for conceptualizing this process is illustrated with the help of Figures 12D-4 and 12D-5.

4. Sampling and "sync" frequencies

The selection of a sampling interval, and an observation period has a profound effect on the estimated spectrum when the total number of samples is limited. As we discussed in the Fourier analysis section, a value of T_N which is exactly a multiple of the Fourier period will produce an exact spectrum up to a frequency of N/T_N. The sampling interval, $\Delta t = T_N/(2N+1)$, may determine how many unique samples of a particular sinusoidal component are obtained. Consider the effect of the sampling interval on a single sinewave as shown in Figure 12D-6. This is effectively the same as sampling a single period of the sinewave over many points as shown in Figure 12D-7.
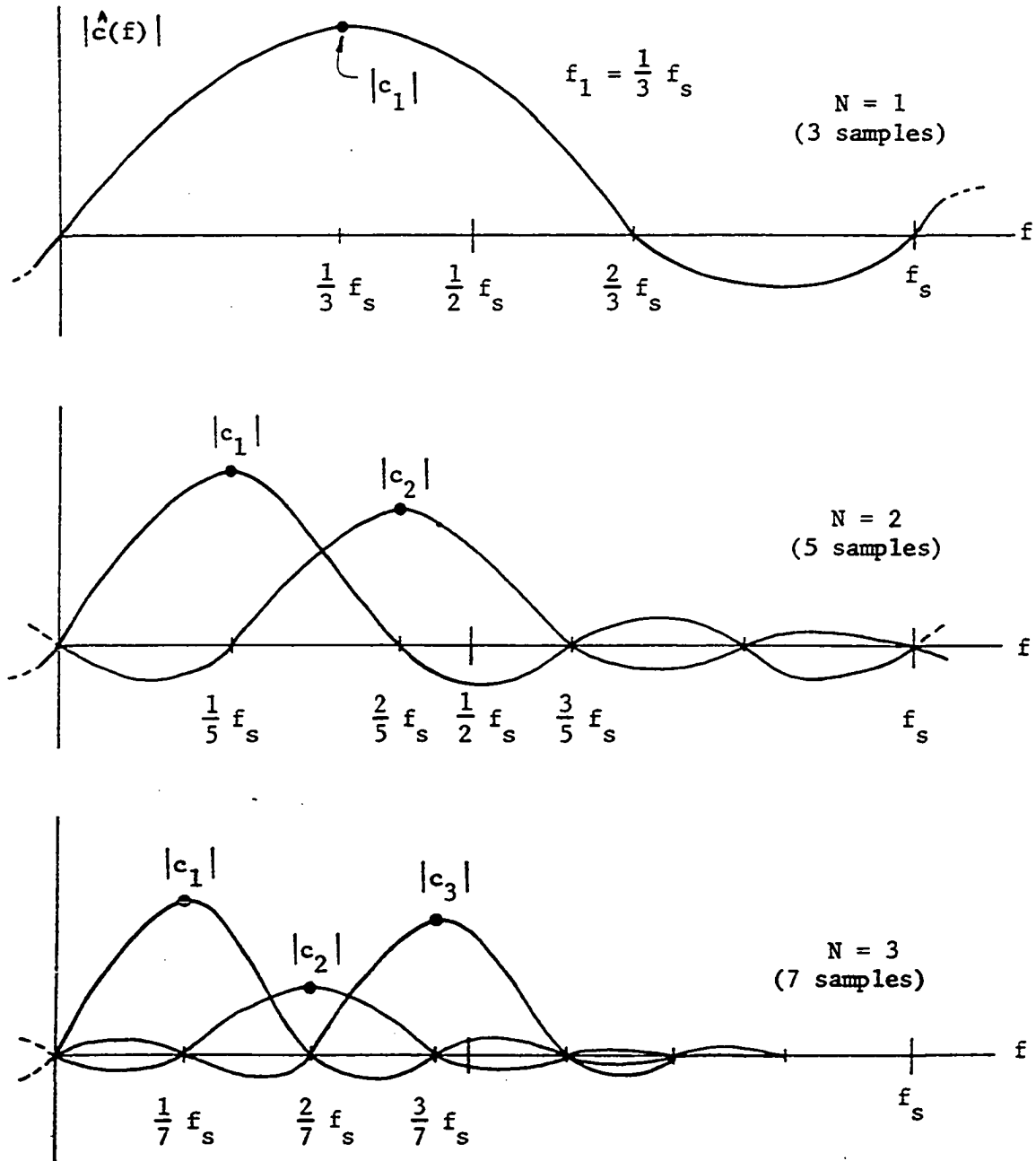
Figure 12D-4. Conceptual Presentation for Illustrating the Distribution of Spectral Power as the Number of Samples Increases
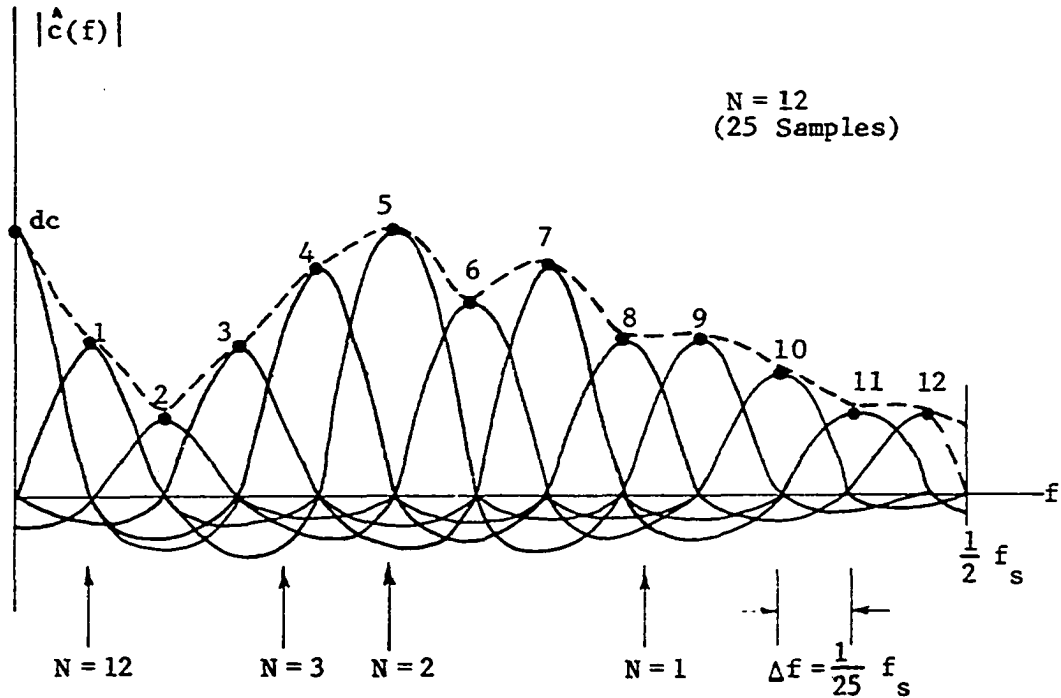
Figure 12D-5. Conceptual Presentation for a
Large Number of Samples

This way of looking at the sampling process led to the discovery of
unique sampling frequencies we will call "sync" frequencies. When the
spectrum of x(t) contains a sinewave component corresponding to one of
these sync frequencies, the number of unique samples of this spectral com-
ponent is limited to a finite number, n_p.

To determine these frequencies, consider the single sinewave in Figure
12D-8. We can define a remainder period ΔL such that:

$$2\Delta L = T - n_p \Delta t \qquad n = 3,4,\ldots \qquad \Delta L \leq 0 \qquad (12D.22)$$
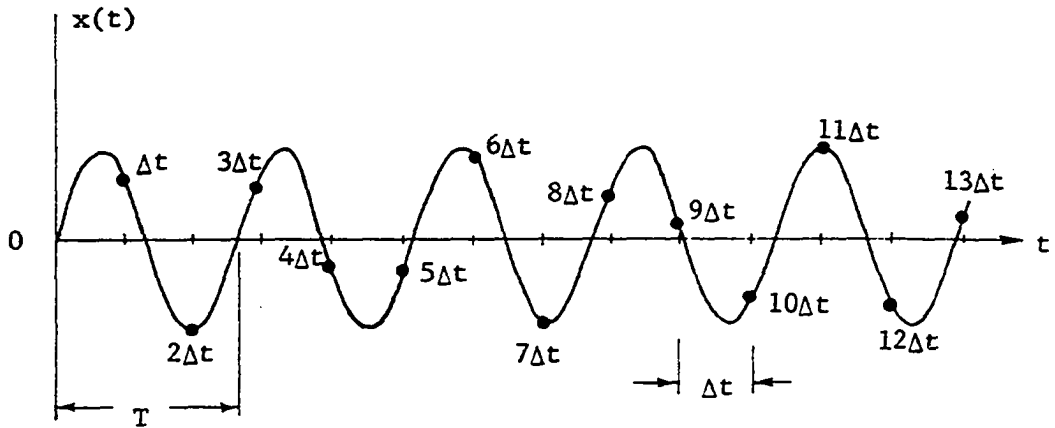
Figure 12D-6. Sampling a Single Sinewave
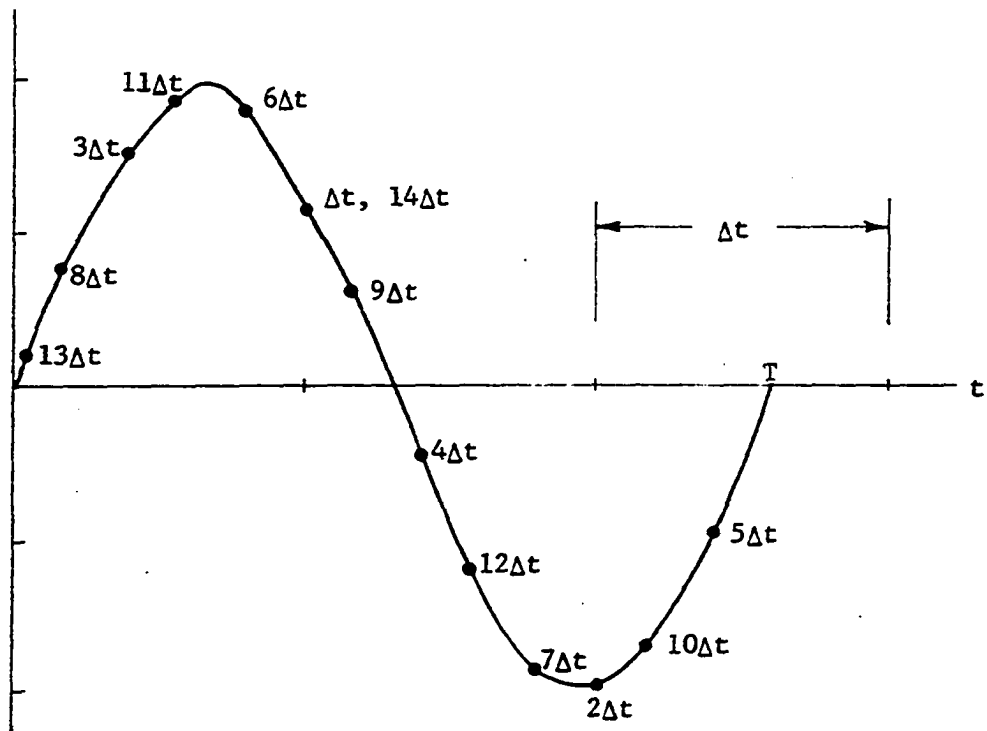
Figure 12D-7. Equivalent Sampling Information
for One Period of a Single Sinewave
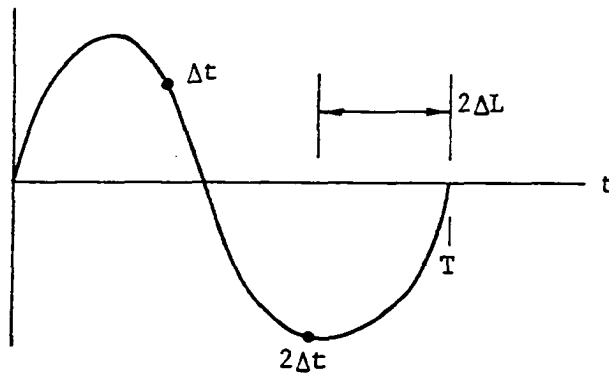
Figure 12D-8. Single Period Sampling of a Single Sinewave
Showing Remainder Period, ΔL

The integer, n_p, represents the number of increments in a period, T, before the cycle repeats and ΔL is one-half of the remaining period length.

For, $\Delta L = 0$, the sync frequency and unique sampling interval are defined by:

$$\Delta L = 0 \qquad \Delta t = \frac{1}{n_p} T \qquad f_{sn} = \frac{n_p}{T} \qquad (12D.23)$$

For a 3 Hz sinewave and, $n_p = 7$ unique samples, the sync frequency would be 21 Hz and the sampling interval would be 1/21 seconds. It should be noted that any integer multiple of a sync frequency is still a sync frequency. For, $\Delta L > 0$, the total number of periods sampled must accumulate until $n_p \Delta L = T$. The sync frequency and unique sampling interval become:

$$\Delta L > 0 \qquad \Delta t = (\frac{1}{2} - \frac{1}{n_p})T \quad , \qquad f_{sn} = (\frac{2n_p}{n_p - 2}) \frac{1}{T}$$

$$(12D.24)$$

$$n_p = 3,4,5,\ldots(2N+1)$$

For the previous example, the sync frequency would be 42/5 Hz and the sampling interval would be 5/42 seconds.

Another way to view sync frequencies is to select a given sampling frequency, f_s, and determine where in the spectrum these frequencies will occur. They will occur at frequencies corresponding to:

$$f = \frac{1}{n_p} f_s \qquad \text{and} \qquad f = (\frac{1}{2} - \frac{1}{n_p}) f_s \qquad (12D.25)$$

$$\Delta L = 0 \qquad\qquad\qquad \Delta L > 0$$

The location of these frequencies with respect to the discrete spectrum is shown in Figure 12D-9 for $3 \le n_p \le 10$. This figure should be compared to those in Part 4 of this section. From the figure it can be seen that the frequency $f_s/3$ has the fewest unique samples of all the sampled frequency components. For $n_p = 3$, the critical Fourier frequencies are

$$1/7 \ f_s, \quad 2/7 \ f_s, \quad 3/7 \ f_s$$

as shown in the figure. Only the first component corresponds to a sync frequency.

As stated previously, the total number of independent samples for any given sync frequency is n_p. It does not improve resolution to sample for an observation interval longer than, $T_N = n_p \Delta t$. There is an exception to this however if the sinewave is corrupted by noise. With a signal that has additive noise, the resolution accuracy can be improved by increasing the observation period because this will provide an averaging effect for each of the unique sample values defined for the noiseless case.
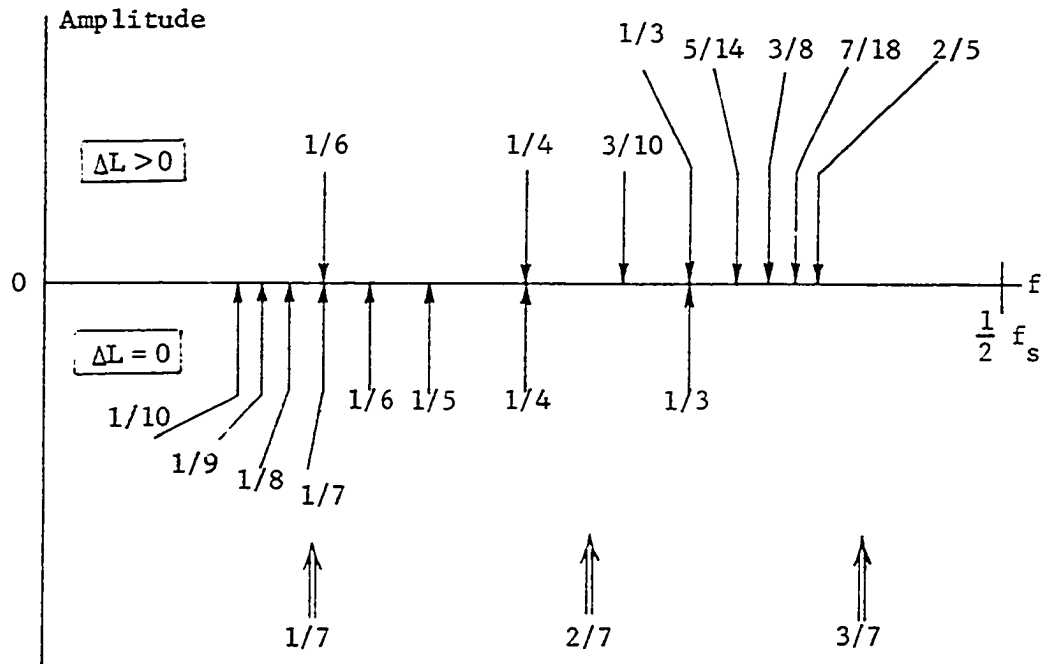
Figure 12D-9. The Locations of the Principle Sync
Frequencies as Referenced to the
Sampling Frequency, f_s

5. Noisy data

When "ideal" data is corrupted by noise or unwanted statistical
variations, the collective parameters which characterize the process
become functions of a random variable. The estimated averages will fluc-
tuate according to how the data is taken and how much data is observed.

The effect of noise can be reduced only by increasing the amount of
data taken and applying averaging techniques or by smoothing the data
record according to some a priori knowledge of the generating process.
Quite often, data is smoothed by applying digital filtering to remove

the high frequency noise mixed with the desired data. In spectral analysis, noise effects are reduced both by selective filtering and by spectrum averaging.

Selective filtering (also called notch, bandpass, highpass, lowpass, or rejection filtering) can be used when the desired spectrum is limited to some specified frequency range or ranges. This type of processing requires a knowledge of the "possible" spectral characteristics of the signal. Selective filtering and preprocessing of the data function were discussed in Chapter IX.

Spectrum averaging can be implemented when several spectral estimates for the same process are available. In the discussion of the Blackman-Tukey method of spectral analysis in Chapter IX, it was noted that the estimated spectrum is the convolution of the "true" spectrum with the spectral window function (Equation 9E.5). This is only true for the expected value of $\hat{P}(f)$. In other words, $\hat{P}(f)$, is a random function and several spectral estimates must be averaged before the composite estimate approaches the ideal case specified by Equation (9E.5). In this sense, even the smoothed estimate of the power spectrum given by $E\{\hat{P}(f)\}$ is still a very idealized concept.

There are essentially two ways to determine an average frequency spectrum in time series analysis. First, if the time series is used to generate a discrete autocovariance function which is then Fourier analyzed, the resulting discrete power spectral density function will be a set of spectral amplitudes and discrete frequencies. Several of these power spectral density records may be averaged to determine an average power

spectrum. In some instances it will be necessary to average the absolute values of the amplitudes to avoid the conceptual problem of dealing with theoretically impossible negative components. This can also be handled by windowing or other such techniques.

Second, if the amplitude spectrum is calculated directly, the Fourier coefficients will be complex and one must chose one of two methods of averaging complex numbers. The first type of average is called the vector or coherent average. This processing involves averaging first the real parts and then the imaginary parts of all the complex numbers. It may be written as:

$$\text{Ave}\{c_n\} = \frac{1}{N} \sum_{k=1}^{N} a_k + j \frac{1}{N} \sum_{k=1}^{N} b_k$$

(12D.26)

$$c_k = a_k + jb_k$$

It is called a coherent average because it is usually used when the phase information is important. The second type of complex number average is called the algebraic or incoherent average. For this processing, one averages the absolute magnitudes and then the phases of all the complex numbers. The algebraic average is represented by

$$\text{Ave}\{c_n\} = \overline{c_n} \, e^{+j \overline{\theta_n}}$$

(12D.27)

where:

$$\overline{c_n} = \frac{1}{N} \sum_{k=1}^{N} |c_k|$$

(12D.28)

$$\overline{\theta_n} = \frac{1}{N} \sum_{k=1}^{N} \theta_k$$

(12D.29)

The equations for the vector or coherent average have been worked out using the familiar Fourier series notation given in Equation A2.2 in Appendix II. The reader is cautioned to realize that the time records must be phase connected or measured with respect to the same absolute phase reference or the advantage of a coherent average cannot be realized.

A particular data set denoted by the subscript, m, is corrupted with noise and is written as

$$\tilde{x}_m(k\Delta t) = x(k\Delta t) + \epsilon_{mk} \tag{12D.30}$$

where the tilde accent denotes a measured value and ϵ_{mk} denotes an additive noise time series for the m-th record. The estimated Fourier coefficients for the m-th record and the corresponding error contributions may be written as:

$$\hat{a}_{mo} = \frac{1}{2N+1} \sum_{k=-N}^{+N} \tilde{x}_m(k\Delta t) \tag{12D.31}$$

$$= \frac{1}{2N+1} \sum_{k=-N}^{+N} x(k\Delta t) + \frac{1}{2N+1} \sum_{k=-N}^{+N} \epsilon_{mk} \tag{12D.32}$$

$$= \bar{x} + \overline{\Delta\epsilon_m} \tag{12D.33}$$

$$\hat{a}_{mn} = \frac{2}{2N+1} \sum_{k=-N}^{+N} \tilde{x}_m(k\Delta t) \cos\left(\frac{2\pi}{T} nk\Delta t\right) \tag{12D.34}$$

$$= \hat{a}_n + \Delta a_{mn} \tag{12D.35}$$

$$\hat{b}_{mn} = \frac{2}{2N+1} \sum_{k=-N}^{+N} \tilde{x}_m(k\Delta t) \sin\left(\frac{2\pi}{T} nk\Delta t\right) \tag{12D.36}$$

$$= \hat{b}_n + \Delta b_{mn} \tag{12D.37}$$

The coefficients $\hat{a}_n$ and $\hat{b}_n$ are the estimates obtained without noise corruption and are denoted by:

$$\hat{a}_n = \frac{2}{2N+1} \sum_{k=-N}^{+N} x(k\Delta t) \cos \left(\frac{2\pi}{T} nk\Delta t\right) \tag{12D.38}$$

$$\hat{b}_n = \frac{2}{2N+1} \sum_{k=-N}^{+N} x(k\Delta t) \sin \left(\frac{2\pi}{T} nk\Delta t\right) \tag{12D.39}$$

The contributions to these estimates caused by the noise corruption are given by:

$$\Delta a_{mn} = \frac{2}{2N+1} \sum_{k=-N}^{+N} \epsilon_{mk} \cos \left(\frac{2\pi}{T} nk\Delta t\right) \tag{12D.40}$$

$$\Delta b_{mn} = \frac{1}{2N+1} \sum_{k=-N}^{+N} \epsilon_{mk} \sin \left(\frac{2\pi}{T} nk\Delta t\right) \tag{12D.41}$$

If there are MM independent records to be averaged, the average values for the estimated coefficients are calculated as:

$$\text{Ave}\{\hat{a}_{mn}\} = \frac{1}{MM} \sum_{r=1}^{MM} \hat{a}_{rn}$$

$$= \hat{a}_n + \overline{\Delta a_n} \tag{12D.42}$$

$$\text{Ave}\{\hat{b}_{mn}\} = \frac{1}{MM} \sum_{r=1}^{MM} \hat{b}_{rn}$$

$$= \hat{b}_n + \overline{\Delta b_n} \tag{12D.43}$$

The error term $\overline{\Delta a_n}$ and $\overline{\Delta b_n}$ can be calculated from:

$$\overline{\Delta a_n} = \frac{1}{MM} \sum_{r=1}^{MM} \Delta a_{rn} = \frac{1}{MM} \sum_{r=1}^{MM} \frac{2}{2N+1} \sum_{k=-N}^{+N} \epsilon_{rk} \cos \left(\frac{2\pi}{T} nk\Delta t\right) \tag{12D.44}$$

$$\overline{\Delta b_n} = \frac{1}{MM} \sum_{r=1}^{MM} \Delta b_{rn} = \frac{1}{MM} \sum_{r=1}^{MM} \frac{2}{2N+1} \sum_{k=-N}^{+N} \epsilon_{rk} \cos \left(\frac{2\pi}{T} nk\Delta t\right) \tag{12D.45}$$

Actual data records are numerically processed by computing $\hat{a}_{mn}$ and $\hat{b}_{mn}$ for each record and then numerically averaging over all MM records to obtain $\text{Ave}\{\hat{a}_{mn}\}$ and $\text{Ave}\{\hat{b}_{mn}\}$. The uncorrupted estimates of the spectral amplitudes are obtained by solving Equations 12D.42 and 12D.43 to get:

$$\hat{a}_n = \text{Ave}\{\hat{a}_{mn}\} - \overline{\Delta a_n} \tag{12D.46}$$

$$\hat{b}_n = \text{Ave}\{\hat{b}_{mn}\} - \overline{\Delta b_n} \tag{12D.47}$$

As the number of data points becomes very large, the estimates converge to the "true" values, a_n and b_n. The error terms $\overline{\Delta a_n}$ and $\overline{\Delta b_n}$ can be statistically specified if the statistical parameters of the noise series, ϵ_{mk}, is known. This will allow one to obtain error limits and variance estimates on $\hat{a}_n$ and $\hat{b}_n$.

A similar analysis for the algebraic or incoherent average can be derived. Starting with an absolute magnitude estimate for each spectral component of the m-th data record we obtain:

$$|\hat{c}_{mn}| = \frac{1}{2} [\hat{a}_n^2 + \hat{b}_n^2 + 2(\hat{a}_n \Delta a_{mn} + \hat{b}_n \Delta b_{mn}) + \Delta a_{mn}^2 + \Delta b_{mn}^2]^{\frac{1}{2}} \tag{12D.48}$$

The incoherent amplitude average becomes:

$$\text{Ave}\{|\hat{c}_{mn}|\} = \frac{1}{MM} \sum_{r=1}^{MM} |\hat{c}_{rn}| \tag{12D.49}$$

The reader should contrast this estimate with the coherent amplitude estimate given by:

$$\frac{1}{2} [\hat{a}_n^2 + \hat{b}_n^2 + 2(\hat{a}_n \overline{\Delta a_n} + \hat{b}_n \overline{\Delta b_n}) + \overline{\Delta a_n}^2 + \overline{\Delta b_n}^2]^{\frac{1}{2}} \tag{12D.50}$$

The advantage of a coherent average over the incoherent average for obtaining an amplitude resolution limit will be discussed in the chapter on interpretation of estimated spectra.

6. Detection of a single sinewave in bandlimited white Gaussian noise

A single frequency sinewave can be detected in bandlimited white Gaussian noise if the signal-to-noise ratio is large enough. In statistical detection theory (Whalen, 1971) the presence of a sinewave is determined by the change in the output of an envelope detector. Since the noise alone has a Rayleigh distribution and the signal plus noise has a Rician distribution it is possible to determine the probability of detection as a function of signal-to-noise ratio for a given detection threshold. In spectral analysis the same types of effects are involved. A presentation of some basic ideas for statistical detection of periodic components in an estimated spectrum are presented in Chapter XIX. A simple presentation for a single sinewave and "ideal" noise will now be given.

To begin, we define a time series that is the sum of a single frequency sinusoid and a white noise sequence:

$$x(k\Delta t) = \xi(k\Delta t) + [c_1 e^{+j \frac{2\pi}{T_1} k\Delta t} + c_1^* e^{-j \frac{2\pi}{T_1} k\Delta t}] \qquad (12D.51)$$

The white noise sequence (Appendix I, Part G) was defined as:

$$E\{\xi(k\Delta t)\} = 0, \quad E\{\xi(k\Delta t)\xi(p\Delta t)\} = 0 \quad , \quad k \neq p$$

$$E\{\xi^2(k\Delta t)\} = \sigma_\xi^2 = P_N \qquad (12D.52)$$

The questions to be answered are:

1. What are the important characteristics of the amplitude spectrum estimated from one or more sample records of the process?

2. What is the effect of increasing the number of samples?

Define a sample realization $\{x(k\Delta t): k = 0, \pm1, \pm2, \ldots, \pm N\}$ of the time series in (12D.51) as $(2N + 1)$ samples taken at an interval, $\Delta t = 1/f_s$. Assume that no aliasing occurs and that for any sample record the average value is approximately zero. A discrete Fourier transform applied to the sample time series will give (Equation 19D.3):

$$\hat{c}_n = \frac{1}{2N+1} \sum_{k=-N}^{+N} \xi(k\Delta t) e^{-j \frac{2\pi}{2N+1} nk}$$

$$+ c_1 \hat{\delta}(\frac{2\pi}{T_1} - n\Delta f) + c_1^* \hat{\delta}(-\frac{2\pi}{T_1} - n\Delta f) \qquad (12D.53)$$

$$\{n = 0, \pm1, \pm2, \ldots, \pm N\}$$

Representing the noise components with Equations 19C.3 and 19C.4 and the estimated amplitudes of c_1 in the complex form $B_n e^{-j\phi_n}$ gives:

$$\hat{c}_n = \frac{1}{2N+1} (\hat{\alpha}_n - j \hat{\beta}_n) + B_n e^{-j\phi_n} \qquad (12D.54)$$

$$= [\frac{\hat{\alpha}_n}{2N+1} + B_n \cos \phi_n] - j[\frac{\hat{\beta}_n}{2N+1} + B_n \sin \phi_n] \qquad (12D.55)$$

For a large number of samples the spectral mixing formula gives a good approximation for the amplitude c_1. The <u>large sample approximation</u> is

$$B_1 e^{-j\phi_1} \simeq |c_1| e^{-j\theta_1}$$

$$B_{-1} e^{-j\phi_{-1}} \simeq |c_1| e^{+j\theta_1}$$

(12D.56)

$$B_n \simeq 0 \qquad n \neq \pm 1$$

and:

$$\hat{c}_n = \frac{1}{2N+1} (\hat{\alpha}_n - j \hat{\beta}_n) \qquad n \neq \pm 1$$

(12D.57)

$$\hat{c}_1 = \frac{1}{2N+1} (\hat{\alpha}_1 - j \hat{\beta}_1) + |c_1| e^{-j\theta_1}$$

(12D.58)

If a large number of <u>phase connected</u> samples are available, a <u>coherent</u> <u>average</u> (Equation 12D.26) may be taken which yields:

$$\mathrm{Ave}\{\hat{c}_n\} = E\{\frac{\hat{\alpha}_n}{2N+1}\} - j \, E\{\frac{\hat{\beta}_n}{2N+1}\} = 0$$

(12D.59)

$$\mathrm{Ave}\{\hat{c}_1\} = E\{\frac{\hat{\alpha}_1}{2N+1} + |c_1| \cos \theta_1\} - j \, E\{\frac{\hat{\beta}_1}{2N+1} + |c_1| \sin \theta_1\}$$

$$= c_1$$

(12D.60)

This performance is very good but it takes large amounts of data. If the complex amplitudes are <u>incoherently averaged</u> the resulting estimate

$$|\hat{c}_n| = [(\frac{\hat{\alpha}_n}{2N+1})^2 + (\frac{\hat{\beta}_n}{2N+1})^2]^{\frac{1}{2}} \qquad n \neq \pm 1$$

(12D.61)

is Rayleigh distributed (Equation 19C.7). The resulting estimate for $|\hat{c}_1|$ has a Rician distribution (Whalen, 1971):

$$|\hat{c}_1| = [(\frac{\hat{\alpha}_1}{2N+1} + |c_1| \cos \theta_1)^2 + (\frac{\hat{\beta}_1}{2N+1} + |c_1| \sin \theta_1)^2]^{\frac{1}{2}}$$

(12D.62)

A statistical criterion for detection can be developed using the concepts of average spectral density and the Rician density function. The Marcum Q-Function is used to test the value of $|\hat{c}_1|$ against a threshold determined by $\text{Ave}\{\hat{c}_n\}$. The author plans to develop this idea in a future paper.

The same concepts can be applied to Equation 12D.54 the only effect is the change of $|c_1|e^{-j\theta_1}$ to $B_1 e^{-j\phi_1}$ caused by the spectral mixing effect.

The reader is referred to Chapter XIX, Section C where more properties of the DFT and Gaussian noise are discussed. In particular, a relatively simple criterion is given for testing a noise spectrum to see if it contains a periodic component.

XIII. PREDICTIVE DECONVOLUTION

An analog or digital filter convolves an input, $x(t)$, with the filter's impulse response, $h(t)$, to give an output, $y(t)$. The central problem of deconvolution is: given the output $y(t)$ and either $x(t)$ or $h(t)$, can the third function be uniquely determined? The answer is very definitely no. Deconvolution involves finding the inverse filter for $h(t)$ and this demands that the reciprocal of the transfer function of $h(t)$ exist for all frequencies of interest.

To provide a practical basis for the problem of deconvolution it is necessary that the class of possible filters be restricted to those for which the inverse filter exists and is well-behaved. This restriction may appear to be too severe but it turns out that much scientific data processing and spectral analysis problems can be modeled with such a class of filter. A class of filters variously called <u>prediction error filters</u>, <u>digital Wiener filters</u>, <u>least-squares inverse filters</u>, <u>least-squares deconvolution filters</u>, <u>prewhitening filters</u>, or <u>recursive digital filters</u> have been successfully used in the deconvolution of geophysical data (Peacock and Treitel, 1969).

Predictive deconvolution techniques are usually applied to a degenerate class of time series characterized by a known component and a purely random component. The desired objective is to take a measured time series, $x(t)$, and decompose it into a completely predictive component, $z(t)$, and a random or uncorrelated component, $\eta(t)$.

In the analysis of practical time series and especially when applying autoregressive analysis techniques, it is assumed that the time series $\{z(t): t = 0, \pm1, \pm2, \ldots\}$ can be characterized by a finite number of unique parameters (these will be discussed shortly). The uncorrelated component for these analysis techniques is represented by the white noise sequence $\{\xi(t): t = 0, 1, 2, \ldots\}$. Characteristics of a white noise process with finite variance are discussed in Chapter XIV.

For the rest of this chapter, the time index $\{t = 0, \pm1, \pm2, \ldots\}$ will be used as shorthand notation for $\{t = k\Delta t: k = 0, \pm1, \pm2, \ldots\}$. This notation is common in the literature and so is the convention of assuming $\Delta t = 1$. This convention will be used except where the explicit omission of Δt may cause confusion.

The three most commonly used mathematical models for representing a measured time series are the Fourier series, the autoregressive series, and the convolution of the known and random components. The Fourier series representation may be written as the sum of a white noise sequence (see Equation 14.3) and a complex Fourier series with complex amplitudes, c_n and Fourier period T_F:

$$x(t) = \xi(t) + \sum_{n=-M}^{+M} c_n e^{+j \frac{2\pi n}{T_F} t} = \xi(t) + z(t) \qquad (13.1)$$

The predictable component, $z(t)$, is characterized by the $2M + 1$ complex amplitudes and the Fourier period, T_F. This constitutes the finite number of unique parameters for this representation.

The second representation is an autoregressive series (see Chapter XIV and Appendix I) of order K:

$$x(t) = \xi(t) + \sum_{n=1}^{K} a_n x(t-n)$$ (13.2)

The predictable component is characterized by the finite number of amplitude coefficients $\{a_n: n = 1, 2, \ldots K\}$. The power spectral density function for this process model is both continuous and bandlimited. The resulting autocovariance function is infinite and nonperiodic.

It is reasonable for the reader to wonder at this point if a process can be modeled as the sum of a Fourier series and an autoregressive series. The answer is, yes, a process that has a power spectral density function that has both continuous and discrete components should be represented as the sum of both models (Cooper and McGillem, 1971, Ch. 6). The autocorrelation function for such a model will be infinite and contain periodic and nonperiodic components.

The third common model is the convolution of a white noise sequence, $\eta(t)$, with a completely known time series, $z(t)$, to give:

$$y(t) = z(t) * \eta(t) = \sum_{n} z(n) \, \eta(t-n)$$ (13.3)

It is this model that is used by Peacock and Treitel (1969) to develop a scheme of predictive deconvolution. The notation $y(t)$ is used for this model to avoid confusion with the autoregressive process model which yields similiar results.

The desired least-squares deconvolution filter which characterizes $z(t)$ is the one which ideally transforms $y(t)$ into a white noise sequence

and hence

$$y(t) * b(t) = z(t) * \eta(t) * b(t) = \eta(t) \tag{13.4}$$

or:

$$y(t) * b(t) = \eta(t) \tag{13.5}$$

The deconvolution filter and the predictable component are now related by:

$$z(t) * b(t) = 1 \tag{13.6}$$

If both $z(t)$ and $b(t)$ are modeled using predictive filters, $b(t)$ can be referred to as the inverse filter characterizing $z(t)$. This is why the technique is often called least-squares inverse filtering. Peacock and Treitel (1969) develop a general technique whereby the data function $y(t)$ is used to generate a filter $b(t)$ which describes the deconvolved component, $z(t)$. $z(t)$ can be described as a filter or convolving function which transforms a white noise input, $\eta(t)$, into the time series, $y(t)$. What this really means is that <u>the spectral function representing $y(t)$ is</u> <u>limited to a class of functions that can be described as the output of a</u> <u>real filter with white noise input.</u> Also, the inverse filter must exist. Before continuing, we will digress to examine Equation 13.1 and to put it into an alternate but especially interesting form. First substitute Equation 11.12 into (13.1) to get:

$$x(t) = \xi(t) + \frac{1}{2N+1} \sum_{n=-M}^{+M} \sum_{k=-N}^{+N} x(k\Delta t) e^{-j\frac{2\pi}{T_F}nk\Delta t} e^{+j\frac{2\pi n}{T_F}t} \tag{13.7}$$

By interchanging summation this can be written as:

$$x(t) = \xi(t) + \sum_{k=-N}^{+N} x(k\Delta t) \left\{ \frac{1}{2N+1} \sum_{n=-M}^{+M} e^{-j\frac{2\pi}{T_F}n(k\Delta t - t)} \right\} \qquad (13.8)$$

Now the $k\Delta t$ dependence is factored out of the term in brackets and the series is written in a more compact form as

$$x(t) = \xi(t) + \sum_{k=-N}^{+N} \alpha_k(t)\, x\,(k\Delta t) \qquad t = 0, \pm\Delta t, \pm 2\Delta t, \ldots \pm N\Delta t. \qquad (13.9)$$

where:

$$\alpha_k(t) = \frac{1}{2N+1} \sum_{n=-M}^{+M} e^{-j\frac{2\pi}{T_F}n(k\Delta t - t)} \qquad (13.10)$$

$$= \frac{1}{2N+1} \left\{ 1 + 2 \sum_{n=1}^{M} \cos\left[\frac{2\pi}{T_F} n(k\Delta t - t)\right] \right\} \qquad (13.11)$$

It is interesting to note that (13.9) is similar in form to (13.2) except that the coefficients, $\alpha_k(t)$, are functionally dependent on the index t. Also, the coefficients are even in both t and $k\Delta t$ and are another form of the estimated Kronecker delta function (Equation 11.19). This difference between (13.2) and (13.9) accounts for the difference in the two types of time series representations. The indices for the representation of (13.9) do not have to be symmetrical about t = 0 and could just as well be written as

$$x(t) = \xi(t) + \sum_{k=0}^{2N} \alpha_k(t)\, x\,(k\Delta t) \qquad t = 0, \Delta t, \ldots 2N\Delta t \qquad (13.12)$$

with $\alpha_k(t)$ now being symmetrical about the point, $t = (N+1)\Delta t$.

If the time series contains a single frequency spectral component where the period is fairly well-known, the complex Fourier amplitude can be obtained by using the estimator (Equation 11.15):

$$\hat{C}(f_o) = \frac{1}{2N+1} \sum_{k=-N}^{+N} x(k\Delta t)e^{-j\frac{2\pi}{T_o}k\Delta t} \qquad (13.13)$$

This component is then removed from the data by (See Appendix II)

$$\tilde{x}(t) = x(t) - 2\left|\hat{C}(f_o)\right| \cos\left(\frac{2\pi}{T_o} t + \phi_o\right) \qquad (13.14)$$

where ϕ_o is the phase angle of $\hat{C}(f_o)$. The numerical algorithm for this estimation will take the form:

$$\text{Re}\{\hat{C}(f_o)\} = \frac{1}{2N+1} \sum_{k=1}^{2N+1} x(k\Delta t) \cos\left[\frac{2\pi}{T_o} (k-N-1)\Delta t\right] \qquad (13.15)$$

$$\text{I}_m\{\hat{C}(f_o)\} = \frac{-1}{2N+1} \sum_{k=1}^{2N+1} x(k\Delta t) \sin\left[\frac{2\pi}{T_o} (k-N-1)\Delta t\right] \qquad (13.16)$$

$$\left|\hat{C}(f_o)\right| = \left[\text{Re}^2\{\hat{C}\} + \text{Im}^2\{\hat{C}\}\right]^{\frac{1}{2}} \qquad (13.17)$$

$$\phi_o = \text{ARCTAN}\left[\frac{\text{Im}\{\hat{C}\}}{\text{Re}\{\hat{C}\}}\right] \qquad (13.18)$$

$$\tilde{x}(k\Delta t) = x(k\Delta t) - 2\left|\hat{C}(f_o)\right| \cos\left[\frac{2\pi}{T_o} (k-N-1)\Delta t + \phi_o\right] \qquad (13.19)$$

PROGRAM 06 in Appendix III has been written to implement the estimator described above. The modified time series, $\tilde{x}(t)$, may also be spectrum analyzed to determine a "residue" spectrum. If the period T_o is not exactly known, the complex amplitude can still be found by using approximation techniques. For example a discrete Fourier transform estimation using x(t) would give approximate spectral components to use as starting values.

We now proceed to derive the mathematical properties and methods involved in determining a suitable predictive deconvolution technique. The predictive filtering viewpoint and the autoregression analysis viewpoint will both be presented since they are mathematically equivalent.

The discrete convolution formula for a digital filter (Equation 5C.4) is

$$y(t) = \sum_{n}^{t} h(t-n) x(n) \qquad t = 0, \pm 1, \pm 2, \ldots \qquad (13.20)$$

where the lower range of the index, n, depends on the length, $K-1$, of the digital filter. The sampled impulse response of the filter is limited in time to the series $\{h(n\Delta t): n = 0, 1, 2, \ldots (K-1)\}$ where $h(n\Delta t) = 0$ for $k \geq K$. K is called the length of the filter and the lower limit on n becomes $(t-K+1)$. The filter coefficients have been normalized by Δt. Linear prediction can be formulated in terms of a filter output by considering $h(t)$ to be a linear prediction operator with prediction distance $\alpha \Delta t$. The output of the filter will be an estimate of the input time series at some future time $t + \alpha$. This is represented by:

$$y(t) = \sum_{n}^{t} h(t-n) x(n) = \hat{x}(t+\alpha) \qquad (13.21)$$

The best linear prediction in a least-squares sense is made by a filter with coefficients that minimize the total mean-square prediction error:

$$M = \sum_{t} e^2(t+\alpha) = \sum_{t} [x(t+\alpha) - \hat{x}(t+\alpha)]^2 \qquad t = 0, \pm 1, \pm 2, \ldots \qquad (13.22)$$

The error of the prediction, $\epsilon(t+\alpha)$, is the difference between the "true" and predicted values of the time series:

$$\epsilon(t+\alpha) = x(t+\alpha) - \hat{x}(t+\alpha) = x(t+\alpha) - \sum_{n}^{t} x(n) h(t-n) \qquad (13.23)$$

The total mean-square error can be written in terms of the infinite time series and the filter coefficients:

$$M = \sum_t \left[x(t + \alpha) - \sum_n^t x(n)\, h\,(t - n) \right]^2 \tag{13.24}$$

A system of K equations can be used to determine the K unknown filter coefficients that will minimize M. This system of equations is obtained by the following minimizations:

$$\frac{\partial M}{\partial h(k)} = 0 \quad k = 0, 1, 2, \ldots, (K - 1) \tag{13.25}$$

The k-th linear equation is derived from

$$\frac{\partial M}{\partial h(k)} = -2 \sum_t \left[x(t + \alpha) - \sum_n^t x(n)\, h\,(t - n) \right] x(t - k) = 0 \tag{13.26}$$

This may be written in the more usual form as

$$\sum_t \left[\sum_n^t x(n)\, h\,(t - n) \right] x\,(t - \tau) = \sum_t x(t + \alpha)\, x\,(t - \tau) \tag{13.27}$$
$$\tau = 0, 1, 2, \ldots, K - 1.$$

or:

$$\sum_{n=0}^{K-1} h(n)\, r\,(\tau - n) = \sum_t x(t + \alpha)\, x\,(t - \tau) \tag{13.28}$$
$$\tau = 0, 1, 2, \ldots, K - 1$$

If we make the following substitutions

$$r(\tau - n) = \sum_t x(t)\, x\,(t - \tau + n) \tag{13.29}$$

$$r(\tau + \alpha) = \sum_t x(t + \alpha)\, x\,(t - \tau)$$

we can write the system of equations given in (13.28) in terms of the co-variance matrix and filter coefficients as (remembering $r(\tau) = r(-\tau)$):

$$
\begin{bmatrix}
r(0) & r(1) & \cdots & r(K-1) \\
r(1) & r(0) & \cdots & r(K-2) \\
\cdot & \cdot & \cdots & \cdot \\
\cdot & \cdot & \cdots & r(1) \\
r(K-1) & r(K-2) & \cdots & r(1)\ r(0)
\end{bmatrix}
\begin{bmatrix}
h(0) \\
h(1) \\
\cdot \\
\cdot \\
h(K-1)
\end{bmatrix}
=
\begin{bmatrix}
r(\alpha) \\
r(\alpha+1) \\
\cdot \\
\cdot \\
r(\alpha+K-1)
\end{bmatrix}
\tag{13.30}
$$

The covariance matrix is made up of elements:

$$
r(\tau) = \sum_t x(t)\, x\,(t-\tau) = r(-\tau) \tag{13.31}
$$

The system of equations represented by (13.30) is solved for the filter coefficients by inverting the covariance matrix. The least-squares prediction operator represented by $h(t)$ can be used for the prediction:

$$
\hat{x}(t+\alpha) = \sum_n^t h(t-n)\, x\,(n) \tag{13.32}
$$

The prediction error operator is defined as

$$
\{g(n)\} = 1, \overbrace{0, 0 \ldots, 0}^{\alpha-1\ \text{zeros}}, -h(0), -h(1), \ldots, -h(K-1).
$$

$$
= g(0),\ g(1),\ \ldots,\ g(\alpha+K). \tag{13.33}
$$

which may be used directly to obtain the error of an α-step prediction:

$$
\epsilon(t+\alpha) = \sum_{n=0}^{\alpha+K} g(n)\, x\,(t+\alpha-n) \tag{13.34}
$$

Equation 13.34 is also an alternate representation of (13.23).

The least-squares prediction operator characterized in Equations 13.30 and 13.32 contains the elements of a <u>prediction filter</u> while the least-

squares prediction error operator of (13.33) represents a <u>prediction error</u> <u>filter</u>. Before looking at the central problem of predictive deconvolution and filtering we will digress to consider the autoregression approach to the same analysis.

For autoregressive processes modeled by (13.2), the <u>best</u> linear one-step predictor in a least-squares sense (Appendix I and Koopmans, 1974) is given by:

$$\hat{x}(t+1) = x(t+1) - \xi(t+1) = \sum_{n=1}^{K} a_n x(t+1-n) \tag{13.35a}$$

$$= a_1 x(t) + a_2 x(t-1) + \ldots + a_K x(t-K) \tag{13.35b}$$

The one-step prediction error is the expected value of the mean-square error:

$$E\{((x(t+1) - \hat{x}(t+1))^2\} = E\{\xi^2(t+1)\} = \sigma^2 \tag{13.36}$$

Koopmans (1974) has shown that the best α-step predictor in a least-square sense for an autoregressive series is ($\alpha \leq K+1$):

$$\hat{x}(t+\alpha) = \sum_{n=1}^{\alpha-1} a_n \hat{x}(t+\alpha-n) + \sum_{n=\alpha}^{K} a_n x(t+\alpha-n) \tag{13.37}$$

$$\hat{x}(t+\alpha) = a_1 \hat{x}(t+\alpha-1) + a_2 \hat{x}(t+\alpha-2) + \ldots a_{\alpha-1} \hat{x}(t+1)$$

$$+ a_\alpha x(t) + a_{\alpha+1} x(t-1) + \ldots a_K x(t+\alpha-K) \tag{13.38}$$

The α-step prediction error is ($\alpha \geq 2$):

$$E\{(x(t+\alpha) - \hat{x}(t+\alpha))^2\} = E\{\xi^2(t+\alpha)\} = \sigma^2[1 + \sum_{n=1}^{\alpha-1} a_n^2] \tag{13.39}$$

The coefficients $\{a_n: n = 1, 2, 3, \ldots K\}$ of the autoregression can be obtained by solving the matrix of autocovariances specified by the Yule-Walker equations and derived in Chapter XIV (Equation 14.47). In the notation of this chapter, the solution is:

$$\begin{bmatrix} a_1 \\ a_2 \\ \cdot \\ \cdot \\ \cdot \\ a_K \end{bmatrix} = \begin{bmatrix} r(0) & r(1) & \cdot\cdot & r(K-1) \\ r(1) & r(0) & \cdot\cdot & r(K-2) \\ \cdot & \cdot & \cdot & \cdot \\ \cdot & \cdot & \cdot & \cdot \\ \cdot & \cdot & \cdot & \cdot \\ r(K-1) & r(K-2) & \cdot\cdot & r(0) \end{bmatrix}^{-1} \begin{bmatrix} r(1) \\ r(2) \\ \cdot \\ \cdot \\ \cdot \\ r(K) \end{bmatrix} \qquad (13.40)$$

For a one-step predictor ($\alpha = 1$) Equations 13.40 and 13.30 give the same coefficients. The relationship between the filter coefficients and autoregressive coefficients is expressed as:

$$h(n - 1) = a_n \qquad n = 1, 2, 3, \ldots, K \qquad (13.41)$$

Although we see that the predictive filter and autoregression are two seemingly separate viewpoints on prediction and prediction error for time series, they produce identical results for the one-step predictor. This equivalence will become important later on when maximum entropy spectral analysis is derived in terms of predictive filters and autoregression.

The deconvolution operator, $b(t)$ is determined using the one-step prediction operator and the condition given by Equation 13.6. The basis for the existence of this operator is the fact that the autocorrelation function for $y(t)$ differs from that for $z(t)$ only by a constant scale factor. This will now be shown. Using an analogy to Equation 5B.8, we know that the spectral density of $y(t)$ is equal to the product of the

spectral densities of $z(t)$ and $\eta(t)$

$$S_y(\omega) = S_z(\omega) S_\eta(\omega) \tag{13.42}$$

and consequently the convolution of their autocorrelation functions is:

$$R_{yy}(\tau) = R_{zz}(\tau) * R_{\eta\eta}(\tau) \tag{13.43}$$

From theory we know that the autocorrelation function for white noise is a delta function with strength σ_η^2:

$$R_\eta(\tau) = \sigma_\eta^2 \, \delta(\tau) \tag{13.44}$$

The convolution integral of (13.40) becomes

$$R_{yy}(\tau) = \sigma_\eta^2 \, R_{zz}(\tau) \tag{13.45}$$

and we see that the output and input autocorrelation functions differ only by a constant amplitude scaling factor, σ_η^2. We can also conclude that the power spectral density function amplitudes differ by the same scale factor.

The property of (13.45) has been used by Peacock and Treitel (1969) to develop a predictive filter for deconvolving $z(t)$ and $\eta(t)$. The matrix of (13.30) is augmented by adding the estimated variance of the white noise sequence (see Equation 14.44)

$$\sigma_\eta^2 = r(0) + \sum_{n=1}^{K} r(n) \, h(n-1) \tag{13.46a}$$

$$= R_{yy}(0) + \sum_{n=1}^{K} R_{yy}(n) \, h(n-1) \tag{13.46b}$$

to give:

$$
\begin{bmatrix}
r(0) & r(1) & .. & r(K) \\
r(1) & r(0) & .. & r(K-1) \\
. & . & . & . \\
. & . & . & . \\
. & . & . & . \\
r(K) & r(K-1) & .. & r(0)
\end{bmatrix}_{yy}
\begin{bmatrix}
1 \\
-h(0) \\
-h(1) \\
. \\
. \\
-h(K-1)
\end{bmatrix}
=
\begin{bmatrix}
\sigma_\eta^2 \\
0 \\
0 \\
. \\
. \\
0
\end{bmatrix}
\qquad (13.47)
$$

The column vector $[h]$ forms a one-step prediction error operator which operates on $[r]_{yy}$ to give the one-step prediction error, σ_η^2. The augmented matrix equation (13.47) is identical in form to that determined by augmenting (14.46) or (13.40) to give:

$$
\begin{bmatrix}
r(0) & r(1) & .. & r(K) \\
r(1) & r(0) & .. & r(K-1) \\
. & . & . & . \\
. & . & . & . \\
. & . & . & . \\
r(K) & r(K-1) & .. & r(0)
\end{bmatrix}_{yy}
\begin{bmatrix}
1 \\
-a_1 \\
-a_2 \\
. \\
. \\
-a_K
\end{bmatrix}
=
\begin{bmatrix}
\sigma_\xi^2 \\
0 \\
0 \\
. \\
. \\
0
\end{bmatrix}
\qquad (13.48)
$$

Again we see that predictive filtering and autoregression are equivalent viewpoints. By comparing (13.48) and (13.47) with (13.5) and (13.6) we see that the deconvolution filter or predictive deconvolution operator is characterized by the following system of equations:

$$
\begin{bmatrix}
r(0) & r(1) & .. & r(K) \\
r(1) & r(0) & .. & r(K-1) \\
. & . & & . \\
. & . & & . \\
. & . & & . \\
r(K) & r(K-1) & .. & r(0)
\end{bmatrix}_{yy}
\begin{bmatrix}
b_o \\
b_1 \\
. \\
. \\
. \\
b_k
\end{bmatrix}
=
\begin{bmatrix}
1 \\
0 \\
0 \\
. \\
. \\
0
\end{bmatrix}
\qquad (13.49)
$$

The deconvolution operator is seen to be just a scaled version of $h(n)$ or a_n as:

$$b_o = \frac{1}{\sigma_\xi^2} \qquad\qquad b_o = \frac{1}{\sigma_n^2}$$

$$\tag{13.50}$$

$$b_n = -a_n \qquad\qquad b_n = h(n-1)$$

Deconvolution is performed using Equation 13.5. The power spectral density function for $y(t)$ is characterized by $z(t)$ or the inverse of $b(t)$. This will be shown in Chapter XIV.

XIV. AUTOREGRESSIVE SPECTRAL ESTIMATION

The estimation of a continuous power spectral density function using autoregressive techniques is based on the fact that any weakly stationary (covariance stationary) stochastic process with a continuous spectrum can be represented by an infinite moving average (Koopmans, 1974).

A moving average process is defined by the series

$$y(t) = \sum_{n=-\infty}^{+\infty} b_n \xi(t-n) \qquad t = 0, \pm1, \pm2, \ldots \qquad (14.1)$$

where the coefficients, b_n, are restricted to:

$$\sum_{n=-\infty}^{+\infty} b_n^2 < \infty \qquad (14.2)$$

The time series $\{y(t): t = 0, \pm1, \pm2, \ldots \}$ is completely characterized by the coefficients $\{b_n\}$ and can be thought of as a linear transformation of the white noise process represented by $\xi(t)$. The white noise time series $\{\xi(t): t = 0, \pm1, \pm2, \ldots \}$ characterizes the white noise process and is completely described by its mean, autocovariances, and spectral density. The mean of the white noise process is zero

$$E\{\xi(t)\} = 0 \qquad (14.3)$$

and the autocovariances are:

$$C(k) = E\{\xi(t) \, \xi(t-k)\} = \begin{cases} \sigma^2, & k = 0 \\ 0, & k \neq 0 \end{cases} \qquad (14.4)$$

The power spectral density function is the Fourier transform of the auto-

covariance function:

$$S_{\xi}(\omega) = \Delta t \sum_{k=-\infty}^{+\infty} C(k) e^{-j\omega k \Delta t} = \sigma^2 \Delta t \qquad (14.5)$$

The reader should be made aware that the notation in this chapter will differ from that in Appendix I. Also, subscripted variables and functions may appear with actual subscripts or with an index in parentheses. The sampling interval in all equations will be represented by Δt.

For practical analysis considerations, the time series generated by a moving average process is one-sided:

$$y(t) = \sum_{n=0}^{K} b_n \xi(t-n) \qquad (14.6)$$

The process and the resulting time series are characterized by the $K+1$ coefficients $\{b_n: n = 0, 1, 2, 3, \ldots K\}$. The value of $y(t)$ depends only upon the b_n's and $K+1$ present and past values of $\xi(t)$.

The time-series for a one-sided moving average process can be synthesized numerically by first generating the white noise sequence with a random number generator and then doing the linear operations described by Equation 14.6. This gives

$$y(t) = b_0 \xi(t) + b_1 \xi(t-1) + \ldots + b_K \xi(t-K) \qquad (14.7)$$

for all $t = 0, \pm 1, \pm 2, \ldots$.

The power spectrum for a moving average process is obtained by using a digital filtering analogy. A digital filter convolves the white noise sequence with the filter coefficients $\{b_n\}$ to produce the output time series. Since the spectrum of the input white noise sequence is flat, the

spectrum of the output time series will be the amplitude response of the filter multiplied by the constant input spectrum.

A look at the convolution and z-transform properties of a digital filter will help provide better understanding of the autoregressive spectral estimator. The output, y(t), of a digital filter is the convolution of an input time series, x(t), with the filter weights $\{b_k\}$:

$$y(t) = \sum_{k=-\infty}^{+\infty} b_k x(t-k) \qquad t = 0, \pm1, \pm2, \ldots \qquad (14.8)$$

To obtain the filter <u>weighting sequence</u> we define the impulse response of a linear filter, g(t), as the filter output in response to a delta function input. In the sampling domain, the sampled impulse response or weighting sequence is:

$$b_n = \frac{1}{\Delta t} g(n\Delta t) \qquad (14.9)$$

From z-transform theory we know that the convolution theorem in the transform domain (Equation 5A.8) is:

$$Y(Z) = G(Z)X(Z) \qquad (14.10)$$

The next step is to define what is meant by the transfer function, $G(Z)$.

From basic filter theory we know that a complex transfer function, $G(\omega)$, is defined for sinusoidal inputs $(x(t) = \sin \omega t)$ by using the relation

$$y(t) = |G(\omega)| \sin(\omega t + \phi(\omega)) \qquad (14.11)$$

and for complex sinusoidal inputs $(x(t) = e^{+j\omega t})$ as:

$$y(t) = |G(\omega)| e^{+j\phi(\omega)} e^{+j\omega t} \qquad (14.12)$$

In the same manner, the transfer function for the digital filter is obtained by applying a complex sinusoidal input $(x(t) = e^{+j\omega t})$ and factoring the output into the product of the input and a transfer function as shown in (14.12). When this is done for the convolution sequence given in (14.8) the result is:

$$y(t) = \sum_{k=-\infty}^{+\infty} b_k e^{+j\omega(t-k\Delta t)} = e^{+j\omega t} \sum_{k=-\infty}^{+\infty} b_k e^{-j\omega k\Delta t} \qquad (14.13)$$

The complex transfer function for the digital filter can now be identified as:

$$G(\omega) = \sum_{k=-\infty}^{+\infty} b_k e^{-j\omega k\Delta t} \qquad (14.14)$$

The filter weights or sampled impulse response can be determined from the transfer function by the transform:

$$b_k = \frac{1}{2\pi} \int_{-\pi}^{+\pi} G(\omega) e^{+j\omega k\Delta t} d\omega \qquad (14.15)$$

The single-sided z-transform for a causal filter is determined from (14.14) by substituting $Z = e^{+j\omega\Delta t}$ to generate the Z-transform of the filter weighting series:

$$G(Z) = B(Z) = \sum_{n=0}^{K} b_n Z^{-n} \qquad (14.16)$$

The continuous spectral density for the moving average process can now be determined by driving the digital filter with white noise and determining the output spectrum. The relationship between input and output spectral densities (Equation 5B.8) becomes:

$$S_y(\omega) = |G(\omega)|^2 S_x(\omega)$$

$$= |G(\omega)|^2 S_\xi(\omega) \tag{14.17}$$

Using (14.5) and (14.14) the final result is:

$$S_y(\omega) = \Delta t \sigma^2 \left| \sum_{k=-\infty}^{+\infty} b_k e^{-j\omega k \Delta t} \right|^2 \tag{14.18}$$

Likewise, the power spectral density for the one-sided process becomes:

$$S_y(\omega) = \Delta t \sigma^2 \left| \sum_{n=0}^{K} b_n e^{-j\omega k \Delta t} \right|^2 \tag{14.19}$$

The continuous spectral density can also be obtained by evaluation of the z-transform on the unit circle:

$$S_y(\omega) = \Delta t \sigma^2 |B(Z)|^2, \quad Z = e^{+j\omega \Delta t}, \quad |\omega| \le \frac{\pi}{\Delta t} \tag{14.20}$$

The continuous spectral density function for a moving average process is periodic with period $2\pi/\Delta t$. Usually only the principal spectrum, $|\omega| \le \pi/\Delta t$, is of interest.

We now define a time series $\{x(t): t = 0, \pm 1, \pm 2, \ldots \}$ as representing a weakly stationary (covariance stationary) finite autoregressive process if it satisfies the K-th order autoregressive series:

$$\sum_{n=0}^{K} a_n x(t - n) = \xi(t) \qquad t = 0, \pm 1, \pm 2 \ldots \tag{14.21}$$

The autoregression must satisfy the conditions (Koopmans, 1974)

$$E\{x(s) \xi(t)\} = 0 \quad \text{for all } s < t \tag{14.22}$$

and:

$$a_o = 1, \quad a_K \neq 0, \quad \sum_{n=0}^{K} a_n^2 < \infty \tag{14.23}$$

The finite autoregressive series is now written as:

$$x(t) - \sum_{n=1}^{K} a_n x(t-n) = \xi(t) \tag{14.24a}$$

$$x(t) - a_1 x(t-1) - a_2 x(t-2) - \ldots - a_K x(t-K) = \xi(t) \tag{14.24b}$$

The power spectrum for a finite autoregressive series can be obtain both from a digital filtering analogy and from a one-to-one correspondence with a moving average process. A digital filter operating on the time series $\{x(t): t = 0, \pm 1, \pm 2 \ldots \}$ produces the white noise sequence $\{\xi(t): t = 0, \pm 1, \pm 2, \ldots \}$. This special type of filter is referred to as a prewhitening filter by most authors (see Chapter IX). It is a simple matter to define the relationship between input and output spectral densities as

$$S_x(\omega) \, |A(\omega)|^2 = S_\xi(\omega) \tag{14.25}$$

and consequently:

$$S_x(\omega) = \frac{1}{|A(\omega)|^2} S_\xi(\omega) = \frac{\sigma^2 \Delta t}{|A(\omega)|^2} \tag{14.26}$$

The z-transform of the digital filter is

$$A(Z) = \sum_{n=0}^{K} a_n Z^{-n} \tag{14.27}$$

and the transfer function in the frequence domain is obtained by evaluating $A(Z)$ on the unit circle:

$$\left| A(\omega) \right| = \left| A(Z) \right| \Big|_{Z=e^{+j\omega\Delta t}} = \left| \sum_{n=0}^{K} a_n e^{-j\omega n \Delta t} \right| \tag{14.28}$$

Koopmans (1974, p. 218) has shown that if A(Z) has no zeros on or outside the unit circle, the linear filter can always be inverted and $1/A(\omega)$ is square integrable.

The equivalence of a finite moving average and a finite autoregressive series can be shown by applying a Fourier series expansion for the inverted filter and constraining the Fourier coefficients to those which will satisfy the boundary conditions of Equations 14.22 and 14.23. The infinite moving average formulation is

$$\frac{1}{A(\omega)} = \sum_{k=-\infty}^{+\infty} b_k e^{-j\omega k \Delta t} = \left| G(\omega) \right| e^{+j\phi(\omega)} \tag{14.29}$$

and it follows from Equations 14.1, 14.12, 14.13, and 14.14 that the finite autoregressive series can be expressed as a moving average:

$$x(t) = \sum_{k=-\infty}^{+\infty} b_k \xi(t-k) \tag{14.30}$$

In order for the moving average to satisfy the boundary conditions in Equations 14.22 and 14.23 it is necessary and sufficient (Koopmans, 1974) that:

$$E\{x(s)\,\xi(t)\} = 0 \tag{14.31}$$

for $s = (t-1)$, $(t-2)$, ... This can be shown by taking the expected value using Equation 14.30:

$$E\{x(s)\,\xi(t)\} = \sum_{k=-\infty}^{+\infty} b_k\, E\{\xi(s-k)\,\xi(t)\} \tag{14.32}$$

Using the identity, $E\{\xi(s-k)\,\xi(t)\} = \delta(s-j-t)\sigma^2$, (14.32) can be further reduced to show:

$$\sum_{k=-\infty}^{+\infty} b_k\, \delta(s-j-t)\sigma^2 = b_{s-t}\sigma^2 = 0 \tag{14.33}$$

and this implies the boundary condition:

$$b_{-1} = b_{-2} = b_{-3} = \ldots = 0 \tag{14.34}$$

For $s = t$, the expected value in (14.32) becomes

$$E\{x(t)\,\xi(t)\} = b_0\sigma^2 \tag{14.35}$$

but from Equation 14.24a we know that

$$E\{x(t)\,\xi(t)\} = E\{\xi^2(t)\} = \sigma^2 \tag{14.36}$$

so that $b_0 = 1$ is the final boundary condition.

In conclusion, a weakly stationary time series satisfying Equations 14.24 will have a one-sided moving average representation given by:

$$x(t) = 1 + \sum_{n=1}^{K} b_n\xi(t-n) \tag{14.37}$$

For a covariance stationary finite autoregression to exist, it is sufficient that all the zeros of $B(Z)$ lie inside the unit circle. The z-transform of a one-sided moving average is related to the z-transform of the autoregression as:

$$A(Z) = \frac{1}{B(Z)} \tag{14.38}$$

The continuous power spectral density function for a finite auto-regression is written as:

$$S_x(\omega) = \sigma^2 \Delta t \left| 1 + \sum_{n=1}^{K} b_n e^{-j\omega n \Delta t} \right|^2 \tag{14.39}$$

or:

$$S_x(\omega) = \frac{\sigma^2 \Delta t}{\left| 1 - \sum_{n=1}^{K} a_n e^{-j\omega n \Delta t} \right|^2} \tag{14.40}$$

The stationary autocovariances for the autoregressive process are defined as:

$$C(k) = E\{x(t) \, x(t-k)\} = C(-k) \tag{14.41}$$

The Yule-Walker equations (Equation A1.31) relate the autoregression co-efficients, a_n, and the stationary autocovariances:

$$C(k) = \sum_{n=1}^{K} a_n C(k-n), \quad k = 1, 2, \ldots K \tag{14.42a}$$

$$C(k) = a_1 C(k-1) + a_2 C(k-2) + \ldots a_K C(k-K) \tag{14.42b}$$

A useful estimate of the variance of the white noise sequence can be obtained by combining Equations 14.36 and 14.37 to give:

$$E\{x(t) \, \xi(t)\} = E\{x(t) \sum_{n=0}^{K} a_n x(t-n)\} = \sum_{n=0}^{K} a_n C(k) = \sigma^2 \tag{14.43}$$

This estimate may be written as:

$$\sigma^2 = C(0) + \sum_{n=1}^{K} a_n C(n) \tag{14.44}$$

To obtain the estimated power spectral density of a finite sample $\{\hat{x}(t): t = 0, 1, 2, \ldots (M-1)\}$ of the "true" time series $\{x(t)\}$, the estimated autocovariances, $\hat{C}(k)$, and the estimated autoregressive coefficients, $\hat{a}_n$, must be determined by appropriate numerical estimation procedures.

One commonly used approach to this estimation problem is to compute estimated autocovariances from the definition:

$$\hat{C}(k) = \frac{1}{M-k} \sum_{t=0}^{M-k} \hat{x}(t)\hat{x}(t-k) \qquad (14.45)$$

Next the Yule-Walker equations are used to define a linear set of equations in $\hat{C}(k)$ and $\hat{a}_n$:

$$\begin{bmatrix} \hat{C}(1) \\ \hat{C}(2) \\ \cdot \\ \cdot \\ \cdot \\ \hat{C}(K) \end{bmatrix} = \begin{bmatrix} \hat{C}(0) & \hat{C}(1) & \ldots & \hat{C}(K-1) \\ \hat{C}(1) & \hat{C}(0) & & \hat{C}(K-2) \\ \cdot & \cdot & & \cdot \\ \cdot & \cdot & & \cdot \\ \cdot & \cdot & & \cdot \\ \hat{C}(K-1) & \hat{C}(K-1) & \ldots & \hat{C}(0) \end{bmatrix} \begin{bmatrix} \hat{a}_1 \\ \hat{a}_2 \\ \cdot \\ \cdot \\ \cdot \\ \hat{a}_K \end{bmatrix} \qquad (14.46)$$

For initial calculations, the order of the process has been estimated as K. The $K \times K$ covariance matrix is inverted and the autoregressive coefficients are computed from:

$$\begin{bmatrix} \hat{a}_1 \\ \hat{a}_2 \\ \cdot \\ \cdot \\ \cdot \\ \hat{a}_k \end{bmatrix} = \begin{bmatrix} \hat{C}(0) & \ldots & \hat{C}(K-1) \\ \hat{C}(1) & \ldots & \hat{C}(K-2) \\ \cdot & \cdot \cdot \cdot & \cdot \\ \cdot & \cdot \cdot \cdot & \cdot \\ \cdot & \cdot \cdot \cdot & \cdot \\ \hat{C}(K-1) & \cdot \cdot \cdot & \hat{C}(0) \end{bmatrix}^{-1} \begin{bmatrix} \hat{C}(1) \\ \hat{C}(2) \\ \cdot \\ \cdot \\ \cdot \\ \hat{C}(K) \end{bmatrix} \qquad (14.47)$$

The spectrum of the estimated white noise sequence is generally not a con-

stant unless the sample is very large. The estimated autocovariance function for the approximate white noise sequence is written as:

$$\hat{R}_{\hat{\xi}}(k) = E\{\hat{\xi}(t) \, \hat{\xi}(t-k)\} \tag{14.48}$$

Substituting the autoregressive series of Equation 14.24a for both $\hat{\xi}(t)$ and $\hat{\xi}(t-k)$ gives

$$\hat{R}_{\hat{\xi}}(k) = E\{\sum_{n=0}^{K} \hat{a}_n \hat{x}(t-n) \sum_{p=0}^{K} \hat{a}_p \hat{x}(t-p-k)\}$$

$$= \sum_{n=0}^{K} \hat{a}_n \sum_{p=0}^{K} \hat{a}_p E\{\hat{x}(t-n) \, \hat{x}(t-p-k)\}$$

$$= \sum_{n=0}^{K} \sum_{p=0}^{K} \hat{a}_n \hat{a}_p \hat{C}(n-p+k) \tag{14.49}$$

for $k = 0, \pm 1, \pm 2, \ldots \pm (M-K)$.

The estimated spectral function $\hat{S}_{\hat{\xi}}(\omega)$ can be obtained from $\hat{R}_{\hat{\xi}}(k)$ by using a lag window function and a digital Fourier transform. A spectral density estimate for the white noise sequence can also be obtained using Equation 14.44 to give:

$$\hat{\sigma}^2 = \sum_{n=0}^{K} \hat{a}_n \hat{C}(n) \tag{14.50}$$

The estimated spectral density for these numerical techniques can be written as

$$\hat{S}_x(\omega) = \frac{\hat{S}_{\hat{\xi}}(\omega)}{|1 - \sum_{n=1}^{K} \hat{a}_n e^{-j\omega n \Delta t}|^2} \tag{14.51}$$

or:

$$\hat{S}_x(\omega) = \frac{\hat{\sigma}^2 \Delta t}{\left|1 - \sum_{n=1}^{K} \hat{a}_n e^{-j\omega n \Delta t}\right|^2} \tag{14.52}$$

Other methods of obtaining best estimates of $\hat{C}(k)$ and $\hat{a}_n$ may also be used effectively. Most methods employ a least-squares estimate that also constrains the covariance matrix so it will remain positive definite. This will constrain the spectral estimators to be positive over the entire frequency range. More about these estimators and the proper constraints will be given in Chapter XV.

XV. MAXIMUM ENTROPY SPECTRAL ESTIMATION

A. Introduction

A new criterion for estimating the continuous power spectral density function for a random time series (Stanley, 1975) was first proposed by Burg (1967). This estimator, called the Maximum Entropy Method (MEM), essentially maximizes the average entropy (Newman, 1977) over the information bandwidth using the estimated autocorrelation function. MEM was developed as a technique to minimize the effects of observer bias and reduce certain types of processing error on the spectral estimates. For example, one of the most noticeable differences between MEM processing and other commonly used techniques is that no window function selection is required.

It is important for the reader to realize that MEM spectral analysis is not meant to be a replacement for other techniques and it is not vastly superior to others. As with any estimation technique, MEM has its own strengths and weaknesses based upon an assumed process model. When reading the published literature on MEM it is most important to carefully assess the various assumptions and boundary conditions used to derive the published results.

As discussed previously in Chapter IX, all spectral estimators must use a particular model to fit empirical data. In addition, most apply smoothing and all apply extrapolation or a periodic extension to the data to obtain infinite data functions which conform to the selected criteria. Once an infinite estimate is obtained, the spectral density can be found using basic theory (Chapter IV). A summary of the commonly used models will help to put MEM spectral analysis in proper perspective.

The model for Fourier transform spectral analysis is based upon a periodic extension of the empirical data function. Constraints on this extension include assuming that the observation period T_N is equal to the Fourier period T_F, that the signal is bandlimited, and that the number of discrete spectral components does not exceed the number of data samples (adequate sampling). This model gives excellent results for many applications but can have serious deficiencies if the true process is not periodic. In Fourier transform spectral analysis only the amplitude spectrum is usually computed because the power spectrum is a trivial extension (Chapter XII, Section C). Many users object to using a periodic extension assumption and an amplitude spectrum for analyzing data. These users often prefer the Blackman-Tukey method.

The Blackman-Tukey model for spectral analysis assumes a zero extension of the estimated autocovariance function. This zero extension assumption is emphasized by the use of a lag window function which guarantees a zero value beyond some chosen lag value τ_m. Although this assumption is often unrealistic, it gives good results in many applications. Users of the Blackman-Tukey method most often complain about lack of spectral resolution, inefficient computation and use of empirical data, and negative spectral components.

A rigorous discussion of the properties of the various spectral estimators was given in Chapters VIII, IX, and X. As a rule the most commonly used power spectrum estimators compute an estimate of the autocovariance function, apply a window function to this estimate, and obtain the power spectrum from the Fourier transform of the result. This technique produces

an estimate that has the following deficiencies:

1. The inverse transform cannot reproduce the original estimated autocovariance function.

2. The lag window introduces spectral smoothing which decreases spectral resolution.

3. The lag window may produce a modified autocovariance function which could result in negative spectral components.

4. Most estimates of the autocovariance function use less data as the lag value increases thereby increasing statistical variability.

5. The estimate of the autocovariance function may be badly truncated.

6. The arbitrary choice of a lag window function may tempt the observer to choose the one that produces the "most agreeable" spectrum.

All of these deficiencies can be minimized or eliminated by using the MEM spectral estimator. The following results are obtained with MEM:

1. The estimate is constrained so that the inverse transform will exactly reproduce the original estimated autocovariance function.

2. MEM does not explicity use a lag window function and empirical test results show it produces a frequency resolution superior to other methods when short data records are employed.

3. MEM constrains the autocovariance matrix to be nonnegative definite so that only positive spectral components are produced.

4. MEM incorporates nearly all of the input data function for each step in the autocovariance estimate and hence reduces the problem of statistical variability for large lag values.

5. MEM produces an estimated autocovariance function that can be ex-
   trapolated to any desired order of lag and consequently eliminates
   the truncation problem.

6. Since MEM is a data adaptive method, the selection of a lag win-
   dow is implicit in the process and its use is transparent to the
   observer.

The maximum entropy criterion for spectral analysis will not reduce the
intrinsic spectral estimation errors (Chapter IX) of aliasing, statistical
variability, and lack of stationarity. These continue to be important
practical problems associated with all spectral estimation methods and
must be dealt with on an individual basis.

The Maximum Entropy Method of spectral analysis has the following
limitations and known deficiencies:

1. The validity of the spectral estimate relies on the assumption
   that the measured process can be adequately modeled by a finite
   autoregressive series. This requires a "noise-like" data function
   and a spectrum that is both continuous and bandlimited.

2. The observer must select an arbitrary order for the autoregressive
   process that is used to model the data. This selection intro-
   duces observer bias into the estimate because it controls the
   amount of spectral smoothing and hence resolution. A nonsub-
   jective solution to the problem of selecting an optimum order has
   not yet been solved (Parzen, 1969).

3. For estimations using a large order autoregression, the MEM algor-
   ithm may become numerically unstable. This occurs because the

locations of the zeros of the characteristic polynomial shift

slightly due to numerical truncation and fall very near or on the

unit circle.

In spite of these deficiencies, the MEM technique represents a powerful

tool for the estimation of time series spectra. Along with FFT, Blackman-

Tukey, and autoregressive techniques it should become a widely used method

of data analysis. Its properties and applications will now be presented

along with some derivations of fundamental concepts.

B. Fundamental Descriptions for MEM

The Maximum Entropy Method can be simply described as a technique for

obtaining an infinite autocovariance function from finite data. The em-

pirical time series is modeled with a finite order autoregressive series

and the resulting spectral estimate is constrained by maximizing the

average entropy. Practical algorithms may compute either the estimated

autocovariances or the autoregressive coefficients. The power spectral

density function is obtained by taking the Fourier transform of the auto-

covariance function or by using the autoregressive spectral estimator.

More than one viewpoint can be used to summarize the fundamental

characteristics of MEM spectral analysis. The three most common view-

points will now be discussed. The original viewpoint is that MEM is

equivalent to maximizing the average spectral entropy of a Gaussian, band-

limited time series subject to the constraint that the estimated power

spectral density and the estimated autocorrelation function form an exact

Fourier transform pair (Chen and Stegen, 1974; Newman, 1977). This can

also be interpreted as determining an optimum power spectral density func-

tion that keeps the entropy of the empirical time series stationary with respect to the selection of extrapolated values of the estimated autocorrelation function (Radoski et al., 1975).

A second viewpoint is that MEM is equivalent to an "optimum" method for extrapolating a truncated autocovariance function (Veltman et al., 1972). The criterion for "optimum" is that the entropy of the time series model must be maximized at each step of the extrapolation. Van den Bos (1971) has demonstrated that this criterion is equivalent to fitting the data with a finite autoregressive process model with a least-square-error criterion. This is sometimes referred to in the literature as fitting an all-pole model to the data. This nomenclature comes from the z-Transform description of the transfer function used to model the power spectrum (Stanley, 1975). This type of estimator contains only poles (no zeros except at the origin) in the z-plane.

The third viewpoint is that MEM is equivalent to modeling the desired spectrum with the output of a filter driven with white noise. The empirical data function is processed to obtain the estimated filter spectral response. The filter has been variously termed a prewhitening filter, a Weiner prediction filter, and a least-squares inverse filter (see Chapter XIII). An equivalent mathematical model for the empirical data function is the convoltuion of a finite autoregressive series and a white noise series (Radoski et al., 1975). In this type of processing the input time series is converted to a white noise sequence (See Equation 14.24a) and the prewhitening filter is used to characterize the spectrum (Ulrych, 1972b).

A fourth viewpoint, which is actually a combination of the others, is that the entropy loss of the filter should be maximized subject to the constraint that the inverse transform of the MEM spectral estimate yield the exact autocorrelation values. As with the third viewpoint, a filter is found that can generate the correct autocorrelation function when driven with white noise but it must also reduce the entropy by a maximal amount. This viewpoint emphasizes the First Principle of Data Reduction (Chapter VII) because it minimizes the biasing effects of missing data.

C. Entropy Definitions for MEM

The concept of entropy is used in many scientific disciplines. Entropy as a thermodynamic state function in statistical mechanics is a measure of the randomness of the system. Entropy quantifies the lack of knowledge about the exact state of the system at any instant in time. In information theory (Beckmann, 1967) the entropy of a source of information is defined as the average self-information per state of the system. In communication systems the entropy is often called the average information rate in bits-per-symbol. The entropy of a signal will be maximum when all states or symbols are equally likely. Two concepts that will be used in MEM derivations are those of a entropy power and entropy loss in a linear filter. Mathematical definitions will now be given for the various entropy quantities.

The entropy of a discrete system of N states, E_n, with probabilities, p_n, is given by:

$$H = - \sum_{n=1}^{N} p_n \ln(p_n) \tag{15C.1}$$

If H is maximized subject to the constraint that the sum of all probabilities is equal to unity, the distribution of probabilities that yields maximum entropy is given by (Beckmann, 1967):

$$p_n = \frac{1}{N} \qquad n = 1, 2, 3, \ldots, N \tag{15C.2}$$

A convenient definition for the entropy of a continuous distribution of a single variable is (Goldman, 1953; Beckmann, 1967):

$$H = -\int p(x) \ln(p(x)) dx \tag{15C.3}$$

If H is maximized subject to the constraint that the variance of x remains constant, the calculus of variations solution gives a Gaussian distribution. The entropy of a Gaussian distribution is given by:

$$H = \ln(2\pi e \sigma_x^2)^{\frac{1}{2}} \tag{15C.4}$$

It is also true that, for a constant entropy, a Gaussian distribution has the smallest variance of all possible distributions.

An excellent discussion on the effect of a linear transformation on entropy has been given by Goldman (1953). In essence Goldman shows that the entropy of a signal vector y_i produced by a linear transformation of the vector x_i is given by

$$H_y = H_x + \ln \left| a_{ij} \right| \tag{15C.5}$$

where $\left| a_{ij} \right|$ is the determinant of the transformation matrix defined by:

$$y_i = \sum_{j=1}^{N} a_{ij} x_j \tag{15C.6}$$

Random noise may be characterized by sampling points in the time domain which are statistically independent and have distributions which are Gaussian. The entropy per degree-of-freedom for random noise is

$$h_n = \ln(2\pi e\, \sigma_n^2)^{\frac{1}{2}} \qquad (15C.7)$$

where σ_n^2 is the variance of the noise. To obtain the total entropy it is necessary to multiply by the Nyquist frequency, $f_N = 1/2\Delta t$, and the duration or observation period, T_N, of the signal:

$$H_n = 2f_N T_N h_n \qquad (15C.8)$$

The entropy power (Goldman, 1953) of a signal is:

$$P_e = \frac{1}{2\pi e}\, e^{2h_n} \qquad (15C.9)$$

For Gaussian noise the entropy power is equal to the variance. Entropy power is always less than or equal to the time average power.

Entropy loss in a linear filter is a function only of the frequency response of the filter and is most easily described in the frequency domain. The derivation for entropy change in a linear filter is analogous to that for a linear transformation since filtering is a linear transformation process. For N sampling points in the frequency domain the entropy at the output, H_y, is related to the entropy at the input, H_x, using (Goldman, 1953)

$$H_y = H_x + \sum_{n=1}^{N} \ln(G_o^2 |G(f_n)|^2) \qquad (15C.10)$$

where G_o is the filter gain and $G(f)$ is the normalized frequency response. In the limit as the frequency sampling interval goes to zero and the

frequency response becomes continuous, the entropy change becomes:

$$H_y = H_x + T_N \int_0^{f_N} \ln(G_o^2 |G(f)|^2) df \qquad (15C.11)$$

The entropy-per-degree-of-freedom can be obtained by dividing (15C.11) by $2f_N T_N$:

$$h_y = h_x + \frac{1}{2f_N} \int_0^{f_N} \ln(G_o^2 |G(f)|^2) df \qquad (15C.12)$$

The change in entropy is obtained both from the filter shape and the filter gain. The integral can be separated into:

$$\frac{1}{2f_N} \int_0^{f_N} \ln|G(f)|^2 df + \ln(G_o) \qquad (15C.13)$$

In most of the literature and for the rest of this text the filter gain is assumed to be normalized to unity and only the integral term is considered.

The entropy power at the output of the filter is given by:

$$P_e = \frac{1}{2\pi e} e^{2h_y} \qquad (15C.14)$$

If the class of power spectra to be analyzed by MEM is restricted to those that can be represented by a linear filter of finite length, we can define an average spectral entropy density or spectral entropy rate as:

$$h_x = \frac{1}{4f_N} \int_{-f_N}^{+f_N} \ln[S_x(f)] df \qquad (15C.15)$$

The power spectral density function, $S_x(f)$, is two-sided and analogous to $|G(f)|^2$. This is the definition that will be used for MEM (Lacoss, 1971).

D. Mathematical Bases for MEM

A good mathematical description of maximum entropy spectral analysis can be presented using any or all of the viewpoints discussed in Section B. Three somewhat independent derivations will now be given.

1. Maximum average spectral entropy basis

The basis first proposed by Burg (unpublished 1967) maximizes the spectral entropy subject to the constraint that the inverse Fourier transform gives the exact values of the finite autocorrelation function. For a Gaussian process with a continuous bandlimited power spectrum, this entropy measure (Equation 15C.15; Smylie et al., 1973) is represented by the integral:

$$h_x = \frac{1}{4f_N} \int_{-f_N}^{+f_N} \ln[S_x(f)]df \qquad (15D.1)$$

Restrictions on $S_x(f)$ are that it be nonzero in the Nyquist frequency interval and that it be representable as the power transfer function of a linear filter. $S_x(f)$ is considered to be the "true" power spectral density of the process and f_N is the maximum frequency of nonzero spectral content. This would be the folding frequency for a sampling system or the Nyquist frequency for a bandlimited signal.

From previous theoretical considerations we know that the power spectral density function and the autocorrelation function form a Fourier transform pair as represented by the Wiener-Khinchine relations (Equation 4A.9). From transform theory it follows that the inverse Fourier transform

of the continuous and bandlimited spectral density produces an autocorrelation function which may exist over the entire autocorrelation domain. It also follows that the autocorrelation function cannot be finite in extent because two finite functions cannot form an exact Fourier transform pair (uncertainty principle). If either the autocorrelation function or the spectral density are exactly known, the other may be computed using the transformation:

$$\mathcal{F}^{-1}\{S_x(f)\} = \int_{-f_N}^{+f_N} S_x(f)e^{+j2\pi f\tau}df = R_x(\tau) \tag{15D.2}$$

A capital R is now used to represent autocorrelation but it has the same meaning as small r in Chapter XIII.

Of course for practical problems the data function is finite and only an estimate of the true power spectrum can be obtained. A finite data function produces an estimated autocorrelation that is both truncated <u>and</u> statistically variable. Both of these important effects must be accounted for in a practical MEM spectral estimator. As a start we will first consider the problem of truncation.

To be able to satisfy Equation 15D.2 the truncated autocorrelation function must be extrapolated in some optimum manner. To examine this possibility the autocorrelation function is separated into a "known" component, $\hat{R}_x(\tau)$, defined in the interval $|\tau| \leq \tau_m$ and an "unknown" component $\tilde{R}_x(\tau)$ representing the autocorrelation for all lags $|\tau| > \tau_m$. The inverse transform relationship of (15D.2) can now be separated into the two components:

$$\int_{-f_N}^{+f_N} \overset{\mathtt{A}}{S}_x(f)e^{+j2\pi f\tau}\,df = \overset{\mathtt{A}}{R}_x(\tau) \qquad |\tau| \le \tau_m \qquad\qquad (15D.3)$$

$$\int_{-f_N}^{+f_N} \overset{\mathtt{A}}{S}_x(f)e^{+j2\pi f\tau}\,df = \tilde{R}_x(\tau) \qquad |\tau| > \tau_m \qquad\qquad (15D.4)$$

τ_m will be defined as the maximum lag at which values for $R_x(\tau)$ are known. The so-called "known" component plays a dual role in MEM analysis. For developing the theory it is assumed to be a truncated version of the exact or "true" autocorrelation function while in actual application it is an estimate based on empirical data. For the analysis to follow it will be assumed to be exact while in Sections F and G it will be an estimate.

When the maximum entropy estimate satisfying (15D.3) is obtained, the "unknown" component given by (15D.4) is completely specified. It can be referred to as a maximum entropy extrapolation of the autocorrelation function. From this viewpoint the maximum entropy criterion is equivalent to the a priori assumption that the "best" spectral estimate must be the most random of all possible estimates that is still consistent with the "known" (but truncated) autocorrelation function. This also means that the extrapolated part of the autocorrelation function adds the least amount of "information" to the spectrum.

The derivation that now follows is based on the calculus of variations material presented in Part J of Appendix I. The entropy measure that will be maximized is given in Equation 15D.1 and the constraint equation will be a sampled version of (15D.3). The extra degrees-of-freedom which allow h_x to be maximized are represented by Equation 15D.4.

First, the use of a sampled version of Equation 15D.3 must be justified. Now because we are interested only in $S(f)$ defined in the interval $|f| \leq f_N$ it is possible to represent $S(f)$ either by Equation 15D.2 or as a periodic function with period $2f_N$. The mathematical restriction imposed by this representation is that we never try to use it for $|f| > f_N$. The fact that a continuous and periodic spectrum can be represented by an infinite sum of sampled autocorrelation values (Stanley, 1975) leads to the selection of the following infinite series and basis set for $S(f)$:

$$S_x(f) = \Delta\tau \sum_{k=-\infty}^{+\infty} R_x(k\Delta\tau)e^{-j2\pi f k\Delta\tau} \qquad (f_N \leq \frac{1}{2\Delta\tau}) \qquad (15D.5)$$

The sampling period in the autocorrelation domain is related to the spectral width by $\Delta\tau = 1/2f_N$. To verify that this basis is valid, it is substituted into the following sampled version of (15D.2):

$$\int_{-f_N}^{+f_N} S_x(f)e^{+j2\pi f n\Delta\tau}df = R_x(n\Delta\tau) \qquad (15D.6)$$

After substitution, integration and summation can be interchanged to give the form:

$$\Delta\tau \sum_{k=-\infty}^{+\infty} R_x(k\Delta\tau) \int_{-f_N}^{+f_N} e^{+j2\pi f(n-k)\Delta\tau}df = R_x(n\Delta\tau) \qquad (15D.7)$$

To show that this is an identity, the form of the integral is compared with the representation of the Kronecker delta function given in Equation A2.33. This representation is obtained by identifying $f_N = 1/2\Delta\tau$ and $T = 2f_N$ to give:

$$\Delta\tau \int_{-f_N}^{+f_N} e^{+j2\pi f(n-k)\Delta\tau}df = \delta_{nk} \qquad (15D.8)$$

The identity in Equation 15D.7 becomes

$$\sum_{k=-\infty}^{+\infty} R_x(k\Delta\tau)\delta_{nk} = R_x(n\Delta\tau) \tag{15D.9}$$

and we have shown the representation in (15D.5) to be valid.

A corresponding sampled representation for Equation 15D.3 is obtained by defining a maximum known lag index $M = \tau_m/\Delta\tau$. This gives $2M+1$ known lags to define the bandlimited spectrum. The constraint equation and corresponding series definition for $\hat{S}(f)$ become:

$$\int_{-f_N}^{+f_N} \hat{S}_x(f)e^{+j2\pi fn\Delta\tau}df = \hat{R}_x(n\Delta\tau) \tag{15D.10}$$

$$\{n = 0, \pm1, \pm2, \ldots, \pm M\}$$

$$\hat{S}_x(f) = \Delta\tau \sum_{k=-M}^{+M} \hat{R}_x(k\Delta\tau)e^{-j2\pi fk\Delta\tau} \tag{15D.11}$$

From the calculus-of-variations solution and Equations 15D.1 and 15D.10 we can identify the following terms for the Euler-Lagrange equation:

$$F(f,\hat{S}_x(f)) = \frac{1}{4f_N} \ln[\hat{S}_x(f)] \tag{15D.12}$$

$$Q_n(f,\hat{S}_x(f)) = \hat{S}_x(f)e^{+j2\pi fn\Delta\tau} \tag{15D.13}$$

The Euler-Lagrange equation is:

$$\frac{\partial}{\partial\hat{S}_x(f)} [F(f,\hat{S}_x(f)) - \sum_{n=-M}^{+M} \lambda_x(n)Q_n(f,\hat{S}_x(f))] = 0 \tag{15D.14}$$

The partial derivatives are

$$\frac{\partial F}{\partial S} = \frac{1}{4f_N \hat{S}_x(f)} \qquad \frac{\partial Q}{\partial S} = e^{+j2\pi f n \Delta \tau} \qquad (15D.15)$$

and the equation is evaluated to be:

$$\frac{1}{4f_N \hat{S}_x(f)} - \sum_{n=-M}^{+M} \lambda_x(n) e^{+j2\pi f n \Delta \tau} = 0 \qquad (15D.16)$$

From this solution we see that both the Lagrange multipliers and the inverse spectrum must be finite. This reaffirms the constraint of nonzero $\hat{S}(f)$ on MEM spectral estimates.

The next step in the solution is to solve the Euler-Lagrange equation for $\hat{S}_x(f)$ in terms of the Lagrangian multipliers, $\lambda_x(n)$, and frequency, f. This solution is substituted into the constraint equation and the 2M+1 values of the autocorrelation function are used to solve for the 2M+1 values of $\lambda_x(n)$, the Lagrange multipliers. The solution is completed when the $\lambda_x(n)$ are used in the explicit equation for $\hat{S}_x(f)$. The explicit equation is obtained by rearranging (15D.16):

$$\hat{S}_x(f) = \frac{1}{4f_N} \left[\sum_{n=-M}^{+M} \lambda_x(n) e^{+j2\pi f n \Delta \tau} \right]^{-1} \qquad (15D.17)$$

It is pointed out at this time that Equation 15D.16 is a finite and sampled version of Equation 15E.6.

The direct method of solving 15D.17 is to use a Laurent series expansion and equate it term-for-term to Equation 15D.11. An alternate method which derives the spectral estimate directly in terms of the autocorrela-

tion coefficients used in the Burg algorithm (Section G) will be presented.

The derivation essentially follows one given by Ulrych in Smylie et al.,

(1973).

The z-transforms of Equations 15D.17 and 15D.5 are equated to give:

$$\Delta\tau R(z) = \frac{1}{4f_N \Lambda(z)} \qquad\qquad z = e^{-j2\pi f \Delta\tau} \qquad (15D.18)$$

The polynomial, $\Lambda(z)$, represents the double-sided z-transform of the series

in Equation 15D.17 and, as such, is an ideal (not estimated) representation

of the Lagrange multipliers. Conceptually, $R(z)$ is also the infinitely

long Laurent series expansion of $1/\Lambda(z)$. If the z-transform of (15D.11) is

represented by $\Delta\tau \hat{R}(z)$, then $R(z)$ and $\hat{R}(z)$ must have equal coefficients for

like powers of z. We also know that $\lambda_x(n) = \lambda^*(-n)$ and $R_x(n\Delta\tau) = R_x^*(-n\Delta\tau)$

because $\hat{S}_x(f)$ must be a real function. Since these coefficients are Hermi-

tian, the polynomials $R(z)$ and $\Lambda(z)$ can be factored into the product of two

polynomials and Equation 15D.18 can now be written as (Smylie et al, 1973):

$$\Delta\tau C(z)C^*(1/z^*) = \frac{1}{4f_N Q(z)Q^*(1/z^*)} \qquad (15D.19)$$

The new polynomials are defined by:

$$R(z) = C(z)C^*(1/z^*) \qquad (15D.20)$$

$$\Lambda(z) = Q(z)Q^*(1/z^*) \qquad (15D.21)$$

The symbol Q for the polynomial must not be confused with that for the

generalized function in the Euler-Lagrange equation of (15D.13). A similar

process for obtaining a polynomial product is the spectral factorization

for rational spectral densities discussed in standard texts on signal anal-

ysis (Cooper and McGillem, 1971).

The system of equations which represent the maximum entropy solution,

for example Equation 13.48 in matrix form, can be written in series form as

$$\sum_{k=0}^{K} a_K(n)\hat{R}_x(k+n) = -P_K \delta_o(k) \qquad (15D.22)$$

where $a_K(0) = -1$ and $\delta_o(k)$ is the Kronecker delta function. The mean-square

error of the estimate will be represented by P_K which is equivalent to the

notation $\hat{\sigma}_K^2$.

We now implement a mathematical technique that will help simplify the

solution. The system of equations represented by (15D.22) is augmented with

the arbitrary series

$$\begin{aligned} h(k) &= 0 \qquad \{k = 0, 1, 2, \ldots, K\} \\ &\neq 0 \qquad \{k = -1, -2, -3, \ldots, -K\} \end{aligned} \qquad (15D.23)$$

to give:

$$\sum_{n=0}^{K} a_K(n)\hat{R}_x(k+n) = -P_K \delta_o(k) - h(k)$$
$$\{k = 0, \pm 1, \pm 2, \ldots, \pm K\} \qquad (15D.24)$$

The z-transform of (15D.24) is the start of the solution:

$$A(z)\hat{R}(z) = P_K + H(z) \qquad (15D.25)$$

$$A(z) = 1 - a_K(1)z - a_K(2)z^2 - \ldots - a_K(K)z^K \qquad (15D.26)$$

$$H(z) = h(-1)z^{-1} + h(-2)z^{-2} + \ldots + h(-K)z^{-K} \qquad (15D.27)$$

$A(z)$ is the z-transform of the digital filter (Chapter XIV) characterizing the autoregressive process.

Since $\hat{R}(z)$ also consists of Hermitian coefficients it likewise can be factorized into the special form

$$\hat{R}(z) = U(z)U^*(1/z^*) = U(z)V(z)/z^K \tag{15D.28}$$

where the product polynomials are defined by:

$$U(z) = u_0 + u_1 z + \ldots + u_K z^K \tag{15D.29}$$

$$V(z) = u_0^* z^K + u_1^* z^{K-1} + \ldots + u_K^* \tag{15D.30}$$

Substituting (15D.28) into (15D.25) and dividing gives the desired result:

$$A(z)U(z) = \frac{P_K z^K}{V(z)} + \frac{H(z)z^N}{V(z)} \tag{15D.31}$$

The rather elaborate means by which we have arrived at Equation 15D.31 are necessary so that the concluding steps, including a polynomial division, are easier.

Typical terms on the left-hand side of (15D.31) are:

$$A(z)U(z) = u_0 + [u_1 - a_K(1)u_0]z + \ldots + [u_K - u_0 a_K(K)]z^K \ldots$$

$$- [u_K a_K(K-1) + a_K(K)u_{K-1}]z^{2K-1} - u_K a_K(K)z^{2K} \tag{15D.32}$$

This is a polynomial of degree $+2K$. Typical terms for the polynomial divisions on the right hand side are:

$$\frac{P_K z^K}{V(z)} + \frac{H(z)z^K}{V(z)} = [\frac{P_K}{u_0^*} + (\frac{h_{-1}}{u_0^*} - \frac{u_1^*}{u_0^{*2}})z^{-1} + \ldots + (\cdot)z^{-K}] \tag{15D.33}$$

Since the exponents on the left-hand side are positive and those on the right-hand are negative, equating equal powers of z on both sides of Equation 15D.31 gives the trivial result:

$$u_o = \frac{P_K}{u_o^*} \tag{15D.34}$$

The coefficients of all other powers of z are zero so (15D.31) reduces to the result:

$$A(z)U(z) = u_o = \frac{P_K}{u_o^*} \tag{15D.35}$$

In a similar manner we can also obtain the result:

$$A^*(1/z^*)U^*(1/z^*) = u_o^* = \frac{P_K}{u_o} \tag{15D.36}$$

Combining these results and relating them to (15D.28) gives the z-transform of $\hat{R}_x(k\Delta\tau)$ in terms of the z-transform of the autoregressive series:

$$\hat{R}(z) = U(z)U^*(1/z^*) = \frac{P_K}{A(z)A^*(1/z^*)} \tag{15D.37}$$

Substituting this result into Equation 15D.11 and evaluating the z-transform on the unit circle between 0 and π gives the maximum entropy estimate of the power spectral density function:

$$\hat{S}_x(f) = \frac{\Delta\tau P_K}{A(e^{-j2\pi f\Delta\tau})A^*(e^{-j2\pi f\Delta\tau})} \tag{15D.38}$$

From Equation 15D.26 we get the identity

$$A(e^{-j2\pi f\Delta\tau}) = 1 - \sum_{k=1}^{K} a_K(k)e^{-j2\pi fk\Delta\tau} \qquad (15D.39)$$

and Equation 15D.38 can be put in the usual form given by Equation 15F.1.
In the cause of academic curiosity we can determine the Lagrange multipliers
from

$$\Lambda(Z) = \frac{1}{2P_K} A(Z)A^*(1/Z^*) \qquad (15D.40)$$

where:

$$\Lambda(Z) = \sum_{n=-K}^{K} \lambda_x(n)Z^{-n} \qquad (15D.41)$$

The solution is obtained by equating like powers of Z in the equations:

$$\sum_{n=-K}^{+K} \lambda_x(n)Z^{-n} = [1 - \sum_{k=1}^{K} a_K(k)Z^k][1 - \sum_{k=1}^{K} a_K(k)Z^{-k}] \qquad (15D.42)$$

This completes the derivation of the maximum entropy spectral estimate.
Alternate derivations are given in the next two parts of this section.

2. Autocorrelation function extrapolation

The following description of the MEM spectral estimator is based on
the desirable property that the autocovariance matrix for a real finite
autoregressive process must be semipositive definite (Veltman et al., 1972).
This implies that the determinant of the autocovariance matrix must be non-
negative. This condition guarantees that the resulting estimated power
spectral density function will be nonnegative over the interval $|f| \leq f_N$.
The analysis using the autocovariance matrix is based on the fact that it
can be used to obtain the estimated spectrum by applying the Fourier trans-

form directly or by generating the autoregressive coefficients (Chapter XIV) and using the autoregressive spectral estimator.

As in the previous section we will assume that the first $2N+1$ autocorrelations are known exactly and that the process is stationary and Gaussian. The maximum entropy extrapolation problem is to find the $(N+1)$ autocovariance value by maximizing the entropy defined by the autocovariance matrix.

To simplify the matrix notation for this section we will use the abbreviation $r(n) = R_x(n\Delta\tau)$. The autocovariance matrix of order N will be represented by $R(N)$ where the matrix elements are defined by:

$$R_{ij} = r(j - i) \tag{15D.43}$$

The autocovariance matrix for an $(N+1)$-th order autoregressive process is given by:

$$R(N) = \begin{bmatrix} r(0) & r(1) & \cdots & r(N) \\ r(-1) & r(0) & \cdots & r(N-1) \\ \cdot & \cdot & \cdots & \cdot \\ r(-N) & r(-N+1) & \cdot & r(0) \end{bmatrix} \tag{15D.44}$$

For real processes the correlation function is even, $r(n) = r(-n)$, so it would be possible to rewrite the matrix with all positive subscripts. To emphasize the fact that the function is double-sided we will keep the negative notation for the moment.

The autocovariance matrix, $R(N)$, is extrapolated to one order higher, $R(N+1)$, by maximizing the entropy measure defined by (Van den Bos, 1971 and Smylie et al., 1973):

$$h = \ln\{(2\pi e)^{N+2} \det[R(N+1)]\}^{\frac{1}{2}} \qquad (15D.45)$$

This is the entropy of a $N+2$ dimensional Gaussian probability density function with covariance matrix $R(N+1)$. To maximize h with respect to the unknown correlation, $r(N+1)$, the first derivative is set to zero:

$$\frac{\partial h}{\partial r(N+1)} = \frac{\frac{1}{2}}{(2\pi e)^{N+2} \det[R(N+1)]} \frac{\partial \det[R(N+1)]}{\partial r(N+1)} = 0 \qquad (15D.46)$$

This is equivalent to finding $r(N+1)$ such that:

$$\frac{\partial \det[R(N+1)]}{\partial r(N+1)} = 0 \qquad (15D.47)$$

From Equation 15D.46 we see that $R(N+1)$ must be positive definite so that $\det[R(N+1)]$ is positive and nonzero. The derivative of $\det[R(N+1)]$ is obtained by first reducing $R(N+1)$ to the next lower order (this is the matrix minor of element $R_{N+2,N+2}$) and then applying a lowering operator to all indices. This gives:

$$\frac{\partial \det[R(N+1)]}{\partial r(N+1)} = \det \begin{bmatrix} r(-1) & r(0) & \ldots & r(N-1) \\ r(-2) & r(-1) & \ldots & r(N-2) \\ \ldots & \ldots & \ldots & \ldots \\ r(-N-1) & r(-N) & \ldots & r(-1) \end{bmatrix} = 0 \qquad (15D.48)$$

Two additional useful properties of $\det[R(N+1)]$ can also be demonstrated. The first is that it is a quadratic function of $r(N+1)$:

$$\det[R(N+1)] = \alpha_0 + \alpha_1 r(N+1) + \alpha_2 r^2(N+1) \qquad (15D.49)$$

This is obtained by actually expanding $\det[R(N+1)]$, setting $r(-m) = r(m)$, and collecting terms. The coefficients α_0, α_1, and α_2 are functions only

of the elements of R(N). The second property is that the second derivative of $\det[R(N+1)]$ is always negative

$$\frac{\partial^2 \det[R(N+1)]}{\partial r^2(N+1)} = -2 \det[R(N-1)] \qquad (15D.50)$$

because $\det[R(N-1)] > 0$. From the quadratic representation we can immediately identify the coefficient α_2 to be:

$$\alpha_2 = -\det[R(N-1)] \qquad (15D.51)$$

The quadratic now takes the form:

$$\det[R(N+1)] = \alpha_o + \alpha_1 r(N+1) - |\alpha_2| r^2(N+1) \qquad (15D.52)$$

A typical plot of $\det[R(N+1)]$ as a function of $r(N+1)$ is a parabola that is concave down. A valid solution can exist only in the region $\det[R(N+1)] > 0$. The parabolic form also guarantees that there is only one maximum in the valid region. Since the ordinate values of the parabola are symmetrical about the maximum, it also follows that maximizing the entropy is equivalent to choosing a value for $r(N+1)$ that lies at the midpoint (Veltman et al., 1972) of the region where $\det[R(N+1)] > 0$.

The final solution for the unknown autocorrelation value is obtained by differentiating Equation 15D.52 and solving for $r(N+1)$:

$$\frac{\partial \det[R(N+1)]}{\partial r(N+1)} = \alpha_1 - 2|\alpha_2| r(N+1) = 0 \qquad (15D.53)$$

$$r(N+1) = \frac{\alpha_1}{2|\alpha_2|} = \frac{\alpha_1}{2 \det[R(N-1)]} \qquad (15D.54)$$

A satisfactory solution requires that α_1 be nonzero otherwise the extrapolation would terminate. The determination of α_1 requires several matrix manipulations starting with Equation 15D.48. To eliminate notation complications caused by negative indices the even property of r(n) is invoked to give:

$$\det \begin{bmatrix} r(1) & r(0) & \ldots & r(N-1) \\ r(2) & r(1) & \ldots & r(N-2) \\ \cdot & \cdot & \cdots & \cdot \\ r(N) & r(N-1) & \ldots & r(0) \\ r(N+1) & r(N) & \ldots & r(1) \end{bmatrix} = 0 \qquad (15D.55)$$

Expanding the determinant using the last row and the method of minors produces the result:

$$r(N+1) \det [R(N-1)] + \sum_{k=1}^{N} r(k)(-1)^{N+k+1} M_{N+1,k} = 0 \qquad (15D.56)$$

The $M_{N+1,k}$ are the corresponding matrix minors of the elements in the bottom row. Finally we can identify the coefficient α_1 as:

$$\alpha_1 = - \sum_{k=1}^{N} r(k)(-1)^{N+k+1} M_{N+1,k} \qquad (15D.57)$$

In conclusion, the MEM extrapolation algorithm is simply a step-by-step computation of higher order autocorrelations to achieve an arbitrarily high order matrix. The matrix manipulations indicated by Equation 15D.57 are not implemented in practical algorithms because of the computational effort involved. In the next section an equivalent estimate based on an autoregressive model is derived that has better computational efficiency.

3. Autoregressive or predictive-filter basis

The third mathematical description of MEM involves the definition and calculation of a prewhitening or predictive filter. In Chapter XIII it was shown that predictive filtering and autoregression are equivalent viewpoints. Before starting a detailed analysis it will be helpful to briefly review some basic system analysis concepts that will help tie together the equivalent viewpoints.

A continuous-time, linear, time-invariant system with a single input $x(t)$ and a single output $y(t)$ is illustrated in Figure 15D.1. The differential equation which describes the system is given by:

$$a_M \frac{d^M y}{dt^M} + a_{M-1} \frac{d^{M-1} y}{dt^{M-1}} + \ldots + a_o y =$$

$$b_K \frac{d^K x}{dt^K} + b_{K-1} \frac{d^{K-1} x}{dt^{K-1}} + \ldots + b_o x \qquad (15D.58)$$
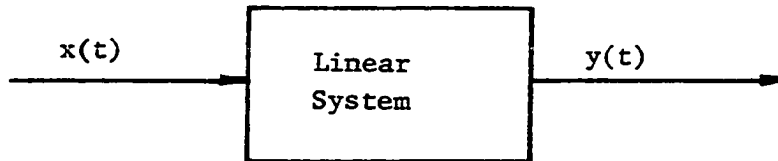
Figure 15D-1. Continuous-time, Linear, Time-invariant System.

An equivalent discrete-time system, is likewise described by a linear difference equation (Stanley, 1975) with constant coefficients as given by:

$$a_o y(n) + a_1 y(n-1) + a_2 y(n-2) + \ldots + a_M y(n-M) =$$

$$b_o x(n) + b_1 x(n-1) + \ldots + b_K x(n-k) \qquad (15D.59)$$

The z-transform definition for the transfer function of a discrete-time system is obtained from (15D.59) by applying a unit impulse:

$$H(Z) = \frac{b_o + b_1 Z^{-1} + b_2 Z^{-2} + \ldots + b_k Z^{-K}}{a_o + a_1 Z^{-1} + a_2 Z^{-2} + \ldots + a_M Z^{-M}} \qquad (15D.60)$$

A special form of this transfer function is used in MEM spectral analysis and is called the "all-pole" model. The terminology "all-pole" model (Van den Bos, 1971) in the literature refers to a transfer function that has no zeros in the z-plane. As a consequence, the numerator polynomial in Equation 15D.60 has all zero coefficients except for b_o.

If the input to the filter is white noise we say the output time series, $y(t)$, was generated by a moving average process (See Chapter XIV), Equations 14.6 and 14.19). The output time series power spectral density is completely characterized by the coefficients, b_n.

If the input to the filter generates an output which is white noise we refer to the input time series as representing a finite autoregressive process of order M. The power spectral density function is completely specified by the coefficients, a_n (Equation 14.40). The "all-pole" model is represented by the finite autoregressive series given in Equation 14.24.

The Yule-Walker equations are used to relate the finite autoregression coefficients, a_n, and the stationary autocovariances. These relationships are presented in detail in Equation 14.42. This linear set of equations is expressed in matrix form in Equation 14.46. After manipulating the matrix form, changing the notation so $\hat{C}(n) = r(n)$, and adding a row of order $N+1$, the Yule-Walker equations can be expressed as:

$$
\begin{bmatrix}
r(1) & r(0) & \ldots & r(N-1) \\
r(2) & r(1) & \ldots & r(N-2) \\
\ldots & \ldots & \ldots & \ldots \\
r(N+1) & r(N) & \ldots & r(1)
\end{bmatrix}
\begin{bmatrix}
1 \\
-a_1 \\
\vdots \\
-a_N
\end{bmatrix}
=
\begin{bmatrix}
0 \\
0 \\
\vdots \\
0
\end{bmatrix}
\qquad (15D.61)
$$

This is a homogeneous system of $N+1$ linear equations and from Cramers rule the characteristic determinant of the system must be zero; therefore:

$$
\det
\begin{bmatrix}
r(1) & r(0) & \ldots & r(N-1) \\
r(2) & r(1) & \ldots & r(N-2) \\
\ldots & \ldots & \ldots & \ldots \\
r(N+1) & r(N) & \ldots & r(1)
\end{bmatrix}
= 0
\qquad (15D.62)
$$

Since this solution is identical to that obtained by maximizing the entropy (Equation 15D.55) the autoregressive model is equivalent when the autocorrelations are known exactly. If it is desirable to obtain the extrapolated autocorrelation values using an autoregressive model, they are easily obtained from the following modification of Equation 14.42a:

$$
r(N+1) = \sum_{n=1}^{N} a_n r(N+1-n)
\qquad (15D.63)
$$

This requires a knowledge of exactly N values of a_n and N values of $r(k)$. The power spectrum obtained from the autoregressive coefficients is equal to that obtained by a Fourier transform of the autocorrelations. The autoregressive technique is superior to the extrapolation method in the last section because the coefficients, a_n, are easily obtained from the known autocorrelations by using Equation 14.47. The practical implementation of an MEM spectral estimator is presented in Sections F and G.

E. The Companion Function for $R_x(\tau)$

At the beginning of the author's research, one of the first problems attempted was to relate the maximum entropy viewpoint of spectral analysis to the Wiener-Khinchine relations (Equations 4A.8 and 4A.9). The concepts of MEM were not well-understood and it was hoped that this approach would provide the needed insight. The result of this effort was the development of the generalized calculus-of-variations formulation for integral constraints given in Part J of Appendix I. The maximum entropy measure discussed in the previous section and its integral constraint equation are an application of the calculus-of-variations solution that was derived.

This approach to the investigation of the properties of MEM led to the discovery of a companion function, $\lambda_x(\tau)$, for the autocorrelation function, $R_x(\tau)$, which for a certain class of processes gives an equivalent description of the power spectrum of the process. The results that follow will seem peculiar because the constraint equation completely specifies $S_x(f)$ and thus allows no degrees of freedom. The reasons for presenting this unusual approach are to show that MEM is consistent with the Wiener-Khinechine relations for specific classes of spectral functions and to show the discovery of the companion function.

The entropy measure to be maximized is given in Equation 15D.1 and the integral constraint equation is given by the Fourier transform relationship:

$$\int_{-\infty}^{+\infty} S_x(f) e^{+j2\pi f\tau} df = R_x(\tau) \tag{15E.1}$$

Comparing Equations 15D.1 and 15E.1 with Equations A1.72 and A1.73 in Part J of Appendix I we can identify:

$$F(f, S_x(f)) = \ln[S_x(f)] \qquad (15E.2)$$

$$Q(\tau, f, S_x(f)) = S_x(f)e^{+j2\pi f\tau} \qquad (15E.3)$$

The factor $(4f_N)^{-1}$ will be neglected in this section.

The appropriate Euler-Lagrange equation is (Equation A1.83):

$$\frac{\partial F}{\partial S} - \int_{-\infty}^{+\infty} \lambda_x(\tau) \frac{\partial Q}{\partial S} \, d\tau = 0 \qquad (15E.4)$$

Evaluating the partial derivatives in (15E.4) and solving for $S_x(f)$ in terms of $\lambda_x(\tau)$ and f gives the solution:

$$\frac{\partial F}{\partial S} = \frac{1}{S_x(f)} \qquad \frac{\partial Q}{\partial S} = e^{+j2\pi f\tau} \qquad (15E.5)$$

$$\frac{1}{S_x(f)} - \int_{-\infty}^{+\infty} \lambda_x(\tau)e^{+j2\pi f\tau} d\tau = 0 \qquad (15E.6)$$

This important result (See also Equation 15D.16) states that the complex conjugate of the Fourier transform of the continuous Lagrangian multiplier, $\lambda_x(\tau)$, is equal to the reciprocal of the power spectral density function for the process:

$$\frac{1}{S_x(f)} = \mathcal{F}^*\{\lambda_x(\tau)\} \qquad (15E.7)$$

This representation is restricted to processes which have a well-behaved reciprocal spectral density. The spectral density must be continuous and nonzero for all f. This limits the representation to stochastic processes when the frequency is not bandlimited. For bandlimited processes the dis-

cussion in Section D applies and the reciprocal spectral density is always well behaved.

Continuing with the calculus-of-variations method, the solution for $S_x(f)$ is substituted into the constraint equation to give the relationship between $\lambda_x(\tau)$ and $R_x(\tau)$:

$$\int_{-\infty}^{+\infty} \frac{1}{\mathcal{F}^*\{\lambda_x(\tau)\}} e^{+j2\pi f\tau} df = R_x(\tau) \tag{15E.8}$$

This integral equation can be solved for $\lambda_x(\tau)$ as a function of $R_x(\tau)$ by taking the direct Fourier transform of both sides. This procedure gives the following results:

$$1 = \mathcal{F}\{R_x(\tau)\} \mathcal{F}^*\{\lambda_x(\tau)\} \tag{15E.9}$$

$$\lambda_x(\tau) = \int_{-\infty}^{+\infty} \frac{1}{\mathcal{F}\{R_x(\tau)\}} e^{-j2\pi f\tau} df \tag{15E.10}$$

Finally the solution for $\lambda_x(\tau)$ is used in (15E.6) to derive equations for $S_x(f)$ as a function of $\lambda_x(\tau)$ and $R_x(\tau)$:

$$S_x(f) = \frac{1}{\mathcal{F}^*\{\lambda_x(\tau)\}} = \mathcal{F}\{R_x(\tau)\} \tag{15E.11}$$

The power spectral density function, $S_x(f)$, is specified completely by the Fourier transform of the autocorrelation function (Wiener-Khinchine relations) or alternately by the reciprocal of the complex conjugate of the Fourier transform of the continuous Lagrangian multiplier function, $\lambda_x(\tau)$. Because of this analogy, the function $\lambda_x(\tau)$ will be called a companion function for the autocorrelation function, $R_x(\tau)$.

After a considerable amount of effort was expended on trying to determine an interpretation for the companion function, a simple solution was seen that now will appear trivially obvious. Consider Equation 15E.9 for the case of a "real" process. The autocorrelation function is real and even and so is the companion function. The equation can then be rewritten as

$$1 = \mathcal{F}\{S_x(\tau)\}\mathcal{F}\{\lambda_x(\tau)\} \tag{15E.12}$$

or

$$1 = S_x(f)\Lambda_x(f) \tag{15E.13}$$

where $\Lambda_x(f)$ is the spectral function represented by the Fourier transform of $\lambda_x(\tau)$. Comparing Equation 15E.12 with Equation 5B.8 we can make the following interpretations:

1. Equation 15E.12 represents a linear filter operating on a stochastic input to produce a white noise output. In short: an ideal prewhitening filter.

2. $S_x(f)$ and $R_x(\tau)$ represent the filter input.

3. $\Lambda_x(f)$ and $\lambda_x(f)$ represent the filter transfer function where $\Lambda_x(f) = |H(f)|^2$.

4. The output spectral density function represents white noise with unity amplitude, $S_y(f) = 1$.

The Fourier transform relationships in (15E.12) can be replaced by the following convolution integral:

$$\delta(\tau) = \int_{-\infty}^{+\infty} R_x(t)\lambda_x(\tau - t)dt \tag{15E.14}$$

This is yet another way of representing the ideal prewhitening filter.

Equation 15E.14 is analogous to (14.21) for a finite autoregressive process. Also compare (15E.13) and (14.25).

In summary we can say that the companion function, $\lambda_x(\tau)$, represents an ideal linear prewhitening filter and that the filter transfer function is specified by:

$$|H(f)|^2 = \mathcal{F}\{\lambda_x(f)\} \tag{15E.15}$$

F. MEM for Discrete and Finite Data

For empirical data records the data function is finite and the estimated autocorrelation function is also discrete and finite. Furthermore the autocorrelation function is also statistically variable with the variability increasing with lag. The exact autocorrelations used in the previous sections will now have to be replaced with estimates. The second factor that enters the picture is the selection of the order of the process used to do the modeling. The order affects the resolution of the estimator and the numerical stability of the computer algorithm.

Practical methods of implementing the MEM spectral estimator use the autoregressive model and compute the coefficients directly. This approach has the simplest numerical implementation because it can be done recursively and avoids the matrix manipulation needed in other approaches. This direct approach is the only practical one for large orders. The presentation to follow will show the methods employed to control statistical variability and to select a suitable order.

To begin we will define all of the terms used in the autoregressive spectral estimator given by (Equation 14.52)

$$\hat{S}_K(f) = \frac{\hat{\sigma}_K^2 \Delta\tau}{\left| 1 - \sum_{k=1}^{K} a_K(k) e^{-j2\pi fk\Delta\tau} \right|^2}$$ (15F.1)

where:

f = frequency at which the spectral density is estimated. f is limited to the range, $|f| \le f_N$.

f_N = the Nyquist frequency or folding frequency determined by the sampling rate, $f_N = 1/2\Delta\tau$. It will be tacitly assumed that the data function has been suitably preprocessed to eliminate aliasing.

$\Delta\tau$ = sampling interval or lag interval between samples in the autocorrelation domain. The lag interval is also equal to the sampling interval in the time domain, $\Delta\tau = \Delta t$.

K = the order of the autoregression used to model the process. For most applications K is never larger than approximately one-third of the total number of data function samples.

$a_K(k)$ = $\{a_K(k): k = 1, 2, \ldots, K\}$ the estimated autoregressive coefficients used to model the empirical data function. A boundary condition for physical realizability is: $a_K(K) < 1$.

$\hat{S}_K(f)$ = Estimated power spectral density function at frequency f for a K-th order autoregressive approximation to the process.

$\hat{\sigma}_K^2$ = total mean-square error for a K-th order autoregressive model of the process. This is also the one-step prediction error given in Equation 13.36. It is also the estimated variance of the white noise sequence produced by removing the predictability in the data

function (Equations 14.43, 14.44, and 14.48). This is sometimes referred to as the total error power of the prediction.

The system of equations used to represent the maximum entropy solution was discussed in Chapters XIII and XIV (Equations 13.48 and 14.47). This matrix formulation is repeated below in the notation that will be used in this section:

$$
\begin{bmatrix}
\hat{r}(0) & \hat{r}(1) & . & . & \hat{r}(K) \\
\hat{r}(1) & \hat{r}(0) & . & . & \hat{r}(K-1) \\
. & . & . & & . \\
. & . & . & & . \\
. & . & . & & . \\
. & . & . & & . \\
\hat{r}(K) & \hat{r}(K-1) & . & . & \hat{r}(0)
\end{bmatrix}
\begin{bmatrix}
1 \\
-a_K(1) \\
-a_K(2) \\
. \\
. \\
. \\
-a_K(K)
\end{bmatrix}
=
\begin{bmatrix}
\hat{\sigma}_K^2 \\
0 \\
0 \\
. \\
. \\
. \\
0
\end{bmatrix}
\qquad (15F.2)
$$

We can now get down to the crux of the problem encountered in the practical application of MEM, autoregressive, or any other spectral estimation technique:

How does one obtain "good" estimates of the autocorrelations, $\hat{r}(n)$, or the autoregressive coefficients, $a_K(k)$, directly from the finite data function?

To begin, consider estimating the autocorrelation function:

$$
r(n) = E\{x(t)x(t-n)\} \qquad (15F.3)
$$

For a finite data function defined by $\{x(t): t = 0, 1, 2, \ldots, N-1\}$ an unbiased estimator is:

$$
\hat{r}(n) = \frac{1}{N - |n|} \sum_{q=0}^{N-|n|-1} x(q)x(q + |n|) \qquad (15F.4)
$$

It is unbiased because for large N it converges to the theoretical values defined by Equation 15F.3. This estimator becomes unsatisfactor for large lags because the amount of the data record used is so small that the variability of the estimate becomes intolerably large (Jenkins & Watts, 1968). A common solution to this that appears in much of the literature is to bias the estimator with a triangular window function (Schwartz and Shaw, 1975):

$$\hat{r}'(n) = (1 - \frac{|n|}{N})\hat{r}(n) \qquad (15F.5)$$

This choice is adequate for some applications of spectral analysis and is a special case of the Blackman-Tukey method discussed previously. It is undesirable in many applications because it causes smoothing in the estimated spectrum. The estimator in Equation 15F.4 may actually produce an FFT with negative components. In fact there is no assurance that the covariance matrix will be positive definite (Jenkins & Watts, 1968).

We now proceed to demonstrate the computation of the autoregressive coefficients directly. An earlier paper by Levinson (1947) gives an excellent discussion on linear prediction and the least-squares prediction error criterion for obtaining the "best" filter coefficients. J. P. Burg (1968) modified the Levinson algorithm to give an estimate that would guarantee that $|a_1(1)|$ would not exceed unity (Ulrych, 1972b). A brief presentation of linear filtering and prediction patterned after Levinson's treatment will now be given followed by a derivation of Burg's recursion method.

Linear filtering and prediction can be briefly explained with the help of Figure 15F-1. As much as possible, notation will be patterned after Chapters XIII and XIV. A known signal x(k) is corrupted by white noise $\xi(k)$

to generate a corrupted signal y(k). This corrupted signal represents the data function in the spectral estimation process. The data function is then "optimally" filtered by a convolution with h(n). The "best" estimate of x(k) represented by $\hat{x}(k)$ appears at the output of the filter. The estimation error for the k-th sample is represented by $\mathcal{E}(k)$. The following equations apply

$$y(k) = x(k) + \mathcal{E}(k) \qquad\qquad (15F.6)$$

$$\mathcal{E}(k) = x(k) - \hat{x}(k) \qquad\qquad (15F.7)$$

$$\hat{x}(k) = \sum_{n=0}^{K} h(n)y(k-n) \qquad\qquad (15F.8)$$

where K is the order of the estimate.
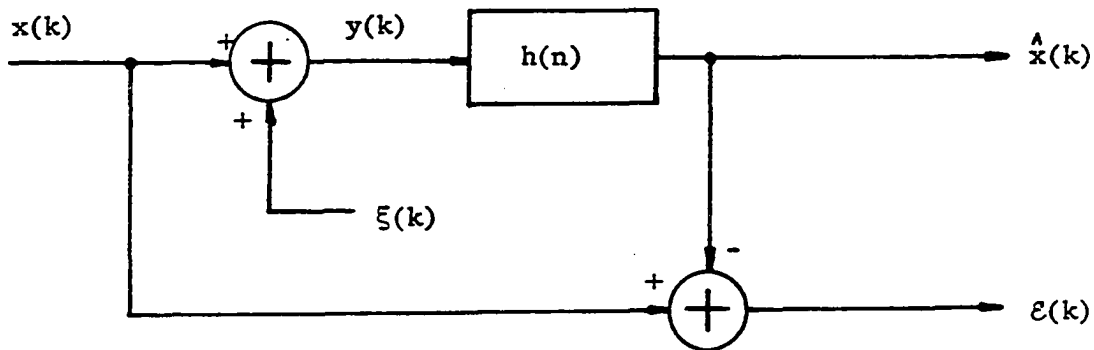
Figure 15F-1. Linear Filtering and Prediction

A measure of the quality of the estimate is the expected value of the mean-square error (Equation 13.36):

$$E\{\mathcal{E}^2(k)\} = E\{[x(k) - \sum_{n=0}^{K} h(n)y(k-n)]^2\} \qquad\qquad (15F.9)$$

$$\{k = 0, \pm 1, \pm 2, \ldots, \pm\infty\}$$

Denoting this error by M_e and expanding the expected value using Equation 15F.6 gives:

$$M_e = E\{x^2(k)\} - 2 \sum_{n=0}^{K} h(n)E\{x(k)x(k-n)\}$$

$$- 2 \sum_{n=0}^{K} h(n)E\{x(k)\xi(k-n)\}$$

$$+ \sum_{n=0}^{K} \sum_{m=0}^{K} h(n)h(m)E\{y(k-n)y(k-m)\} \qquad (15F.10)$$

By recognizing the appropriate autocorrelations and assuming $x(k)$ and $\xi(k)$ are totally uncorrelated we get:

$$M_e = R_x(0) - 2 \sum_{n=0}^{K} h(n)R_x(n)$$

$$+ \sum_{n=0}^{K} \sum_{m=0}^{K} h(n)h(m)R_y(m-n) \qquad (15F.11)$$

It is important to note that $R_y(m-n)$ represents the autocorrelation function of the generated or measured data.

The best estimation in a least-square error sense for the filter coefficients is obtained when M_e is minimized with respect to the $h(n)$. The partial derivatives

$$\frac{\partial M_e}{\partial h(k)} = 0 \qquad \{k = 0, 1, 2, \dots, K\} \qquad (15F.12)$$

are evaluated to give

$$\frac{\partial M_e}{\partial h(k)} = -2 R_x(k) + 2 \sum_{n=0}^{K} h(n)R_y(k-n) = 0 \qquad (15F.13)$$

which for a system of $K+1$ equations:

$$\sum_{n=0}^{K} h(n)R_y(m-n) = R_x(m) \qquad m = 0, 1, \ldots, K \qquad (15F.14)$$

The minimum error of the estimation is obtained by substitution of (15F.14) into the double summation of (15F.11) to give:

$$M_e(\min) = R_x(0) - \sum_{n=0}^{K} h(n)R_x(n) \qquad (15F.15)$$

The optimum filter gives a best estimate of the $x(k)$ in a least-squares sense. The solution to the system of equations given by (15F.14) is presented as an iterative technique in Levinson's paper and is referred to as the <u>Levinson algorithm.</u> This completes the presentation on linear filtering and prediction except to state that the infinite data model used would have to be modified for finite data before it could be applied to a practical filter synthesis problem.

The Burg recursion also determines the linear prediction-error filter coefficients and minimizes the mean-square error of the estimate. The appropriate system of equations for the Burg recursion given by Equation 15F.2 is analogous to Equation 15F.14 augmented by Equation 15F.15. It is interesting to note that Equations 15F.2 can also be written in series form (See Equation 15D.22) as:

$$\sum_{n=1}^{K} a_k(n)\hat{r}(k+n) = \hat{r}(k) - \hat{\alpha}_K^2 \delta_o(k) \qquad \{k = 0, 1, 2, \ldots, K\} \qquad (15F.16)$$

The best linear one-step predictor in a least-square error sense is given by (Equation 13.35):

$$\hat{x}(t) = \sum_{n=1}^{K} a_k(n)x(t-n) \qquad (15F.17)$$

The one-step prediction error for a K-th order autoregressive model is the total mean-square error:

$$\sigma_K^2 = E\{[x(t) - \hat{x}(t)]^2\} \qquad (15F.18)$$

$$\sigma_K^2 = E\{[x(t) - \sum_{n=1}^{K} a_K(n)x(t-n)]^2\} \qquad (15F.19)$$

For a finite data function defined by $\{x(n): n = 0, 1, 2, \ldots, (N-1)\}$ Burg suggests defining both a _forward_ prediction error and a _backward_ prediction error:

$$\mathcal{E}_f(q) = x(q) - \sum_{n=1}^{K} a_K(n)x(q-n) \qquad (15F.20)$$

$$\mathcal{E}_b(q-1) = x(q-1) - \sum_{n=1}^{K} a_K(n)x(q+n) \qquad (15F.21)$$

To eliminate end effects the predictor subscripts must be limited to

$$\text{forward:} \qquad K \leq q \leq (N-1) \qquad (15F.22)$$

$$\text{backward:} \qquad 1 \leq q \leq (N-K-1) \qquad (15F.23)$$

$$\text{inclusive:} \qquad K \leq q \leq (N-K-1) \qquad (15F.24)$$

where K is the order of the estimate and $N > K$ is the total number of data samples. The mean-square error of a K-th order prediction would now be defined as the mean of the error for both forward and backward predictions. For N data samples:

$$M_K = \frac{1}{2(N-1)} \sum_{q=k}^{(N-K-1)} [\mathcal{E}_f^2(q) + \mathcal{E}_b^2(q-1)] \tag{15F.25}$$

The solution proceeds by minimizing M_K with respect to the $a_K(n)$ in a recursive manner and solving the system of equations for the $a_K(n)$. A procedure for implementing the Burg recursion in a manner similar to the Levinson algorithm has been outlined by Anderson (1974). A derivation of this technique and a computer algorithm for implementation will be given in Section G.

G. Burg MEM Recursion Algorithm

This algorithm determines estimates of the autoregressive coefficients $a_K(n)$ which are "best" in the following senses:

1. The coefficients generate a maximum entropy spectral estimate when used in Equation 15F.1.

2. The entropy loss in a linear predictive filter is maximized.

3. The estimated mean-square error of a K-th order prediction, $\hat{\sigma}_K^2$, is minimized.

4. Equations 15F.2 are satisfied in a least-square error sense.

5. $|a_K(K)|$ cannot exceed unity (Ulrych, 1972b).

6. The autocovariance matrix is positive definite.

7. No zero extension of the data is needed and no window function is used explicitly.

For a finite data function defined by

$$\{x(t): t = 1, 2, 3, \ldots, N\} \tag{15G.1}$$

the average mean-square total prediction error for a K-th order process can be written as:

$$M_K = \frac{1}{2(N-K)} \sum_{t=1}^{N-K} [x(t) - \sum_{k=1}^{K} a_K(k)x(t+k)]^2$$

$$+ \frac{1}{2(N-K)} \sum_{t=1}^{N-K} [x(t+K) - \sum_{k=1}^{K} a_K(k)x(t+K-k)]^2 \qquad (15G.2)$$

The reader should convince himself that the equation above is identical in every respect to Equation 15F.25. The form and subscript notation now used are more convenient and closely conform to those used by Anderson (1974).

The implementation of Equation 15G.2 by the minimization of M_K is done with a recursion which starts with order $K = 1$ and progresses to some maximum value $K = 2, 3, \ldots, K_m$. This procedure generates a 2×2, 3×3, $\ldots$, $K_m \times K_m$ autocovariance matrix which is both positive definite and maximizes the entropy. By generalizing this procedure it can be shown that the autoregressive coefficients are related by (Smylie et al., 1973):

$$a_K(k) = a_{K-1}(k) - a_K(K)a_{K-1}(K-k) \qquad (15G.3)$$

$$K = 2, 3, \ldots, (N-1)$$

$$k = 1, 2, \ldots, (K-1)$$

Using the notation, $P_K = \hat{\sigma}_K^2$, a recursion for P_K is obtained by using Equation 15G.3 in Equations 15F.2 or 15F.16. It is:

$$P_K = P_{K-1}[1 - a_K^2(K)] \qquad (15G.4)$$

$$P_0 = \frac{1}{N} \sum_{t=1}^{N} x_t^2 = \hat{r}(0) \qquad (15G.5)$$

At each step in the recursive process P_K is the minimum value of M_K at that step. As can be shown using (15G.3) the only degree of freedom at each new step is the coefficient $a_K(K)$. To obtain the least-squares solution, the average prediction error should be minimized with respect to $a_K(K)$. This gives the following system of equations:

$$\frac{\partial M_K}{\partial a_K(K)} = 0 \qquad K = 1, 2, \ldots, K_m \qquad (15G.6)$$

It will be seen shortly that the solution for $a_K(K)$ which minimizes M_K is a function only of $x(t)$ and can be calculated directly.

Another important feature of the technique is that the estimated auto-correlation functions can also be obtained recursively (analogous to the Yule-Walker equations) as

$$\hat{r}(m) = \sum_{q=1}^{m} a_m(q) \hat{r}(m-q) \qquad (15G.7)$$

where $\hat{r}(0)$ is given by Equation 15G.5. This is analogous to the system of equations represented by (14.42).

A convenient formulation of the solutions represented by (15G.6) has been given by Andersen (1974) and will now be summarized. First define $a_K(0) = -1$ so M_K in Equation 15G.2 can be rewritten as:

$$M_K = \frac{1}{2(N-K)} \sum_{t=1}^{N-K} \left[\left(-\sum_{k=0}^{K} a_K(k) x(t+k) \right)^2 \right.$$

$$\left. + \left(-\sum_{k=0}^{K} a_K(k) x(t+K-k) \right)^2 \right. \qquad (15G.8)$$

Next define $a_K(k) = 0$, $k \geq K$ in the recursion of Equation 15G.3 (except for

the term shown explicitly as $a_K(K)$) and substitute into (15G.8). With a change of sign inside the squared terms the results are easily determined to be

$$M_K = \frac{1}{2(N-K)} \sum_{t=1}^{N-K} [(B_K(t) - a_K(K)B_K'(t))^2$$

$$+ (B_K'(t) - a_K(K)B_K(t))^2]$$ (15G.9)

where:

$$B_K(t) = \sum_{k=0}^{K} a_{K-1}(k)x(t+k)$$ (15G.10)

$$B_K'(t) = \sum_{k=0}^{K} a_{K-1}(K-k)x(t+K-k)$$ (15G.11)

$$t = 1, 2, \ldots, N-K$$

The value of $a_K(K)$ which minimizes M_K as defined by Equation 15G.6 is easily determined since $B_K(t)$ and $B_K'(t)$ are both independent of $a_K(K)$. Taking the partial derivatives of Equation 15G.9 as described by Equation 15G.6, we obtain the desired result:

$$a_K(K) = \frac{2 \sum_{t=1}^{N-K} B_K(t)B_K'(t)}{\sum_{t=1}^{N-K} B_K^2(t) + B_K'^2(t)}$$ (15G.12)

A simple example of a first order autoregression will illustrate the difference between estimating $a_K(K)$ with the Burg technique and using the estimated autocorrelations. The Burg technique gives:

$$a_1(1) = \frac{2 \sum\limits_{t=1}^{N-1} x(t)x(t+1)}{\sum\limits_{t=1}^{N-1} [x^2(t) + x^2(t+1)]} \qquad (15G.13)$$

The direct method gives:

$$a_1(1) = \frac{\hat{r}(1)}{\hat{r}(0)} = \frac{N}{N-1} \frac{\sum\limits_{t=1}^{N-1} x(t)x(t+1)}{\sum\limits_{t=1}^{N} x^2(t)} \qquad (15G.14)$$

Both estimates are unbiased. The condition $|a_K(K)| < 1$ can be shown by applying triangle inequalities to (15G.12).

The final task that remains is to demonstrate useful recursion formulas for $B_K(t)$ and $B_K'(t)$. Using (15G.3) in (15G.10) and (15G.11) and paying careful attention to the valid range of indices and previous definitions for $a_K(k)$ outside the normal ranges gives:

$$B_K(t) = B_{K-1}(t) - a_{K-1}(K-1)B_{K-1}'(t) \qquad (15G.15)$$

$$B_K'(t) = B_{K-1}'(t+1) - a_{K-1}(K-1)B_{K-1}(t+1) \qquad (15G.16)$$

$$K = 2, 3, \ldots, K_m \qquad (15G.17)$$

$$t = 1, 2, \ldots, (N-K) \qquad (15G.18)$$

$$B_1(t) = x_t \qquad\qquad B_1'(t) = x(t+1) \qquad (15G.19)$$

This completes the presentation on the Burg MEM Recursion Algorithm except for a few summary comments.

It should be strongly emphasized that the Burg recursion reduces but does not eliminate the effects of statistical variability in the estimated coefficients. Also the effect of numerical truncation in a computer implementation of the technique may introduce zeros in the numerator of Equation 15F.1. The statistical variability of M_K, and consequently $a_K(K)$, increases with K. This can be interpreted as a reduction in the amount of data used for the estimate. The reader can verify this by examining Equations 15G.9, 15G.10, and 15G.11. The quality of the estimate of $S_K(f)$ as a function of K is best evaluated using both P_K(or M_K) and the variance of the estimate of P_K. We know from previous work that $E\{P_K\} = \sigma_K^2$. These factors will be discussed more in Chapter XIX.

XVI. ONE-BIT AUTOCORRELATION SPECTRUM

Although the one-bit autocorrelation scheme of digital spectral analysis is well-known and widely used in radio astronomy (Weinreb, 1963), the method is not presented in most textbooks. This computationally simple digital technique makes use of the fact that only _phase_ information is necessary for the determination of the shape of the power spectral density function of a Gaussian process. Amplitude information is necessary only for the determination of the amplitude scale factor of the spectral density.

To implement this technique, the data function, x(t) is processed by first sending it through a zero-crossing detector and then clipping the output to obtain digital logic levels. This process is described mathematically as

$$y(t) = \text{sgn}\{x(t)\} \tag{16.1}$$

or:

$$y(t) = \begin{cases} +1 & x(t) \geq 0 \\ -1 & x(t) < 0 \end{cases} \tag{16.2}$$

The digital signal, y(t), is then sampled at a uniform clock rate to code the samples for digital processing. The resulting digitized time series can be used to obtain the estimated autocorrelation function of y(t) by the following correlation process:

$$\hat{\rho}_y(\tau) = \frac{1}{N} \sum_{k=1}^{N} y(k\Delta t) y(k\Delta t + \tau) \tag{16.3}$$

The estimate of the normalized autocorrelation function of the "unclipped" signal is now obtained by the Van Vleck relation:

$$\hat{\rho}_x(\tau) = \sin[\frac{\pi}{2} \hat{\rho}_y(\tau)]$$ (16.4)

Finally, a normalized estimate of the power spectral density of the process is obtained by the Fourier transform:

$$\hat{S}_x(\omega) = K \mathcal{F}\{\hat{\rho}_x(\tau)\}$$ (16.5)

The amplitude scale factor, K, may be found by measuring the power in the data function, x(t).

A complete discussion of one-bit autocorrelation spectral analysis is given in Weinreb (1963). He derives the Van Vleck relation and also the mean and variance for the one-bit autocorrelation function estimate. He shows that, in terms of a large number of samples, N, the mean of the estimate is approximated by

$$\langle \hat{\rho}_x \rangle \simeq \rho_x[1 + \frac{\pi^2}{8N} (\rho_y^2 - 1)]$$ (16.6)

and the variance by:

$$\hat{\sigma}_x^2 \simeq \frac{\pi^2}{4N} (1 - \rho_x^2)(1 - \rho_y^2)$$ (16.7)

The hardware implementation of a simple one-bit crosscorrelator is relatively simple. The block diagram of a crosscorrelator designed by the author for radio astronomy research is shown in Figure 16-1. It is also possible to use the same system for autocorrelation if y(t) is a time-delayed version of x(t).

For autocorrelation, it is simpler to provide the necessary time delay (or lag) by sampling the input signal and using digital delay techniques. The block diagram for a simple one-bit autocorrelator is shown in Figure 16-2.

One-bit autocorrelation techniques can be applied only when large amounts of data are available. The method offers simplicity in exchange for large data sets. Small data sets require the extrapolation and smoothing techniques inherent in methods such as MEM.
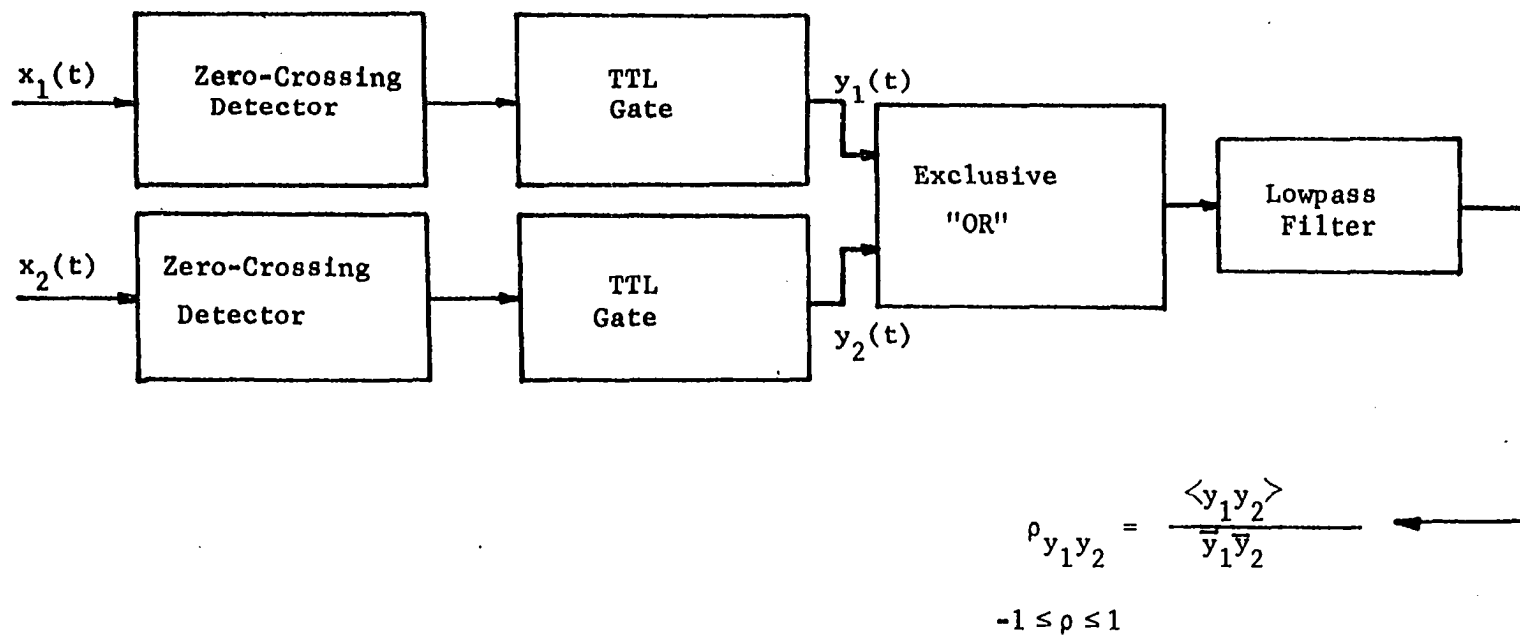
Figure 16-1. One-Bit Crosscorrelator
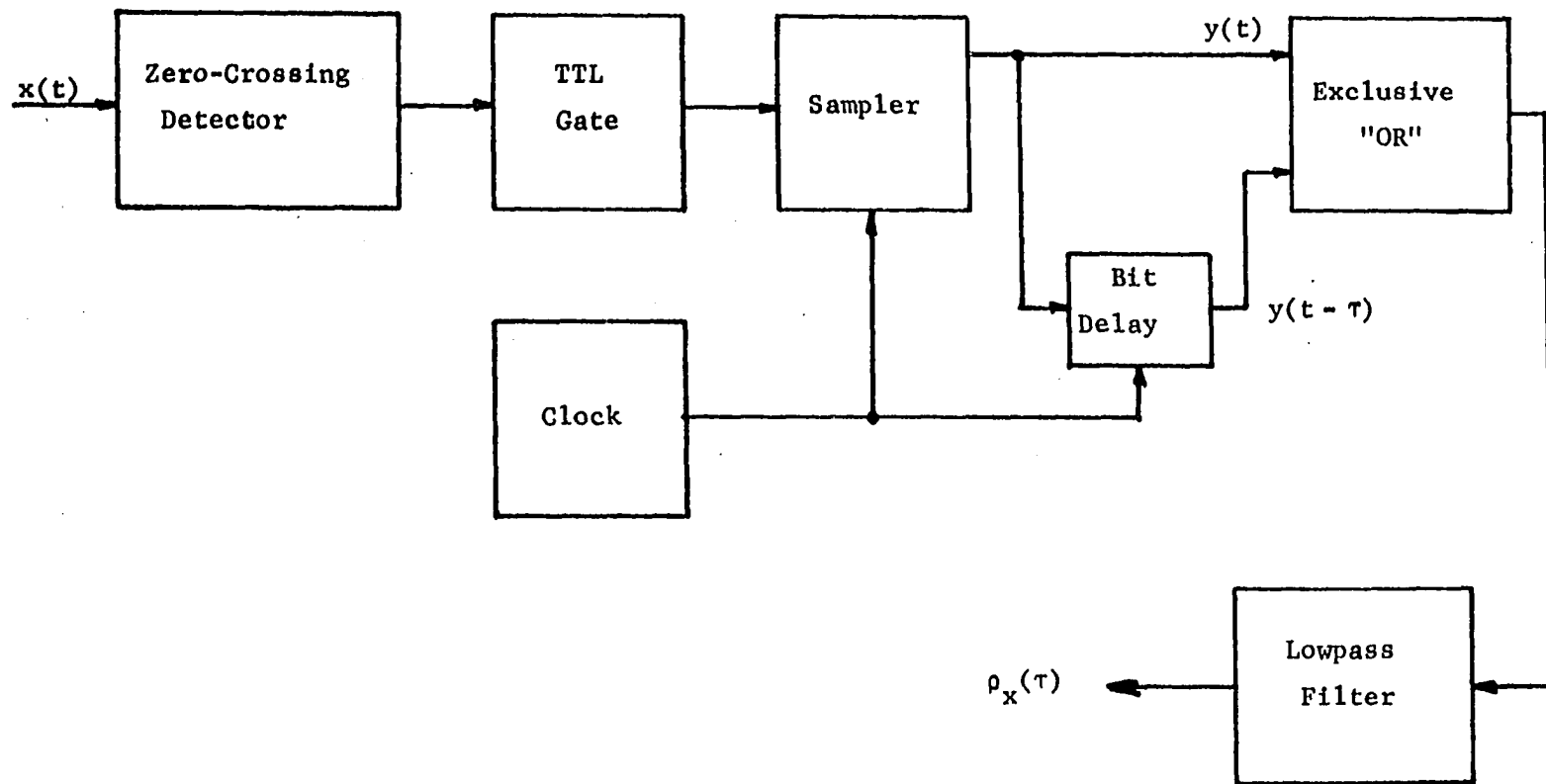
Figure 16-2. Simple One-Bit Autocorrelator

XVII. DATA REDUCTION SCHEMES

The various computer programs written for data reduction are described in this chapter. Each discussion includes an introduction, a list of program variables, and an example run. Programs 01, 02, 03, and 04 are intended primarily to be tutorial aids. Programs 05, 06, and 07 are user oriented and designed to be used to process data. For this reason, the last programs will be explained in much more detail. Listings of the programs are given in Appendix III while further examples of their use are given in various chapters. The printed outputs for the programs are also given in Appendix III and the reader must refer to them for the examples. Each program number is keyed to an example in the appendix.

A. PROGRAM 01 - Discrete Fourier Transform Testing

1. Introduction

This program was written to illustrate the digital Fourier transform and its inverse as derived in the text. The program consists of two subroutines which can be used to illustrate various sampling effects on the estimates of the Fourier coefficients. The program is provided for user experimentation and as an example. It is not intended for routine data processing.

SUBROUTINE FSRS computes an output time series corresponding to input Fourier coefficients. It is a program implementation of Equation 12D.1. The program equations follow the more familiar Fourier series form given by Equation A2.2 in Appendix II.

SUBROUTINE LNSPTM computes the Fourier coefficients from an input time series. It is a program implementation of Equation 12D.5. The program equations are the digital form of Equations A2.4 and A2.5 in Appendix II.

2. Input/output data definitions

A(I) =	Fourier coefficients corresponding to the cosine integral or even part of the input time series.
B(I) =	Fourier coefficients corresponding to the sine integral or odd part of the input time series.
CMAG(I) =	Absolute magnitude of the i-th Fourier coefficient.
CMAGDB(I) =	Absolute magnitude in dB.
CPHASE(I) =	Phase angle of the i-th Fourier coefficient referenced to the center of the input time series.
DCV =	Average or 'dc' value of the input time series.
FX(I) =	Output time series generated by SUBROUTINE FSRS.
FVALUE(I) =	Input time series for SUBROUTINE LNSPTM.
NS =	Total number of input samples of the time series (must be odd).
TDEL =	Equivalent sampling interval in seconds.
TF =	Fourier period, seconds.
TN =	Observation period, seconds.
XDELTA =	Sample times for the output time series.

3. Example

The input for the example program is the Fourier coefficients $a_1 = 4$, $b_3 = 1$. The Fourier frequency is one Hertz and 21 samples are taken in an observation period of 3.1 seconds.

The program generates its own analysis data by using SUBROUTINE FSRS and the Fourier period ("true" period), T_F.

The complex Fourier amplitudes are computed from these 21 samples using SUBROUTINE LNSPTM. The user must remember that this routine requires neither a sampling time nor an observation period. These are only used to interprete the output results.

The last step is the computation of the estimated time series with a factor of four increase in time resolution. This output can be compared to the "true" series to judge the quality of the estimate.

The numerical results for this example are compared in Figure 12D-3.

The quality and numerical stability of the estimate can often be judged by applying Parseval's theorem to the results. First, the complex amplitudes are determined using (A2.13):

$$c_o = 0 \qquad c_1 = 2 \qquad \underline{c}_1 = 2$$

$$c_3 = -\frac{1}{2}j \qquad \underline{c}_3 = +\frac{1}{2}j$$

Second, from Equation 12.A8, the sum of the squared amplitudes gives:

$$R(0) = \sum_{n=-3}^{+3} |c_n|^2 = 8.50 \text{ volts}^2$$

From the estimated time series, the result approximated by (12B.29) is

$$\hat{P} = \frac{1}{2N+1} \sum_{k=1}^{2N+1} x_k^2 \simeq 8.70 \text{ volts}^2$$

and finally, from the estimated complex coefficients (with $c_o = -0.132$):

$$\hat{P} = |\hat{c}_o|^2 + 2 \sum_{n=1}^{M} |\hat{c}_n|^2 = 8.67 \text{ volts}^2$$

The estimates give good results when compared to the true value thus indicating good quality and numerical stability. Refer to PROGRAM 05 for more details on this method of verifying results.

B. PROGRAM 02 - Estimated Kronecker Delta Function

1. Introduction

This program evaluates the approximation to the Kronecker delta function. It is included to show the high degree of accuracy in approximating Equation 12D.11. Figure 11-1 shows another application of the program. The practical usefulness of the routine is limited to analysis and testing of signal processing schemes.

2. Input/output data definitions

DELTQR = Matrix elements of the estimated Kronecker delta.

M = Maximum row order.

N = Maximum column order.

Q = Row index of DELTQR.

R = Column index of DELTQR.

RF = Fourier period in seconds.

TN = Observation period in seconds.

3. Example

The example run illustrates the result when the Fourier period and the observation period are equal. DELTQR is defined for both positive and negative indices. Diagonal elements are unity and off-diagonal elements are better than thirteen orders of magnitude smaller.

C. PROGRAM 03 - Estimated Spectral Amplitudes using Kronecker Delta

1. Introduction

   This program is a simple example of the application of the estimated

Kronecker delta function to computing spectral estimates. The algorithm is

specialized to real (zero phase angle) amplitudes and must be rewritten for

complex amplitudes if the user so desires. The routine is intended as an

example of spectral mixing errors caused by an observation period unequal

to a multiple of the Fourier period. Equation 11.20 is a prototype for the

algorithm.

2. Input/output data definitions

   C(Q) =   Estimated spectral amplitudes.

   CTRUE(I) = Input ('true') spectral amplitudes.

      M =   Maximum index on input spectral amplitudes.

      N =   Index corresponding to $2N+1$ samples.

      Q =   Index for double-sided spectral amplitudes.

      TN = Observation period in seconds.

      TF = Fourier period in seconds.

3. Example

   The data function has a Fourier frequency of 1 Hertz ($T_F = 1$) and has

been sampled 21 times in a period of 3.1 seconds. The true spectral com-

ponents are 2.0 and 0.38 at 1 and 3 Hertz respectively. The estimated

spectral components at zero frequency and intervals of $(3.1)^{-1}$ Hertz are

listed in the printout.

   At 0.968 and 2.90 Hz., the estimates are 2.038 and 0.356 respectively.

Although these are reasonably accurate, spectral mixing has introduced

several large components at other frequencies. The component at 0.645 Hz. is -0.253 which is approaching the size of the true component at 3 Hz. This effect is present in every spectral estimator and must be considered when evaluating the quality of the estimate. Notice also that the average value of the estimate is not zero.

D. PROGRAM 04 - Discrete Fourier Transform Analysis

1. Introduction

This program evaluates the discrete Fourier transform in its most fundamental form. The complex coefficients evaluated are those necessary for the complex series representation (Equations A2.8 and A2.9). The algorithms evaluate Equations 12D.5 and 12D.6 and also do linear regression on the input data to remove an undesired linear trend. For purposes of better evaluation, the estimated complex amplitudes are used to generate an estimated time function with four times more time resolution than the input.

SUBROUTINE LNSPTM computes the complex Fourier coefficients based on the input time series and observation period. The algorithm is an implementation of Equation 12D.5.

SUBROUTINE FSRS is used to generate a time series from Fourier coefficients and time period information. The algorithm is an implementation of Equation 12D.6.

2. Input/output data definitions

A(I) =   In-phase or "real" component of the DFT output.

B(I) =   Quadrature or "imaginary" component of the DFT output.

BZERO =   Intercept point from linear regression.

B1 =   Slope from linear regression.

CDB =   Component power in dB relative to unity total power.

CMAGDB =   Magnitude of each spectral component in dB relative to the computed amplitude after scaling.

CMAG =   Magnitude of the estimated Fourier coefficient.

CPHASE =   Phase of the estimated Fourier component in degrees.

CMAGN(I) =   Normalized magnitude relative to unity total power.

CPHASN(I) =   Phase in degrees.

DCV =   Average or dc-value of the input time series.

FREQ =   Frequency corresponding to each amplitude estimate.

FSAVE(I) =   Initial input time series data saved for comparison purposes.

FVALUE(I) =   Input time series data after linear regression.

FX(I) =   Estimated time series with increased resolution.

LINREG =   A user selected data preprocessing option. LINREG = 0 chooses the input data function for spectral estimation while LINREG = 1 selects the time series after linear regression modification.

NLS =   Number of data samples for use in SUBROUTINE LNSPTM.

NS =   Number of data samples in the input time series.

SCALE =   User selected scale factor for computing spectral amplitudes in relative dB.

TDEL =   Data sampling interval is seconds.

TF =   Fourier period in seconds.

TN =   Observation period in seconds.

YBAR =   Average value of the input time series.

YF(I) =   Sample values of the straight line determined by linear regression.

3. Example

Time series data for the example was provided by Mr. Wai Ling Tsui (Tsui, 1976). The time series is 41 samples of the output of a phase-switched interferometer. The radio source is Hercules A (3C348) and the data was taken 29 July 1975.

The scientific objective is to obtain an estimate of the natural fringe frequency of the source. This is obtained by computing the digital Fourier transform of the time series data shown in Figure 17D-1. The resulting estimated spectrum is given in Figure 17D-2. The plot is smoother than the printed data because zero-filling (concatenation) was used to improve the output resolution. The peak used to estimate the fringe frequency occurs at 2.11×10^{-3} Hertz. The true fringe frequency is predicted to be 1.95×10^{-3} Hertz. This result is typical of what might be expected for DFT spectral estimation.
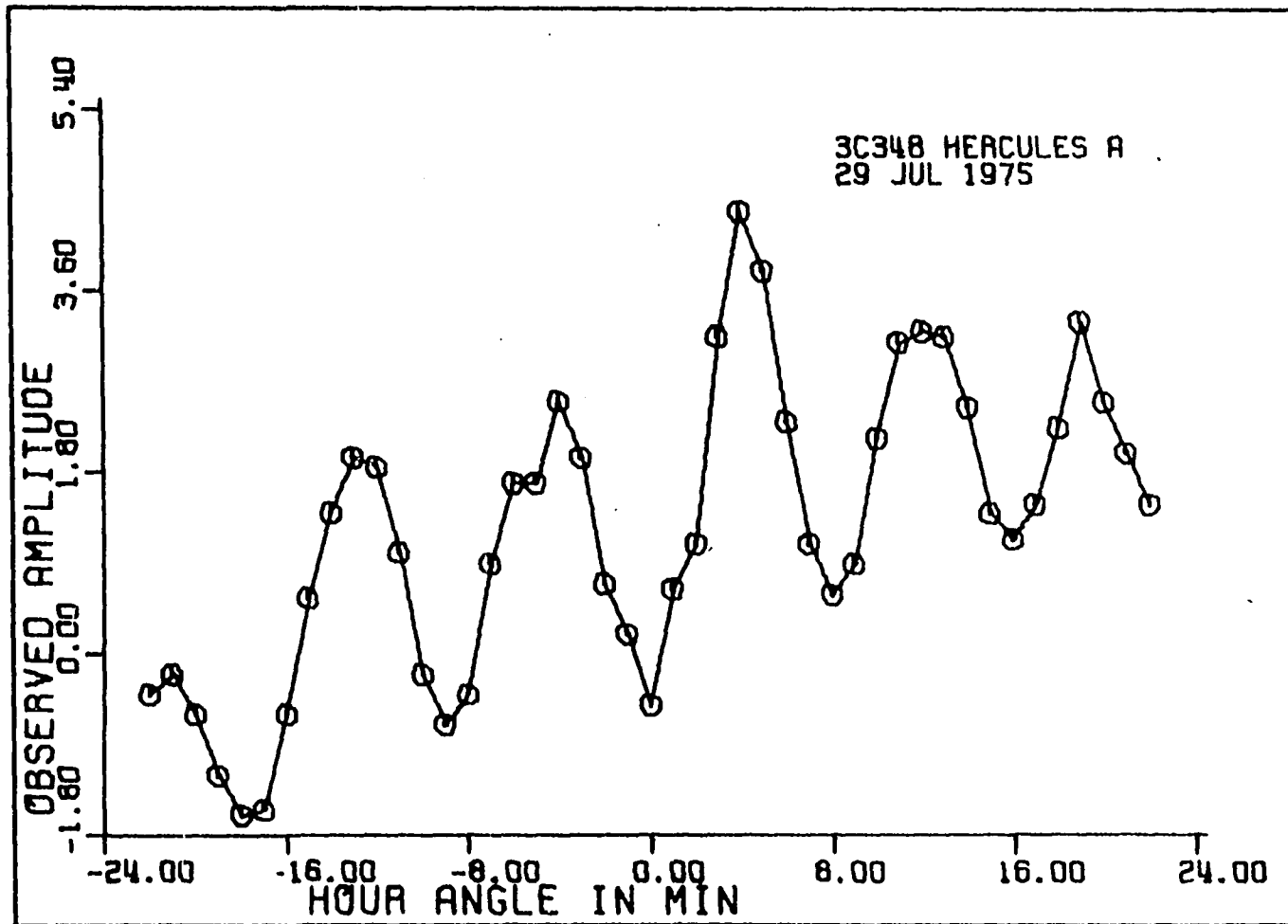
Figure 17D-1. Time Series Data for the DFT Example
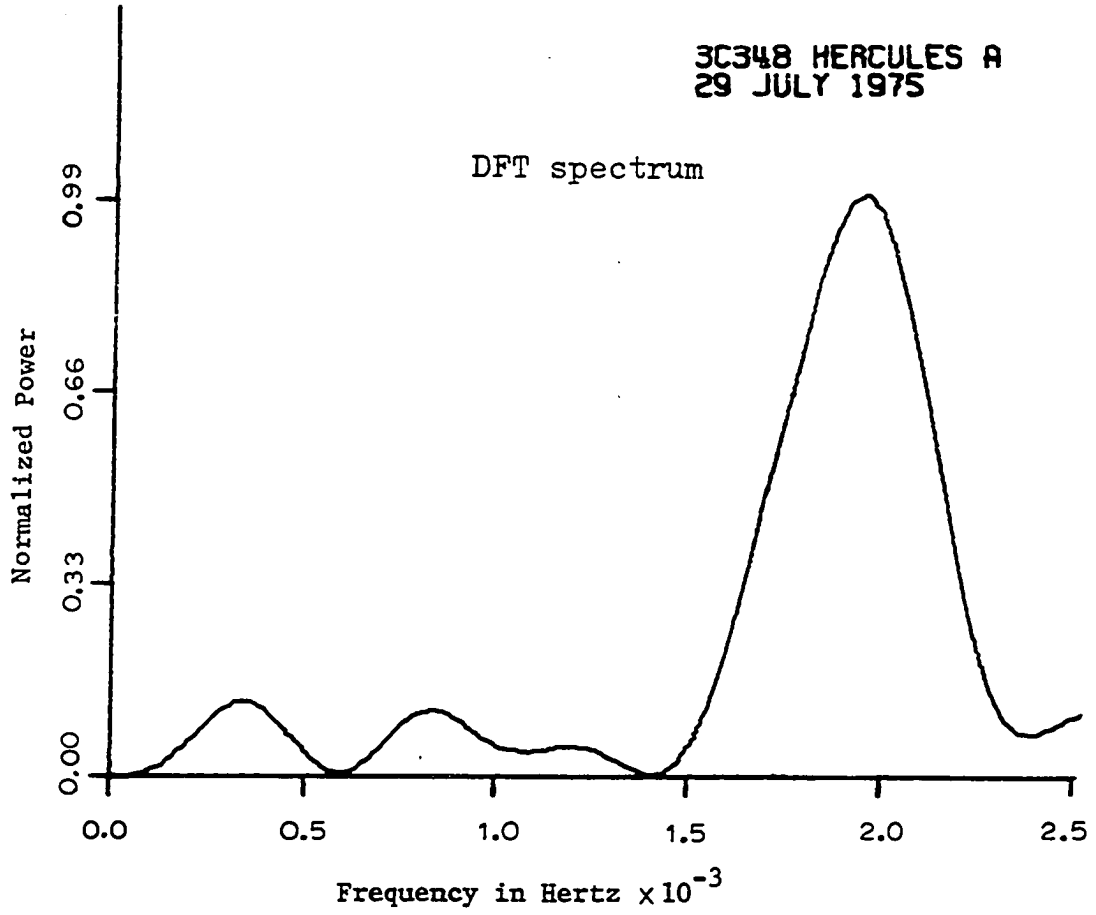
Figure 17D-2. DFT Spectral Estimation

E. PROGRAM 05 - Fast Fourier Transform Spectral Analysis

1. Introduction

This program implements a Fast Fourier Transform (FFT) routine to do spectral analysis. It is intended to be used for routine data processing and has features which include such preprocessing options as average value removal and data conversion to standard variable form. Output data options are also included that provide suppression of unwanted output during routine operations.

The program will accept an arbitrary number of input data points and a resolution option provides an increase in output resolution (but not accuracy) that is helpful in analyzing and plotting results. These features are accomplished by adding zeros (zero filling or concatenation) to the time series to bring the total number of input data values to a factor of 2^n where n is an integer. The FFT subroutine must have 2^n data points to operate properly. Another feature is that, in addition to giving the usual aliased FFT output for 2^n points, the program does proper scaling and computes the true amplitude spectral density function. It also monitors the Nyquist frequency to guarantee that no output above the folding frequency is given. Finally, an estimate of the double-sided power spectral density function is given using the squared-amplitude definition.

SUBROUTINE FFAST is adapted from a FFT routine given by Stearns (1975, Appendix B). The method is described as time decomposition with input bit reversal.

A flow diagram describing the essential features of the program is given in Figures 17E-1a and 17E-1b.
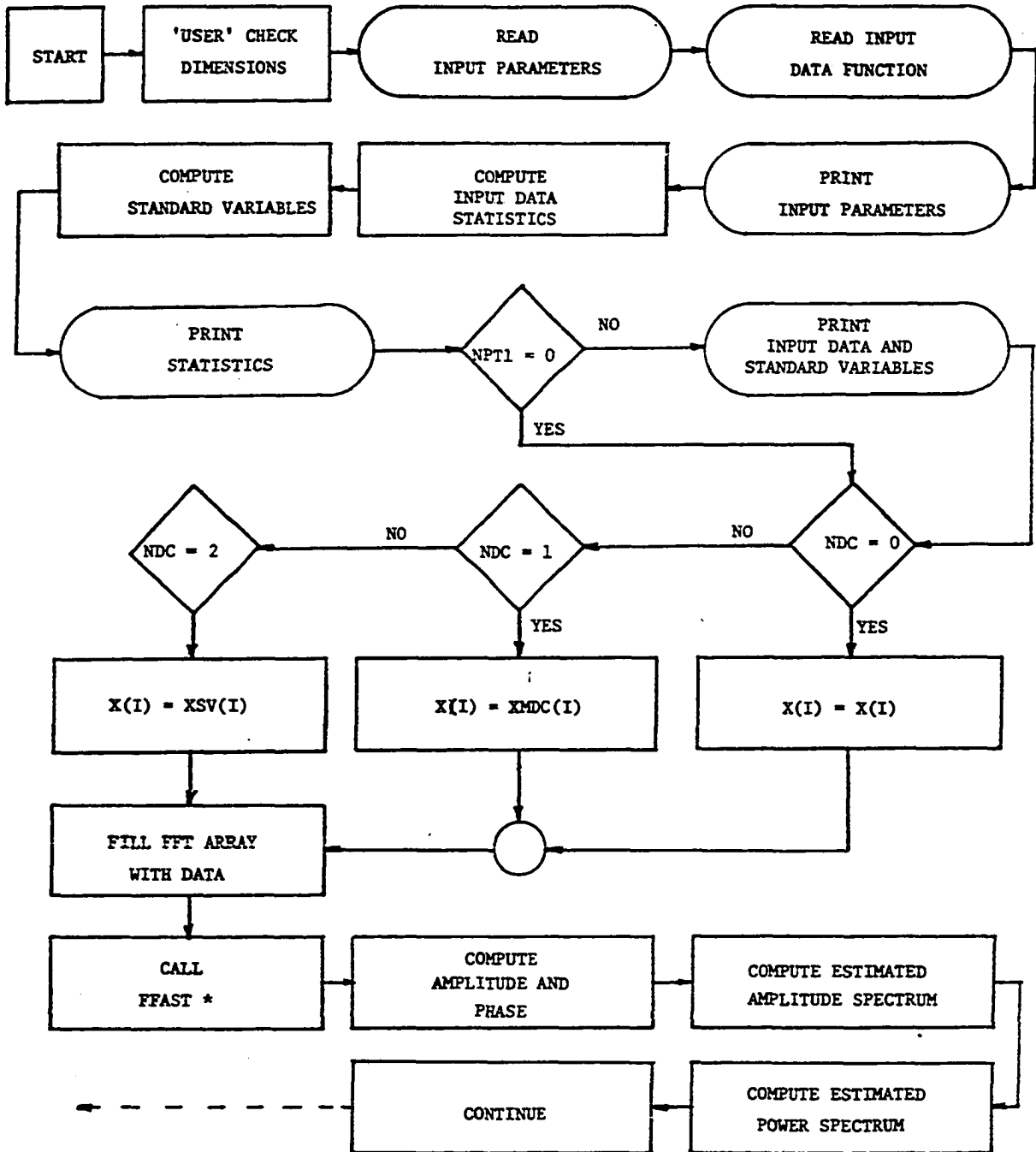
Figure 17E-1a.   PROGRAM 05:   Fast Fourier
Transform Amplitude Spectral
Density
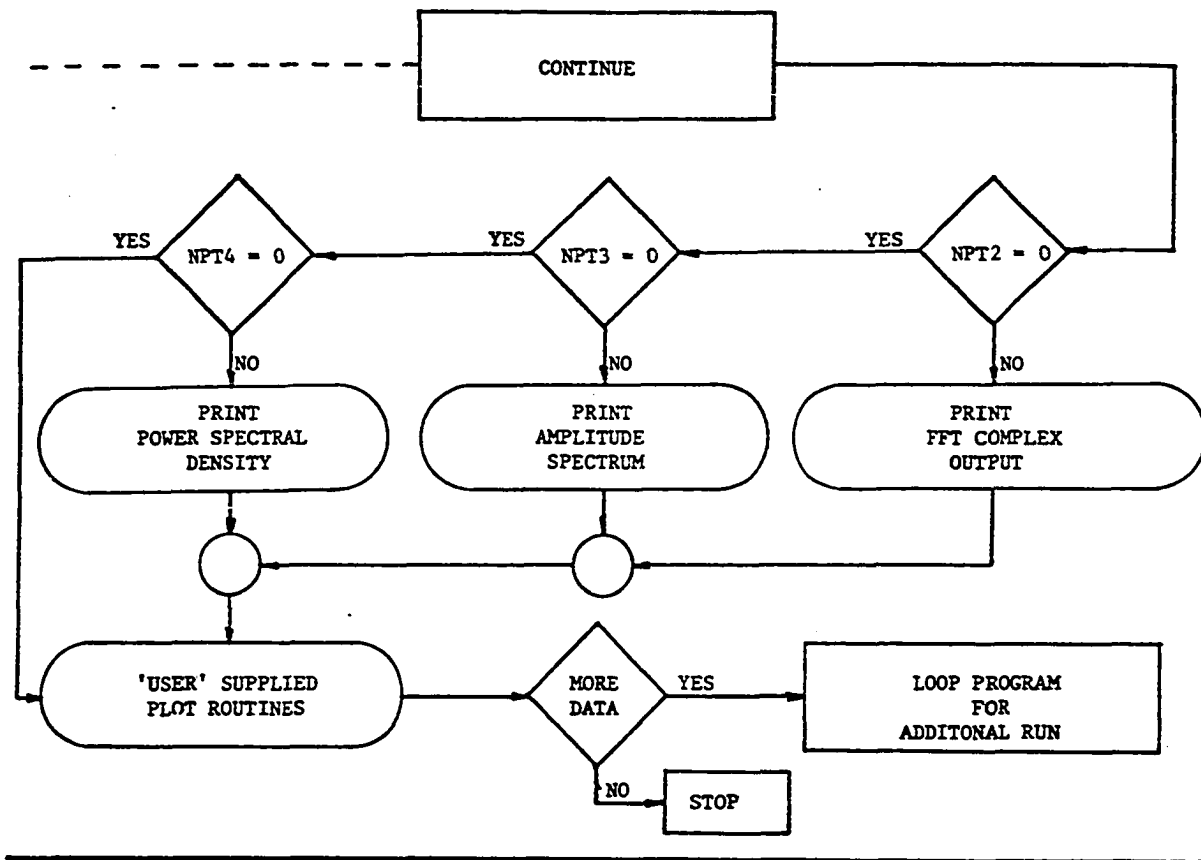
SUBROUTINE FFAST
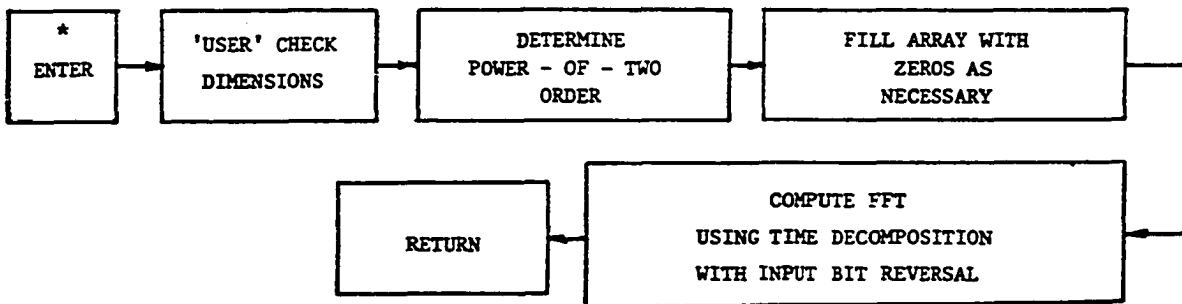
Figure 17E-1b. PROGRAM 05

2. Input data definitions

NDC = The processing option for the input data function. The user has a choice of letting the FFT operate directly on the input data function X(T), (NDC = 0), the zero-mean data function XMDC(T), (NDC = 1), or the data function converted to standard variable form XSV(T), (NDC = 2).

NRESL = The resolution option for the FFT display. A nonzero selection will add a power-of-two resolution increase for the FFT output. For example, NRESL = 3 will increase the output display resolution by a factor of 2^3.

NS = The total number of time samples in the input data function. The user must dimension program variables accordingly.

PTOPT = A printing option used to control the printed output of the program and used to suppress unwanted output. PTOPT is a binary word of the form: (NPT1, NPT2, NPT3, NPT4). NPT1 controls the printing of the input data functions. NPT2 controls the printing of the FFT complex output. NPT3 controls the printing of the amplitude spectral density. NPT4 controls the printing of the power spectral density. Use a 1 if printing is desired and a 0 to suppress printing.

SNAME = A name or label in FORMAT (5A4) used to identify the data record.

XTDELT = Sampling interval for the input time series, seconds.

X(T) = Input time series data. Units of volts will be assumed for simplified presentation.

3. <u>Output statistics</u>

DCV =   Average value or estimated mean of the data function, Volts.

XBAR2 =   Mean-square value of the input data function, Volts^2.

XVAR =   Unbiased estimate of the variance of the input data function, Volts^2.

STDEV =   Standard deviation, Volts.

4. <u>Output data definitions</u>

A(N) =   In-phase or "real" component of the FFT output, Volts.

B(N) =   Quadrature or "imaginary" component of the FFT output, Volts.

CMAG(I) = Absolute magnitude of the discrete spectral component obtained from the discrete Fourier transform (DFT), Volts.

FMAG(N) = Absolute magnitude of the FFT output, Volts.

F.PHASE(N)=Phase angle of the FFT output MOD π, Degrees.

FR(I) =   Fourier frequencies of the spectral estimates, Hertz.

KMAX =   Total number of independent and nonredundant spectral components.

N =   2 * KMAX, the total number of data pairs used in the FFT subroutine.

S(I) =   The estimate of the double-sided power spectral density function, Volts^2/Hz (Watts/Hz in 1 ohm). The printout gives only the positive frequency values.

XX(I) =   The estimate of the double-sided amplitude spectral density function, Volts/Hz. The printout gives only positive frequency values.

XMDC(I) = The input time series with the average (or 'dc') value removed.

XSV(T) = The input time series converted to standard variables which are derived from X(T) by subtracting the average value and dividing by the standard deviation.

XTIME(I) = Sample times for the input data function in seconds. This indexed time is used for plotting routines.

5. Example

An excellent example for illustrating many of the features of the FFT is given by Stearns (1975). The following example incorporates the same essential features. The data function may be written in the continuous form as:

$$f(t) = \begin{cases} e^{-t} \sin t & t \geq 0 \\ 0 & \text{otherwise.} \end{cases} \qquad (17E.1)$$

The Fourier transform of this function is determined from integral tables to be:

$$F(j\omega) = \int_0^\infty e^{-t} \sin t \, e^{-j\omega t} dt = \frac{1}{(2 - \omega^2) + j2\omega} \qquad (17E.2)$$

The absolute magnitude of the Fourier transform is:

$$|F(j\omega)| = \frac{1}{(4 + \omega^4)^{\frac{1}{2}}} \qquad (17E.3)$$

This is the amplitude spectral density estimated by the program. The program prints only the positive frequency values because the transform is

symmetrical. For the reader's interest, the phase function is:

$$\theta_F(\omega) = ARCTAN\left[\frac{-2\omega}{(2 - \omega^2)}\right] \qquad (17E.4)$$

The program does not compute this result because we are assuming interest only in the spectral densities.

The program input is 15 samples of Equation 17E.1 starting at zero and going in steps of $\Delta t = 0.3$ seconds. The estimated amplitude spectral density is shown in Figure 17E-2 and compared with the exact results given by Equation 17E.3. The folding frequency for the given sampling rate is:

$$f_f = \frac{1}{2\Delta t} = 1.67 \text{ Hz.}$$

As would be expected, the estimated amplitude spectral density shows the effects of aliasing due to components in $|F(j\omega)|$ beyond the folding frequency. Also, the truncation effect of finite sampling introduces further high frequency components. The estimated amplitude for $f = 1.46$ Hz is 106% too high while that for $f = 0.21$ Hz is only 0.3% too high. These effects are common in most FFT spectral estimates.

Figure 17E-3 shows the estimate when the resolution is increased by a factor of 2^2 (NRESL = 2). It is important to notice that the accuracy of the estimate remains unchanged and only the resolution is increased. Figure 17E-4 shows the estimated power spectral density for the increased resolution.
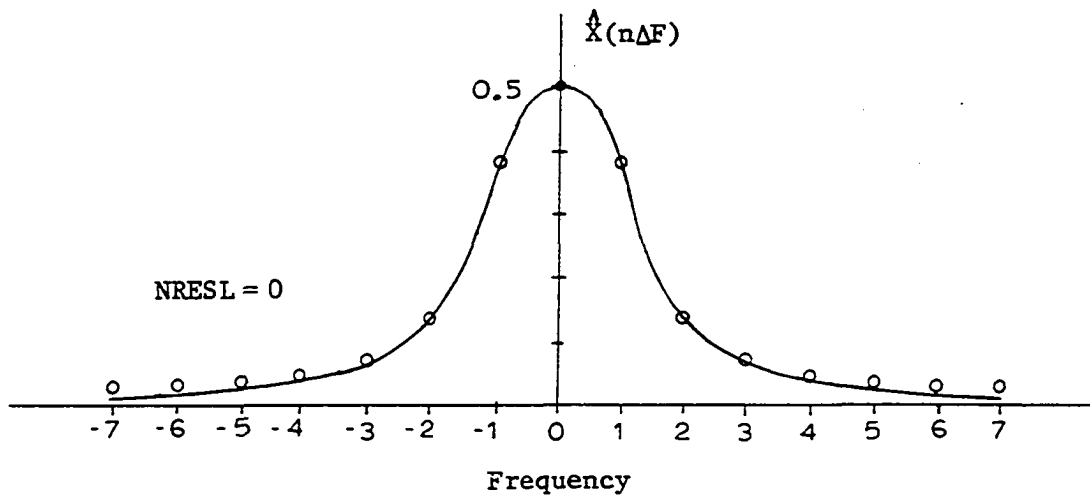
Figure 17E-2. Basic Resolution of FFT Estimate
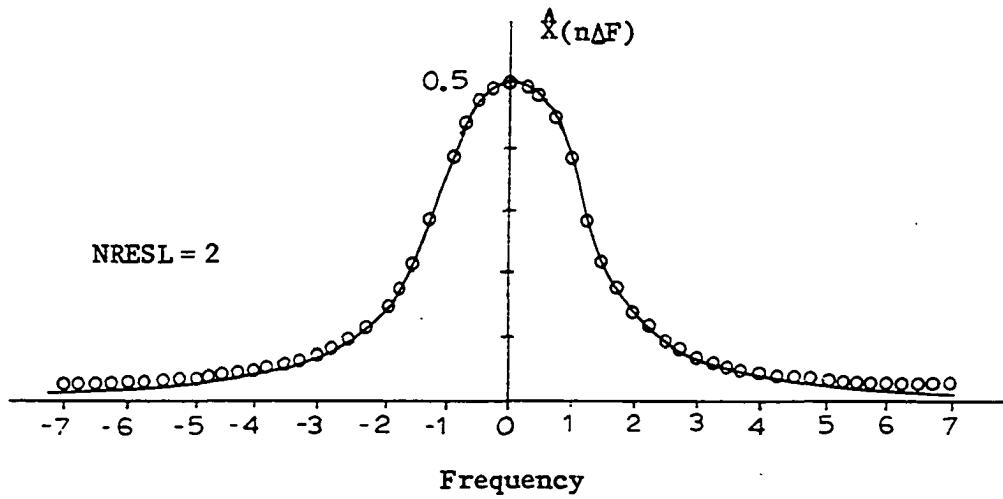
Figure 17E-3. Increased Resolution for FFT Estimate

$$|\hat{X}(n\Delta F)|^2$$
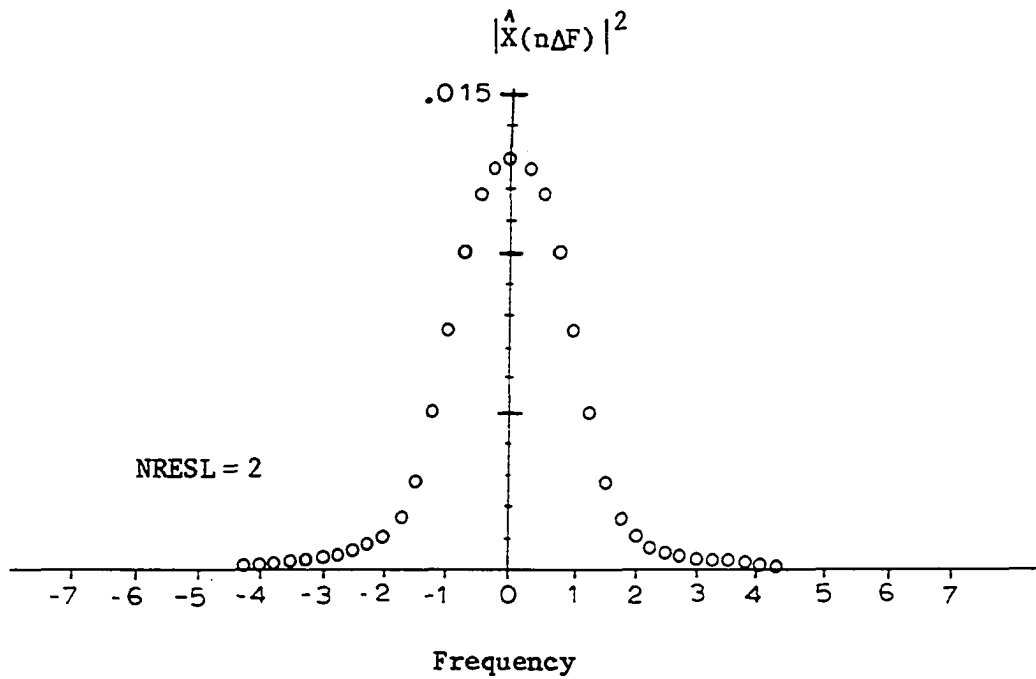
Figure 17E-4. FFT Estimate Proportional to
the Power Spectrum

Parseval's theorem provides a useful check of the stability and accuracy of the estimate and can be used to verify the correctness of the program. Using integral tables it is possible to show that:

$$\int_0^\infty (e^{-t} \sin t)^2 dt = \frac{1}{2\pi} \int_{-\infty}^{+\infty} \frac{d\omega}{4 + \omega^4} = 1/8 \quad \text{volts}^2/\text{Hz}$$

The integral in the frequency domain can be numerically integrated by the following routine to give

$$\Delta F \hat{X}(0) + 2\Delta F \sum_{n=1}^{7} \hat{X}^2(n\Delta F) = 0.1249 \quad \text{volts}^2/\text{Hz}$$

where:

$$\Delta F = \frac{1}{2\ \mathrm{KMAX}\ \Delta t} = 0.208 \quad \mathrm{Hz.}$$

In the time domain, the result is:

$$\Delta t \sum_{i=1}^{15} x_i^2 = 0.1248 \quad \mathrm{volts^2/Hz}$$

These results may be compared directly with the standard deviation of the input data function. These agreements are very good even though aliasing has produced an estimate with considerable error near the folding frequency.

Printed along with the amplitude spectral density function are the absolute magnitudes of the Fourier series components that would be used to represent the input data function. These amplitudes are related to the density function by the equation:

$$\hat{c}_n = \Delta F\ \hat{X}\ (n\Delta F)$$

Refer also to Equation 11.13.

An example of the effects of white Gaussian noise on the estimate is given in Chapter XIX and a detailed discussion presented in Chapter XII, Section D.

F. PROGRAM 06 - Estimation of Single-Sinewave Parameters

1. _Introduction_

This program implements a digital Fourier transform amplitude spectral estimate for a single frequency component with a frequency that may be continuously varied. The input is assumed to be a single-frequency sinewave

plus bandlimited Gaussian noise. For a selected frequency below the Nyquist frequency, it will compute a "best" fit. The fit is "best" in the sense that the amplitude and phase represent an orthogonal component of a discrete Fourier series which can represent the input data function.

The estimate is improved if the input data is first preprocessed to remove any linear trends. To guarantee a zero-mean data function, the program computes the mean value and removes it before doing the spectral estimate. The actual algorithms are based on Equations 13.13 through 13.18. These results will be presented here in a slightly different manner to provide a better understanding of the estimator.

A continuous complex amplitude estimate (not an amplitude density) is defined as

$$\hat{C}(f_o) = \frac{1}{2N+1} \sum_{k=-N}^{+N} x(k\Delta t) e^{-j \frac{2\pi}{T_o} k\Delta t} \tag{17F.1}$$

where $\Delta t = T_N/(2N+1)$. Discrete coefficients are defined at the frequencies corresponding to $f_o = n/T_N$. In general, the continuous complex amplitude is defined for any frequency between zero and the Nyquist frequency.

If $\hat{C}(f_o)$ is represented in complex notation

$$\hat{C}(f_o) = \alpha(f_o) + j\beta(f_o) \tag{17F.2}$$

the complex components can be computed from the following algorithms:

$$\alpha(f_o) = \frac{1}{2N+1} \sum_{k=1}^{2N+1} x(k\Delta t) \cos\left[\frac{2\pi}{T_o}(k-N-1)\Delta t\right] \tag{17F.3}$$

$$\beta(f_o) = \frac{-1}{2N+1} \sum_{k=1}^{2N+1} x(k\Delta t) \sin\left[\frac{2\pi}{T_o}(k-N-1)\Delta t\right] \tag{17F.4}$$

This method of defining the summation index forces the phase angle to be referenced to the center of the input time series. From Fourier analysis (Appendix II), the complex amplitudes are related to the usual a and b co-efficients as follows (Equation A2.13):

$$a_n = C_n + C_n^*$$ (17F.5)

$$b_n = j(C_n - C_n^*)$$ (17F.6)

For the definition of continuous estimates this becomes:

$$a(f_o) = 2 \alpha (f_o)$$ (17F.7)

$$b(f_o) = -2 \beta (f_o)$$ (17F.8)

The absolute magnitude of a complex amplitude estimate is:

$$|\hat{C}(f_o)| = [\alpha^2(f_o) + \beta^2(f_o)]^{\frac{1}{2}} = \frac{1}{2} [a^2(f_o) + b^2(f_o)]^{\frac{1}{2}}$$ (17F.9)

The absolute magnitude of a real frequency component is the sum of both positive and negative frequency contributions:

$$d(f_o) = 2|\hat{C}(f_o)|$$ (17F.10)

The phase angle for the complex component is

$$\phi_c(f_o) = \text{ARCTAN} \left[\frac{\beta(f_o)}{\alpha(f_o)}\right]$$ (17F.11)

while for the real component it is:

$$\phi_d(f_o) = \phi_c(f_o) - 270^o$$ (17F.12)

The terminology "real" and "complex" refer to the observable sinusoid and its double-sided mathematical representation. Finally the "residue" time series is defined as:

$$x_r(k\Delta t) = x(k\Delta t) - d(f_o) \sin \left[\frac{2\pi}{T_o} (k - N - 1)\Delta t\right] \qquad (17F.13)$$

The program output prints the input parameters and the input data function statistics. The input time series and the zero-mean time series are also printed. Next, the magnitude, frequency, and phase of the best-fit sinewave are given. The "residue" time series is computed and its statistics are printed. Finally, the zero-mean input, sampled sinewave, and residue are printed.

It should be emphasized that this technique is not superior to doing a complete FFT on the input data. It has advantages in its simplicity and selectable frequency but the FFT gives an estimate of all components as compared to only one.

2. <u>Input/output data definitions</u>

CMAG = Absolute magnitude of the complex coefficient defined in Equation 11.15 and evaluated at the chosen frequency.

CPHASE = Phase angle of the complex coefficient in degrees.

DMAG = Amplitude of the "best-fit' sinewave.

DPHASE = Phase angle of the "best-fit" sinewave in degrees referenced to the center of the input time series.

FREQ = Frequency in Hertz at which the "best-fit" sinewave is evaluated.

FS(I) = Sinewave estimate evaluated at the sampling times.

NS =   The total number of time samples in the input data function.

SNAME =   A name or label in FORMAT (5A4) used to identify the data
            record.

TDELT =   Sampling interval for the input time series, seconds.

TZERO =   Period for which the sinewave approximation is evaluated.

X(I) =   Input time series data.

XMDC(I) =   The input time series with the average value removed to give
            a zero-mean time series.

XR(I) =   This is a time series generated by subtracting the sinewave
            from the zero-mean input data. It is referred to as the
            "Residue" time series.

3. Input/output statistics

DCV =   Average value or estimated mean of the time series.

STDEV =   Standard deviation.

XBAR2 =   Mean-square value.

XVAR =   Unbiased estimate of the variance.

4. Example

The time series data for this example is the same as used for PROGRAM
04 except a linear regression analysis has been performed to remove any
linear trend. The first printout, the input parameters, shows the total
number of samples (NS = 41), the period of the desired spectral component
(T_o = 49.26 seconds), and the sampling interval (Δt = 60 seconds). The sta-
tistics for the input data function are computed and printed to be used for
comparison with final results. For this example, the input time series

and zero-mean time series are equal because the data was previously processed to remove the mean value.

The next output is the desired "best-fit" sinewave describing the input time series

$$f_s = 128.46 \ \sin(\frac{2\pi}{T_o} \ t - 1.839) \qquad (17F.14)$$

where:

$T_o = 4.926 \times 10^2$ seconds.

$\text{Frequency} = \frac{1}{T_o} = 2.03 \times 10^{-3}$ Hz.

$\text{Phase} = -105.34$ degrees

A statistical measure of the quality of this estimate can be obtained by applying Rayleigh statistics as discussed in Chapter XIX, Section C. First we assume that the time series is bandlimited Gaussian noise and test the hypothesis that the output amplitude spectral density was generated exclusively by noise. The expected value of the Rayleigh output is computed as:

$$E\{\hat{X}(f)\} \simeq (\frac{\pi}{4})^{\frac{1}{2}} \Delta t \ (NS \ \overline{x^2})^{\frac{1}{2}} \qquad (17F.15)$$

For $\Delta t = 60$, $NS = 41$, and $\overline{x^2} = 1.4904 \times 10^4$, the expected value becomes:

$$E\{\hat{X}(f)\} = 4.1566 \times 10^4 = (\frac{\pi}{2})^{\frac{1}{2}} \sigma_x \qquad (17F.16)$$

The estimated sinewave amplitude is converted to an equivalent amplitude spectral density by:

$$\hat{X}_d \simeq NS \ \Delta t \ (\frac{DMAG}{2}) \qquad (17F.17)$$

For DMAG = 128.5, the estimated amplitude density becomes:

$$\hat{X}_d \simeq 15.8055 \times 10^4$$

Since we know that $\sigma_x = 3.3165 \times 10^4$, the estimated amplitude is at the 4.766 sigma-level on the Rayleigh distribution. The probability that an a priori selected sample at this frequency could be due to random noise is:

$$P_f = P(\hat{X} > 4.766 \ \sigma_x) = \text{Exp}[-\frac{1}{2} (4.766)^2] = 1.17 \times 10^{-5} \tag{17F.18}$$

This is an extremely low probability. The probability that any amplitude estimated by a Fourier transform would exceed this value with only noise input is given by:

$$\hat{P}_f = 1 - (1 - P_f)^{NS} = 4.789 \times 10^{-4} \tag{17F.19}$$

This is also a low probability. A more detailed discussion of how to interpret estimated spectra is given in Chapter XIX, Section C.

To give the reader a relative idea of the quality of the sinewave fit, the zero-mean data function, "best-fit" sinewave, and "residue" time series are plotted together in Figure 17F-1.
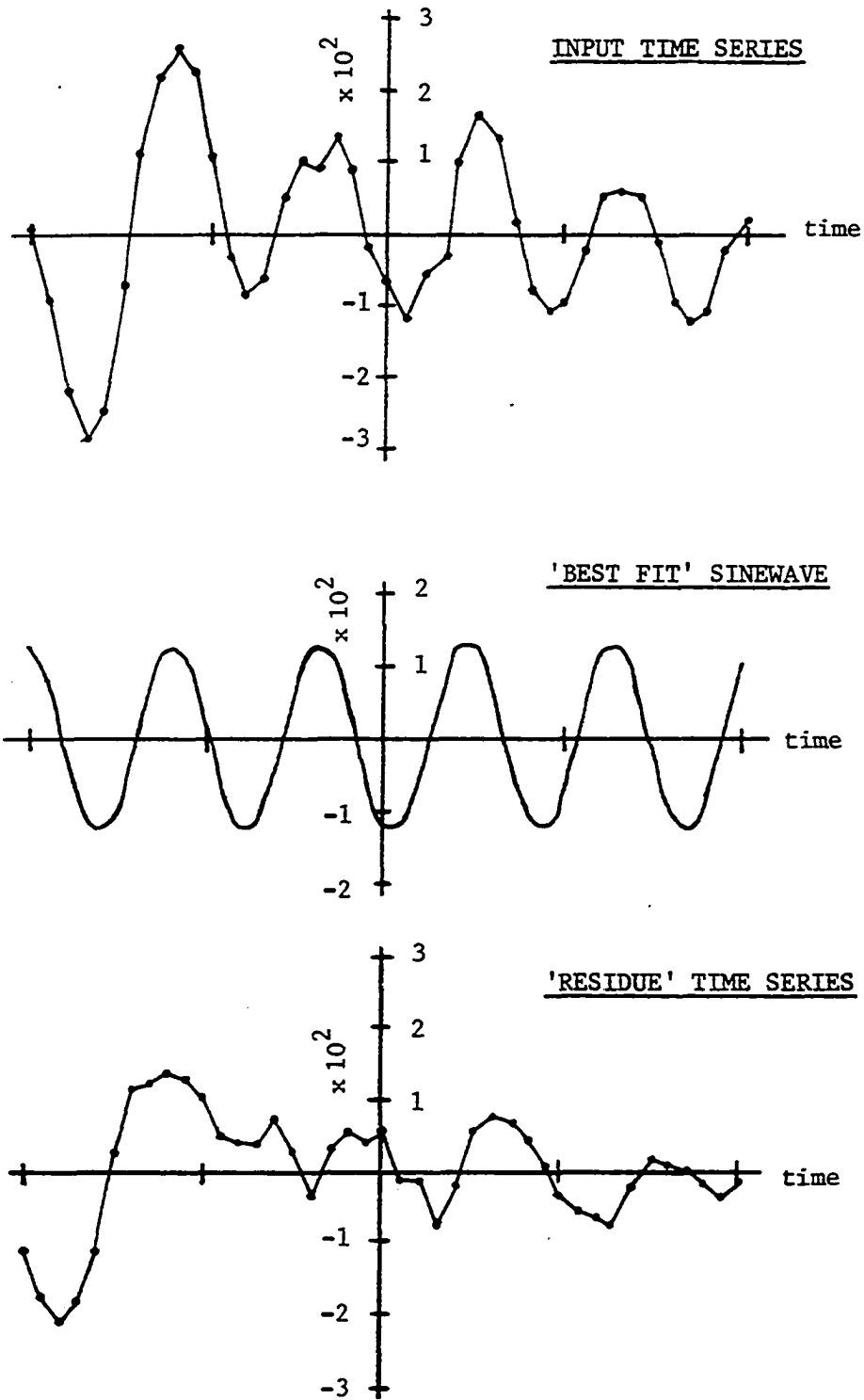
Figure 17F-1. Single-sinewave Parameter Estimation

G. PROGRAM 07 - Maximum Entropy Spectral Analysis

1. Introduction

This program computes the maximum entropy estimate of the power spectral density function of a finite time series. A finite autoregressive series is used to model the input data function and the power spectrum is computed using the autoregressive spectral estimator given by Equation 15F.1. The estimates of the autoregressive coefficients are obtained from the Burg MEM recursion algorithm described in Chapter XV, Section G.

The program is intended to be used for routine data processing and has been user oriented as much as possible. Processing features include user selected spectral output display resolution and autoregressive order. A selectable printing option has been included so that routine or unwanted output can be suppressed. Selectable data preprocessing options include removing the average value, linear trend removal, and converting the input to standard variables.

Printed output includes the input data parameters, input time series, data function statistics before and after linear regression, time series after linear trend removal, standard variables, MEM starting values, intermediate coefficients (optional), summary of iterative results, maximum filter length, error power, estimated autoregressive coefficients, peak value of the estimated spectrum, total spectral power, and the normalized power spectral density estimate.

The folding frequency is computed from the input data and the program inhibits the calculation or printing of any aliased output. The spectrum is scaled such that the output is the positive frequency half of a double-

sided spectrum. Since the spectral power has been normalized to unity, the program integrates the spectral density to obtain the total power in the estimated spectrum which may then be compared with unity. This provides a reasonable check on the quality of the estimate and the numerical stability of the algorithms.

SUBROUTINE ATOREG recursively computes estimates of the autoregressive coefficients using the Berg algorithm. A detailed description of the routine is given in the flow diagram of Figure 17G-1. The equation numbers refer to those equations in the text which are implemented in the subroutine.

SUBROUTINE MEMSPM computes the power spectral density estimate using the autoregressive coefficients from ATOREG. This algorithm implements Equation 15F.1.

A simple flow diagram describing the essential features of the entire program is given in Figures 17G-2a and 17G-2b.

SUBROUTINE ATOREG

```
T = 1,N
    P = P + X(T)**2
PZERO = P/N
```
The mean-square value is computed in the main program. (Equation 15G.5)

```
K = 1
B1(1) = X(1)
B2(N - 1) = X(N)

T = 2,N - 1
    B1(T) = B2(T - 1) = X(T)
```
Compute starting values for B1 and B2. (Equation 15G.19)

```
XNOM = XDEN = 0.

T = 1,N - K
    XNOM = XNOM + B1(T)*B2(T)
    XDEN = XDEN + B1(T)**2 + B2(T)**2

A1(1) = 2.*XNOM/XDEN
P(1) = PZERO*(1.-A1(1)*A1(1))
PRINT,A1(1),P(1),P(0)
```
Compute the K = 1 values of AK(K) and P(K). (Equation 15G.12)

(Equation 15G.4)

○ ─ ─ ─ ─ ─ ─ ─ ─ ─── Iterate

```
K = K + 1
```
Increment the order K.

```
T = 1,K - 1
    AA(T) = AK(T)

T = 1,N - K
    B1(T) = B1(T) - AA(K - 1)*B2(T)
    B2(T) = B2(T + 1)-AA(K - 1)*B1(T + 1)
```
Compute the autoregressive coefficients AK(T) using recursive equations for increasing values of K up to K = MM. (Equations 15G.10, 15G.11, 15G.15, 15G.16)

```
XNOM = XDEN = 0.

T = 1,N - K
    XNOM = XNOM + B1(T)*B2(T)
    XDEN = XDEN + B1(T)**2 + B2(T)**2
AK(K) = 2.*XNOM/XDEN
```
Compute the highest order coefficient AK(K) for a Kth order process. (Equation 15G.12)

```
P(K) = P(K - 1)*(1.- AK(K)**2)
```
Compute the mean-square prediction error. (Equation 15G.4)

Figure 17G-1. Burg MEM Recursion Algorithm for Computing Estimates of the Autoregressive Coefficients

SUBROUTINE ATOREG (CONT.)

T = 1, K - 1
    AK(T) = AA(T) - AK(K) *AA(K - T)
    PRINT, K, T, AK(K)
	Compute the estimated autoregres-
	sive coefficients for a Kth order
	model of the process. Printing of
	intermediate values is optional.
	(Equation 15G.3)

NO
K = MM - - - - - - ──► Iterate

YES

T = 1, K PRINT, T, AK(T), P(T)	Print a summary of the iterative results for increasing values of K.

PRINT, K, P(K) T = 1, MM PRINT, T, AK(T)	Print the final order and corres- ponding error power. Print all of the autoregressive coefficients for a Kth order estimate.

RETURN

Figure 17G-1.   (Continued)

Figure 17G-2a. Main Program Flow Diagram.

SUBROUTINE ATOREG
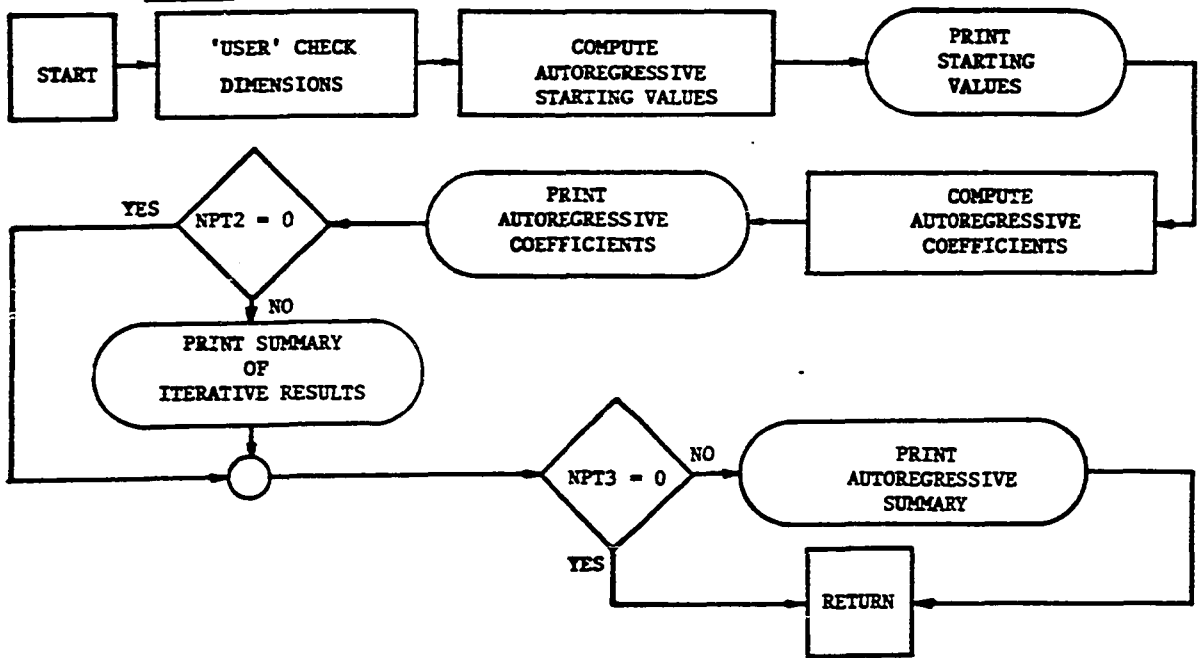
SUBROUTINE MEMSPM
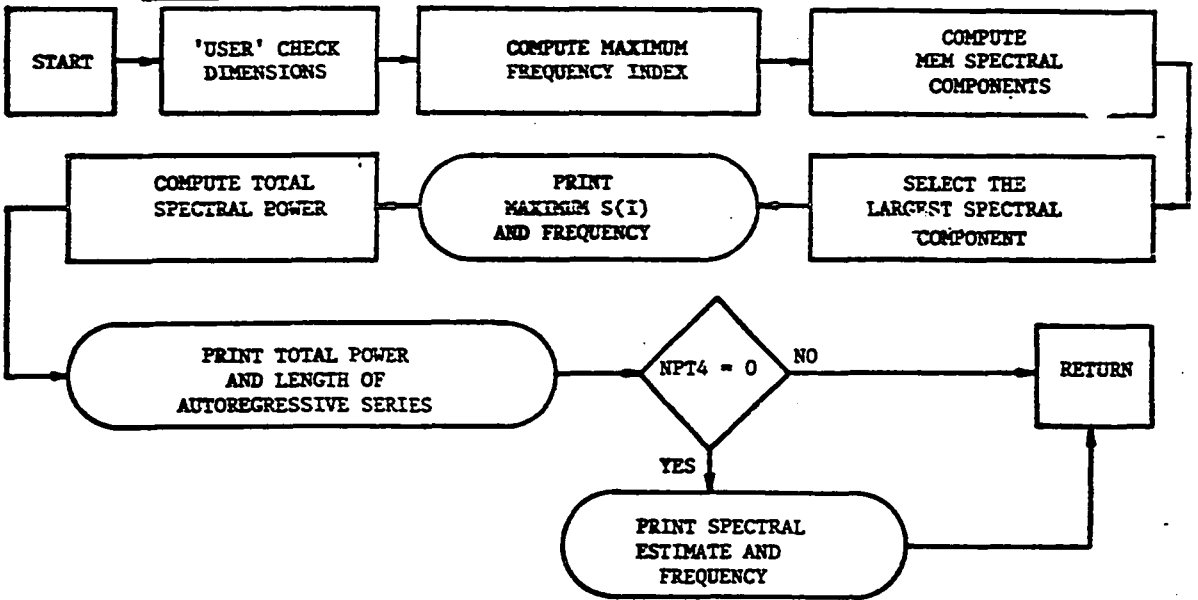
Figure 17G-2b. Subroutine Flow Diagrams

2. <u>Input data definitions</u>

FDELT = Output frequency display resolution of the MEM spectral estimate in Hz. If the user selects FDELT = 0., the program will default to a value equal to four times the Fourier resolution.

LINREG = A user selected data preprocessing option. Spectral estimation may be performed using XSV(I), XNORM(I), XMDC(I) or X(I) by choosing LINREG = 3, 2, 1, 0 respectively.

MM = User selected value for the maximum order of the MEM model. This is the maximum number of autoregressive coefficients used to characterize the input time series.

NS = Total number of input data samples. User must dimension program variables accordingly.

PTOPT = A printing option used to control the printed output of the program and used to suppress unwanted output. PTOPT is a binary word of the form: (NPT1, NPT2, NPT3, NPT4). <u>NPT1</u> controls the printing of the input data function and standard variables. <u>NPT2</u> controls the printing of the summary of iterative MEM results. <u>NPT3</u> controls the printing of the autoregressive estimation summary. <u>NPT4</u> controls the printing of the MEM normalized spectral density.

SNAME = A name or label in FORMAT (5A4) used to identify the data record.

XTDELT = Sampling interval for the input time series, seconds.

X(I) = Input time series data. Units of volts will be assumed for simplified presentation.

3. <u>Input data function statistics</u>

$\bar{x}$ = XDC = Average value or estimated mean value of the data function, volts.

$\overline{x^2}$ = PT = Mean-square value of the input data function, volts^2.

σ_x^2 = PZERO3 = Unbiased estimate of the variance of the input data function, volts^2.

σ_x = STDEV3 = Standard deviation, volts.

4. <u>Linear regression</u>

b_o = BZERO = Intercept point from linear regression.

b_1 = BX1 = Slope from linear regression

σ_x^2 = PZERO2 = Variance of the data function after removal of the linear trend.

σ_x = STDEV2 = Standard deviation.

5. <u>Output data definitions</u>

A1(1) =   Starting value of the autoregressive coefficients for the MEM recursion algorithm.

AK(K) =   K-th autoregressive coefficient for an MM-th order process.

FDELT =   Output resolution of the MEM spectral estimate, Hz.

FR(I) =   Frequency points at which the spectral estimate is computed, Hz.

K =   ·   Index for the autoregressive coefficients.

L =   Index for spectral components.

NMAX =   Maximum spectral index number computed on the basis of aliasing.

P(0) = Normalized total power for the time series (equal to the variance).

P(1) = Starting value of the mean-square estimation error for the MEM recursion algorithm.

P(K) = Mean-square estimation error for the K-th order autoregressive estimate.

PT = Total power (or variance) for the data function after linear regression.

S(I) = MEM estimate of the output power spectral density (or second-moment density) function, watts/Hz. The printout gives the positive frequency half of the double-sided density function.

SBIG = Largest spectral component in the estimated spectrum.

SPLOT(I) = The relative power spectral density with respect to the largest component.

XMDC(I) = Input data function with the average value removed.

XNORM(I) = Data function after linear regression.

XSV(I) = The input data function converted to standard variables after linear trend removal.

XTIME = Sample times for the input data function, seconds. This indexed time is used for plotting routines.

6. Example

The time series data in PROGRAM 04 will also be used for this example because it provides a demonstration of the resolution differences between the DFT and MEM. A 9th order autoregressive estimate was chosen for the 41-point time series and the selected output resolution was 2.5×10^{-5} Hz. This

is approximately four times more resolution than the default value in the program. All the printing options were chosen so that the output features could be demonstrated.

Since the raw data exhibits a pronounced average value as well as a linear trend, it was decided that the estimated spectrum would be computed on XSV(I), the input data function after removing the linear trend and converting to standard variables. The input data before and after removing the linear trend is shown in Figure 17G-3. The time series after pre-processing is shown in Figure 17G-4. This is the series for which the spectrum will be estimated. Notice from the data function statistics after linear regression that the variance has been reduced to approximately 61% of its previous value.

The MEM starting values are printed so the user may see the total power (mean-square value) in the data function and the error power in a first order estimate. A summary of iterative results is printed to illustrate the trends in the reduction of the total error power and the extrapolated coefficient, {AK(K): K = 1, 2, ... MM}. The mean-square estimation error follows the typical trend of decreasing rapidly with order until some minimum level is reached. Figure 17G-5 illustrates this effect.

The autoregressive estimation summary gives the mean-square estimation error for the chosen order (MM = 9) of the estimate and the best-fit auto-regressive coefficients. The error power indicates a white noise contribution of only 8.6% to the total spectral power.

The maximum entropy power spectral density estimation output prints the spectral density in watts/Hz as well as relative amplitudes in dB. The numerical integration to obtain total power produces a result very close to unity and this indicates good numerical stability. The largest spectral component occurs at a frequency of 1.925×10^{-3} Hz. Plots of the power spectrum in watts/Hz and in relative dB are shown in Figures 17G-6 and 17G-7.

These results should be contrasted with the DFT estimate given by PROGRAM 04. Comparing Figures 17D-2 and 17G-6 we see the spectral peak is much sharper for MEM. Also the fringe frequency estimate given by MEM is much closer to the true frequency (1.95×10^{-3} Hz.) than that given by the DFT. A further discussion of MEM resolution and this example is given in Chapter XIX.
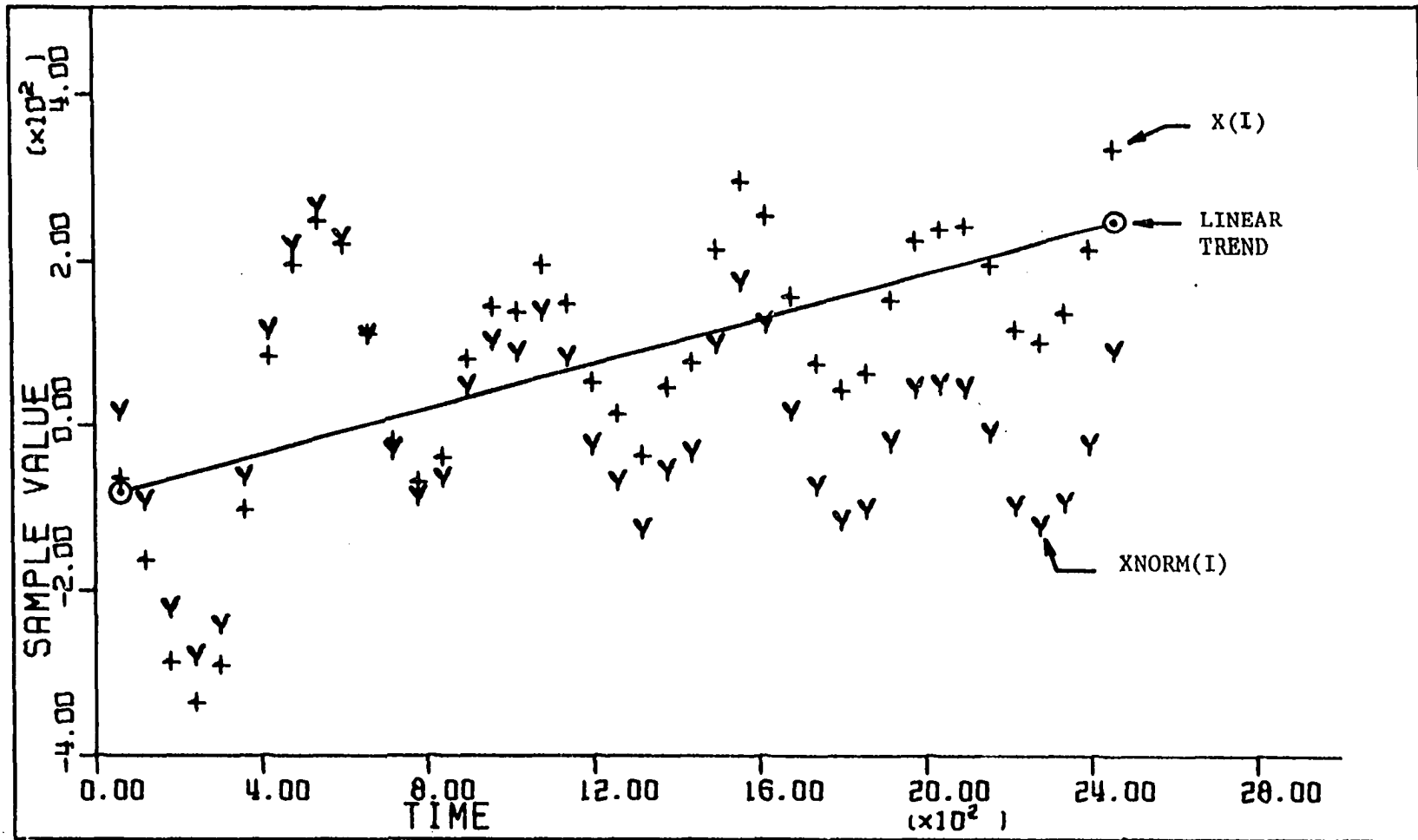
Figure 17G.3. Time Series Data
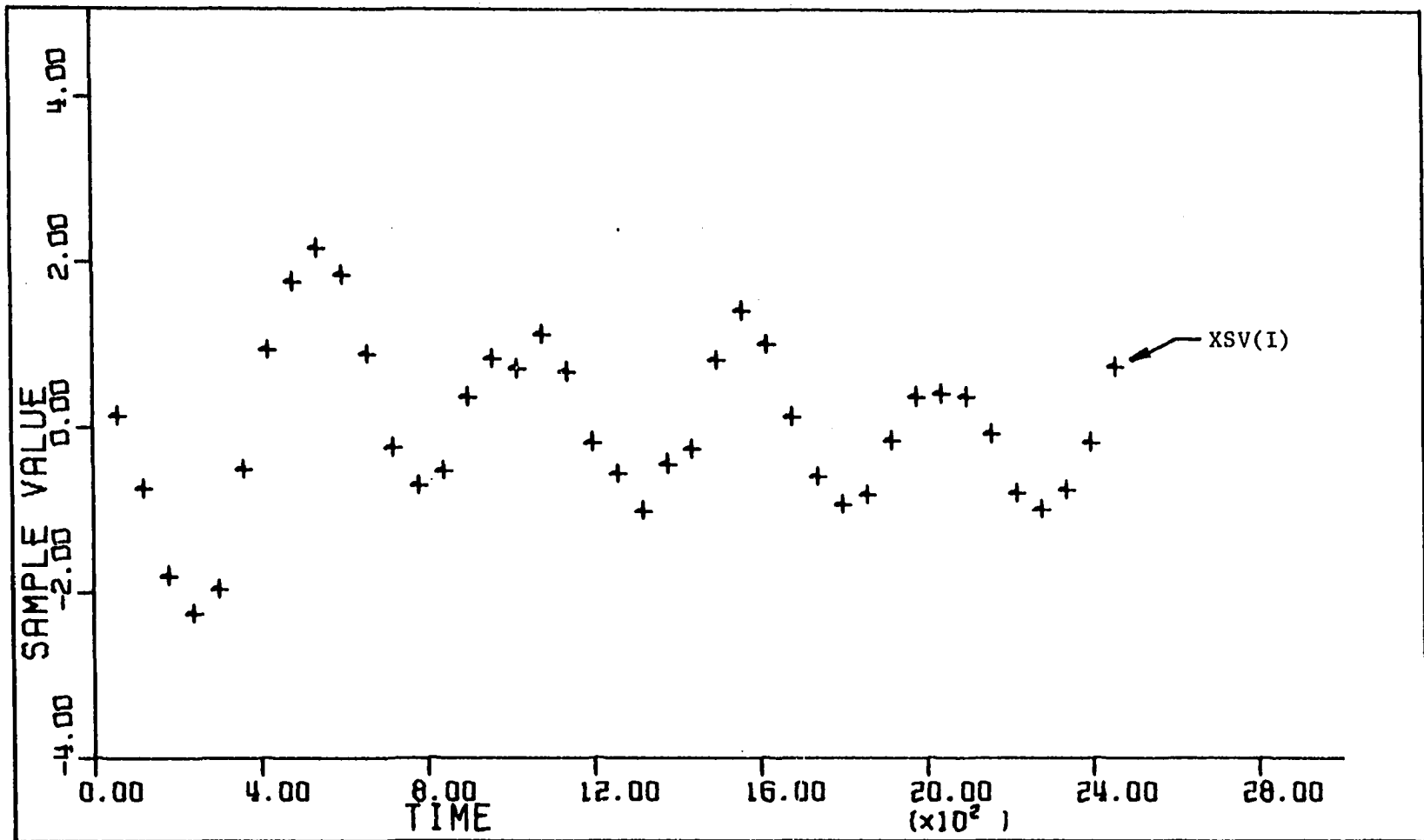
Figure 17G-4. Time Series Standard Variables
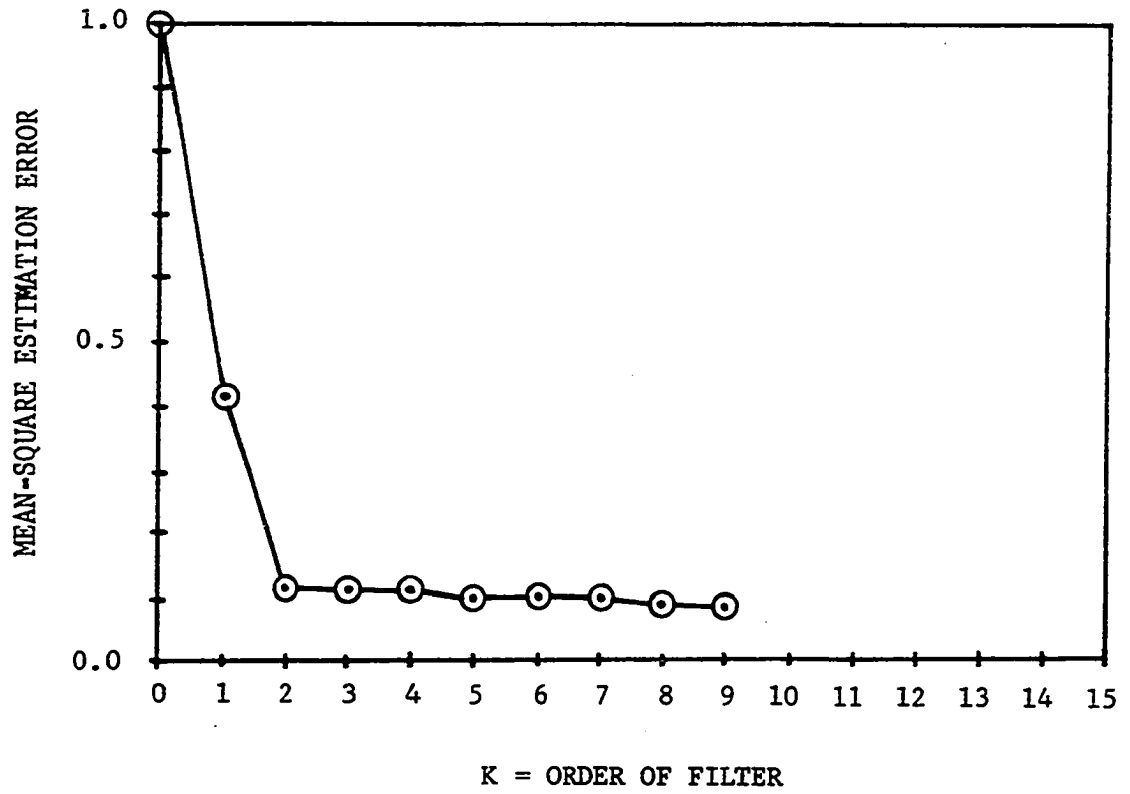
Figure 17G-5.   Estimation Error as a Function of
               the Order of the Estimate
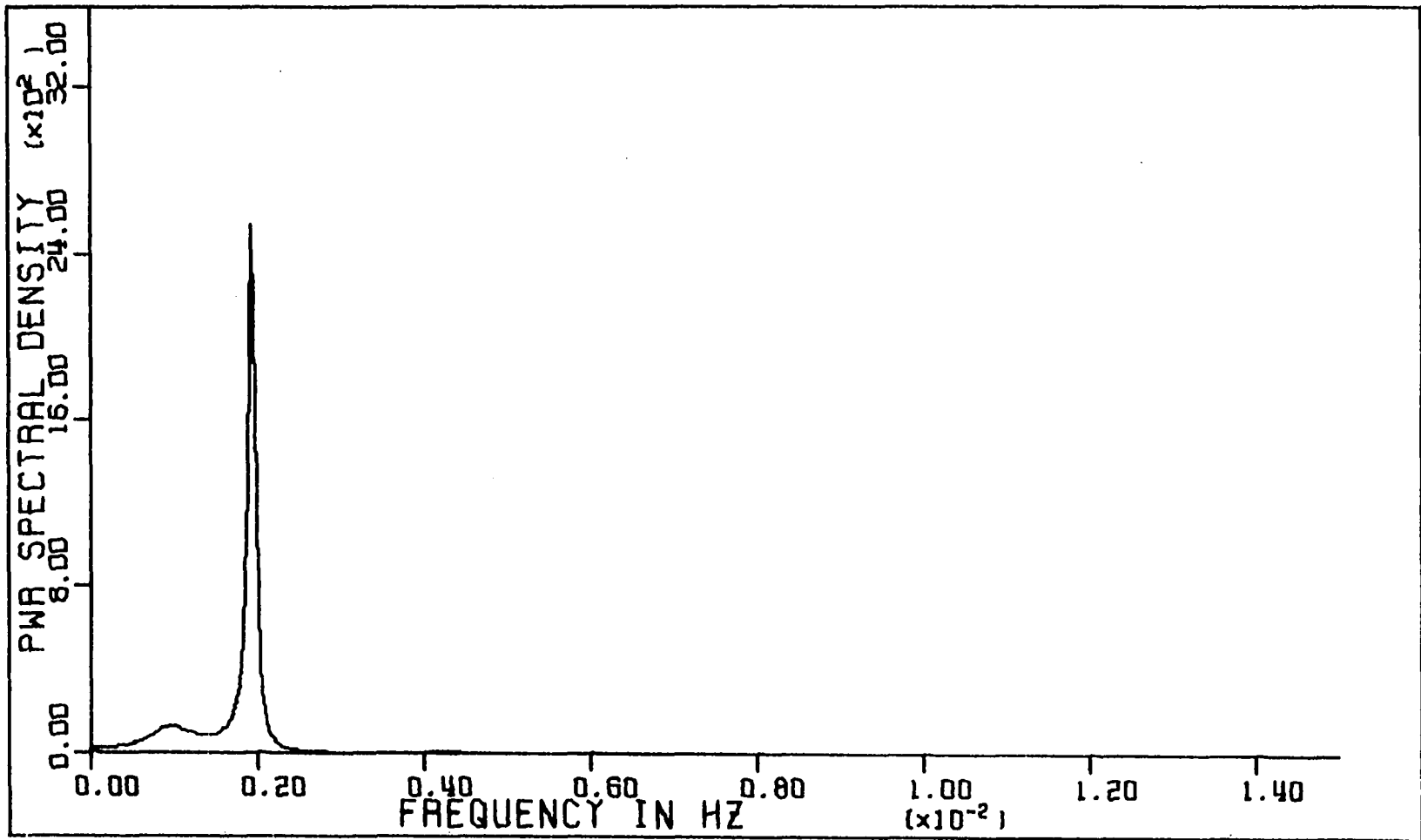
Figure 17G-6. Power Spectrum, HER A 7/29/75
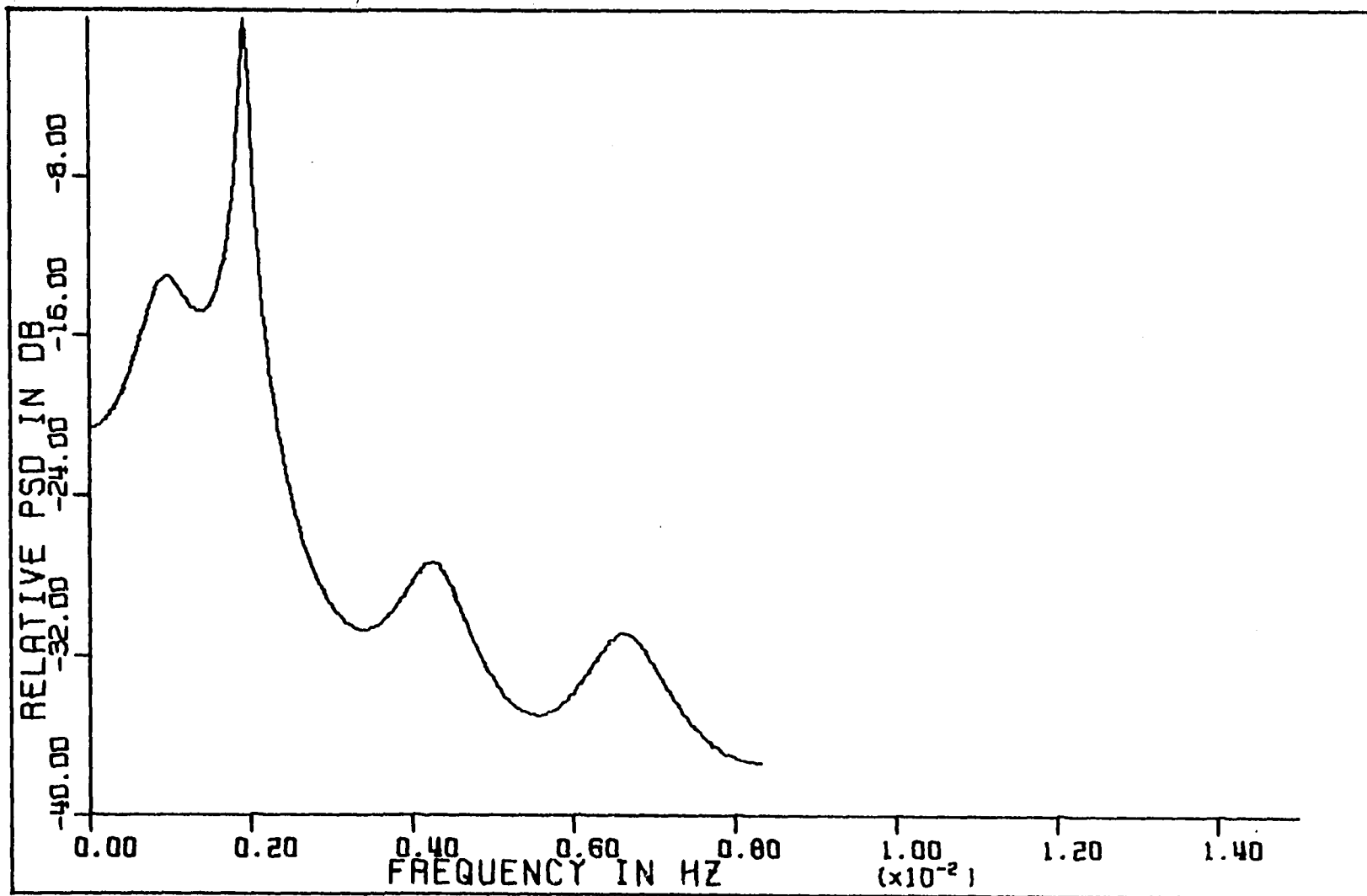
Figure 17G-7. Power Spectrum, HER A 7/29/75

XVIII. MAXIMUM ENTROPY AND FOURIER TRANSFORMS

A. Introduction

This chapter is devoted to a summary of the properties, similarities, and differences in DFT and MEM spectral estimation. These techniques are emphasized because they represent two of the most basic philosophies on spectral estimation: periodic extension in the time domain (DFT) and extrapolation in the autocorrelation domain (MEM). Throughout the presentation we will keep in mind the fact that spectral analysis is usually employed to detect periodicities in a data function and to determine the "strength" and "realness" of the estimated component. This presentation is by no means exhaustive in its coverage nor does it present the variety of viewpoints that are possible. Also, much of the material is redundant in the fact that it may be found in various forms elsewhere in the text.

B. Fourier Transform Spectrum Summary

Since the DFT is a discrete implementation of the Fourier transform it is helpful to discuss these properties first. A time function $\{x(t):-\infty \leq t \leq +\infty\}$ and its amplitude spectral density function $\{X(j\omega):-\infty \leq \omega \leq +\infty\}$ form a Fourier transform pair $(\omega = 2\pi f)$:

$$X(j\omega) = \int_{-\infty}^{+\infty} x(t)^{-j\omega t} dt \qquad (18B.1)$$

$$x(t) = \int_{-\infty}^{+\infty} X(j\omega) e^{+j\omega t} df \qquad (18B.2)$$

The Fourier transform does not exist for all possible types of data functions, a good example being white noise. If the Fourier transform is to exist, it must be piecewise continuous on every finite interval (Riemann

integrability) and it must have a finite average value (necessary). A sufficient (but not necessary) condition is that it be absolutely integrable.

Examples of functions which are most easily analyzed by Fourier transform techniques are single pulse waveforms and time functions modified by a finite data window. These types of transforms are commonly determined both analytically and numerically.

The Fourier transform has the following useful properties:

1. The real part of $X(j\omega)$ is an even function in ω; $\text{Re}\{X(j\omega)\} = \text{Re}\{X(-j\omega)\}$.

2. The imaginary part of $X(j\omega)$ is an odd function; $\text{Im}\{X(j\omega)\} = -\text{Im}\{X(-j\omega)\}$.

3. The amplitude spectrum is an even function; $|X(j\omega)| = |X(-j\omega)|$.

Although not specifically a property, the majority of the functions analyzed using the Fourier transform are time limited: $x(t) = 0$ for $|t| \geq t_{max}$. This produces an amplitude spectrum of infinite extent. The absolute magnitude squared, $|X(j\omega)|^2$, of the amplitude spectral density function is called the energy spectrum of $x(t)$. This concept is used to relate time and frequency in the definition of Parseval's theorem:

$$\int_{-\infty}^{+\infty} |X(j\omega)|^2 df = \int_{-\infty}^{+\infty} |x(t)|^2 dt \qquad (18B.3)$$

The energy spectrum of white noise does not exist because the Fourier transform is undefined.

C. DFT Spectrum Summary

A discrete Fourier transform pair can be obtained from Equations 18B.1 and 18B.2 by using a Riemann sum approximation for the integrals. For a sampled time function, $\{x(k\Delta t): k = -N, -N+1, \ldots, 0, \ldots, N-1, N\}$, containing $(2N+1)$ samples of an infinite time series, the discrete Fourier transform (DFT) is defined by:

$$X(jn\Delta\omega) = \Delta t \sum_{k=-N}^{+N} x(k\Delta t)e^{-jn\Delta\omega k\Delta t} \tag{18C.1}$$

$$x(k\Delta t) = \frac{\Delta\omega}{2\pi} \sum_{n=-N}^{+N} X(jn\Delta\omega)e^{+jn\Delta\omega k\Delta t} \tag{18C.2}$$

There is absolutely no restrictions on the type of function used to obtain a DFT. However, if the DFT is used to make an estimate of the amplitude spectral density function or energy spectrum of a continuous time function, $x(t)$, the _quality_ of the estimate will depend not only on the "true" properties of $x(t)$ but also on the limited ability of $x(k\Delta t)$ to faithfully represent $x(t)$. The commonly used _estimates_ for $X(j\omega)$ and $x(t)$ in terms of the sample function $x(k\Delta t)$ and its DFT are:

$$\hat{X}(j\omega) = \Delta t \sum_{k=-N}^{+N} x(k\Delta t)e^{-j\omega k\Delta t} \tag{18C.3}$$

$$\hat{x}(t) = \frac{\Delta\omega}{2\pi} \sum_{n=-N}^{+N} X(jn\Delta\omega)e^{+jn\Delta\omega t} \tag{18C.4}$$

The DFT has the following properties:

1. The real part of $X(jn\Delta\omega)$ is even.

2. The imaginary part of $X(jn\Delta\omega)$ is odd.

3. The discrete amplitude spectrum, $|X(jn\Delta\omega)|$, is even.

4. The frequency interval of the estimate is: $\Delta\omega = 2\pi/(2N+1)\Delta t$.

From the sample function $x(k\Delta t)$, the estimated Fourier series is computed using (18C.4) and has the following properties:

1. $\hat{x}(t) = x(k\Delta t)$: $t = 0, \pm\Delta t, \pm 2\Delta t, \ldots, \pm N\Delta t$.

2. $\hat{x}(t)$ is periodic with period, $T_N = (2N+1)\Delta t$.

The amplitude spectral density computed using (18C.3) has the following properties:

1. It is periodic with period $2\pi/\Delta t$, $\hat{X}(j\omega + j2\pi/\Delta t) = \hat{X}(j\omega)$.

2. $\hat{X}(j\omega) = \hat{X}^*(-j\omega)$.

3. The estimated amplitude spectrum is even, $|\hat{X}(j\omega)| = |\hat{X}(-j\omega)|$, and is uniquely evaluated in the range, $0 \leq \omega \leq \pi/\Delta t$.

Parceval's theorem for the DFT is given by:

$$\Delta t \sum_{k=-N}^{+N} x^2(k\Delta t) = \frac{1}{(2N+1)\Delta t} \sum_{n=-N}^{+N} |X(jn\Delta\omega)|^2 \qquad (18C.5)$$

An interesting property of the DFT concerns the concatenation of zero's to the data function. The new data function defined by

$$\begin{aligned} y(k\Delta t) &= x(k\Delta t) & \{k = 0, \pm 1, +2, \ldots, \pm N\} \\ &= 0 & \{k = \pm(N+1), \ldots, \pm M\} \end{aligned} \qquad (18C.6)$$

improves the resolution (not "accuracy") of $X(jn\Delta\omega)$ by decreasing $\Delta\omega$. This artifice produces a more continuous and hence pleasing display of the result. For a single time pulse there is no loss of accuracy but for a truly periodic function the period becomes distorted and an additional estimation error is introduced.

D. Wiener-Khinchine Relations

The concept of a _power_ spectral density function (as opposed to the amplitude spectrum) is based on the definition of a time autocorrelation function for a wide-sense stationary random process. The autocorrelation function and the power spectral density function form a Fourier transform pair called the Wiener-Khinchine relations. The advantage of this concept is that the autocorrelation and power spectrum are defined for both periodic and random components. A disadvantage is that more numerical computation is required than for the DFT. The power spectrum of a random process is presented in Appendix I, Part F and in various other chapters.

Applications of the Wiener-Khinchine relations include the Blackman-Tukey method, the maximum entropy method, and the filtering method of spectral analysis. An important model for all of this methods is discussed in Chapter V. Most important are the time domain convolution integral (Equation 5A.1), the autocorrelation domain convolution integral (Equation 5B.5), and the linear filter power spectrum relationship (Equation 5B.8).

E. MEM Spectral Theory Summary

Any process with a bandlimited, finite, and continuous power spectrum can be represented by an infinite moving average (Equation 14.1). The filtering analogy of a moving average process is the linear transformation of white noise. The time series at the output of the filter can be represented arbitrarily close by a K-th order (K possibly infinite) autoregressive series (Equation 14.21). The maximum entropy method maximizes the entropy of the spectrum (Equation 15D.1) subject to the constraint that the inverse Fourier transform of the bandlimited power spectral density function (Equation 15F.1)

for a finite number of sampled autocorrelations be exact (Equation 15D.10). This is equivalent to a least-square error fitting of the time series with a finite number of autoregressive coefficients. Given enough data, this fit can be made arbitrarily close by increasing the order.

F. MEM and DFT Comparisons

The biggest contrast between DFT and MEM spectral estimators is that the former is an amplitude spectrum and the latter a power spectrum. They also differ in the fundamental way they approach the theoretical need for infinite data. The DFT assumes a periodic extension of the sampled data function, $x(k\Delta t)$, while MEM estimates an extrapolated autocorrelation function based on an autoregressive model. Practical applications have shown that extrapolation results in an estimator with superior resolving power. Increases by a factor of 4-5 over DFT have been reported in the literature (Ulrych et. el., 1973).

For bandlimited random processes, the power spectrum estimate of MEM converges with increasing amounts of data while the DFT estimate does not. The spectral amplitudes for the DFT estimate, $|\hat{X}(jn\Delta\omega)|$, are always Rayleigh distributed for Gaussian noise no matter what the record length.

The DFT spectral estimate is periodic, bandlimited, and discrete because of the periodic extension assumption and the Nyquist sampling theorem. The MEM spectral estimate is periodic, bandlimited, and continuous because of the autoregressive model. Both can be designed to give an estimate that is continuous in frequency although practical resolution is usually limited by the required computing effort.

The DFT estimate is "optimum" in the sense that $\hat{x}(t)$ (Equation 18C.4) exactly reproduces the original time series, $x(k\Delta t)$, at the points $t = k\Delta t$. The mean-square error of the time domain representation is thus constrained to zero:

$$E\{[x(k\Delta t) - \hat{x}(k\Delta t)]^2\} = 0 \qquad (18F.1)$$

Because the estimator was also constrained in frequency (bandlimited) it also provides the "smoothest" extrapolation between data points, $x(k\Delta t)$, consistent with the restriction that $\hat{x}(t)$ be periodic. The accuracy with which the spectral estimate, $\hat{X}(jn\Delta\omega)$, agrees with the "true" spectrum, $X(j\omega) = \mathcal{F}\{x(t)\}$, depends upon how well $x(t)$ is modeled by a bandlimited periodic function.

The MEM estimate is "optimum" in the sense that the spectral entropy (Equation 15D.1) is minimized while constraining the estimated autocorrelation function to be the exact inverse Fourier transform of the power spectral density. The mean-square error in the time domain is minimized by choosing autoregressive coefficients which minimize (Equation 13.36):

$$E\{[x(k\Delta t) - \hat{x}(k\Delta t)]^2\} = \sigma_\xi^2 \qquad (18F.2)$$

An interesting parallel between the DFT and MEM can be developed using ideas presented in Chapter XIII. Equation 13.9 represented the Fourier series in a form similar to autoregression. The autoregressive approach starts with the best linear one-step predictor in a least-squares sense:

$$\hat{x}(k+1) = \sum_{n=1}^{K} a_n x(k+1-n) \qquad (18F.3)$$

Using a complex representation for a sinusoid of frequency, f, we have:

$$x(k) = Ae^{+j2\pi f k \Delta t} \tag{18F.4}$$

If, ideally, the prediction error is to be zero, $\hat{x}(k+1) - x(k+1) = 0$, then substituting Equation 18F.4 into 18F.3 gives the condition for the complex coefficients as:

$$Ae^{+j2\pi f(k+1)\Delta t} = \sum_{n=1}^{K} a_n e^{+j2\pi f(k+1-n)\Delta t} \tag{18F.5}$$

This can also be written as:

$$1 = \sum_{n=1}^{K} a_n e^{-j2\pi f n \Delta t} \tag{18F.6}$$

The solution for a_n from (18F.5) is given as:

$$a_n = \frac{1}{K} e^{+j2\pi f n \Delta t} \tag{18F.7}$$

These are the complex coefficients needed to perfectly predict (or filter) the single-frequency sinusoid.

For more than one sinusoid the solution is much more involved. Consider the representation

$$x(k) = \sum_{p=1}^{M} A_p e^{+j\lambda_p k} \tag{18F.8}$$

where $\lambda_p = 2\pi f_p \Delta t$. The condition for the complex coefficients now becomes:

$$\sum_{p=1}^{M} A_p e^{+j\lambda_p(k+1)} = \sum_{n=1}^{K} a_n \sum_{p=1}^{M} A_p e^{+j\lambda_p(k+1-n)} \tag{18F.9}$$

The solution for a_n is given by

$$a_n = \frac{1}{K} \left[\sum_{p=1}^{M} A_p e^{+j\lambda_p(k+1)} \right]\left[\sum_{p=1}^{M} A_p e^{+j\lambda_p(k+1-n)} \right]^{-1} \qquad (18F.10)$$

which reduces to (18F.7) for $M = 1$. Notice the k dependence of a_n when more one frequency is involved. This means that a_n depends on time which is not allowed for autoregressive coefficients. In conclusion, MEM cannot represent the Fourier series given by (18F.8). These representations may be contrasted with the Fourier series representation of Equations 11.9 and 11.10 to determine further comparisons.

XIX. INTERPRETATION OF ESTIMATED SPECTRA

A. Introduction

A study of the properties of the various spectral estimators is only part of the task necessary for the practical application of spectral theory in research. Even after careful selection and implementation of a good estimator one is faced with the task of interpretation of the computed results. In this chapter we will concentrate on the DFT (FFT) and MEM techniques. The important properties that affect the interpretation of the results of these estimates are presented along with practical examples. Two of the most important concepts presented are the detection criterion for a sinewave in Gaussian noise using the FFT and the effects of data length and autoregressive order on the estimated frequency for MEM. The summaries on resolution limits and common estimation errors should be especially helpful for designing the data taking and processing methods.

B. Data Function Models

It is helpful in the interpretation of estimated spectra to keep in mind a suitable model for the process. Three possible models were suggested in Chapter XIII that seem to be able to describe most empirical data functions. These models are:

1. Fourier series plus bandlimited Gaussian noise.

$$y(t) = \xi(t) + \sum_{n=-M}^{+M} c_n e^{+j \frac{2\pi n}{T_F} t} \qquad (19B.1)$$

2. Autoregressive series of order K.

$$y(k) = \xi(k) + \sum_{n=1}^{K} a_n x(k - n) \qquad (19B.2)$$

3. Convolution of a known function and bandlimited white Gaussian noise.

$$y(k) = z(k) * \eta(k) \qquad (19B.3)$$

Strictly speaking, the amplitude spectral density does not exist for these models because they do not have Fourier transforms. As a practical matter however only a limited time record is ever observed and thus the actual empirical data model is the product of $y(t)$ and a suitable time domain window:

$$x(t) = y(t) \cdot w(t) \qquad (19B.4)$$

$$w(t) \neq 0 \qquad |t| \leq t_m \qquad (19B.5)$$
$$= 0 \qquad \text{otherwise}$$

The Fourier transform of $x(t)$ exists for all of the suggested models. The effect of the window function and random noise on the estimated amplitude spectrum are a topic of discussion in this chapter.

The power spectral density function exists for all the models of $y(t)$ because they all have well-defined autocorrelation functions. The "unwindowed" power spectrum is usually referred to as the "true" spectrum and the quality of the estimate is judged against the "true". This is not a really fair comparison in many cases because of the degrading effects of data windowing. Whenever possible, an estimate should be compared to the spectrum of the "windowed" function.

For purposes of reference, the power spectral density functions of the models will now be given. For all cases, the spectral models will be obtained from the following:

$$E\{y(t)\, y\,(\tau - t)\} = R_y(\tau) \tag{19B.6}$$

$$\mathcal{F}\{R_y(\tau)\} = S_y(f) \tag{19B.7}$$

$$\mathcal{F}\{E\{\xi(t)\, \xi\,(\tau - t)\}\} = S_\xi(f) \tag{19B.8}$$

The spectra of the models are:

1. Fourier series plus bandlimited Gaussian noise.

$$S_y(f) = S_\xi(f) + \sum_{n=-M}^{+M} |c_n|^2 \, 2\pi\delta(\frac{n}{T_F} - f) \tag{19B.9}$$

2. Autoregressive series of order K.

$$S_y(f) = \frac{S_\xi(f)}{\left| 1 - \sum_{n=1}^{K} a_n e^{-j2\pi f n \Delta t} \right|^2} \tag{19B.10}$$

$$S_\xi(f) = \sigma_\xi^2 \, \Delta t \qquad |f| \le f_N \tag{19B.11}$$
$$= 0 \qquad\qquad \text{otherwise}$$

$$f_N = \frac{1}{2\Delta t}$$

3. Convolution of a known function and bandlimited white Gaussian noise.

$$S_y(f) = S_z(f) S_\xi(f) \tag{19B.12}$$

$$S_z(f) = H(j\omega)H^*(j\omega) \qquad \text{(convolution filter)} \qquad (19B.13)$$

$$S_\xi(f) = \sigma_\xi^2 \, \Delta t \qquad |f| \le f_N \qquad (19B.14)$$
$$= 0 \qquad \text{otherwise}$$

$$f_N = \frac{1}{2\Delta t}$$

There are many pathological functions which do not fit these models and whose spectra are not well-estimated but for the majority of noisy data, these models are adequate. Also, there seems to be a reluctance on the part of some theorists to accept the noise model restrictions of finite bandwidth and Gaussian distribution on the noise model. Bandlimiting is not a problem either conceptually or practically as all measurement techniques cause bandlimiting. The Gaussian assumption is harder to justify conceptually but for practical applications the Central Limit Theorem usually applies because of all the linear operations associated with signal processing. In most communication and signal processing systems the narrow-band filtering (linear filtering) generates Gaussian noise.

C. DFT and Gaussian Noise

The DFT is still commonly used for analyzing noisy or almost random data in spite of the fact that nearly every book on signal processing cautions that the DFT estimate for random noise does not converge. This misuse is probably a result of the following circumstances:

1. The FFT is readily available and the Fourier transform method of estimating an amplitude spectrum is widely understood.

2. The autocorrelation method of estimating a power spectrum is more difficult and the Blackman-Tukey approach is not as widely understood.

3. The data window effect (Equation 19B.4) allows the existence of a DFT for x(t). It also allows for a statistical interpretation of the estimate and for spectral smoothing techniques.

The application of the DFT to a limited time record of bandlimited Gaussian noise will now be presented.

The complex Fourier amplitudes for a random signal defined by $\{\xi(k): k = 0, \pm 1, \pm 2, \ldots, \pm N\}$ are given by the complex series:

$$\hat{c}_n = \frac{1}{2N+1} \sum_{k=-N}^{+N} \xi(k) e^{-j \frac{2\pi}{2N+1} nk} \tag{19C.1}$$

The sampling interval in time is Δt and is represented at times, $t = k\Delta t$, by the index k. An alternate representation for (19C.1) is given by

$$\hat{c}_n = \frac{1}{2N+1} (\hat{\alpha}_n - j\hat{\beta}_n) \tag{19C.2}$$

where

$$\hat{\alpha}_n = \xi(0) + \sum_{k=1}^{N} [\xi(k) + \xi(-k)] \cos \left(\frac{2\pi}{2N+1} nk\right) \tag{19C.3}$$

$$\hat{\beta}_n = \sum_{k=1}^{N} [\xi(k) - \xi(-k)] \sin \left(\frac{2\pi}{2N+1} nk\right) \tag{19C.4}$$

$$\hat{c}_n = \hat{c}_{-n} \tag{19C.5}$$

$\hat{\alpha}_n$ and $\hat{\beta}_n$ are both Gaussian because the operations described by (19C.3) and (19C.4) are just scaling and linear combinations of the Gaussian random variables, $\xi(k)$. Even when $\xi(k)$ is not Gaussian the central limit theorem applies and the linear combinations of many samples makes $\hat{\alpha}_n$ and $\hat{\beta}_n$ tend to be Gaussian.

The discrete amplitude spectrum is estimated by scaling the absolute value of the complex Fourier amplitudes $(\Delta f = 1/(2N+1)\Delta t)$:

$$\left| \hat{X}(n\Delta f) \right| = (2N+1)\Delta t \left| \hat{c}_n \right| \qquad (19C.6)$$

In terms of the $\hat{\alpha}_n$ and $\hat{\beta}_n$, the estimated amplitude spectrum is:

$$\left| \hat{X}(n\Delta f) \right| = \Delta t (\hat{\alpha}_n^2 + \hat{\beta}_n^2)^{\frac{1}{2}} \qquad (19C.7)$$

From statistical communication theory (Whalen, 1971) we know that $\hat{X}(n\Delta f)$ represents an envelope function and hence is <u>Rayleigh</u> distributed. Since the Rayleigh characteristic does not depend upon the number of samples used in the estimate, the amplitudes remain Rayleigh distributed no matter how much data is used. For this reason the amplitude spectral estimate is said to be nonconvergent.

Figures 19C-1 and 19C-2 show the estimated amplitude spectra for sample records of a bandlimited white Gaussian noise process. The "parent" Gaussian process has the following properties:

1. Mean: $E\{\xi(k)\} = 0$.

2. Mean-Square: $E\{\xi^2(k)\} = 1$.

3. Variance: $E\{(\xi(k) - E\{\xi(k)\})^2\} = 1$.

4. Power Spectrum: $S_\xi(f) = 1/\Delta t$, $|f| \leq f_N$.

The first sample data record with $M = 32$ points has the following properties:

1. Mean: $\langle \hat{\xi}(k) \rangle = 3.25 \times 10^{-2}$

2. Mean-Square: $\langle \hat{\xi}^2(k) \rangle = 1.39$

3. Variance: $\langle (\hat{\xi}(k) - \langle \hat{\xi}(k) \rangle)^2 \rangle = 1.43$

The nonnegative half of the estimated amplitude spectrum shown in Figure 19C-1 has the following properties $\{ n = 0, 1, 2, \ldots, (\frac{M}{2} - 1) \}$:

1. Spectrum: Rayleigh distributed

2. Mean: $\langle |\hat{X}(n\Delta f)| \rangle = 5.94$

3. Mean-Square: $\langle |\hat{X}(n\Delta f)|^2 \rangle = 43.8$

4. Variance: $\langle (|\hat{X}(n\Delta f)| - \langle |\hat{X}(n\Delta f)| \rangle)^2 \rangle = 9.06$

The second sample record with $M = 256$ points has the following properties:

1. Mean: $\langle \hat{\xi}(k) \rangle = -1.52 \times 10^{-2}$

2. Mean-Square: $\langle \hat{\xi}^2(k) \rangle = 0.979$

3. Variance: $\langle (\hat{\xi}(k) - \langle \hat{\xi}(k) \rangle)^2 \rangle = 0.982$

The nonnegative half of the estimated amplitude spectrum shown in Figure 19C-2 has the following properties $\{ n = 0, 1, 2, \ldots, (\frac{M}{2} - 1) \}$:

1. Spectrum: Rayleigh distributed

2. Mean: $\langle |\hat{X}(n\Delta f)| \rangle = 13.8$

3. Mean-Square: $\langle |\hat{X}(n\Delta f)|^2 \rangle = 250.$

4. Variance: $\langle (|\hat{X}(n\Delta f)| - \langle |\hat{X}(n\Delta f)| \rangle)^2 \rangle = 61.4$

Parceval's theorem for the DFT as given in (18C.5) can be rewritten in terms of the present quantities to be:

$$\Delta t \, M \langle \hat{\xi}^2(k) \rangle \simeq \Delta f [M \langle |\hat{X}(n\Delta f)|^2 \rangle - |\hat{X}(0)|^2] \qquad (19C.8)$$

For $\Delta t = 1$ and $\Delta f = 1/M\Delta t$ the estimates above (for $M = 256$) give
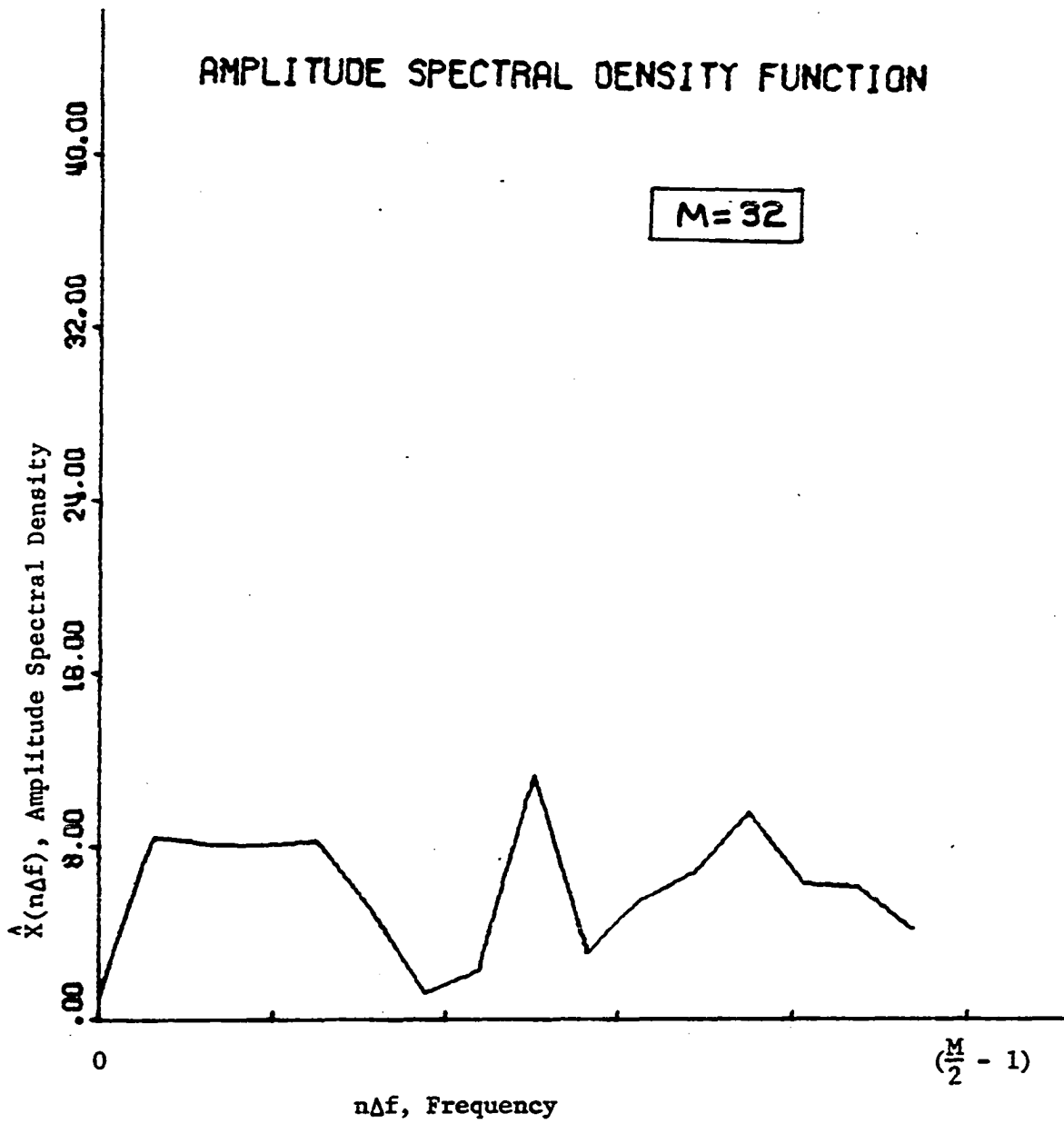
Figure 19C-1. Estimated Amplitude Spectral
Density for Gaussian Noise (M = 32)

$$\Delta t \, M \langle \hat{\xi}^2(k) \rangle \simeq 251.$$

and:

$$\Delta f [M \langle |\hat{X}(n\Delta f)|^2 \rangle - |\hat{X}(0)|^2] \simeq 250.$$

This is in excellent agreement. We also know from theory that, for a truly Rayleigh distribution, the mean and mean-square values should be related as:

$$E\{ |\hat{X}(n\Delta f)|^2 \} = \frac{4}{\pi} E^2 \{ |\hat{X}(n\Delta f)| \} \qquad (19C.9)$$

For estimates, the approximation is:

$$\langle |\hat{X}(n\Delta f)|^2 \rangle \simeq \frac{4}{\pi} \langle |\hat{X}(n\Delta f)| \rangle^2 \qquad (19C.10)$$

For the estimate shown in Figure 19C-2 the ratio of right to left-hand-side of (19C.10) is 0.970 which is a three-percent difference.

Combining Equations 19C.10 and 19C.8 gives an important result that relates the average value of the output amplitude spectrum to the input data. The theoretical result is

$$E\{ |\hat{X}(n\Delta f)| \} = (\frac{\pi}{4})^{\frac{1}{2}} [(\Delta t)^2 M E\{\xi^2(k)\} + \frac{|x(0)|^2}{M}]^{\frac{1}{2}} \qquad (19C.11)$$

while for estimates the approximation is:

$$\langle |\hat{X}(n\Delta f)| \rangle \simeq (\frac{\pi}{4})^{\frac{1}{2}} [(\Delta t)^2 M \langle \hat{\xi}^2(k) \rangle + \frac{|\hat{X}(0)|^2}{M}]^{\frac{1}{2}} \qquad (19C.12)$$

$$\{ n = 0, 1, 2, \ldots, (\frac{M}{2} - 1) \}$$

The reader should again be reminded that all the equations are written in terms of only the nonnegative part of the double-sided amplitude spectrum.
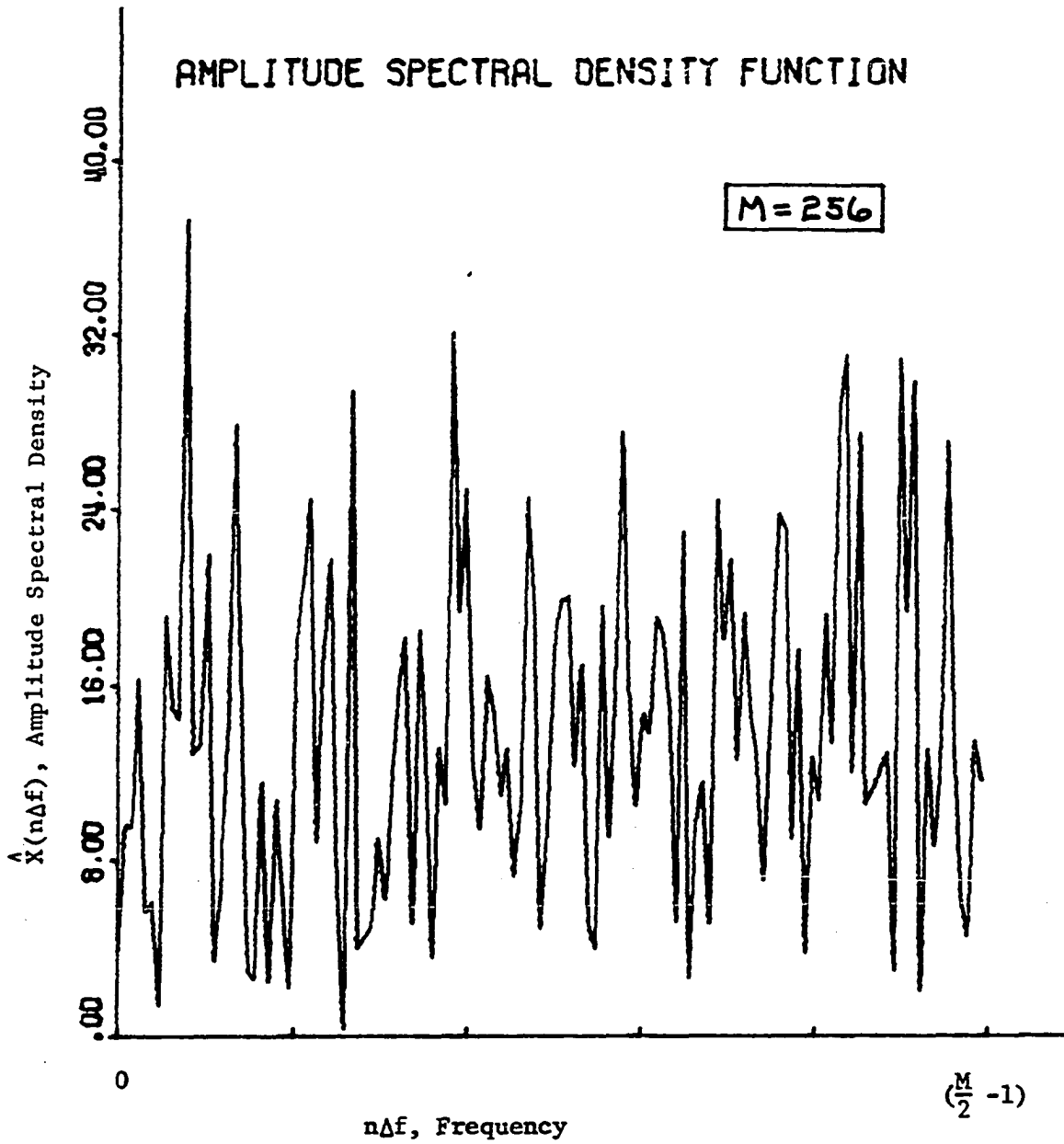
Figure 19C-2. Estimated Amplitude Spectral
Density for Gaussian Noise (M = 256)

Using the notation

$$\sigma_o^2 = \frac{1}{2} [(\Delta t)^2 M \langle \hat{\xi}^2(k) \rangle + \frac{|X(0)|^2}{M}] \tag{19C.13}$$

it is possible to express the characteristics of the Rayleigh distribution compactly as:

1. Mean: $\langle |\hat{X}(n\Delta f)| \rangle \simeq (\frac{\pi}{2})^{\frac{1}{2}} \sigma_o$ (19C.14)

2. Mean-Square: $\langle |\hat{X}(n\Delta f)|^2 \rangle \simeq 2\sigma_o^2$ (19C.15)

3. Variance: $\langle (|\hat{X}(n\Delta f)| - \langle |\hat{X}(n\Delta f)| \rangle)^2 \rangle \simeq (2 - \frac{\pi}{2})\sigma_o^2$ (19C.16)

For the example with $M = 256$, Equation 19C.13 gives $(\sigma_o^2 = 125.3)$.

In this section we have shown that the amplitude spectrum estimates are Rayleigh distributed both in an ensemble sense and across frequency.

The statistical properties of a DFT estimate of the amplitude spectrum of Gaussian noise can be used to develop a simple test for the detection of a periodic component in the spectrum both over frequency and in an ensemble sense.

First, at an a priori selected frequency $a\Delta f$, the amplitude estimates are Rayleigh distributed over an ensemble of spectral estimates. The probability that a single estimate, $|\hat{X}_a|$, from one ensemble function will exceed a selected threshold X_o is given by:

$$P_o = P(|\hat{X}_a| \leq X_o) = \exp[-\hat{X}_o^2/2\sigma_o^2] \tag{19C.17}$$

This is analogous to the well-known "false alarm" probability for statistical detection (Whalen, 1971, Ch. 8) when using a Rayleigh envelope function (Whalen, 1971, Ch. 4). The detection criterion for testing an ensemble of spectral estimates for a periodic component at $a\Delta f$ is developed by selecting

a confidence limit using (19C.17) and (19C.13) and testing all $\overset{\Lambda}{X}_a$'s against the computed threshold X_o.

Second, for a single sample record of the estimated amplitude spectrum the amplitude estimates are Rayleigh distributed over frequency. The probability that any single estimate, $|\overset{\Lambda}{X}(n\Delta f)|$, will not exceed a selected threshold X_o is given by:

$$P(\,|\overset{\Lambda}{X}(n\Delta f)|\, \le X_o) = (1 - P_o) \qquad (19C.18)$$

This is simply one minus the false alarm probability. Using the theorem of joint probability and the multiplication theorem (Beckmann, 1967, p. 19) leads to the probability that any of the M/2 independent amplitude estimates will not exceed a threshold X_o:

$$P(\overset{\Lambda}{X}_1, \overset{\Lambda}{X}_2, \ldots, \overset{\Lambda}{X}_{M/2} \le X_o) = (1 - P_o)^{M/2} \qquad (19C.19)$$

Likewise the probability that one or more amplitudes in a single spectral estimate will exceed X_o is given by:

$$\overset{\Lambda}{P}_o = 1 - (1 - P_o)^{M/2} \qquad (19C.20)$$

Equation 19C.20 can be used to test the largest spectral component to see how likely it would be to achieve that given level. If $\max\{\overset{\Lambda}{X}(n\Delta f)\}$ exceeds some chosen confidence threshold X_o, we can use this test to determine the likelihood of a periodic component. As an example, for the record $M = 256$, the largest amplitude is:

$$\max\{\,|\overset{\Lambda}{X}(n\Delta f)|\,\} = |\overset{\Lambda}{X}(10\Delta f)| = 37.4 \qquad (19C.21)$$

Computing σ_o^2 using (19C.13), the test probability using (19C.17) is:

$$P_o = \exp[-(37.4)^2/2(125.3)] = 3.77 \times 10^{-3} \qquad (19C.22)$$

The probability that at least one of the amplitudes would be as large as $\hat{X}(10\Delta f)$ is:

$$\hat{P} = 1 - (1 - P_o)^{128} = 0.38 \qquad (19C.23)$$

This is a very likely occurrence so we can assume that the spectrum represented by Figure 19C-2 is due exclusively to random noise.

The threshold for a confidence limit of 0.01 is obtained by solving Equations 19C.20 and 19C.17 for X_o. The solution is as follows:

$$\hat{P} = 0.01 = 1 - (1 - P_o)^{128}$$

$$P_o = 7.85 \times 10^{-5}$$

$$\sigma_o^2 = 125.3$$

$$X_o = 48.7$$

If any of the estimated amplitudes had exceeded this level it would have been strong evidence for a periodic component in the data. This technique is recommended as a method of detecting a periodic component in noisy data by using the DFT.

A second example will now be given that includes both sinewave detection and the effect of increasing the total number of phase coherent samples (as discussed in the next section). A test signal of the form

$$y(k\Delta t) = \xi(k\Delta t) + A \sin(2\pi f k \Delta t + 0.77) \qquad (19C.24)$$

was generated using; Gaussian noise with zero mean and unity variance, $A = 0.707$, and $f = 0.249$. PROGRAM 05 was used to obtain amplitude spectrum estimates for data records of various lengths. The results and conclusions will now be discussed.

Table 19C-1 is a summary of results for various data samples. The Rayleigh mean and standard deviation are shown along with the confidence thresholds computed for the 0.05, 0.01, and 0.001 confidence limits. The largest amplitude, its frequency, and probability of occurrence are also shown. Figure 19C-3 shows plots of the amplitude spectral density function for the various phase-coherent sample lengths. The effect of the sinewave component "growing" out of the noise is very evident.

The sinewave component is easily detected for $M = 256$ as shown in Figure 19C-3(d). The probability of occurrence of a component this large from noise alone is only 1.5×10^{-5}. This corresponds to a DFT spectral signal-to-noise ratio (Chapter XIX, Section E) of 31.9 or +15.0 dB (Equation 19E.4). These numbers agree quite well with envelope detection theory (Whalen, 1971, Chapter 8). From this we conclude that enough samples should be taken so that $\underline{SNR}_n$ (Equation 19E.4) is greater than 12 - 15 dB.

This last example was intended to illustrate the effect of increased sampling on the detection of a sinewave component in noise and to indicate the number of samples necessary for a good probability of detection.

Table 19C-1. Summary of Results for the Example of the Detection of a Sinewave in Gaussian Noise.

NS = M	$\langle|\hat{X}|\rangle$	σ_o	X_o @0.95	X_o @0.99	X_o @0.999	$\max\{\hat{X}(n\Delta f)\}$	$n\Delta f$ Hertz	$\hat{P}$ for X_{max}
32	5.32	4.24	14.4	16.3	--	9.5	0.375 $\pm$.031	0.74
64	7.62	6.08	21.8	24.4	--	16.3	0.109 $\pm$.015	0.59
128	10.9	8.72	32.9	36.5	--	30.6	0.250 $\pm$.0078	0.127
256	14.1	11.26	44.5	48.9	54.6	63.6	0.250 $\pm$.0039	1.5×10^{-5}
512	21.1	16.80	69.3	75.7	83.8	115.8	0.250 $\pm$.0019	1.23×10^{-8}
1024	28.6	22.80	97.8	106.1	116.9	322.7	0.249 $\pm$.0009	1.6×10^{-41}

AMPLITUDE SPECTRAL DENSITY FUNCTION

AMPLITUDE SPECTRAL DENSITY FUNCTION

(a)
NS = 32

(b)
NS = 64
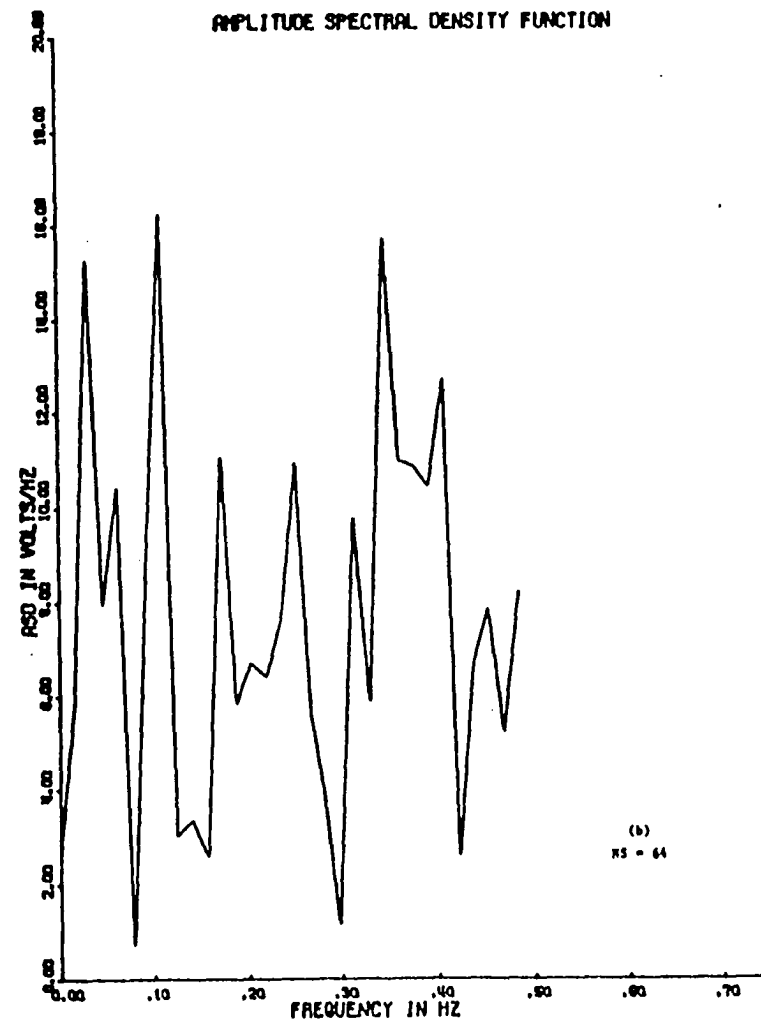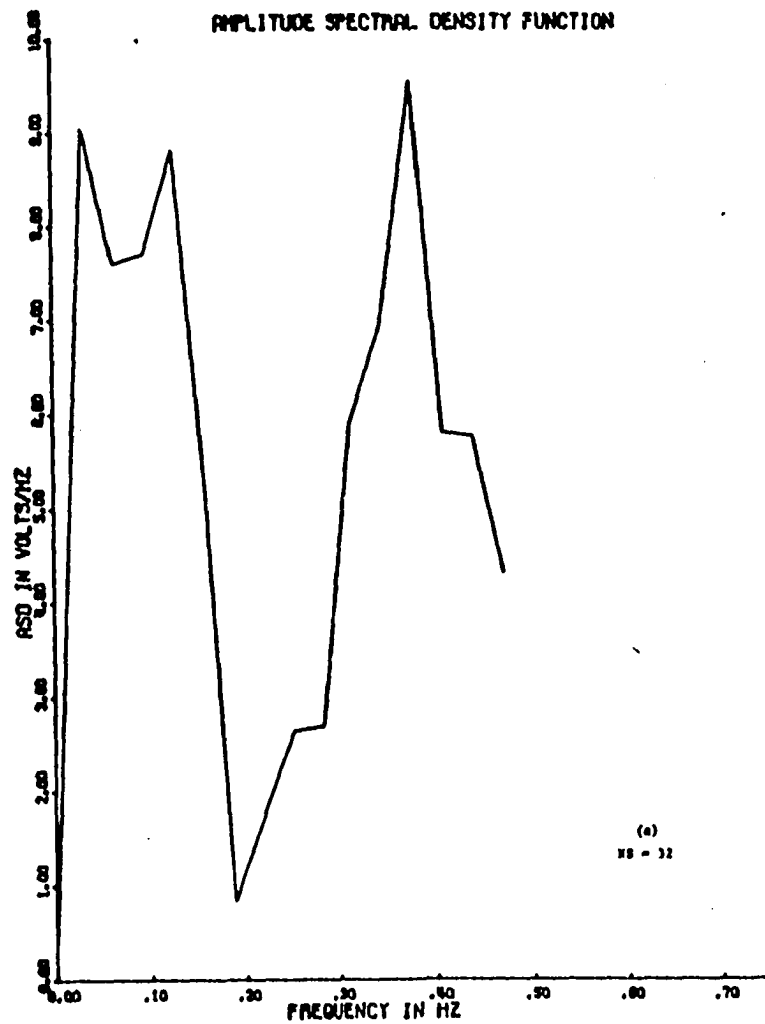
Figure 19C-3. Example Results for the Detection of a Sinewave in Gaussian Noise
as the Number of Coherent Samples is Increased
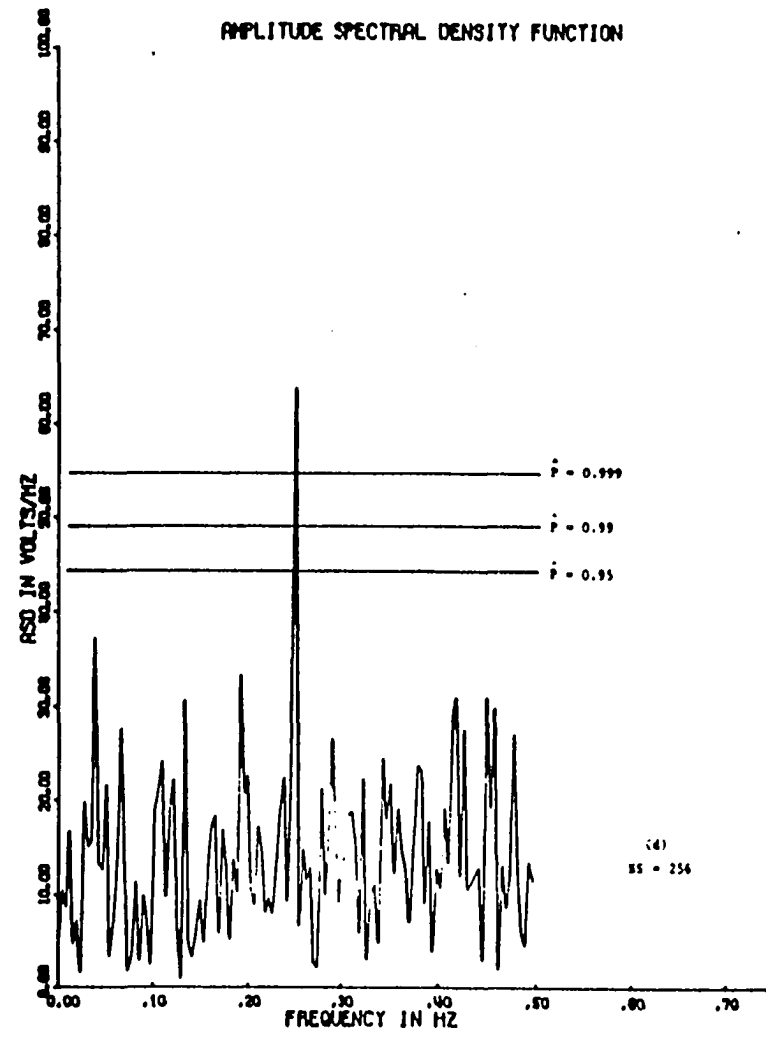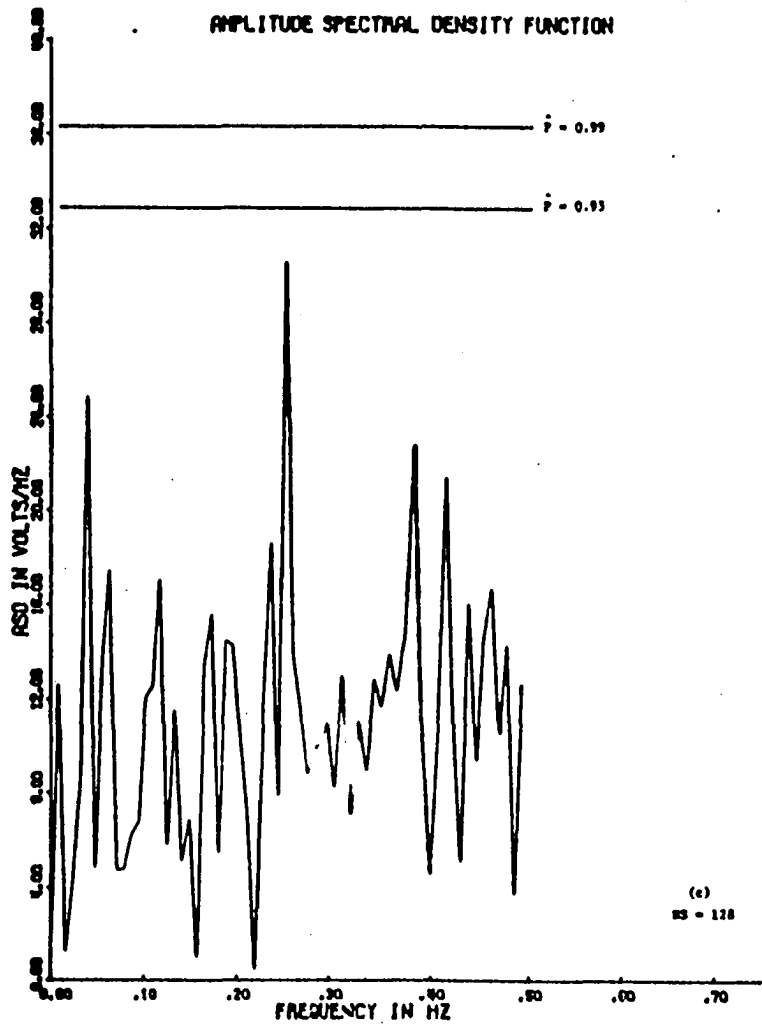
Figure 19C-3. (Continued)
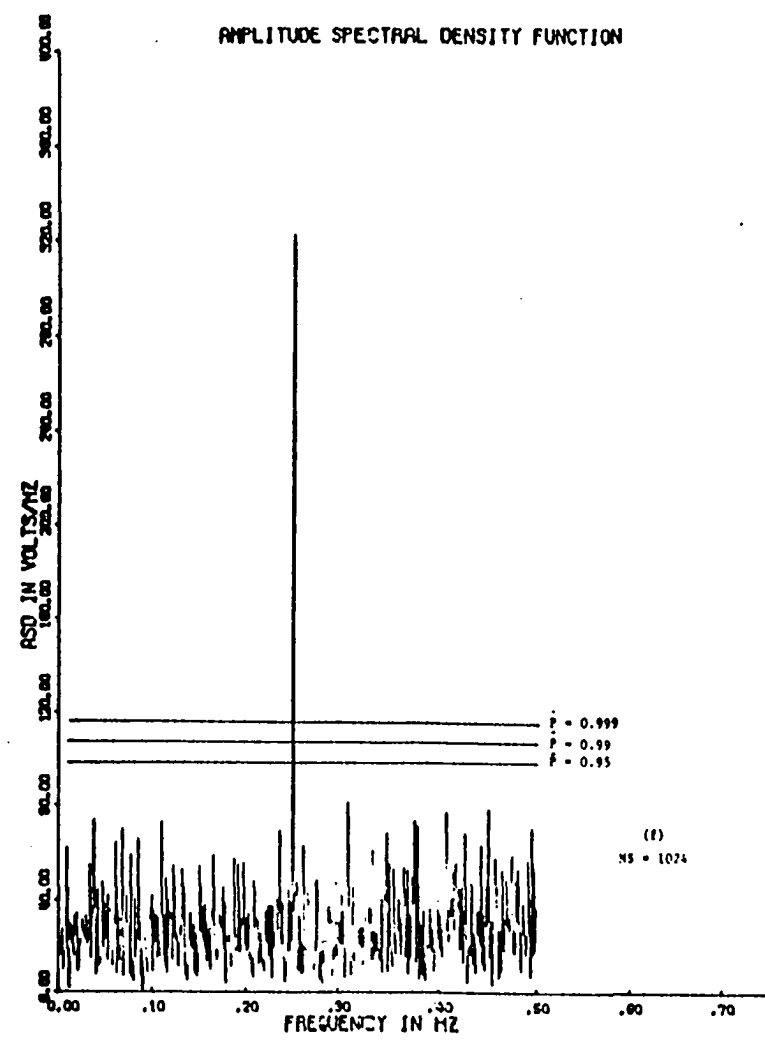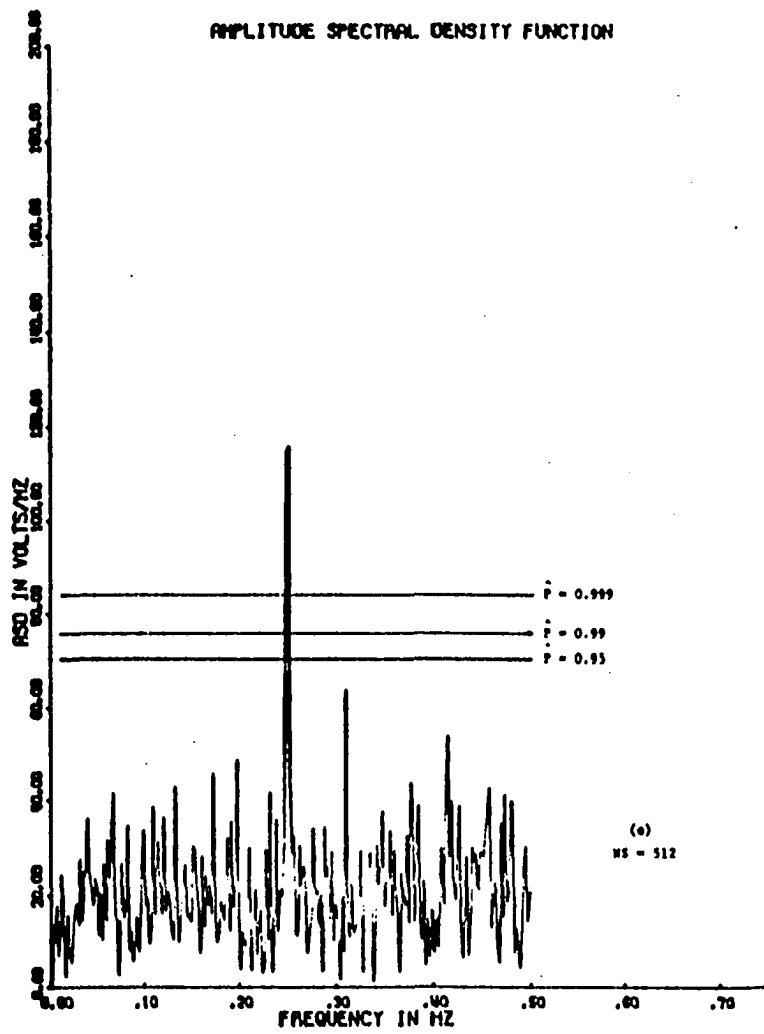
Figure 19C-3. (Continued)

D. DFT and Spectral Averaging

In Chapter XII the sampling and estimation problem was discussed and some groundwork was done on spectral averaging for noisy periodic signals. In Section C of the present chapter, the DFT amplitude spectrum estimate was characterized for a bandlimited Gaussian noise sample. In this section we will look at simple methods of spectral averaging and how they affect the estimate of the amplitude spectral density function.

· For a Gaussian noise input, the amplitude estimate given by Equation 19C.7 has an average value given by Equation 19C.14. For large samples the mean converges to:

$$E\{|\hat{X}(n\Delta f)|\} = \Delta t (\frac{\pi}{4} M E\{\xi^2(k)\})^{\frac{1}{2}} \qquad (19D.1)$$

The mean value depends on the sampling interval, the total number of samples, and the variance of the input noise.

Now consider a finite data function $\{x(k\Delta t): k = 0, \pm 1, \pm 2, \ldots, \pm N\}$ represented by Equation 19B.1 and a rectangular data window function of width, $T_N = (2N + 1)\Delta t$:

$$x(k\Delta t) = \xi(k\Delta t) + \sum_{m=-M}^{+M} c_m e^{+j \frac{2\pi m}{T_F} k\Delta t} \qquad (19D.2)$$

The amplitude spectral density is estimated using the sum of the DFT of $\xi(k\Delta t)$ and the spectral mixing formula (Equation 11.19):

$$\hat{X}(n\Delta f) = \Delta t \sum_{k=-N}^{+N} \xi(k\Delta t) e^{-j \frac{2\pi}{2N+1} nk}$$

$$+ T_N \sum_{m=-M}^{+M} c_m \hat{\delta}(\frac{2\pi m}{T_F} - n\Delta f) \qquad (19D.3)$$

If we represent the second term of (19D.3) by the estimate, $\hat{A}(n\Delta f)$, of the "true" spectrum and the first term by Equations 19C.3 and 19C.4 the result is:

$$\hat{X}(n\Delta f) = \Delta t(\hat{\alpha}_n - j\hat{\beta}_n) + \hat{A}(n\Delta f) \tag{19D.4}$$

Since the estimate $\hat{A}$ is complex it can be represented as

$$\hat{A}(n\Delta f) = A_n e^{-j\theta_n} \tag{19D.5}$$

and the estimated amplitude spectrum can be expressed in complex form as:

$$\hat{X}(n\Delta f) = [\Delta t\hat{\alpha}_n + A_n \cos\theta_n] - j[\Delta t\hat{\beta}_n + A_n \sin\theta_n] \tag{19D.6}$$

The terms A_n and θ_n are really the noiseless estimates of $|X(n\Delta f)|$ and $\arg\{X(n\Delta f)\}$ discussed in Chapter XII. These estimates are corrupted only by the spectral mixing effect. The terms $\hat{\alpha}_n$ and $\hat{\beta}_n$ are Gaussian random variables which represent the effects of noise. To adequately represent the effects of record averaging, the terms in Equation 19D.6 need a subscript denoting the record number. If the record number is denoted by the subscript m then the following double subscript notation is needed:

$$\hat{X}_m(n\Delta f) = [\Delta t\,\hat{\alpha}_{nm} + A_{nm} \cos\theta_{nm}] - j[\Delta t\,\hat{\beta}_{nm} + A_{nm} \sin\theta_{nm}] \tag{19D.7}$$

The __vector__ or __coherent__ average for R records is expressed as:

$$Ave\{\hat{X}_m(n\Delta f)\} = [\Delta t\,\frac{1}{R}\sum_{m=1}^{R}\hat{\alpha}_{nm} + \frac{1}{R}\sum_{m=1}^{R}A_{nm}\cos\theta_{nm}]$$

$$-j[\Delta t\,\frac{1}{R}\sum_{m=1}^{R}\hat{\beta}_{nm} + \frac{1}{R}\sum_{m=1}^{R}A_{nm}\sin\theta_{nm}] \tag{19D.8}$$

For large numbers of records the noise averages out and the result may be written in abbreviated notation as:

$$\text{Ave}\{\hat{X}(n\Delta f)\} = \text{Ave}\{A_n \cos\theta_n\} - j\ \text{Ave}\{A_n \sin\theta_n\} \qquad (19D.9)$$

The _algebraic_ or _incoherent average_ is obtained by averaging the magnitude and phase separately. The magnitude and phase of $\hat{X}(n\Delta f)$ are:

$$|\hat{X}(n\Delta f)| = [A_n^2 + (\Delta t)^2(\hat{\alpha}_n^2 + \hat{\beta}_n^2) + 2\Delta t\ A_n(\hat{\alpha}_n \cos\theta_n + \hat{\beta}_n \sin\theta_n)]^{\frac{1}{2}} \qquad (19D.10)$$

$$\text{Arg}\{\hat{X}(n\Delta f)\} = \text{Arctan}\left[\frac{-(\Delta t\ \hat{\beta}_n + A_n \sin\theta_n)}{(\Delta t\ \hat{\alpha}_n + A_n \cos\theta_n)}\right] \qquad (19D.11)$$

Since only the average magnitude is desired for an amplitude spectral density estimate the two types of averages give the final results:

1. Vector or coherent average.

$$\text{Ave}\{|\hat{X}(n\Delta f)|\} = [\text{Ave}\{A_n \cos\theta_n\}^2 + \text{Ave}\{A_n \sin\theta_n\}^2]^{\frac{1}{2}} \qquad (19D.12)$$

2. Algebraic or incoherent average.

$$\text{Ave}\{|\hat{X}(n\Delta f)|\} = [\text{Ave}\{A_n^2\} + (\Delta t)^2\ \text{Ave}\{\hat{\alpha}_n^2 + \hat{\beta}_n^2\}]^{\frac{1}{2}} \qquad (19D.13)$$

The quality of the estimate of the amplitude spectrum is affected both by the observation period T_N (or the total number of samples for fixed Δt) and by the number of records averaged. Equations 19D.12 and 19D.13 are the final results assuming that enough records have been averaged that the variability of the estimated average can be neglected.

According to the spectral mixing theory of Chapter XI, as the observation period T_N increases, the estimate $\hat{A}$ converges to the "true" amplitude:

$$A_n e^{-j\theta_n} \simeq X(n\Delta f) = T_N c_n \qquad (19D.14)$$

and the <u>coherent average</u> gives:

$$\text{Ave}\{|\hat{X}(n\Delta f)|\} \simeq |X(n\Delta f)| \qquad (19D.15)$$

<u>If</u> the records are <u>not phase connected</u>, the phase angles θ_n become random functions of the record number with a uniform distribution $(-\pi, +\pi)$ and the coherent average becomes zero. Normally the phase connection will be approximately correct and θ_n will have a Gaussian distribution around the mean angle. If phase connecting cannot be guaranteed the coherent average should not be used. The coherent average is a fickle performer as an estimator and must be used with caution.

To assess the performance of the incoherent average we need to express it in an alternate form by using Equations 19C.7 and 19C.14 to give:

$$\text{Ave}\{\hat{\alpha}_n^2 + \hat{\beta}_n^2\} = \frac{1}{(\Delta t)^2}(\frac{\pi}{2})\sigma_o^2 \qquad (19D.16)$$

This is used in 19D.13 to obtain the alternate representation:

$$\text{Ave}\{|\hat{X}(n\Delta f)|\} = [\text{Ave}\{A_n^2\} + (\frac{\pi}{2})\sigma_o^2]^{\frac{1}{2}} \qquad (19D.17)$$

From (19D.3) we see that A_n^2 increases as T_N^2 while from (19C.13) σ_o^2 increases only as T_N $(M = T_N/\Delta t)$. Since A_n is always positive, the estimate for large T_N converges to:

$$\text{Ave}\{|\hat{X}(n\Delta f)|\} \simeq \text{Ave}\{A_n\} \qquad (19D.18)$$

For $\text{Ave}\{A_n\} = 0$, the estimate of (19D.17) converges to that of (19C.14).

The amplitudes A_{nm} are statistically variable because the samples are not phase connected and because of spectral mixing effects. Because the phase reference for several arbitrary records is random and approximately uniformly distributed, A_{nm} will have a Gaussian distribution about some average value that has a fixed bias from the true value, $|X(n\Delta f)|$.

E. DFT Signal-To-Noise Ratio Concepts

The concept of a spectral signal-to-noise ratio seems like a natural extension of the presentation in Section D and may contribute to a better understanding of the spectral averaging concept. If we define a signal-to noise ratio for a Fourier frequency $n\Delta f$ as

$$\underline{SNR}_n = \frac{2|c_n|^2}{\frac{1}{M}\langle\xi^2(k)\rangle} \tag{19E.1}$$

and use the relations,

$$\sigma_o^2 \simeq \frac{1}{2} \Delta t\, T_N\, \langle\xi^2(k)\rangle \tag{19E.2}$$

$$|c_n| = \frac{1}{T_N}\, |\hat{X}(n\Delta f)| \tag{19E.3}$$

the SNR at $n\Delta f$ becomes $(M = T_N/\Delta t)$:

$$\underline{SNR}_n = \frac{|\hat{X}(n\Delta f)|^2}{\sigma_o^2} \tag{19E.4}$$

The average value of the estimated amplitude A_n can be represented as a correction factor γ_n times the "true" amplitude:

$$\text{Ave}\{A_n\} = \gamma_n\, |\hat{X}(n\Delta f)| \tag{19E.5}$$

If we identify the total number of samples as $M = T_N/\Delta t$ then Equation 19D.17 may be written as:

$$\text{Ave}\{|\hat{X}(n\Delta f)|\} = (\frac{\pi}{2})^{\frac{1}{2}}\sigma_o[1 + (\frac{2}{\pi})\gamma_n^2 \underline{\text{SNR}}_n]^{\frac{1}{2}} \qquad (19E.6)$$

This equation expresses the average amplitude spectral density as a function of the signal-to-noise power ratio for a spectral component represented by the complex Fourier coefficient, c_n.

For a sufficiently long sample of a model consisting of Gaussian noise with a single periodic component represented by c_m, the spectral mixing correction factor, γ_n, is unity for $n = m$ and zero for all other n. This leads to the approximations:

$$\text{Ave}\{|\hat{X}(n\Delta f)|\} \simeq (\frac{\pi}{2})^{\frac{1}{2}}\sigma_o \qquad n \neq m \qquad (19E.7)$$

$$\text{Ave}\{|\hat{X}(m\Delta f)|\} \simeq (\frac{\pi}{2})^{\frac{1}{2}}\sigma_o[1 + (\frac{2}{\pi}) \underline{\text{SNR}}_m]^{\frac{1}{2}} \qquad (19E.8)$$

For a single sinewave we will briefly introduce another concept with the help fo Equation 19E.8. Applying Parceval's theorem (Equation 18C.5) we get

$$\Delta t \sum_{k=-N}^{+N} x^2(k) = \frac{1}{(2N+1)\Delta t} \sum_{n=-N}^{+N} \text{Ave}\{|\hat{X}(n\Delta f)|\}^2 \qquad (19E.9)$$

or after many manipulations:

$$M(\Delta t)^2 \langle x^2(k) \rangle = \frac{\pi}{2} \sigma_o^2[1 + \frac{2}{\pi} \underline{\text{SNR}}_m] \qquad (19E.10)$$

The presence of a sinewave increases the mean-square value of x(k) as indicated by Equation 19E.10. If the removal of a spectral component $m\Delta f$ · decreases $\langle x^2(k) \rangle$ by an amount that is statistically more significant than

the removal of a random component, then (19E.10) could be the basis of a criterion for detecting a single sinewave component in noisy data.

The author plans to publish additional work with these topics in a future paper.

F. MEM in the Z-Transform Domain

In Chapter XV it was shown that the maximum entropy spectral estimator could be represented by (Equations 15D.38 and 15D.39):

$$\hat{S}_x(f) = \frac{\Delta\tau P_K}{Q(Z)Q^*(Z)} = \frac{\Delta\tau P_K}{|Q(Z)|^2} \tag{19F.1}$$

where:

$$Z = e^{+j2\pi f\Delta\tau} \qquad\qquad |f| \le \frac{1}{2\Delta\tau} \tag{19F.2}$$

$$Q(Z) = 1 - \sum_{k=1}^{K} a_K(k)Z^{-k} \tag{19F.3}$$

Remember that $\Delta\tau$ is the sampling interval in the autocorrelation domain, that $a_K(k)$ represents the coefficients for a K-th order autoregressive model of the time series, and that P_K is the minimum mean-square error of the one-step prediction. The properties of the spectral estimator can be related to the properties of the complex polynomial $Q(Z)$ and the associated coefficients, $a_K(k)$.

The orders of the polynomial and the process are always the same. $Q(Z)$ also represents the z-transform of the "best" least-squares linear prediction filter for the process. For this reason $|Q(Z)|^2$ will be called the absolute value squared of the filter transfer function or simply the power transfer function. We will use the abbreviated notation

$$G(f) = |Q(Z)|^2 = |Q(e^{+j2\pi f \Delta \tau})|^2 \qquad (19F.4)$$

to indicate that Z is evaluated on the unit circle so that $G(f)$ is real. The notation is not precise but generally there is no confusion as to meaning. Another notation option will be the substitution of $\Delta \tau = 1/2f_N$ into some of the equations so that the effect of the Nyquist frequency limit can be displayed directly:

$$Z = e^{+j\pi f/f_N} \qquad |f| \le f_N \qquad (19F.5)$$

As a simple example we will look at a first order process with associated polynomial and power transfer function:

$$Q(Z) = 1 - a_1(1)Z^{-1} \qquad (19F.6)$$

$$|Q(Z)|^2 = [1 - a_1(1)Z^{-1}][1 - a_1(1)Z^{+1}]$$

$$= -a_1 Z^{-1} + [1 + a_1^2(1)] - a_1 Z^{+1} \qquad (19F.7)$$

$$G(f) = 1 + a_1^2(1) - 2a_1(1) \cos(\pi f/f_N) \qquad (19F.8)$$

The zero of $Q(Z)$ occurs at $Z_1 = a_1(1)$ and those of $|Q(Z)|^2$ at $Z_{1,2} = a_1(1)$, $1/a_1(1)$. Figure 19F-1 shows the estimated power spectral density for different values of $a_1(1)$.

Now consider a second order process:

$$Q(Z) = 1 - a_2(1)Z^{-1} - a_2(2)Z^{-2} \qquad (19F.9)$$

$$|Q(Z)|^2 = -a_2(2)Z^{-2} - a_2(1)[1 - a_2(2)]Z^{-1}$$

$$+ [1 + a_2^2(1) + a_2^2(2)] - a_2(1)[1 - a_2(2)]Z^1 - a_2(2)Z^2 \qquad (19F.10)$$
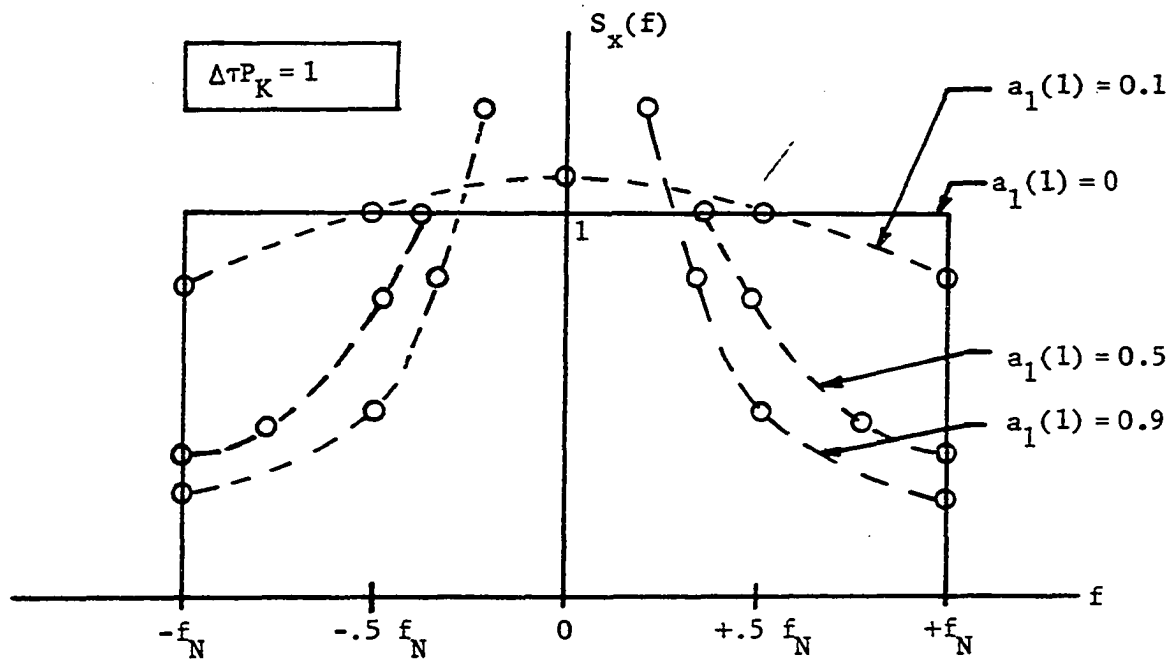
Figure 19F-1. First-Order Spectra

$$G(f) = [1 + a_2^2(1) + a_2^2(2)] - 2a_2(2) \cos (2\pi f/f_N)$$

$$- 2a_2(1)[1 - a_2(2)] \cos (\pi f/f_N) \qquad (19F.11)$$

The zeros of Q(Z) now occur at:

$$z_{1,2} = \frac{1}{2} a_2(1) \pm \frac{1}{2} [a_2^2(1) + 4a_2(2)]^{\frac{1}{2}} \qquad (19F.12)$$

An excellent example for a second order autoregressive time series is given by Fuller (1976, p. 55):

$$x(t) - x(t-1) + 0.89\, x(t-2) = \xi(t) \qquad (19F.13)$$

$$a_2(1) = 1 \qquad\qquad a_2(2) = -0.89 \qquad (19F.14)$$

The zeros of Q(Z) now occur at:

$$z_{1,2} = 0.500 \pm j\, 0.800$$

$$= 0.943\, e^{\pm j\, 1.01} \tag{19F.15}$$

A plot of the locations of both zeros is shown in Figure 19F-2. The auto-correlation function for this process has the appearance of an exponentially damped sinusoid. The power transfer function is:

$$G(f) = 2.79 + 1.78 \cos (2\pi f / f_N) - 3.78 \cos (\pi f / f_N) \tag{19F.16}$$
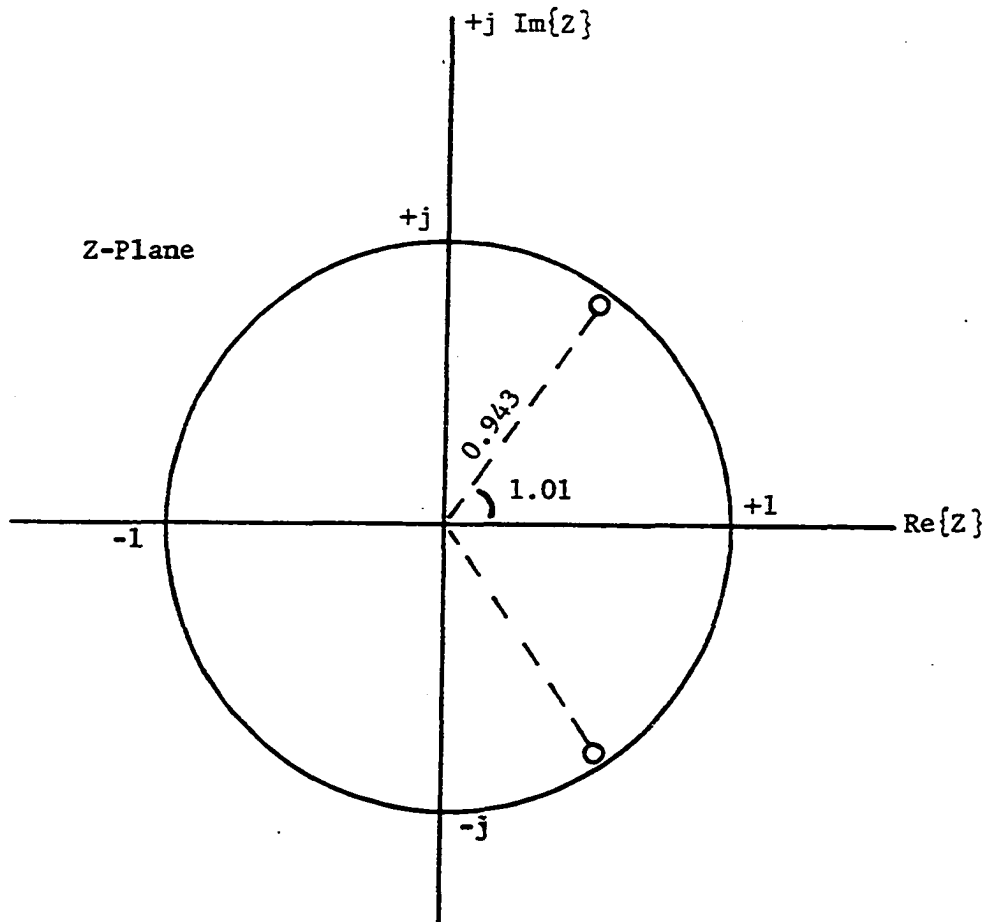
Figure 19F-2. Zeros of $Q(Z) = 1 - Z^{-1} + 0.89\, Z^{-2}$
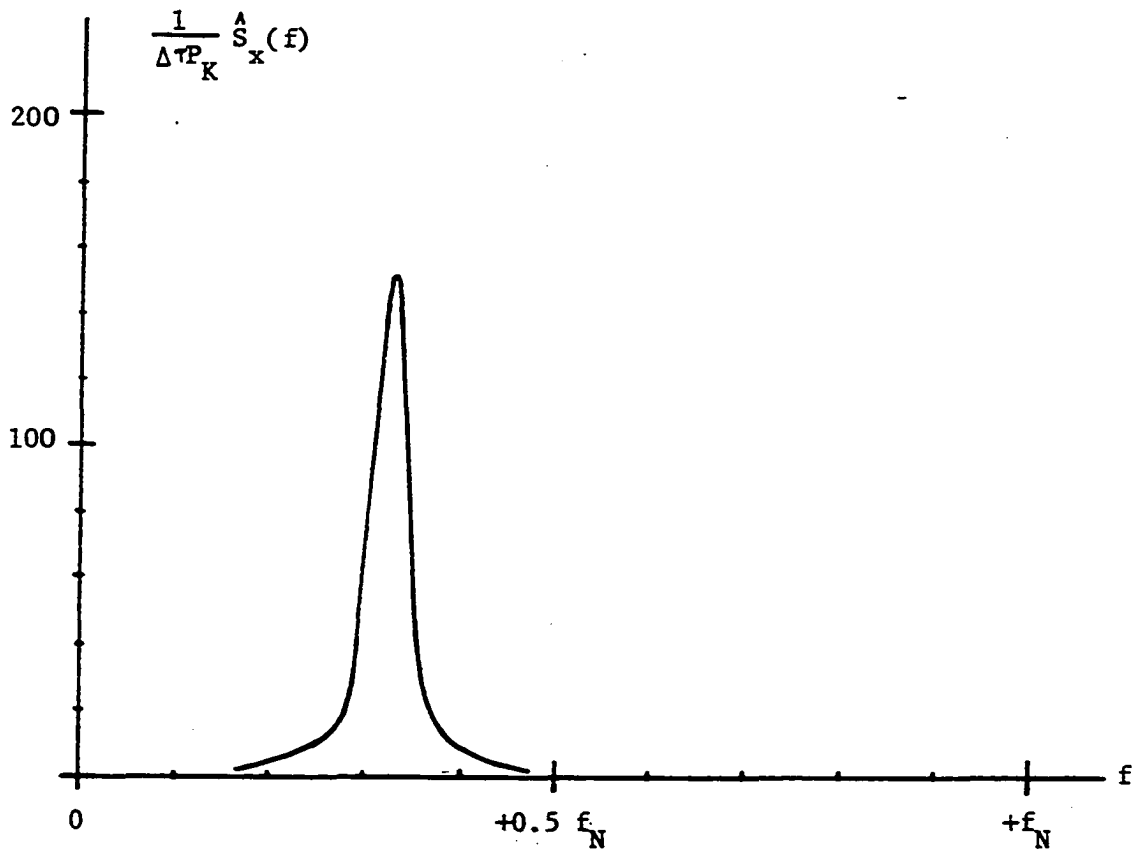
$$\frac{1}{\Delta \tau P_K} \hat{S}_x(f)$$

Figure 19F-3. Typical Spectral Peak for MEM

A plot of $\frac{1}{\Delta \tau P_K} S_x(f) = \frac{1}{G(f)}$ is shown in Figure 19F-3. A multitude of the properties of MEM spectral estimators can now be summarized using the second order process as a typical example. These properties are:

1. Q(Z) gives a complete description of the spectral estimate and the location of its zeros carry important information about the spectral shape.

2. Q(Z) is defined so that all of its zeros lie inside the unit circle.

3. For second and higher orders, the zeros of Q(Z) may be complex. Zeros lying close to the unit circle are capable of representing nearly periodic structure and thus allow MEM to estimate both noise and quasi-periodic components. Zeros off the real axis always come in complex conjugate pairs.

4. For each quasi-periodic component, two orders are needed for Q(Z) because the zeros must come in complex conjugate pairs. Thus to describe five quasi-periodic components the polynomial must be of at least order ten.

5. The Burg recursion restricts the K-th autoregressive component to the range: $0 < a_K(K) < 1$ thereby assuring a positive definite covariance matrix and the absence of zeros lying _exactly_ on the unit circle.

6. The frequency of a zero that is sufficiently isolated from other zeros can be obtained approximately by:

$$f_p \simeq \frac{f_N}{\pi} \text{ARCTAN}\{\frac{\text{Im}\{Z_p\}}{\text{Re}\{Z_p\}}\} \qquad (19F.17)$$

For the Fuller example, $f_p \simeq 0.322 \; f_N$.

7. Some estimates can give a very sharp peak as illustrated by Figure 19F-3. When designing a numerical algorithm for the estimator one must guarantee that no spectral peaks are missing. A quality check can be performed by integrating $S_x(f)$ to see if it gives the total power.

When the approximate peak locations are known an expanded resolution as illustrated by Figure 19F-4 may be economical.

Another approach to determining the location of spectral peaks is to determine the zeros of Q(Z) directly from a polynomial solving routine:

$$Q(Z) = (Z - Z_1)(Z - Z_2)(Z - Z_3) \ldots (Z - Z_K)/Z^K \qquad (19F.18)$$

This works especially well if the zeros are well separated and the order is within reasonable limits. This approach also has the advantage that the stability of the zero locations and their separation from the unit circle can be more directly observed as K is increased. An example of this approach will be given in Section H of this chapter.
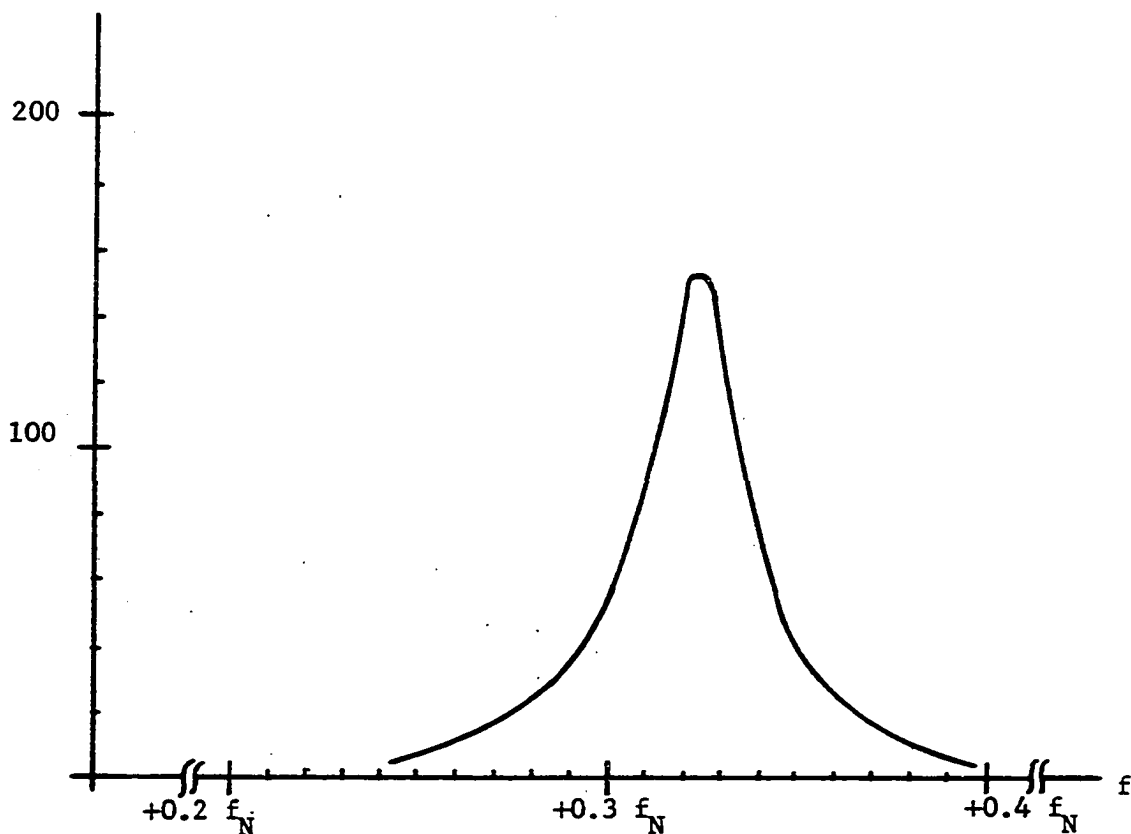
Figure 19F-4. Expanded Resolution of Spectral Peak
Showing the General Shape to be Expected

G. MEM Resolution and Stability

This section is essentially an extension of the last section with an emphasis on the resolution and stability properties of the MEM spectral estimate. The estimator given by Equations 15F.1 or 19F.1 is shown to be continuous, however, for a practical computer implementation, it is discrete. The practical display resolution, Δf, is limited by the amount of computational effort one is willing to invest into Equation 15F.1. A discrete estimator will be represented by

$$\hat{S}_x(n\Delta f) = \frac{\Delta T P_K}{\left| 1 - \sum_{k=1}^{K} a_K(k) e^{-j2\pi m\Delta f k \Delta T} \right|^2} \tag{19G.1}$$

where:

$$\{n = 0, \pm 1, \pm 2, \ldots, \pm(f_N/\Delta f)\} \tag{19G.2}$$

The analogy between MEM and digital filtering will be fully exploited in this section. To begin we redefine the complex polynomial to agree with

$$H(Z) = \frac{1}{Q(Z)} = \frac{Z^K}{D(Z)} \tag{19G.3}$$

where:

$$D(Z) = d_K(0) + d_K(1)Z + d_K(2)Z^2 + \ldots + d_K(K)Z^K \tag{19G.4}$$

$$D(Z) = (Z - Z_1)(Z - Z_2)(Z - Z_3) \ldots (Z - Z_K) \tag{19G.5}$$

$$Z = e^{+j2\pi f \Delta T} \tag{19G.6}$$

The coefficients of D(Z) can be identified with those of Q(Z) by the following:

$$d_K(K) = 1 \qquad d_K(K - k) = -a_K(k) \qquad (19G.7)$$

The complex transfer function $H(Z)$ represents the moving-average filter model. The zeros of $Q(Z)$ are also the zeros of $D(Z)$. The K-th order zero of $H(Z)$ at zero represents a phase angle of $K\pi f/f_N$ at f but has no effect on the spectrum. The MEM power spectrum can also be determined by:

$$\hat{S}_x(f) = \Delta T P_K \left. H(Z) H^*(Z) \right|_{Z = e^{+j2\pi f \Delta T}} \qquad (19G.8)$$

It is common practice to represent each factor of Equation 19G.5 as an amplitude and phase

$$(Z - Z_n) = r_n e^{+j\theta_n} \qquad (19G.9)$$

so that (19G.5) can be expressed in an alternate form as:

$$D(Z) = r_1 r_2 r_3 \cdots r_K e^{+j(\theta_1 + \theta_2 + \ldots + \theta_K)} \qquad (19G.10)$$

The magnitudes, r_n, represent the magnitudes of a vector from the zero location to a location on the unit circle and θ_K is the angle this vector makes with the abscissa. The filter transfer function can now be written as:

$$H(Z) = \frac{e^{+j(K\pi f/f_N - \theta_1 - \theta_2 \ldots - \theta_K)}}{r_1 r_2 r_3 \cdots r_K} \qquad (19G.11)$$

The spectral estimate becomes:

$$\hat{S}_x(f) = \frac{\Delta T P_K}{(r_1 r_2 r_3 \cdots r_K)^2} \qquad (19G.12)$$

The concept of a complex frequency location to describe the zeros of $D(Z)$ will now be given. Its use will become apparent later. A complex frequency Ω_n is defined as

$$\Omega_n = \beta_n + j\,\alpha_n \tag{19G.13}$$

and is used to describe the location of a zero of $D(Z)$ in complex notation:

$$Z_n = e^{+j\pi\Omega_n/f_N} \tag{19G.14}$$

$$Z_n = e^{-\pi\alpha_n/f_N}\, e^{+j\pi\beta_n/f_N} \tag{19G.15}$$

The factors in (19G.9) are expressed in terms of a complex frequency as:

$$(Z - Z_n) = (Z - e^{+j2\pi\Omega_n/f_N}) \tag{19G.16}$$

On the unit circle we get

$$(Z - Z_n) = [e^{+j\pi f/f_N} - e^{-\pi\alpha_n/f_N}\, e^{+j\pi\beta_n/f_N}] \tag{19G.17}$$

or alternately:

$$(Z - Z_n) = e^{+j\pi f/f_N}[1 - e^{-\pi\alpha_n/f_N}\, e^{+j\pi(\beta_n - f)/f_N}] \tag{19G.18}$$

The absolute magnitude of (19G.18) is:

$$|Z - Z_n| = r_n = \{1 + e^{-2\pi\alpha_n/f_N} - 2e^{-\pi\alpha_n/f_N} \cos\,(\pi(\beta_n - f)/f_N)\}^{\frac{1}{2}} \tag{19G.19}$$

The spectral shape of Equation 19G.12 is dominated by the function $|Z - Z_n|^2$ near an isolated zero, Z_n, that is close to the unit circle. The function r_n^2 is conceptually very important because it represents the generic shape factor of the MEM spectral estimator near all isolated zeros of $D(Z)$

when the zero is near the unit circle (small α_n). r_n^2 is a function of both parameters, α_n and β_n, and of the frequency variable f. This is the reason for the concept of a complex frequency to represent the zero. In general we can use (19G.12) to represent the spectral estimate with the amplitude terms r_n^2 formally defined for each zero Z_n as:

$$r_n^2(f) = [1 + e^{-2\pi\alpha_n/f_N} - 2e^{-\pi\alpha_n/f_N} \cos(\pi(\beta_n - f)/f_N)] \qquad (19G.20)$$

with:

$$\alpha_n = -\frac{f_N}{\pi} \ln\{|Z_n|\} \qquad \alpha_n > 0 \qquad (19G.21)$$

$$\beta_n = \frac{f_N}{\pi} \text{Arg}\{Z_n\} \qquad -f_N \le \beta_n \le +f_N \qquad (19G.22)$$

Consider the example shown in Figure 19G-1 for a 3rd-order process with a zero on the real axis and a single complex conjugate pair. For frequencies very near the zero, Z_3, we have $\pi f/f_N \simeq \theta_3$ and $f \simeq \beta_3$. The estimated spectral density is approximately:

$$\hat{S}_x(f) = \frac{\Delta T P_K}{r_1^2(\beta_3) r_2^2(\beta_3)[1 + e^{-2\pi\alpha_3/f_N} - 2e^{-\pi\alpha_3/f_N} \cos(\pi(\beta_3 - f)/f_N)]}$$

$$(19G.23)$$

For $\alpha_n \ll f_N$ the spectral peak is influenced only by the closest zero and occurs at $f = \beta_3$. The estimated spectral density has a peak of:

$$\hat{S}_x(f) = \frac{\Delta T P_K}{r_1^2(\beta_3) r_2^2(\beta_3)[1 + e^{-2\pi\alpha_3/f_N} - 2e^{-\pi\alpha_3/f_N}]} \qquad (19G.24)$$

For $\alpha_n \ll f_N$ the peak is symmetrical about $f = \beta_n$. If we define the frequencies $\beta_n \pm \Delta f/2$ as the points where $\hat{S}_x(f)$ is down from the peak value by an amount K_o then the bandwidth Δf can be determined from the expression:
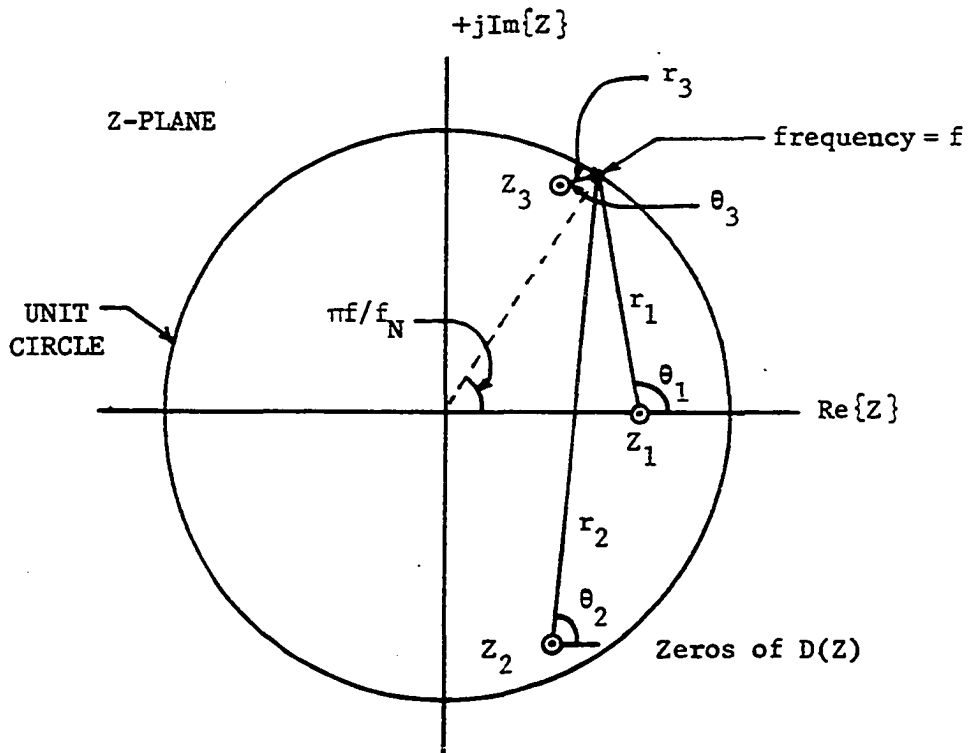
Figure 19G-1. Complex Plane Interpretation of an MEM
Spectral Estimate for a 3rd-Order Process

$$\frac{\left[1 + e^{-2\pi\alpha_n/f_N} - 2e^{-\pi\alpha_n/f_N}\right]}{r_n^2(\beta_n + \Delta f/2)} = \frac{1}{K_o} \qquad (19G.25)$$

The solution for Δf in terms of the cosine function is given by:

$$\cos\left(\frac{\pi\Delta f}{2f_N}\right) = K_2[1 - K_oK_1] \qquad (19G.26)$$

$$K_1 = \frac{[1 + e^{-\pi\alpha_n/f_N} - 2e^{-\pi\alpha_n/f_N}]}{[1 + e^{-2\pi\alpha_n/f_N}]} \qquad K_2 = \frac{1 + e^{-2\pi\alpha_n/f_N}}{2e^{-\pi\alpha_n/f_N}} \qquad (19G.27)$$

$$\frac{\Delta f}{f_N} = \frac{2}{\pi} \text{ARCCOS}\{K_2[1 - K_o K_1]\} \qquad (19G.28)$$

For small α_n, K_2 is very close to unity. As an example, take the solution represented by Equation 19F.15 and Figures 19F-3 and 19F-4. The appropriate factors are:

$$\alpha_n = -\frac{f_N}{\pi} \ln\{0.943\} = -\frac{f_N}{\pi} (-0.0587) \qquad (19G.29)$$

$$K_1 = 1.72 \times 10^{-3} \qquad K_2 \simeq 1.0017$$

Assume a width where the spectrum is down by a factor of $K_o = 2$ and the solution is:

$$\frac{\Delta f_2}{f_N} = \frac{2}{\pi} \text{ARCCOS}\{0.9983\} = 0.0374 \qquad (19G.30)$$

This result can be verified from Figure 19F-4.

Next we consider the spectral resolving ability of MEM for two closely spaced zeros near the unit circle. Assume they are symmetrically spaced about a nominal frequency β_o such that:

$$\beta_1 = \beta_o + \Delta f/2$$
$$\beta_2 = \beta_o - \Delta f/2 \qquad (19G.31)$$

Peaks occur in $\hat{S}_x(f)$ at $f = \beta_1$, β_2 and a valley occurs at $f = \beta_o$.

First assume the zeros are equidistant from the unit circle so $\alpha_1 = \alpha_2 = \alpha_0$. Then the ratio of the dip to one of the peaks can be written as:

$$\frac{r_1^2(\beta_0)\, r_2^2(\beta_0)}{r_1^2(\beta_1)\, r_2^2(\beta_1)} = K_o^{-1} \tag{19G.32}$$

Equation 19G.32 can be evaluated using the results given by (19G.19) and the frequencies, $\beta_o = f$ and $\beta_1 = \beta_o + \Delta f/2$. Expanding the terms gives:

$$\frac{[1 + e^{-2\pi\alpha_o/f_N} - 2e^{-\pi\alpha_o/f_N}\cos(\frac{\pi\Delta f}{2f_N})]^2}{[1 + e^{-2\pi\alpha_o/f_N} - 2e^{-\pi\alpha_o/f_N}][1 + e^{-2\pi\alpha_o/f_N} - 2e^{-\pi\alpha_o/f_N}\cos(\frac{\pi\Delta f}{f_N})]} = K_o \tag{19G.33}$$

This results in a quadratic equation in $\cos(\frac{\pi\Delta f}{2f_N})$ given by

$$[1 + 2K_o K_1]\cos^2(\frac{\pi\Delta f}{2f_N}) - 2K_2 \cos(\frac{\pi\Delta f}{2f_N})$$
$$+ [K_2^2 - K_o K_1 (K_2 + 1)] = 0 \tag{19G.34}$$

where:

$$K_1 = \frac{[1 + e^{-2\pi\alpha_o/f_N} - 2e^{-\pi\alpha_o/f_N}]}{2e^{-\pi\alpha_o/f_N}} \quad \text{and} \quad K_2 = \frac{1 + e^{-2\pi\alpha_o/f_N}}{2e^{-\pi\alpha_o/f_N}} \tag{19G.35}$$

For two zeros spaced from the unit circle such that $\alpha_n = .01$ ($|z_n| \simeq 0.99$) and for a peak-to-valley ratio $K_o = 2$ the quadratic equation can be solved to give:

$$\frac{\Delta f}{f_N} \simeq 0.0556 \tag{19G.36}$$

The solution of (19G.34) must be done with high numerical precision because the coefficients are so close to a value corresponding to $\Delta f = 0$.

These equations illustrate the type of resolution, Δf, needed to evaluate Equation 19G.1 when the zero locations are known from evaluating the polynomials $D(Z)$ or $Q(Z)$. A check on the accuracy of $\hat{S}_x(f)$ is to numerically integrate it to be sure it is equal to the total power. If any peaks are unresolved the integration will yield a value less than the total power.

A solution for resolving power when the zeros are not equidistant from the unit circle is much more difficult. Simplifying assumptions about the location of peaks and valleys are no longer valid. An estimator for the locations of the peaks and valleys as a function of Δf would have to be determined. This more general problem has not been solved.

To determine stability and accuracy of the estimate we need to relate the data to the computation of the zeros of $D(Z)$. This will be done for a second-order process. For a second-order process the polynomial is

$$D(Z) = -a_2(2) - a_2(1)Z + Z^2 \tag{19G.37}$$

and the zero locations are:

$$Z_{1,2} = \frac{1}{2} a_2(1) \pm \frac{1}{2} [a_2^2(1) + 4a_2(2)]^{\frac{1}{2}} \tag{19G.38}$$

If the roots are complex ($a_2(2) < 0$ and $|4a_2(2)| > a_2^2(1)$) the solutions are:

$$Z_{1,2} = \frac{1}{2} a_2(1) \pm \frac{1}{2} j[4|a_2(2)| - a_2^2(1)]^{\frac{1}{2}} \tag{19G.39}$$

Examples of second-order processes can be found in many texts. A good reference is Fuller (1976, p. 54).

For complex roots the following solutions are obtained for the root locations and the sampled autocorrelation function of the process. The absolute values of the roots are:

$$|z_1| = |z_2| = |a_2(2)|^{\frac{1}{2}} \tag{19G.40}$$

The sampled autocorrelation function for positive k is (Fuller, 1976):

$$\hat{R}_x(k\Delta\tau) = A(k\Delta\tau) \sin\left[\frac{\pi\beta}{f_N} k\Delta\tau + \phi\right] \tag{19G.41}$$

$$\cos\left(\frac{\pi\beta}{f_N}\right) = \frac{1}{2} a_2(1) |a_2(2)|^{\frac{1}{2}} \tag{19G.42}$$

$$\tan(\phi) = \left[\frac{1 - a_2(2)}{1 + a_2(2)}\right] \tan\left(\frac{\pi\beta}{f_N}\right) \tag{19G.43}$$

$$A(k\Delta\tau) = \frac{|a_2(2)|^{k/2}}{\sin\phi} \simeq \frac{e^{-2\pi\alpha k\Delta\tau}}{\sin\phi} \tag{19G.44}$$

From the concept of complex frequency we identify:

$$\alpha = -\frac{f_N}{\pi} \ln\{|a_2(2)|^{\frac{1}{2}}\} \tag{19G.45}$$

$$\beta = \frac{f_N}{\pi} \text{ARCCOS}\{\frac{1}{2} a_2(1) |a_2(2)|^{\frac{1}{2}}\} \tag{19G.46}$$

Keeping these results in mind we can now consider the Burg algorithm for MEM and possible sampling effects. First of all we know that $a_K(K)$ is determined by minimizing the error of M_K (Equation 15G.6) in a least squares sense. We also know that the total amount of data used for the estimate (Equation 15G.8) decreases with increasing K. This means that the variance of $a_K(K)$ for a given set of data increases with increasing K. Alternately

for a fixed value of K (K = 2 in our example) the variance decreases with increasing amounts of data. Also as the data increases the <u>variance</u> of the estimated error P_K (Equation 15G.4) decreases. The general trends of these variances are shown in Figure 19G-2. The concept of variance for $a_K(K)$ can be shown using Equation (15G.12) and defining an ensemble with index N to illustrate dependence on sample length:

$$Var\{a_K(K,N)\} = E\{a_K^2(K,N)\} \geq 0 \qquad N < \infty \qquad (19G.47)$$

For large amounts of data the expected values of P_K and $a_K(K)$ tend to zero for large K. For smaller data sets they tend to decrease until the mean is masked by the variability. For some maximum $K = K_m$:

$$E\{a_{K_m}(K_m)\} \simeq 0 \qquad (19G.48)$$

$$E\{P_{K_m}\} = P_{K_m-1}[1 - E^2\{a_{K_m}(K_m)\} \simeq P_{K_m-1} \qquad (19G.49)$$

Typical trends are shown in Figures 19G-3 and 19G-4. For actual data records the masking effect is shown in 19G-5.

The variability of $|a_K(K)|$ directly affects the distance between a zero and the unit circle (Equation 19G.45) thus affecting the peak value. In practical applications this can be seen as a change in peak value for increasing K and as the data record changes.

MEM is becoming more widely known and used because it is an estimator which has better spectral resolution than the DFT for short data records. This effect can be explained for certain types of common sampling situations. The two most common examples are: severe oversampling of short data records
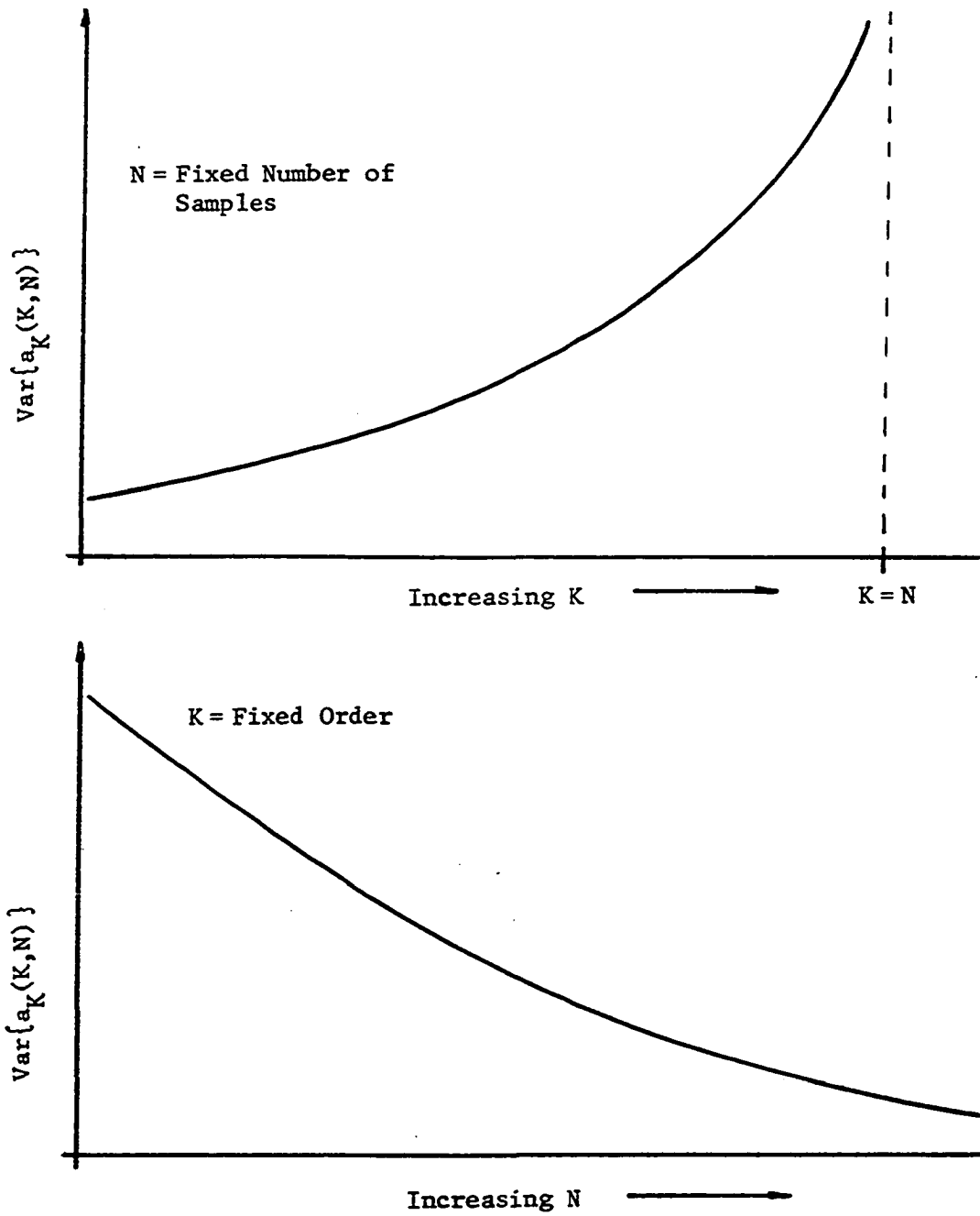
Figure 19G-2. General Trends of the Variability of $a_K(K)$ for Fixed Data Records and for Variable Data Records
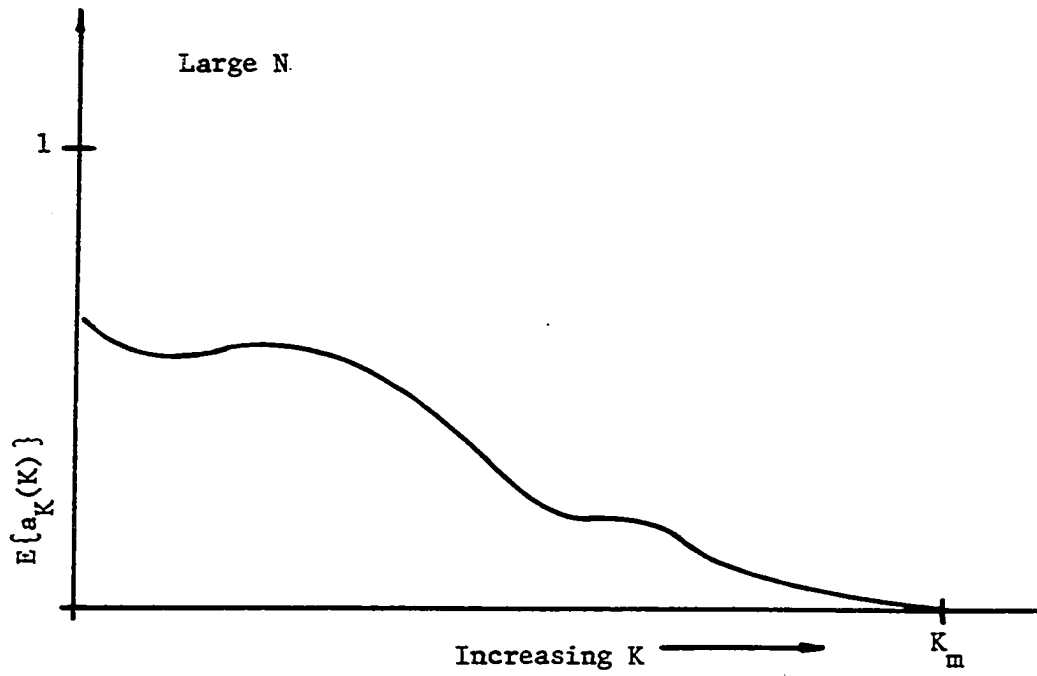
Figure 19G-3. Typical Trend in the Expected Value of
$a_K(K)$ for Large Amounts of Data
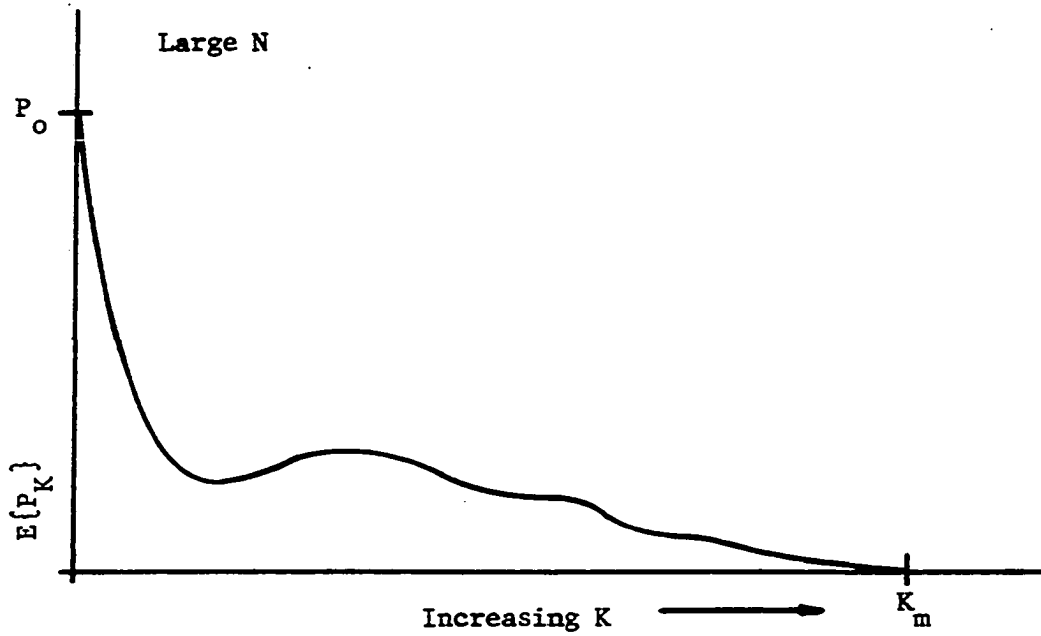
Figure 19G-4. Typical Trend in $E\{P_K\}$ for Large Amounts of Data
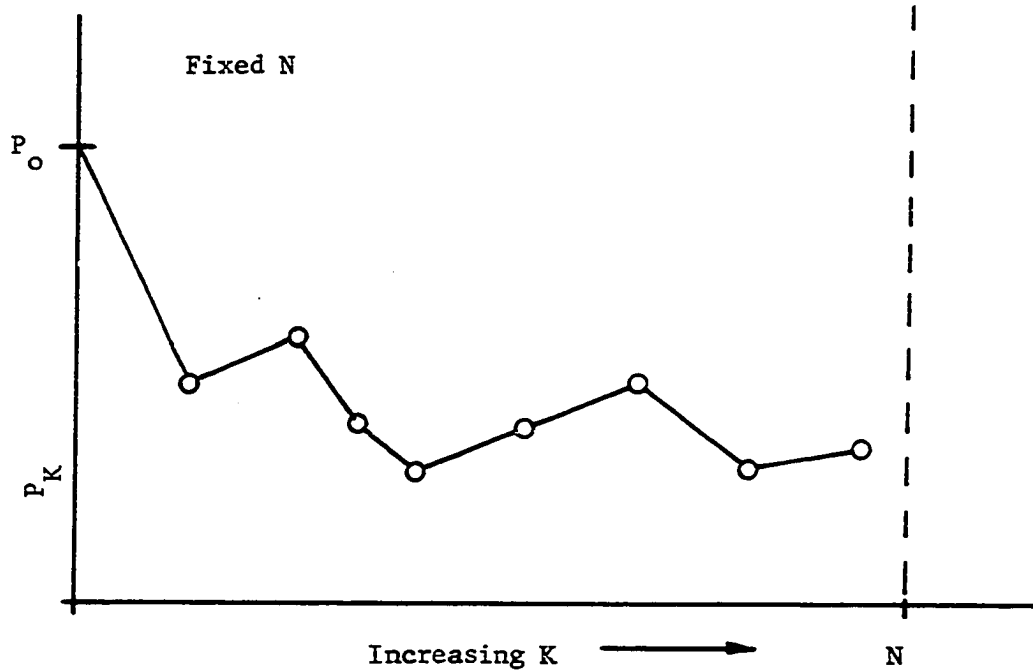
Figure 19G-5. Typical Trend for Actual Estimates of the
Total Mean-Square Error of the One-Step
Prediction

with one periodic component and a reasonable amount of bandlimited noise or

long observation periods with a moderate sampling rate and bandlimited

noise.

Since the autoregressive coefficients can implement both a one-step

predictor in time (Equation 13.35) as well as autocorrelation (Equation

14.42) and since the coefficients are determined by minimizing the mean-

square error (Equation 15G.6) and are not explicitly dependent on the

sampling interval ($\Delta t = \Delta \tau$), the estimate can be considerably improved by

oversampling. Not only does it decrease the variance of $a_K(K)$ due to noise

but once the data record is long enough to include more than about 60% of

a cycle of the sinusoid represented by Equation 19G.41 the extrapolation

property takes over and produces a strong periodic component. The extrapolation is helped by oversampling. For longer records the sampling properties are analogous to those discussed in Chapter XII Section D, Part 4. In effect a single period of $\hat{R}_x(\tau)$ is oversampled and the extrapolation property completes the task of producing a sharp peak.

The effect of increasing the order of the estimate on the spectral resolution is less obvious. For a given fixed record length, increasing the order increases the number of zeros of $D(Z)$. Now only zeros close to the unit circle produce a significant effect on the spectral shape so for given periodicities in the data only these zeros are needed. For a finite and noisy record however these zeros are required to represent a least-squares estimate for all of the data. The net effect is to shift the zeros away from the unit circle. By increasing the order, K, of the estimate, additional zeros are added (additional degrees of freedom for the prediction) that are far from the unit circle thereby having little effect on shape and at the same time allowing the important zeros to move closer to the unit circle. For this reason the spectral resolution is improved (sharper peaks) and the location of the peak is more accurate. The resolution of two closely spaced and equal peaks is a function only of the distance between their zeros and the unit circle. Figure 19G-6 illustrates a spectral representation of the effect of zero location.

A particular zero, Z_n, has a random distribution in a circular sense around some nominal location. The distribution for $|Z_n|$ is a cross section of this circular distribution. When Z_n is close to the unit circle a small change in location has a very gross effect on the amplitude and location of
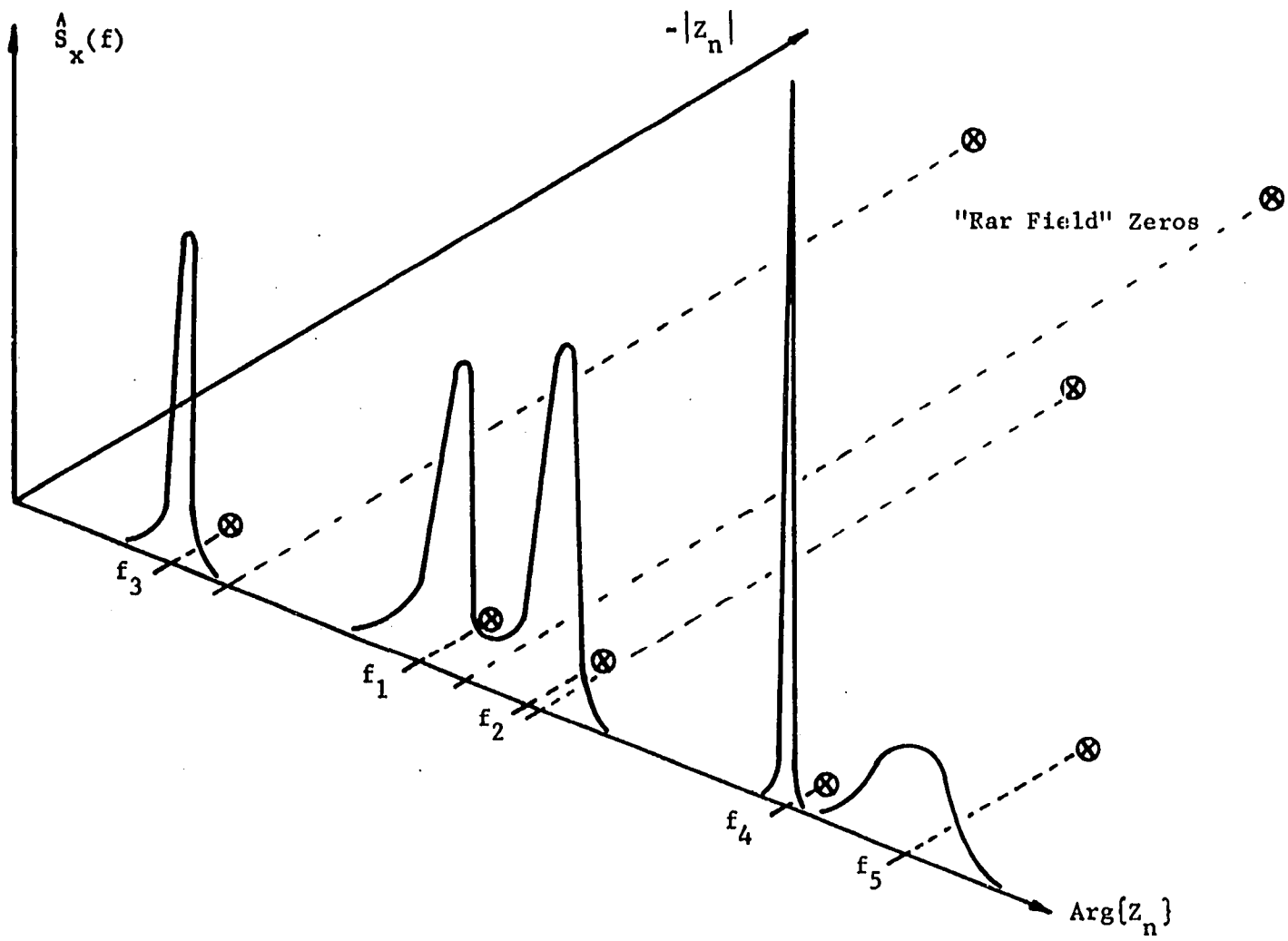
Figure 19G-6. Spectral Representation of the Effect of Zero Location on $\hat{S}_x(f)$

the peak. This shifting and variability can be seen for any practical record. A point of diminishing returns is reached where the average zero location is no longer moved closer to the unit circle by increasing the order, K. The order should not be increased beyond this point. A pictorial representation of this effect for an isolated zero near the unit circle is shown in Figure 19G-7.
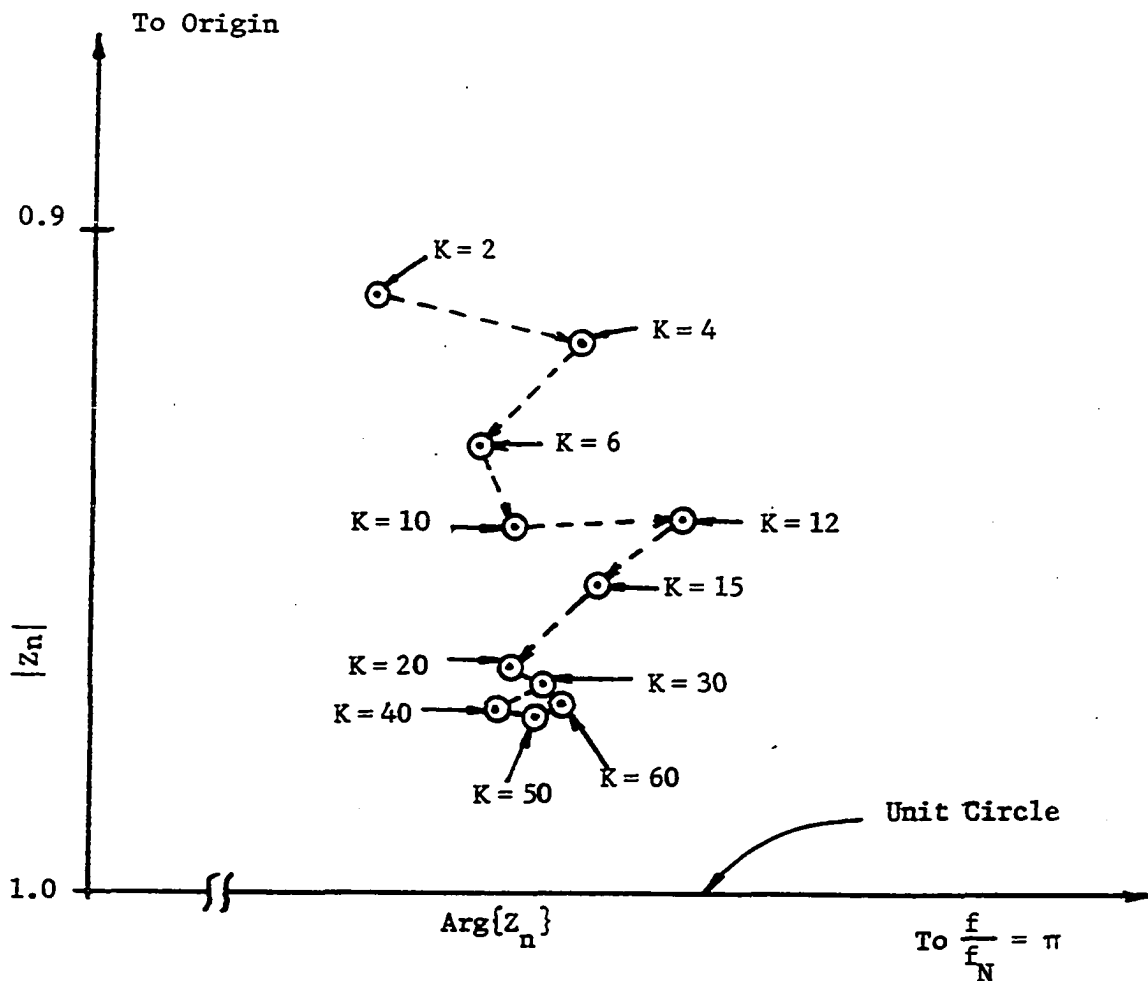
Figure 19G-7. Variability of the Estimated Zero Location
for Increasing Orders of the Estimate

H. DFT and MEM Resolution Limits

1. Introduction

When considering the resolution of a spectral estimator, one must be careful to distinguish between the ability to detect and resolve periodic components and the frequency resolution to which the resulting estimate is displayed. The latter will be referred to as the <u>display resolution</u> while the former will be called the <u>spectral resolution</u> or simply the resolution of the estimator.

An increase in <u>display resolution</u> is only a matter of increasing processor time. It makes the estimate appear more continuous and may be used to produce a more pleasing appearance. High display resolution is particularly needed for MEM because a sharp peak may otherwise be overlooked. For the FFT, higher display resolution may sometimes improve the frequency ambiguity of a spectral peak.

In contrast, the <u>spectral resolution</u> of the estimator is an inherent property that is determined by the "quality" of the estimator and the observation time for the data. It cannot be improved by postprocessing techniques.

2. Display resolution

For MEM spectral analysis the information about sharp spectral peaks is all contained in the zero locations of the complex polynomial, $D(Z)$. These sharp peaks will always be displayed if the frequency interval Δf (Equation 19G.1) is kept small enough. For a given polynomial, the display resolution can be arbitrarily increased by decreasing Δf without affecting estimator quality.

For the FFT, the display resolution problem caused by a sampled spectrum can be minimized by either using a continuous estimator (Equation 11.1) or by concatenation of zeros to the record. Zero concatenation is a well-established technique in FFT analysis and is often used to make the number of data points the required power-of-two. Concatenation forces the FFT to treat the data as though it were a periodic time pulse with a low duty cycle. For large orders of concatenation, the spectral estimate closely approximates that for a single time pulse. Concatenation also increases the apparent observation time thereby causing the apparent amplitudes and frequencies to shift slightly. This can sometimes result in a slightly better estimate of the frequency of peak amplitude. The disadvantage to large order concatenation is increased processing time. A simple DFT does not require zero concatenation.

3. Spectral resolution

The fundamental resolution limit for the DFT is imposed by T_N and was given for two closely spaced sinusoids by Equation 12B.48. The _Rayleigh resolution_ or one-half the bandwidth-between-first-nulls is given by:

$$\Delta B_r = \frac{1}{T_N} \tag{19H.1}$$

This resolution limit assumed a continuous estimator (Equation 11.1) and peaks of equal amplitude. Neither assumption is the case in most practical FFT applications. In most FFT analysis, the estimated location-of-peak is within $\pm \frac{1}{T_N}$ Hz. of the true peak. Zero concatenation does not improve this resolution.

Improvements in the spectral resolution of the DFT can only be obtained by increasing the observation time, T_N.

The spectral resolution for the MEM spectral estimator is limited by the number of independent samples of the time series (observation time, T_N) and the degrees-of-freedom for the spectral estimator (order of the estimated autoregression). Increasing the number of samples decreases the variance of the estimate of the expected values of the autoregressive coefficients. Increasing the order of the estimate allows more degrees-of-freedom to approximate higher order regressions thereby minimizing the error associated with the most prominent spectral peaks. This choice of the degrees-of-freedom is contrasted with the situation for the DFT where the order is fixed.

Mathematical derivations for MEM resolution as a function of the number of samples and the order of the estimate have yet to be published.

4. MEM resolution limits

The resolution limit for MEM spectral analysis in terms of the number of samples and the order of the estimate is much more difficult to assess than for the DFT. For the latter, the degrees-of-freedom are fixed due to the periodic assumption and hence for each two time samples there is an additional pair of orthogonal components. Also, there is no least-mean-square error to be minimized. In MEM the degrees-of-freedom are selected by the user and hence the resolution limit is affected both by the number of samples and the order of the estimate.

The presentation of MEM resolution in Section G of this chapter addresses the properties associated with the location of the zeros of $D(Z)$

but does not present the effects of the number of samples or the order.
Some of the present MEM literature refers to the assumption that MEM uses
all of the data at each step in the recursive algorithm. It does not! End
effects, although minimized in the Burg algorithm (Equations in Chapter XV,
Section G), are not eliminated for higher order autocorrelation components.
Reduction in the amount of data used is clearly evident in the summation
index of Equation 15G.12. End effects cause an increase in the variance of
the autoregressive coefficients as the order is increased (Figure 19G-2)
because of the reduced amounts of data used in the estimate.

Parzen (1969) has suggested, but did not prove, a method for deter-
mining the order based on the variance of the least-mean-square error esti-
mate. Several examples examined by the author show that this technique
produces an estimate that does not have the best resolution inherent in
the estimator. A better criteria is the stability (or variance) of the
location of a critical zero of $D(Z)$.

A general rule is to choose a sample length that will span more than
one-half of the period of the lowest frequency component and chose an order
high enough so that the variance of the zero locations of spectral peaks
of interest is minimized. A detailed example will be given at the end of
this section.

5. DFT resolution limit

From an estimation theory viewpoint, the resolution limit for the DFT
is given by Equation 19H.1. It states simply that the resolution is limited
by the observation time, T_N. From a theoretical viewpoint, the exact effect
of DFT sampling on the estimated amplitude spectrum of a periodic function

is specified by the estimated Kronecker delta function defined in Equation 12D.11 and used in Equation 12D.10.

Figure 11-1 illustrates the bandpass or weighting effect represented by $\hat{\delta}_{rq}(N, T_N, T_F)$ for a single spectral component. The weighting function is specified for each harmonic number or frequency. The true amplitude of the spectral component is slightly reduced with the corresponding power distributed to other frequencies. The resolution limit for smaller amplitudes is limited by the peak value of spurious components. The magnitudes of the spurious components can be related to the "parent" peak by using the spectral mixing formula.

For a large peak at frequency f_L, the principal and spurious complex amplitudes can be obtained from a single term of the series in Equation 11.20:

$$\hat{c}(f_L, \frac{2\pi}{T_N} n) = c_L\{\frac{1}{2N+1} [1 + 2 \sum_{k=1}^{N} \cos(2\pi f_L - \frac{2\pi n}{T_N})k \; \frac{T_N}{2N+1}]\} \tag{19H.2}$$

For estimation purposes, c_L is replaced by its estimate when calculating spurious components. An example of this effect is illustrated in Figure 12D-3. For $T_N = 3.1$, $T_F = 1.0$, and $(2N+1) = 21$, the principal component and frequency are:

$$|c_L| = 2.0 \qquad f_L = 0.968 \text{ Hz}$$

The nearest spurious component has an amplitude and frequency of:

$$|c_{L+1}| = 0.186 \qquad f_{L+1} = 1.29 \text{ Hz}$$

A small adjacent spectral component could not be resolved if its amplitude did not exceed $|c_{L+1}|$.

The location of a spectral peak near zero frequency can be masked by the average value if only a fraction of a cycle is sampled. This type of error is illustrated in Figure 12D-2. Since partial cycles cannot be resolved using the DFT it is highly desirable to remove the average value before processing.

6. Example for MEM

The interferometer data used as an example in Sections D, F, and G of Chapter XVII is also an excellent practical example for illustrating the effect of filter order on the MEM spectral estimator. The output from PROGRAM-07 in Appendix III provides the data used in this example.

The time series (HER A 7/29/75) was processed using a variable filter length, $K = 1 - 15$. The estimated autoregressive coefficients are printed for each order of the estimate. Figure 19H-1 illustrates the variability of the estimated coefficients as a function of the chosen filter length for $K = 1 - 9$. The variation of the magnitude of these estimates directly affects the zero locations of the z-transform polynomial they generate. The most variable coefficient is $a_K(K)$ because it is the independent variable for the one-step prediction.

The estimated coefficients were used to generate the complex polynomial, $D(Z)$, as described in Equations 19G.4 and 19G.5 and the roots were obtained using a polynomial root solver. A summary of the results for filter orders up to ten is shown in Table 19H-1. Each root is described by a top entry which is the magnitude ($|z_n| < 1$) and a bottom entry which is

the phase angle in radians $(-\pi \leq \text{Arg}\{Z_n\} \leq +\pi)$. These root locations are plotted on the unit circle as shown in Figure 19H-2. The zeros representing the principal peak are labled Z_1 and are marked with a dotted line.
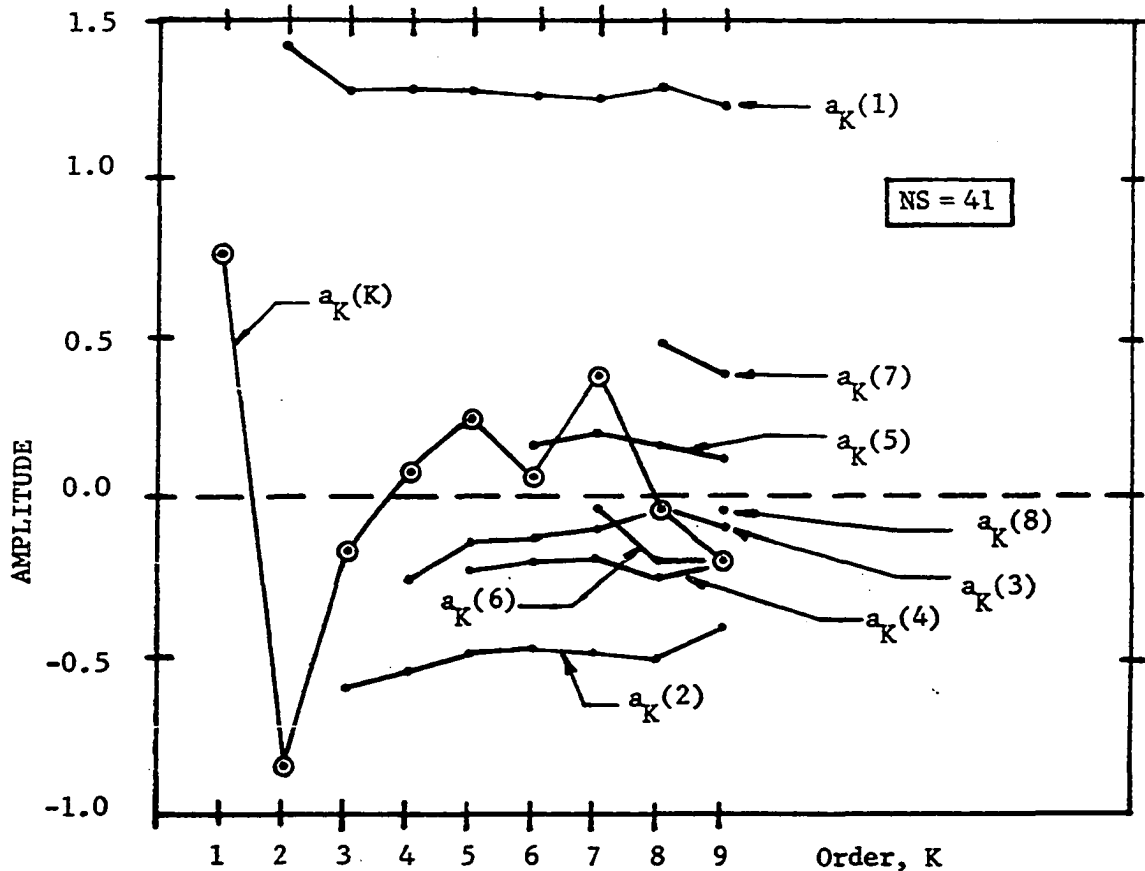
Figure 19H-1. Variability of the Estimated Autoregressive Coefficients as a Function of the Order, K, of the Estimate

The estimated location-of-spectral-peak for Z_1 varies as a function of the order K. Figure 19H-3 illustrates this variation. This characteristic was discussed in Section G and an example plot given in Figure 19G-7.

Table 19H-1. Zeros of the Complex Polynomial, D(Z)

ORDER K	z_1	z_2	z_3	z_4	z_5	z_6	z_7
2	+0.9229 ±.687	--	--	--	--	--	--
3	+0.9446 ±.675	--	--	--	--	+0.2008 + π	--
4	+0.9411 ±.684	--	--	--	--	+0.3824 + π	+0.2100 0
5	+0.9572 ±.707	+0.6275 ±2.30	--	--	--	--	+0.6539 0
6	+0.9267 ±.707	+0.5798 ±2.16	--	--	--	+0.2777 + π	+0.7149 0
7	+0.9681 ±.702	+0.6608 ±2.47	+0.5255 ±1.55	--	--	--	+0.7861 0
8	+0.9718 ±.725	+0.8616 ±2.60	+0.8283 ±1.71	+0.8128 ±.349	--	--	--
9	+0.9816 ±.727	+0.8262 ±2.50	+0.8554 ±1.61	+0.8893 ±.345	--	+0.5255 + π	--
10	+0.9844 ±.725	+0.8021 ±2.58	+0.8302 ±1.56	+0.9097 ±.337	+0.4966 ±2.25	--	--
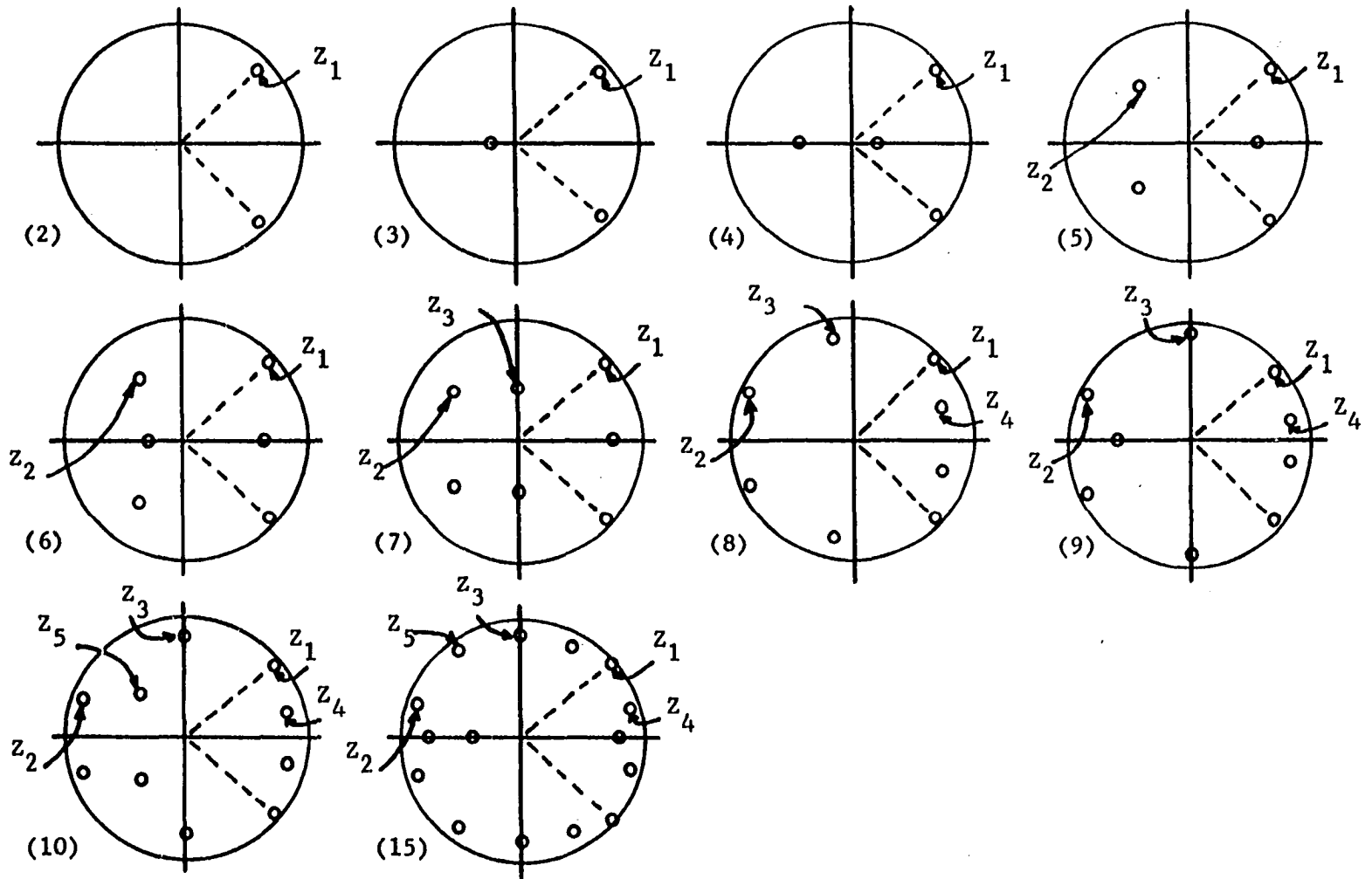
Figure 19H-2. The Effect of Increasing Order on Zero Locations
in the Unit Circle
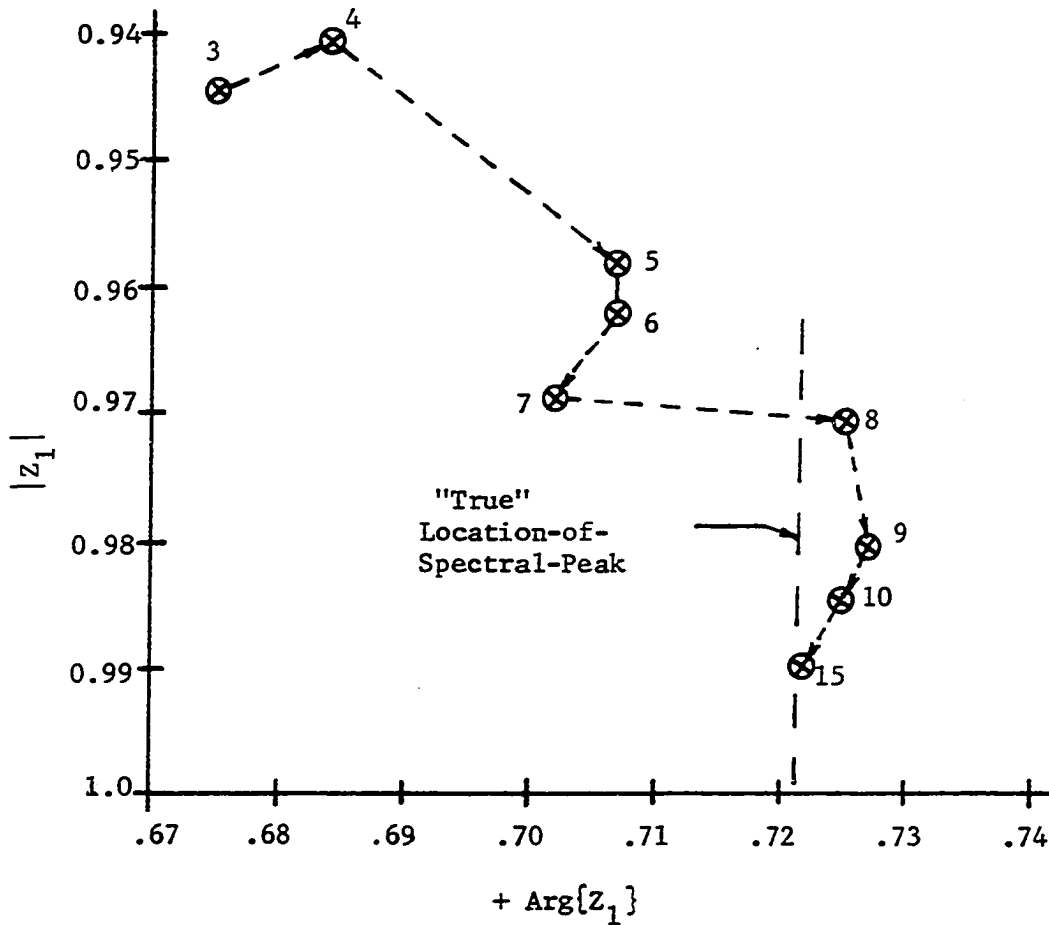
Figure 19H-3. Migration of the Estimated Location of
the Spectral Peak Represented by Z_1

Several interesting features of the MEM spectral estimator are illus-
trated in this example. The first thing we realize is that the mean-square
estimation error is not a suitable measure for selecting the order of the
estimate. From Figure 17G-5 we see that the error decreases very little
beyond order $K = 2$ and yet Figure 19H-3 shows the estimated location-of-
spectral peak improving up to order $K = 15$. This improvement comes about
because the degrees-of-freedom were increased thereby allowing the zero
location to migrate to its preferred position. Also the peak became

sharper as indicated by the magnitude of Z, approaching unity. The important conclusion is that the zero location is a better indicator of the desired order of the estimate.

Figure 19H-2 shows the effect of increasing order on all zero locations. It is important to note that each spectral peak to be resolved requires two additional orders of the polynomial. This is illustrated for order $K = 5$ where two peaks are modeled. In other words, only those zeros in the upper-half-plane have a significant effect on spectral shape. From Table 19H-1 and Figure 19H-2 we also see that the identity of the most important zeros can be preserved over many orders of the estimate. This property also helps in the selection of a maximum order.

The techniques of analysis presented in this example are typical of those that may be used for practical MEM spectral estimation. For each prominent spectral peak a separate plot similar to Figure 19H-3 should be made. The "true" location is marked for reference and illustration. In general an estimate of the true location must be made. Estimates of the total power in a spectral peak must be obtained by computing the _area_ under the peak. This power spectrum technique is in direct contrast to FFT analysis where the _amplitude_ of the peak is important.

I. Review of Common Spectral Estimation Errors

1. _Introduction_

This review of some of the more common errors associated with the estimation of amplitude and power spectra will specifically address the DFT (also FFT) and MEM. The techniques and effects of data preprocessing on errors have been discussed in Chapter IX, Section C. Here we concentrate

on the major effects of observer bias and error and intrinsic estimation errors. Gross observer error, equipment malfunction error and lack of stationarity will not be addressed.

2. Aliasing

Aliasing or the frequency fold-over effect caused by sampling at a rate less than the Nyquist rate has been discussed in Chapters VI and IX. In the FFT literature, aliasing has been given considerable attention while in MEM literature it is seldom mentioned. The reader should be keenly aware that it can occur in both types of analyses.

The effects of aliasing can be minimized or eliminated by careful experimental design such as prefiltering ahead of the sampler. Under certain special circumstances aliasing is desirable. An example of a practical application of aliasing is for the detection of a sinewave in a spectrum much wider than the principal alias. The fold-over effect allows the sinusoid to be detected without an increase in the sampling rate.

For the vast majority of spectral analysis applications aliasing must be eliminated and, when reporting results, it is helpful to inform the reader as to how this was accomplished.

3. Numerical stability and accuracy

Because the word length is finite for digital processing systems, it is possible to introduce noise and instabilities into the various spectral estimation algorithms. Truncation or roundoff error will introduce wide-band noise into the estimate.

Truncation can be serious for MEM because, for good signal-to-noise ratios, it can cause a zero of the characteristic polynomial, D(Z), to lie on the unit circle. Some applications may require the use of double precision or the addition of a small amount of wideband noise to eliminate this effect. A well designed MEM algorithm should check for this effect.

For a majority of practical scientific data processing, numerical stability and accuracy will not be a problem. Only for the cases of very high predictability or very small word length should the user apply special precautions.

4. Spectral smoothing

Spectral smoothing or the loss of spectral resolution caused by a finite observation time is discussed in Chapter IX. Smoothing in FFT analysis is caused by a finite time window. In the Blackman-Tukey method it is caused by a finite lag window. Smoothing in MEM analysis is the result of using a smoothed estimate for extrapolating the autocorrelation function and using a single zero of the complex polynomial, D(Z), to represent a single spectral peak.

The undesirable effect of spectral smoothing can only be reduced by increasing the number of samples (or the observation time). For MEM, improved spectral resolution (over FFT) is the result of using an estimator that has a selectable degrees-of-freedom.

5. Spectral leakage and end effects

Spectral leakage (or spectral mixing) is caused by the finite observation time (finite time window) and is discussed in Chapter IX. The spectral mixing formula derived in Chapter XI is an exact model for representing the affect of a specific DFT estimate on spectral leakage. For MEM, spectral leakage is observed as a shift in the absolute magnitude of the zeros representing spectral peaks. Leakage reduces the ability to resolve minor components because a large peak may have leakage that obscures a minor one. For DFT analysis the spectral mixing formula can be used to place an upper bound on leakage and hence on minor component detection. For MEM, no technique, as yet, exists.

The variability of estimated autocorrelations with increasing lags is caused by the end effect of finite data records. For the Blackman-Tukey method, end effects are minimized by the proper choice of a lag window (Blackman and Tukey, 1958). For MEM, end effects are minimized by the least-squares smoothing used in extrapolating the autocorrelation function. End effects for MEM are further discussed in Section G of Chapter XV.

6. Noise and statistical variability

Sample records of the time series representing a physical process are usually contaminated by random noise inherent in the measurement process. Also, since the sample records are finite, the estimated means of the various parameters have a considerable variability that depends on the length of the sample. These effects introduce random noise and statistical variability into the various spectral estimators.

The effect of noise on the DFT estimate was discussed in Section D of this chapter. Statistical variability due to sampling effects can be analyzed using the spectral mixing model and Rayleigh statistics.

For MEM, measurement noise is modeled as Gaussian noise with a band-limited spectrum. In this model, all noise is treated equally so measurement noise and random processes effects are indistinguishable. Statistical variability appears in the estimated autoregressive coefficients and is caused by noise and sampling effects. Variability is reduced by taking longer sample records.

Spectrum averaging is frequently used in FFT analysis to reduce the effects of statistical variability. In MEM, spectrum averaging and increased sample length are both helpful.

7. Fractional period sampling

All spectral estimators perform poorly if only a fraction of the period of a spectral peak is sampled. For DFT (and FFT) analysis, samples less than $0.9\ T_F$ are unusable as most of the amplitude will appear as a zero frequency component. For all DFT applications, the data taking method must be designed so at least nine-tenths of the period of the lowest frequency component is sampled.

The MEM estimator can give good results when only 60% of a period is sampled. This requires severe oversampling and a reasonable low noise variance. MEM performance is discussed further in Section G of this chapter.

8. Spectral strength or magnitude

Interpretation of the results of a spectral estimate most often involves the selection of the "most prominent" spectral component. For DFT (and FFT) analysis this simply means choosing the highest peak because the height is proportional to the amplitude of a sinusoid at that frequency.

For MEM, the estimate is a power spectral _density_ and the amplitude of a periodic component is proportional to the _area_ under the peak. When analyzing MEM records, one should avoid the temptation of looking at the heights of the components and instead compute the areas for comparison.

9. Location-of-spectral-peak (LOSP)

The location or estimated frequency of a spectral peak is another important property of a spectral estimator. For FFT analysis, the LOSP is affected by the number of samples and the record length and by zero concatenation. If only a fraction of a period of the lowest spectral component is sampled, the LOSP for that component will occur at zero frequency. The LOSP for MEM analysis is affected by the number of samples and the order of the estimate. Typical effects where discussed in Sections G and H of this chapter.

The user must realize that the LOSP is statistically variable from record to record and take this into account when reporting results. If many records are available it is possible to get an estimate of the variance of the LOSP.

10. MEM display resolution

Since the MEM spectral estimator (Equation 15F.1) is continuous with frequency, a digital implementation requires the selection of a display resolution, Δf. For a very sharp peak it is possible that the output will not show the peak because it falls between frequency samples. For this reason a practical MEM program must contain a check for missed spectral peaks. One way is to numerically integrate $\hat{S}_K(\Delta f)$ to see if the total power is recovered. Another way is to compute the zero locations for $D(Z)$ to see if one lies extremely close to the unit circle. MEM display resolution is a practical problem that must always be accounted for by the user.

XX. BIBLIOGRAPHY

Ables, J. G.
    1974   Maximum entropy spectral analysis. Astronomy and Astrophysics,
            Supplement Series 15: 383-393.

Anderson, N.
    1974   On the calculation of filter coefficients for maximum entropy
            spectral analysis. Geophysics 39: 69-72.

Arfken, George
    1970   Mathematical Methods for Physicists. New York: Academic Press.

Bartlett, Maurice Stevenson
    1966   An Introduction to Stochastic Processes with Special Reference
            to Methods and Applications. 2nd ed. Cambridge: Cambridge
            University Press.

Beckmann, Petr
    1967   Probability in Communication Engineering. New York: Harcourt,
            Brace and World.

Bergland, G. D.
    1969   A guided tour of the fast Fourier transform. IEEE Spectrum 6
            (July): 41-52.

Bingham, Christopher, Michael D. Godfrey and John W. Tukey
    1967   Modern techniques of power spectrum estimation. IEEE Transac-
            tions on Audio and Electroacoustics AU-15: 56-79.

Blackburn, James A., Editor
    1970   Spectral Analysis: Methods and Techniques. New York: Marcel
            Dekker, Inc.

Blackman, R. B.
    1965   Linear Data-Smoothing and Prediction in Theory and Practice.
            Reading, Mass.: Addison-Wesley Publishing Company, Inc.

Blackman, R. B. and J. W. Tukey
    1958   The Measurement of Power Spectra. New York: Dover Publica-
            tions, Inc.

Bracewell, R. N.
    1965   The Fourier Transform and Its Applications. New York: McGraw-
            Hill Book Co.

Burg, John Parker
    1967   Maximum entropy spectral analysis. (unpublished) A paper pre-
            sented at the Thirty-Seventh Meeting, Society of Exploration
            Geophysicists. Oklahoma City, Oklahoma, October 31, 1967.

Burg, John Parker
    1968   A new analysis technique for time series data. A paper presented
          at the NATO Advanced Study Institute on Signal Processing,
          Enschede, Netherlands. August.

Burg, John Parker
    1970   New concepts in power spectra estimation. (unpublished) A paper
          presented at the 40th Annual Meeting, Society of Exploration
          Geophysicsts. New Orleans, La., November.

Burg, John Parker
    1972   The relationship between maximum entropy spectra and maximum
          likelihood spectra. Geophysics 37: 375-376.

Butcher, Wade E. and R. J. Sims
    1972   Application of adaptive algorithms to RF antenna arrays. IEEE
          Proceedings 60: 326-327.

Capon, J.
    1969   High-resolution frequency-wavenumber spectrum analysis. IEEE
          Proceedings 57: 1408-1418.

Capon, J., R. J. Greenfield and R. J. Kolker
    1967   Multidimensional maximum-likelihood processing of a large
          aperture seismic array. IEEE Proceedings 55: 192-211.

Carlson, A. Bruce
    1968   Communication Systems: An Introduction to Signals and Noise in
          Electrical Communication. New York: McGraw-Hill Book Co.

Chen, W. Y. and G. R. Stegen
    1974   Experiments with maximum entropy power spectra of sinusoids.
          Journal of Geophysical Research 79: 3019-3022.

Cheng, David K.
    1959   Analysis of Linear Systems. Reading, Mass.: Addison-Wesley
          Publishing Co., Inc.

Cochran, W. T., et al.
    1967   What is the fast Fourier transform? IEEE Transactions on Audio
          and Electroacoustics AU-15: 45-55.

Cohen, Theodore J. and Paul R. Lintz
    1974   Long term periodicities in the sunspot cycle. Nature 250:
          398-399.

Cooley, James W. and J. W. Tukey
    1965   An algorithm for the machine calculation of complex Fourier
          series. Mathematics of Computation 19: 297-301.

Cooley, James W., Peter A. W. Lewis and Peter D. Welch
   1967   Application of the fast Fourier transform to computation of
           Fourier integrals, Fourier series, and convolution integrals.
           IEEE Transactions on Audio and Electroacoustics AU-15: 79-84.

Cooper, George R. and Clare D. McGillem
   1971   Probilistic Methods of Signal and System Analysis. New York:
           Holt, Rinehart and Winston, Inc.

Crain, I. K., P. L. Crain and M. G. Plaut
   1969   Long period Fourier spectrum of geomagnetic reversals. Nature
           223: 283.

Deutsch, Ralph
   1965   Estimation Theory. Englewood Cliffs, N. J.: Prentice-Hall, Inc.

Deutsch, Ralph
   1969   System Analysis Techniques. Englewood Cliffs, N. J.: Prentice-
           Hall, Inc.

Edward, J. A. and M. M. Fitelson
   1973   Notes on maximum-entropy processing. IEEE Transactions on In-
           formation Theory IT-19: 232-234.

Fomalont, Edward B.
   1973   Earth-rotation aperture synthesis. IEEE Proceedings 61: 1211-
           1218. Special issue on radio and radar astronomy.

Frankignoul, Claude
   1974   A cautionary note on the spectral analysis of short internal
           wave records. Journal of Geophysical Research 79: 3459.

Fuller, Wayne A.
   1976   Introduction to Statistical Time Series. New York: John Wiley
           and Sons.

Gage, Douglas W. and David Hestenes
   1973   Comment on the paper 'Jayne's maximum entropy prescription and
           probability theory'. Journal of Statistical Physics 7: 89-90.

Gold, Bernard and Charles M. Rader
   1969   Digital Processing of Signals. New York: McGraw-Hill Book Co.

Goldberg, Samuel
   1958   Introduction to Difference Equations. New York: John Wiley
           and Sons, Inc.

Goldman, Stanford
   1953   Information Theory. New York: Prentice-Hall, Inc.

Griffiths, L. J.
    1969   A simple adaptive algorithm for real-time processing of antenna
            arrays. IEEE Proceedings 57: 1696-1704.

Gulamhusein, Mohamed N. and Frank Fallside
    1973   Short-time spectral analysis and autocorrelation analysis in the
            Walsh domain. IEEE Transactions on Information Theory IT-19:
            615-623.

Hinich, M. J. and C. S. Clay
    1968   The application of the discrete Fourier transform in the estima-
            tion of power spectra, coherence, and bispectra of geophysical
            data. Reviews of Geophysics 6: 347-363.

Jenkins, Gwilym M. and Donald G. Watts
    1968   Spectral Analysis and Its Applications. San Francisco: Holden-
            Day.

Jennison, R. C.
    1961   Fourier Transforms and Convolutions for the Experimentalists.
            New York: Pergamon Press.

Jensen, Oliver G. and Tadeusz Ulrych
    1973   An analysis of the perturbations of Barnard's star. The Astro-
            nomical Journal 78: 1104-1114.

Kailath, Thomas
    1974   A view of three decades of linear filtering theory. IEEE Trans-
            actions on Information Theory IT-20: 146-181.

Koopmans, L. H.
    1974   The Spectral Analysis of Time Series. New York: Academic Press.

Lacoss, Richard T.
    1968   Adaptive combining of wideband array data for optimal reception.
            IEEE Transactions on Geoscience Electronics GE-6: 78-86.

Lacoss, Richard T.
    1971   Data adaptive spectral analysis methods. Geophysics 36: 661-675.

Levinson, Norman
    1947   The Wiener RMS (Root Mean Square) Error Criterion in Filter Design
            and Prediction. Journal of Mathematics and Physics 25: 261-278.
            (New Title: Studies in Applied Mathematics).

Liu, Bede and Toyihisa Kaneko
    1975   Roundoff error in fast Fourier transforms (decimation in time).
            IEEE Proceedings 63: 991-992.

Lucy, L. B.
    1974   An iterative technique for the rectification of observed distri-
            butions. The Astronomical Journal 79: 745-754.

Makhoul, John
    1975   Linear Prediction: A Tutorial Review. IEEE Proceedings 63:
            561-580.

McDonough, R. N.
    1974   Maximum-entropy spatial processing of array data. Geophysics 39:
            843-851.

Meditch, J. S.
    1969   Stochastic Optimal Linear Estimation and Control. New York:
            McGraw-Hill Book Co.

Newman, William I.
    1977   A New Method of Multidimensional Power Spectral Analysis. Astron-
            omy and Astrophysics 54: 369-380.

Oppenheim, Alan V., Editor
    1969   Papers on Digital Signal Processing. Cambridge, Mass.: M.I.T.
            Press.

Oppenheim, Alan V., Guest Editor
    1975   Special issue on signal processing. IEEE Proceedings 63 (April).

Oppenheim, Alan V. and Ronald W. Schafer
    1975   Digital Signal Processing. Englewood Cliffs, N. J.: Prentice-
            Hall, Inc.

Otnes, R. K. and L. Enochson
    1972   Digital Time Series Analysis. New York: John Wiley and Sons.

Palmer, David F.
    1969   Exact formulation of window functions for analog network spectrum
            analyzers. IEEE Transactions of Aerospace and Electronic Systems
            AES-5: 230-235.

Palmer, L. C.
    1974   Course frequency estimation using the discrete Fourier transform.
            IEEE Transactions on Information Theory IT-20: 104-109.

Papoulis, Athanasios
    1962   The Fourier Integral and Its Applications. New York: McGraw-
            Hill Book Co.

Papoulis, Athanasios
    1973   Minimum-bias windows for high-resolution spectral estimates.
            IEEE Transactions on Information Theory IT-19: 9-12.

Parzen, Emanuel
    1969   Multiple time series modeling. Pp. 389-409 in Paruchuri R.
            Krishnaiah (ed.), Multivariate Analysis-II. Proceedings of the
            Second International Symposium on Multivariate Analysis. New
            York: Academic Press.

Peacock, K. L. and Sven Treitel
    1969   Predictive deconvolution: theory and practice. Geophysics 34:
            155-169.

Ponsonby, F. E. B.
    1973   An entropy measure for partially polarized radiation and its
            application to estimating radio sky polarization distributions
            from incomplete 'aperture synthesis' data by the maximum entropy
            method. Royal Astronomical Society, Monthly Notices 163: 369-
            380.

Rabiner, Lawrence R. and Charles M. Rader, Editors
    1972   Digital Signal Processing. New York: IEEE Press, The Institute
            of Electrical and Electronics Engineers.

Radoski, Henry R., Paul F. Fougere and Edward J. Zawalick
    1975   A comparison of power spectral estimates and applications of the
            maximum entropy method. Journal of Geophysical Research 80:
            619-625.

Reference Data for Radio Engineers
    1968   Fifth Edition. New York: Howard W. Sams and Co., Inc.

Robinson, Enders A.
    1967a   Statistical Communication and Detection with Special Reference
            to Digital Data Processing of Radar and Seismic Signals. New
            York: Hafner Publishing Co.

Robinson, Enders A.
    1967b   Multichannel Time Series Analysis with Digital Computer Programs.
            San Francisco: Holden-Day.

Rogers, A. E. E.
    1974   Maximum entropy method for unequally-spaced data in two dimensions
            and numerical tests of its effectiveness. Technical Note 1974-1.
            Northeast Radio Observatory Corporation, Haystack Observatory,
            Westford, Mass. Operated under agreement with Massachusetts
            Institute of Technology.

Schwartz, Mischa
    1970   Information Transmission, Modulation, and Noise. 2nd ed. New
            York: McGraw-Hill Book Co.

Schwartz, Mischa and Leonard Shaw
  1975 Signal Processing: Discrete Spectral Analysis, Detection, and
        Estimation. New York: McGraw-Hill Book Co.

Shannon, C. E. and W. Weaver
  1949 The Mathematical Theory of Communication. Urbana, Illinois: The
        University of Illinois Press.

Smylie, D. E., G. K. C. Clarke and T. J. Ulrych
  1973 Analysis of irregularities in the earth's rotation. Pp. 391-431
        in B. Alder, S. Fernbach and M. Rotenberg (series editors), and
        Bruce A. Bolt (volume editor), Methods in Computational Physics
        Volume 13, Geophysics. New York: Academic Press.

Sneddon, I. N.
  1951 Fourier Transforms. New York: McGraw-Hill Book Co.

Stanley, William D.
  1975 Digital Signal Processing. Reston, Virginia: Reston Publishing
        Company, Inc.

Stearns, Samuel D.
  1975 Digital Signal Analysis. Rochelle Park, New Jersey: Hayden
        Book Company, Inc.

Taub, Herbert and Donald L. Schilling
  1971 Principles of Communication Systems. New York: McGraw-Hill
        Book Co.

Thomas, John B.
  1969 An Introduction to Statistical Communication Theory. New York:
        John Wiley and Sons, Inc.

Todd, Donald E.
  1973 Sampled data reconstruction of deterministic bandlimited signals.
        IEEE Transactions on Information Theory IT-19: 809-811.

Toman, K.
  1965 The spectral shifts of truncated sinusoids. Journal of Geophysi-
        cal Research 70: 1749-1750.

Trench, William F.
  1974 Inversion of Toeplitz band matrices. Mathematics of Computation
        28: 1089.

Tsui, Wai Ling
  1976 Calibration of 26 MHz Interferometer and Measurement of Flux
        Densities of Celestial Radio Sources. M.S. thesis, Iowa State
        University, Ames, Iowa.

Ulrych, T. J.
1972a   Maximum entropy power spectrum of long period geomagnetic re-
versals.   Nature 235:   218-219.

Ulrych, T. J.
1972b   Maximum entropy power spectrum of truncated sinusoids.   Journal
of Geophysical Research 77:   1396-1400.

Ulrych, T. J. and Oliver Jensen
1974   Cross-spectral analysis using maximum entropy.   Geophysics 39:
353-354.

Ulrych, T. J. and D. E. Smylie, O. G. Jensen and G. K. C. Clarke
1973   Predictive filtering and smoothing of short records by using
maximum entropy.   Journal of Geophysical Research 78:   4959-4964.

Van den Bos, A.
1971   Alternate interpretation of maximum entropy special analysis.
IEEE Transactions on Information Theory IT-17:   493-494.

Veltman, B., A. Van den Bos, R. de Bruine, R. de Ruiter and P. Verloren
1972   Some remarks on the use of autocorrelation functions with the
analysis and design of signals.   Pp. 131-140 in J. W. R.
Griffiths,   P. L. Stocklin and C. van Schooneveld (eds.), Signal.
Processing.   Proceedings of the NATO Advanced Study Institute
of Signal Processing.   New York: Academic Press.

Weinreb, Sander
1963   A digital spectral analysis technique and its application to
radio astronomy.   Technical Report 412.   Research Laboratory of
Electronics,   Massachusetts Institute of Technology,   Cambridge,
Massachusetts.

Whalen, A. D.
1971   Detection of Signals in Noise.   New York: Academic Press.

Widrow, B., P. E. Mantey, L. J. Griffiths and B. B. Goode
1967   Adaptive antenna systems.   IEEE Proceedings 55:   2143-2159.

Wiggens, Ralph A. and Enders A. Robinson
1965   Recursive solution to the multichannel filtering problem.
Journal of Geophysical Research 70:   1885-1891.

Young, Hugh D.
1962   Statistical Treatment of Experimental Data.   New York: McGraw-
Hill Book Co.

XXI. APPENDIX I - MATHEMATICAL TECHNIQUES

A. Integration and Riemann Summation

A function $f(x)$ is said to be Riemann integrable if in the limit

$$I_{ab} = \int_a^b f(x)\,dx = \lim_{n \to \infty} \sum_{k=1}^{n} f(a+k\,\frac{b-a}{n})\,\frac{b-a}{n} \qquad (A1.1)$$

where the interval $a - b$ is divided into n segments with each segment having a width of $(b - a)/n$. If the number of segments, n, is not taken to the limit, the Riemann sum will yield an estimate of the definite integral I_{ab}. The actual value of the estimate depends upon how many segments are used and how the sum is taken. For small n, a good technique of estimation is to evaluate the function at the midpoint of the segment for use in the summation. The integral estimate using this procedure becomes:

$$\hat{I}_{ab} = \frac{b-a}{n} \sum_{k=1}^{n} f(a+[k-\frac{1}{2}]\,\frac{b-a}{n}) \qquad (A1.2)$$

Figure A1-1 illustrates this procedure.

For the purposes of this research work it was discovered that a specialized form of the Reimann sum approximation was very well-suited to Fourier series analysis. If we assume that $f(x)$ is shifted so that the origin is at the midpoint of the independent variable and that there are an odd number of segments, the definite integral

$$I_{aa} = \int_{-a}^{+a} f(x)\,dx \qquad (A1.3)$$

can be estimated with the following sums

$$\hat{I}_{aa} = \sum_{k=-N}^{+N} f(k\Delta x)\,\Delta x \qquad (A1.4)$$
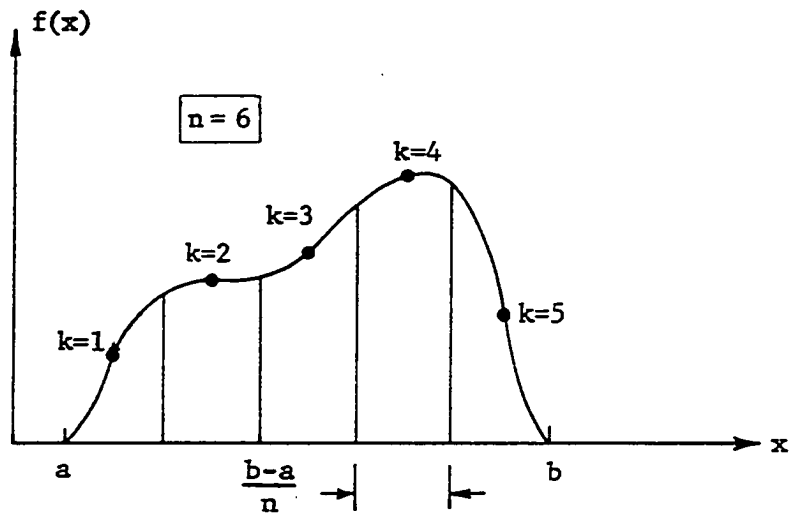
Figure A1-1. Riemann Sum Approximation for a
Definite Integral

$$\hat{I}_{aa} = \frac{2a}{(2N+1)} \sum_{k=-N}^{+N} f(k \frac{2a}{[2N+1]})$$ (A1.5)

where:

$k = 0, \pm 1, \pm 2, \ldots \pm N.$

$n = (2N+1)$, the number of segments - assumed odd.

$\Delta x = \frac{2a}{n} = \frac{2a}{(2N+1)}.$

Figure A1-2 illustrates this procedure.

This particular estimator for the definite integral is used many times throughout this report. Its usefulness is illustrated in several of the derivations involving the estimation of the complex Fourier coefficients for digital Fourier transforms.
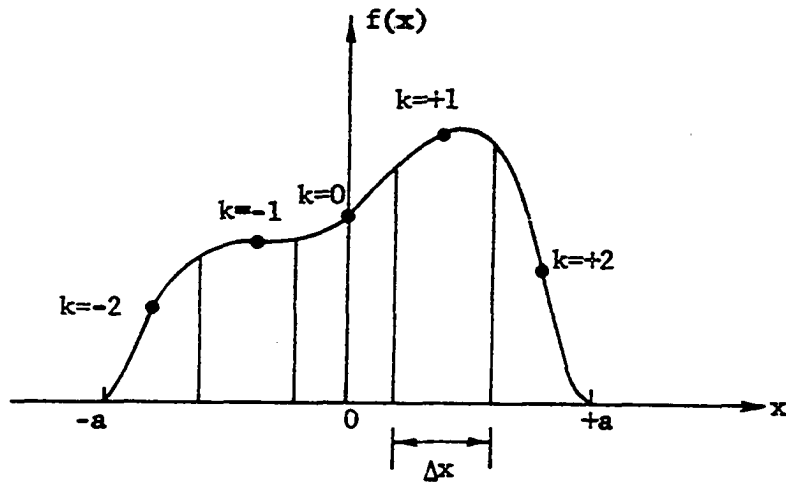
Figure A1-2. Riemann Sum Approximation Used in
Fourier Series Analysis

B. Hilbert Space Vectors

An infinite-dimensional vector space is called a "Hilbert space" and is denoted symbolically by $\mathcal{H}$. In $\mathcal{H}$, the "vectors" are not directed line segments, but rather are complex functions of real variables. We define a "vector" in $\mathcal{H}$ to be a complex function, ψ, of a real variable x. In other words, a "vector" in $\mathcal{H}$ is a rule of correspondence which assigns to each number x, a complex number $\psi(x)$. The vector space is defined as follows:

a) Scalars are the set of all complex numbers, c.

b) The distributive law of addition holds (vector addition):

$$\psi(x) = c_1\psi_1(x) + c_2\psi_2(x) \tag{A1.6}$$

c) The vector inner product is defined to be

$$(\psi_1, \psi_2) = \int_{\text{all } x} \psi_1^*(x)\psi_2(x)dx \qquad (A1.7)$$

with the following properties:

$$(\psi_2, \psi_1) = (\psi_1, \psi_2)^* \qquad (A1.8)$$

$$(c_1\psi_1, c_2\psi_2) = c_1^* c_2 (\psi_1, \psi_2) \qquad (A1.9)$$

$$|(\psi_1, \psi_2)| \leq (\psi_1, \psi_1)^{\frac{1}{2}}(\psi_2, \psi_2)^{\frac{1}{2}} \qquad (A1.10)$$

d) The vector norm is defined as

$$(\psi, \psi) = \int_{\text{all } x} |\psi(x)|^2 dx \qquad (A1.11)$$

and a function $\psi(x)$ must have a finite norm, $(\psi, \psi) < \infty$, to be a vector in $\mathcal{H}$.

e) A set of $\mathcal{H}$-vectors $\{\alpha_n(x)\}$ form a vector basis set in $\mathcal{H}$. The set is said to be complete if any vector in $\mathcal{H}$ can be constructed from a linear combination of the basis vectors $\{\alpha_n(x)\}$. The basis set is orthogonal if the inner product (α_n, α_m) is zero for all $n \neq m$. The basis set is orthonormal if $(\alpha_n, \alpha_m) = \delta_{nm}$ (the Kronecker delta).

f) An orthonormal set of eigenvectors $\{\alpha_n(x)\}$ are said to form an orthonormal basis set in $\mathcal{H}$ if the set is both orthonormal and complete. Any given $\mathcal{H}$-vector, $\psi(x)$, can be written as an infinite-dimensional (infinite series) linear combination of the orthonormal basis set

$$\psi(x) = \sum_{n=1}^{\infty} a_n \alpha_n(x) = \sum_{n=1}^{\infty} (\alpha_n, \psi) \alpha_n(x) \qquad (A1.12)$$

where the a_n's are the <u>complex expansion coefficients</u> (eigen-values of ψ) defined by the inner product:

$$a_n = (\alpha_n, \psi) = \int_{\text{all } x} \alpha_n^*(x) \psi(x) dx \qquad (A1.13)$$

The vector norm of $\psi(x)$ can be written in terms of the expansion coefficients as:

$$(\psi, \psi) = \sum_{n=1}^{\infty} |a_n|^2 \qquad (A1.14)$$

The theory of Hilbert space vectors was successfully applied to Fourier transform theory to give many of the important derivations shown in the text. This formulation also can provide useful insight into the problem of estimating the complex Fourier coefficients.

C. Deterministic Functions

Mathematical functions which are made up of parameters which are completely specified for all time and all values of the independent variables will be called deterministic. This terminology is used to denote that there is no "randomness" associated with the function. For practical purposes, a function of time $x(t)$ is deterministic if it can be exactly characterized by a Fourier series. It is philosophically satisfying to realize that an observable function of time, $x(t)$, must be periodic and therefore represented by a Fourier series if it is to be deterministic. Time functions which are not periodic cannot be completely specified because an infinite observation time is required.

Deterministic time functions are periodic in the time domain and exhibit only line spectra in the frequency domain. Deterministic functions cannot have continuous spectra. A pathological exception to this definition exists for single pulses in time. These functions are known for all time and have an implied period which is infinite. They also are characterized by infinite and continuous power spectra.

D. Noise and Random Processes

A random process will be defined to be a collection of time functions and an associated complete probability description. The entire collection of time functions $x_n(t)$ is called an ensemble of random time functions of which the nth function is called a sample function of the process. In general, only one sample function of a random process can ever be observed; the other $(n-1)$ sample functions represent all other possible realizations which might have occurred but didn't. The following properties of random processes are important for our purposes:

a) Continuous -- Discrete

In a continuous random process, the random variables $x_n(t_k)$ at time t_k can assume any value within a specified range of values. The probability density function is continuous and has no Dirac delta functions in it. A discrete random process is one in which the random variables can assume only certain isolated values. The probability density function contains only Dirac delta functions and does not have a continuous component. A mixed random process is one in which probability density function may have both discrete and continuous properties.

b) Deterministic -- Nondeterministic

If future values of $x_n(t)$ cannot be exactly predicted from observed past values, the process is called nondeterministic. If future values can be completely specified, the process is called deterministic. It is possible for a function to be random over the ensemble but not random with respect to time. An example of this type of process is an ensemble of sinewaves, $x_n(t)$, each with a different amplitude, A_n, where A_n is a random variable. Any sample function of this process would be deterministic with respect to time.

c) Stationary -- Nonstationary

If all of the marginal and joint density functions describing a random process do not depend upon the choice of time origin, the process is said to be stationary. If these density functions do depend upon time, the process is called nonstationary. Most real physical processes are nonstationary to some degree but quite often they can be characterized as stationary for practical considerations.

A process is said to be stationary in the wide sense (or covariance stationary) when the expectation value, $E\{x(t_1)\}$, is independent of the choice of time origin and when $E\{x(t_1)x(t_2)\}$ depends only upon the time difference, $(t_2 - t_1) = \tau$. This guarantees that the mean value, mean-square value, variance, and correlation coefficient are all independent of the choice of time origin.

d) Ergodic -- Nonergodic

A random process is said to be strictly ergodic if the time average of one sample function is equal to the ensemble average. It is

ergodic with respect to its correlation function when the ensemble correlation function is equal to the time autocorrelation function.

For ergodic processes, mean value and higher order moments can be determined by time averages over an infinite interval as well as by ensemble averages:

$$E\{x^n\} = \int_{-\infty}^{+\infty} x^n p(x) dx = \lim_{T \to \infty} \frac{1}{T} \int_{-T/2}^{+T/2} x^n(t) dt \qquad (A1.15)$$

In this report, most random processes will be continuous, nondeterministic, stationary, and ergodic. A sample function of the process will be called "noise" or a random time function. Usually, only one sample function will be available for analysis and its statistical properties will be estimates of the "true" values.

E. Correlation Functions for a Random Process

The _autocorrelation_ function $R_y(t_1, t_2)$ of a random process is defined as the joint moment of the random variables $y(t_1)$ and $y(t_2)$:

$$E\{Y(t_1)Y(t_2)\} = R_y(t_1, t_2) = \int_{-\infty}^{+\infty} dy_1 \int_{-\infty}^{+\infty} y_1 y_2 p(y_1, y_2) dy_2 \qquad (A1.16)$$

The _autocovariance_, $C_y(t_1, t_2)$ of the process is defined as:

$$E\{[Y(t_1) - \overline{Y(t_1)}][Y(t_2) - \overline{Y(t_2)}]\} = C_y(t_1, t_2) \qquad (A1.17)$$

For a "wide-sense" stationary process, the ensemble averages defined above are independent of the choice of time origin and the autocorrelation function becomes

$$R_y(\tau) = E\{Y(t)Y(t + \tau)\} \qquad (A1.18)$$

where $\tau = (t_2 - t_1)$ is called the "lag time". For stationary processes, the <u>time autocorrelation function</u> and <u>time autocovariance function</u> are defined as

$$R_y(\tau) = \lim_{T \to \infty} \frac{1}{T} \int_{-T/2}^{+T/2} y(t)y(t+\tau)dt \qquad (A1.19)$$

and:

$$C_y(\tau) = \lim_{T \to \infty} \frac{1}{T} \int_{-T/2}^{+T/2} [y(t) - \bar{y}(t)][y(t+\tau) - \bar{y}(t+\tau)]dt \qquad (A1.20)$$

For most of the work in this report we will let $x(t)$ represent a random variable with zero mean and then define a <u>zero-mean autocovariance function</u> as:

$$C_x(\tau) = \lim_{T \to \infty} \frac{1}{T} \int_{-T/2}^{+T/2} x(t)x(t+\tau)dt \qquad (A1.21)$$

The autocovariance function is very important in the study of random processes and random time functions because it is used to define the power spectrum of the process.

F. The Power Spectrum of a Random Process

The power spectrum of a random process is defined as the Fourier transform of the autocorrelation function. For a wide-sense stationary random process the autocorrelation function is

$$R_x(\tau) = \lim_{T \to \infty} \frac{1}{T} \int_{-T/2}^{+T/2} x(t)x(t+\tau)dt \qquad (A1.22)$$

where $x(t)$ is a sample function of the process. The autocorrelation function and the power spectral density function, $S_x(\omega)$, (also called the

second moment spectral density) are related by the Wiener Khinchine relations (Cooper and McGillem, 1971, p. 148):

$$S_x(\omega) = \int_{-\infty}^{+\infty} R_x(\tau) e^{-j\omega\tau} d\tau \qquad\qquad (A1.23)$$

$$R_x(\tau) = \frac{1}{2\pi} \int_{-\infty}^{+\infty} S_x(\omega) e^{+j\omega\tau} d\omega \qquad\qquad (A1.24)$$

In theory, a knowledge of the autocorrelation function is equivalent to a knowledge of the power spectral density function.

G. Autoregressive-Moving Average Processes

Stochastic processes which generate a random time series can be successfully modeled as moving average processes, finite autoregressive processes, or autoregressive-moving average processes (Koopmans, 1974, Ch. 7). These models can then be used to generate an infinite time series, a discrete autocovariance function, and a continuous power spectrum. This type of analysis is widely used in statistics and is becoming increasingly important in engineering for studying the spectra of stochastic processes using the maximum entropy method.

A __finite moving average process__ is modeled by the following series

$$x(t) = \sum_{k=-M}^{+M} a_k \xi(t-k) \qquad\qquad (A1.25)$$

where $2M+1$ is the order of the series and the a_k's are real constants. The sequence of uncorrelated random variables, $\xi(t)$: $t = 0, \pm 1, \ldots$, models a white noise process. The common mean for this sequence is $E\{\xi(t)\} = 0$

and the variance $E\{\xi^2(t)\} = \sigma^2$. The finite moving average model can be interpretated as the weighted sum of $2M+1$ random and completely independent impulses, $\xi(t)$, occuring at past and future times which gives the value $x(t)$ at time t. These impulses (called random shocks by Koopmans) are most commonly referred to as <u>innovations</u> at time t (Parzen, 1969). If we impose the requirement of causality and consider models which depend only upon present and past innovations, we obtain a <u>one-sided moving average</u>:

$$x(t) = \sum_{k=0}^{2M} a_k \xi(t-k) \tag{A1.26}$$

The model for a moving average process has wide applicability. In fact, every weakly stationary (covariance stationary) process that has a strictly continuous spectrum can be approximated arbitrarily close (in a mean-square sense) by a finite moving average process. Koopmans (1974, p. 214) shows that every weakly stationary process with a continuous spectrum has an infinite moving average representation.

The <u>scheme of linear autoregression</u> is a technique that is used to approximate the value of a given finite series at a time t by some weighted sum of past values of the series. <u>Finite autoregressive processes</u> are a class of finite parameter models that may be represented by this approach. The finite order autoregression satisfies the equation:

$$\sum_{k=0}^{2M} b_x x(t-k) = \xi(t), \qquad (t = 0, \pm 1, \pm 2, \ldots,) \tag{A1.27}$$

The boundary conditions for this series are

$$b_o = 1, \quad \sum_{k=0}^{2M} b_k^2 < \infty \tag{A1.28}$$

and since the innovations are independent and the x(t)'s and the innovations are mutually independent, the expectations of the following products must be zero:

$$E\{x(s) \, \xi(t)\} = 0 \quad \text{for all } s \leq t - 1 \tag{A1.29}$$

$$E\{\xi(s) \, \xi(t)\} = 0 \quad \text{for all } s \neq t \tag{A1.30}$$

The <u>autocovariance matrix elements</u> for a stationary process are defined as:

$$E\{x(t - p) \, x(t - k)\} = C(p - k) \tag{A1.31}$$

The autocovariance matrix elements can be related to the expansion constants, b_k, and to each other by the <u>Yule-Walker equations</u>. These equations are derived by multiplying both sides of Equation A1.27 by $x(t - p)$ and taking the expectation:

$$E\left\{x(t - p) \sum_{k=0}^{2M} b_k x(t - k)\right\} = \sum_{k=0}^{2M} b_k E\{x(t - p)x(t - k)\}$$

$$= E\{x(t - p) \, \xi(t)\} = 0 \tag{A1.32}$$

$$p = 1, 2, \ldots, 2M$$

Substituting into (A1.32) with the definition of the autocovariance matrix elements gives:

$$\sum_{k=0}^{2M} b_k C(p - k) = C(p) + \sum_{k=1}^{2M} b_k C(p - k) = 0 \tag{A1.33}$$

This gives the Yule-Walker equations ($b_o = 1$):

$$\sum_{k=1}^{2M} b_k C(p - k) = -C(p) \tag{A1.34}$$

Equation A1.32 is similiar to an orthogonality statement about the auto-covariance elements and the Yule-Walker equations express a particular autocovariance as a weighted sum of the others.

The variance for the process is defined as the expectation of the product of $x(t)$ and $\xi(t)$:

$$E\{x(t)\,\xi(t)\} = \sum_{k=0}^{2M} b_k C(k) = \sigma^2 \tag{A1.35}$$

This equation is used to estimate the variance of the process from the autocovariances and the autoregressive coefficients. In maximum entropy spectral estimation, this variance is called the error power of the process and is minimized by a least-squares criterion.

An autoregressive series can also be used as a linear predictor. The series can be extrapolated one unit ahead in time by using the following equation:

$$x(t+1) = \xi(t+1) - \sum_{k=1}^{2M} b_k x(t+1-k) \tag{A1.36}$$

The **best** linear one step predictor (in a least-squares sense) is given by (Koopmans, 1974, p. 228):

$$\hat{x}(t) = -\sum_{k=1}^{2M} b_k x(t+1-k) \tag{A1.37}$$

The one-step prediction error is equal to the innovation variance:

$$E\{[x(t+1) - \hat{x}(t)]^2\} = E\{\xi^2(t+1)\} = \sigma^2 \tag{A1.38}$$

The autoregressive process can be thought of as high order Markov process. That is, the state or value of the series at time t depends only

upon the previous states or values. Markov processes are important to the study of random variables, probability, and discrete-time random processes (Thomas, 1969, p. 114).

Mixed autoregressive-moving average processes are modeled by a combination of finite autoregressions and finite moving averages (Koopmans, 1974, p. 240):

$$\sum_{p=0}^{q} d_p x(t-p) = \sum_{k=0}^{r} a_k \xi(t-k) \tag{A1.39}$$

This type of model can be viewed as a linear filter with an output of $x(t)$ in response to a white noise input, $\xi(t)$. The transfer function for the filter can be obtained from the z-transform as:

$$H(\omega) = \frac{\sum_{k=0}^{r} a_k e^{-j\omega k}}{\sum_{p=0}^{q} d_p e^{-j\omega p}} \tag{A1.40}$$

The autoregressive-moving average process can also be modeled by a high-order recursive filter. The output of the filter, $y(t)$, is described by (Otnes and Enochson, 1972, p. 89):

$$y(t) = \sum_{p=0}^{q} g_p x(t-p) + \sum_{k=1}^{r} h_k y(t-k) \tag{A1.41}$$

The filter is modeled by the parameters, g_p and h_k. The complex transfer function for this filter is:

$$H(\omega) = \frac{\sum_{p=0}^{q} g_p e^{-j\omega p \Delta t}}{1 - \sum_{k=1}^{r} h_k e^{-j\omega k \Delta t}} \tag{A1.42}$$

H. The Power Spectrum of an Autoregressive-Moving Average Process

By using a filtering model, the power spectrum for a moving average process can be estimated by ($\omega = 2\pi k \Delta t$)

$$S_x(\omega) = \frac{\sigma^2}{2\pi} \left| \sum_{k=0}^{2M} a_k e^{-j\omega k} \right|^2 \tag{A1.43}$$

where x(t) is modeled as the output of a digital filter with white noise input $\xi(t)$ and a complex transfer function of:

$$H(\omega) = \sum_{k=0}^{2M} a_k e^{-j\omega k} \tag{A1.44}$$

The spectrum for a finite autoregressive process can be defined from the theory of inverting linear filters and z-transforms (Koopmans, 1974, p. 217):

$$S_x(\omega) = \frac{\sigma^2}{2\pi} \frac{1}{|H(\omega)|^2} = \frac{\sigma^2}{2\pi} \frac{1}{\left| \sum_{k=0}^{2M} b_k e^{-j\omega k} \right|^2} \tag{A1.45}$$

The spectrum for a autoregressive-moving average process is given by:

$$S_x(\omega) = \frac{\sigma^2}{2\pi} |H(\omega)|^2 = \frac{\sigma^2}{2\pi} \frac{\left| \sum_{k=0}^{r} a_k e^{-j\omega k} \right|^2}{\left| \sum_{p=0}^{q} d_p e^{-j\omega p} \right|^2} \tag{A1.46}$$

I. Window Functions

The concept of a window function is very useful in the study of spectral analysis and sampled data systems. The window function serves as a mathematical tool to "bridge the gap" between theoretical concepts and empirical analysis techniques. Its most important use is to model the effect of finite data and finite observation times on estimated autocorrelation functions and estimated power spectra. There are three types of window functions to consider; the data window, the lag window, and the spectral window.

The data window (also called the observation window) models the effect of a finite observation time. A continuous time function, $x(t)$, which may hypothetically exist for all time, can be observed for only a finite time, T_N. This function may be periodic, stochastic, or mixed and its spectral bandwidth may be very large but all of its properties must be determined from those values in the observation interval, T_N, which are known. From this finite observation, one usually tries to obtain estimates of such characteristic parameters as average value, mean-square value, autocorrelation function, and power spectral density function. The length of observation time (width of the data window) has a profound effect on this estimate.

The inherent process of observation forces all data windows to be rectangular functions. The observed data function, denoted by a circumflex accent, is the product of the real function and the data window function:

$$\hat{x}(t) = h_d(t)x(t) \qquad (A1.47)$$

The estimated properties of x(t) will generally be different than the "true" properties of x(t). As a general rule, when the observation time T_N becomes large, the properties of $\hat{x}(t)$ become good estimates of the properties of x(t) and the effect of a finite observation time becomes minimized. This is especially true when the spectral bandwidth of x(t) is limited. The effect of finite observations on the amplitude spectral function can be seen by taking the Fourier transform of both sides of Equation A1.47. The resulting estimated amplitude spectrum, assuming the Fourier transform of x(t) exists, is obtained as:

$$\hat{X}(\omega) = \frac{1}{2\pi} \int_{-\infty}^{+\infty} H_d(\omega - \lambda) x(\lambda) d\lambda \tag{A1.48}$$

This convolution of the data window spectral function with the "true" amplitude spectrum causes a spectral smoothing effect and a loss in spectral resolution. Also, the spectral window will introduce spectral mixing. A rectangular window causes the most spectral mixing and to minimize this, some type of window smoothing may be employed. A data function can be tapered at each end to minimize the discontinuity caused by the observation. Various types of data windows and an analysis of their performance can be found in Otnes and Enochson (1972, p. 281).

The lag window is used primarily to model the effect of a finite autocovariance function, $C_o(\tau)$, where τ is called the lag time or simply the lag. In the Blackman-Tukey method of spectral analysis, the lag window is also used to reduce the effect of statistical variance by emphasizing lag values close to zero lag. The apparent or observed autocovariance function, $C_o(\tau)$ must be finite because the time function, x(t), is observed

only for a finite time. An unbiased estimate for the autocovariance function has been defined as (Blackman and Tukey, 1958):

$$C_o(\tau) = \frac{1}{T_N - |\tau|} \int_{-(T_N - |\tau|)/2}^{+(T_N - |\tau|)/2} x(t - \tau/2)x(t + \tau/2)dt \qquad |\tau| < T_N \qquad (A1.49)$$

This definition produces an autocovariance function which is even and estimated over the lag interval $-T_N \leq \tau \leq +T_N$. For statistical reasons, this estimate is best for values of lag time near zero. The variance of the estimate becomes very large as the lag time approaches $\underline{+}T_N$. Blackman and Tukey suggest using a lag window function to modify the shape of $C_o(\tau)$ so that lag times near zero are emphasized.

The apparent or observed autocovariance function, when multiplied by a suitable weighting function (lag window function), is called the modified apparent autocovariance function and its Fourier transform gives a smoothed estimate of the power spectrum of $x(t)$. This modification produces an autocovariance estimator that is defined by the equation

$$\hat{C}(\tau) = D(\tau)C_o(\tau) \qquad (A1.50)$$

where the lag window function, $D(\tau)$, may be chosen from a variety of functions that are commonly used for the purpose of spectral smoothing.

Lag window functions have been very rigorously investigated for their properties in an effort to produce a window function which will maximize spectral resolution and minimize spectral "leakage". Names for window functions commonly used in the literature include; Hanning window, Hamming

window, Goodman window, Parzen window, Goodman-Enochson-Otnes window, and Bartlett window. Generally speaking, all lag windows have a general shape like a cosine bell or a smoothed sinc function. A rectangular window is commonly used in theoretical treatments of spectral analysis but usually not in practice because it has severe leakage problems. Further discussions of window functions can be found in Otnes and Enochson (1972), Koopmans (1974), Blackman and Tukey (1958), and Papoulis (1973).

The spectral window function models the spectral smoothing effect produced by a lag window. The spectral window function is defined as the Fourier transform of the lag window function. The expected value of a collection of estimated spectral density functions is the convolution of the spectral window function with the "true" spectral density of x(t). The various relationships between the lag and spectral windows and the "true" and estimated spectra are summarized below:

$$P(f) = \mathcal{F}\{C(\tau)\} \qquad \text{(true spectrum)} \qquad (A1.51)$$

$$\hat{P}(f) = \mathcal{F}\{\hat{C}(\tau)\} \qquad \text{(a single spectral estimate)} \qquad (A1.52)$$

$$= \mathcal{F}\{C_0(\tau)D(\tau)\} \qquad (A1.53)$$

$$Q(f) = \mathcal{F}\{D(\tau)\} \qquad \text{(spectral window)} \qquad (A1.54)$$

$$E\{\hat{P}(f)\} = \int_{-\infty}^{+\infty} Q(f-\lambda)P(\lambda)d\lambda \qquad \text{(spectral smoothing)} \qquad (A1.55)$$

J. Calculus of Variations

The calculus of variations problem with constant Lagrangian multipliers and integral constraints is formulated as follows:

1) Given a definite integral

$$H = \int_a^b F(x,p(x))dx \qquad\qquad (A1.56)$$

the problem is to maximize H with respect to the function p(x) where p(x) has N constraints as given by:

$$\int_a^b Q_k(x,p(x))dx = \phi_k \qquad k = 1, 2, 3, \ldots N. \qquad (A1.57)$$

The integrals must all be finite and the limits of integration are over all defined values of the independent variable, x. $F(x,p(x))$ and $Q_k(x,p(x))$ are explicit functions of x and p(x). p(x) is a function of x alone.

2) Substitute for the function to be maximized (in this case p(x)) the following modified function which has N arbitrary "perturbation" functions:

$$\hat{P}(x) = P(x) + e_1\eta_1(x) + e_2\eta_2(x) + \ldots e_N\eta_N(x) \qquad (A1.58)$$

$$\hat{P}(x) = P(x) + \sum_{k=1}^{N} e_k\eta_k(x) \qquad (A1.59)$$

This produces a function with p(x) and N additional degrees of freedom.

3) Next, form the following auxiliary function

$$w = H(e_1, e_2, \ldots e_N) + \sum_{k=1}^{N} \lambda_k [\int_a^b Q_k dx - \phi_k] \qquad (A1.60)$$

where $Q_k = Q_k(p(x), e_1\eta_1, e_2\eta_2, \ldots e_N\eta_N)$.

4) w is minimized with respect to each e_k by evaluating the following derivatives at all $e_k = 0$:

$$\left.\frac{\partial w}{\partial e_1}\right|_{\text{all } e_k = 0} = 0 \qquad\qquad \left.\frac{\partial w}{\partial e_2}\right|_{\text{all } e_k = 0} = 0$$

$$\cdots \qquad \left. \frac{\partial w}{\partial \epsilon_N} \right|_{\text{all } \epsilon_k = 0} = 0 \qquad\qquad (A1.61)$$

This procedure will yield N equations that can be used to solve for N constraint constants. The partial derivatives can be expanded by noting that:

$$\frac{\partial w}{\partial \epsilon_k} = \frac{\partial w}{\partial \hat{p}} \frac{\partial \hat{p}}{\partial \epsilon_k} \qquad\qquad \frac{\partial Q}{\partial \epsilon_k} = \frac{\partial Q}{\partial \hat{p}} \frac{\partial \hat{p}}{\partial \epsilon_k}$$

$$\frac{\partial \hat{p}}{\partial \epsilon_k} = \eta_k(x) \qquad\qquad (A1.62)$$

All the partial derivatives become:

$$\left. \frac{\partial w}{\partial \epsilon_k} \right|_{\text{all } \epsilon_k = 0} = \int_a^b \left. \frac{\partial F}{\partial \epsilon_k} \right|_{\text{all } \epsilon_k = 0} dx$$

$$+ \sum_{m=1}^{N} \lambda_m \left[\int_a^b \left. \frac{\partial Q_m}{\partial \epsilon_k} \right|_{\text{all } \epsilon_k = 0} dx - \left. \frac{\partial \phi_m}{\partial \epsilon_k} \right|_{\text{all } \epsilon_k = 0} \right] \qquad (A1.63)$$

The partial derivatives for F, Q_m, and ϕ_m are written as follows:

$$\left. \frac{\partial F}{\partial \epsilon_k} \right|_{\text{all } \epsilon_k = 0} = \left. \frac{\partial}{\partial \epsilon_k} \left[F(x, p(x) + \epsilon_1 \eta_1 + \epsilon_2 \eta_2 + \cdots \epsilon_N \epsilon_N) \right] \right|_{\text{all } \epsilon_k = 0}$$

$$= \left. \frac{\partial F}{\partial \hat{p}} \frac{\partial \hat{p}}{\partial \epsilon_k} \right|_{\text{all } \epsilon_k = 0} = \left. \eta_k(x) \frac{\partial F}{\partial \hat{p}} \right|_{\text{all } \epsilon_k = 0} \qquad (A1.64)$$

$$\frac{\partial Q_m}{\partial \epsilon_k}\bigg|_{\text{all } \epsilon_k = 0} = \eta_k(x) \frac{\partial Q_m}{\partial \hat{p}}\bigg|_{\text{all } \epsilon_k = 0} \qquad (A1.65)$$

$$\frac{\partial \phi_m}{\partial \epsilon_k} = 0 \qquad (A1.66)$$

The partial derivatives for w are reduced to:

$$\frac{\partial w}{\partial \epsilon_k}\bigg|_{\text{all } \epsilon_k = 0} = \int_a^b \eta_k(x) \left[\frac{\partial F}{\partial \hat{p}}\bigg|_{\text{all } \epsilon_k = 0} + \sum_{m=1}^{N} \lambda_m \frac{\partial Q_m}{\partial \hat{p}}\bigg|_{\text{all } \epsilon_k = 0} \right] dx = 0 \qquad (A1.67)$$

5) Since the integral of Equation is zero for any **arbitrary** "perturbation" function $\eta_k(x)$, only two possibilities exist. Either $\eta_k(x) = 0$ which is the trivial solution or else:

$$\left[\frac{\partial F}{\partial \hat{p}(x)}\bigg|_{\text{all } \epsilon_k = 0} \pm \sum_{m=1}^{N} \lambda_m \frac{\partial Q_m}{\partial \hat{p}(x)}\bigg|_{\text{all } \epsilon_k = 0} \right] = 0 \qquad (A1.68)$$

Equation A1.68 is called the Euler-Lagrange equation and may be written in an alternate way as:

$$\frac{\partial}{\partial \hat{p}(x)}\left[F(x,\hat{p}(x)) \pm \sum_{m=1}^{N} \lambda_m Q_m(x,\hat{p}(x)) \right]\bigg|_{\text{all } \epsilon_k = 0} = 0 \qquad (A1.69)$$

The Euler-Lagrange equation will generally contain N Lagrange multipliers, the independent variable x, and the dependent variable $p(x)$.

6) The Euler-Lagrange equation is solved for $p(x)$ in terms of the λ_m's and x. This solution will generally be very complicated and quite often transcendental. The explicit solution for $p(x)$ will be

represented by $V(x, \lambda_1, \lambda_2, \ldots \lambda_N)$. This solution is then substituted into the N constraint equations

$$\int_a^b Q_k(x, V(x, \lambda_1, \lambda_2, \ldots \lambda_N)) dx = \phi_k \qquad (A1.70)$$

and the N equations are solved for the N values of λ_m, the Lagrangian multipliers.

7) The solution is completed when these λ_m's are used in the explicit equation for $p(x)$ to give:

$$p(x) = V(x, \lambda_1, \lambda_2, \ldots \lambda_N) \qquad (A1.71)$$

The calculus of variations problem with a continuous Lagrangian multiplier function is formulated as follows:

1) Given the definite integral

$$H = \int_a^b F(x, p(x)) dx \qquad (A1.72)$$

the constraints are now assumed to form a continuous function and the constraining equation becomes

$$\int_a^b Q(\tau, x, p(x)) dx = \phi(\tau) \qquad (A1.73)$$

where the continuous parameter τ replaces the index k.

2) Substitute for the function to be maximized, the following modified function which contains an arbitrary "perturbation" function $\eta(\tau, x)$ and an $\epsilon(\tau)$ continuous multiplier that is independent of x. The modified function becomes:

$$\hat{p}(x) = p(x) + \int_{\text{all } \tau} \epsilon(\tau) \eta(\tau, x) d\tau \qquad (A1.74)$$

Note that the interval of τ for $\phi(\tau)$ must be the same as that for $\epsilon(\tau)$ and $\eta(\tau,x)$ or there will not be enough "degrees of freedom" in the product $\epsilon(\tau)\eta(\tau,x)$.

3) Next, form the following auxiliary function using $\overset{\Lambda}{p}(x)$:

$$w = H(\epsilon,\tau) \pm \int_{\text{all } \tau} \lambda(\tau) \; [\int_a^b Q(\tau,x,\overset{\Lambda}{p})dx - \phi(\tau)]d\tau \qquad (A1.75)$$

4) Calculate the partial derivatives of w with respect to $\epsilon(\tau)$ and evaluate this partial derivative at $\epsilon(\tau) = 0$ to minimize the function w at the point $\overset{\Lambda}{p}(x) = p(x)$.

The partial derivatives are expanded as before:

$$\frac{\partial w}{\partial \epsilon(\tau)}\bigg|_{\epsilon(\tau)=0} = \frac{\partial w}{\partial \overset{\Lambda}{p}} \frac{\partial \overset{\Lambda}{p}}{\partial \epsilon(\tau)}\bigg|_{\epsilon(\tau)=0} \qquad (A1.76)$$

$$\frac{\partial F}{\partial \epsilon(\tau)}\bigg|_{\epsilon(\tau)=0} = \frac{\partial F}{\partial \overset{\Lambda}{p}} \frac{\partial \overset{\Lambda}{p}}{\partial \epsilon(\tau)}\bigg|_{\epsilon(\tau)=0} \qquad (A1.77)$$

$$\frac{\partial Q}{\partial \epsilon(\tau)}\bigg|_{\epsilon(\tau)=0} = \frac{\partial Q}{\partial \overset{\Lambda}{p}} \frac{\partial \overset{\Lambda}{p}}{\partial \epsilon(\tau)}\bigg|_{\epsilon(\tau)=0} \qquad (A1.78)$$

It is important to note that the partial derivative of $\overset{\Lambda}{p}(x)$ with respect to $\epsilon(\tau)$ can be reduced to a function of x alone as follows:

$$\frac{\partial \overset{\Lambda}{p}}{\partial \epsilon(\tau)}\bigg|_{\epsilon(\tau)=0} = \frac{\partial}{\partial \epsilon(\tau)}[p(x) + \int_{\text{all } \tau} \epsilon(\tau)\eta(\tau,x)d\tau]\bigg|_{\epsilon(\tau)=0}$$

$$= \int_{\text{all } \tau} [\epsilon(\tau) \frac{\partial \eta}{\partial \epsilon(\tau)} + \eta \frac{\partial \epsilon(\tau)}{\partial \epsilon(\tau)}]d\tau\bigg|_{\epsilon(\tau)=0}$$

$$= \int_{\text{all } \tau} \eta(\tau,x)d\tau \qquad (A1.79)$$

The integral of $\eta(\tau,x)$ over τ leaves a function of x alone, therefore:

$$\left.\frac{\partial \hat{p}(x)}{\partial \epsilon(\tau)}\right|_{\epsilon(\tau)=0} = \int_{all\ \tau} \eta(\tau,x)\,d\tau = K(x) \tag{A1.80}$$

With these various partial derivative expansions, the partial derivative of w becomes:

$$\left.\frac{\partial w}{\partial \epsilon(\tau)}\right|_{\epsilon(\tau)=0} = \int_a^b \left.\frac{\partial F}{\partial \epsilon(\tau)}\right|_{\epsilon(\tau)=0} dx \pm \int_{all\ \tau} \int_a^b \lambda(\tau)\frac{\partial Q}{\partial \epsilon(\tau)}\,dx\,d\tau \tag{A1.81}$$

Combining the integrals and reducing gives:

$$\left.\frac{\partial w}{\partial \epsilon(\tau)}\right|_{\epsilon(\tau)=0} = \int_a^b K(x) \left[\left.\frac{\partial F}{\partial \hat{p}}\right|_{\epsilon(\tau)=0} \pm \int_{all\ \tau} \lambda(\tau)\left.\frac{\partial Q}{\partial \hat{p}}\right|_{\epsilon(\tau)=0}\,d\tau\right]dx = 0 \tag{A1.82}$$

5) Since the integral is zero for every <u>arbitrary</u> "perturbation" function $K(x)$, the only nontrivial solution is:

$$\left.\frac{\partial F(x,\hat{p}(x))}{\partial \hat{p}(x)}\right|_{\epsilon(\tau)=0} \pm \int_{all\ \tau} \lambda(\tau)\left.\frac{\partial Q(\tau,x,\hat{p}(x))}{\partial \hat{p}(x)}\right|_{\epsilon(\tau)=0}\,d\tau = 0 \tag{A1.83}$$

Equation A1.83 is the Euler-Lagrange equation for a continuous constraint function defined by an integral constraint. This equation will contain a continuous Lagrangian multiplier, $\lambda(\tau)$, the independent variable x, and the dependent variable, p(x).

6) The Euler-Lagrange equation must be solved for p(x) in terms of the multiplier function $\lambda(\tau)$ and x. In general the solution will involve a transcendental equation in p(x). An explicit solution would be:

$$p(x) = V_\lambda(x,\lambda(\tau)) \tag{A1.84}$$

7) This value of p(x) is then substituted into the constraint equation to give:

$$\int_a^b Q(t,x,V_\lambda(x,\lambda(\tau)))dx = \phi(\tau) \qquad (A1.85)$$

This integral equation must be solved to yield $\lambda(\tau)$ as some function of $\phi(\tau)$ represented by:

$$\lambda(\tau) = R_\phi(\phi(\tau)) \qquad (A1.86)$$

Again this solution may be transcendental.

8) The solution for p(x) to maximize H is completed when the solution for $\lambda(\tau)$ is used in Equation A1.84 to give:

$$p(x) = V_\lambda(x,R_\phi) \qquad (A1.87)$$

XXII. APPENDIX II - FOURIER ANALYSIS

A. Fourier Series - Equivalent Mathematical Forms

A continuous function $f(x)$ is periodic in x if it is defined for all real x and if

$$f(x + nT) = f(x) \tag{A2.1}$$

where T is called the period of $f(x)$ and n is any positive or negative integer including zero.

The familiar Fourier series representation of $f(x)$ is given as:

$$f(x) = a_o + \sum_{n=1}^{\infty}(a_n \cos \frac{2\pi n}{T} x + b_n \sin \frac{2\pi n}{T} x) \tag{A2.2}$$

The Fourier coefficients for (A2.2) are computed by the following integrals:

$$a_o = \frac{1}{T} \int_{-T/2}^{+T/2} f(x) dx \tag{A2.3}$$

$$a_n = \frac{2}{T} \int_{-T/2}^{+T/2} f(x) \cos(\frac{2\pi n}{T} x) dx \tag{A2.4}$$

$$b_n = \frac{2}{T} \int_{-T/2}^{+T/2} f(x) \sin(\frac{2\pi n}{T} x) dx \tag{A2.5}$$

The complex representation of a Fourier series is obtained by using Euler's equation, $e^{j\alpha} = \cos\alpha + j\sin\alpha$, to replace the sin and cos terms of (A2.2). When this is done, the series can be written as:

$$f(x) = k_o + \sum_{n=1}^{\infty}[k_n e^{+j\frac{2\pi n}{T}} + k_n^* e^{-j\frac{2\pi n}{T}x}] \tag{A2.6}$$

The complex coefficients are related to the a's and b's as follows:

$$k_o = a_o \qquad\qquad |k_n| = \frac{1}{2}(a_n^2 + b_n^2)^{\frac{1}{2}}$$

(A2.7)

$$k_n = \frac{1}{2}(a_n - j\,b_n) \qquad\qquad \phi_n = Arctan\left(\frac{-b_n}{a_n}\right)$$

The complex series representation is most often seen in the following compact form

$$f(x) = \sum_{n=-\infty}^{+\infty} c_n e^{+j\frac{2\pi n}{T}x}$$

(A2.8)

$$c_n = \frac{1}{T}\int_{-T/2}^{+T/2} f(x)e^{-j\frac{2\pi n}{T}x}\,dx$$

(A2.9)

with $c_{-n} = c_n^*$.

Another common representation of the Fourier series is the phase angle representation. This representation is obtained from Equation A2.2 by using the substitutions $a_n = d_n\cos\phi_n$ and $b_n = -d_n\sin\phi_n$. After several trignometric manipulations we obtain:

$$f(x) = a_o + \sum_{n=1}^{\infty} d_n\cos\left(\frac{2\pi n}{T}x + \phi_n\right)$$

(A2.10)

The values for d_n, and ϕ_n are computed from the a's and b's as follows:

$$d_n = (a_n^2 + b_n^2)^{\frac{1}{2}}$$

(A2.11)

$$\phi_n = Arctan\left(\frac{-b_n}{a_n}\right)$$

The relationships between the complex representations and the phase angle representations are summarized below:

a) $a_n = k_n + k_n^*$ $k_n = \frac{1}{2}(a_n - j\,b_n)$

$b_n = j(k_n - k_n^*)$ $k_n^* = \frac{1}{2}(a_n + j\,b_n)$ (A2.12)

b) $a_n = c_n + c_{-n}$ $c_n = \frac{1}{2}(a_n - j\,b_n)$

$b_n = j(c_n - c_{-n})$ $c_{-n} = \frac{1}{2}(a_n + j\,b_n)$ (A2.13)

$|c_n| = \frac{1}{2}(a_n^2 + b_n^2)^{\frac{1}{2}}$ $\phi_n = \mathrm{Arctan}(\dfrac{-b_n}{a_n})$ (A2.14)

c) $a_n = d_n \cos\phi_n$ $d_n = (a_n^2 + b_n^2)^{\frac{1}{2}}$

$b_n = -d_n \sin\phi_n$ $\phi_n = \mathrm{Arctan}(\dfrac{-b_n}{a_n})$ (A2.15)

$c_n = \frac{1}{2} d_n e^{+j\phi_n}$ $d_n = 2|c_n|$

$c_{-n} = \frac{1}{2} d_n e^{-j\phi_n}$ $\phi_n = \mathrm{Arctan}[\dfrac{\mathrm{Im}\{c_n\}}{\mathrm{Re}\{c_n\}}]$ (A2.16)

Each representation of the Fourier series has its useful applications. Quite often the phase angle representation is used in discussions of network theory and wave propagation. For data analysis, the compact complex representation is used because it is identical to the digital Fourier transform and also because it is notationally convenient.

B. Fourier Series - Discrete Independent Variable

An infinite periodic time series can be represented by a digital Fourier series. Using the compact complex representation and assuming equally spaced x-values we get:

$$f(k\Delta x) = \sum_{n=-M}^{+M} c_n e^{+j\frac{2\pi n}{T}k\Delta x} \qquad / \qquad (A2.17)$$

There are only $(2M+1)$ values of c_n because for a finite number of values of $f(x)$ in the Fourier period, T, only a finite number of complex amplitudes can be uniquely specified. This result points out the important fact that a digital Fourier series must, of necessity, be spectrally limited. The complex amplitudes can be exactly specified by the following digital routine which is obtained by using a Riemann sum approximation for the integral of (A2.9):

$$c_n = \frac{\Delta x}{T} \sum_{k=-M}^{+M} f(k\Delta x) e^{-j\frac{2\pi}{T}nk\Delta x} \qquad (A2.18)$$

Equations A2.17 and A2.18 form a digital Fourier transform pair if the increment Δx is such that $\Delta x = T/(2M+1)$. The c_n's calculated from (A2.18) can then be used in (A2.17) to reproduce the exact $f(k\Delta x)$-values.

C. Fourier Transform Pair

The Fourier series can be used to derive the Fourier integral and Fourier transform. If a Fourier integral is to exist for an arbitrary function $f(x)$ (not necessarily periodic) the function must be piecewise continuous on every finite interval (Riemann integrability), it must have a finite average value, and it must be absolutely integrable (sufficient but not necessary).

The Fourier integral may be written as

$$f(x) = \frac{1}{\pi} \int_0^\infty [A(w) \cos wx + B(w) \sin wx] dw \qquad (A2.19)$$

where:

$$A(w) = \int_{-\infty}^{+\infty} f(u) \cos wu \, du \qquad \text{(A2.20)}$$

$$B(w) = \int_{-\infty}^{+\infty} f(u) \sin wu \, du \qquad \text{(A2.21)}$$

The Fourier transform is the complex representation of the Fourier integral. Using Euler's equation, the Fourier integral becomes

$$f(x) = \frac{1}{2\pi} \int_{0}^{+\infty} [e^{-jwx} \int_{-\infty}^{+\infty} f(u)e^{+jwu} du + e^{+jwx} \int_{-\infty}^{+\infty} f(u)e^{-jwu} du] dw \qquad \text{(A2.22)}$$

which can be reduced to:

$$f(x) = \frac{1}{2\pi} \int_{-\infty}^{+\infty} e^{+jwx} [\int_{-\infty}^{+\infty} f(u)e^{-jwu} du] dw \qquad \text{(A2.23)}$$

Equation A2.23 is used to define the Fourier transform pair:

$$f(x) = \frac{1}{2\pi} \int_{-\infty}^{+\infty} e^{+jwx} F(w) \, dw \qquad \text{(A2.24)}$$

$$F(w) = \int_{-\infty}^{+\infty} f(x)e^{-jwx} dx \qquad \text{(A2.25)}$$

Many functions that appear in physics and mathematics are formulated in terms of the Fourier transform and thus are associated with Fourier transform pairs. Two common examples are: 1) position and momentum in quantum mechanics and 2) autocorrelation and power spectral density in signal processing. The autocorrelation function, $R(\tau)$ of a random process and the power spectral density function, $S(\omega)$, of that process form a Fourier transform pair:

$$S(\omega) = \int_{-\infty}^{+\infty} R(\tau)e^{-j\omega\tau} d\tau \qquad \text{(A2.26)}$$

$$R(\tau) = \frac{1}{2\pi} \int_{-\infty}^{+\infty} S(\omega)e^{+j\omega\tau}d\omega \qquad (A2.27)$$

An alternate mathematical form that is often seen is obtained by substituting $2\pi f = \omega$ to give:

$$P(f) = \int_{-\infty}^{+\infty} R(\tau)e^{-j2\pi f\tau}d\tau \qquad (A2.28)$$

$$R(\tau) = \int_{-\infty}^{+\infty} P(f)e^{+j2\pi f\tau}df \qquad (A2.29)$$

D. Digital Fourier Transform

The digital (discrete) Fourier transform is obtained by using a Riemann sum approximation for the integral of Equation (A2.24):

$$f(k\Delta x) = \frac{1}{2\pi} \Delta w \sum_{n=-N}^{+N} F(n\Delta w)e^{+jn\Delta wk\Delta x} \qquad (A2.30)$$

The spectral amplitudes are obtained from the sample values of $f(k\Delta x)$ by the Riemann sum:

$$F(n\Delta w) = \Delta x \sum_{k=-\infty}^{+\infty} f(k\Delta x)e^{-jn\Delta wk\Delta x} \qquad (A2.31)$$

Other mathematical forms of these equations are often used to develop the theory and practical application of digital Fourier transforms.

E. Special Functions

There are several special functions which occur repeatedly in the mathematics associated with Fourier analysis. Three of the most important are the Kronecker delta, the Dirac delta and the sinc function. The fol-

lowing tabulations of the various forms of these three functions are included because they have proved to be valuable for use in a variety of derivations.

The Kronecker delta plays an important part in Einstein summation notation and in the formulation of digital Fourier analysis. The Kronecker delta is defined as follows:

$$\delta_{kn} = \begin{cases} 1 & k = n \quad k,n \text{ are integers} \\ 0 & k \neq n \end{cases} \tag{A2.32}$$

Some of the various mathematical forms for the Kronecker delta function are:

$$\delta_{kn} = \frac{\sin \pi(k - n)}{\pi(k - n)} \tag{A2.33}$$

$$\delta_{kn} = \frac{1}{T} \int_{-T/2}^{+T/2} e^{+j\frac{2\pi}{T}(k-n)x} \, dx \tag{A2.34}$$

$$\delta_{kn} = \frac{1}{2\pi} \int_{-\pi}^{+\pi} e^{+j\theta(k-n)} \, d\theta \qquad (T = 2\pi) \tag{A2.35}$$

$$\delta_{kn} = \frac{2}{T} \int_{-T/2}^{+T/2} \cos(\frac{2\pi}{T} kt) \cos(\frac{2\pi}{T} nt) \, dt \tag{A2.36}$$

$$\delta_{kn} = \sum_{p=-M}^{+M} \frac{1}{2M+1} e^{+j\frac{2\pi}{(2M+1)}(k-n)p} \tag{A2.37}$$

This last form was discovered in the derivation of the spectral mixing formula and can also be written alternately as:

$$\delta_{kn} = \frac{1}{(2M+1)} [1 + 2 \sum_{p=1}^{M} \cos \frac{2\pi}{2M+1}(k - n)p] \tag{A2.38}$$

The validity of this equation was shown using a double precision computer program. The magnitude of the indexes was shown to be restricted to the ranges; $0 \le k \le M$, $0 \le n \le M$.

The Dirac delta function (or impulse function) plays the same type of mathematical role in continuous functions as the Kronecker delta does in discrete functions. The Dirac delta is defined as follows:

$$\delta(x-y) = \begin{cases} \infty & x = y \\ 0 & \text{otherwise} \end{cases} \qquad (A2.39)$$

$$\int_{\text{all } x} \delta(x-y)dx = 1 \qquad (A2.40)$$

$$\int_{\text{all } x} f(x)\delta(x-y)dx = f(y) \qquad (A2.41)$$

Equation A2.41 is the sifting (or sampling) property of the Dirac delta. The Dirac delta function also has the following integral definition (Cauchy principle value):

$$\delta(x-y) = \int_{-\infty}^{+\infty} e^{+j2\pi(x-y)\lambda} d\lambda \qquad (A2.42)$$

The Dirac delta can also be represented in the following mathematical forms:

$$\delta(x-y) = \lim_{T \to \infty} T \frac{\sin \pi T(x-y)}{\pi T(x-y)} \qquad (A2.43)$$

$$\delta(x-y) = \lim_{T \to \infty} T e^{-\pi T^2(x-y)^2} \qquad (A2.44)$$

$$\delta(x \pm y) = \lim_{T \to \infty} \frac{T}{\pi} \frac{\sin(x \pm y)T}{(x \pm y)T} \qquad (A2.45)$$

For conceptual purposes, the Dirac delta is often represented by a rectangle function of height T, width 1/T, and unity area:

$$\delta(x-y) = \lim_{T \to \infty} T \, \text{rect}\{T(x-y)\} \tag{A2.46}$$

The sinc function appears in most discussions of Fourier analysis and sampling theory. It is the Fourier transform of a rectangle function and can be used to approximate a Dirac delta function. The normalized sinc function is defined as

$$\text{sinc}(x) = \frac{\sin \pi x}{\pi x} \tag{A2.47}$$

and has the following integral definitions:

$$\int_{-\infty}^{+\infty} \frac{\sin \pi x}{\pi x} \, dx = 1$$

$$\int_{0}^{+\infty} \frac{\sin mx}{x} \, dx = \begin{cases} \pi/2 & m > 0 \\ 0 & m = 0 \\ -\pi/2 & m < 0 \end{cases} \tag{A2.48}$$

A more generalized form of the sinc function can be written as:

$$AT_m \, \text{sinc}(r) = AT_m \left[\frac{\sin(\omega - \omega_0)T_m}{(\omega - \omega_0)T_m} \right] \tag{A2.49}$$

Figure A2-1 show a plot of the generalized sinc function. The peak amplitude of AT_m occurs at $\omega = \omega_0$. The zeros of the sinc function occur at $\omega = \omega_0 \pm n \frac{\pi}{T_m}$, $n = 1, 2, 3 \ldots$ and the bandwidth between first nulls is $\text{BWFN} = 2\pi/T_m$.
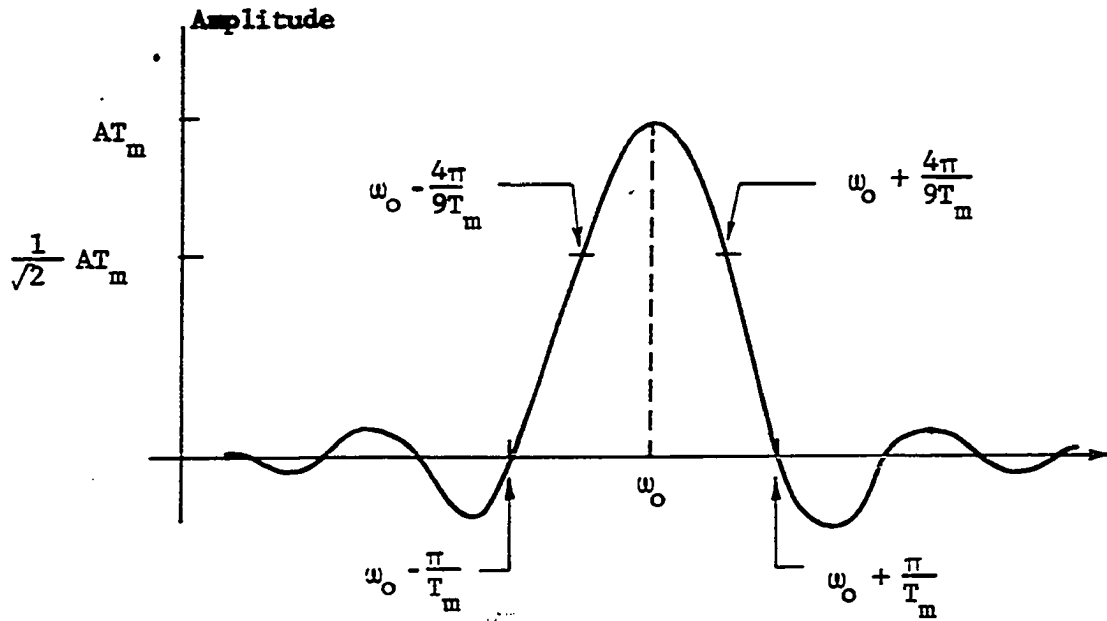
Figure A2-1.   A Generalized Sinc Function

The sinc function has the following useful mathematical properties:

$$\frac{1}{2\pi} \int_{-\infty}^{+\infty} AT_m \left[\frac{\sin(\omega - \omega_o)T_m}{(\omega - \omega_o)T_m} \right] d\omega = \frac{A}{2} \qquad (A2.50)$$

$$\lim_{T_m \to \infty} AT_m \left[\frac{\sin(\omega - \omega_o)T_m}{(\omega - \omega_o)T_m} \right] = \pi A \, \delta(\omega - \omega_o) \qquad (A2.51)$$

```
$JCB    'RUSSELL',TIME=30,PAGES=75
C
C                    PROGRAM 01
C
C       DISCRETE FOURIER TRANSFORM TESTING
C
C       THIS PROGRAM IS USED TO ANALYZE THE EFFECT OF
C       VARIOUS SAMPLING CONDITIONS ON THE DISCRETE FOURIER
C       TRANSFORM ESTIMATE OF THE SPECTRUM OF A TIME SERIES.
C       THE INPUT TIME SERIES IS GENERATED IN THE PROGRAM.
C
1              DIMENSION FVALUE(201),FX(804),A(400),B(400)
2              DO 5 I=1,400
3              A(I)=0.0
4     5        B(I)=0.0
C
C          INPUT DATA VALUES
C
5              A(1)=4.0
6              B(3)=1.0
C
7              TF=1.0
8              TN=3.1
9              NS=21
10             FNS=NS
11             TDEL=TN/FNS
12             SCALE=2.0
C
13             NLS=NS
14             NMAX=(NS-1)/2
15             DCV=0.0
C
C          GENERATE DATA VALUES, EQUATION(120.1)
C
16             CALL FSRS(FX,A,B,DCV,NS,TDEL,TF)
17             PRINT 9
18    9        FORMAT('1',11X,'K',7X,'TIME',13X,'F(TIME)'/)
19             DO 10 I=1,NS
20             FVALUE(I)=FX(I)
21             II=I-NMAX-1
22             XDELTA=II*TDEL
23    10       PRINT,II,XDELTA,FX(I)
C
C       COMPUTE COMPLEX FOURIER AMPLITUDES, EQUATION(120.5)
C
24             CALL LNSPTM(FVALUE,A,B,NLS,DCV)
25             PRINT 34
26    34       FORMAT('1',4X,'N',3X,'CC-VALUE',4X,'CMAG',8X
              1,'CPHASE',6X,'FREC-HZ',7X,'CMAG-DB'/)
```

```
27       NLMAX=(NLS-1)/2
28       DO 35 I=1,NLMAX
29       XI=I
30       CMAG=((A(I)*A(I)+B(I)*B(I))**0.5)/2.
31       CM=CMAG/SCALE
32       CMAGDB=20.*ALOG10(CM)
33       ATEST=B(I)/A(I)
34       ATEST=ATEST*ATEST
35       ATEST=ATEST**0.5
36       AT=1000.-ATEST
37       IF(AT) 20,20,21
38    20 CPHASE=.3899889E
39       GO TO 22
40    21 CONTINUE
41       BA=-B(I)/A(I)
42       CPHASE=ATAN(BA)
43       CPHASE=CPHASE*57.29577
44       FNLS=NLS
45    22 FREQ=XI/(TDEL*FNLS)
46    35 PRINT 36,I,DCV,CMAG,CPHASE,FREQ,CMAGDB
47    36 FORMAT(I6,4E12.3,F10.2)
      C
      C       COMPUTE THE ESTIMATED TIME SERIES, EQUATION(120.6)
      C
48       NS=4*NS-3
49       TDEL=TDEL/4
50       NMAX=(NS-1)/2
51       TF=TN
52       CALL FSRS(FX,A,B,DCV,NS,TDEL,TF)
53       PRINT 90
54    90 FORMAT('1',11X,'K',7X,'TIME',11X
        1,'ESTIMATED F(TIME)'/)
55       DO 100 I=1,NS
56       II=I-NMAX-1
57       XDELTA=II*TDEL
58   100 PRINT,II,XDELTA,FX(I)
59   501 STOP
60       END
      C              LINE SPECTRUM SUBROUTINE
      C
      C       THIS SUBROUTINE GENERATES THE FOURIER COEFFICIENTS
      C       A AND B FOR NLS SAMPLES OF THE FUNCTION, FVALUE.
      C
61       SUBROUTINE LNSPTM(FVALUE,A,B,NLS,DCV)
62       DIMENSION FVALUE(201),A(400),B(400)
63       NLMAX=(NLS-1)/2
64       PI=3.1415926
65       XNN=NLS
```

```
66          DCV=0.
67          DO 15 J=1,NLS
68    15    CCV=DCV+FVALUE(J)
69          DCV=DCV/XNN
70          DO 16 J=1,NLS
71    16    FVALUE(J)=FVALUE(J)-DCV
72          DO 10 N=1,NLMAX
73          ASUM=0.
74          BSUM=0.
75          XN=N
76          DO 5 J=1,NLS
77          JJ=J-NLMAX-1
78          XJJ=JJ
79          ARG=2.0*PI*XN*XJJ/XNN
80          ASUM=CCS(ARG)*FVALUE(J)+ASUM
81    5     BSUM=SIN(ARG)*FVALUE(J)+BSUM
82          A(N)=2.0*ASUM/XNN
83    10    B(N)=2.0*BSUM/XNN
84          DO 17 J=1,NLS
85    17    FVALUE(J)=FVALUE(J)+DCV
86          RETURN
87          END
      C                    FOURIER SERIES SUBROUTINE
      C
      C     THIS SUBROUTINE GENERATES SAMPLES OF THE DATA
      C     FUNCTION, FX(I), USING THE FOURIER COEFFICIENTS,
      C     A(I), B(I), AND DC-VALUE, DCV, AND THE NUMBER OF
      C     DESIRED SAMPLES, NS.  TDEL IS THE SAMPLING PERIOD
      C     AND TF IS THE FOURIER PERICD.
      C
88          SUBROUTINE FSRS(FX,A,B,DCV,NS,TDEL,TF)
89          DIMENSION FX(804),A(400),B(400)
90          NMAX=(NS-1)/2
91          PI=3.1415926
92          XNS=NS
93          DO 10 I=1,NS
94          K=I-NMAX-1
95          XK=K
96          FXK=0.
97          DO 5 N=1,NMAX
98          XN=N
99          ARG=(2.0*PI*XN*XK*TDEL)/TF
100   5     FXK=FXK+A(N)*CCS(ARG)+B(N)*SIN(ARG)
101   10    FX(I)= FXK + DCV
102         RETURN
103         END

      SENTRY
```

K	TIME	F(TIME)
-10	-0.14761906E 01	-0.43695220E 01
-9	-0.13285706E 01	-0.18057656E 01
-8	-0.11809526E 01	0.19474606E 01
-7	-0.10333336E 01	0.33248621E 01
-6	-0.88571416E 00	0.38468333E 01
-5	-0.73609506E 00	-0.12738646E 01
-4	-0.59047606E 00	-0.23795637E 01
-3	-0.44285706E 00	-0.46255336E 01
-2	-0.29523806E 00	-0.46376026E 00
-1	-0.14761906E 00	0.20479116E 01
0	0.00000000E 00	0.40000000E 01
1	0.14761906E 00	0.27506666E 01
2	0.29523806E 00	-0.17796446E 01
3	0.44285706E 00	-0.28643366E 01
4	0.59047606E 00	-0.43618396E 01
5	0.73809506E 00	0.67598776E 00
6	0.88571416E 00	0.21777136E 01
7	0.10333336E 01	0.45003666E 01
8	0.11809526E 01	0.14154276E 01
9	0.13285706E 01	-0.19651156E 01
10	0.14761906E 01	-0.35214186E 01

N	DC-VALUE	CMAG	CPHASE	FREQ-HZ	CMAG-DB
1	-0.132E 00	0.146E 00	-0.424E 00	0.323E 00	-22.71
2	-0.132E 00	0.222E 00	-0.593E 00	0.645E 00	-19.08
3	-0.132E 00	0.200E 01	-0.105E 00	0.968E 00	0.02
4	-0.132E 00	0.186E 00	0.164E 01	0.129E 01	-20.65
5	-0.132E 00	0.741E-01	0.716E 01	0.161E 01	-28.62
6	-0.132E 00	0.427E-01	0.207E 02	0.194E 01	-33.42
7	-0.132E 00	0.363E-01	0.488E 02	0.226E 01	-34.82
8	-0.132E 00	0.647E-01	0.771E 02	0.258E 01	-29.81
9	-0.132E 00	0.380E 00	0.888E 02	0.290E 01	-14.42
10	-0.132E 00	0.261E 00	-0.895E 02	0.323E 01	-17.69

K	TIME	ESTIMATED F(TIME)
-40	-0.14761904E 01	-0.43851715 01
-39	-0.14392858E 01	-0.41727816 01
-38	-0.14023808E 01	-0.36666636 01
-37	-0.13654766E 01	-0.29586966E 01
-36	-0.13285708E 01	-0.18057716 01
-35	-0.12916668E 01	-0.64036356 00
-34	-0.12547618E 01	0.46285608 00
-33	-0.12178568E 01	0.13489338 01
-32	-0.11809522E 01	0.19474708 01
-31	-0.11440478E 01	0.23048938 01
-30	-0.11071428E 01	0.25609668 01
-29	-0.10702378E 01	0.28735658 01
-28	-0.10333338E 01	0.33248088 01
-27	-0.99642838 00	0.38568748 01
-26	-0.95952368 00	0.42766356 01
-25	-0.92261988 00	0.43347178 01
-24	-0.88571418 00	0.38467588 01
-23	-0.84880638 00	0.27982798 01
-22	-0.81150458 00	0.13767418 01
-21	-0.77499988 00	-0.91077038E-01
-20	-0.73809508 00	-0.12738848 01
-19	-0.70119038 00	-0.15755658 01
-18	-0.66428558 00	-0.22367938 01
-17	-0.62738088 00	-0.22705058 01
-16	-0.59047608 00	-0.23755910 01
-15	-0.55357138 00	-0.27749658 01
-14	-0.51666658 00	-0.34550258 01
-13	-0.47976188 00	-0.41908858 01
-12	-0.44285708 00	-0.46255208 01
-11	-0.40595238 00	-0.44466668 01
-10	-0.36904758 00	-0.35472168 01
-9	-0.33214288 00	-0.20936718 01
-8	-0.29523808 00	-0.46373458 00
-7	-0.25833338 00	0.91804118 00
-6	-0.22142858 00	0.17688148 01
-5	-0.18452388 00	0.20676848 01
-4	-0.14761908 00	0.20478658 01
-3	-0.11071438 00	0.20642038 01
-2	-0.73809508E-01	0.24005298 01
-1	-0.36904758E-01	0.31161058 01
0	0.00000008 00	0.35555748 01
1	0.36904758E-01	0.46659998 01
2	0.73809508E-01	0.47536758 01
3	0.11071438E 00	0.40765288 01

4	0.1476150E 00	0.2750656E 01
5	0.1845238E 00	0.1132101E 01
6	0.2214285E 00	-0.3392093E 00
7	0.2593333E 00	-0.1335740E 01
8	0.2952380E 00	-0.1775624E 01
9	0.3321422E 00	-0.1855581E 01
10	0.3690475E 00	-0.1896126E 01
11	0.4059523E 00	-0.2159636E 01
12	0.4428570E 00	-0.2864324E 01
13	0.4797618E 00	-0.3742486E 01
14	0.5166665E 00	-0.4497952E 01
15	0.5535713E 00	-0.4773554E 01
16	0.5904760E 00	-0.4361814E 01
17	0.6273808E 00	-0.3304071E 01
18	0.6642855E 00	-0.1871200E 01
19	0.7011903E 00	-0.4393817E 00
20	0.7380950E 00	0.6759574E 00
21	0.7749998E 00	0.1347073E 01
22	0.8119045E 00	0.1664277E 01
23	0.8488093E 00	0.1861163E 01
24	0.8857141E 00	0.2177700E 01
25	0.9226188E 00	0.2730844E 01
26	0.9595236E 00	0.3454321E 01
27	0.9964283E 00	0.4131682E 01
28	0.1033333E 01	0.4500347E 01
29	0.1070237E 01	0.4372299E 01
30	0.1107142E 01	0.3714053E 01
31	0.1144047E 01	0.2653052E 01
32	0.1180952E 01	0.1415442E 01
33	0.1217856E 01	0.2318068E 00
34	0.1254761E 01	-0.7435662E 00
35	0.1291666E 01	-0.1466540E 01
36	0.1328570E 01	-0.1985106E 01
37	0.1365476E 01	-0.2389432E 01
38	0.1402380E 01	-0.2759990E 01
39	0.1439285E 01	-0.3137555E 01
40	0.1476150E 01	-0.3521374E 01

sSTOP

```
$JOB    'RUSSELL S',TIME=10,PAGES=50
C
C                     PROGRAM 32
C
C       ESTIMATED KRONECKER DELTA FUNCTION
C
C       THIS ROUTINE EVALUATES THE APPROXIMATION TO THE
C       KRONECKER DELTA FUNCTION.  DOUBLE PRECISION IS USED
C       TO RESOLVE THE EXACT VALUES OF THE OFF-DIAGONAL
C       ELEMENTS.
C
1               REAL*8 THETA,AMAT,DELTOR,DNN,DQ,DR,TF,TN,DK,PI,DCOS
2               INTEGER Q,R
C
C                     INPUT DATA
3               N=5
4               M=5
5               TN=1.
6               TF=1.

7               NN=2*N+1
8               DNN=NN
9               MM=2*M+1
10              PI=3.1415926535897
C
11              PRINT 85
12      85      FORMAT('1',5X,'Q',7X,'R',7X,'DELTQR',16X,'DELTQR'/)
13              DO 80  I=1,NN
14              Q=I-N-1
15              DQ=Q
16              DO 80 L=1,MM
17              R=L-M-1
18              DR=R
19              AMAT=0.0
20              DO 50 K=1,N
21              DK=K
22              THETA=2.*PI*DK*TN*(DQ/TN-DR/TF)/DNN
23      50      AMAT=DCOS(THETA)+AMAT
24              DELTQR=(1.+2.*AMAT)/DNN
25      80      PRINT 81,Q,R,DELTQR,DELTQR
26      81      FORMAT(I8,I6,F10.5,D28.16)
27              STOP
28              END


        $ENTRY
```

Q	R	DELT GR	DELT QR
-5	-5	1.00000	0.10000000000000000D 01
-5	-4	0.00000	0.3024600771859489D-13
-5	-3	-0.00000	-0.3138903278712943D-13
-5	-2	0.00000	0.3372302437298913D-13
-5	-1	-0.00000	-0.3740442299328028D-13
-5	0	0.00000	0.4321543123353422D-13
-5	1	-0.00000	-0.5189787993293232D-13
-5	2	0.00000	0.6615667609692496D-13
-5	3	-0.00000	-0.9027122483861272D-13
-5	4	0.00000	0.1430421437863639D-12
-5	5	-0.00000	-0.3030101422299677D-12
-4	-5	0.00000	0.3024600771859489D-13
-4	-4	1.00000	0.10000000000000000D 01
-4	-3	0.00000	0.3024600771859489D-13
-4	-2	-0.00000	-0.3138903278712943D-13
-4	-1	0.00000	0.3372302437298913D-13
-4	0	-0.00000	-0.3740442299328028D-13
-4	1	0.00000	0.4321543123353422D-13
-4	2	-0.00000	-0.5189787993293232D-13
-4	3	0.00000	0.6615667609692496D-13
-4	4	-0.00000	-0.9027122483861272D-13
-4	5	0.00000	0.1430421437863639D-12
-3	-5	-0.00000	-0.3138903278712943D-13
-3	-4	0.00000	0.3024600771859489D-13
-3	-3	1.00000	0.10000000000000000D 01
-3	-2	0.00000	0.3024600771859489D-13
-3	-1	-0.00000	-0.3136903278712943D-13
-3	0	0.00000	0.3372302437298913D-13
-3	1	-0.00000	-0.3740442299328028D-13
-3	2	0.00000	0.4321543123353422D-13
-3	3	-0.00000	-0.5189787993293232D-13
-3	4	0.00000	0.6615667609692496D-13
-3	5	-0.00000	-0.9027122483861272D-13
-2	-5	0.00000	0.3372302437298913D-13
-2	-4	-0.00000	-0.3138903278712943D-13
-2	-3	0.00000	0.3024600771859489D-13
-2	-2	1.00000	0.10000000000000000D 01
-2	-1	0.00000	0.3024600771859489D-13
-2	0	-0.00000	-0.3138903278712943D-13
-2	1	0.00000	0.3372302437298913D-13
-2	2	-0.00000	-0.3740442299328028D-13
-2	3	0.00000	0.4321543123353422D-13
-2	4	-0.00000	-0.5189787993293232D-13
-2	5	0.00000	0.6615667609692496D-13
-1	-5	-0.00000	-0.3740442299328028D-13
-1	-4	0.00000	0.3372302437298913D-13
-1	-3	-0.00000	-0.3138903278712943D-13

-1	-2	0.00000	0.3024600771859489D-13
-1	-1	1.00000	0.1000000000000000D 01
-1	0	0.00000	0.3024600771859489D-13
-1	1	-0.00000	-0.3138903278712943D-13
-1	2	0.00000	0.3372302437298913D-13
-1	3	-0.00000	-0.3740442299328028D-13
-1	4	0.00000	0.4321543123353422D-13
-1	5	-0.00000	-0.5189787993293232D-13
0	-5	0.00000	0.4321543123353422D-13
0	-4	-0.00000	-0.3740442299328028D-13
0	-3	0.00000	0.3372302437298913D-13
0	-2	-0.00000	-0.3138903278712943D-13
0	-1	0.00000	0.3024600771859489D-13
0	0	1.00000	0.1000000000000000D 01
0	1	0.00000	0.3024600771859489D-13
0	2	-0.00000	-0.3138903278712943D-13
0	3	0.00000	0.3372302437298913D-13
0	4	-0.00000	-0.3740442299328028D-13
0	5	0.00000	0.4321543123353422D-13
1	-5	-0.00000	-0.5189787993293232D-13
1	-4	0.00000	0.4321543123353422D-13
1	-3	-0.00000	-0.3740442299328028D-13
1	-2	0.00000	0.3372302437298913D-13
1	-1	-0.00000	-0.3138903278712943D-13
1	0	0.00000	0.3024600771859489D-13
1	1	1.00000	0.1000000000000000D 01
1	2	0.00000	0.3024600771859489D-13
1	3	-0.00000	-0.3138903278712943D-13
1	4	0.00000	0.3372302437298913D-13
1	5	-0.00000	-0.3740442299328028D-13
2	-5	0.00000	0.6615667609692496D-13
2	-4	-0.00000	-0.5189787993293232D-13
2	-3	0.00000	0.4321543123353422D-13
2	-2	-0.00000	-0.3740442299328028D-13
2	-1	0.00000	0.3372302437298913D-13
2	0	-0.00000	-0.3138903278712943D-13
2	1	0.00000	0.3024600771859489D-13
2	2	1.00000	0.1000000000000000D 01
2	3	0.00000	0.3024600771859489D-13
2	4	-0.00000	-0.3138903278712943D-13
2	5	0.00000	0.3372302437298913D-13
3	-5	-0.00000	-0.9027122483861272D-13
3	-4	0.00000	0.6615667609692496D-13
3	-3	-0.00000	-0.5189787993293232D-13
3	-2	0.00000	0.4321543123353422D-13
3	-1	-0.00000	-0.3740442299328028D-13
3	0	0.00000	0.3372302437298913D-13
3	1	-0.00000	-0.3138903278712943D-13
3	2	0.00000	0.3024600771859489D-13

3	3	1.00000	0.1000000000000000D 01
3	4	0.00000	0.30246007718594899D-13
3	5	-0.00000	-0.31389032787129943D-13
4	-5	0.00000	0.14304214378636390D-12
4	-4	-0.00000	-0.90271224838612720D-13
4	-3	0.00000	0.66156676096924960D-13
4	-2	-0.00000	-0.51897879932932320D-13
4	-1	0.00000	0.43215431233534220D-13
4	0	-0.00000	-0.37404422993280280D-13
4	1	0.00000	0.33723024372989130D-13
4	2	-0.00000	-0.31389032787129430D-13
4	3	0.00000	0.30246007718594890D-13
4	4	1.00000	0.1000000000000000D 01
4	5	0.00000	0.30246007718594890D-13
5	-5	-0.00000	-0.30301014222996770D-12
5	-4	0.00000	0.14304214378636390D-12
5	-3	-0.00000	-0.90271224838612720D-13
5	-2	0.00000	0.66156676096924960D-13
5	-1	-0.00000	-0.51897879932932320D-13
5	0	0.00000	0.43215431233534220D-13
5	1	-0.00000	-0.37404422993280280D-13
5	2	0.00000	0.33723024372989130D-13
5	3	-0.00000	-0.31389032787129430D-13
5	4	0.00000	0.30246007718594890D-13
5	5	1.00000	0.1000000000000000D 01

$STOP

```
&JCB    *RUSSELL*,TIME=30,PAGES=75
C
C                   PROGRAM C3
C
C       ESTIMATED SPECTRAL AMPLITUDES USING KFONECKER DELTA
C
C       THIS ROUTINE EVALUATES THE APPROXIMATION TO THE
C       KRONECKER DELTA FUNCTION AND USES IT TO CALCULATE
C       THE ESTIMATED AMPLITUDES WHEN THE REAL AMPLITUDES
C       ARE SPECIFIED.  DOUBLE PRECISION IS USED TO RESOLVE
C       THE EXACT VALUES OF THE OFF-DIAGONAL ELEMENTS.
C
1               REAL*8 THETA,AMAT,DELTCR,DNN,DQ,DR,TF,TN,DK,PI,DCOS
2               REAL*8 CTRUE(400),CSUM,CMPLX(400)
3               INTEGER Q,R
C
4               DO 5 I=1,400
5         5     CTRUE(I)=0.0
C
C                       INPUT DATA
C
6               N=10
7               M=3
8               TN=3.1
9               TF=1.0
10              CTRUE(5)=2.00
11              CTRUE(7)=0.380
12              CTRUE(3)=CTRUE(5)
13              CTRUE(1)=CTRUE(7)
C
14              NN=2*N+1
15              DNN=NN
16              MM=2*M+1
17              PI=3.1415926535897
C
18              PRINT 65
19        65    FORMAT('1',5X,'Q',7X,'C(Q)',16X,'C(Q)',/)
20              DO 90 I=1,NN
21              Q=I-N-1
22              DQ=Q
C
23              CSUM=0.0
24              DO 80 L=1,MM
25              R=L-M-1
26              DR=R
C
27              AMAT=0.0
28              DO 50 K=1,N
29              DK=K
30              THETA=2.*PI*DK*TN*(DQ/TN-DR/TF)/DNN
31        50    AMAT=DCOS(THETA)+AMAT
```

```
32    C     DELTRG=(1.+2.*AMAT)/CNA
33    C
34    80    CSUM=CTFUE(L)*CELTFQ+CSUM
35    90    CMPLX(I)=CSUM
36    91    PRINT 91,Q,CSUM
37          FORMAT(I8,F10.3,C28.16)
38          STOP
            END
```

$SENTRY

Q	C(Q)	C(Q)
-10	0.084	0.84340736434789670-01
-9	0.396	0.35573511776523240 00
-8	0.089	-0.69165903515962340-01
-7	0.042	0.42058553044246380-01
-6	0.010	-0.104081022887404310-01
-5	0.032	-0.31735510903318160-01
-4	0.149	0.14857664057673100 00
-3	2.036	0.20378214713480040 01
-2	0.253	-0.25347770405849830 00
-1	0.176	0.17648231655208000 00
0	0.161	-0.16134397573661850 00

Q	C(Q)	C(Q)
0	0.176	0.17648231655208600 00
1	0.253	-0.25347770405849830 00
2	2.036	0.20378214713480040 01
3	0.149	0.14857664057673100 00
4	0.032	-0.31735510903318160-01
5	0.010	-0.10408102387404310-01
6	0.042	0.42058553044246380-01
7	0.089	-0.69165903515962340-01
8	0.396	0.35573511776523240 00
9	0.084	0.84340736434789670-01
10		

$STOP

```
      $JOB    'RUSSELL',TIME=30,PAGES=75
      C
      C                       PROGRAM 04
      C
      C      DISCRETE FOURIER TRANSFORM ANALYSIS
      C
      C      THIS PROGRAM CAN BE USED TO GENERATE A DIGITAL
      C      FOURIER TRANSFORM FROM TIME SERIES DATA.  IT WILL
      C      ALSO DO A FIRST-ORDER LINEAR REGRESSION ANALYSIS
      C      ON THE INPUT DATA TO REMOVE THE DC-VALUE AND ANY
      C      LINEAR TREND.  THE ESTIMATED FOURIER COEFFICIENTS
      C      ARE THEN USED TO COMPUTE AN ESTIMATED TIME SERIES.
      C
  1          DIMENSION FVALUE(201),FSAVE(201),FX(804),A(400)
  2          DIMENSION CMAGN(400),CPHASN(400),B(400),YF(201)
  3          DO 2 I=1,400
  4          A(I)=0.0
  5    2     B(I)=0.0
      C
      C      INPUT DATA VALUES
      C
  6          LINREG=1
  7          NS=41
  8          TDEL=60.
  9          TF=1.0
 10          FNS=NS
 11          TN=FNS*TDEL
 12          SCALE=52.0
      C
 13          NLS=NS
 14          NMAX=(NS-1)/2
 15          DCV=0.0
      C
      C      READ DATA CARDS AND PRINT DATA VALUES
      C
 16          READ(5,3)(FVALUE(I),I=1,NS)
 17    3     FORMAT(10X,F14.2)
 18          PRINT 6
 19    6     FORMAT('1',11X,'K',7X,'TIME',13X,'F(TIME)'/)
 20          DO 10 I=1,NS
 21          XDELTA=I*TDEL
 22   10     PRINT,I,XDELTA,FVALUE(I)
      C
      C      DO A FIRST-ORDER LINEAR REGRESSION ANALYSIS TO
      C      REMOVE THE DC-VALUE AND ANY LINEAR TREND.
      C      IF LINREG=0, THE LINEAR REGRESSION IS SKIPPED.
      C      BZERO IS THE Y-INTERCEPT, B1 IS THE SLOPE, AND YBAR
      C      IS THE AVERAGE OF THE DATA VALUES.
      C
```

```
23              IF(LINREG)28,28,17
24       17     KSUM=0
25              KSUM2=0
26              YKSUM=0.0
27              YSUM=0.0
28              DC 19 K=1,NS
29              KSUM=KSUM+K
30              KSUM2=KSUM2+(K**2)
31              YKSUM=YKSUM+K*FVALUE(K)
32       19     YSUM=YSUM+FVALUE(K)
33              XBAR=(TDEL*KSUM)/FNS
34              YBAR=YSUM/FNS
35              XSUM2=(TDEL**2)*KSUM2
36              XYSUM=TDEL*YKSUM
37              B1=(XYSUM-XBAR*YBAR*FNS)/(XSUM2-FNS*(XBAR**2))
38              BZERO=YBAR-B1*XBAR
39              PRINT 25
40       25     FORMAT('1',10X,'BZERO',10X,'B1',14X,'YBAR'/)
41              PRINT,BZERO,B1,YBAR
42              DO 27 K=1,NS
43              YF(K)=BZERO+B1*K*TDEL
44              FSAVE(K)=FVALUE(K)
45       27     FVALUE(K)=FVALUE(K)-YF(K)
         C
         C      THE TIME SERIES HAS NOW BEEN CORRECTED FOR ANY
         C      LINEAR TREND AND THE DC-VALUE HAS BEEN REMOVED.
         C      THE MODIFIED TIME SERIES IS NOW PRINTED.
         C
46       28     CONTINUE
47              PRINT 29
48       29     FORMAT('1',11X,'K',7X,'TIME',13X,'F(TIME)'/)
49              DC 30 I=1,NS
50              II=I-NMAX-1
51              XDELTA=II*TDEL
52       30     PRINT,II,XDELTA,FVALUE(I)
         C
         C      COMPUTE COMPLEX FOURIER AMPLITUDES, EQUATION(120.5)
         C
53              CALL LNSFTM(FVALUE,A,B,NLS,DCV)
54              PRINT 34
55       34     FORMAT('1',4X,'N',2X,'DC-VALUE',5X,'CMAG',10X
                1,'CPHASE',8X,'FREC-HZ',3X,'CMAG-DB'/)
56              NLMAX=(NLS-1)/2
57              DC 35 I=1,NLMAX
58              XI=I
59              CMAG=((A(I)*A(I)+B(I)*B(I))**0.5)/2.
60              CM=CMAG/SCALE
61              CMAGDB=20.*ALOG10(CM)
```

```
62            ATEST=B(I)/A(I)
63            ATEST=ATEST*ATEST
64            ATEST=ATEST**0.5
65            AT=1000.-ATEST
66            IF(AT) 20,20,21
67    20      CPHASE=.8888888
68            GO TO 22
69    21      CONTINUE
70            BA=-B(I)/A(I)
71            CPHASE=ATAN(BA)
72            CPHASE=CPHASE*57.29577
73            FNLS=NLS
74    22      FREQ=XI/(TDEL*FNLS)
75            CMAGN(I)=CMAG
76            CPHASN(I)=CPHASE
77    35      PRINT 36,I,CCV,CMAG,CPHASE,FREQ,CMAGDB
78    36      FORMAT(I6,4E12.3,F10.2)
      C
      C      THE TOTAL POWER IN THE SIGNAL IS NOW DETERMINED BY
      C      SUMMING THE SQUARES OF THE COMPLEX AMPLITUDES.  THE
      C      COMPLEX AMPLITUDES ARE SCALED BY THE SQUARE ROOT
      C      OF THIS TOTAL POWER SO THAT ALL AMPLITUDES CAN BE
      C      REFERENCED TO THE TOTAL POWER.  THIS NORMALIZATION
      C      WILL HELP IN SELECTING THE MOST STATISTICALLY
      C      SIGNIFICANT SPECTRAL COMPONENTS.
      C
79            PRINT 43
80    43      FORMAT('1',4X,'N',3X,'MAGNITUDE',5X,'PHASE',8X
      1.'FREQUENCY',4X,'DB RELATIVE TO'/
      2,48X,'UNITY TOTAL POWER'/)
81            TPWR=0.0
82            DO 40 J=1,NLMAX
83    40      TPWR=TPWR+CMAGN(J)*CMAGN(J)
84            TPWR=TPWR**0.5
85            DO 45 J=1,NLMAX
86            CMAGN(J)=CMAGN(J)/TPWR
87            XJ=J
88            FREQ=XJ/(TDEL*FNS)
89            CDB=20.*ALOG10(CMAGN(J))
90    45      PRINT 46,J,CMAGN(J),CPHASN(J),FREQ,CDB
91    46      FORMAT(I6,3E13.3,F10.2)
      C
      C      COMPUTE THE ESTIMATED TIME SERIES, EQUATION(12D.6)
      C
92            NS=4*NS-3
93            TDEL=TDEL/4
94            NMAX=(NS-1)/2
95            TF=TN
```

```
96          CALL FSRS(FX,A,E,CCV,NS,TDEL,TF)
97          PRINT 90
98    90    FORMAT('1',11X,'K',7X,'TIME',11X
      1.'ESTIMATED F(TIME)'/)              /
99          DO 100 I=1,NS
100         II=I-NMAX-1
101         XDELTA=II*TDEL
102   100   PRINT,II,XDELTA,FX(I)
103   501   STOP
104         END
      C              LINE SPECTRUM SUBROUTINE
      C
      C     THIS SUBROUTINE GENERATES THE FOURIER COEFFICIENTS
      C     A AND B FOR NLS SAMPLES OF THE FUNCTION, FVALUE.
      C

105         SUBROUTINE LNSPTM(FVALUE,A,B,NLS,CCV)
106         DIMENSION FVALUE(201),A(400),B(400)
107         NLMAX=(NLS-1)/2
108         PI=3.1415926
109         XNN=NLS
110         DCV=0.
111         DO 15 J=1,NLS
112   15    DCV=DCV+FVALUE(J)
113         DCV=DCV/XNN
114         DO 16 J=1,NLS
115   16    FVALUE(J)=FVALUE(J)-DCV
116         DO 10 N=1,NLMAX
117         ASUM=0.
118         BSUM=0.
119         XN=N
120         DO 5 J=1,NLS
121         JJ=J-NLMAX-1
122         XJJ=JJ
123         ARG=2.0*PI*XN*XJJ/XNN
124         ASUM=COS(ARG)*FVALUE(J)+ASUM
125   5     BSUM=SIN(ARG)*FVALUE(J)+BSUM
126         A(N)=2.0*ASUM/XNN
127   10    B(N)=2.0*BSUM/XNN
128         DO 17 J=1,NLS
129   17    FVALUE(J)=FVALUE(J)+DCV
130         RETURN
131         END
```

```
C                     FOURIER SERIES SUBROUTINE
C
C       THIS SUBROUTINE GENERATES SAMPLES OF THE DATA
C       FUNCTION, FX(I), USING THE FOURIER COEFFICIENTS,
C       A(I), B(I), AND DC-VALUE, DCV, AND THE NUMBER OF
C       DESIRED SAMPLES, NS.  TDEL IS THE SAMPLING PERIOD
C       AND TF IS THE FOURIER PERIOD.
C
132            SUBROUTINE FSRS(FX,A,B,DCV,NS,TDEL,TF)
133            DIMENSION FX(804),A(400),B(400)
134            NMAX=(NS-1)/2
135            PI=3.1415926
136            XNS=NS
137            DO 10 I=1,NS
138            K=I-NMAX-1
139            XK=K
140            FXK=0.
141            DO 5 N=1,NMAX
142            XN=N
143            ARG=(2.0*PI*XN*XK*TDEL)/TF
144     5      FXK=FXK+A(N)*CCS(ARG)+B(N)*SIN(ARG)
145    10      FX(I)= FXK + DCV
146            RETURN
147            END

        $ENTRY
```

K	TIME	F(TIME)
1	0.6000000E 02	−0.6392999E 02
2	0.1200000E 03	−0.1643E00E 03
3	0.1800000E 03	−C.2860801E C3
4	0.2400000E 03	−0.3361799E C3
5	0.3000000E 03	−C.2902000E 03
6	0.3600000F 03	−C.1010600E C3
7	0.4200000E 03	C.8405000E 02
8	0.4800000F 03	C.1996200E 03
9	0.5400000E 03	0.2508900E 03
10	0.6000000E 03	C.2205500E 03
11	0.6600000E 03	C.1111300CL C3
12	0.7200000E 03	−0.2083000E 02
13	0.7800000E 03	−C.6872000E 02
14	0.8400000E 03	−C.3719000E 02
15	0.9000000E 03	0.7363000E 02
16	C.9600000E 03	C.1437900E C3
17	0.1020000F 04	0.1360600E C3
18	0.1080000E 04	0.1957700E 03
19	0.1140000E 04	0.1478500E 03
20	0.1200000E 04	0.5160001E 02
21	0.1260000E 04	C.1438000E 02
22	0.1320000E 04	−C.3524001E 02
23	0.1380000E 04	0.4507001E 02
24	0.1440000E 04	C.7931000E 02
25	0.1500000E 04	0.2137900E C3
26	0.1560000E 04	0.2970300E 03
27	0.1620000E 04	0.2961999E C3
28	0.1680000E 04	0.1554100E C3
29	0.1740000E 04	C.7478000E 02
30	0.1800000E 04	C.4120000E 02
31	0.1860000E 04	0.6267000E 02
32	0.1920000E 04	0.1924000E C3
33	0.1980000E 04	0.2246000E 03
34	0.2040000E 04	0.2379900E C3
35	0.2100000E 04	C.2414100E C3
36	0.2160000E 04	C.1943700E 03
37	0.2220000E 04	0.1155000E 03
38	0.2280000E 04	0.9912000E 02
39	0.2340000E 04	0.1357500E 03
40	0.2400000E 04	0.2149100E C3
41	0.2460000E 04	0.3344900E 03

	BZERO	F1	YEAR
	-0.8834317E 02	0.1359553E 00	0.6296040E 02

K	TIME	F(TIME)
-20	-0.1200000E 04	0.1825586E 02
-19	-0.1140000E 04	-0.9235146E 02
-18	-0.1080000E 04	-0.2222088E 03
-17	-0.1020000E 04	-0.2804658E 03
-16	-0.9600000E 03	-0.2426434E 03
-15	-0.9000000E 03	-0.6166072E 02
-14	-0.8400000E 03	0.1152920E 03
-13	-0.7800000E 03	0.2187047E 03
-12	-0.7200000E 03	0.2656074E 03
-11	-0.6600000E 03	0.2273200E 03
-10	-0.6000000E 03	0.1097426E 03
-9	-0.5400000E 03	-0.3037460E 02
-8	-0.4800000E 03	-0.6642151E 02
-7	-0.4200000E 03	-0.6304926E 02
-6	-0.3600000E 03	0.4561346E 02
-5	-0.3000000E 03	0.1016161E 03
-4	-0.2400000E 03	0.6772882E 02
-3	-0.1800000E 03	0.1372815E 03
-2	-0.1200000E 03	0.8120419E 02
-1	-0.6000000E 02	-0.2320311E 02
0	0.0000000E 00	-0.6858046E 02
1	0.6000000E 02	-0.1263578E 03
2	0.1200000E 03	-0.9420509E 02
3	0.1800000E 03	-0.3212239E 02
4	0.2400000E 03	0.5816032E 02
5	0.3000000E 03	0.1732830E 03
6	0.3600000E 03	0.1242556E 03
7	0.4200000E 03	0.1534833E 02
8	0.4800000E 03	-0.7343896E 02
9	0.5400000E 03	-0.1151763E 03
10	0.6000000E 03	-0.1018636E 03
11	0.6600000E 03	-0.2029077E 02
12	0.7200000E 03	0.4375177E 02
13	0.7800000E 03	0.4654453E 02
14	0.8400000E 03	0.4424731E 02
15	0.9000000E 03	-0.1095016E 02
16	0.9600000E 03	-0.9797739E 02
17	0.1020000E 04	-0.1225140E 03
18	0.1080000E 04	-0.9404208E 02
19	0.1140000E 04	-0.2303931E 02
20	0.1200000E 04	0.8838345E 02

N	DC-VALUE	CMAG	CPHASE	FREC-HZ	CMAG-DB
1	0.662E-04	0.269E 02	0.344E 02	0.407E-03	-5.83
2	0.662E-04	0.249E 02	-0.905E 01	0.813E-03	-6.49
3	0.662E-04	0.245E 02	-0.731E 02	0.122E-02	-6.64
4	0.662E-04	0.312E 02	-0.873E 02	0.163E-02	-4.53
5	0.662E-04	0.640E 02	-0.152E 02	0.203E-02	1.70
6	0.662E-04	0.163E 02	0.586E 01	0.244E-02	-10.20
7	0.662E-04	0.333E 01	0.889E 00	0.285E-02	-23.96
8	0.662E-04	0.743E 01	0.315E 01	0.325E-02	-17.01
9	0.662E-04	0.258E 01	-0.160E 02	0.366E-02	-26.18
10	0.662E-04	0.352E 01	0.866E 01	0.407E-02	-23.48
11	0.662E-04	0.521E 01	0.643E 02	0.447E-02	-20.09
12	0.662E-04	0.150E 01	0.391E 02	0.488E-02	-30.87
13	0.662E-04	0.373E 01	0.219E 02	0.526E-02	-24.24
14	0.662E-04	0.380E 01	0.172E 02	0.569E-02	-22.84
15	0.662E-04	0.137E 01	0.118E 01	0.610E-02	-31.70
16	0.662E-04	0.382E 01	0.603E 02	0.650E-02	-22.79
17	0.662E-04	0.267E 01	0.369E 02	0.691E-02	-25.87
18	0.662E-04	0.321E 01	0.738E 02	0.732E-02	-24.30
19	0.662E-04	0.164E 01	-0.267E 02	0.772E-02	-30.10
20	0.662E-04	0.230E 01	0.450E 02	0.813E-02	-27.19

N	MAGNITUDE	PHASE	FREQUENCY	DB RELATIVE TO UNITY TOTAL POWER
1	0.311E 00	0.344E 02	0.407E-03	-10.14
2	0.289E 00	-0.905E 01	0.813E-03	-10.80
3	0.284E 00	-0.731E 02	0.122E-02	-10.94
4	0.362E 00	-0.873E 02	0.163E-02	-8.84
5	0.741E 00	-0.152E 02	0.203E-02	-2.61
6	0.188E 00	0.586E 01	0.244E-02	-14.50
7	0.386E-01	0.889E 00	0.285E-02	-28.26
8	0.860E-01	0.315E 01	0.325E-02	-21.31
9	0.299E-01	-0.160E 02	0.366E-02	-30.48
10	0.408E-01	0.866E 01	0.407E-02	-27.79
11	0.603E-01	0.643E 02	0.447E-02	-24.39
12	0.174E-01	0.391E 02	0.488E-02	-35.18
13	0.374E-01	0.219E 02	0.528E-02	-28.54
14	0.440E-01	0.172E 02	0.569E-02	-27.14
15	0.158E-01	0.118E 01	0.610E-02	-36.01
16	0.442E-01	0.603E 02	0.650E-02	-27.06
17	0.310E-01	0.369E 02	0.691E-02	-30.18
18	0.372E-01	0.738E 02	0.732E-02	-28.60
19	0.190E-01	-0.267E 02	0.772E-02	-34.40
20	0.266E-01	0.450E 02	0.813E-02	-31.50

K	TIME	ESTIMATED F(TIME)
-80	-0.1200000E 04	0.1625310E 02
-79	-0.1185000E 04	-0.1350116E 02
-78	-0.1170000E 04	-0.4065467E 02
-77	-0.1155000E 04	-0.6612059E 02
-76	-0.1140000E 04	-0.5234979E 02
-75	-0.1125000E 04	-0.1217645E 03
-74	-0.1110000E 04	-0.1548497E 03
-73	-0.1095000E 04	-0.1655864E 03
-72	-0.1080000E 04	-0.2222081E 03
-71	-0.1065000E 04	-0.2488539E 03
-70	-0.1050000E 04	-0.2671575E 03
-69	-0.1035000E 04	-0.2771402E 03
-68	-0.1020000E 04	-0.2704617E 03
-67	-0.1005000E 04	-0.2785950E 03
-66	-0.9900000E 03	-0.2733059E 03
-65	-0.9750000E 03	-0.2621352E 03
-64	-0.9600000E 03	-0.2426437E 03
-63	-0.9450000E 03	-0.2121370E 03
-62	-0.9300000E 03	-0.1656788E 03
-61	-0.9150000E 03	-0.1180927E 03
-60	-0.9000000E 03	-0.6165892E 02
-59	-0.8850000E 03	-0.6536420E 01
-58	-0.8700000E 03	0.4234529E 02
-57	-0.8550000E 03	0.8270328E 02
-56	-0.8400000E 03	0.1152906E 03
-55	-0.8250000E 03	0.1429113E 03
-54	-0.8100000E 03	0.1666262E 03
-53	-0.7950000E 03	0.1940724E 03
-52	-0.7800000E 03	0.2187049E 03
-51	-0.7650000E 03	0.2402622E 03
-50	-0.7500000E 03	0.2560557E 03
-49	-0.7350000E 03	0.2645730E 03
-48	-0.7200000E 03	0.2658035E 03
-47	-0.7050000E 03	0.2613250E 03
-46	-0.6900000E 03	0.2530081E 03
-45	-0.6750000E 03	0.2418421E 03
-44	-0.6600000E 03	0.2273185E 03
-43	-0.6450000E 03	0.2077964E 03
-42	-0.6300000E 03	0.1810204E 03
-41	-0.6150000E 03	0.1484016E 03
-40	-0.6000000E 03	0.1097420E 03
-39	-0.5850000E 03	0.6869198E 02
-38	-0.5700000E 03	0.3016054E 02
-37	-0.5550000E 03	-0.3476593E 01
-36	-0.5400000E 03	-0.7037477E 02
-35	-0.5250000E 03	-0.5082777E 02

-34	-0.5100000E 03	-0.6624619E 02
-33	-0.4950000E 03	-0.7799013E 02
-32	-0.4800000E 03	-0.8642059E 02
-31	-0.4650000E 03	-0.9063297E 02
-30	-0.4500000E 03	-0.8859418E 02
-29	-0.4350000E 03	-0.7989761E 02
-28	-0.4200000E 03	-0.6304919E 02
-27	-0.4050000E 03	-0.3947273E 02
-26	-0.3900000E 03	-0.1150681E 02
-25	-0.3750000E 03	0.1784879E 02
-24	-0.3600000E 03	0.4561244E 02
-23	-0.3450000E 03	0.6928053E 02
-22	-0.3300000E 03	0.8703726E 02
-21	-0.3150000E 03	0.9784479E 02
-20	-0.3000000E 03	0.1016160E 03
-19	-0.2850000E 03	0.9948602E 02
-18	-0.2700000E 03	0.9398491E 02
-17	-0.2550000E 03	0.8877206E 02
-16	-0.2400000E 03	0.8772876E 02
-15	-0.2250000E 03	0.9354007E 02
-14	-0.2100000E 03	0.1062932E 03
-13	-0.1950000E 03	0.1226140E 03
-12	-0.1800000E 03	0.1372807E 03
-11	-0.1650000E 03	0.1431210E 03
-10	-0.1500000E 03	0.1355520E 03
-9	-0.1350000E 03	0.1136869E 03
-8	-0.1200000E 03	0.8120360E 02
-7	-0.1050000E 03	0.4508919E 02
-6	-0.9000000E 02	0.1294637E 02
-5	-0.7500000E 02	-0.1006115E 02
-4	-0.6000000E 02	-0.2320346E 02
-3	-0.4500000E 02	-0.3018306E 02
-2	-0.3000000E 02	-0.3709712E 02
-1	-0.1500000E 02	-0.4929091E 02
0	0.0000000E 00	-0.6858044E 02
1	0.1500000E 02	-0.9217192E 02
2	0.3000000E 02	-0.1138118E 03
3	0.4500000E 02	-0.1266343E 03
4	0.6000000E 02	-0.1263581E 03
5	0.7500000E 02	-0.1133115E 03
6	0.9000000E 02	-0.9232533E 02
7	0.1050000E 03	-0.7054535E 02
8	0.1200000E 03	-0.5420451E 02
9	0.1350000E 03	-0.4586327E 02
10	0.1500000E 03	-0.4337198E 02
11	0.1650000E 03	-0.4059869E 02
12	0.1800000E 03	-0.3212219E 02
13	0.1950000E 03	-0.1223556E 02

14	0.21000000E 03	0.19084424E 02
15	0.22500000E 03	0.58032275E 02
16	0.24000000E 03	0.95160013E 02
17	0.25500000F 03	0.13284431E 02
18	0.27000000E 02	0.15744744E 03
19	0.28500000E 03	0.17057220E 03
20	0.30000000E 03	0.17328288E 03
21	0.31500000E 03	0.16816662E 03
22	0.33000000E 03	0.15746110E 03
23	0.34500000E 02	0.14291294E 03
24	0.36000000E 03	0.12425544E C2
25	0.37500000E 03	0.10141147E 03
26	0.39000000E 03	0.74654846E 02
27	0.40500000E 03	0.45242254E C2
28	0.42000000F 03	0.15349068E 02
29	0.43500000E 03	-0.12661058E C2
30	0.45000000E 03	-0.37077982F 02
31	0.46500000E 03	-0.57188358E 02
32	0.48000000F 03	-0.73437628E 02
33	0.49500000E 03	-0.86820018E 02
34	0.51000000F 03	-0.92205798E C2
35	0.52500000E 03	-0.10726407E 02
36	0.54000000E 03	-0.11517761E 03
37	0.55500000E 03	-0.11561625E 03
38	0.57000000E 03	-0.11866813E 03
39	0.58500000E 03	-0.11297148E 03
40	0.60000000E 02	-0.10166388E C3
41	0.61500000E 03	-0.85820698E 02
42	0.63000000F 03	-0.65854038E 02
43	0.64500000E 03	-0.43416328E C2
44	0.66000000E 03	-0.20291411E 02
45	0.67500000E 03	0.15676558E C1
46	0.69000000E 03	0.20309348E 02
47	0.70500000E 03	0.34553638E 02
48	0.72000000F 02	0.43751978E C2
49	0.73500000E 03	0.48358228E 02
50	0.75000000E 03	0.49560508E 02
51	0.76500000E 03	0.45401608E 02
52	0.78000000E 03	0.48944858E 02
53	0.79500000E 03	0.48933278E C2
54	0.81000000E 03	0.48985208E 02
55	0.82500000E 03	0.47916938E 02
56	0.84000000E 03	0.44244658E C2
57	0.85500000E 03	0.36753408E 02
58	0.87000000E 03	0.24856528E 02
59	0.88500000E 03	0.67078548E C1
60	0.90000000E 03	-0.10949953E 02
61	0.91500000E 03	-0.32580518E 02

62	0.9300000E	03	-0.5597472E	02
63	0.9450000E	03	-0.7826826E	02
64	0.9600000E	03	-0.9797656E	02
65	0.9750000E	03	-0.1132027E	03
66	0.9900000E	03	-0.1224752E	03
67	0.1005000E	04	-0.1263107E	03
68	0.1020000E	04	-0.1225146E	03
69	0.1035000E	04	-0.1160630E	03
70	0.1050000E	04	-0.1083329E	03
71	0.1065000E	04	-0.1009923E	03
72	0.1080000E	04	-0.9404175E	02
73	0.1095000E	04	-0.8554649E	02
74	0.1110000E	04	-0.7237814E	02
75	0.1125000E	04	-0.5176640E	02
76	0.1140000E	04	-0.2304001E	02
77	0.1155000E	04	0.1129809E	02
78	0.1170000E	04	0.4576476E	02
79	0.1185000E	04	0.7345763E	02
80	0.1200000E	04	0.8238284E	02

$STOP

```
$JOB   'RUSSELL',TIME=30,PAGES=75
C                       PROGRAM 05
C
C      FAST FOURIER TRANSFORM SPECTRAL DENSITY
C
C      THIS PROGRAM ILLUSTRATES A SIMPLE EXAMPLE FOR THE
C      USE OF THE FAST FOURIER TRANSFORM.  SUBROUTINE FFAST
C      CAN BE USED IN OTHER PROGRAMS WHERE HIGH SPEED
C      PROCESSING IS NEEDED.  THE SUBROUTINE CONTAINS A
C      ZERO FILLING ROUTINE TO ACCOMODATE ANY LENGTH DATA
C      AND ANY DESIRED DISPLAY RESOLUTION.
C
1          DIMENSION A(1024),B(1024),CMAG(1024)
2          DIMENSION FMAG(1024),FPHASE(1024),FR(1024)
3          DIMENSION S(1024),SNAME(5),XX(1024)
4          DIMENSION X(1024),XMDC(1024),XSV(1024),XTIME(1024)
C
C      READ INPUT DATA -- THE TIME SERIES, X(I), THE
C      NUMBER OF DATA SAMPLES, NS, THE SAMPLING INTERVAL,
C      DELTA-T, THE DESIRED FFT RESOLUTION OPTION, NRESL,
C      THE DC-REMOVAL OPTION, NDC, AND THE PRINT OPTIONS,
C      NPT1, NPT2, NPT3, NPT4.
C
5    4     READ(5,5,END=501) NPT1,NPT2,NPT3,NPT4,NDC
          +,NRESL,NS,XTDELT,SNAME
6    5     FORMAT(4I1,I6,2I5,E18.7,11X,5A4)
C
C          **** USER SPECIFIED READ FORMAT ****
C
7          READ(5,10)(X(I),I=1,NS)
8    10    FORMAT(E14.7)
C
C          *************************************************
C
C       PRINT INPUT DATA
C
9          PRINT 15,NPT1,NPT2,NPT3,NPT4,NDC,
          + NRESL,NS,XTDELT
10   15    FORMAT('1',17X,'FAST FOURIER TRANSFORM',
          +1X,'SPECTRAL ANALYSIS'///,10X,'PTOPT',3X,
          +'NDC',3X,'NRESL',3X,'NS',6X,'TDELT-SEC.'//,10X,
          +4I1,5X,I1,2I7,E18.7///)
C
C       COMPUTE THE AVERAGE (OR DC-VALUE), THE MEAN-SQUARE,
C       THE VARIANCE, AND THE STANDARD DEVIATION.
C
11         XNS=FLOAT(NS)
12         DCV=0.0
13         XBAR2=0.0
```

```
14              DO 20 I=1,NS
15              DCV=DCV+X(I)
16      20      XBAR2=XBAR2+X(I)*X(I)
17              DCV=DCV/XNS
18              XBAR2=XBAR2/XNS
19              XVAR=(XBAR2-DCV*DCV)*XNS/(XNS-1.)
20              STDEV=XVAR**0.5
        C
        C       COMPUTE THE ZERO-MEAN DATA FUNCTION AND TRANSFORM
        C       THE DATA TO STANDARD VARIABLES BY DIVIDING EACH
        C       ZERO-MEAN DATA VALUE BY THE STANDARD DEVIATION.
        C
21              DO 25 I=1,NS
22              XTIME(I)=FLOAT(I-1)*XTDELT
23              XMDC(I)=X(I)-DCV
24      25      XSV(I)=XMDC(I)/STDEV
        C
25              PRINT 30,SNAME,DCV,XBAR2,XVAR,STDEV
26      30      FORMAT(' ',///,10X,'INPUT DATA FUNCTION STATISTICS:'
        +,2X,5A4,//,8X,'AVERAGE',5X,'MEAN-SQUARE',5X,
        +'VARIANCE',5X,'STANDARD DEVIATION',//,5X,E12.5
        +,3X,E12.5,3X,E12.5,3X,E12.5,///)
        C
27              IF(NPT1 .EQ. 0) GO TO 50
28              PRINT 35
29      35      FORMAT(' ',7X,'T',3X,'INPUT DATA FUNCTION',3X
        +,'ZERO MEAN',5X,'STANDARD VARIABLES',/)
30              DO 40 I=1,NS
31      40      PRINT 45,I,X(I),XMDC(I),XSV(I)
32      45      FORMAT(' ',I8,3E18.7)
        C
        C       SELECT THE DESIRED FORM OF THE DATA FUNCTION
        C       FOR FFT PROCESSING.
        C
33      50      NDC=NDC-1
34       .      IF(NDC) 75,55,65
35      55      DO 60 I=1,NS
36      60      X(I)=XMDC(I)
37              GO TO 75
38      65      DO 70 I=1,NS
39      70      X(I)=XSV(I)
        C
        C       THE INPUT TIME SERIES HAS BEEN PREPROCESSED INTO
        C       A CONVIENENT FORM.  THE FFT COEFFICIENTS ARE NOW
        C       COMPUTED.
        C
        C       FILL THE FFT ARRAY WITH TIME SERIES DATA AND
        C       COMPUTE THE REAL AND IMAGINARY COMPONENTS OF THE
        C       COMPLEX FOURIER AMPLITUDE COEFFICIENTS.
        C
```

```
40    75        CONTINUE
41              DO 80 I=1,NS
42              A(I)=X(I)
43    80        B(I)=0.0
44              K=0
45              CALL FFAST(A,B,NS,NRESL,K)
46              N=2**(K+NRESL)
47              KMAX=2**(K+NRESL-1)
      C
      C         CONVERT THE REAL AND IMAGINARY COMPONENTS INTO
      C         MAGNITUDE AND PHASE COMPONENTS.
      C
48              DO 85 I=1,N
49              FMAG(I)=(A(I)*A(I)+B(I)*B(I))**0.5
50    85        FPHASE(I)=57.29577*ATAN2(B(I),A(I))
      C
      C         COMPUTE THE ESTIMATED DISCRETE FOURIER AMPLITUDE
      C         SPECTRUM BY SCALING.
      C
51              XN=FLOAT(N)
52              DO 90 I=1,KMAX
53              L=I-1
54              XL=FLOAT(L)
55              XX(I)=FMAG(I)*XTDELT
56              CMAG(I)=FMAG(I)/XN
57    90        FR(I)=XL/(XN*XTDELT)
      C
      C         COMPUTE THE ESTIMATED POWER SPECTRAL DENSITY
      C         FUNCTION.
      C
58              DO 95 I=1,KMAX
59              L=I-1
60    95        S(I)=CMAG(I)*CMAG(I)*XTDELT*XN
      C
      C         PRINT RESULTS
      C
61              IF(NPT2 .EQ. 0 ) GO TO 115
62              PRINT 100
63    100       FORMAT('1',10X,'FFT COMPLEX OUTPUT',//,9X,'N',6X,
              +'FMAG',7X,'FPHASE',6X,'A(N)',8X,'B(N)',/)
64              DO 105 I=1,N
65    105       PRINT 110,I,FMAG(I),FPHASE(I),A(I),B(I)
66    110       FORMAT(' ',I9,4E12.3)
      C
67    115       IF(NPT3 .EQ. 0) GO TO 135
68              PRINT 120
69    120       FORMAT('1',10X,'AMPLITUDE SPECTRAL DENSITY',//,
              +9X,'L',6X,'FREQUENCY-HZ',5X
              +,'MAG XX(W)-V/HZ',7X,'CMAG-DFT',/)
```

```
70           DO 125 I=1,KMAX
71           L=I-1
72    125    PRINT 130,L,FR(I),XX(I),CMAG(I)
73    130    FORMAT(' ',I9,3E18.7)
      C
74    135    IF(NPT4 .EQ. 0) GO TO 499
75           PRINT 140
76    140    FORMAT('1',10X,'POWER SPECTRAL DENSITY',//,9X,'L',
      +7X,'FREQUENCY-HZ',6X,'MAG S(I)-W/HZ',//)
77           DO 145 I=1,KMAX
78           L=I-1
79    145    PRINT 150,L,FR(I),S(I)
80    150    FORMAT(' ',I9,2E19.7)
81    499    CONTINUE
      C
      C        **** USER SUPPLIED PLOT ROUTINES ****
      C
      C        @@ INPUTS @@
      C
      C     TIME VARIABLE, XTIME(I).
      C     INPUT DATA FUNCTION, X(I).
      C     DATA FUNCTION WITH DC-VALUE REMOVED, XMDC(I).
      C     STANDARD VARIABLES, XSV(I).
      C
      C        @@ OUTPUTS @@
      C
      C     FREQUENCY VARIABLE IN HERTZ, FR(I).
      C     AMPLITUDE SPECTRAL DENSITY, XX(I).
      C     POWER SPECTRAL DENSITY, S(I).
      C
82           GO TO 4
83    501    STOP
84           END
      C
      C     FAST FOURIER TRANSFORM SUBROUTINE
      C
85           SUBROUTINE FFAST(A,B,NS,NRESL,K)
      C
86           DIMENSION A(1024),B(1024)
      C
      C     TEST THE TOTAL NUMBER OF POINTS AND IF NS IS N.E.
      C     TO 2**K, FILL THE REMAINING TIME SERIES ARRAY, A(I)
      C     WITH ZEROS.  IF ADDITIONAL DISPLAY RESOLUTION IS
      C     DESIRED, ZERO-FILLING CAN BE IMPLEMENTED BY
      C     SELECTING THE RESOLUTION CONSTANT, NRESL.
      C
      C
      C     DETERMINE THE POWER-OF-TWO ORDER, K.
      C
```

```
87              ZNS=FLOAT(NS)
88               XK=ALOG(ZNS)/ALOG(2.0)
89               K=INT(XK)
90               N=2**K
91               IF(NS.GT.N) K=K+1
92               N=2**(K+NRESL)
    C
    C           ZERO-FILL.
    C
93               NSP1=NS+1
94               DO 5 I=NSP1,N
95               A(I)=0.0
96      5        B(I)=0.0
    C
    C           COMPUTE THE FFT ON N DATA POINTS USING TIME
    C           DECOMPOSITION WITH INPUT BIT REVERSAL.
    C
97               MR=0
98               NN=N-1
99               DO 20 M=1,NN
100              L=N
101     10       L=L/2
102              IF(MR+L.GT.NN) GO TO 10
103              MR=MOD(MR,L)+L
104              IF(MR.LE.M) GO TO 20
105              TR=A(M+1)
106              A(M+1)=A(MR+1)
107              A(MR+1)=TR
108              TI=B(M+1)
109              B(MR+1)=TI
110     20       CONTINUE
111              L=1
112     30       IF(L.GE.N) RETURN
113              ISTEP=2*L
114             EL=FLOAT(L)
115              DO 4 M=1,L
116              Z=3.1415926*FLOAT(1-M)/EL
117              WR=COS(Z)
118              WI=SIN(Z)
119              DO 4 I=M,N,ISTEP
120              J=I+L
121              TR=WR*A(J)-WI*B(J)
122              TI=WR*B(J)+WI*A(J)
123              A(J)=A(I)-TR
124              B(J)=B(I)-TI
125              A(I)=A(I)+TR
126     4        B(I)=B(I)+TI
127              L=ISTEP
128              GO TO 30
129              END
```

FAST FOURIER TRANSFORM SPECTRAL ANALYSIS

PTOPT	NDC	NRESL	NS	TDELT-SEC.
1111	0	0	15	0.3000000E 00

INPUT DATA FUNCTION STATISTICS: EXP(-T)SIN(T)

AVERAGE	MEAN-SQUARE	VARIANCE	STANDARD DEVIATION
0.11129E 00	0.27733E-01	0.16443E-01	0.12823E 00

T	INPUT DATA FUNCTION	ZERO MEAN	STANDARD VARIABLES
1	0.0000000E 00	-0.1112922E 00	-0.8679157E 00
2	0.2189268E 00	0.1076345E 00	0.8393911E 00
3	0.3098824E 00	0.1985902E 00	0.1548711E 01
4	0.3184770E 00	0.2071847E 00	0.1615736E 01
5	0.2807248E 00	0.1694326E 00	0.1321324E 01
6	0.2225712E 00	0.1112790E 00	0.8678120E 00
7	0.1609759E 00	0.4968363E-01	0.3874592E 00
8	0.1057055E 00	-0.5586743E-02	-0.4356838E-01
9	0.6127660E-01	-0.5001564E-01	-0.3900484E 00
10	0.2872230E-01	-0.8256990E-01	-0.6439236E 00
11	0.7026002E-02	-0.1042662E 00	-0.8131231E 00
12	-0.5818199E-02	-0.1171104E 00	-0.9132890E 00
13	-0.1209130E-01	-0.1233835E 00	-0.9622099E 00
14	-0.1392170E-01	-0.1252139E 00	-0.9764843E 00
15	-0.1306980E-01	-0.1243620E 00	-0.9698405E 00

FFT COMPLEX OUTPUT

N	FMAG	FPHASE	A(N)	B(N)
1	0.167E 01	0.000E 00	0.167E 01	0.000E 00
2	0.127E 01	-0.836E 02	0.141E 00	-0.126E 01
3	0.473E 00	-0.134E 03	-0.326E 00	-0.343E 00
4	0.226E 00	-0.153E 03	-0.201E 00	-0.103E 00
5	0.140E 00	-0.164E 03	-0.135E 00	-0.379E-01
6	0.105E 00	-0.172E 03	-0.104E 00	-0.144E-01
7	0.887E-01	-0.177E 03	-0.886E-01	-0.491E-02

8	0.819E-01	-0.179E 03	-0.819E-01	-0.130E-02
9	0.799E-01	0.180E 03	-0.799E-01	0.000E 00
10	0.819E-01	0.179E 03	-0.819E-01	0.130E-02
11	0.887E-01	0.177E 03	-0.886E-01	0.491E-02
12	0.105E 00	0.172E 03	-0.104E 00	0.144E-01
13	0.140E 00	0.164E 03	-0.135E 00	0.379E-01
14	0.226E 00	0.153E 03	-0.201E 00	0.103E 00
15	0.473E 00	0.134E 03	-0.326E 00	0.343E 00
16	0.127E 01	0.836E 02	0.141E 00	0.126E 01

AMPLITUDE SPECTRAL DENSITY

L	FREQUENCY-HZ	MAG XX(W)-V/HZ	CMAG-DFT
0	0.0000000E 00	0.5008157E 00	0.1043366E 00
1	0.2083333E 00	0.3807855E 00	0.7933033E-01
2	0.4166666E 00	0.1419684E 00	0.2957676E-01
3	0.6249999E 00	0.6781936E-01	0.1412904E-01
4	0.8333333E 00	0.4204089E-01	0.8758519E-02
5	0.1041666E 01	0.3137103E-01	0.6535631E-02
6	0.1249999E 01	0.2661949E-01	0.5545728E-02
7	0.1458333E 01	0.2456124E-01	0.5116925E-02

POWER SPECTRAL DENSITY

L	FREQUENCY-HZ	MAG S(I)-W/HZ
0	0.0000000E 00	0.5225342E-01
1	0.2083333E 00	0.3020782E-01
2	0.4166666E 00	0.4198965E-02
3	0.6249999E 00	0.9582227E-03
4	0.8333333E 00	0.3682158E-03
5	0.1041666E 01	0.2050294E-03
6	0.1249999E 01	0.1476245E-03
7	0.1458333E 01	0.1256780E-03

```
      $JOB   'RUSSELL',TIME=30,PAGES=75
      C
      C                PROGRAM 06
      C
      C     ESTIMATION OF SINGLE-SINEWAVE PARAMETERS
      C
      C     THIS PROGRAM COMPUTES THE BEST FIT OF A SINGLE-
      C     FREQUENCY SINEWAVE TO AN INPUT TIME SERIES WHEN
      C     THE SINEWAVE PERIOD IS KNOWN OR ESTIMATED.
      C
  1         DIMENSION X(1000),FS(1000),XR(1000),XMDC(1000)
  2         DIMENSION SNAME(5),XTIME(1000)
      C
      C     READ INPUT PARAMETERS
      C
  3   4     READ(5,5,END=501) NS,TZERO,TDELT,SNAME
  4   5     FORMAT(I5,5X,2E16.6,7X,5A4)
      C
      C     **** USER SPECIFIED READ FORMAT ****
      C
  5         READ(5,10)(X(I),I=1,NS)
  6   10    FORMAT(E14.7)
      C
      C     ********************************************
      C
      C     PRINT INPUT PARAMETERS
      C
  7         PRINT 15,NS,TZERO,TDELT
  8   15    FORMAT('1',9X,'ESTIMATION OF SINGLE-SINEWAVE ',
           +'PARAMETERS'///,11X,'INPUT PARAMETERS:'//,11X
           +,'NS',5X,'TZERO-SEC.',7X,'TDELT-SEC.'//
           +,I14,2E17.7)
      C
      C     COMPUTE THE AVERAGE, MEAN-SQUARE, VARIANCE, AND
      C     STANDARD DEVIATION OF THE INPUT TIME SERIES.
      C
  9         XNS=NS
 10         DCV=0.0
 11         XBAR2=0.0
 12         DO 20 I=1,NS
 13         DCV=DCV+X(I)
 14   20    XBAR2=XBAR2+X(I)*X(I)
 15         DCV=DCV/XNS
 16         XBAR2=XBAR2/XNS
 17         XVAR=(XBAR2-DCV*DCV)*XNS/(XNS-1.)
 18         STDEV=XVAR**0.5
      C
      C     COMPUTE THE ZERO-MEAN DATA FUNCTION
      C
```

```
19            DO 25 I=1,NS
20       25   XMDC(I)=X(I)-DCV
         C
         C    PRINT THE INPUT TIME SERIES STATISTICS, INPUT
         C    TIME SERIES, AND ZERO-MEAN DATA FUNCTION.
         C
21            PRINT 30,SNAME,DCV,XBAR2,XVAR,STDEV
22       30   FORMAT(' '///,10X,'INPUT DATA FUNCTION STATISTICS:'
         +,2X,5A4//,8X,'AVERAGE',4X,'MEAN-SQUARE',4X
         +,'VARIANCE',3X,'STANDARD DEVIATION'//3X,4E14.5///)
23            PRINT 31
24       31   FORMAT(' ',5X,'T',4X,'INPUT TIME SERIES'
         +,4X,'ZERO-MEAN TIME SERIES'/)
25            DO 35 I=1,NS
26       35   PRINT 36,I,X(I),XMDC(I)
27       36   FORMAT(I7,E18.4,E21.4)
         C
         C    COMPUTE EQUATIONS (13.15) AND (13.16) USING THE
         C    ZERO MEAN DATA FUNCTION.
         C
28            N=(NS-1)/2
29            PI=3.1415926
30            ZED=(2.*PI*TDELT)/TZERO
31            ALPHA=0.0
32            BETA=0.0
33            DO 40 I=1,NS
34            L=I-N-1
35            XL=L
36            ALPHA=ALPHA+XMDC(I)*COS(XL*ZED)
37       40   BETA=BETA+XMDC(I)*SIN(XL*ZED)
         C
38            ALPHA=ALPHA/XNS
39            BETA=-BETA/XNS
         C
         C    COMPUTE THE MAGITUDE AND PHASE OF THE COMPLEX
         C    AMPLITUDE COEFFICIENT GIVEN BY EQUATIONS
         C    (13.17) AND (13.18).
         C
40            CMAG=(ALPHA*ALPHA+BETA*BETA)**0.5
41            CPHASE=57.29577*ATAN2(BETA,ALPHA)
         C
         C    COMPUTE THE MAGNITUDE AND PHASE OF A SINGLE-
         C    FREQUENCY SINEWAVE WHICH IS A BEST FIT.
         C
42            DMAG=2.*CMAG
43            DPHASE=CPHASE-270.
         C
         C    PRINT THE FREQUENCY, MAGNITUDE, AND PHASE OF THE
         C    SINEWAVE.
         C
```

```
44            FREQ=1./TZERO
45            PRINT 45,FREQ,DMAG,DPHASE
46       45   FORMAT('1',7X,'BEST-FIT SINEWAVE:'//,7X
             +,'FREQUENCY',7X,'DMAG',8X,'DPHASE-DEG'//,4X,
             +3E14.4///)
     C
     C        COMPUTE THE "RESIDUE" TIME SERIES AND
     C        ITS STATISTICS.
     C
47            DPHASE=2.*PI*DPHASE/360.
48            DO 50 I=1,NS
49            L=I-N-1
50            XL=L
51       50   XR(I)=XMDC(I)-DMAG*SIN(XL*ZED+DPHASE)
52            DCV=0.0
53            XBAR2=0.0
54            DO 60 I=1,NS
55            DCV=DCV+XR(I)
56       60   XBAR2=XBAR2+XR(I)*XR(I)
57            DCV=DCV/XNS
58            XBAR2=XBAR2/XNS
59            XVAR=(XBAR2-DCV*DCV)*XNS/(XNS-1.)
60            STDEV=XVAR**0.5
     C
     C        PRINT THE "RESIDUE" TIME SERIES STATISTICS.
     C
61            PRINT 70,DCV,XBAR2,XVAR,STDEV
62       70   FORMAT(' ',10X,'RESIDUE TIME SERIES STATISTICS:'//
             +,8X,'AVERAGE',4X,'MEAN-SQUARE',4X,'VARIANCE'
             +,3X,'STANDARD DEVIATION'//3X,4E14.5///)
     C
     C        PRINT THE ZERO-MEAN DATA FUNCTION, BEST FIT
     C        SINEWAVE, AND RESIDUE TIME SERIES.
     C
63            PRINT 75
64       75   FORMAT(' '///,14X,'REFERENCE',26X,'RESIDUE'/,
             +6X,'T',6X,'TIME SERIES',7X,'SINEWAVE'
             +,8X,'TIME SERIES'//)
65            DO 80 I=1,NS
66            L=I-N-1
67            XL=L
68            XTIME(I)=FLOAT(I-1)*TDELT
69            FS(I)=DMAG*SIN(XL*ZED+DPHASE)
70       80   PRINT 90,L,XMDC(I),FS(I),XR(I)
71       90   FORMAT(I7,3E17.4)
     C
     C        **** USER SUPPLIED PLOT ROUTINES ****
     C
     C                    @@ INPUTS @@
     C
```

```
C      TIME VARIABLE, XTIME(I).
C      INPUT DATA FUNCTION, X(I).
C      ZERO-MEAN DATA FUNCTION, XMDC(I).
C
C                aa OUTPUTS aa
C
C      SINEWAVE FUNCTION, FS(I).
C      "RESIDUE" TIME SERIES, XR(I).
C
C      ***************************************
C
72         GO TO 4
73    501  STOP
74         END
```

ESTIMATION OF SINGLE-SINEWAVE PARAMETERS

INPUT PARAMETERS:

NS	TZERO-SEC.	TDELT-SEC.
41	0.4926101E 03	0.6000000E 02

INPUT DATA FUNCTION STATISTICS: HER A 7/29/75 LINREG

AVERAGE	MEAN-SQUARE	VARIANCE	STANDARD DEVIATION
0.72944E-04	0.14904E 05	0.15276E 05	0.12360E 03

T	INPUT TIME SERIES	ZERO-MEAN TIME SERIES
1	0.1626E 02	0.1626E 02
2	-0.9235E 02	-0.9235E 02
3	-0.2222E 03	-0.2222E 03
4	-0.2805E 03	-0.2805E 03
5	-0.2426E 03	-0.2426E 03
6	-0.6166E 02	-0.6166E 02
7	0.1153E 03	0.1153E 03
8	0.2187E 03	0.2187E 03
9	0.2553E 03	0.2658E 03

10	0.2273E 03	0.2273E 03
11	0.1097E 03	0.1097E 03
12	-0.3037E 02	-0.3037E 02
13	-0.8642E 02	-0.8642E 02
14	-0.6305E 02	-0.6305E 02
15	0.4561E 02	0.4561E 02
16	0.1016E 03	0.1016E 03
17	0.8773E 02	0.8773E 02
18	0.1373E 03	0.1373E 03
19	0.8120E 02	0.8120E 02
20	-0.2320E 02	-0.2320E 02
21	-0.6858E 02	-0.6858E 02
22	-0.1264E 03	-0.1264E 03
23	-0.5421E 02	-0.5421E 02
24	-0.3212E 02	-0.3212E 02
25	0.9816E 02	0.9816E 02
26	0.1733E 03	0.1733E 03
27	0.1243E 03	0.1243E 03
28	0.1535E 02	0.1535E 02
29	-0.7344E 02	-0.7344E 02
30	-0.1152E 03	-0.1152E 03
31	-0.1019E 03	-0.1019E 03
32	-0.2029E 02	-0.2029E 02
33	0.4375E 02	0.4375E 02
34	0.4894E 02	0.4894E 02
35	0.4425E 02	0.4425E 02
36	-0.1095E 02	-0.1095E 02
37	-0.9798E 02	-0.9798E 02
38	-0.1225E 03	-0.1225E 03
39	-0.9404E 02	-0.9404E 02
40	-0.2304E 02	-0.2304E 02
41	0.8838E 02	0.8838E 02

BEST-FIT SINEWAVE:

FREQUENCY	DMAG	DPHASE-DEG
0.2030E-02	0.1285E 03	-0.1053E 03

RESIDUE TIME SERIES STATISTICS:

AVERAGE	MEAN-SQUARE	VARIANCE	STANDARD DEVIATION
0.15755E 00	0.66434E 04	0.68095E 04	0.82520E 02

T	REFERENCE TIME SERIES	SINEWAVE	RESIDUE TIME SERIES
-20	0.1626E 02	0.1273E 03	-0.1110E 03
-19	-0.9235E 02	0.7988E 02	-0.1722E 03
-18	-0.2222E 03	-0.1209E 02	-0.2101E 03
-17	-0.2805E 03	-0.9731E 02	-0.1832E 03
-16	-0.2426E 03	-0.1283E 03	-0.1144E 03
-15	-0.6166E 02	-0.8770E 02	0.2604E 02
-14	0.1153E 03	0.1774E 01	0.1135E 03
-13	0.2187E 03	0.9026E 02	0.1284E 03
-12	0.2658E 03	0.1284E 03	0.1374E 03
-11	0.2273E 03	0.9496E 02	0.1324E 03
-10	0.1097E 03	0.8551E 01	0.1012E 03
-9	-0.3037E 02	-0.8262E 02	0.5225E 02
-8	-0.8642E 02	-0.1277E 03	0.4130E 02
-7	-0.6305E 02	-0.1016E 03	0.3855E 02
-6	0.4561E 02	-0.1882E 02	0.6443E 02
-5	0.1016E 03	0.7446E 02	0.2716E 02
-4	0.8773E 02	0.1262E 03	-0.3848E 02
-3	0.1373E 03	0.1076E 03	0.2969E 02
-2	0.8120E 02	0.2897E 02	0.5224E 02
-1	-0.2320E 02	-0.6581E 02	0.4260E 02
0	-0.6858E 02	-0.1239E 03	0.5530E 02
1	-0.1264E 03	-0.1129E 03	-0.1348E 02
2	-0.5421E 02	-0.3893E 02	-0.1528E 02
3	-0.3212E 02	0.5573E 02	-0.8885E 02
4	0.9816E 02	0.1208E 03	-0.2259E 02
5	0.1733E 03	0.1174E 03	0.5584E 02
6	0.1243E 03	0.4864E 02	0.7562E 02
7	0.1535E 02	-0.4729E 02	0.6264E 02
8	-0.7344E 02	-0.1169E 03	0.4340E 02
9	-0.1152E 03	-0.1212E 03	0.6065E 01
10	-0.1019E 03	-0.5803E 02	-0.4383E 02
11	-0.2029E 02	0.3754E 02	-0.5783E 02
12	0.4375E 02	0.1122E 03	-0.6843E 02
13	0.4894E 02	0.1243E 03	-0.7531E 02
14	0.4425E 02	0.6705E 02	-0.2280E 02
15	-0.1095E 02	-0.2755E 02	0.1660E 02
16	-0.9798E 02	-0.1068E 03	0.8809E 01
17	-0.1225E 03	-0.1265E 03	0.3960E 01
18	-0.9404E 02	-0.7563E 02	-0.1841E 02
19	-0.2304E 02	0.1738E 02	-0.4042E 02
20	0.8838E 02	0.1007E 03	-0.1232E 02

```
$JOB    *RUSSELL*,TIME=30,PAGES=75
C
C                       PROGRAM 07
C
C       MAXIMUM ENTROPY SPECTRAL ANALYSIS
C
C       THIS PROGRAM COMPUTES THE MAXIMUM ENTROPY SPECTRAL
C       ESTIMATE FOR A TIME SERIES.  THE PROGRAM WILL DO A
C       FIRST ORDER LINEAR REGRESSION ANALYSIS, IF DESIRED,
C       AND ALSO CONVERT THE DATA TO STANDARD VARIABLES.
C
1               DIMENSION AK(100),FR(1000)
2               DIMENSION S(1000),SPLOT(1000),SNAME(5)
3               DIMENSION X(1000),XMDC(1000),XNORM(1000)
4               DIMENSION XSV(1000),XTIME(1000)
C
C       READ INPUT DATA --  THE TIME SERIES, X(I), THE
C       NUMBER OF DATA SAMPLES, NS, THE MAXIMUM NUMBER OF
C       COEFFICIENTS TO BE CALCULATED, MM, THE SAMPLING
C       INTERVAL, DELTA-T, AND THE DESIRED RESOLUTION IN
C       THE MEM SPECTRAL ESTIMATE, DELTA-F.  SNAME IS A USER
C       DEFINED LABEL FOR THE INPUT DATA SET. LINREG IS
C       A PROCESSING OPTION.  NPT1, NPT2, NPT3, NPT4, ARE
C       PRINT OPTIONS.
C
5       4       READ(5,5,END=501) NPT1,NPT2,NPT3,NPT4
        +,LINREG,NS,MM,XTDELT,FDELT,SNAME
6       5       FORMAT(4I1,I6,2I5,E13.3,E15.3,5A4)
7               N=NS
8               XN=FLOAT(N)
9               IF(FDELT) 501,6,7
10      6       FDELT=.25/(FLOAT(NS)*XTDELT)
11      7        CONTINUE
C
C           **** USER SPECIFIED READ FORMAT ****
C
C       READ INPUT DATA FUNCTION.
C
12              READ(5,10)(X(I),I=1,N)
13      10      FORMAT(10X,F14.2)
C           *****************************************
C
C       PRINT INPUT DATA.
C
14              PRINT 15
15      15      FORMAT('1',17X,'MAXIMUM ENTROPY SPECTRAL ANALYSIS',
        +///,9X,'PTOPT',2X,'LINREG',3X,'NS',5X,'MM',
        +3X,'DELTA-T, SEC',3X,'DELTA-F, HZ'/)
16              PRINT 20,NPT1,NPT2,NPT3,NPT4,LINREG,NS,MM,XTDELT,FDELT
17      20      FORMAT(' ',9X,4I1,4X,I1,3X,I5,I7,E15.7,E16.7)
```

```
      C
      C      DO A FIRST ORDER LINEAR REGRESSION ANALYSIS TO
      C      REMOVE ANY LINEAR TREND AND COMPUTE THE
      C      AVERAGE VALUE.
      C
18  25     KSUM=0
19         KSUM2=0
20         XKSUM=0.0
21         XSUM=0.0
22        XDC=0.
      C
      C      COMPUTE THE AVERAGE VALUE.
      C
23         DO 30 K=1,N
24  30     XDC=XDC+X(K)
25         XDC=XDC/XN
26         DO 35 K=1,N
27  35     XMDC(K)=X(K)-XDC
      C
      C      COMPUTE LINEAR REGRESSION.
      C
28         DO 40 K=1,N
29         KSUM=KSUM+K
30         KSUM2=KSUM2+(K**2 )
31        XKSUM=XKSUM+FLOAT(K)*X(K)
32  40     XSUM=XSUM+X(K)
33        XTBAR=XTDELT*FLOAT(KSUM)/XN
34         XBAR=XSUM/XN
35        XTSUM2=XTDELT**2*FLOAT(KSUM2)
36         XTSUM=XTDELT*XKSUM
37         BX1=(XTSUM-XTBAR*XBAR*XN)/(XTSUM2-XN*(XTBAR**2.))
38         BZERO=XBAR-BX1*XTBAR
39         DO 45 K=1,N
40  45     XNORM(K)=X(K)-BZERO-BX1*K*XTDELT
      C
      C      THE TIME SERIES HAS NOW BEEN CORRECTED FOR ANY
      C      LINEAR TREND AND THE DC-VALUE HAS BEEN REMOVED.
      C
      C
      C      COMPUTE THE STATISTICS FOR THE VARIOUS FORMS OF
      C      THE DATA FUNCTION.  ALSO, TRANSFORM THE DATA INTO
      C      STANDARD VARIABLES BY DIVIDING EACH ZERO-MEAN DATA
      C      VALUE BY THE STANDARD DEVIATION.
      C
41  50     PZERO1=0.0
42         PZERO2=0.0
43         PZERO3=0.0
44         DO 55 I=1,N
45         PZERO1=PZERO1+X(I)*X(I)
```

```
46          PZERO2=PZERO2+XNORM(I)*XNORM(I)
47    55     PZERO3=PZERO3+(X(I)-XDC)*(X(I)-XDC)
48          PT=PZERO1/XN
49          PZERO1=PZERO1/(XN-1.)
50          PZERO2=PZERO2/(XN-1.)
51          PZERO3=PZERO3/(XN-1.)
52          STDEV2=PZERO2**0.5
53          STDEV3=PZERO3**0.5
54          DO 60 I=1,N
55          XI=I
56          XTIME(I)=XI*XTDELT
57    60     XSV(I)=XNORM(I)/STDEV2
      C
58          PRINT 65,SNAME,XDC,PT,PZERO3,STDEV3
59    65    FORMAT(' ',///,10X,'INPUT DATA FUNCTION STATISTICS:',
      +2X,5A4,//,8X,'AVERAGE',5X,'MEAN-SQUARE',5X,
      +'VARIANCE',4X,'STANDARD DEVIATION',//,5X,E12.5
      +,3X,E12.5,3X,E12.5,3X,E12.5,///)
      C
60          PRINT 70,BZERO,BX1,PZERO2,STDEV2
61    70    FORMAT(' ',9X,'DATA FUNCTION STATISTICS AFTER',/,10X,
      +'LINEAR REGRESSION:',//,8X,'BZERO',11X,'B1',10X,
      +'VARIANCE',4X,'STANDARD DEVIATION',//,5X,E12.5
      +,3X,E12.5,3X,E12.5,3X,E12.5,///)
      C
62          IF(NPT1 .EQ.  0) GO TO 90
63          PRINT 75
64    75    FORMAT(' ',7X,'T',3X,'INPUT DATA FUNCTION',4X,
      +'LINREG',7X,'STANDARD VARIABLES',/)
65          DO 80 I=1,N
66    80     PRINT 85,I,X(I),XNORM(I),XSV(I)
67    85    FORMAT(' ',I8,3E18.7)
      C
68    90     IF(LINREG .EQ. 3) GO TO 115
69          LINREG=LINREG-1
70          PZERO=PZERO1
71          IF(LINREG) 125,95,105
      C
72    95     DO 100 I=1,N
73    100    X(I)=XMDC(I)
74          PZERO=PZERO3
75          GO TO 125
      C
76    105    DO 110 I=1,N
77    110    X(I)=XNORM(I)
78          PZERO=PZERO2
79          GO TO 125
      C
```

```
80    115       DO 120 I=1,N
81    120       X(I)=XSV(I)
82              PZERO=1.
83    125       CONTINUE
      C
      C        THE INPUT TIME SERIES HAS BEEN PREPROCESSED INTO A
      C        CONVENIENT FORM.  THE MEM AUTOREGRESSIVE COEFFI-
      C        CIENTS ARE NOW COMPUTED.  INPUT VARIABLES ARE X(I),
      C        PZERO,N,PT,MM,XTDELT,AND FDELT.
      C
84              CALL ATOREG(X,PZERO,N,PT,MM,XTDELT,FDELT,
               +PK,AK,K,NPT2,NPT3)
      C
      C        THE AUTOREGRESSIVE COEFFICIENTS, AK(T), HAVE NOW
      C        BEEN ESTIMATED USING A LEAST-SQUARE ERROR
      C        CRITERION.  THESE COEFFICIENTS ARE NOW USED IN THE
      C        MEM SPECTRAL ESTIMATOR TO OBTAIN AN ESTIMATE OF THE
      C        POWER SPECTRAL DENSITY FUNCTION.
      C
85              CALL MEMSPM(NS,K,XTDELT,FDELT,PK,AK,S,NMAX,
               +SBIG,IMAX,NPT4)
      C
      C        COMPUTE SPECTRAL AMPLITUDES IN DB AND
      C        FREQUENCIES FOR PLOTTING.
      C
86              NMP1=NMAX+1
87              DO 499 I=1,NMP1
88              L=I-1
89              FR(I)=FLOAT(L)*FDELT
90              SPLOT(I)=10.*ALOG10(S(I)/SBIG)
91              STEST=SPLOT(I)+40.
92              IF(STEST) 498,498,499
93    498       SPLOT(I)=-40.
94    499       CONTINUE
      C
      C           **** USER SUPPLIED PLOT ROUTINES ****
      C           @@ INPUTS @@
      C
      C
      C        TIME VARIABLE, XTIME(I).
      C        INPUT DATA FUNCTION, X(I).
      C        DATA FUNCTION WITH DC-VALUE REMOVED, XMDC(I).
      C        DATA FUNCTION AFTER LINEAR REGRESSION, XNORM(I).
      C         STANDARD VARIABLES,XSV(I).
      C
      C           @@ OUTPUTS @@
      C
      C        FREQUENCY VARIABLE IN HERTZ, FR(I).
      C        POWER SPECTRAL DENSITY FUNCTION, S(I).
      C        RELATIVE PSD IN DB, SPLOT(I).
```

```
        C
 95             GO TO 4
 96     501     STOP
 97             END
        C
        C       THIS SUBROUTINE ESTIMATES THE AUTOREGRESSIVE
        C       COEFFICIENTS USING A MAXIMUM ENTROPY CRITERION
        C       AND A MINIMUM LEAST SQUARE ERROR.
        C

 98             SUBROUTINE ATOREG(X,PZERO,N,PT,MM,XTDELT,FDELT,
       +PK,AK,K,NPT2,NPT3)
        C
 99             DIMENSION AA(100),AK(100),AKSAVE(100)
100             DIMENSION B1(1000),B2(1000),P(1000),X(1000)
        C
101             INTEGER T,TP1
        C
        C       COMPUTE THE STARTING VALUES, B1(T), B2(T), AK(1),
        C       AND P(1) FOR THE RECURSIVE EQUATIONS.
        C
102             K=1
103             B1(1)=X(1)
104             NM1=N-1
105             B2(NM1)=X(N)
106             DO 5 T=2,NM1
107             B1(T)=X(T)
108     5       B2(T-1)=X(T)
109             XNOM=0.
110            XDEN=0.
111             NMK=N-K
112             DO 10 T=1,NMK
113             XNOM=XNOM+B1(T)*B2(T)
114     10      XDEN=XDEN+B1(T)*B1(T)+B2(T)*B2(T)
115             AK(1)=2.*XNOM/XDEN
116             AKSAVE(1)=AK(1)
117             P(1)=PZERO*(1.-AK(1)*AK(1))
118             PRINT 15
119     15      FORMAT('1',7X,'MEM STARTING VALUES:',//,6X,'K',8X,
       +'A1(1)',11X,'P(1)',8X,'P(0)',5X,'TOTAL POWER',/)
120             PRINT 20,K,AK(1),P(1),PZERO,PT
121     20      FORMAT(I7,E17.7,3E12.3///)
        C
        C       COMPUTE AK(T) VALUES USING RECURSIVE EQUATIONS
        C
122     25      K=K+1
123             NMK=N-K
124             KM1=K-1
```

```
125            DO 30 T=1,KM1
126     30     AA(T)=AK(T)
127            DO 35 T=1,NMK
128            TP1=T+1
129            B1(T)=B1(T)-AA(KM1)*B2(T)
130     35     B2(T)=B2(TP1)-AA(KM1)*B1(TP1)
131            XNOM=0.
132            XDEN=0.
133            DO 40 T=1,NMK
134            XNOM=XNOM+B1(T)*B2(T)
135     40     XDEN=XDEN+B1(T)*B1(T)+B2(T)*B2(T)
136            AK(K)=2.*XNOM/XDEN
137            AKSAVE(K)=AK(K)
138            P(K)=P(KM1)*(1.-AK(K)*AK(K))
139            DO 45 T=1,KM1
140            KMT=K-T
141     44     AK(T)=AA(T)-AK(K)*AA(KMT)
        C
        C
        C      TO INHIBIT THE PRINTING OF ALL IMMEDIATE FILTER
        C      CALCULATIONS AND COEFFICIENTS, CHANGE STATEMENTS
        C      45, 50, AND 51 TO COMMENTS AND CHANGE THE RANGE
        C      OF THE DO-LOOP FROM STATEMENT 45 TO STATEMENT 44.
        C
142     45     PRINT 46,K,T,AK(T)
143     46     FORMAT(' ',2I8,E18.7)
144     50      PRINT 51
145     51      FORMAT(///)
146             IF(MM-K)52,55,25
147     52      PRINT 53
148     55      IF(NPT2.EQ.0) GO TO 71
149     53      FORMAT(' ',10X,'*** ERROR IN ATOREG ***',//)
150             PRINT 60
151     60      FORMAT(' ',7X,'SUMMARY OF ITERATIVE RESULTS',//,
               +5X,'INDEX',3X,'COEFFICIENT',6X,'ERROR POWER',
               +//,7X,'K',8X,'AK(K)',13X,'P(K)',/)
152             PK=P(K)
153             DO 65 I=1,K
154     65      PRINT 70,I,AKSAVE(I),P(I)
155     70      FORMAT(I8,3E17.7//)
156     71      PRINT 75,K,P(K)
157     75      FORMAT('1', 9X,'AUTOREGRESSIVE ESTIMATION SUMMARY',
               +///,8X,'LENGTH, K=',I3,3X,'ERROR POWER, P(K)=',
               +E13.7,///,8X,'ORDER',3X,
               +'AUTOREGRESSIVE COEFFICIENTS',//,
               +8X,'T',9X,'AK(T)',//)
158             IF(NPT3 .EQ. 0) GO TO 90
159             DO 80 T=1,MM
160     80      PRINT 85,T,AK(T)
161     85      FORMAT(' ',I8,E18.7)
```

472

```
162    90      RETURN
163            END
       C
       C       THIS SUBROUTINE EVALUATES THE MEM SPECTRUM USING
       C       THE CALCULATED COEFFICIENTS, AK(T), AND THE
       C       SPECIFIED FREQUENCY INCREMENT, DELTA-F. THE ROUTINE
       C       CALCULATES THE NYQUIST FREQUENCY AND LIMITS THE
       C       FREQUENCY RANGE ACCORDINGLY.  THIS ELIMINATES THE
       C       POSSIBILITY OF COMPUTING ALIASED SPECTRA.
       C

164            SUBROUTINE MEMSPM(NS,K,XTDELT,FDELT,PK,AK,S,NMAX
              +,SBIG,IMAX,NPT4)
       C
165            DIMENSION AK(100),S(1000)
       C
166            PI=3.1415926
167            NMAX=INT(1./(2.*XTDELT*FDELT))
168            NMP1=NMAX+1
169            PRINT 1
170    1       FORMAT('1',12X,'MEM POWER SPECTRAL DENSITY',1X,
              +'ESTIMATION',///)
171            DO 10 I=1,NMP1
172            L=I-1
173            XL=FLOAT(L)
174            PHI=2.*PI*XL*FDELT*XTDELT
175            ALPHA=0.0
176            BETA=0.0
177            DO 5 J=1,K
178            ALPHA=AK(J)*COS(J*PHI)+ALPHA
179    5       BETA=AK(J)*SIN(J*PHI)+BETA
180            D=(1.-ALPHA)*(1.-ALPHA)+BETA*BETA
181    10      S(I)=PK*XTDELT/D
182            PRINT 14
183    14      FORMAT(' ',5X,'THE LARGEST SPECTRAL COMPONENT IS:',
              +//,7X,'L',4X,'FREQUENCY',7X,'AMPLITUDE',/)
184            SBIG=0.0
185            DO 15 I=2,NMP1
186            XS=S(I )
187    15      IF(XS.GT.SBIG)SBIG=XS
188            IS=0
189    20      IS=IS+1
190            STEST=S(IS)-SBIG
191            IF(STEST) 20,21,21
192    21      IMAX=IS-1
193            FREQ=IMAX*FDELT
194            PRINT 25,IMAX,FREQ,SBIG
195    25      FORMAT(' ',I7,E12.4,E16.4,///)
196            PS=0.0
```

```
197          DO 30 I=2,NMAX
198   30     PS=PS+S(I)*FDELT
199          PS=PS+S(1)*FDELT/2.+S(NMP1)*FDELT/2.
200          PS=2.*PS
201          PRINT 31,K,PS
202   31     FORMAT(' ',5X,'THE TOTAL POWER IN THE ESTIMATED',
             +1X,'SPECTRUM IS',//,6X,'LENGTH,K=',I3,5X,
             +'POWER=',E13.7,/////)
      C
203          IF(NPT4 .EQ. 0) GO TO 45
204          PRINT 35
205   35     FORMAT(' ',6X,'L',6X,'FREQ-HZ',6X,'NORMALIZED',
             +3X,'TOTAL POWER',3X,'RELATIVE',/,27X,'SPECTRAL',
             +19X,'AMPLITUDE',/,27X,'DENSITY',7X,'DB',13X,'DB',/)
206          DO 40 I=1,NMP1
207          L=I-1
208          FREQ=L*FDELT
209          PS1=S(I)*FDELT
210          PS1=10.*ALOG10(PS1)
211          PS2=S(I)/SBIG
212          PS2=10.*ALOG10(PS2)
213   40     PRINT 41,L,FREQ,S(I),PS1,PS2
214   41     FORMAT(' ',I7,2E13.3,F11.1,F14.1)
215   45     RETURN
216          END
```

MAXIMUM ENTROPY SPECTRAL ANALYSIS

PTOPT	LINREG	NS	MM	DELTA-T, SEC	DELTA-F, HZ
1111	3	41	15	0.6000000E 02	0.2500000E-04

INPUT DATA FUNCTION STATISTICS: HER A 7/29/75

AVERAGE	MEAN-SQUARE	VARIANCE	STANDARD DEVIATION
0.82960E 02	0.31102E 05	0.24825E 05	0.15756E 03

DATA FUNCTION STATISTICS AFTER
LINEAR REGRESSION:

BZERO	B1	VARIANCE	STANDARD DEVIATION
-0.88342E 02	0.13595E 02	0.15276E 05	0.12360E 03

T	INPUT DATA FUNCTION	LINREG	STANDARD VARIABLES
1	-0.6392999E 02	0.1625516E 02	0.1315165E 00
2	-0.1643800E 03	-0.9235213E 02	-0.7471983E 00
3	-0.2860801E 03	-0.2222099E 03	-0.1797842E 01
4	-0.3361799E 03	-0.2804666E 03	-0.2269185E 01
5	-0.2902000E 03	-0.2426439E 03	-0.1963172E 01
6	-0.1010600E 03	-0.6166125E 02	-0.4988860E 00
7	0.8405000E 02	0.1152915E 03	0.9327948E 00
8	0.1956200E 03	0.2187041E 03	0.1769481E 01
9	0.2508800E 03	0.2658066E 03	0.2150576E 01
10	0.2205500E 03	0.2273195E 03	0.1839186E 01
11	0.1111300E 03	0.1097423E 03	0.8878980E 00
12	-0.2083000E 02	-0.3037497E 02	-0.2457564E 00
13	-0.6872000E 02	-0.8642226E 02	-0.6992212E 00
14	-0.3719000E 02	-0.6304955E 02	-0.5101184E 00
15	0.7963000E 02	0.4561317E 02	0.3690450E 00
16	0.1437900E 03	0.1016159E 03	0.8221490E 00
17	0.1380600E 03	0.8772861E 02	0.7097906E 00
18	0.1957700E 03	0.1372812E 03	0.1110708E 01
19	0.1478500E 03	0.8120407E 02	0.6570022E 00
20	0.5160001E 02	-0.2320322E 02	-0.1877315E 00
21	0.1438000E 02	-0.6858051E 02	-0.5548680E 00
22	-0.3524001E 02	-0.1263578E 03	-0.1022329E 01
23	0.4507001E 02	-0.5420503E 02	-0.4385596E 00
24	0.7531000E 02	-0.3212231E 02	-0.2598937E 00
25	0.2137500E 03	0.9816025E 02	0.7941904E 00
26	0.2970300E 03	0.1732830E 03	0.1401990E 01
27	0.2561599E 03	0.1242556E 03	0.1005322E 01
28	0.1554100E 03	0.1534859E 02	0.1241816E 00
29	0.7478000E 02	-0.7343871E 02	-0.5941745E 00
30	0.4120000E 02	-0.1151760E 03	-0.9318605E 00
31	0.6267000E 02	-0.1018633E 03	-0.8241505E 00
32	0.1524000E 03	-0.2029053E 02	-0.1641656E 00
33	0.2246000E 03	0.4375220E 02	0.3539882E 00
34	0.2379500E 03	0.4894458E 02	0.3959985E 00
35	0.2414100E 03	0.4424756E 02	0.3579961E 00
36	0.1943700E 03	-0.1094971E 02	-0.8859134E-01
37	0.1155000E 03	-0.9797690E 02	-0.7927070E 00
38	0.9912000E 02	-0.1225141E 03	-0.9912317E 00
39	0.1357500E 03	-0.9404160E 02	-0.7608674E 00
40	0.2149100E 03	-0.2303882E 02	-0.1864014E 00
41	0.3344900E 03	0.8838379E 02	0.7150915E 00

MEM STARTING VALUES:

K		A1(1)	P(1)	P(0)	TOTAL POWER
1		0.7703549E 00	0.407E 00	0.100E 01	0.311E 05
2	1	0.1426599E 01			
3	1	0.1273918E 01			
3	2	-0.5961846E 00			
4	1	0.1286666E 01			
4	2	-0.5537803E 00			
4	3	-0.2698378E 00			
5	1	0.1269886E 01			
5	2	-0.4901221E 00			
5	3	-0.1391941E 00			
5	4	-0.2324146E 00			
6	1	0.1255294E 01			
6	2	-0.4757471E 00			
6	3	-0.1305848E 00			
6	4	-0.2021002E 00			
6	5	0.1573693E 00			
7	1	0.1249800E 01			
7	2	-0.4897244E 00			
7	3	-0.1126345E 00			
7	4	-0.1905018E 00			
7	5	0.1996245E 00			
7	6	-0.4964290E-01			

8	1	0.1277999E 01
8	2	-0.5054857E 00
8	3	-0.4925478E-01
8	4	-0.2509851E 00
8	5	0.1638636E 00
8	6	-0.2051279E 00
8	7	0.4856238E 00

9	1	0.1214496E 01
9	2	-0.4083553E 00
9	3	-0.9026274E-01
9	4	-0.2182105E 00
9	5	0.1136636E 00
9	6	-0.2149794E 00
9	7	0.3845207E 00
9	8	-0.6188023E-01

10	1	0.1196949E 01
10	2	-0.4137836E 00
10	3	-0.5655117E-01
10	4	-0.2370692E 00
10	5	0.1236346E 00
10	6	-0.2341216E 00
10	7	0.3766007E 00
10	8	-0.9770262E-01
10	9	-0.9347177E-01

11	1	0.1195743E 01
11	2	-0.4150690E 00
11	3	-0.5789482E-01
11	4	-0.2318900E 00
11	5	0.1204148E 00
11	6	-0.2324213E 00
11	7	0.3733404E 00
11	8	-0.9848028E-01
11	9	-0.9916228E-01
11	10	-0.7126266E-01

1 2	1	0.1195573E 01
1 2	2	-0.4159462E 00
1 2	3	-0.5911542E-01
1 2	4	-0.2331021E 00
1 2	5	0.1250103E 00
1 2	6	-0.2352822E 00
1 2	7	0.3748226E 00
1 2	8	-0.1013346E 00
1 2	9	-0.9987491E-01
1 2	1 0	-0.7637179E-01
1 2	1 1	0.9661391E-03

1 3	1	0.1195349E 01
1 3	2	-0.4159285E 00
1 3	3	-0.6050623E-01
1 3	4	-0.2349269E 00
1 3	5	0.1231648E 00
1 3	6	-0.2284563E 00
1 3	7	0.3705379E 00
1 3	8	-0.9905803E-01
1 3	9	-0.1041199E 00
1 3	1 0	-0.7744831E-01
1 3	1 1	-0.6608676E-02
1 3	1 2	0.9463485E-02

1 4	1	0.1198529E 01
1 4	2	-0.4175817E 00
1 4	3	-0.5935176E-01
1 4	4	-0.2213914E 00
1 4	5	0.1413535E 00
1 4	6	-0.2111518E 00
1 4	7	0.3058087E 00
1 4	8	-0.5914903E-01
1 4	9	-0.1256355E 00
1 4	1 0	-0.3641000E-01
1 4	1 1	0.3961150E-02
1 4	1 2	0.8212191E-01
1 4	1 3	-0.2270263E 00

1 5	1	0.1184735E 01
1 5	2	-0.3996562E 00

```
15      3      -0.6583589E-01
15      4      -0.2217042E  00
15      5       0.1442283E  00
15      6      -0.2012320E  00
15      7       0.3104789E  00
15      8      -0.8329493E-01
15      9      -0.1089634E  00
15     10      -0.4757093E-01
15     11       0.2144169E-01
15     12       0.8680815E-01
15     13      -0.1940551E  00
15     14       0.8005691E-01
```

SUMMARY OF ITERATIVE RESULTS

INDEX	COEFFICIENT	ERROR POWER
K	AK(K)	P(K)
1	0.7703549E 00	0.4065534E 00
2	-0.8518724E 00	0.1115230E 00
3	-0.1792291E 00	0.1079406E 00
4	0.7112604E-01	0.1073945E 00
5	0.2359126E 00	0.1014174E 00
6	0.6185063E-01	0.1010294E 00
7	0.8881867E-01	0.1002324E 00
8	-0.3174950E 00	0.9012860E-01
9	-0.2000117E 00	0.8652300E-01
10	-0.8772367E-01	0.8585715E-01
11	-0.1375243E-01	0.8584088E-01
12	-0.1230915E-01	0.8582783E-01
13	-0.1821105E-01	0.8579934E-01
14	0.1746899E 00	0.8318102E-01
15	0.7895762E-01	0.8266240E-01

AUTOREGRESSIVE ESTIMATION SUMMARY

LENGTH, K= 15   ERROR POWER, P(K)=0.8266240E-01

ORDER   AUTOREGRESSIVE COEFFICIENTS

T   AK(T)

T	AK(T)
1	0.1184735E 01
2	-0.3996562E 00
3	-0.6583589E-01
4	-0.2217042E 00
5	0.1442283E 00
6	-0.2012320E 00
7	0.3104789E 00
8	-0.8329493E-01
9	-0.1089634E 00
10	-0.4757093E-01
11	0.2144169E-01
12	0.8680815E-01
13	-0.1940551E 00
14	0.8005691E-01
15	0.7895762E-01

MEM POWER SPECTRAL DENSITY ESTIMATION

THE LARGEST SPECTRAL COMPONENT IS:

L	FREQUENCY	AMPLITUDE
77	0.1925E-02	0.4210E 04

THE TOTAL POWER IN THE ESTIMATED SPECTRUM IS

LENGTH,K= 15   POWER=0.9988377E 00

L	FREQ-HZ	NORMALIZED SPECTRAL DENSITY	TOTAL POWER DB	RELATIVE AMPLITUDE DB
0	0.000E 00	0.287E 02	-31.4	-21.7
1	0.250E-04	0.287E 02	-31.4	-21.7
2	0.500E-04	0.286E 02	-31.5	-21.7
3	0.750E-04	0.285E 02	-31.5	-21.7
4	0.100E-03	0.284E 02	-31.5	-21.7
5	0.125E-03	0.282E 02	-31.5	-21.7
6	0.150E-03	0.280E 02	-31.5	-21.8
7	0.175E-03	0.278E 02	-31.6	-21.8
8	0.200E-03	0.277E 02	-31.6	-21.8
9	0.225E-03	0.275E 02	-31.6	-21.8
10	0.250E-03	0.274E 02	-31.6	-21.9
11	0.275E-03	0.273E 02	-31.7	-21.9
12	0.300E-03	0.273E 02	-31.7	-21.9
13	0.325E-03	0.274E 02	-31.6	-21.9
14	0.350E-03	0.276E 02	-31.6	-21.8
15	0.375E-03	0.279E 02	-31.6	-21.8
16	0.400E-03	0.283E 02	-31.5	-21.7
17	0.425E-03	0.288E 02	-31.4	-21.6
18	0.450E-03	0.295E 02	-31.3	-21.5
19	0.475E-03	0.304E 02	-31.2	-21.4
20	0.500E-03	0.315E 02	-31.0	-21.3
21	0.525E-03	0.328E 02	-30.9	-21.1
22	0.550E-03	0.344E 02	-30.7	-20.9
23	0.575E-03	0.363E 02	-30.4	-20.6
24	0.600E-03	0.387E 02	-30.1	-20.4
25	0.625E-03	0.415E 02	-29.8	-20.1
26	0.650E-03	0.449E 02	-29.5	-19.7
27	0.675E-03	0.490E 02	-29.1	-19.3
28	0.700E-03	0.539E 02	-28.7	-18.9
29	0.725E-03	0.599E 02	-28.2	-18.5
30	0.750E-03	0.672E 02	-27.7	-18.0
31	0.775E-03	0.761E 02	-27.2	-17.4
32	0.800E-03	0.869E 02	-26.6	-16.9
33	0.825E-03	0.100E 03	-26.0	-16.2
34	0.850E-03	0.116E 03	-25.4	-15.6
35	0.875E-03	0.134E 03	-24.8	-15.0
36	0.900E-03	0.154E 03	-24.1	-14.4
37	0.925E-03	0.175E 03	-23.6	-13.8
38	0.950E-03	0.193E 03	-23.2	-13.4
39	0.975E-03	0.205E 03	-22.9	-13.1
40	0.100E-02	0.209E 03	-22.8	-13.0
41	0.102E-02	0.203E 03	-22.9	-13.2
42	0.105E-02	0.189E 03	-23.3	-13.5
43	0.108E-02	0.171E 03	-23.7	-13.9
44	0.110E-02	0.151E 03	-24.2	-14.4
45	0.112E-02	0.133E 03	-24.8	-15.0

46	0.115E-02	0.116E 03	-25.4	-15.6
47	0.117E-02	0.102E 03	-25.9	-16.1
48	0.120E-02	0.908E 02	-26.4	-16.7
49	0.123E-02	0.813E 02	-26.9	-17.1
50	0.125E-02	0.735E 02	-27.4	-17.6
51	0.127E-02	0.672E 02	-27.7	-18.0
52	0.130E-02	0.622E 02	-28.1	-18.3
53	0.132E-02	0.581E 02	-28.4	-18.6
54	0.135E-02	0.550E 02	-28.6	-18.8
55	0.137E-02	0.527E 02	-28.8	-19.0
56	0.140E-02	0.510E 02	-28.9	-19.2
57	0.142E-02	0.499E 02	-29.0	-19.3
58	0.145E-02	0.495E 02	-29.1	-19.3
59	0.148E-02	0.496E 02	-29.1	-19.3
60	0.150E-02	0.503E 02	-29.0	-19.2
61	0.152E-02	0.517E 02	-28.9	-19.1
62	0.155E-02	0.538E 02	-28.7	-18.9
63	0.157E-02	0.569E 02	-28.5	-18.7
64	0.160E-02	0.610E 02	-28.2	-18.4
65	0.163E-02	0.666E 02	-27.8	-18.0
66	0.165E-02	0.741E 02	-27.3	-17.5
67	0.167E-02	0.842E 02	-26.8	-17.0
68	0.170E-02	0.981E 02	-26.1	-16.3
69	0.172E-02	0.118E 03	-25.3	-15.5
70	0.175E-02	0.146E 03	-24.4	-14.6
71	0.178E-02	0.191E 03	-23.2	-13.4
72	0.180E-02	0.264E 03	-21.8	-12.0
73	0.182E-02	0.398E 03	-20.0	-10.2
74	0.185E-02	0.677E 03	-17.7	-7.9
75	0.188E-02	0.138E 04	-14.6	-4.8
76	0.190E-02	0.338E 04	-10.7	-0.9
77	0.192E-02	0.421E 04	-9.8	0.0
78	0.195E-02	0.171E 04	-13.7	-3.9
79	0.197E-02	0.734E 03	-17.4	-7.6
80	0.200E-02	0.385E 03	-20.2	-10.4
81	0.203E-02	0.232E 03	-22.4	-12.6
82	0.205E-02	0.154E 03	-24.1	-14.4
83	0.207E-02	0.109E 03	-25.6	-15.9
84	0.210E-02	0.812E 02	-26.9	-17.1
85	0.212E-02	0.628E 02	-28.0	-18.3
86	0.215E-02	0.501E 02	-29.0	-19.2
87	0.218E-02	0.410E 02	-29.9	-20.1
88	0.220E-02	0.342E 02	-30.7	-20.9
89	0.222E-02	0.291E 02	-31.4	-21.6
90	0.225E-02	0.251E 02	-32.0	-22.2
91	0.228E-02	0.220E 02	-32.6	-22.8
92	0.230E-02	0.195E 02	-33.1	-23.3
93	0.233E-02	0.175E 02	-33.6	-23.8
94	0.235E-02	0.158E 02	-34.0	-24.3
95	0.237E-02	0.144E 02	-34.4	-24.7

96	0.240E-02	0.133E 02	-34.8	-25.0
97	0.243E-02	0.123E 02	-35.1	-25.3
98	0.245E-02	0.115E 02	-35.4	-25.7
99	0.247E-02	0.108E 02	-35.7	-25.9
100	0.250E-02	0.101E 02	-36.0	-26.2
101	0.252E-02	0.962E 01	-36.2	-26.4
102	0.255E-02	0.916E 01	-36.4	-26.6
103	0.258E-02	0.876E 01	-36.6	-26.8
104	0.260E-02	0.840E 01	-36.8	-27.0
105	0.262E-02	0.808E 01	-36.9	-27.2
106	0.265E-02	0.779E 01	-37.1	-27.3
107	0.268E-02	0.752E 01	-37.3	-27.5
108	0.270E-02	0.727E 01	-37.4	-27.6
109	0.273E-02	0.704E 01	-37.5	-27.8
110	0.275E-02	0.681E 01	-37.7	-27.9
111	0.277E-02	0.659E 01	-37.8	-28.1
112	0.280E-02	0.637E 01	-38.0	-28.2
113	0.283E-02	0.616E 01	-38.1	-28.3
114	0.285E-02	0.594E 01	-38.3	-28.5
115	0.288E-02	0.572E 01	-38.4	-28.7
116	0.290E-02	0.550E 01	-38.6	-28.8
117	0.292E-02	0.528E 01	-38.8	-29.0
118	0.295E-02	0.505E 01	-39.0	-29.2
119	0.298E-02	0.483E 01	-39.2	-29.4
120	0.300E-02	0.461E 01	-39.4	-29.6
121	0.302E-02	0.439E 01	-39.6	-29.8
122	0.305E-02	0.418E 01	-39.8	-30.0
123	0.308E-02	0.398E 01	-40.0	-30.2
124	0.310E-02	0.378E 01	-40.2	-30.5
125	0.313E-02	0.359E 01	-40.5	-30.7
126	0.315E-02	0.341E 01	-40.7	-30.9
127	0.317E-02	0.324E 01	-40.9	-31.1
128	0.320E-02	0.308E 01	-41.1	-31.4
129	0.323E-02	0.294E 01	-41.3	-31.6
130	0.325E-02	0.280E 01	-41.5	-31.8
131	0.328E-02	0.268E 01	-41.7	-32.0
132	0.330E-02	0.256E 01	-41.9	-32.2
133	0.332E-02	0.246E 01	-42.1	-32.3
134	0.335E-02	0.237E 01	-42.3	-32.5
135	0.338E-02	0.229E 01	-42.4	-32.7
136	0.340E-02	0.221E 01	-42.6	-32.8
137	0.343E-02	0.215E 01	-42.7	-32.9
138	0.345E-02	0.209E 01	-42.8	-33.0
139	0.348E-02	0.205E 01	-42.9	-33.1
140	0.350E-02	0.201E 01	-43.0	-33.2
141	0.353E-02	0.198E 01	-43.1	-33.3
142	0.355E-02	0.195E 01	-43.1	-33.3
143	0.357E-02	0.194E 01	-43.1	-33.4
144	0.360E-02	0.193E 01	-43.2	-33.4
145	0.363E-02	0.193E 01	-43.2	-33.4

146	0.365E-02	0.194E 01	-43.1	-33.4
147	0.368E-02	0.196E 01	-43.1	-33.3
148	0.370E-02	0.199E 01	-43.0	-33.3
149	0.372E-02	0.202E 01	-43.0	-33.2
150	0.375E-02	0.207E 01	-42.9	-33.1
151	0.378E-02	0.213E 01	-42.7	-33.0
152	0.380E-02	0.220E 01	-42.6	-32.8
153	0.383E-02	0.229E 01	-42.4	-32.7
154	0.385E-02	0.239E 01	-42.2	-32.5
155	0.388E-02	0.250E 01	-42.0	-32.3
156	0.390E-02	0.264E 01	-41.8	-32.0
157	0.392E-02	0.280E 01	-41.5	-31.8
158	0.395E-02	0.298E 01	-41.3	-31.5
159	0.397E-02	0.319E 01	-41.0	-31.2
160	0.400E-02	0.343E 01	-40.7	-30.9
161	0.402E-02	0.369E 01	-40.3	-30.6
162	0.405E-02	0.399E 01	-40.0	-30.2
163	0.407E-02	0.432E 01	-39.7	-29.9
164	0.410E-02	0.466E 01	-39.3	-29.6
165	0.412E-02	0.502E 01	-39.0	-29.2
166	0.415E-02	0.538E 01	-38.7	-28.9
167	0.417E-02	0.570E 01	-38.5	-28.7
168	0.420E-02	0.597E 01	-38.3	-28.5
169	0.422E-02	0.614E 01	-38.1	-28.4
170	0.425E-02	0.620E 01	-38.1	-28.3
171	0.427E-02	0.613E 01	-38.1	-28.4
172	0.430E-02	0.594E 01	-38.3	-28.5
173	0.432E-02	0.564E 01	-38.5	-28.7
174	0.435E-02	0.527E 01	-38.8	-29.0
175	0.437E-02	0.486E 01	-39.2	-29.4
176	0.440E-02	0.444E 01	-39.5	-29.8
177	0.442E-02	0.403E 01	-40.0	-30.2
178	0.445E-02	0.364E 01	-40.4	-30.6
179	0.447E-02	0.329E 01	-40.8	-31.1
180	0.450E-02	0.298E 01	-41.3	-31.5
181	0.452E-02	0.270E 01	-41.7	-31.9
182	0.455E-02	0.246E 01	-42.1	-32.3
183	0.457E-02	0.225E 01	-42.5	-32.7
184	0.460E-02	0.206E 01	-42.9	-33.1
185	0.463E-02	0.190E 01	-43.2	-33.5
186	0.465E-02	0.176E 01	-43.6	-33.8
187	0.467E-02	0.164E 01	-43.9	-34.1
188	0.470E-02	0.153E 01	-44.2	-34.4
189	0.472E-02	0.144E 01	-44.4	-34.7
190	0.475E-02	0.136E 01	-44.7	-34.9
191	0.477E-02	0.129E 01	-44.9	-35.1
192	0.480E-02	0.123E 01	-45.1	-35.3
193	0.482E-02	0.118E 01	-45.3	-35.5
194	0.485E-02	0.114E 01	-45.5	-35.7
195	0.487E-02	0.110E 01	-45.6	-35.8

196	0.490E-02	0.107E 01	-45.7	-35.9
197	0.492E-02	0.104E 01	-45.8	-36.1
198	0.495E-02	0.102E 01	-45.9	-36.1
199	0.497E-02	0.101E 01	-46.0	-36.2
200	0.500E-02	0.993E 00	-46.1	-36.3
201	0.502E-02	0.984E 00	-46.1	-36.3
202	0.505E-02	0.978E 00	-46.1	-36.3
203	0.508E-02	0.976E 00	-46.1	-36.3
204	0.510E-02	0.977E 00	-46.1	-36.3
205	0.512E-02	0.981E 00	-46.1	-36.3
206	0.515E-02	0.988E 00	-46.1	-36.3
207	0.517E-02	0.998E 00	-46.0	-36.3
208	0.520E-02	0.101E 01	-46.0	-36.2
209	0.522E-02	0.103E 01	-45.9	-36.1
210	0.525E-02	0.104E 01	-45.8	-36.1
211	0.527E-02	0.106E 01	-45.8	-36.0
212	0.530E-02	0.108E 01	-45.7	-35.9
213	0.532E-02	0.111E 01	-45.6	-35.8
214	0.535E-02	0.113E 01	-45.5	-35.7
215	0.537E-02	0.115E 01	-45.4	-35.6
216	0.540E-02	0.118E 01	-45.3	-35.5
217	0.542E-02	0.121E 01	-45.2	-35.4
218	0.545E-02	0.123E 01	-45.1	-35.3
219	0.547E-02	0.125E 01	-45.0	-35.3
220	0.550E-02	0.127E 01	-45.0	-35.2
221	0.552E-02	0.129E 01	-44.9	-35.1
222	0.555E-02	0.131E 01	-44.9	-35.1
223	0.557E-02	0.132E 01	-44.8	-35.1
224	0.560E-02	0.132E 01	-44.8	-35.0
225	0.562E-02	0.132E 01	-44.8	-35.0
226	0.565E-02	0.132E 01	-44.8	-35.0
227	0.567E-02	0.131E 01	-44.8	-35.1
228	0.570E-02	0.130E 01	-44.9	-35.1
229	0.573E-02	0.129E 01	-44.9	-35.1
230	0.575E-02	0.127E 01	-45.0	-35.2
231	0.577E-02	0.125E 01	-45.1	-35.3
232	0.580E-02	0.123E 01	-45.1	-35.4
233	0.582E-02	0.120E 01	-45.2	-35.4
234	0.585E-02	0.118E 01	-45.3	-35.5
235	0.587E-02	0.116E 01	-45.4	-35.6
236	0.590E-02	0.113E 01	-45.5	-35.7
237	0.592E-02	0.111E 01	-45.6	-35.8
238	0.595E-02	0.109E 01	-45.7	-35.9
239	0.597E-02	0.107E 01	-45.7	-36.0
240	0.600E-02	0.105E 01	-45.8	-36.0
241	0.602E-02	0.103E 01	-45.9	-36.1
242	0.605E-02	0.102E 01	-45.9	-36.2
243	0.607E-02	0.101E 01	-46.0	-36.2
244	0.610E-02	0.100E 01	-46.0	-36.2
245	0.612E-02	0.997E 00	-46.0	-36.3

246	0.615E-02	0.995E 00	-46.0	-36.3
247	0.618E-02	0.996E 00	-46.0	-36.3
248	0.620E-02	0.100E 01	-46.0	-36.2
249	0.622E-02	0.101E 01	-46.0	-36.2
250	0.625E-02	0.102E 01	-45.9	-36.2
251	0.627E-02	0.103E 01	-45.9	-36.1
252	0.630E-02	0.105E 01	-45.8	-36.0
253	0.632E-02	0.107E 01	-45.7	-35.9
254	0.635E-02	0.110E 01	-45.6	-35.8
255	0.637E-02	0.113E 01	-45.5	-35.7
256	0.640E-02	0.117E 01	-45.3	-35.6
257	0.642E-02	0.121E 01	-45.2	-35.4
258	0.645E-02	0.126E 01	-45.0	-35.2
259	0.647E-02	0.131E 01	-44.8	-35.1
260	0.650E-02	0.138E 01	-44.6	-34.9
261	0.652E-02	0.144E 01	-44.4	-34.6
262	0.555E-02	0.152E 01	-44.2	-34.4
263	0.657E-02	0.160E 01	-44.0	-34.2
264	0.660E-02	0.169E 01	-43.7	-34.0
265	0.662E-02	0.178E 01	-43.5	-33.7
266	0.665E-02	0.188E 01	-43.3	-33.5
267	0.667E-02	0.198E 01	-43.1	-33.3
268	0.670E-02	0.208E 01	-42.8	-33.1
269	0.672E-02	0.218E 01	-42.6	-32.9
270	0.675E-02	0.226E 01	-42.5	-32.7
271	0.677E-02	0.233E 01	-42.3	-32.6
272	0.680E-02	0.238E 01	-42.2	-32.5
273	0.683E-02	0.241E 01	-42.2	-32.4
274	0.685E-02	0.241E 01	-42.2	-32.4
275	0.687E-02	0.238E 01	-42.2	-32.5
276	0.690E-02	0.233E 01	-42.3	-32.6
277	0.692E-02	0.225E 01	-42.5	-32.7
278	0.695E-02	0.216E 01	-42.7	-32.9
279	0.697E-02	0.205E 01	-42.9	-33.1
280	0.700E-02	0.193E 01	-43.2	-33.4
281	0.702E-02	0.181E 01	-43.4	-33.7
282	0.705E-02	0.169E 01	-43.7	-34.0
283	0.707E-02	0.157E 01	-44.0	-34.3
284	0.710E-02	0.147E 01	-44.4	-34.6
285	0.712E-02	0.136E 01	-44.7	-34.9
286	0.715E-02	0.127E 01	-45.0	-35.2
287	0.717E-02	0.118E 01	-45.3	-35.5
288	0.720E-02	0.110E 01	-45.6	-35.8
289	0.722E-02	0.103E 01	-45.9	-36.1
290	0.725E-02	0.969E 00	-46.2	-36.4
291	0.728E-02	0.912E 00	-46.4	-36.6
292	0.730E-02	0.860E 00	-46.7	-36.9
293	0.732E-02	0.814E 00	-46.9	-37.1
294	0.735E-02	0.772E 00	-47.1	-37.4
295	0.737E-02	0.735E 00	-47.4	-37.6

296	0.7740E-02	0.702E 00	-47.6	-37.8
297	0.7742E-02	0.672E 00	-47.7	-38.0
298	0.7745E-02	0.646E 00	-47.9	-38.1
299	0.7747E-02	0.622E 00	-48.1	-38.3
300	0.7750E-02	0.601E 00	-48.2	-38.5
301	0.7752E-02	0.582E 00	-48.4	-38.6
302	0.7755E-02	0.566E 00	-48.5	-38.7
303	0.7757E-02	0.551E 00	-48.6	-38.8
304	0.7760E-02	0.538E 00	-48.7	-38.9
305	0.7762E-02	0.527E 00	-48.8	-39.0
306	0.7765E-02	0.517E 00	-48.9	-39.1
307	0.7767E-02	0.509E 00	-49.0	-39.2
308	0.7770E-02	0.501E 00	-49.0	-39.2
309	0.7772E-02	0.495E 00	-49.1	-39.3
310	0.7775E-02	0.490E 00	-49.1	-39.3
311	0.7777E-02	0.486E 00	-49.2	-39.4
312	0.7780E-02	0.482E 00	-49.2	-39.4
313	0.7782E-02	0.480E 00	-49.2	-39.4
314	0.7785E-02	0.478E 00	-49.2	-39.4
315	0.7787E-02	0.477E 00	-49.2	-39.5
316	0.7790E-02	0.476E 00	-49.2	-39.5
317	0.7793E-02	0.476E 00	-49.2	-39.5
318	0.7795E-02	0.477E 00	-49.2	-39.5
319	0.7797E-02	0.478E 00	-49.2	-39.5
320	0.800E-02	0.479E 00	-49.2	-39.4
321	0.802E-02	0.480E 00	-49.2	-39.4
322	0.805E-02	0.482E 00	-49.2	-39.4
323	0.807E-02	0.484E 00	-49.2	-39.4
324	0.810E-02	0.486E 00	-49.2	-39.4
325	0.812E-02	0.488E 00	-49.1	-39.4
326	0.815E-02	0.490E 00	-49.1	-39.3
327	0.817E-02	0.491E 00	-49.1	-39.3
328	0.820E-02	0.493E 00	-49.1	-39.3
329	0.822E-02	0.494E 00	-49.1	-39.3
330	0.825E-02	0.496E 00	-49.1	-39.3
331	0.827E-02	0.497E 00	-49.1	-39.3
332	0.830E-02	0.497E 00	-49.1	-39.3
333	0.832E-02	0.497E 00	-49.1	-39.3